United States
Department of
Agriculture

**Agricultural
Research
Service**

ARS-80

April 1990

Small Watershed Model (SWAM) for Water, Sediment, and Chemical Movement

Supporting Documentation

ABSTRACT

DeCoursey Donn G., coordinator. 1990. Small Watershed Model (SWAM) for Water, Sediment, and Chemical Movement: Supporting Documentation. U.S. Department of Agriculture, Agricultural Research Service, ARS-80, 276 pp.

This publication presents the theoretical basis for some of the components of SWAM, a model for estimating the movement of runoff, sediment, plant nutrients, and chemicals from small agricultural watersheds.

KEYWORDS: ammonium transfer, crop-residue-derived nutrients, groundwater transport, labile phosphorus, nutrient cycling, nutrient release, nutrient transport, pesticide dissipation, pesticide sorption, pesticide transport, sediment-adsorbed nutrients, soluble phosphorus.

Small Watershed Model (SWAM) for Water, Sediment, and Chemical Movement

Supporting Documentation

PREFACE

Section 208 of Public Law 92-500, the 1972 amendments of the Clean Water Act, places emphasis on nonpoint-source pollution. Planning required by this legislation emphasizes the need for methods to assess nonpoint sources of pollution under various management practices and recommend treatment to reduce nonpoint pollution to acceptable levels.

Given the expertise within the research staff of the Agricultural Research Service (ARS) and in response to the high priority needs of action agencies, the National Program Staff (NPS) developed plans for a concerted national effort to develop mathematical models for evaluation of nonpoint-source pollution. A steering committee (NPS Scientists) for the effort met with a technical work group in October 1977 to initiate the program. This was followed by a workshop of interested ARS scientists in February 1978.

A major objective of that meeting was the development of a plan of action to assemble a model that would estimate runoff, sediment, plant nutrient, and pesticide movement in a field. That effort culminated in the development and publication in May 1980 of "CREAMS, a Field Scale Model for Chemicals, Runoff, and Erosion from Agricultural Management Systems," edited by Water G. Knisel, Jr.

A second objective of the meeting was the development of plans to extend the modeling effort from the field scale to the basin scale. Plans were to do this using an intermediate step, development of a small watershed model. The small watershed model (SWAM) would be a research tool in extrapolation of data from field to basin scales. The small watershed modeling effort was originally designed to use the CREAMS model concepts to simulate responses from field sized areas. These responses were to be routed through stream channels, adding other field responses as they were encountered, to a given point downstream. Because the small watershed model was to be much larger than a single field in size, it was designed to include the contribution of groundwater and the effects of movement through surface impoundments, such as small lakes and ponds. In all cases, water, sediment, and agricultural chemicals (pesticides and nutrients) were traced.

Concepts, upon which SWAM was developed, have changed very little. However modular design has enabled the development team to use the most current technology in all components; thus the source area response uses the most recent CREAMS model, OPUS, developed by R.E. Smith, Fort Collins, CO. The channel routing and groundwater subsystems have been updated considerably, and the pond model completely rewritten. Documentation and information for potential users are being prepared, as of this date, and will be available in the next few months.

A large number of ARS scientists have contributed to the development of SWAM. Many of those scientists contributed by providing algorithms of specific subprocesses. Many of those processes are described in papers presented in this document. Not all of the concepts described in these papers have been incorporated in SWAM, but many of them have been. However, the papers themselves provide valuable information to others interested in simulating the processes. Authors of material upon which these scientists drew are acknowledged throughout the publication.

The purpose of this publication is to provide support for subprocesses used in SWAM. SWAM is a very comprehensive model made up of many subsystems: thus its documentation must be very concise. In order not to detract from the objective in writing a description of the model, details of many of the subprocesses are described as supporting documentation and presented in this report.

Questions relative to the overall structure of SWAM and supporting documentation should be addressed to me or to the authors of specific subprocesses.

Donn G. DeCoursey
Project Coordinator
USDA-ARS
P.O. Box E
301 South Howes
Fort Collins, CO 80522

ACKNOWLEDGMENTS

CONTENTS

ESTIMATING PESTICIDE SORPTION COEFFICIENTS
FOR SOILS AND SEDIMENTS

R.E. Green and S.W. Karickhoff

ABSTRACT

An approach is presented for estimating pesticide sorption coefficients for
soils and sediments when such coefficients are not available by direct
measurement. Pesticide sorption estimates can be based either on the affinity
of soil organic carbon for hydrophobic pesticides or on experimentally derived
relationships between sorption and surface area of soil constituents.
Assumptions inherent in both approaches are defined and evaluated in the context
of environmental assessments for which sorption parameters are required.
Published partition coefficients for a large number of pesticides are summarized
in the appendix.

INTRODUCTION

Mathematical prediction of the distribution of a pesticide in the environment
after its application to agricultural fields requires measured or estimated
values of the distribution coefficients. These coefficients represent relative
concentrations of the pesticide in various phases: liquid (solution phase),
solid (sorbed phase) and gas (vapor phase). In this paper we are concerned with
the distribution of pesticides between the solution and sorbed phases, that is,
the distribution which dominates the mobility of pesticides associated with
soils or sediments.

The importance of pesticide sorption from solution on the environmental fate of
pesticides is widely recognized. The physical-chemical nature of the sorption
process for a variety of chemicals on organic and mineral surfaces has been
exhaustively reviewed (for example, Bailey and White 1964, Hamaker and Thompson
1972, Weber 1972, Weed and Weber 1974, Green 1974). Understanding the
mechanisms or magnitude of specific pesticide-sorbent interactions does not,
however, help substantially in assessments of pesticide distribution and impact
in the environment, unless sorption information is integrated with other
information on fate processes. Complex mathematical models have been developed
to accomplish this integration, but with considerable simplification in the
description of individual processes (for example, the ARM and HSPF models of EPA
or the CREAMS and SWAM models of ARS/USDA). The incorporation of a large number
of processes (physical, chemical, and biological) into a complex model usually
requires sacrificing detail in the description of any given process. The
principal reason for simplification is the lack of independently measured input
parameters needed in a detailed mathematical description of the process for a
variety of relevant environmental conditions. Such is the case for sorption of
pesticides. Although some progress has been made in identifying sorption
mechanisms, the complexity of sorption from solution on mixed colloids, such as
soils and sediments, has precluded rigorous theoretical analysis. Thus most
characterizations of pesticide sorption on soils are empirical simplications.

The most attractive simplification is that which can utilize existing or easily
developed data on pesticides and soils or sediments to provide sorption
estimates which are sufficiently accurate for a given modeling objective.
Currently, an approach which is widely accepted for management-oriented models
is a linear approximation of the sorbed-concentration/solution concentration
relationship, and expression of sorbed concentration with reference to organic
carbon content rather than to the mass of the whole soil or sediment (see, for
example, Hamaker and Thompson 1972, Chiou et al. 1979, Rao and Davidson 1980,
Kenaga and Goring 1980, Karickhoff 1981, McCall et al. 1981, Briggs 1981a and b,
Lyman 1982b, and Chiou et al. 1983). An alternative approach is to express
sorption on the basis of soil or sediment surface area rather than mass (Pionke
and deAngelis 1980); however, this surface area calculation also weights

_____

Professor of Soil Science, Department of Agronomy and Soil Science, University
of Hawaii, Honolulu, HI 96822, and Research Chemist, U. S. Environmental
Protection Agency, Athens, GA 30513.

sorption heavily toward organic carbon content. The organic carbon basis has gained the most acceptance because organic carbon content is commonly measured in soils and sediments, in contrast to surface area, which must be estimated from other soil properties. The coefficients obtained by both of these procedures are acceptable as input in the SWAM model (Pionke et al. 1985). However, it is important that the limitations of both simplified sorption approaches be understood by the model user and that inherent errors associated with their use be recognized and even quantified when possible.

The principal objective of this paper is to present a rational approach for estimating pesticide sorption coefficients for soils and sediments when such coefficients are not available by direct measurement. The general approach is based on the findings of numerous researchers whose data and conclusions provide some consensus for our recommendations. Several summaries of sorption data and octanol-water partition data for pesticides have been published in the past several years, increasing the likelihood that at least one of the estimation approaches suggested herein will provide the coefficient required for a given pesticide.

This paper first describes the K_{oc} approach for estimating pesticide sorption coefficients, including the assumptions inherent in the method and the implications of these assumptions. Indirect methods of estimating K_{oc} values for pesticides are then described and evaluated. Following this, the alternative approach of estimating pesticide distribution coefficients on a surface area basis is presented. Then a scheme to assist a potential user of the model in selecting an appropriate estimation procedure is outlined. Finally, various sources of existing data are identified and described, and K_{oc} prediction equations obtained from various sources are presented.

SORPTION ESTIMATES BASED ON PARTITIONING OF PESTICIDE
ON ORGANIC CARBON

A number of simplifying assumptions are inherent in the organic-carbon-referenced method of representing sorption of pesticides (K_{oc} approach). The errors in predicting pesticide distribution which are caused by violation of the assumptions in actual field situations are difficult to assess. The impact and importance of such errors will depend on the objective of the modeling effort and the sensitivity of model output to variation in sorption parameters. The following discussion will, hopefully, aid the prospective modeler in understanding the advantages and limitations of the K_{oc} approach.

The principal assumptions are (1) equilibrium in the sorption-desorption process, (2) linearity of the sorption isotherm, (3) singularity of the isotherm for sorption and desorption (sorption is reversible), and (4) sorption is limited to the organic component of the soil or sediment. Using the notation of Pionke et al. (1985) the assumed relationship between sorbed concentration C_s (mg pesticide per kg dry soil or sediment) and the solution concentration C_{sol} (mg pesticide per L solution) is

$$C_s = K_d C_{sol} \tag{1}$$

where K_d is the pesticide sorption distribution coefficient having units of L/kg. Whereas C_s represents pesticide sorption per unit mass of dry soil or sediment, C_s can also be adjusted to represent the amount of pesticide sorbed per unit mass of organic carbon, i.e.,

$$^{oc}C_s = K_{oc} C_{sol} \tag{2}$$

with K_{oc} also having units of L/kg when the mass of organic carbon is expressed in kilograms. If f_{oc} = (mass organic carbon)/(mass dry soil or sediment), K_{oc} is given by $K_{oc} = K_d / f_{oc}$, and $^{oc}C_s = C_s / f_{oc}$. Thus equation 2 represents a linear sorption isotherm which is referenced to organic carbon content, and K_{oc} is a distribution coefficient which describes the distribution of a pesticide between the aqueous phase and the soil organic phase. This approach is most appropriate for hydrophobic pesticides, that is nonionic pesticides with a water solubility less than about 10^{-3} M, but may be practically suitable for many pesticides which are slightly polar and too water soluble to be considered hydrophobic. Each of the assumptions inherent in using equation 2 to describe sorption in environmental assessments is discussed briefly.

Assumption of Equilibrium

Although there are a variety of laboratory methods available to measure sorption from solution (Green et al. 1980), the most commonly used method is "batch equilibration" in which a known mass of soil or sediment is equilibrated with an aqueous pesticide solution of known initial concentration until apparent equilibrium in the sorption process is achieved; the pesticide concentration in the aqueous phase is subsequently measured and sorption is calculated from the change in pesticide concentration in solution. It is doubtful that true equilibrium is reached in a few hours for sorbents high in organic carbon, especially if sorption is relatively high. Karickhoff (1980) suggests that the sorption process has a rapid component and a slower component, the rate of the latter depending largely on movement of solute to less accessible sorption sites; his analysis on one sediment indicated that the rate coefficient for the slow component varied inversely as the sorption partition coefficient.

For most practical applications laboratory measurements probably produce sorption coefficients which represent macroscale equilibrium quite well, even though equilibrium may not be reached at internal sorbent surfaces. The question to be answered, then, is whether or not an equilibrium sorption coefficient measured in the laboratory is appropriate for use in pesticide transport models to represent partition of the pesticide between the aqueous and sorbed states. This question is difficult to answer in a general sense because field systems being simulated may or may not be near equilibrium. In near-static soil-water systems, such as a soil profile at field capacity without evapotranspiration, equilibrium is likely approached, and an equilibrium sorption coefficient may provide a good estimate of pesticide distribution in the soil. Laboratory results of Green and Obien (1969) for equilibration of atrazine in pots of soil at various water contents encourage such a conclusion. On the other hand, during infiltration and redistribution of water in soils, the equilibrium sorption coefficient appears to overpredict pesticide retardation in both laboratory columns and the field. Bilkert and Rao (1985) found that for two nematicides (neither hydrophobic) the equilibrium K_d of equation 1 had to be multiplied by a factor of about 0.4 to successfully predict the position of a pesticide peak in soil columns or in a field soil profile. Assuming equilibrium conditions for dynamic systems will result in calculating too much pesticide in the sorbed state for the sorption process and too little in the sorbed state for the desorption process. Pionke et al. (1985) present a rationale for treating the chemical system in the SWAM Model as an equilibrium system.

Assumption of Linearity

The linear relationship (equations 1 and 2) is a desirable simplification for models as it allows simpler mathematical solutions. For many environmental contexts, e.g., runoff and stream flow, the linear approximation is probably quite accurate and acceptable in terms of other errors associated with the estimation of water and sediment transport. Karickhoff (1981) cites evidence that for hydrophobic polycyclic aromatic compounds sorbed on natural sediments the sorption isotherms are linear if the equilibrium concentration of solute in the aqueous phase is below 10^{-5} M (1 to 3 ppm) or less than one-half the solute solubility in water, whichever is lower. At the higher concentrations encountered in surface soils soon after application of a pesticide to the soil, the linear assumption may result in sorption estimates that are too high by 2- to 3-fold or even more, depending on the extent of isotherm nonlinearity and the concentration of solute in solution. In an analysis of data from the literature for a large spectrum of organic compounds and numerous sorbents, Rao and Davidson (1980) found the exponent N, in the Freundlich equation $S = K_f C^N$, to have a mean value of 0.87 with a coefficient of variation of 14.8%. These data included measurements made with solution concentrations far above the 10^{-5} M limit mentioned previously, but the results emphasize the difficulty of using a single sorption coefficient for all model applications. When N departs significantly from unity (N=1) the apparent K_d may change substantially with changes in pesticide concentration in solution. The error which results from assuming a linear relationship when the Freundlich equation (a power function) is the appropriate mathematical form was given in tabular form by Hamaker and Thompson (1972) and in graphical form by Rao and Davidson (1980).

Assumption of Singularity

An additional uncertainty in the measurement and application of sorption data is the question of whether a single sorption isotherm can represent both sorption and desorption of the pesticide. Numerous investigators have shown, by simply reversing the sorption experimental procedure, that less organic solute is desorbed from the colloid over a given solution concentration interval than was sorbed initially. This apparent nonsingularity, often called sorption hysteresis, has been assessed experimentally and from the literature by Rao and Davidson (1980); they conclude "that while nonsingularity of pesticide adsorption-desorption isotherms may often be an artifact, it could be real and significant for certain compounds'." Calculation of the error introduced by assuming singularity of a nonsingular Freundlich isotherm showed that the error is greater at low solution concentrations (i.e., far away from the maximum solution concentration at which desorption was initiated) and decreases with increasing nonlinearity of the isotherm (Rao and Davidson 1980). Again, perhaps this error is acceptable for a comprehensive environmental model, but the impact should be evaluated by sensitivity analysis.

Assumption of Partitioning on Organic Carbon

The three assumptions above are inherent in the use of equation 1. Adoption of equation 2 as a further simplification is attended by some additional assumptions, which if invalid will introduce more error. It appears that the errors associated with the assumption of partitioning pesticides on organic carbon may be much larger than those resulting from the first three assumptions. If the model user is to avoid unacceptably large errors which may lead to inappropriate conclusions from model calculations, an awareness of the limits of applicability of the partitioning assumption is necessary.

If equation 2 were to be strictly correct and universal in its application, even if only among so-called hydrophobic organic pollutants, the following assumptions would have to be valid: (1) Sorption occurs only on the organic component of the soil, i.e., the mineral component has little or no effect; (2) the organic matter in all soils and sediments is the same with respect to its performance as a sorbent for a given hydrophobic organic solute; (3) the effects of variations in other factors, such as ionic strength of the solution, pH, and temperature, have little or no impact on the amount of pesticide sorbed.

Clearly, none of these assumptions is valid in the strict sense, so that use of organic-carbon-referenced sorption will introduce errors, the magnitude of which depends on how severely the assumptions are violated in a given system. Opinions concerning the K_{oc} approach for environmental assessments range from enthusiastic support (Chiou et al. 1979) to skepticism (Mingelgrin and Gerstl 1983). The application of this concept has been proposed and also questioned repeatedly since its introduction relative to pesticides in the early 1960's. Acceptance of the approach has been encouraged by the increasing need for calculation procedures applicable to hundreds of organic chemicals in hazard assessments for a wide range of environmental conditions.

The importance and urgency of developing a generalized procedure justifies some sacrifice in scientific rigor and accuracy. On the other hand, theoretical justification for the K_{oc} approach has been provided by Karickhoff (1981, 1984), who identifies the organic-carbon/hydrophobic-chemical interaction as a "first-order" effect in contrast to the "second-order" effects of other factors of lesser importance. In practice, one must know when "second-order" effects are important. For example, Mingelgrin and Gerstl (1983) challenge the use of the partitioning concept (i.e., that hydrophobic organic chemicals are partitioned between water and the organic component of soils or sediments in a manner analogous to partitioning between two immiscible solvents); they contend that other mechanisms may play a dominant role, e.g., pesticide-clay-water interactions. These authors illustrate their point by showing the variability in K_{om} (sorption coefficient referenced to organic matter rather than organic carbon) for 12 compounds sorbed on soils or sediments having a wide range of organic matter contents. The largest variation in K_{om} was for parathion (factor of 50 between the largest and smallest value) and the smallest was for dieldrin (factor of 3). The variability that one might anticipate in K_{oc} values for a given compound is indicated by the coefficient of variability calculated for 43 chemicals by Rao and Davidson (1980). Many important pesticides have polar functional groups that preclude strictly hydrophobic behavior, and several

others are weak acids or bases, requiring that care be exercised in applying the K_{oc} approach indiscriminantly to all pesticides. The scheme proposed in this paper for determining a distribution coefficient for a given pesticide-soil system recognizes the need for alternative procedures for nonhydrophobic chemicals.

The role of clays in sorption of organic chemicals is addressed quantitatively by Karickhoff (1984). His analysis of a few sets of experimental data suggests that swelling clays may have important effects on sorption of some hydrophobic organics in sediments having low organic carbon contents, but when the ratio of clay to organic carbon is less than 30, contributions of mineral surfaces are masked regardless of the clay content. Thus, further scrutiny of the available data and continued research in this area will help to define applications in which the K_{oc} approach is acceptable.

Finding an Appropriate K_{oc} Value

Once one has decided to use the K_{oc} approach for a reasonably hydrophobic pesticide, the next step is to find the appropriate K_{oc} value. Several tabulations of K_{oc} values for a large number of pesticides are now available; these sources are given in a later section, "Sources of Sorption Data...." If a K_{oc} value is not available for a given pesticide, it may be possible to calculate an approximate K_{oc} from the octanol-water partition coefficient (K_{ow}), if one exists for the pesticide of interest. The K_{ow}-based prediction of K_{oc} and other indirect methods of estimating K_{oc} are presented in the next section. Additional error will usually be introduced by indirect approaches; these errors should be evaluated in the context of variability in K_{oc} associated with variation of organic carbon content of soils in a watershed. More research is needed to quantify the relative magnitude of errors contributed by various sources of variation mentioned in this section.

INDIRECT METHODS OF ESTIMATING K_{oc}

Estimating the sorption of uncharged organics, as discussed above, can often be reduced to estimating K_{oc}, which, when combined with organic carbon content, yields an estimate of the soil/water distribution coefficient, K_d.

The approach used in estimating K_{oc} combines thermodynamic theory and empirical correlation to relate sorption parameters to widely measured properties of pesticides and soils. Theory is used to suggest the mathematical form relating the physical properties, and experimental data are used to empirically establish constants (by calibration) in the mathematical equation. This approach is far preferable to complete reliance on empirical correlation which precludes extrapolation out of the narrow range of substances or system properties upon which it is based.

K_{oc} can be expressed as a ratio of solute activity coefficients in the aqueous phase, γ^w, and organic carbon phase, γ^{oc}, thus $K_{oc} = \gamma^w / \gamma^{oc}$. Activity coefficients quantify pesticide affinity for a given phase. In considering K_{oc} for a series of uncharged pesticides, one would expect variations in K_{oc} to be dominated by variations in aqueous phase affinity. This derives from the dissimilarity of the organic solute with the aqueous medium, with variations in γ^w from solute to solute comparable to variations in aqueous solubilities. For uncharged solutes, one would expect much less variability in affinity for soil organic matter (γ^{oc}). Water outcompetes organic solutes for polar sites on soil surfaces, substantially reducing hydrophilic-bonding contributions for uncharged chemicals. Futhermore, lipophilic interactions with soil organic matter are not highly variable from solute to solute, and their differences in K_{oc} are dominated by γ^w (Chiou et al. 1983, has recently addressed γ^{oc} variability explicitly). The aqueous phase activity coefficient, γ^w, provides the thermodynamic link relating K_{oc} to other solute properties, such as water solubility, molecular surface area, or octanol-water partition coefficient. Table 1 is a tabulation of semiempirical equations for estimating K_{oc} from solute physical properties, such as solubility in water (S), melting point (mp), and octanol-water partition coefficient (K_{ow}). These equations are generally applicable for uncharged pesticides of limited water solubility ($< 10^{-3}$ M) that are not susceptible to speciation changes or other complex formation in soil suspensions of interest. Soil organic matter dominance of sorption is presumed, so the ratio of clay/organic carbon must be < 40; otherwise, mineral

Table 1.—Semiempirical equations for estimating K_{oc} from solute physical properties

	Calibration Compounds[1]	K_{oc} Range	Number of Compounds	r^2	Reference
a. log K_{oc} = -0.68 log S(μg/ml) + 4.273	pn, ha, aa, ch	10-10^6	23	0.93	Hassett et al. 1980
b. log K_{oc}[2] = -0.557 log S(μmole/L) + 4.277	ch	10-10^5	15	0.99	Chiou et al. 1979
c. log K_{oc} = -0.83 log S(mole fraction)[3] - 0.01(mp-25°C)[4] - 0.93	pn, ch, ct, cb, op	10^2-10^6	47	0.93	Karickhoff 1984
d. log K_{oc}[2] = -0.729 log S(molar) - 0.0073 (mp - 25°C) + 0.24	pn, ch	10-10^5	12	0.996	Chiou et al. 1983
e. log K_{oc}[2] = -0.808 log [v̄S(molar)][5] - 0.0081 (mp - 25°C) - 0.74	pn, ch	10-10^5	12	0.997	Chiou et al. 1983
f. log K_{oc}[2] = 0.904 log K_{ow} - 0.539	pn, ch	10-10^5	12	0.989	Chiou et al. 1983
g. log K_{oc} = 1.029 log K_{ow} - 0.18	ch, ct, cb, op, ur, pa	10-10^5	13	0.91	Rao and Davidson 1982
h. log K_{oc} = log K_{ow} - 0.317	pn, ha, aa, ch	10-10^6	23	0.98	Hassett et al. 1980
i. log K_{oc} = 0.72 log K_{ow} + 0.49	ch, mb	10^2-10^4	13	0.95	Schwarzenbach and Westall 1981

1/ pn-polynuclear aromatic hydrocarbons; ha-heteronuclear aromatic hydrocarbons; aa-aromatic amines; ch-chlorinated hydrocarbons; ct-chloro-s-triazines; cb-carbamates; op-organophosphates; ur-uracils; pa-phenoxy acids; mb-methylated benzenes.
2/ Original data expressed as K_{om}; the factor 1.74 was used to convert K_{om} to K_{oc}; K_{oc} = 1.74 K_{om}.
3/ For hydrophobic compounds, the solubility, S(mole fraction) ≈ S(molar) x 18/1000.
4/ mp - melting point in degrees Celsius; reference temperature 25°C; for liquids mp set at 25°C, crystal term vanishes.
5/ v̄ pure solute molar volume (L/mole).

contributions should be addressed. The reader is cautioned that the generalized equations in Table 1 are expected to give only approximate estimates of K_{oc}. An equation developed for a broad range of chemical structures will likely give questionable results for pesticides which are not well represented by the chemicals used to develop the equation.

SORPTION ESTIMATES BASED ON SPECIFIC SURFACE
OF SOIL OR SEDIMENT

An alternative to the organic-carbon-referenced sorption approach may be desirable for some pesticide-soil combinations. For example, if the chemical is nonhydrophobic the relationship between K_d and f_{oc} may not be reliable. The K_{oc} approach may also be inappropriate for soils or sediments having a clay/organic-carbon ratio which is sufficiently high (perhaps > 40) for the clay contribution to pesticide sorption to be a significant part of the total sorption.

Pionke and DeAngelis (1980) developed an estimation methodology which allows one to predict K_d values for a large number of pesticides on the basis of the relationship of K_d to either the organic carbon content or the specific surface of the soil or sediment. The specific surface (SS) was calculated from the equation

$$SS = 100 \ (\% \ OC) + 2.0 \ (\% \ clay) + 0.4 \ (\% \ silt) + 0.005 \ (\% \ sand).$$

The coefficients for mineral fractions in the equation were taken from the work of Young and Onstad (1976), while the coefficient for % OC was determined from data presented by Bailey and White (1964), with the assumption that most clay in intact soils would exhibit the surface area of kaolinite (20 m^2/g). The Pionke-DeAngelis method is based on linear regressions between measured K_d values for 35 pesticides and either % OC or SS; the SS calculation is heavily weighted toward organic carbon, i.e. % OC dominates except where % clay is large and % OC is very small. It was designed to give results similar to the K_{oc} calculation (Pionke, personal communication). For a diverse group of pesticides the equation $K_d = mSS$ gave consistently higher coefficients of determination than did the equation $K_d = m \ (\% \ OC) + b$; thus the authors recommended the surface area approach.

To extend the relationship between K_d and soil surface area to other pesticides which were not included in the original data set, Pionke and DeAngelis developed curves relating m values from the two equations to published R_f values from soil-thin-layer chromatography (Helling 1971). Since R_f values were available for about 100 pesticides, the R_f-m relationship obtained for the original group of pesticides could then be used to predict m values for many other pesticides for which R_f values had been measured. The procedure requires an assumption that the standard soil on which the R_f values were measured (Hagerstown silty clay loam) is reasonably representative of the soils for which the predictions of pesticide sorption are to be made. The authors present data of Helling (1971) which show that R_f values for the Hagerstown soil were representative of the average mobility of 13 pesticides on a number of fine textured soils. However, the Hagerstown data did not adequately represent R_f results for two coarse-textured soils.

While the soil-thin-layer procedure is a good way to characterize relative mobilities of a large number of pesticides, it is risky to assume that the relationship between R_f and m values can be applied to any soil of interest, even if the soil is fine textured. In the present context we are interested in predicting a sorption coefficient for a specific pesticide on a specific soil, which may not be well represented by the average mobility of the pesticide on many soils. However, in spite of this principal limitation of the Pionke-DeAngelis method, the approach does provide an alternative for pesticide-soil combinations for which the K_{oc} method appears inappropriate. The reader is encouraged to consult the paper by Pionke and DeAngelis for details.

SELECTING A SORPTION COEFFICIENT FOR A GIVEN COMBINATION
OF PESTICIDE AND SOIL OR SEDIMENT

In the event that it is not possible or practical to measure an appropriate distribution coefficient for a specific pesticide-soil combination, then an

estimation procedure must be followed. The following decision sequence provides a systematic approach to obtaining an estimate of a sorption coefficient.

Required information:

1. The nature of the chemical. Five useful groupings of chemicals are (a) hydrophobic (solubility in water less than 10^{-3}M or about 300 mg/L); (b) sufficiently polar so that solubility in water exceeds 10^{-3} M, but not cationic or a weak acid or weak base; (c) a weak base; (d) a weak acid; (e) a cation.

2. Soil or sediment properties. The nature of the pesticide and the associated procedure used to obtain an appropriate sorption coefficient will determine what soil or sediment properties are required. In general, the order of priority for required data will be (a) organic carbon content, (b) clay, silt, and sand contents, (c) pH. Organic carbon content is required for both the K_{oc} approach and the surface area approach. Percentages of the various textural separates are required for the surface area approach and will aid in estimating the mineral contribution to sorption. The pH is needed only if the pesticide of interest is an acid or base.

A scheme for obtaining a sorption coefficient for a given pesticide in a given soil or sediment is shown in Figure 1. Each decision or action step is numbered for easy reference in the following discussion. While an attempt has been made to provide a definitive procedure that can be followed by anyone with a basic understanding of the chemistry of pesticides and soils, there are a number of points of uncertainty that will be encountered in using the scheme. For example, the definition of "hydrophobic" is somewhat arbitrary, but the criterion of $< 10^{-3}$ M solubility in water is a useful, though perhaps conservative, upper boundary for hydrophobic compounds. Other criteria for decisions, such as in steps 2 and 11 are based on experimental evidence but may not be appropriate for all soil-pesticide combinations. Experience in using the scheme in Figure 1 will hopefully lead to procedural improvements.

Some brief explanations or directions associated with several steps in Figure 1 are given below to assist in the use of the scheme.

<u>Steps 1 and 8 through 20</u>

The use of the K_{oc} approach is most appropriate for organic chemicals of limited solubility in water. Karickhoff (1984) has suggested a solubility of $< 10^{-3}$ M, or about 100 to 300 mg/L, for most pesticides. K_{oc} values are available in the literature for many chemicals with much higher solubilities in water, but the reliability of the K_{oc} approach is more questionable for these pesticides than for hydrophobic chemicals.

There are unique problems associated with estimating sorption coefficients for weak acids and weak bases due to significant changes in sorption mechanism and quantity sorbed with changes in soil pH. Two generally accepted assumptions for such pesticide-soil systems provide guidelines for estimating K_d values for weak acids and weak bases. One assumption is that the pH at colloid surfaces is lower than in a bulk soil-water suspension, such as in the 1:1 soil:water slurry often used for pH measurement. A reasonable estimate of surface acidity (pH_s) is two pH units lower than the bulk suspension pH, i.e., $pH_s = pH - 2.0$. The other assumption is that in aqueous solutions the ratio of molecular to ionic species is 1:1 when pH = pK_a. Most weakly acidic pesticides are in predominantly ionic (negatively charged) form at the pH of most agricultural soils, while most weakly basic pesticides are in molecular form. In either case as soil pH decreases toward a value equal to the pK_a of the pesticide, sorption tends to increase because the acidic pesticide has more of the molecular species at low pH and the basic pesticide has more of the protonated (positive) ionic species at low pH.

The colloidal surfaces of most agricultural soils have a net negative charge and thus have an affinity for positively charged species of bases but not much affinity for negatively charged species of acids. Pionke and DeAngelis (1980) adopted the following approximations: 50% of the basic pesticide is positively charged when the measured soil suspension pH minus 1.0 equals the pK_a, and 50% of the acidic pesticide is negatively charged when soil suspension pH equals the pK_a. These workers suggest that if measured pH minus 2 is one or more pH units
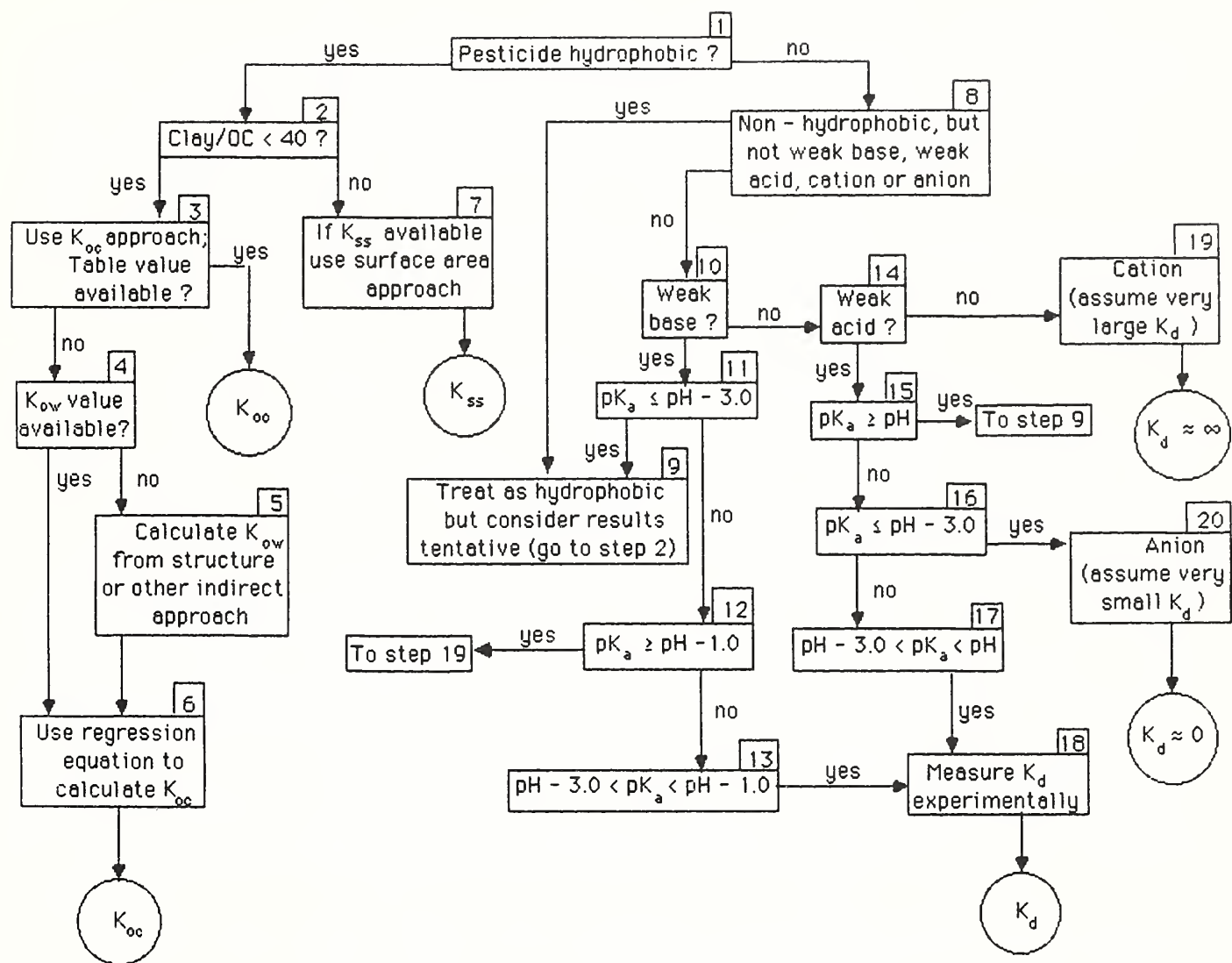
Figure 1
A scheme for obtaining sorption coefficients.

above the pK_a of the pesticide, the effect of pH on K_d can be considered insignificant. This limiting criterion can be summarized by $pK_a \leq$ (soil pH -3). In the absence of other more rational approaches, the above rule is adopted for weak bases in the scheme in Figure 1 (see step 11). Additional useful criteria have been suggested by Pionke (personal communication) and are included in the sequence for weak bases and weak acids in Figure 1. These criteria should be considered tentative since they have not been confirmed experimentally. The rationale for each step is given to aid the reader in evaluating the procedure.

The relevant equilibrium for weak bases is

$$RH_2^+ \rightleftharpoons RH + H^+$$

Then $K_a = \{[RH][H^+]\}/[RH_2^+]$

or $pK_a = pH_s + p[RH/RH_2^+]$.

Assuming $pH_s = pH - 2.0$, we get

$$pK_a = pH - 2.0 + p[RH/RH_2^+].$$

If we require $[RH] \geq 10[RH_2^+]$

or $[RH]/[RH_2^+] \geq 10$

for a compound to be considered hydrophobic (in addition to the solubility criterion), then $pK_a \leq pH - 3.0$ is the appropriate criterion (step 11). Conversely, if $[RH]/[RH_2^+] < 0.1$, then the compound would be expected to behave like a cation because 90% or more is positively charged. Thus, for a weak base to be considered cationic, $pK_a \geq pH - 2.0 + p(0.1)$ or $pK_a \geq pH - 1.0$, as given in step 12. For pH/pK_a relationships which are intermediate to the above extreme cases (i.e., the chemical cannot be considered either molecular or cationic but rather a mixture of both species), a measured value of K_d is required (step 18).

Many acidic pesticides are negatively charged at prevailing soil pH values and thus are not hydrophobic. However, a procedure analogous to that suggested for weak bases can be rationalized for weak acids.

$$RH \rightleftharpoons R^- + H^+$$

$$K_a = \{[R^-][H^+]\}/[RH]$$

or $pK_a = pH_s + p[R^-/RH]$

Again, with $pH_s = pH - 2.0$ as assumed earlier for the computation with weak bases, $pK_a = pH - 2.0 + p[R^-/RH]$. If we require $[R^-/RH] \geq 10$ (corresponding to 90% or more in the anion form) for the weak acid to be considered anionic, then the appropriate numerical criterion is given by

$$pK_a \leq pH - 2.0 + p[10]$$

or $pK_a \leq pH - 3.0$

as shown in step 16. For the unusual case in which an acidic pesticide may be hydrophobic, a more restrictive criterion such as $[R^-/RH] < 0.01$ may be desirable to ensure a very small fraction of the mobile anionic species. Thus, $pK_a \geq pH - 2.0 + p[0.01]$ or $pK_a \geq pH$, as given in step 15, is the appropriate criterion. Intermediate pK_a values (step 17) would require that the K_d be measured experimentally. Values of pK_a for several basic pesticides are given by Pionke and DeAngelis (1980).

Steps 2 and 7

The K_{oc} approach assumes no contribution of the mineral fraction of a soil or sediment to sorption of a hydrophobic chemical. However, when the organic carbon content of the sorbent is low relative to the clay content, the clay may contribute to sorption (Minglegrin and Gerstl 1983; Karickhoff 1984). Karickhoff (1984) found a threshold for swelling-clay contribution to sorption at an f_{cm}/f_{oc} ratio of about 30/1 for clay mineral fraction (f_{cm}) to organic

carbon fraction (f_{oc}). This ratio can be expected to vary with clay type, swelling clays being more active in sorption than nonswelling clays. At the present time there is no quantitative method of correcting for mineral contribution to sorption, but a threshold of about 40 for f_{cm}/f_{oc} may be a reasonable value to adopt in view of the suggestion by Karickhoff of 25 to 60 for neutral organics with polar functional groups and >60 for nonpolar organics.

Steps 3 and 4

Sources of K_{oc} and K_{ow} data for a large number of pesticides are given in a later section in this chapter. It is anticipated that such data will be developed in the near future for all commercially available pesticides used on field crops.

SOURCES OF SORPTION DATA, OCTANOL-WATER PARTITION DATA
AND OTHER INFORMATION PERTINENT TO SORPTION ESTIMATES

It is our intention in this section to direct the reader to the principal published summaries of pesticide sorption data. New data continue to be published so that any published summary is soon dated. It would be a major service to model users if some agency would undertake the ongoing accumulation, categorization, and development of a computer retrieval system for all environmentally relevant distribution coefficients. An admirable attempt in this direction has been initiated by Ralph Nash, USDA-ARS, Pesticide Degradation Laboratory, Beltsville, MD.

A well-organized and well-documented data set which could be easily accessed by potential users would have tremendous value in the future. However, at the present time one must rely on existing published summaries of data or find individual published research papers dealing with specific chemicals of interest. Several of the summary-type papers have presented regression equations, calculated with the data base at hand, which further summarize the relationships of measured K_d or K_f to organic carbon content or the relationship of K_{oc} to K_{ow} or solubility in water. In general, such regression equations summarize a large body of data obtained from various sources; use of such equations has the advantage of generality of application but the disadvantage of incorporating a high level of variability which is inherent in the procedure of lumping data from many sources.

The following selected sources of data are given in the order that the manuscripts were first made available or published. Original measured sorption data are included in a number of summaries of sorption data. Usually the source of the original data is cited in the summary paper.

1. <u>Hamaker and Thompson (1972)</u>. This comprehensive paper on sorption processes in soils tabulates the following data for a large number of pesticides:

    -- Average K_d and C.V. (coefficient of variation)
    -- Average K_f and 1/n (Freundlich constants) and C.V.
    -- Average K_{oc} derived from K_d or K_f and the C.V. for K_{oc}
    -- Range of organic carbon contents (%) of soils or sediments in sorption experiments
    -- Range of pesticide concentrations in solution
    -- Equilibration times
    -- Temperatures
    -- Number of soils used in each study

The authors have provided separate data summaries for soils containing more than 8.7% organic carbon.

2. <u>Kenaga and Goring (1980)</u>. This report was first made available in a symposium proceedings in 1978. It lists 170 chemicals (principally pesticides) and provides average values of K_{oc}, K_{ow}, water solubility (WS), and bioconcentration factor (BCF). No estimate of variability is given, but references to the original sources of the data are provided. Using the appropriate data for all chemicals in the table, Kenaga and Goring calculated regression coefficients for the linear equations relating pairs of coefficients (in log form). For example:

11

$$\log K_{oc} = 1.377 + 0.544 (\log K_{ow}) \tag{3}$$

$$\log K_{oc} = 3.64 - 0.55 (\log WS) \tag{4}$$

The correlation coefficients for equations 3 and 4 were 0.86 and -0.84, respectively, and the 95% confidence limits on $\log K_{oc}$ were ± 1.37 and ± 1.23, respectively. The considerable prediction error represented by these confidence intervals is likely the result of including such a wide variety of chemicals in a single regression. The prediction error is expected to be much less for regressions accomplished with chemicals of similar structure and properties.

3. Rao and Davidson (1980). This summary provides mean values of K_d or K_f and the associated derived values of K_{oc} and $\ln K_{oc}$ (they used the base e logarithm here) for 44 chemicals, most of which are herbicides. Coefficients of variation and the number of soils included in the measurements for each chemical are also given. In addition, K_{ow} values are provided for 67 chemicals. A linear regression of $\log K_{oc}$ on $\log K_{ow}$ for the sorption data of 13 pesticides presented in this paper resulted in the equation

$$\log K_{oc} = 1.029 \log K_{ow} - 0.18 \tag{5}$$

with $r^2 = 0.91$. This equation differs considerably from equation 3 (above) of Kenaga and Goring.

It is of interest that the coefficient of variation for $\ln K_{oc}$ was found to be much lower than the C.V. for K_{oc} for most pesticides. Also the geometric mean of K_{oc} was generally lower than the arithmetic mean.

4. Pionke and DeAngelis (1980). This paper is summarized in a previous section entitled "Sorption Estimates Based on Specific Surface of Soil or Sediment." Tabular sorption data are presented for 35 pesticides. Distribution coefficients for these chemicals can be calculated for a given soil from the organic carbon content (% OC) or the specific surface area (SS, m^2/gm) using the regression equations $K_d = m$ (% OC) + b or $K_d = m$ (SS). Also, the relationships developed for the 35 chemicals can be used to determine K_d values for about 100 pesticides for which soil-thin-layer chromatography R_f values are available.

5. Briggs (1981a). This paper seeks to establish a general relationship between the partition coefficients for organic chemicals sorbed on soil organic matter (K_{om}) and the octanol-water partition coefficients (K_{ow}) of the same chemicals. The K_{om} of Briggs is related to K_{oc} by $K_{om} = K_{oc}/1.724$. Initially, sorption measurements for 72 chemicals were made on four soils at four solution concentrations. The resulting sorption isotherms were sufficiently linear to justify calculation of K_{om} values for each chemical on each of the four soils (organic matter percentages ranged from 1.09 to 4.25%). This group of chemicals included only 12 pesticides, most of which were substituted urea compounds. Subsequent measurements of K_{om} for other chemicals (including some pesticides) on one or more soils were made at only one solution concentration. Tabular values of $\log K_{om}$, $\log K_{ow}$, and $\log WS$ are given for all chemicals. Also, the linear regression of $\log K_{om}$ on $\log K_{ow}$ was accomplished for each chemical group (13 groups). The average correlation coefficient for all of the regressions was 0.95.

Other recent papers present original measured K_{om} or K_{oc} results for a limited number of pesticide-soil combinations. For example, Briggs (1981b) examined the relationship of K_{om} and K_{ow} for 24 chemicals, 12 of which were pesticides; this study involved 17 soils, having organic matter contents varying from 0.19 to 6.62% (corresponding to organic carbon contents of 0.11 to 3.84%). The chemicals were mostly substituted phenylurea herbicides. Another recent study (Rao et al. 1984) included five herbicides and three insecticides sorbed on seven soils and particle-size separates of the same soils. K_{oc} values calculated from measured sorption on these soils were compared with K_{oc} values from the literature and with values calculated from pesticide solubility and melting point. Twofold differences in K_{oc} values for a given chemical existed

between the three sets of data. Karickhoff (1981) found that variation between measured and computed K_{oc} values was comparable to deviations in measured K_{oc} values reported for a given compound on widely different sediments or soils.

To assist potential model users in finding sorption coefficients (K_{oc} or K_{ss}) or octanol-water partition coefficients (K_{ow}) for specific pesticides, we have provided an alphabetical listing of the pesticides for which such data are available in the above sources. The list is given in the appendix. As additional sources of data become available, the list can be updated periodically by the user. Commonly accepted chemical names have been used.

REFERENCES

Bailey, G. W., and White, J. L. 1964. Review of adsorption and desorption of organic pesticides by soil colloids, with implications concerning pesticide bioactivity. J. Agric. Food Chem. 12:324-332.

Bilkert, J. N., and Rao, P. S. C. 1985. Sorption and leaching of three nonfumigant nematicides in soils. J. Environ. Sci. Health, B20(1):1-26.

Briggs, G. G. 1981a. Theoretical and experimental relationships between soil adsorption, octanol-water partition coefficients, water solubilities, bioconcentration factors, and the parachor. J. Agric. Food Chem. 29:1050-1059.

Briggs, G. G. 1981b. Adsorption of pesticides by some Australian soils. Aust. J. Soil Res. 19:61-68.

Chiou, C. T.; Peters, L. J.; and Freed, V. H. 1979. A physical concept of soil-water equilibria for nonionic organic compounds. Science 206:831-832.

Chiou, C. T.; Porter, P. E.; and Schmedding, D. W. 1983. Partition equilibria of nonionic organic compounds between soil organic matter and water. Environ. Sci. Technol. 17:227-231.

Green, R. E., and Obien, S. R. 1969. Herbicide equilibrium in soils in relation to soil water content. Weed Sci. 17:514-519.

Green, R. E. 1974. Pesticide-clay-water interactions. In W. D. Guenzi (ed.), Pesticides in Soil and Water, pp. 3-37. Soil Science Society of America, Madison, WI.

Green, R. E.; Davidson, J. M.; and Biggar, J. W. 1980. An assessment of methods for determining adsorption-desorption of organic chemicals. In A. Banin and V. Kafkafi (eds.), Agrochemicals in Soils, pp. 73-82. Pergamon Press Inc., New York.

Hamaker, J. W., and Thompson, J. M. 1972. Adsorption. In C.A.I. Goring and J. W. Hamaker (eds.), Organic Chemicals in the Soil Environment, Chapter 2, Vol. 1. Marcel Dekker, Inc., New, York.

Hassett, J. J.; Means, J. C.; Banwart, W. L.; and Wood, S. G. 1980. Sorption properties of sediments and energy-related pollutants. EPA-600/3-80-041. U.S. Environmental Protection Agency.

Helling, C. S. 1971. Pesticide mobility in soils. III. Influence of soil properties. Soil Sci. Soc. Am. Proc. 35:743-748.

Karickoff, S. W. 1980. Sorption kinetics of hydrophobic pollutants in natural sediments. In R.A. Baker (ed.), Contaminants and Sediments, Chapter 11, Vol. 2. Ann Arbor Science Publishers, Inc., Ann Arbor, MI.

Karickhoff, S. W. 1981. Semi-empirical estimation of sorption of hydrophobic pollutants on natural sediments and soils. Chemosphere 10:833-846.

Karickhoff, S. W. 1984. Organic pollutant sorption in aquatic systems. J. Hydraulic Eng. 110:707-735.

Kenaga, E. E., and Goring, C. A. I. 1980. Relationship between water solubility, soil sorption, octanol-water partitioning and concentration of chemicals in biota. In J. G. Eaton, P. R. Parrish, and A. C. Hendriks (eds.), Aquatic Toxicology. ASTM STP 707, pp. 78. Philadelphia: Amer. Soc. Testing and Materials.

Lyman, W. J. 1982b. Adsorption coefficients for soils and sediments. In W. J. Lyman, W. F. Reehl, and D. H. Rosenblatt (eds.), Handbook of Chemical Property Estimation Methods, pp. 4-1 to 4-32. McGraw-Hill Book Co., New York.

McCall, P. J.; Laskowski, D. A.; Swann, R. L.; and Dishburger, H. J. 1981. Measurement of sorption coefficients of organic chemicals and their use in environmental fate analysis. In Test Protocols for Environmental Fate and Movement of Toxicants, Symposium Proceedings, pp. 89-109. Association of Official Analytical Chemists 94th Annual Meeting. AOAC, Arlington, VA.

Mingelgrin, U., and Gerstl, Z. 1983. Reevaluation of partitioning as a mechanism of nonionic chemicals adsorption in soils. J. Environ. Qual. 12:1-11.

Pionke, H. B., and DeAngelis, R.J. 1980. Method for distributing pesticide loss in field runoff between the solution and adsorbed phase. Chapt. 19. In CREAMS, A Field Scale model for Chemicals, Runoff, and Erosion from Agricultural Management System, USDA Conservation Research Report No. 26, pp. 607-643.

Pionke, H. B.; Kunishi, H. M.; Schnabel, R. R.; and others. 1985. SWAM--The chemical models used in the channel system. In D.G. DeCoursey (ed.), Proc. Natural Resour. Modeling Symposium, Pingree Park, Colo. Oct. 16-21, 1983, USDA-ARS, ARS-30, pp. 155-159.

Rao, P. S. C., and Davidson, J. M. 1980. Estimation of pesticide retention and transformation parameters required in non-point source pollution models. In M. R. Overcash and J. M. Davidson (eds.), Environmental Impact of Nonpoint Source Pollution, 67 pp. Ann Arbor Science Publishers, Inc., Ann Arbor, MI.

Rao, P. S. C., and Davidson, J. M. 1982. Retention and transformation of selected pesticides and phosphorus in soil-water systems: A critical review. EPA-600/3-82-060. U.S. Environmental Protection Agency.

Rao, P. S. C.; Berkheiser, V. E.; and Ou, L. T. 1984. Estimation of parameters for modeling the behavior of selected pesticides and orthophosphate. EPA-600/3-84-019, 181 pp. U.S. Environmental Protection Agency.

Schwartzenbach, R. P., and Westall, J. 1981. Transport of nonpolar organic compounds from surfacewater to groundwater. Environ. Sci. Tech. 15:1360-1367.

Weber, J. B. 1972. Interaction of organic pesticides with particulate matter in aquatic and soil systems. In R. F. Gould (ed.), Fate of Organic Pesticides in the Aquatic Environment. Advan. Chem. Ser. No. 11, Amer. Chem. Soc., Wash. D. C.

Weed, S. B., and Weber, J. B. 1974. Pesticide-organic matter interactions. In W.D. Guenzi (ed.), Pesticides in Soil and Water, pp. 39-66. Soil Sci. Soc. Am., Madison, Wis.

Young, R. A., and Onstad, C. A. 1976. Predicting particle-size composition of eroded soil. Transactions of the ASAE 19:1071-1075.

APPENDIX: PESTICIDE K_{oc} AND K_{ow} VALUES
FROM PUBLISHED SUMMARIES[1]

Sources of data are indicated by the letters in brackets after table values; the source references are given at the end of the table. An attempt was made to round off numbers to avoid an inference of unrealistic precision, but the data are presented here with no evaluation of either accuracy or precision. The reader is encouraged to check the original sources for details.

Chemical	K_{oc}[2]	K_{ow}[2]
Alachlor	190[B]	830[B], 434[C]
Aldicarb	42[E]	5.0[C], 37[E]
Aldicarb sulfone	3[E]	0.3[E]
Aldrin	410[B], 48600[E]	25,000,000[E]
Altosid	-	176[C]
Ametryn	380[A], 392[B], 388[C]	-
Asulam	300[B]	-
Atrazine	102[A], 149[B], 163[C], 111[G]	476[B], 212[C], 226[C]
Azobenzene	1340[E]	6610[E]
Benefin	10700[B]	-
Benomyl	-	264[C]
Bentazon	0[B]	220[B]
Bifenox	-	174[C]
Bromacil	72[B], [C]	104[C]
Butralin	8200[B]	-
Captafol	2070[E]	6760[E]
Captan	198[E]	224[B], 33[C], 347[E]
Carbaryl	230[B], 298[G], 104[E], 121[F]	230[B], 651[C], 209[E]
Carbofuran	29[C], 40[G]	40[B], 207[C]
Carbon tetrachloride	-	436[B]
Carbophenothion	45400[B]	-
Chloramben	21[B]	13[C]
Chloramben, methyl ester	507[B], [A]	-
Chloramben, NH_4^+ salt	13[A]	-
Chlorbromuron	217[A], 460[B], 996[C], 377[E], 364[F]	1230[E]
Chlordane	-	2110[C]
Chlorfenvinphos	293[E]	1260[E]
Chloroneb	1160[B], 1650[C]	-
6-Chloropicolinic acid	9[B]	0.02[B]
Chloroxuron	3200[B], 4340[C]	-
Chlorpropham	590[A],[B], 245[A], 816[C]	1160[C]
Chlorpyrifos	13600[B]	97700[B], 2060[C], 66000[C], 129000[C]
Chlorpyrifos, methyl	3300[B]	14750[B], 1970[C], 20400[C]
Chlorthiamid	107[B], 98[C]	-
Chlortoluron	104[E], 105[F]	257[E]
Crotoxyphos	173[A], 170[B] 75[C]	-
Crufomate	-	2780[B]
Cyanazine	200[B], 116[G]	150[B]
Cycloate	345[A],[B]	-
2,4-D	32[A], 23[A], 20[B],[C]	37[B], 416[C], 443[C], 646[C]
2,4-D, amine	109[C]	-
Dalapon	-	6[B], 5.7[C]
Dalapon, Na salt	-	1[C]
DBCP	129[B]	-
DDD	-	1047000[B], 115000[C]

15

DDE, p,p -	-	490000[C]
DDE	-	583000[B], 73400[C]
DDT	131000[A], 355000[A], 229000[A], 238000[B], 243000[C],	960000[B] 370000[C] 1549000[C]
DDT, p,p -	-	1549000[C]
Dialifor	-	49300[B], 49000[C]
Diallate	1900[B]	-
Diamidfos	30[A], 32[B]	-
Diazinon	227[E]	1052[C], 1288[E]
Dicamba	4[A], 0.4[B], 2[C]	3[C]
Dichlobenil	164[A], 235[B], 224[C]	787[C]
Dichlofenthion	-	137000[B], 138000[C]
3,6-Dichloropicolinic acid	2[B]	-
cis-1,3-Dichloropropene	26[A], 23[B], 798(Telone)[C]	-
trans-1,3-Dichloropropene	28[A], 26[B], 1380(Telone)[C]	-
Dichlorovos	-	25[B], 195[C]
Dicifol	-	3460[C]
Dieldrin	12780[E]	4930[C], 1585000[E]
Diflubenzuron	6790[B]	-
Dimethoate	9[E]	0.51[B], 6[E]
Dimethylamine	435[C]	-
Dinitramine	4000[B]	-
Dinoseb	124[B]	4900[B], 198[C]
Diphenylamine	598[E]	2630[E]
Dipropetryn	1170[B], 1180[C]	-
Disulfoton	1780[B], 1600[C]	-
Diuron	902[A], 400[B], 383[C], 161[E], 191[F],534[G]	94[B], 650[C], 479[E]
DMU	286[E], 319[F]	871[E]
DSMA	770[B]	-
Endrin	-	218000[B], 1620[C]
EPTC	283[A], 240[B]	-
Ethion	15400[B]	-
Ethoxychlor	-	1180[C]
Ethylene dibromide	32[A], 44[B]	-
Fenamiphos	329[E]	1510[E]
Fenitrothion	-	2400[B], 2300[C]
Fenuron	0.6[A], 27[B], 42[C], 13[E], 26[F]	10[B], 9[E]
Fluchloralin	3600[B]	-
Fluometuron	175[B], 66[E]	22[B], 263[E]
Folpet	1850[E]	4270[E]
Fonofos	770[G]	-
Glyphosate	2640[B]	-
HCB	- 1660000[C]	
Heptachlor	-	7370[C]
Hexachlorobenzene	3900[B]	-
Hydroxyatrazine	888[A]	-
Ipazine	2570[A], 1660[B]	2900[B]
Isocil	130[B]	-
Isopropalin	75250[B]	-
Leptofos	-	4120[C]
Leptophos	9300[B]	2020000[B], 2042000[C]
Lindane	1940[A], 911[B], 1080[C]	643[C]
Linuron	653[A], 820[B], 863[C], 267[E], 229[F]	154[B], 575[E]
Malathion	1800[C]	780[B], 230[C], 776[C]
Methazole	2620[B]	-
Methiocarb	207[E]	832[E]

Methomyl	160[B]	2[B], 12[C]
Methoxychlor	80000[B]	47500[B], 2050[C], 120000[C]
Methyl isothiocyanate	6[B]	-
Methyl parathion	9800[B], 5100[C]	82[B], 2080[C]
Methyl urea	59[C]	-
Metobromuron	60[A],[B], 272[C], 104[E], 100[F]	240[E]
Metoxuron	55[E], 69[F]	44[E]
Metribuzin	95[B], 91[G]	-
Mexacarbate	-	1370[B]
Monolinuron	198[A], 200[B], 284[C], 69[E], 66[F]	40[B], 200[E]
Monuron	163[A], 100[B], 184[C], 50[E], 59[F]	29[B], 133[C], 96[E]
MSMA	-	8.0×10^{-4}[C]
Naphthalene	1300[B], 414[E]	2040[B], 2290[E]
Napropamide	680[B]	-
Neburon	2300[B], 3110[C]	-
Nitralin	960[B]	-
Nitralin ($R_1 = C_3H_7$; $R_2 = CH_3$)	500500[A]	-
Nitrapyrin	420[B], 271[A], 238[A], 172[E]	2590[B], 1050[E]
Nitrofen	-	1240[C]
Norfluorazon	1910[B]	-
Oryzalin [D]	-	-
Oxadiazon	3240[B]	-
Oxamyl	5[E]	0.3[E]
Paraquat	15500[B]	-
Paraquat.2HCl	-	1[C]
Parathion	4800[B], 10650[C] 1040[E]	6400[B], 6450[C], 8510[E]
p-Chloroaniline	562[C]	-
Pebulate	719[A], 630[B]	-
Pentachlorophenol	900[B]	102000[B], 14300 [C]
Permethrin	33300[F]	753[C], 3981000[F]
Phenol	52[E]	29[E]
Phenylurea	76[C]	-
Phorate	3200[B], 655[E] 3260 [C]	823[C], 18200[E]
Phosalone	-	20100[B], 20000[C]
Phosmet	-	677[B], 676[C]
Picloram	13[A], 17[B], 26[C]	2[B], [C]
Profluralin	8600[B]	-
Prometone	74[A], 350[B]	-
Prometryn	311[A], 810[B], 614[C]	-
Pronamide	200[B]	-
Propachlor	265[B], 102[G]	560[B], 41[C]
Propanil	-	106[C]
Propazine	152[A], 160[B], 154[C]	785[B]
Propham	51[A], [B], 88[E]	398[E]
Propoxur	-	33[B], 28[C]
Pyrazon	120[B]	
Ronnel	-	46400[B], 75900[C]
Silvex (fenoprop)	2600[B]	-
Simazine	159[A], 135[B], 138[C], 47[E]	155[B], 88[C], 32[E]
2,4,5-T	42[A], 40[A], 53[B], 80[C]	4[B], 7[C]
2,4,5-T, butyl ester	-	64000[C]
2,4,5-T, octyl ester	-	909[C]
Tebuthiuron	620[B]	-
Terbacil	51[B], 41[C]	78[C]
Terbufos	-	167[C]

Terbutryn	700[B]	-
Tetrachloroethylene	-	758[B]
Thiabendazole	1720[B]	-
Toxaphene	-	1700[C]
Triallate	2220[B]	-
Trichlorfon	-	3[B]
1,2,4-Trichlorobenzene	-	15000[B]
Triclopyr	27[B]	3[B]
Triclopyr (butoxyethyl ester)	-	12300[B]
Triclopyr (triethylamine salt)	-	3[B]
Trietazine	600[B]	2200[B]
Trifluralin	13700[B]	220000[B], 1150[C]

---

[1]Source of data references:
  A: Hamaker and Thompson (1972)
  B: Kenaga and Goring (1980)
  C: Rao and Davidson (1980)
  E: Briggs (1981a)
  F: Briggs (1981b)
  G: Rao et al. (1984)
 Reference E values are given as log K_{om}; we converted them to K_{oc}.
 Reference F values are given as K_{om}; we converted them to K_{oc}.
[2]K_{oc} units are L/Kg; K_{ow} is dimensionless.

METHODS FOR ESTIMATING PESTICIDE DISSIPATION FROM SOILS

Ralph G. Nash

ABSTRACT

Pesticide users and regulators need to know the amount of pesticide remaining on a field at any given time. Measuring every pesticide under every use condition is not feasible. Consequently, estimation methods have been developed. Methods which incorporate temperature into measured dissipation rates appear the most useful at present.

INTRODUCTION

Determining the amount of a pesticide in or on soil without direct measurement at any given time is not an exact science. First, the amount of pesticide that reaches the soil depends upon the amount applied, application method, formulation, the pesticide itself, ground cover (plants or crop residue), and the amount that washes off the plants after application. Second, the dissipation (or persistence) of a pesticide depends upon the characteristics of the pesticide itself, formulation, placement, soil and climatic factors, erosion, and possibly mechanical removal by plants and animals.

This paper is concerned primarily with pesticide dissipation from soil, as described by a lumped parameter, k_s. This parameter is a rate constant for the combined processes that affect the persistence of the pesticide on the soil (surface), in the rhizosphere (topsoil), and below the rhizosphere (subsoil). A finite pesticide amount in or on the soil is assumed to be known either from direct application or from direct measurement at time zero (C_0). For this discussion, the following limitations will be assumed or imposed: (1) method of application will not be considered; (2) the pesticide is assumed to be uniformly applied, or the application parameters are defined; (3) pesticide vapor diffusion from the plants to the soil or from deeper soil depths to rhizosphere soil is considered negligible; and (4) pesticide partitioning within the soil, mass transport within and below the soil, and pesticide washoff from plants onto the soil are not considered. Their appearance in the outline and in a brief discussion within the body of the paper is for purposes of design completeness only.

DISCUSSION

Pesticide content in or on soil is more accurately measured than estimated. Unfortunately, measuring every pesticide under every use condition is neither feasible nor desirable. Consequently, it is the responsibility of researchers to develop estimation methods. Methods used to estimate pesticide dissipation basically include either empirically derived equations developed from pesticide dissipation measurements or conceptually derived equations based on the physicochemical characteristics of the pesticide and environmental parameters.

Conceptual and Observed Considerations

Edwards (1966) proposed a series of line segments to model the dissipation of pesticides applied to a field. Based on the same dissipation pattern, Nash (1980) and Nash and Isensee (this volume) proposed a logarithmic model (fig. 1). With either approach, the dissipation pattern is similar. Initially, the highest loss rates occur during application. Under certain circumstances, application losses may be large, and considerable engineering effort has been expended to limit these losses. Losses during application occur primarily over a short period, perhaps <5 min, but may take as much as 1 h (Seiber and Woodrow, 1983). Secondly, volatilization loss apparently occurs for almost all pesticides, primarily because of their distribution over a large surface area or volume, and may be considerable. Volatilization losses are governed by the pesticide vapor pressure, method of application (surface-applied vs. soil-incorporated), formulation, temperature, soil

Soil scientist, USDA-ARS, Pesticide Degradation Laboratory, B-050, BARC-West, Beltsville, MD 20705

moisture and organic content, relative humidity, wind velocity, and smoothness or roughness of the soil surface. Volatilization losses may be short-term for pesticides that degrade rapidly or long-term for the more persistent pesticides (Nash and Beall, 1980a; Nash et al., 1977). Most data indicate volatilization loss rates are reduced greatly after a few hours, or a few days at the most, even for the most persistent pesticides; however, losses apparently continue for as long as the pesticide remains (Nash and Beall, 1980a; Spencer and Cliath, 1972). Following volatilization, soil penetration, soil adsorption, or soil leaching, or all to a lesser or greater degree, become dominant factors that govern the pesticide dissipation from soil. Finally, degradation (usually biological but sometimes partially chemical) of the pesticide becomes paramount in the disappearance of most pesticides.

Distribution

During application. Obviously, if the soil is the target, most of the applied pesticide will reach the soil, except possibly under some aerial applications. If a volatile pesticide is surface applied, considerable amounts may be lost in a short period of time unless immediately incorporated into the rhizosphere (Nash, 1983a). Many pesticides, however, are applied directly to plants either to protect them from insects and diseases or to kill them. Usually when pesticide application is to the plant, some pesticide reaches the soil. Therefore, during foliar application there will be a distribution of the pesticide primarily among the foliage (target) and soil and air (nontarget). The distribution will depend upon the amount intercepted by the foliage and, as indicated previously, the method of application, formulation, weather, and possibly the physicochemical characteristics of the pesticide itself.

There is no easy way to determine the pesticide distribution between the soil, plant, and air without making measurements. The major reason is that the distribution site, system, and conditions are specific. Usually soil and plant samples are taken or several catchments are placed randomly on the soil surface during application to determine target and off-target pesticide amount. Recently, Willis et al. (1983) determined initial pesticide load on cotton from equations developed from cotton pesticide dissipation rates. This would seem a useful technique wherever dissipation type information is gathered on plants or soil and where the harvested foliage is from a known field area. A more comprehensive review of application principles is given by Hartley and Graham-Bryce (1980).
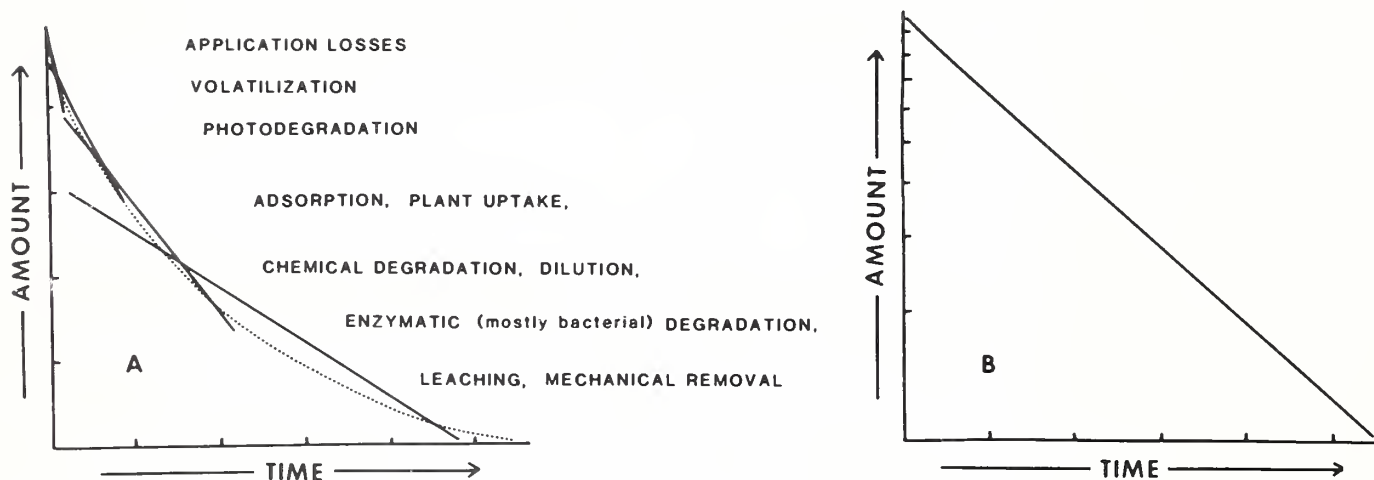
Figure 1.--Pesticide losses (dissipation) from soil: (A) arithmetic amount with time (adapted from Edwards, 1966) and (B) logarithmic amount with time (Nash, 1980).

<u>Subsequent to application</u>. Nash (1983a,b), Nash and Beall (1980b), Nash et
al. (1977), Gile (1983), Gile and Gillet (1979), and Gile et al. (1980) have
determined pesticide distribution in various environmental components in
chamber studies (table 1). A significant portion of most pesticides, whether
foliar-applied or soil-applied, ultimately migrates to the atmosphere. The
exceptions, in the cited studies, were the very insoluble and nonvolatile
ethylenebis (dithiocarbamate) fungicides, maneb and zineb, and certain
pesticides incorporated into the rhizosphere.

The three major recipients of field-applied pesticides will be the soil, crop,
and air. The atmosphere is not a target like the soil and plants are, but more
of a sink (Glotfelty, 1978) into which some of the pesticide in or on soil
dissipates.

Table 1.—Pesticide distribution at end of experiment in terrestrial chambers and field

Pesticide	Applied to	Distribution, % of applied						Reference
		Soil	Plant	Air	Leachate	Animal	Total	
				CHAMBER				
2,4-D B E	ryegrass	15	27	19	–	0.001	61	Gile, 1983
Maneb	tomatoes	[1]22	[1]43	3	0.05	–	67	Nash and Beall, 1980b
Zineb	tomatoes	[1]22	[1]37	5	0.05	–	64	Nash and Beall, 1980b
Heptachlor[2]	fallow surface soil	30	–	51	–	–	81	Nash, 1983b
Trifluralin	"	7	–	60	–	–	67	Nash, 1983b
Lindane	"	13	–	78	–	–	91	Nash, 1983b
Chlordane	"	61	–	50	–	–	111	Nash, 1983b
Dieldrin	"	73	–	35	–	–	109	Nash, 1983b
Endrin	"	70	–	33	–	–	103	Nash, 1983b
p,p'-DDT	"	111	–	11	–	–	122	Nash, 1983b
DDTR[3]	cotton	24	[4]61	15	–	–	100	Nash et al., 1977
Toxaphene	"	20	[4]56	24	–	–	100	Nash et al., 1977
Butylate EC[5]	rhizosphere	18	5	–	–	–	[6]23	Nash, 1983a
Butylate ME[5]	"	69	5	–	–	–	[6]74	Nash, 1983a
Heptachlor[2]	"	69	0.2	15	–	–	84	Nash, 1983a
Lindane	"	65	0.2	12	–	–	77	Nash, 1983a
Dieldrin	"	66	0.1	3	–	–	69	Nash, 1983a
Bromacil[7]	various plant spp.	34	34	32	–	0.3	69	Gile et al., 1980
Trifluralin[7]	"	15	21	62	–	2	79	Gile et al., 1980
Dieldrin[7]	"	44	48	5	–	3	72	Gile and Gillet, 1979
Simazine[7]	"	35	43	21	–	0.8	91	Gile and Gillet, 1979
2,4,5-T IO E[7]	"	35	52	12	–	0.7	103	Gile and Gillet, 1979
PCNB	seeds in rhizosphere	59	16	[8]24	0.3	0.06	99	Gile and Gillet, 1979
PCP	"	65	9	[8]25	0.03	0.3	99	Gile and Gillet, 1979
Dieldrin	"	85	11	[8]3	0.04	0.2	99	Gile and Gillet, 1979
HCB	seeds in rhizosphere	46	5	[8]45	0.2	0.03	96	Gile and Gillet, 1979
Captan	"	19	8	[8]73	0.01	0.3	100	Gile and Gillet, 1979
Dieldrin	alfalfa and ryegrass	44	26	[8]26	–	1.6	98	Gile and Gillet, 1979
				FIELD				
Toxaphene	cotton	18-58	28	6-17	–	–	[9]46	Willis et al., 1983
DDT[9]	"	9	19	11	–	–	28	Willis et al., 1983

[1] In these studies a significant portion of the application was found on the chamber walls; therefore,   the chamber wall amount was
divided proportionately between the soil and plant.
[2] Heptachlor plus heptachlor epoxide.
[3] Total DDT residues.
[4] Estimated.
[5] EC = emulsifiable concentrate and ME = microencapsulated formulations.
[6] A significant portion of these did go to the air, but degradation most likely resulted in much of
    that not accounted for.
[7] Based on ^{14}C-residues.
[8] Includes estimated aerial losses, which in some cases is questionable.
[9] Represents soil and cotton only, because aerial portion was determined as losses from the cotton.

Partitioning (Partition Coefficients - K)

Partitioning of a pesticide in soil is the separating and subsequent equilibration of the pesticide into the several soil components: Soil particulates (both mineral and organic), soil water, soil, air, soil biota, and atmosphere above the soil. Partitioning among the components can be defined by partition coefficients:

$$K_d = \frac{P_S}{P_W}; \quad K_s = \frac{P_A}{P_S}; \quad K_h = \frac{P_A}{P_W}; \quad K_{bcf} = \frac{P_B}{P_S}$$

where P = pesticide concentration in a matrix, S = soil, W = water, A = air and atmosphere, and B = biota. For most pesticides (especially hydrophobic), the separation and equilibration process is rapid relative to losses from each component. Therefore, time is usually ignored and thermodynamic principles are applicable rather than kinetic principles. K_d has been discussed thoroughly elsewhere (Green and Karickhoff, this volume; Pionke and DeAngelis, 1980). K_s probably cannot be separated from K_h, and K_h is defined by Henry's law constant. K_{bcf} in soil has not been studied per se, though considerable literature exists on soil fauna and flora pesticide uptake. In soil, however, K_{bcf} probably can be treated as a component of the organic matter without serious error. A more thorough discussion of the theoretical aspects of pesticide partitioning in soil can be found in Hartley and Graham-Bryce (1980).

Pesticide Dissipation From Soil

Hamaker (1972a), Leistra (1978), and Soulas (1982) have studied the theoretical rates of pesticide degradation and decline in soils, and the latter two have developed mathematical models. Hamaker suggests that the rate laws are of two basic types: rate = kc^n and rate = $k_1 c/(k_2 + c)$, where c is concentration, n is the order of equation, k is the rate constant, k_1 is a maximum rate approached with increasing concentration, and k_2 is a pseudoequilibrium constant. Hamaker found that the former (a power-rate model) usually was the most useful for estimating pesticide dissipation rates, perhaps because not enough observations are made, and that too many complex parameters affect dissipation of pesticides from soils. The latter (a hyperbolic rate model) depends upon pesticide concentration.

The series of straight lines in figure 1A can be reconstructed as a continuous curve (dashed). Further, if the logarithm of the pesticide amount is plotted versus time, a linear relationship is often possible (fig. 1B). Because this relationship is exponential, it is usually referred to as pseudo first-order kinetics. The dissipation from soils of most pesticides [especially the chlorinated hydrocarbon insecticides (fig. 2) and certain herbicides] is nearly always exponential and has been demonstrated by the data contained in the ECD database (Nash and Osborne, 1980).

Ideally, when dissipation results primarily from biological adaptive mechanisms, such as a microbial population buildup or enzymatic adaptation, the dissipation curve is more like that depicted in figure 3. Initially, dissipation is slow, but as an adaptive microbial population builds up or an enzyme adapts, the dissipation rate increases such that the situation could be as shown in figure 4 and demonstrated by Obrigawitch et al. (1982, 1983).

Some of the dissipation processes listed above (most physical and chemical and photochemical transformations and degradations) occur as first-order rate processes under ideal conditions. Other processes [volatilization and some microbial degradations (Nash, 1980; Walker, 1974)] also give the appearance of first-order rate losses. When combined, as in field soil, the pesticide loss from the several dissipation processes nearly always follows a simple exponential equation (hereafter referred to as exponential time-based or normal ETB). This greatly simplifies the development of equations for describing or estimating pesticide loss from soil and allows the use of the kinetic concept of half-life (referred to as half-concentration time, $C_{1/2}$, in this paper).

The ETB equation is given by the expression:

$$C_d = C_o \, e^{-k_s d} \tag{1}$$

where C_d = pesticide concentration on d = day, C_o = initial pesticide concentration or concentration on d = 0, e = 2.718, and k_s = dissipation rate constant. Although use of generalized equation [1] to estimate dissipation from soil is useful, the specifically derived equation is theoretically valid only for the particular data set from which it was derived. For example, equation [1] calibrated to the observed dissipation of a pesticide incorporated into a cold soil would very much underestimate pesticide dissipation from a warm soil.

Pesticide dissipation is not only a function of time but also a function of all environmental factors (e.g., temperature, wind velocity, rainfall, and the soil). If dissipation is dependent upon one environmental factor under ideal conditions (chemical degradation, for example, as a function of time and

Insecticide Dissipation From Soil
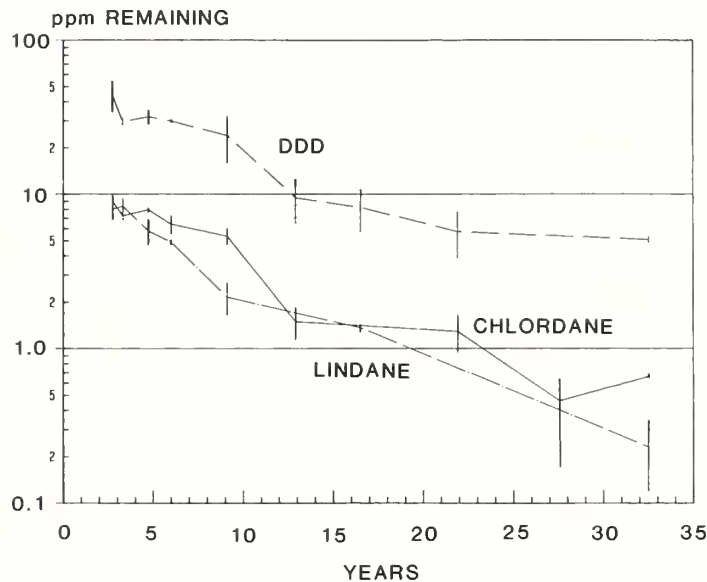
Figure 2.--Long-term persistence of chlorinated
hydrocarbon insecticides in soil
(Nash, 1983d).

ONE APPLICATION
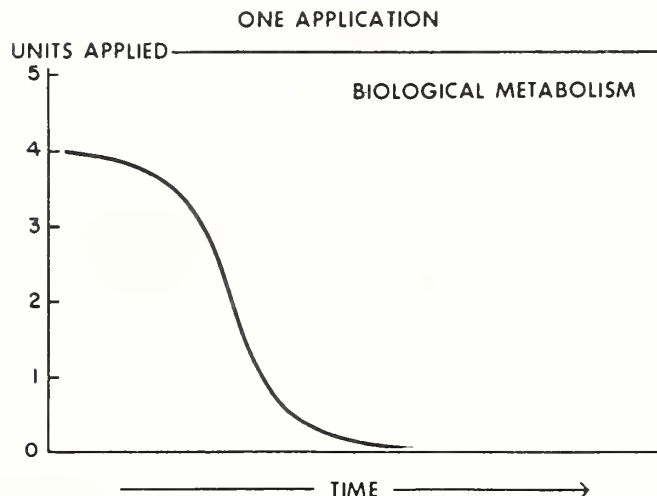
Figure 3.--Pesticide degradation from microbially
adaptive organisms under ideal
conditions (Kearney et al., 1969).

Carbofuran Dissipation From Soil
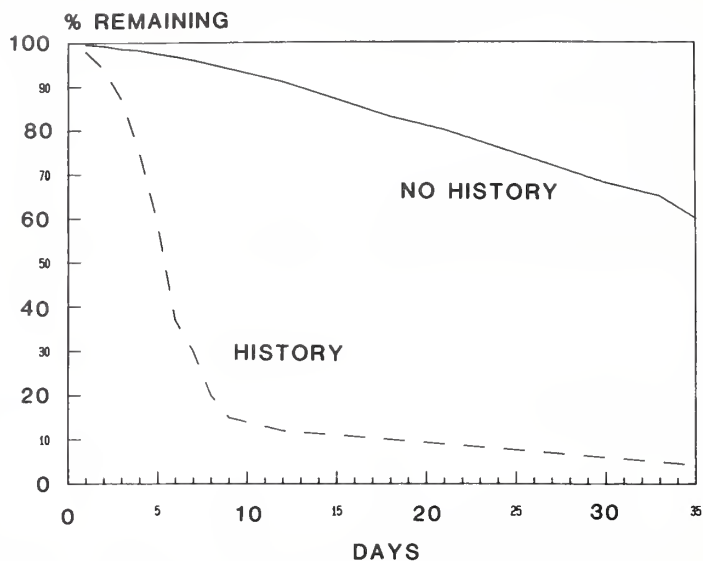
Figure 4.—Carbofuran remaining in soils having
a history or no history of carbamate-
type pesticide applications, indicating
an adaptative microbial population in
the history soils (adapted from Kaufman
and Edwards, 1983).

temperature), pesticide loss can be predicted accurately by use of classical
kinetic equations, e.g., the Arrhenius equation. Ideal conditions rarely exist
in the field, however, and dissipation is controlled by multiple soil and
environmental factors. A more thorough discussion of the factors that
influence pesticide dissipation from soil is given in Nash (1980).

Soil and Environmental Parameters

The management choices, soil and environmental parameters, and pesticide
properties are outlined in table 2. Both the soil parameters, as they pertain
to pesticide dissipation, and the environmental parameters are discussed
elsewhere (Nash, 1980).

The combined dissipation rate (k_s) value has been derived experimentally
using several methods. Walker (1974, 1976a-c) demonstrated that nonvolatile
herbicide dissipation from both several surface and rhizosphere soils followed
ETB equations and that this dissipation depended upon temperature and soil
moisture. Walker and collaborators (1974; 1976a-c; 1978; 1981; 1983)
determined herbicide dissipation at two or more temperatures under laboratory
conditions and found $C_{1/2}$ values (k_s rather than $C_{1/2}$ values were used
for this paper) from ETB equations. The activation energy (ΔE) from the
Arrhenius equation was determined:

$$k_s = k_o \, e^{-\Delta E/RT} \tag{2}$$

where k_s = dissipation rate, k_o = frequency factor, R = 8.315 J mole^{-1},
and T = °K. Then by knowing the ΔE and the k_{s1} value at T1, a k_{s2} value
can be estimated at T2. For example, in table 3 it was found that ΔE for
asulam in Regina clay over a temperature range of 5 to 30°C was 40.1 kJ
mole^{-1}. From table 4 [table 2 of Nash (1980) is partially reproduced here
for convenience], the k_{s1} at 10°C and 20% soil moisture content = 0.0141.
Modifying equation [2] to

$$k_{s1} = k_{s2} \, e^{-\Delta E/R(1/T1 - 1/T2)} \tag{3}$$

where T1 and T2 = 10 and 40 °C, respectively; k_{s2} = 0.0718 at 40°C, which is
close to the k_s of 0.0774 reported in table 4. Other k_s values can be
calculated with equal confidence from these data.

Table 2.--Outline of the parameters and variables that
influence pesticide content on or in soil

A. Management choices
   1. Pesticide
   2. Application
      a. Amount per area or volume
      b. Formulation
      c. Method or placement
      d. Plant cover or crop residue interception
   3. Irrigation
      a. Incidences
      b. Amount
      c. Intensity
      d. Subsequent washoff from plant cover or crop residue
B. Climatic parameters
   1. Average daily temperature
   2. Average daily wind velocity
   3. Average daily relative humidity
   4. Average daily solar radiation
   5. Precipitation
      a. Incidences
      b. Amount
      c. Intensity
      d. Subsequent washoff from plant cover or crop residue
C. Soil parameters and behavior
   1. Type
   2. Organic matter content
   3. Moisture content
   4. Soil pH

D. Pesticide's physical, chemical, and biological
   properties
   1. Molecular weight
   2. Transition temperatures
      a. Melting point
      b. Boiling point
      c. Decomposition
   3. Vapor pressure
   4. Heat of vaporization
   5. Dissipation activation energy
   6. Water solubility
   7. Leaching index
   8. Partition coefficients
      a. Octanol/water (K_{ow})
      b. Adsorption
         (1) Soil (K_d)
         (2) Organic carbon (K_{oc})
      c. Henry's law (K_h)
      d. Bioconcentration factor (K_{bcf})
   9. Disassociation
      a. Acid (pK_a)
      b. Base (pK_b)
   10. Rate reactions
      a. Volatilization (k_a)
         (1). Soil-air (k_a)
         (2). Plant-air (k_t)
         (3). Crop residue-air (k_c)
      b. Photolysis (k_p)
      c. Hydrolysis (k_w)
      d. Biodegradation (k_i)
      e. Oxidation (k_o)
      f. Reduction (k_r)
      g. Leaching (k_g)
      h. Diffusion (k_f)
      i. Desorption (k_d)
      j. Biosorption (k_b)
      k. Bioelimination (k_1)
      l. Complexation (k_e)
      m. Lumped (of above) (k_s)

Table 3.--Calculated dissipation activation energies (ΔE) and soil-moisture influence (b), which describe pesticide dissipation from soil

Pesticide	Conditions	[1]SM [2]SMT %	ΔE kJ mole^{-1}	°C	b[3]	Reference
Alachlor	s l rhizosphere, 10-30 °C	[1]8.4	28.9 ± 0.6	20	0.60 ± 0.01	Zimdahl and Clark, 1982
Alachlor	c l rhizosphere, 10-30 °C	[1]1.5	32.4 ± 13.9	20	0.61 ± 0.09	"
Asulam	Regina c rhizosphere, 10-40 °C	[1]20	[4]40.1 ± 8.2**			Smith and Walker, 1977
"	"	[1]26	23.5 ± 5.5**			"
"	" ,10-30 °C	[1]34	41.7 ± 9.3**			"
"	"	[1]40	42.3 ± 10.8			"
"	" ,20-40% SM			10	1.41 ± 0.37*	"
"	"			15	1.02 ± 0.19**	"
"	"			20	1.45 ± 0.17**	"
"	"			25	0.77 ± 0.11**	"
"	"			30	1.14 ± 0.29*	"
"	"			40	0.15 ± 0.04ns	"
Atrazine	3 soils, rhizosphere, 5-25 °C	[2]70	49.0 ± 3.2			Walker and Zimdahl, 1981
"	" ,70% SMT			25	0.63 ± 0.15	"
"	s l rhizosphere	[2]60	69.9 ± 4.5	20	0.16 ± 0.10	Walker, 1978
Azinphosmethyl	si l rhizoshere, 6-40 °C	[2]50	57.3 ± 5.5**			Yaron et al., 1974
"	" 27-50%			25	0.74 ± 12**	"
Carbofuran	6 soils, 10-1500 kPa SMT			15-35	[5]0.88 ± 0.34	Ou et al., 1982
"	Cecil and Webster rhizosphere, 15-27 °C	10-1500 kPa	70.6 ± 12.0			"
"	Cecil, 27-35 °C	10-100 kPa	18.8 ± 7.5			"
"	"	1500 kPa	75.7			"
"	Webster, 27-35 °C	10-1500 kPa	4.3 ± 10.0			"
"	Grenada, 27-35 °C	10-100 kPa	33.3 ± 11.5			"
"	"	1500 kPa	36.0			"
Carbofuran	Sharpsburg, 27-35 °C	10-1500 kPa	48.0 ± 21.7			"
"	Houston, 27-35 °C	10-1500 kPa	130.8 ± 20.6			"
Chlorsulfuron	s l, 10-30 °C	[1]12	58.9			Walker and Brown, 1983
"	", 6-12% SM			20-30	1.12	"
Chlorthal-dimethyl			92.0 ± 5.5		0.99 ± 0.13	Walker, 1978
p,p'-DDT	Houston Black c surface 30-50 °c day, 25-35 °C night	dry	37.4			Baker and Applegate, 1970
"	Pinal g l surface "	dry	41.1			"
"	Pima si c surface "	dry	38.6			"
Dieldrin	Gilla si l rhizosphere, 20-30 °C	[1]10	64.3			Farmer et al., 1972
Dinitramine	c l rhizosphere, 10-30 °C	[1]17	96.6 ± 35.9			Poku and Zimdahl, 1980
"	Wickham s l rhizosphere, 10-30 °C	[1]9.6	88.7 ± 19.9			"
"	c l rhizosphere, 2.2-22% SM			30	1.06 ± 0.17	"
"	Wickham s l rhizoshpere, 0.5-12% SM			30	0.99 ± 0.11	"
Fluchloralin	Sharkey si c rhizosphere, 4-25 °C	[1]34	33.6			Brewer et al., 1982
"	Crowley si l rhizosphere, 4-25 °C	[1]27	40.7			"
Isopropalin	Aerobic Weld l, 15-30 °C	[1]20	65			Gingerich α Zimdahl, 1976
"	"	[1]20	66			
Linuron	2 soils, 5-25 °C	[2]70	36.7 ± 1.1	25	0.84 ± 0.04	Walker and Zimdahl, 1981
	s l rhizosphere	[2]60	28.8 ± 3.8	20	0.47 ± 0.03	Walker, 1978
"	Gravel Pits s l rhizsosphere, 5-30 °C	[1]4	38.5 ± 6.1**			Walker, 1976b
"	"	[1]12	24.6 ± 2.0**			"
"	Gravel Pits s l rhizosphere, 4-12% SM			5	0.24 ± 0.01	Walker, 1976b
"	"			10	0.24 ± 0.17	"
"	"			15	0.21 ± 0.01	"
"	"			20	0.25 ± 0.01	"

Table 3.--Calculated dissipation activation energies (ΔE) and soil-moisture influence (b), which describe pesticide dissipation from soil--Continued

Pesticide	Conditions	[1]SM [2]SMT %	ΔE kJ mole^{-1}	Soil moisture equation °C	b[3]	Reference
Linuron	Gravel Pits sl rhizoshere, 4-16% SM			25	0.20 ± 0.04**	Walker, 1976b
"	" ,4-16% SM			30	[6]-0.38 ± 0.01	"
Metamitron	2 soils, 5-25 °C	[2]60	46.6 ± 5.1	20	1.00 ± 0.03	Walker, 1978
Metolachlor	3 soil rhizosphere, 5-25 °C	[2]70	48.5 ± 3.8	25	0.95 ± 0.08	Walker and Zimdahl, 1981
"	s l rhizosphere, 10-30 °C	[1]8.5	30.4 ± 10.5	20	0.79 ± 0.03	Zimdahl and Clark, 1982
"	c l rhizosphere, 10-30 °C	[1]11.5	26.0 ± 15.7	20	0.59 ± 0.21	"
Metribuzin	s l rhizosphere	[2]60	65.0 ± 4.4	20	0.71 ± 0.09	Walker, 1978
Methyl	Houston Black c surface,		23.6 ± 8.2*			Baker and
Oryzalin parathion	Aerobic Weld l, 15-30 °C 30-50 °C 8h day 25-30 night	[1]20	72			Gingerich & Zimdahl, 1976 Applegate, 1970
"	Pima si c surface, "		20.1 ± 6.3*			"
"	Pinal g l surface, "		21.0 ± 5.8**			"
Profluralin	Crowley si l rhizosphere, 4-25 °C	[1]27	35.6			Brewer et al., 1982
"	Sharkey si c "	[1]34	35.4			"
Prometryn	s l			25	2.76 ± 0.28	Walker, 1976a
"	Gravel Pits sl rhizosphere,	[1]11.5	93.4 ± 13.1			"
"	" 15-25 °C	[1]6-6.6	52.1 ± 5.7			"
"	" ,6.6-11.5% SM			15	2.63 ± 0.06**	"
"	" ,4.8-13.2% SM			25	2.93 ± 0.26**	"
Pronamide	Gravel Pits s l rhizosphere, 15-25 °C	[1]11.8	50.6 ± 8.1			Walker, 1970
"	Little Cherry s l rhizoshpere, 15-25 °C	[1]12.0	60.6 ± 0.8			"
"	" ,15-30 °C	7.5	27.5 ± 4.5			"
"	Soakwaters c l, 15-25 °C	[1]16.3-17.8	79.2 ± 0.7			"
"	Gallas Ley s c, "	[1]16.7	68.9 ± 1.3			"
Pronamide	Water Meadows c l, 15-25 °C	[1]29.5	62.9 ± 0.9			Walker, 1970
"	Little Cherry s l, 7.5-12% SM			15	1.0	"
"	" , 3.5-10% SM			30	0.47	"
"	Gravel Pits s l, 4.1-11.9% SM			25	2.6	"
"	Little Cherry s l, 4.0-12.1% SM			25	0.79	"
"	Soakwaters c l, 6.4-16.3% SM			25	0.95	"
"	Gallas Ley s c, 6.2-16.7% SM			25	0.80	"
"	Water Meadows c l, 14.8-29.1% SM			25	0.49	"
"	s l rhizosphere	[2]60	74.6 ± 5.5	20	0.68 ± 0.15	Walker, 1978
Propachlor	s l rhizosphere, 10-30 °C	[1]8.5	77.9 ± 20.5	20	1.50 ± 0.53	Zimdahl and Clark, 1982
"	c l rhizosphere, "	[1]11.5	94.5 ± 15.6	20	1.24 ± 0.25	"
Simazine	s l rhizosphere 10-30 °C	[2]60	69.5 ± 3.2	20	0.55 ± 0.09	Walker, 1978
"	16 soil surfaces, "	[2]20-90	48.2 ± 12.1	20	0.46 ± 0.41	Walker et al., 1983
"	, 8.5-25 °C		61.7			Burschel, 1961
"	Gravel Pits s l, 5-30 °C	[1]4	56.3 ± 0.8**			Walker, 1976b
"	"	[1]12	56.2 ± 1.6**			"
"	" , 15-25 °C	[1]6-6.6	79.2 ± 2.5			"
"	" , 4-12% SM			5	0.48 ± 0.03	"
"	"			10	0.50 ± 0.02	"
"	"			15	0.57 ± 0.02	"
"	"			20	0.51 ± 0.01	"
"	" , 4-16% SM			25	0.39 ± 0.05**	"
"	" , 4-12% SM			30	0.54 ± 0.004	"
"	" , 4.8-10.7% SM			25	0.73 ± 0.07**	"

[1] SM = soil moisture content on a weight per weight basis.
[2] SMT = soil moisture tension content of 33 kPa, assuming field capacity is approximately equal to 33 kPa.
[3] exponential b in soil-moisture equation $k_s = a\ SM^b$.
[4] * and ** = 95 and 99% confidence level, respectively.
[5] Using SMT in kPa.
[6] Questionable.

Table 4.--Effect of soil type, organic matter content, moisture content, temperature, and pH on dissipation (k_s values) of pesticides in rhizosphere soil

Pesticide	Soil Type	pH	OM[1]	5°C SM2	5°C k_s	10°C SM	10°C k_s	14-15°C SM	14-15°C k_s	20°C SM	20°C k_s	25°C SM	25°C k_s	28-30°C SM	28-30°C k_s	40°C SM	40°C k_s	Reference
			(%)	(%)		(%)		(%)		(%)		(%)		(%)		(%)		
Asulam	Regina c	7.7	7.2									20	0.0590	20	0.582	20	0.0774	Smith and Walker, 1977
"	"	7.7	7.2									26	.0723	26	.0596	26	.0792	
"	"	7.7	7.2									34	.0957	34	.1052	34	.0814	"
"	"	7.7	7.2									40	.0970	40	.1174	40	.0868	"
EPTC	Tripp vfsl	8.0	1.0									0.5	3.0015**					Obrigawitch et al., 1982
"	"											1.6	.0144**					"
"	"											3.0	.055**					"
"	"											13.0	.066**					"
"	"											16.0	.72**					"
"	Kennobec sil4	6.6	2.4	100	0.0201**			10	.0604**			10.0	.063**					"
"	Kennobec sil5	6.6	2.4	100	.0763**			10	.312			10.0	.443					"
Linuron	Gravel Pits sl	7.0	2.0	4.0	.0065	4.0	.0083	4.0	.0104	4.0	.0122	4.0	.0154	4.0	.0293			Walker, 1976b
"	"	7.0	2.0									8.0	.0165					"
"	"	7.0	2.0	12.0	.0084	12.0	.0110	12.0	.0131	12.0	.0162	12.0	.0187	12.0	.0193			"
"	"	7.0	2.0									16.0	.0204					"
Prometryn	"	7.0	2.0									11.2	.0176					Walker, 1976a
"	"	7.0	2.0					11.5	.0062			11.4	.0191					"
"	"	7.0	2.0									13.2	.0188					"
"	"	7.0	2.0									4.8	.0012					"
"	"	7.0	2.0					6.6	.0014			6.0	.0029					"
"	"	7.0	2.0									7.9	.0084					"
"	"	7.0	2.0									9.7	.0152					"
"	"	7.0	2.0									10.7	.0167					"
"	"	7.0	2.0									11.2	.0234					"
"	"	7.0	2.0					11.5	.0062			11.4	.0276					"
"	"	7.0	2.0									13.2	.0229					"

Table 4.—Effect of soil type, organic matter content, moisture content, temperature, and pH on dissipation (k_s values) of pesticides in rhizosphere soil--Continued

Pesticide	Soil			Temperature														Reference
	Type	pH	OM[1]	5°C		10°C		14-15°C		20°C		25°C		28-30°C		40°C		
				SM[2]	k_s	SM	k_s	SM	k_s	SM	k_s	SM	k_s	SM	k_s	SM	k_s	
				(%)		(%)		(%)		(%)		(%)		(%)		(%)		
Pronamide	Gravel Pits sl	6.1	1.8					11.7	0.0091			4.1	0.0116					Walker, 1976c
"	Little Cherry sl	6.9	1.4					12.0	.0099			4.0	.0096					"
"	Soakwaters cl	6.1	1.4					17.8	.0110			6.4	.0124					"
"	Gallas Ley sc	6.9	2.9					16.7	.0062			6.2	.0074					"
"	Water Meadows cl	7.2	5.3					29.5	.0082			14.8	.0142					"
"	Gravel Pits sl	6.1	1.8									11.9	.0217					"
"	Little Cherry sl	6.9	1.4									12.1	.0231					"
"	Soakwaters cl	6.1	1.4									16.3	.0301					"
"	Gallas Ley sl	6.9	2.9									16.7	.0165					"
"	Water Meadows cl	7.2	5.3									29.1	.0198					"
"	Little Cherry sl	6.1	2.0					7.5	.0062					3.5	0.0077			"
"	"	6.1	2.0											7.5	.0110			"
"	"	6.1	2.0											10.0	.0127			"
Simazine	Gravel Pits sl	7.0	2.0	4.0	.0033	4.0	.0050	4.0	.0075	4.0	.0116	4.0	.0173	4.0	.0239			Walker, 1976b
"	"	7.0	2.0									8.0	.0248					"
"	"	7.0	2.0	12.0	.0056	12.0	.0087	12.0	.0131	12.0	.0204	12.0	.0267	12.0	.0433			"
"	"	7.0	2.0									16.0	.0301					"
"	"	7.0	2.0									4.8	.0082					Walker, 1976a
"	"	7.0	2.0					6.6	.0030			6.0	.0091					"
"	"	7.0	2.0									7.9	.0109					"
"	"	7.0	2.0									9.7	.0131					"
"	"	7.0	2.0									10.7	.0149					"

1 Organic matter.
2 Soil moisture.
3 99% confidence level.
4 No previous EPTC history.
5 Previous EPTC history.

29

Walker (1974) found that the effect of soil moisture (SM) on herbicide persistence could be empirically derived:

$$C_{1/2} = a\ SM^{-b} \quad \text{or} \quad k_s = a\ SM^b \qquad [4]$$

where a and b are constants. Like the Arrhenius equation, a k_s value at a different soil moisture can be calculated from a modification of equation [4]:

$$k_{s2} = k_{s1}\ \frac{SM_2^{\ b}}{SM_1^{\ b}} \qquad [5]$$

(i.e., for asulam from table 4: k_{s1} = 0.044 at 20% SM and 20°C, and from table 3: b = 1.45; the calculated k_{s2} = 0.1202 at 40% SM and 20°C, which is close to the k_s value of 0.1127 value given in table 4.)

Further, by substituting equation [5] into [3], a new k_s value can be estimated for any soil moisture content and temperature [i.e. asulam k_{s1} = 0.0261 at 20% SM and 15°C (table 4); b = 1.02, and ΔE = 40.1 kJ mole^{-1} in table 3; k_{s2} = 0.121 at 40% SM and 30°C, which is close to the given k_s value of 0.1174 in table 4].

Subsequently, by computer programming and using weather data to ascertain soil moisture and temperature, Walker and collaborators (Walker, 1974, 1976a-c, 1978; Walker and Barnes, 1981; Walker et al., 1983; Walker and Zimdahl, 1981) have simulated dissipation of several herbicides from both surface and rhizosphere soil quite accurately, but in other cases (possibly those that have greater daily soil moisture and temperature fluctuations or with higher organic matter content) the simulation usually overestimated herbicide persistence (Walker et al., 1983). Therefore, it would appear that for several pesticides data from carefully conducted laboratory experiments under several soil temperature and moisture regimes (such as some in England that are fairly uniform) could be used with confidence to estimate or describe pesticide dissipation in the field. Table 3 gives the activation energy value (ΔE) and soil-moisture value (b), which can be inserted into equations [3] and [5], respectively, to determine dissipation of several pesticides from soil under various temperature and soil-moisture conditions.

The weather variables can be used to develop dissipation equations empirically (Hill et al., 1982; Nigg et al., 1977). A convenient way to do this is to cumulate the weather variables on a daily basis [i.e., daily mean air temperature (AT), wind run (W) (maximum or minimum may be useful under certain circumstances, also), and relative humidity (RH), rain incidences (RI), rain intensity (I) or daily rainfall (R)]:

$$C_d = C_o e^{-k\ AT} \qquad [6]$$

Equation [6] will be referred to as integral-variable ETB equation. Further, equation [6] can be expanded to include more than one environmental factor through step-wise regression:

$$C_d = C_o e^{-k1\ AT\ +\ k2\ W} \qquad [7]$$

Fortunately, the availability of automatic environmental recording devices and computer statistical analyses has greatly reduced the work of factoring weather data into the equations. Unfortunately, very few data sets in existence have the necessary environmental variables available for use in equation [7], which limits its use. I have used cumulative mean daily air, surface soil, and rhizosphere soil temperatures; cumulative mean daily relative humidity and wind run; cumulative pan evaporation (cm of water evaporated from an open pan); rainfall; and number of rain incidences as weather variables in equation [7] (Nash, 1983c). Other parameters could also be included. With computer, the importance of each weather variable was determined by step-wise regression statistical analysis, which usually identified the one (or two) variable(s) that explained much of the variation.

Equation [7] becomes most useful when data are collected during a period of variable weather conditions. For example, the dissipation of deltamethrin (a synthetic pyrethroid insecticide) during a year in the Canadian Providence of

Alberta followed equation [1] for the first 85 days, then a different rate as the weather cooled during the winter and then warmed during the spring (figure 5A) (Hill and Schaalje, 1985). When replotting the data (figure 5B) using cumulative mean daily temperature, the data appeared to follow equation [1] over the whole time period.

The several methods available to describe pesticide dissipation from soil indicate that none of the methods is wholly acceptable for all conditions. Rather, it has been a search for acceptable methods. The following sections demonstrate the use, advantages, and disadvantages of some of the methods available.

Nash (1980) (Environmental Chemical Dissipation Database - ECD, see appendix 1) devised a scheme for collecting soil and environmental parameters from literature reporting pesticide dissipation. This information has been stored in computer and contains about 1100 items (Nash and Osborne, 1980). The file is available for use by anyone. The significance of this information allows one rapidly to obtain and compare the experimental information to his/her own situation.

Rhizosphere. Some pesticides are incorporated into the soil or can be incorporated into soil upon tillage after a soil surface or plant application. Often in the past, the more persistent chlorinated hydrocarbon insecticides did become incorporated into the soil because the residues remaining on soil surface or plant were incorporated during the next tillage.

Much of the data available on dissipation of pesticides from rhizosphere soil can be expressed mathematically by the ETB equation. This holds true especially for the more persistent chlorinated hydrocarbon insecticides (Edwards, 1966; Nash and Woolson, 1967). An example of pesticide dissipation from rhizosphere soil in long-term plots is shown in figure 2. These plots were established in 1949 at Beltsville, Maryland (Nash and Woolson, 1967) in which 22.4 kg ha^{-1} chlordane and lindane and 89.6 kg ha^{-1} p,p'-DDD were thoroughly mixed into an Evesboro loamy sand before placing into field plots to a depth of about 25 cm. Initial concentrations were about 9, 9, and 36 ppm, respectively. Chlordane, p,p'-DDD, and lindane dissipation was described by an ETB equation with greater than 87% of the variation accounted for (table 5).

The data of Nash (1983a) were subjected to both ETB and integral-variable ETB approaches for describing pesticide dissipation from soil. Several pesticides were incorporated into 5 cm of rhizosphere soil, which was sampled periodically and analyzed for amount of pesticide remaining (table 6). Concurrently, relative humidity, soil and air temperatures, and soil moisture were measured and cumulated daily. In this case (table 7) the pesticide dissipation rate from rhizosphere soil was described better by ETB equations than
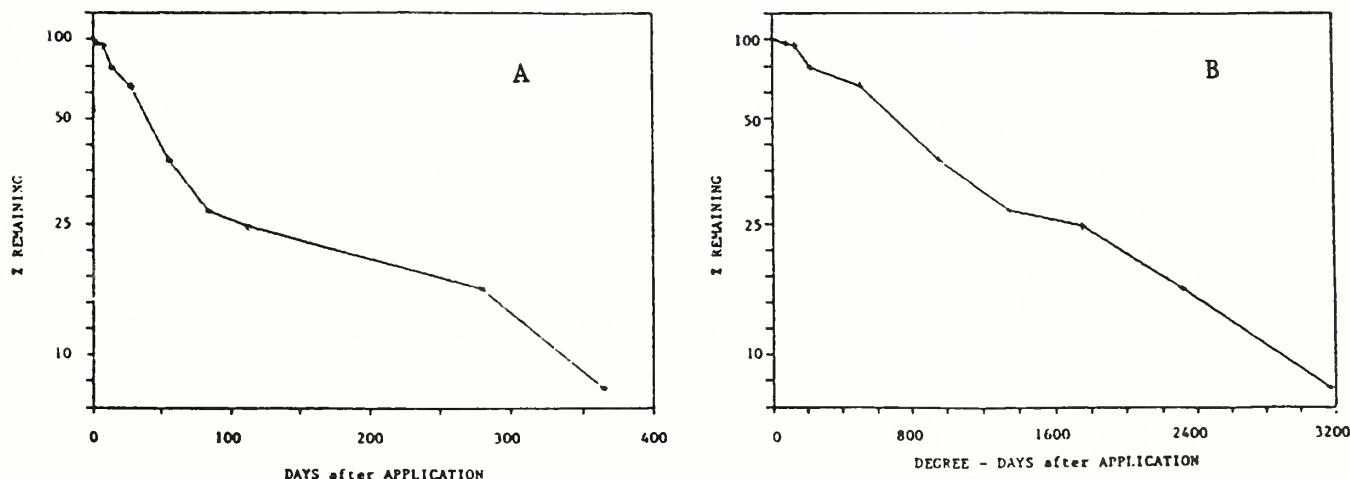
Figure 5.--Dissipation of deltamethrin with time (A) and with cumulative daily mean temperature (B). Correlation coefficient (r^2) for A and B were 0.89 and 0.99, respectively (adapted from Hill and Schaalje, 1985).

Table 5.--Normal exponential time-based (ETB) equations
describing long-term insecticide dissipation from
Evesboro loamy sand soil (Unpub. author's data)

Insecticide[1]	Equation[2]	r^2 [3] %	$c_{1/2}$ [4] years
Chlordane	$C_d = 10.6 \; e^{-0.00027 \; d}$	91**	7.03
p,p'-DDD	$C_d = 41 \quad e^{-0.00021 \; d}$	87**	9.04
Lindane	$C_d = 9.9 \; e^{-0.0032 \; d}$	98**	5.93

[1] Total residues (includes typical contaminants for these
insecticides).
[2] d = day.
[3] Coefficient of determination x 100 (gives % variation
accounted for) and ** = 99% confidence level.
[4] Time for original concentration to be reduced by one-half.

integral-variable ETB equations. However, the variation accounted for was near
50%, except in the observed pesticide dissipation rate for lindane and
emulsifiable concentrated butylate formulation.

The integral-variable ETB equations should have been as good or better than
normal ETB equations. The fact that the integral-variable ETB equations often
did not describe the data as well as the normal ETB indicates that cumulating
the variables, other than time, was a poor choice. Nevertheless, incorporating
such variables as temperature may be quite useful for estimation purposes.

Surface. Dissipation of most pesticides is more rapid from surface soil than
from rhizosphere soil (Nash, 1983a,b) (table 8, dieldrin and heptachlor). For
many pesticides, volatilization becomes a more predominant dissipating pathway
from soil surfaces compared to rhizosphere soil. Further, much greater
environmental variations in temperature, wind run, soil moisture, solar
radiation, and relative humidity occur on soil surface than in rhizosphere
soil. The importance of including the effects of the environmental variables
in any pesticide dissipation equation from soil surfaces is manifest.

Data available from the author (tables 7 to 9) indicated that temperature
(cumulative daily for soils or air), soil moisture (cumulative daily), and rain
(cumulative daily for rain amount or incidences) are the most highly correlated
with pesticide dissipation. Rain incidences perhaps are more important for
pesticides remaining on the soil surface, and cumulative rain perhaps was the
most important variable in one data set (table 8).

Further observations have indicated that a single rate is inadequate for
pesticide dissipation from soil surfaces (Hamaker and Goring, 1976; Hill and
Schaalje, 1985; Savage and Jordan, 1980). Therefore, a two-compartment
exponential model has been proposed (Hamaker and Goring, 1976; Hill and
Schaalje, 1985):

$$C_d = C_o \; e^{-(k_s+k_r)d} + C_o \; \frac{k_r}{(k_s+k_r-k_d)} \; [e^{-k_d d} - e^{-(k_s+k_r)d}] \qquad [8]$$

where k_r = retained residue and k_d = degradation. The data of Hill and
Schaalje (1985) indicates it has considerable validity. Further, Hill and
Schaalje (1985) included °day (d-d) in the model, which as discussed
previously, aids in reducing some of the error because of temperature
fluctuations.

An ETB is a regression equation that describes only the data set from which it
was derived. Thus, application of a given ETB k_s value to predict dissipation
under different conditions should be done with caution. Similarly, an
integral-variable ETB equation is a regression equation that describes only the
data from which it was derived, but it would be more generally applicable
because temperature affects are reduced.

Subsoil. Little is known about pesticide dissipation from subsoil. For
purposes of this paper, the worst case will be assumed to apply [for example,

Table 6.—Pesticide content in the rhizosphere in microagroecosystems as influenced by time and environmental variables (Nash, 1983a)

| Day | Environmental variable[1] | | | | Pesticide[2] (ppm) | | | | |
| | RH | ST | AT | SM | Butylate | | Heptachlor | Lindane | Dieldrin |
	%	°C	°C	%	EC	ME	EC	EC	EC
0.38	1	1	1	1	2.97	4.02	1.35	1.24	1.24
0.63	15	5	6	55	2.73	3.91	1.11	1.25	1.37
1.63	77	27	27	265	3.82	3.23	1.11	1.27	1.34
3.63	174	67	68	656	2.24	3.00	1.16	1.31	1.32
6.42	376	129	133	1130	2.02	3.27	1.05	1.13	0.98
10.33	625	217	222	1795	2.00	3.16	0.72	0.81	1.02
14.33	853	297	306	2575	1.77	2.90	1.07	1.04	1.10
17.58	1009	360	375	3244	1.46	2.99	0.88	0.92	0.89
21.58	1245	456	472	3904	1.30	3.54	1.04	1.09	1.05
24.33	1457	532	549	4289	1.56	3.14	0.99	1.06	1.19
27.58	1658	605	623	4937	1.58	2.66	1.05	0.97	1.06
30.58	1885	675	695	5458	1.41	1.97	0.84	0.82	0.83
34.42	2154	780	800	6000	1.04	2.68	0.87	0.86	0.92
38.42	2432	883	905	6640	1.14	2.90	0.83	0.90	0.90
41.67	2662	967	990	7212	1.05	2.18	0.92	0.99	0.98
45.50	2954	1078	1100	7859	0.76	2.49	0.89	1.03	1.04
48.58	3182	1162	1182	8296	0.90	2.47	0.74	0.83	0.88
52.58	3469	1270	1292	8956	0.63	2.35	0.92	0.94	0.96

[1] RH, ST, AT, and SM = cumulative daily relative humidity, soil temperature, air temperature, and soil moisture (in percent of 33 kPa moisture tension), respectively.

[2] EC = emulsifiable concentrate and ME = microencapsulated formulation.

Table 7.--Normal time-based versus integral-variable time-based equations for determining pesticide dissipation (C = ppm) from rhizosphere (Nash, 1983a) (see Table 6 for input data specifics)

| Pesticide | NORMAL ETB | | Integral-variable ETB and PFTB | |
	Equation[1]	r^2 in %[2]	Equation[3]	r^2 in %[2]
Lindane	$C = 1.16\ e^{-(0.0058\pm0.0016)\,d}$	83**	None None	
Heptachlor	$C = 1.1\ e^{-(0.0058\pm0.0017)\,d}$	40**	None	
Dieldrin	$C = 1.2\ e^{-(0.006\pm0.0015)\,d}$	47**	None	
Butylate ME[4]	$C = 3.5\ e^{-(0.008\pm0.002)\,d}$	59**	$C = 2.33\ e^{-0.0046\,SM}$	29**
Butylate EC[5]	$C = 2.78\ e^{-(0.026\pm0.002)\,d}$	90**	$C = 2.77\ e^{-0.0015\,SM}$	89**

[1] d = day.

[2] Coefficient of determination x 100 (gives % variation accounted for), ** = 99% confidence levels.

[3] SM = cumulative daily soil moisture (in percent of 33 kPa moisture tension).

[4] ME = microencapsulated.

[5] EC = emulsifiable concentrate.

Table 8.--Normal time-based versus integral-variable time-based equations for determining pesticide dissipation (% remaining) from soil surface or rhizosphere (Wegoreck, 1977) (data available from author of this paper)

Pesticide	Conditions	Normal ETB		Integral-variable ETB	
		Equation[1]	r^2 in %[2]	Equation[3]	r^2 in %[2]
Carbaryl	mixed into sl	$\% = 123\ e^{-(0.173 \pm 0.008)d}$	99[**]	$\% = 65.4\ e^{-0.014\ AT}$	92[**]
"	mixed into humus	$\% = 102\ e^{-(0.17\ \pm 0.008)d}$	99[**]	$\% = 54.6\ e^{-0.013\ AT}$	90[**]
"	soil surface	$\% = 143\ e^{-(0.17\ \pm 0.013)d}$	98[**]	$\% = 75.9\ e^{-0.063\ R}$	98[**]
Dieldrin	mixed into sl	$\% = 101\ e^{-(0.0015 \pm 0.0002)d}$	91[**]	$\% = 103.5\ e^{-0.000096\ ST}$	88[**]
"	mixed into humus	$\% = 97.5 e^{-(0.0015 \pm 0.005)d}$	74[*]	$\% = 102.5\ e^{-0.0001\ ST}$	91[**]
"	soil surface	$\% = 106\ e^{-(0.0065 \pm 0.002)d}$	99[**]	$\% = 101.5\ e^{-0.00034\ ST}$	97[**]
Heptachlor	mixed into sl	$\% = 91\ e^{-(0.0031 \pm 0.006)d}$	84[**]	$\% = 90\ e^{-0.00176\ R}$	86[**]
"	mixed into humus	$\% = 109\ e^{-(0.0043 \pm 0.0007)d}$	89[**]	$\% = 110\ e^{-0.0025\ R}$	92[**]
"	soil surface	$\% = 89.4 e^{-(0.007\ \pm 0.005)d}$	97[**]	$\% = 90\ e^{-0.0685\ RI}$	79[*]

[1] d = day.
[2] Coefficient of determination x 100 (gives % variation accounted for), * = 95 and ** = 99% confidence levels.
[3] AT, R, ST, and RI = cumulative daily air temperature, rain in cm, soil temperature, and rain incidence, respectively.

Table 9.--Normal time-based versus integral-variable time-based equations for determining pesticide dissipation from a soil surface (Nash, 1983b) (data available from author)

Pesticide	Normal ETB and PFTB		Integral-variable ETB	
	Equation[1]	r^2 in %[2]	Equation[3]	r^2 in %[2]
Trifluralin	$\% = 100\ e^{-0.26\ d}$	96[**]	$\% = 100\ e^{-0.01\ AT}$	97[**]
Lindane	$\% = 67\ e^{-0.16\ d}$	90[**]	$\% = 71\ e^{-0.0026\ SM}$	94[**]
Heptachlor	$\% = 68\ e^{-0.28\ d}$	98[**]	$\% = 71\ e^{-0.01\ AT}$	98[**]
Heptachlor epoxide	$\% = 110\ e^{-0.07\ d}$	91[**]	$\% = 108\ e^{-0.0026\ AT}$	90[**]
trans-Chlordane	$\% = 110\ e^{-0.068\ d}$	99[**]	$\% = 109\ e^{-0.0025\ AT}$	98[**]
cis-Chlordane	$\% = 110\ e^{-0.052\ d}$	98[**]	$\% = 110\ e^{-0.0019\ AT}$	95[**]
Dieldrin	$\% = 100\ e^{-0.036\ d}$	99[**]	$\% = 100\ e^{-0.0013\ AT}$	99[**]
Endrin	$\% = 81\ d^{-0.04}$	88[**]	$\% = 81\ e^{-0.006\ AT + 0.0023\ SM}$	96[**]
DDD	$\% = 74\ e^{0.06\ d}$	71[*]	$\% = 75\ e^{0.0013\ AT}$	77[*]

[1] d = day.
[2] Coefficient of determination x 100 (gives % variatairion accounted for).

linuron degraded as rapidly at 30-60 cm depth as at 0-10 cm and metribuzin nearly so (Kempson-Jones and Hance, 1979)]. The pesticide in subsoil is ·more likely to transform chemically rather than to degrade completely. Hydrolysis presumably occurs and possibly some oxidation and reduction. Biological degradation presumably decreases rapidly with depth.

Some transport through the subsoil is now known to occur for several pesticides (Cohen et al., 1984; Helling et al., 1984). Presumably this occurs by both diffusion (short range) and leaching (long range), and presumably leaching becomes more dominant with depth, because organic matter content decreases rapidly with depth below the rhizosphere. The rate of pesticide diffusion in subsoil under nonleaching conditions is not presently known but is considered slow compared to leaching except for high-vapor-pressure pesticides.

Pesticide Dissociation (pK_a)

A number of pesticides, being weak acids and bases, can ionize in aqueous solutions. Ionization greatly increases the sorptivity of the bases and decreases the sorptivity of the acids. The degree of ionization is usually dependent upon the soil pH value, particularly at the colloidal surfaces, which may be 1.0 to 2.0 pH units below that determined for the intact soil. The degree of pesticide ionization at the colloidal surface will affect its partitioning between the soil particulates and soil water and the rate of exchange between the two components.

Most of the commonly used acid and base pesticides have pK_a's below 4 or above 8 (Pionke and DeAngelis, 1980). Most agricultural soils in the Eastern United States are above pH 5.5 and in the Western United States below pH 8.0. Even if the pH of the colloidal surface is considered 2 pH units less than that of the intact soil, most of the acid pesticides will be at least 90% ionized, and most of the basic pesticides will be at least 90% nonionized. One should keep in mind also that pH values can change with soil moisture content and temperature.

Harris and Hayes (1982) provide mechanisms for estimating pesticide ionization should no value be found in the literature and ionization be suspected.

The percent dissociation (D) for anionic (acidic) pesticides is found from the following:

$$\log D = pH - pK_a \qquad [9]$$

and

$$\% D = \frac{D \times 100}{D + 1} \qquad [10]$$

For protonated (basic) pesticides pK_a is found from pK_b by

$$pK_a = 14 - pK_b$$

and % D as above. [11]

If the % D is large and the user could obtain estimates of K_d for the ionized and unchanged species, then a new K_d can be computed from a method provided by Pionke and DeAngelis (1980).

Pesticide Dissipation Pathways and Rate Constants (k)

Soils are not static, especially during the summer. Pesticides volatilize with little of the vaporous pesticide returning to the soil. Pesticides hydrolyze irreversibly. Various other transformations and degradation processes occur, which all reduce C_d. These processes usually go in one direction and usually are relatively slow compared to equilibration, i.e., the partitioning and dissociation. Therefore, a computational approach to estimating C_d as opposed to the empirical/experimental approach can be done, also:

$$C_d = C_o \, e^{-(k_a+k_p+k_w+k_i+k_o+k_r+k_g+k_f+k_e+k_b-k_d-k_l)d} \qquad [12]$$

here C_d = concentration on any day = d; C_o = initial soil

concentration; and k_a, k_p, k_w, k_i, k_o, k_r, k_g, k_f, k_e, k_b, k_d, and k_l = volatilization, photolysis, hydrolysis, biodegradation,

oxidation, reduction, leaching, diffusion, complexation, biosorption desorption, and bioelimination rates, respectively.

Bioelimination (k_l) i.e., from root exudation of foliar-applied and stem-translocated pesticide and physically introduced to soil by mobile soil fauna seemingly could enrich the soil pesticide pool, but probably is not a measurable factor and can be omitted from the equation. Likewise, desorption (k_d) from soil could enrich the available pool but most likely would be rate controlling if its occurrence was measurable. Therefore, for all practical purposes desorption can be omitted. Photolysis (k_p) is of little importance, except for certain photosensitive surface-applied pesticides. Oxidation (k_o) and reduction (k_r) depict a transitory, difficultly predictable state, which overall may or may not enhance dissipation. Leaching (k_g) and diffusion (k_f) are pesticide transport from one soil volume (surface, rhizosphere, subsoil) to another. In equation [12] leaching (k_l) and diffusion (k_f) are considered to be decreases in pesticide amount in the soil volume under consideration (i.e., soil surface or rhizosphere). But, when gaseous diffusion is not to the atmosphere, then both leaching and diffusion would carry a (+) sign in the equation for the soil volume (soil surface, rhizosphere, or subsoil) into which the pesticide is being transported. Complexation (k_e) or formation of "bound" residues, which in most cases for all practical purposes removes the pesticide from the available soil pool, is a dissipation process.

Dissipation mechanisms are beyond the scope of this paper and have been discussed elsewhere. It will suffice here to mention briefly the several dissipation pathways, except for volatilization, because further progress has been made in estimating pesticide volatilization from physicochemical and soil or environmental properties. Many soil pesticide losses are not true kinetics, because of the complexity of the conditions in the environment. An extensive literature survey (Nash, 1980) and regression analysis of dissipation data, however, more often than not indicate that a lumped sum of all these various dissipation (k) pathways gives the appearance of a simple exponential (or ETB) equation with a high degree of statistical significance.

Volatilization (soil-air, k_a)

When dissipation from soil is primarily by volatilization, several theoretical and empirical equations based upon the pesticide's physicochemical properties, and usually some of the soil or environmental properties, have been suggested. These several methods have been reviewed and will not be repeated here (Thomas, 1982). Several of these were developed for pesticide volatilization from rhizosphere soil, hence require some knowledge about the diffusion of the pesticide in or from the soil.

Hartley (1969) provides an equation [16-6 (Thomas, 1982)] to determine flux in air of volatile pesticides and a simpler equation ([16-7]) for less volatile pesticides. Both equations appear quite useful as a first approximation for both rhizosphere and surface soil, but in most cases neither the physicochemical or environmental characteristics are available. Therefore, given the initial concentration and the estimated daily flux, a k_a value could be obtained from equation [1], assuming pseudo first-order kinetics.

Hamaker (1972b) provides equations [16-8, 16-9 (Thomas, 1982)] that can give an estimated daily flux, also. Like the Hartley equations [16-6, 16-7 (Thomas, 1982)], the Hamaker equations show some potential, from estimated flux data, for estimating pesticide dissipation (k_s) from soil.

Mayer et al. (1974) have provided five models for determining pesticide flux [16-11 through 16-31 (Thomas, 1982)]. The Mayer et al. models are quite comprehensive, requiring considerable knowledge about the soil and environmental parameters in addition to those of the pesticide. The Mayer et al. equations appear to provide greater sensitivity, but require more accurately described input parameters. Thus, if the parameters selected are inaccurate, the results could be off further than with less sensitive equations.

Jury et al. (1980) have provided another set of equations [16-32 through 16-47 in Thomas (1982)] for determining daily flux of pesticide. In the examples provided by and according to Thomas (1982), the Jury et al. equations [16-44 and 16-45] did not provide a good estimate.

The major disadvantage of the above Hartley, Hamaker, Mayer, and Jury equations for estimation purposes is that detailed pesticide physicochemical characteristics and environmental parameters are required, and usually are not available. Several data sets (Nash et al., 1977; Nash, 1983a,b; Nash and Beall, 1980a; Taylor, 1978) have demonstrated that flux decline in air above a treated soil or crop apparently follows a series of first-order equation declines.

Ideally we would like to obtain a reasonable k_a estimate from our present knowledge or data sets.

Nash (1983e) observed a relationship between pesticide vapor pressure (VP) and dissipation (k_s) when volatilization was the dominant dissipation process. Under his conditions the relationship was $k_s = 0.03 \, VP^{0.6}$ where VP was in mPa.

The Dow Chemical Company expanded upon this relationship [16-48 and 16-49 (Thomas, 1982)] for determining pesticide volatilization from soil surfaces based upon pesticide VP, water solubility (S), and soil organic carbon adsorption coefficient (K_{oc}). [K_{oc} can be obtained, respectively, from K_{ow} (octanol/water partitioning coefficient)] and K_S (water solubility) by

$$K_{oc} = 0.63 \, K_{ow}, \ = 0.48 \, K_{ow}, \ = 18,750 \, K_s^{-0.606}, \qquad [14-17]$$

$$\text{or} = 4,365 \, K_s^{-0.55}$$

(Karickhoff et al. 1979; Hassett et al., 1980; and Kenaga and Goring, 1980).] The Dow equation was modified and is given here as:

$$k_a = k_s = 325 \, \frac{VP}{K_{oc}S} \, \text{day}^{-1} \qquad [18]$$

Dissipation of pesticides according to the Dow equation [18] is given in table 8. The results were reasonably good even though the estimated value for chlorpyrifos was off over one order of magnitude compared to the measured k_a. Presumably, like other estimation expressions, equation [18] is only valid for Dow's standard conditions of 25°C and 75% of 33 kPa moisture tension (Laskowski et al., 1983 and personal communication, Robert Swann, 17 April 1984). However, by incorporating equation [18] into equations [3 and 5], a rough estimate under different conditions possibly could be obtained. The same could be said for the other methods listed.

Hartley (1969) has provided an equation to estimate the flux (F) of a chemical from nonadsorbing surfaces when given the flux of a reference compound:

$$F_b = \frac{VP_b \, (MW_b)^{1/2}}{VP_a \, (MW_a)^{1/2}} \times F_a \qquad [19]$$
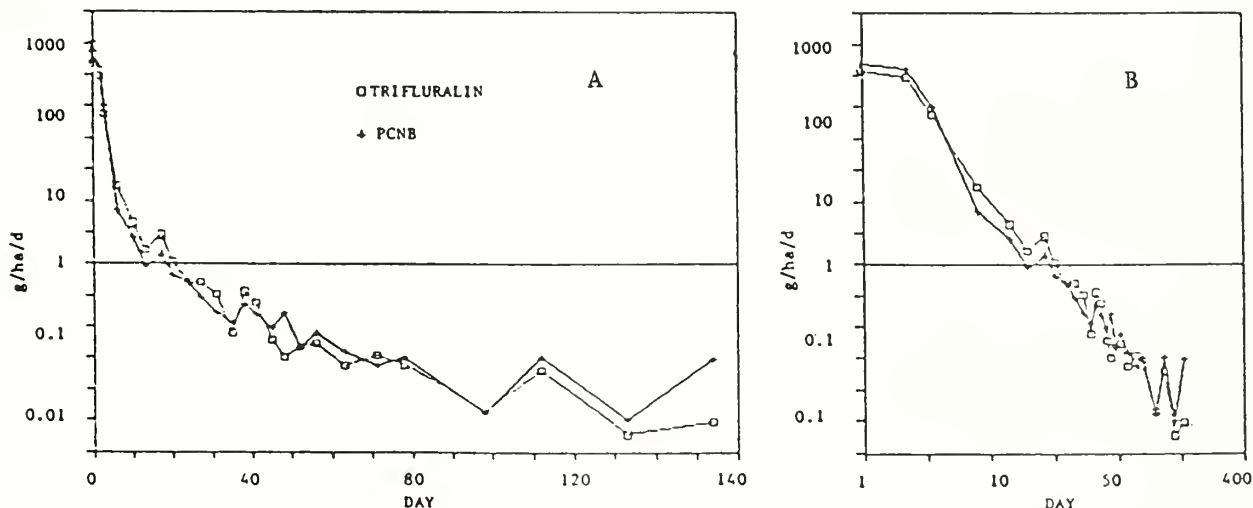
Figure 6.--Decline of trifluralin and PCNB flux in air with time above moist bare soil in chambers. A = normal ETB equation and B = log flux versus log time (Nash, unpublished data).

where MW = molecular weight. The subscripts a and b denote the reference and subject compound, respectively. If volatilization is the primary dissipation pathway, the flux (F) values for the reference compound can be replaced with its k_a value to determine the k_a value of the subject pesticide (table 8). Hartley's equation gives good estimates for compounds of similar vapor pressures. The estimates become less accurate, however, with increased difference in vapor pressures between the reference and subject compound (Nash, 1983e).

One observes upon inspecting equations [18] and [19] that all the elements for Henry's law constant (H)

$$H = \frac{(S)(VP)}{(MW)}$$ [20]

are present, plus whatever influence K_{oc} might have. Therefore, a combination of equations [18] and [19] should provide a reasonable estimate, also

$$k_s = 1.89[H(K_{oc})^{-1}]0.457 \pm 0.053 \ (r^2 = 0.80, \ n = 21)$$ [21]

H in Pa m^3 mol^{-1}. This equation was developed from selected data in Nash (1983b unpublished data, and tables 8 and 9). Equation [21] now incorporates important physicochemical properties, which are available for many pesticides.

Gustafson (personal communication, Monsanto Agric. Co.) suggested a further refinement of model [21], because of some mass transfer resistance to volatilization under very still field conditions or in the relatively mild environmental chambers. "Theory suggests an inverse square root dependence on molecular weight when air-phase transfer controls." Therefore, the same data was regressed after a logarithmic-logarithmic transformation

$$k_s = 3.07 \left(\frac{H}{K_{oc} \ \sqrt{MW}} \right)^{0.453 \pm 0.044}.$$ [22]

Estimated k_s values from equation [21] compared to k_s values from equations [18] and [19] are given in table 8 and equation [18] in table 9. In general, equation [21] fit both the measured laboratory (table 8) and field and chamber measurements (table 9) close. In developing equation [21], the K_{ow} was substituted for K_{oc}, because the K_{ow} can be measured under standard procedures. However, in practice the K_{oc} was found a better parameter. Obviously, K_{oc} has considerable influence on equations [18] and [21] and should be selected carefully.

Equations [18] and [21] do not take into consideration any of the environmental variables. Now however with an estimated k_s value for 25°C, equation [1] can be modified to include temperature. The k_s (equation [1]) was divided by 25 to obtain a time-temperature rate ($-k_{st}$) at 25°C.

$$C_d = C_o \ e^{-k_{st}d-d}$$ [23]

where d-d = degree-days on cumulative daily mean temperature above 0°C for the days under question. (Air temperatures often range as much as 20°C lower than bare soil surface temperatures on bright sunny summer days.) The goodness-of-fit for values calculated from equation [23] versus the observed values found in Table 4 gave $y = 0.93x$ with $r^2 = 0.91$ and $n = 54$.

When dissipation is primarily by volatilization, soil moisture can also influence volatilization greatly, especially for the hydrophobic pesticides. Spencer and Cliath (1972) and Harper et al. (1976) observed that volatilization was greatly reduced when the soil moisture content decreased below the equivalent of about one to three molecular layers of water on the soil particles, a common occurrence during hot sunny summer days on bare soil. Based on the information of Spencer and Cliath (1972) and Harper et al. (1976), the soil moisture tension would be something >10^7 Pa, a soil relative humidity of <93%, and 3 g water (a monomolecular layer = 3 x 10^{-8} cm thick) per 100 m^2 soil surface. Pionke and DeAngelis (1980) [based on papers by Young and Onstad (1976) and Bailey and White (1964)] provide a method to estimate soil-specific surface, which has been modified to SSS = m^{2}g^{-1},

$$SSS = A(\%OC) + \{[B(100-\%M) + (C*\%M)]/100\}(\%c) + 0.04(\%si) + 0.0005(\%s)$$ [24]

Where A = 5-8 (default 10) for OC (organic carbon = 58% organic matter);
B = 0.07-0.3 (def. 0.25) for kaolinite clay or 0.65-1 (def. 0.9) for illite
clay; C = 6-8 (def. 7.5) for montmorillonite (M) and vermiculite clay; and
c = clay, si = silt, and s = sand.

The percent moisture content can be calculated at which dissipation by
volatilization will be greatly reduced. For example, a Galestown (Psammentic
Hapludults) sandy loam soil (from Beltsville, Maryland) has 5.2% organic
matter, 10.5% clay, 22.2% silt, 67.3% sand, and 33 kPa moisture tension of
15.6%. The estimated SSS = 36.8 m^2 g^{-1} soil and % water = 1.1%, would
indicate a considerable decrease in the dissipation rate (k_a) anytime the
soil moisture content dropped below 1.0%, but probably would be proportional to
the percent of soil still covered by a layer of water.

One should keep in mind that none of these methods has received extensive
testing. Thus, they may not be valid for conditions other than those for which
the methods were developed or tested. This holds true especially for the
empirically derived equations. The Hartley (1969), Hamaker (1972b), Mayer et
al. (1974), and Jury et al. (1980) equations for volatilization all suffer the
same shortcomings of the empirically derived equations in that soil (i.e.
temperature and moisture) and environmental parameters are not adequately
tested over a wide range of conditions.

Photolysis (k_p)

Photolysis of a few photosensitive pesticides occurs on soil (Isensee et al.,
1969; Miller and Zepp, 1983), but photolysis is probably a minor dissipation
pathway compared to such pathways as volatilization and biodegradation.
Photolysis on soil most likely is as complex as that in water (Harris, 1982a);
however, photolysis rate is probably sufficiently close to exponential that no
serious error would occur with an ETB equation (Nash and Isensee, 1984).

Hydrolysis (k_a)

Hydrolysis is an important transformation mechanism for many pesticides in
soils. Aqueous pesticide hydrolysis is believed to follow true first-order
kinetics under ideal conditions and has been studied far more extensively than
soil pesticide hydrolysis (Harris, 1982b). Presumably, soil hydrolysis would
follow much the same as that for water.

Biodegradation (k_i)

Of all the dissipation pathways, biodegradation is the most important for most
pesticides, except possibly the chlorinated hydrocarbon insecticides. Although
biodegradation rate appears to follow that depicted in figure 3, the vast
amount of literature available in which biodegradation is paramount indicates a
simple exponential loss (Nash, 1980; Nash and Osborne, 1980). Presumably, the
reason biodegradation rate can be described by ETB equations is because the
soil microorganisms do not depend upon the pesticide as a primary source of
carbon. More likely, the pesticide is a tertiary or quartic source of carbon
for most soil populations. Hence, even though pesticide biodegradation is
incidental to the soil population, it is one of the most important dissipation
pathways. Recently, enhanced biodegradation of carbamate pesticides has been
demonstrated in soils having a history of carbamate applications (fig. 4)
(Kaufman and Edwards, 1983; Obrigawitch et al., 1982, 1983). Even the enhanced
degradation appears to follow an ETB equation.

Oxidation (k_o)

Pesticide oxidation occurs both chemically and biologically. Biological
oxidation probably is more important in the rhizosphere and less important in
the subsoil. An example of the rate of heptachlor oxidation to heptachlor
epoxide is given in figure 5. Oxidation of the pesticide usually leads to a
more stable product than the parent pesticide.

Reduction (k_r)

Pesticide reduction occurs primarily as a biological process. Although
pesticide reduction is not a major transformation mechanism, its occurrence

often leads to enhanced biodegradation in soils and probably to accelerated bound residue formation. For this reason, pesticide rate of reduction is a component that usually cannot be separated from the biodegradation rate.

Leaching (k_g)

Leaching apparently occurs to some degree for all pesticides regardless of the solubility. [Transport by water can be either up or down. Leaching usually refers to transport downward by both gravitational and capillary flow, whereas transport upward is capillary and referred to as "wick" (Hartley and Graham-Bryce, 1980). Leaching may occur in pulses (Helling et al., 1984). This would indicate that pesticide movement is primarily caused by water rather than gaseous diffusion, but whether this is aqueous transport or vaporous transport, or both, as a result of downward saturated water flow washing the soil air is not clear. A leaching "index" as described by Helling (1971) is one way of estimating pesticide leaching in soil by water.

Diffusion (k_f)

Pesticide diffusion in soils occurs in both the aqueous and gaseous phases. Diffusion is an important transport mechanism for the fumigants and therefore is an important dissipation pathway. Several equations exist for describing the pesticide diffusion mechanism (Thomas, 1982; Jury et al., 1980; Farmer et al., 1980; Hartley and Graham-Bryce, 1980).

Desorption (k_d)

In the adsorbed state many pesticides are not likely to be dissipated. Upon desorption, the pesticide becomes more available for dissipation; therefore, desorption often becomes the rate limiting step for dissipation. Several reviews exist on pesticide sorption and desorption mechanisms (Green, 1974; Green and Karickhoff, 1984; Pionke and DeAngelis, 1980; Weed and Weber, 1974).

Bioelimination (k_1)

Bioelimination of sorbed pesticide is probably not an important phenomenon in soils. Biosorption followed by bioelimination would imply only temporary unavailability for dissipation. Bioelimination is probably only a potential and not an important contributing factor in influencing pesticide dissipation rates.

Complexation or "bound" (k_e)

"Bound" residues are generally considered stable, slowly available, and less mobile and bioactive. Therefore, for purposes of this paper complexation can be considered as dissipation. "Bound" residues in soils have been reviewed by Khan (1982) and Kaufman et al. (1976).
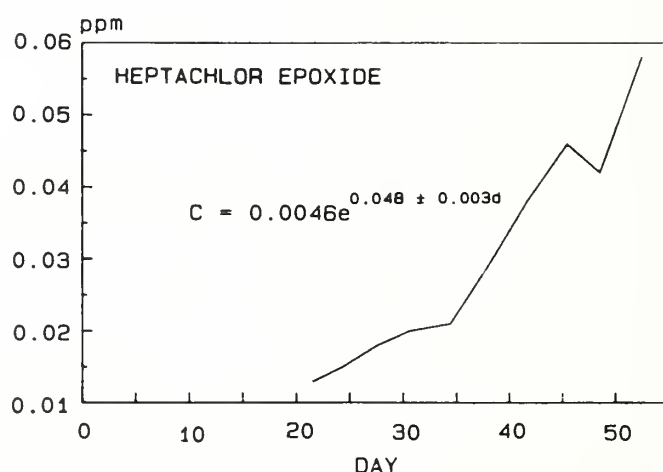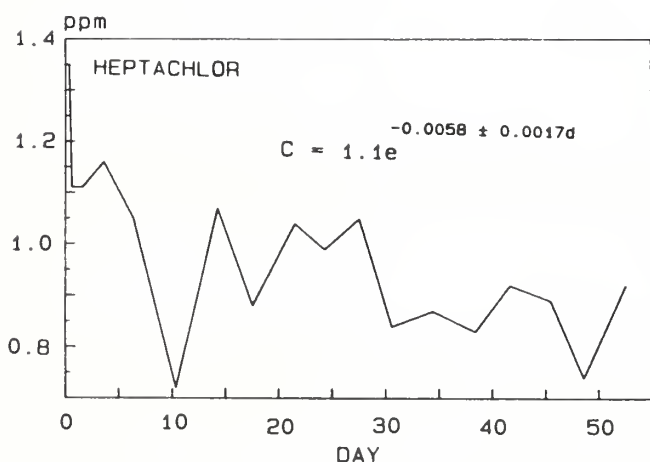
Figure 7.--Oxidation of heptachlor to heptachlor epoxide in chamber soil (Nash, 1983a)

Polymerization (k_m)

Polymerization of pesticides or pesticide degradation products normally does not occur, except at high concentrations. Therefore, it can safely be assumed that polymerization would not occur in the very dilute concentrations found in or on soil.

Pesticide Properties (CP) Database

Eventually some kinetic principles will be applied to estimate pesticide dissipation from soil as more is learned about the pesticides, soils, climate, and dissipation. In the meantime, many pesticide properties (table 2) are being stored in a database by the Model and Database Coordination Laboratory at Beltsville, Maryland.

Classifying Dominant Dissipation Pathways and Dissipation Rates

At any given time, usually one dissipation pathway predominates over all other possible pathways of pesticide loss from soil; however, the dominant pathway may change from one to another throughout the pesticide's persistence in or on soil. The dominant pathway(s) should be estimable from the physico-chemical properties of the pesticide and from measured parameters that are available in the literature. One scheme is to classify the pesticide into three general tendency categories of persistent, moderately persistent, and nonpersistent to moderately persistent (appendix 3):

I. Those that adsorb onto soil mineral (i.e., bipyridinium quaternary salts) or soil organic matter (i.e., hydrophobic chlorinated hydrocarbons).

II. Those that are soluble (relatively) in water (i.e., acids; including their esters; phenols; organophosphates; s-triazines; carbamates; phenylamides; pyrethroids)

III. Those that readily volatilize (i.e., dinitroanilines, thiocarbamates, certain organophosphates)

Category I pesticides have a tendency to adsorb onto soil mineral or organic matter (K_d) and would bioaccumulate (K_{bcf}) in an aqueous system after an initial fast dissipation rate, primarily by volatilization. For the hydrophobic pesticides, volatilization (k_a) would continue slowly throughout the life of the pesticide and would be greatly enhanced under warm, moist soil conditions. Hydrolysis (k_w) and biodegradation (k_i) would be slow to nearly nonexistent. Oxidation would likely occur and lead to a more persistent transformation product. Reduction, when occurring, usually would enhance degradation of the transformed product.

Category II pesticides tend to be soluble in water. Therefore, Category II pesticides tend to be transformed, primarily by hydrolysis (k_w), oxidation (k_o), and reduction (k_r) (or dehalogenation), then dissipate by biodegradation (k_i), and leaching downward (k_g) or upward in the aqueous phase, possibly with some volatilization (k_a).

Category III pesticides are those that volatilize (k_a) and may biodegrade (k_i) rapidly. They would include the high vapor-pressure pesticides, which tend to dissipate very rapidly to moderately slowly.

This classification system does not suggest that less dominant dissipation pathways should be ignored but, rather, serves as an aid to identify the one or two pathways that one should give the most attention to. Appendix 3 presents a scheme to aid in categorizing a pesticide as to its behavior in soil and its likely persistence.

SUMMARY AND CONCLUSIONS

Dissipation of pesticides on surface soil, in rhizosphere soil, and presumably in subsoil usually follows a simple exponential equation, which is a lumped sum of all the loss pathways and the chemical and environmental factors affecting

dissipation. An equation developed from a given data set theoretically is valid only for that data set and should not be used to estimate pesticide dissipation under different conditions without additional testing and calibration. If there are no alternatives, or additional means to test or validate the equation, its application must be considered with a great deal of caution.

Dissipation activation energies (ΔE) (Arrhenius equation) have been determined for several pesticides. The activation energies can be used to estimate pesticide dissipation under conditions like those from which the dissipation activation energies were determined but should be used only with caution under different conditions. Similar to the dissipation activation energy, equations describing soil moisture influence on dissipation have been developed for given situations. These can be used under like conditions but should be used with caution to estimate dissipation under different conditions.

Exponential integral-variable equations are valid only for the data sets from which they were developed, but they may be useful to estimate pesticide dissipation under different conditions, provided caution is taken as described above. Soil moisture and soil or air temperatures were the environmental variables most often associated with the integral-variable equations, and soil moisture and temperature are the two variables addressed in the Arrhenius and soil-moisture-influence equations. The advantage of either Arrhenius plus soil-moisture influence or integral-variable equations over exponential equations is that they use environmental parameters that directly affect dissipation.

A conceptual approach (equation [13]) in which the dissipation rate from each loss pathway is defined and in which environmental influences are reflected has the greatest potential, because true kinetics can be assigned. Unfortunately, separating the several pathways to measure a dissipation pathway accurately under precisely measured environmental (experimental) conditions is rarely possible.

When pesticide dissipation is primarily by volatilization, a k_s value may be developed with empirically derived equations [21 and 22] based upon the pesticide's Henry's law constant and K_{oc}. At the present time, equations [21 and 22] have limited applicability because they may not be universal equations and because of probable bad Henry's law constants and K_{oc} values.

Once a valid k_s value has been obtained at a known temperature (i.e., 25 °C), equation [1] can be modified to include temperature in addition to time (equation [23]).

All of the empirically derived equations are only valid for the data sets from which they were developed. Likewise, many of the theoretical equations may be valid only for the data sets from which they were tested, because assumptions are always made. In principle, however, the theoretical equations based upon sound thermodynamics and kinetics should prove the most useful in the long-run in spite of their present shortcomings.

RECOMMENDATIONS

1. Use of k_s values, primarily from the ECD Database, in an exponential equation is presently the procedure most often used for estimating pesticide concentration in soil at any given time. The k_s value should be derived experimentally onsite or selected from an environmental situation as closely related to the situation under consideration as possible.

2. Where possible, first choice should be use of dissipation activation energies and soil-moisture-influence equations for estimation purposes. When volatilization is the major dissipation pathway, an array of equations is available from which to choose. The simpler methods are apt to be chosen in spite of their kinetic shortcomings. They may give an adequate estimate. Again, the values or equations chosen should be determined by onsite experimentation or from conditions as close as possible to those for which the estimation is intended.

3. Time-temperature equations would be a second choice for those cases where a k_s can be obtained at a known temperature. Time-temperature equations should have wide applicability provided the k_s selected is from conditions (soil surface, rhizosphere, moist or dry soil, subsoil, etc.) to which it will be applied.

4. Where possible, the third choice should be use of integral-variable equations, observing the precautions as listed in recommendation 2. Presumably, a power-function ETB would be better than a normal ETB, because of the nonlinearity effects of the environmental variables.

5. Lastly, equations based on the pesticide's Henry's law constant and K_{oc} values may have applicability for pesticides on moist soil surfaces where volatilization is a major dissipation pathway.

6. Researchers should be cognizant of the needs of modelers and hence should plan their research to provide the environmental parameters necessary for a true kinetic approach to pesticide dissipation from soil.

REFERENCES

Bailey, G.W. and White, J.L. 1964. Review of adsorption and desorption of organic pesticides by soil colloids, with implications concerning pesticide bioactivity. J. Agric. Food Chem. 12:324-332.

Baker, R.D. and Applegate, H.G. 1970. Effect of temperature and ultraviolet radiation on the persistence of methyl parathion and DDT in soils. Agron. J. 62:509-512.

Brewer, F.; Lavy, T.L.; and Talbert, R.E. 1982. Effect of flooding on dinitroaniline persistence in soybean (Glycine max)-rice (Oryza sativa) rotations. Weed Sci. 30:531-539.

Burschel, P. 1961. Untersuchungen uber das Verhalten von Simazin in Boden. Weed Res. 1:131-141.

Cihacek, L. J. and Bremner, J. M. 1979. A simplified ethylene glycol monoethyl ether procedure for assessment of soil surface area. Soil Sci. Soc. Am. J. 43:821-822.

Cohen, S.Z.; Creeger, S.M.; Carsel, R.F.; and Enfield, C.G. 1984. In Treatment and Disposal of Pesticide Wastes. Am. Chem. Soc. Symp. Ser. No. 259. Amer. Chem. Soc. 1155 16th St., NW., Washington, DC 20056.

Edwards, C.A. 1966. Insecticide residues in soils. Residue Rev. 13:83-132.

Farmer, W.J.; Igue, K.; Spencer, W.F.; and Martin, J.P. 1972. Volatility of organochlorine insecticides from soil: I. Effect of concentration, temperature, air flow, and vapor pressure. Soil Sci. Soc. Am. Proc. 36:443-447.

Farmer, W.J.; Yang, M.S.; Letey, J.; and Spencer, W.F. 1980. Hexachlorobenzene: Its vapor pressure and vapor phase diffusion in soil. Soil Sci. Soc. Am. J. 44:676-680.

Garten, C.T. and Trabalka, J.R. 1983. Evaluation of models predicting terrestrial food chain behavior of xenobiotics. Environ. Sci. Technol. 17:590-595.

Gile, J.D. 1983. 2,4-D--Its distribution and effects in a ryegrass ecosystem. J. Environ. Qual. 12:406-412.

Gile, J.D.; Collins, J.C.; and Gillet, J.W. 1980. Fate of selected herbicides in a terrestrial laboratory microcosm. Environ. Sci. Technol. 14:1124-1128.

Gile, J.D. and Gillet, J.W. 1979. Fate of selected fungicides in a terrestrial laboratory ecosystem. J. Agric. Food Chem. 27:1159-1164.

Glotfelty, D.E. 1978. The atmosphere as a sink for applied pesticides. J. Air Pollut. Control Assoc. 28:917-921.

Green, R.E. 1974. Pesticide-clay-water interactions. In W.D. Guenzi (ed.), Pesticides in Soil and Water, pp. 3-37. Soil Sci. Soc. Am., Madison, Wisconsin.

Green, R.E. and Karickhoff, S.W. Estimating pesticide sorption coefficients for soils and sediments. (This volume)

Hamaker, J.W. 1972a. Decomposition: Quantitative aspects. In C.A.A. Goring and J.W. Hamaker (eds.), Organic Chemicals in the Soil Environment. Marcel Dekker, Inc., New York. 1:253-340.

Hamaker, J.W. 1972b. Diffusion and volatilization. In C.A.A. Goring and J.W. Hamaker (eds.), Organic Chemicals in the Soil Environment. Marcel Dekker, Inc., New York. 1:341-397.

Harper, L.A.; White, A.W., Jr.; Bruce, R.R.; Thomas, A.W.; and Leonard, R.A. 1976. Soil and microclimate effects on trifluralin volatilization. J. Environ. Qual. 5:236-242.

Harris, J.C. 1982a. Rate of aqueous photolysis. In W.J. Lyman, W.F. Reehl, and D.H. Rosenblatt (eds.), Handbook of Chemical Property Estimation Methods. Ch. 8. McGraw-Hill Book Co., New York.

Harris, J.C. 1982b. Rate of hydrolysis. In W.J. Lyman, W.F. Reehl, and D.H. Rosenblatt (eds.), Handbook of Chemical Property Estimation Methods. Ch. 7. McGraw-Hill Book Co., New York.

Harris, J.C. and Hayes, M.J. 1982. Acid dissociation constant. In W.J. Lyman, W.F. Reehl, and D.H. Rosenblatt (eds.), Handbook of Chemical Property Estimation Methods. Ch. 6. McGraw-Hill Book Co., New York.

Hartley, G.S. 1969. Evaporation of pesticides. In Pesticidal Formulations Research, Physical and Colloidal Chemical Aspects. Adv. Chem. Ser. 86:115.

Hartley, G.S. and Graham-Bryce, I.J. 1980. Vol. 1, Ch. 3 and 5 and Vol. II, Ch. 14. Physical Principles of Pesticide Behavior. Academic Press, New York.

Hassett, J.J.; Means, J.C.; Banwart, W.L.; and Wood, S.G. 1980. Sorption properties of sediments and energy-related pollutants. EPA-600/3-80-041. 132 pp.

Helling, C.S. 1971. Pesticide mobility in soils II. Applications of soil thin-layer chromatography. Soil Sci. Soc. Am. Proc. 35:737-743.

Helling, C.S. and Turner, B.C. 1968. Pesticide mobility: Determination by soil thin-layer chromatography. Science 162:562-563.

Helling, C.S.; Wehunt, E.J.; Feldmesser, J.; and Kearney, P.C. 1984. Soil leaching and residues in perched ground water. 187th Am. Chem. Soc. Nat'l. Meeting, St. Louis, Missouri. April 8-13, 1984. Pestic. Chem. Div., No. 10.

Hill, B.D. and Schaalje, G.B. 1985. A two-compartment model for the dissipation of deltamethrin on soil. J. Agric. Food Chem. 33:1001-1006.

Isensee, A.R.; Plimmer, J.R.; and Turner, B.C. 1969. Effect of light on the herbicidal activity of some amiben derivatives. Weed Sci. 17:520-523.

Jury, W.A.; Grover, R.; Spencer, W. F.; and Farmer, W.J. 1980. Modeling vapor losses of soil-incorporated trial-late. Soil Sci. Soc. Am. J. 44:445-450.

Karickhoff, S.W.; Brown, D.S.; and Scott, T.A. 1979. Sorption of hydrophobic pollutants on natural sediments. Water Res. 13:241-248.

Kaufman, D.D. and Edwards, D.F. 1983. Pesticide/microbe interaction effects on persistence of pesticides in soil. In J. Miyamoto et al. (eds.), IUPAC pesticide chemistry. Human Welfare and the Environment. pp. 177-182. Pergamon Press, New York.

Kaufman, D.D.; G.G. Still; G.D. Paulson; and S.K. Bandal (eds.). 1976. Bound and Conjugated Pesticide Residues. Am. Chem. Soc. Symp. Ser. 29:1-396.

Kearney, P.C.; Nash, R.G.; and Isensee, A.R. 1969. Persistence of pesticide residues in soils. In M.W. Miller and G.G. Berg (eds.), Chemical Fallout. Charles C. Thomas, Publ., Springfield, Ill. pp. 54-67.

Kempson-Jones, G.F. and Hance, R.J. 1979. Kinetics of linuron and metribuzin degradation in soil. Pestic. Sci. 10:449-454.

Kenaga, E.E. and Goring, C.A.I. 1980. Relationship between water solubility, soil sorption, octanol-water partitioning and concentration of chemicals in biota. In J.C. Eaton, P.R. Parrish, and A.C. Hendricks (eds.), Aquatic Toxicology ASTM 707. Amer. Soc. for Testing and Materials, Philadelphia, PA.

Khan, S.U. 1982. Bound pesticide residues in soil and plants. Residue Rev. 84:1-25.

Laskowski, D.A.; Swann, R.L.; McCall, P.J.; and Bidlack, H.D. 1983. Soil degradation studies. Residue Rev. 85:139-147.

Leistra, M. 1978. Evaluation of rate coefficients for consecutive reactions of pesticides in soil. J. Environ. Sci. Health. B13:343-360.

Mayer, R.; Letey, J.; and Farmer, W.J. 1974. Models for predicting volatilization of soil-incorporated pesticides. Soil Sci. Soc. Am. Proc. 38:563-568.

Miller, G.C. and Zepp, R.G. 1983. Extrapolating photolysis rates from laboratory to the environment. Residue Rev. 85:89-110.

Muhammad, M. 1976. Desorption of adsorbed ametryn and diuron from soils and soil components in relation to rates, mechanisms, and energy of adsorption reactions. Ph.D. Thesis Univ. Microfilms International.

Mustafa, M.A. and Y. Gamar. 1972. Adsorption and desorption of diuron as a function of soil properties. Soil Sci. Soc. Amer. Proc. 36:561-565.

Nash, R.G. 1980. Dissipation rate of pesticides from soil. In W.G. Knisel (ed.), CREAMS: Field Scale Model for Chemicals, Runoff, and Erosion from Agricultural Management Systems. 3:560-594. U.S. Gov't. Printing Office - 1980 0-310-945/SEA-15.

Nash, R.G. 1983a. Distribution of butylate, heptachlor, lindane, and dieldrin emulsifiable concentrated and butylated microencapsulated formulations in microagroecosystem chambers. J. Agric. Food Chem. 31:1195-1201.

Nash, R.G. 1983b. Comparative volatilization and dissipation rates of several pesticides from soil. J. Agric. Food Chem. 31:210-217.

Nash, R.G. 1983c. Integrated and nonintegrated equations for describing pesticide dissipation from soil and air. Am. Soc. Agron. Abstr. p. 36.

Nash, R.G. 1983d. Pesticide distribution and dissipation in a crop environment. Proc. Int'l. Conf. Environ. Hazards of Agrochemicals in Developing Countries. Nov. 8-12, 1983. p. 84. Univ. Alexandria.

Nash, R.G. 1983e. Determining environmental fate of pesticides with microagroecosystems. Residues Rev. 85:199-215.

Nash, R.G. and Beall, M.L., Jr. 1980a. Distribution of silvex, 2,4-D and TCDD applied to turf in chambers and field plots. J. Agric. Food Chem. 28:614-623.

Nash, R.G. and Beall, M.L., Jr. 1980b. Fate of maneb and zineb fungicides in microagroecosystem chambers. J. Agric. Food Chem. 28:322-330.

Nash, R.G.; Beall, M.L., Jr.; and Harris, W.G. 1977. Toxaphene and 1,1,1-trichloro-2,2-bis(p-chlorophenyl)ethane (DDT) losses from cotton in an agroecosystem chamber. J. Agric. Food Chem. 25:336-341.

Nash, R.G. and Osborne, E.M. 1980. Environmental Chemical Dissipation (ECD) File. First Annual Meeting, Soc. Environ. Toxicol. and Chem. November 23-25, Arlington, Va.

Nash, R.G. and Woolson, E.A. 1967. Persistence of chlorinated hydrocarbon insecticides in soils. Science 157:924-927.

Nigg, H.N.; Allen, J.C.; Brooks, R.F.; Edwards, G.J.; Thompson, N.P.; King, R.W.; and Blagg, A.H. 1977. Dislodgeable residues of ethion in Florida citrus and relationships to weather variables. Arch. Environ. Contam. Toxicol. 6:257-267.

Obrigawitch, T.; Martin, A.R.; and Roeth, F.W. 1983. Degradation of thiocarbamate herbicides in soils exhibiting rapid EPTC breakdown. Weed Sci. 31:187-192.

Obrigawitch, T.; Wilson, R.G.; Martin, A.R.; and Roeth, F.W. 1982. The influence of temperature, moisture, and prior EPTC application on the degradation of EPTC in soils. Weed Sci. 30:175-181.

Ou, L.T.; Gancarz, D.H.; Wheeler, W.B.; Rao, P.S.C; and Davidson, J.M. 1982. Influence of soil temperature and soil moisture on degradation and metabolism of carbofuran in soils. J. Environ. Qual. 11:293-298.

Pionke, H.B. and DeAngelis, P.J. 1980. Method for distributing pesticide loss in field runoff between the solution and adsorbed phase. In W.G. Knisel (ed.), CREAMS: Field Scale Model for Chemicals, Runoff, and Erosion from Agricultural Management Systems. U.S. Gov't. Printing Office - 1980 0-310-945/SEA-15. 3:560-594.

Poku, J.A. and Zimdahl, R.L. 1980. Soil persistence of dinitramine. Weed Sci. 28:650-654.

Savage, K.E. and Jordan, T.N. 1980. Persistence of three dinitroaniline herbicides on the soil surface. Weed Sci. 28:105-110.

Schroy, J.M.; Hileman, F.D.; and Cheng, S.C. 1985. "Physical/chemical proper-ties of 2,3,7,8-Tetrachlorodibenzo-p-Dioxin," Aquatic Toxicology and Hazard Assessment: Eighth Symposium, ASTM STP 891, R.C. Bahner and D.J. Hansen, Eds., American Society for Testing and Materials, Philadelphia, pp. 409-421.

Seiber, J.N. and Woodrow, J.E. 1983. Methods for studying pesticide atmospheric dispersal and fate at treated areas. Residue Rev. 85:217-229.

Smith, A.E. and Walker, A. 1977. A quantitative study of asulam in soil. Pestic. Sci. 8:449-456.

Soulas, G. 1982. Mathematical model for microbial degradation of pesticides in the soil. Soil Biol. Biochem. 14:107-115.

Spencer, W.F.; Cliath, M.M.; and Farmer, W.J. 1969. Vapor density of soil-applied dieldrin as related to soil-water content, temperature, and dieldrin concentration. Soil Sci. Soc. Amer. Proc. 33:509-511.

Taylor, A.W. 1978. Post-application volatilization of pesticides under field conditions. J. Air Pollut. Control Assoc. 28:922-927.

Thomas, R.G. 1982. Volatilization from soils. In W.J. Lyman, W.F. Reehl, and D.H. Rosenblatt (eds.), Handbook of Chemical Property Estimation Methods. Ch. 16. McGraw-Hill Book Co., New. York.

Van Bladel, R. and A. Moreale. 1977. Adsorption of herbicide derived p-chloroaniline residues in soils. A predictive equation. J. Soil Sci. 28:93-102.

Walker, A. 1970. Persistence of pronamide in soil. Pestic. Sci. 1:237-239.

Walker, A. 1974. A simulation model for prediction of herbicide persistence. J. Environ. Qual. 3:396-401.

Walker, A. 1976a. Simulation of herbicide persistence in soil. I. Simazine and prometryne. Pestic. Sci. 7:41-49.

Walker, A. 1976b. Simulation of herbicide persistence in soil. II. Simazine and linuron in long-term experiments. Pestic. Sci. 7:50-58.

Walker, A. 1976c. Simulation of herbicide persistence in soil. III. Propyzamide in different soil types. Pestic. Sci. 7:59-64.

Walker, A. 1978. Simulation of the persistence of eight soil-applied herbicides. Weed Res. 18:305-313.

Walker, A. and Barnes, A. 1981. Simulation of herbicide persistence in soil; a revised computer model. Pestic. Sci. 12:123-132.

Walker, A. and Brown, P.A. 1983. Measurement and prediction of chlorsulfuron persistence in soil. Bull. Environ. Contam. Toxicol. 30:365-372.

Walker, A.; Hance, R.J.; Allen, J.G.; Briggs, G.G.; Chen, Yuh-lin; Gaynor, J.D.; Hogue, E.J.; Malquori, A.; Moody, K.; Moyer, J.R.; Pestemer, W.; Rahman, A.; Smith, A.E.; Streibig, J.C.; Torstensson, N.T.L.; Widyanto, L.S.; and Zandvoort, R. 1983. EWRS herbicide-soil working group: Collaborative experiment on simazine persistence in soil. Weed Res. 23:373-383.

Walker, A. and Zimdahl, R.L. 1981. Simulation of the persistence of atrazine, linuron and metolachlor in soil at different sites in the USA. Weed Res. 21:255-265.

Weed, S.B. and Weber, J.B. 1974. Pesticide organic matter interactions. In W.D. Guenzi (ed.), Pesticides in Soil Water. pp. 39-66. Soil Sci. Soc. Am., Madison, Wisconsin.

Wegoreck, W. 1977. Decomposition and accumulation of some insecticides in soil and their diffusion into plants, soil macrofauna and ground water. Annu. Rep. No. 7. Grant No. FG-PO-270. Project No. E21-SWC-a5. Inst. Plant Protection UL. Miczurina 20, 60-318 Poznan, Poland.

Willis, G.H.; McDowell, L.L.; Harper, L.A.; Southwick, L.M.; and Smith, S. 1983. Seasonal disappearance and volatilization of toxaphene and DDT from a cotton field. J. Environ. Qual. 12:80-85.

Yaron, B.; Heuer, B.; and Birk, Y. 1974. Kinetics of azinphosmethyl losses in the soil environment. J. Agric. Food Chem. 22:439-441.

Young, R.A. and Onstad, C.A. 1976. Predicting particle-size composition of eroded soil. Trans. Am. Soc. Agric. Eng. pp. 1071-1075.

Zimdahl, R.L. and Clark, S.K. 1982. Degradation of three acetanilide herbicides in soil. Weed Sci. 30:545-548.

DATA COLLECTION FORM

CHEMical:_____

CAS No:_____   (circle)

RESiDue: Soil surface Rhizosphere Subsoil Air Surface Water Subwater Plant part_____

CoNSTant: k = 0._____ ± 0._____;   Statistics: r^2 = 0._____, n =_____

        Units = _____;   Confidence level: <95%___ , >95%___ , 99%___

Best FIT
equation: ln C_d = _____

        Statistics: r^2 = 0._____, n=_____;   CL: <95%___ , >95%___ , 99%___

SOIL type: _____ (_____)
               (common)   (scientific)

    Particle size (g kg^{-1}): sand____ silt____ clay____ Organic matter_____,

    Bulk density_____Mg m^3, pH_____ , CEC_____meq/100 g, Temperature_____°C or various,

    Moisture_____% or various OF_____kg kg^{-1} or _____%
               (expt)   (33 kPa)   (field capacity)
                                                 (circle)
    Surface: smooth medium rough, Cover: clean trashy stubble-light -medium -heavy

AIR: Temperature_____°C or various, Relative humidity____%, Turbulence _____

    Velocity_____m/s or various, Radiation:____W/m^2, wave length____nm or various,

WATeR: Temperature_____°C or various, Turbulence_____, Other_____

PLaNT: _____ (_____)
        (common)   (scientific)

EXPT: Field_____ Glasshouse_____

     Laboratory_____ Other_____

APPLication: Rate (a.i.)_____

           Formulation_____

           Where: To soil In soil Foliar Other_____
                                        (circle)
           How:_____

CITatioN:_____ (___) (___)
         abbreviation   volume (No.)   pages   (year)

FIELD DESCRIPTION

CHEM a chemical designation (common name)
CAS   Chemical Abstracts Registry Number
RESD residue in environmental component (Rhizoshere Soil Surface Subsoil
      Air Surface Water Subwater Plant part)
CNST k = slope in first-order equation using natural logarithms for
     amount: CD = CO*2.718(KD); where CD = amount on day D; CO = initial
     amount; (KD) is expontional to 2.718; R(2) = coefficient of
     determination with (2) exponential to R; N = number of observations;
     units = for chemical amount; % = % of original
BFIT best-fit equation; ln= natural logarithm. To find CD. substitute ln
     CO for first term in equation. Any (2), (3), or (4) is exponential to D
SOIL type (common and scientific), particle size, organic matter,
     moisture, pH, CEC, temperature, surface, cover
AIR   temperature, relative humidity, velocity, radiation, turbulence
WATR water, temperature, turbulence
PLNT plant name (common and scientific)
EXPT experimental parameters of field, laboratory, or greenhouse
APPL application rate, formulation, where (soil, foliar) and how
CITN citation based upon the ASTM six letter and number Coden (if available)
     system usually found on the journal cover

Appendix 2

Soil Specific-Surface Equation

The SSS equation is based on properties in Bailey and White (1964) for the surface area of Soil constituents

Soil constituent	m^2g^{-1}	mean
Organic matter	500-800	650
Vermiculite	600-800	700
Montmorillonite	600-800	700
Dioctaledral vermiculite	50-800	425
Illite	65-100	83
Chlorite	25-40	33
Kaolinite	7-30	19
Oxides & hydroxes	100-800	450

and equations from Pionke and DeAngelis (1980) for estimating K_d and equations from Young and Onstad (1976) for estimating soil specific area.

The equation was initially expressed with the approximate mean value for each coefficient. Subsequently, the equation was tested against the data in Table 1 of Young and Onstad (1976) by arbitrarily adjusting the % of organic carbon (OC) for all soils to near 3% (three very sandy soils were adjusted to 0.75% OC), the data in Table 1 of Cihacek and Bremner (1979) by arbitrarily adjusting the % montmorillonite clay to near 25% for midwest (U.S.) soils and upward or downward for other soils, the data in Table 2 of Muhammad (1976) by adjusting clay percentages based upon the information given, the data in Table 1 of Van Bladel and Moreale (1977) by adjusting the clay percentages based upon the information given, and the data in Table 1 of Mustafa and Gamar (1972) by adjusting the percent montmorillonite clay to 5, 15, or 25% depending upon suspected soil type. Then the coefficient for OC was adjusted upward, according to Pionke and DeAngelis (1980) and the coefficients for kaolinite, illite and montmorillonite type clays were adjusted upward to fit the above designated data.

The fitted equation, between the measured and estimated values, resulted in a high correlation (r^2=0.93) (estimated = 0.81 measured + 11), but resulted in a large standard error of 23 for the estimate. The fitted equation is conservative, in that it slightly underestimates the measured surface but was considered closer to the real situation because the data may be biased from the arbitrary selected organic carbon and montmorillonite values.

Appendix 3. Scheme for classifying a pesticide as to the probable dominant pathway that will govern its dissipation from soil[1]

Pesticide Name			Classification[2]					
			I		II		III	
Item	Symbol	Units	Value	(x)[3]	Value	(x)[3]	Value	(x)[3]
Water Solubility	WS	$\mu g \; g^{-1}$	<1	( )	>50	( )	<50	( )
Vapor Pressure	VP	Pa	<0.01	( )	>0.01	( )	>0.05	( )
Octanol-water	K_{ow}	$\dfrac{\mu g \; P \; (octanol^{-1})^4}{\mu g \; P \; (water^{-1})}$	>1000	( )	<100	( )	<200	( )
Leaching Index	LI	R_f	<0.1	( )	>0.5	( )	>0.1	( )
Sorption Coefficient	K_d	$\dfrac{\mu g \; P \; (g \; adsorbent^{-1})}{\mu g \; P \; (g \; water^{-1})}$	>10	( )	<5	( )	<10	( )
	K_{oc}	$\dfrac{\mu g \; P \; (g \; adsorbent^{-1})}{\mu g \; P \; (g \; water^{-1})}$	>100	( )	<50	( )	<100	( )
Bioconcentration Factor	K_{bcf}	$\dfrac{\mu g \; P \; (g \; biota^{-1})}{\mu g \; P \; (g \; water^{-1})}$	>1000	( )	<100	( )	<500	( )
Dissipation Rate (rhizosphere or subsoil)	k_s	$\dfrac{\mu g \; P \; (g \; soil^{-1})^5}{day}$	<0.002	( )	<0.05	( )	>0.02	( )
Dissipation Rate (surface soil)	k_s	$\dfrac{\mu g \; P \; (g \; soil^{-1})^5}{day}$	<0.02	( )	<0.5	( )	>0.2	( )
Sum of (x's)				( )		( )		( )

[1]Values arbitrarily selected from Garten and Trabalka (1983), Helling and Turner (1968), Kenaga and Goring (1980), Nash (1980), Pionke and De Angelis (1980), and Weed and Weber (1974).

[2]I,II,III = decreasing order of persistence. See text for details.

[3]Place an "x" for each classification a pesticide falls into.

[4]P = pesticide. [5]P can have any other suitable units.

RELATIONSHIPS AMONG EPC, LABILE P AND SOIL TEST P VALUES

A. M. Wolf, D. E. Baker, H. B. Pionke, and H. M. Kunishi

ABSTRACT

The most biologically available forms of P in soils are the labile P fraction and the P in the soil solution. While laboratory measurements of both labile P and solution P are time consuming and expensive, State and commercial soil testing laboratories routinely perform low-cost soil tests for P for making fertilizer recommendations. The relationships developed in this study allow the labile P and solution P estimates to be made from readily available soil test data.

The relationships among three soil tests for P (Olsen's $NaHCO_3$, Bray I, and Mehlich I), three measurements of labile P (labile ^{32}P, resin P and intercept P) and EPC were examined for a diverse group of noncalcareous agricultural soils. All measurements of labile P were highly correlated with one another ($r^2 \geq 0.83$). When soils were grouped according to geographic location, good relationships were found betwen each labile P measurement and each soil test for P and between EPC and both labile P and soil test P measurements. Bray I was the best predictor of labile P on the North Central and Northeastern soils ($r^2 \geq 0.82$) while the Olsen and Mehlich I soil tests most successfully predicted labile P on soils from the Southeast ($r^2 \geq 0.85$).

From both a soil fertility and environmental perspective there is a growing concern over the loss of P from agricultural land. In conjunction with agriculture management models, the relationships developed in this study provide a tool for evaluating the effects of different soil and water management systems on the loss of the most biologically available P fractions from land.

INTRODUCTION

The ability of a soil to supply phosphorus (P) to plants is dependent upon three factors: the activity of P in the soil solution; the labile quantity of P or the quantity of P in the soil in equilibrium with P in solution; and the phosphate buffer capacity which refers to the ability of a soil to replenish P to the soil solution (Larsen 1967).

The two most important measurements required to characterize the biological availability of P in a soil are the labile P pool and the concentration of P in the soil solution. Soil solution P may be determined by measuring water-soluble P or, more accurately, from an adsorption/desorption isotherm to determine the equilibrium P concentration (EPC) at zero P adsorption (Kunishi and Taylor 1977). Labile P has traditionally been determined using isotopic dilution techniques where ^{32}P is added to a soil and its distribution between the soil and soil solution is determined at a given point in time (Russell et al. 1954). Alternative approaches are to use adsorption/desorption isotherms to estimate the labile P pool in soils (Kunishi and Taylor 1977) or to use an anion saturated resin to extract soil P (Amer et al. 1955).

While the above mentioned tests are performed for research purposes, cost and time considerations do not allow them to be used on a routine basis. Instead, "quick tests" for P, such as Olsen's $NaHCO_3$, Bray I and Mehlich I have been developed (Bray and Kurtz 1945, Olsen et al. 1954, Sabbe and Breland 1974) and are used widely. These tests extract a certain fraction of the P present in the soils, which is often correlated with the labile P pool but is not necessarily equal to it.

If one could quantify the relationships that exist between P extracted by these tests and the labile P and solution P measurements, then the quick tests for P

Director of Merkle Laboratory and Professor of Soil Chemistry, The Pennsylvania State University, University Park, PA, and Soil Scientists, USDA-ARS, University Park, PA and Beltsville, MD, respectively.

could provide useful and easily performed methods for estimating a soil's labile P pool and solution P concentration. With an increase in the use of modeling for the evaluation of agricultural management systems, the development of these relationships is essential.

The primary objectives of this study were 1) to develop an equation or group of equations to describe the relationship(s) between labile P and EPC on a diverse group of non-calcareous soils and 2) to evaluate labile P and EPC as a function of the Olsen, Bray I, and Mehlich I soil tests. Additional experimental objectives were 1) to evaluate the effect of carrier P on the measurement of isotopically determined labile P; 2) to evaluate the relationships among labile P measurements determined by isotopic exchange (labile ^{32}P), by resin extraction (resin P), and from the intercept of adsorption/desorption isotherms (intercept P); and 3) to evaluate the agreement among different soil testing laboratories performing the Olsen, Bray I, and Mehlich I soil tests on the same group of soils.

For ease of discussion, this paper has been divided into two parts. In the first part, studies on the determination of labile P and on the relationships between labile P measurements and EPC will be discussed. In the second part, the Olsen, Bray I and Mehlich I soil test P relationships with the labile P measurements and EPC will be evaluated. Because of the large number of studies included in this paper, each one is discussed independently, and a separate "Summary and Conclusions" section follows the discussion of each. A summary of the most important relationships developed is provided at the end of the paper.

MATERIALS AND METHODS

Collection and Preparation and General Description of Soils

The soils used in this study were noncalcareous agricultural soils which were presently being used or had been used in the past for soil test P calibration studies. The soil types and orders and locations from which the soils were collected and the number of P rates applied to the soils are shown in Table 1. In all, soils from 27 calibration sites were collected from 18 states in the Southeast, South Central, North Central and Northeast regions of the United States. Separate calibration studies had been performed for corn and soybeans on the Wooster and Flanagan soils, and two calibration studies had been performed on the Hagerstown soil using no-till and conventional tillage systems. Soils from both calibration sites on these three soil series were collected (see Table 1).

The textures of the soils used in this study ranged from sandy loams to silty clay loams (Table 1). Following the U. S. Department of Agriculture's classification scheme (Brady 1974), all of these soils would be classified as loams, but they extend over the range of textures--moderately coarse, medium and moderately fine--that fall within this class.

As shown in the table, the soils were from the Ultisol, Alfisol and Mollisol orders. While these three orders represent only a few of those present in the United States, they are present on over 80% of the total land area of the states from which the soils were collected (Buol 1973, Krusekopf 1960, Miller and Quandt, 1984).

The number of P treatments applied to the soils as part of the calibration studies ranged from two to five (Table 1). Five-pound samples were collected from the plow layer (top 6 2/3 inches) from each of the P treatments at all calibration sites, giving a total of 91 soil samples. The soils were collected in a moist state at or below field capacity. After collection, the soils were sealed in plastic bags, returned to Pennsylvania, and stored at 8 C until all samples had been collected.

The movement of soils from Alabama, Georgia, Florida, North Carolina, and South Carolina is restricted by insect and plant quarantines which require that soils transported from these states be sterilized. To meet the requirements of the quarantine, the Hartsells, Benndale, Red Bay, Cecil, Portsmouth and Pacolet soils were sealed in plastic bags and placed in a 75 C drier for a period of one week. After this time, the soils were removed and treated in a manner similar to all other soils.

Table 1
General description of soils collected from experimental P fertility sites

Soil type	Location	Number of P fertilzer treatments	Soil order
Benndale loamy sand	AL	5	Ultisol
Cecil sandy clay loam	GA	5	Ultisol
Cisne silt loam	IL	5	Alfisol
Creldon silt loam	MO	3	Alfisol
Davidson silty clay loam	VA	4	Ultisol
Dickson silt loam*	TN	4	Ultisol
Flanagan silt loam (corn)	IL	3	Mollisol
Flanagan silt loam (soybean)	IL	3	Mollisol
Freehold sandy loam	NJ	2	Ultisol
Hagerstown silt loam (no-till)	PA	3	Alfisol
Hagerstown silt loam (con. till)	PA	3	Alfisol
Hartsells fine sandy loam	AL	5	Ultisol
Hastings silt loam	NE	3	Mollisol
Mattapex silt loam	MD	3	Ultisol
Pacolet sandy clay loam	SC	2	Ultisol
Plano silt loam	WI	3	Mollisol
Portsmouth fine sandy loam	NC	3	Ultisol
Raub silt loam	IN	3	Mollisol
Red Bay fine sandy loam	FL	3	Ultisol
Sharpsburg silty clay loam	NE	3	Mollisol
Tatum silt loam	VA	5	Ultisol
Webster clay loam	IA	3	Mollisol
Webster clay loam	MN	3	Mollisol
Winfield silt loam	MO	3	Alfisol
Woodson silty clay loam	KN	3	Mollisol
Wooster silt loam (corn)	OH	3	Alfisol
Wooster silt loam (soybean)	OH	3	Alfisol
		91	

*The 4th treatment on this soil included manure applications in addition to the high P fertilizer treatment.

A greenhouse experiment was performed to equilibrate the soils by allowing them to go through several wetting and drying cycles. The soils were placed in two-liter pots and planted to a sorghum-sudangrass hybrid which was grown for a period of three weeks. After harvesting, the moist soils were sieved through a 2-mm (9 mesh) sieve and stored at 8 C. Subsamples from all soils were air-dried, resieved and used for the analyses performed in this experiment.

Isotopically Determined Labile P

Isotopically determined labile P was measured on all soils using the method described by Olsen and Sommers (1982) with slight modifications. Measurements were made in duplicate at four levels of carrier P. The carrier levels used were 0, 1.24, 6.20 and 3.10 ug P/g solution giving 0, 3.1, 15.5 and 77.5 ug P/g soil. The procedure involved placing 1.00 g of the air-dried soil samples in 50-ml Oak-Ridge-type centrifuge tubes; adding 25 ml of water or carrier solution; and adding 0.1 ml of a ^{32}P solution which was also 1 x 10^{-6} M in ^{31}P and which provided an activity of approximately 5 uCi to all tubes. Eight drops of chloroform were added to the tubes, which were placed on an end-over-end shaker for 24 hours. After shaking, the samples were centrifuged at 15,000 rpm for 15 minutes in a refrigerated centrifuge at 15 C. The supernatant was filtered through a 0.2 um membrane filter.

To measure ^{32}P in solution, a 0.1-ml aliquot was taken from the filtrate and placed in a vial containing 10 ml of scintillation fluid. The activity of ^{32}P was determined by counting for a period of five minutes or until the counting

error was reduced to 1%. The ^{31}P was measured colorimetrically by the ascorbic acid method (Olsen and Sommers 1982). At the zero level of carrier P, labile P was determined using the equation

$$Labile \ P = P_s/f \qquad\qquad (1)$$

where P_s is the P in solution and f is the fraction of ^{32}P remaining in solution after the 24-hour equilibration period (Olsen and Sommers 1982). For all other levels of carrier P, labile P was determined using the equation

$$Labile \ P = [(S_i/S_f) \ -1]B \qquad\qquad (2)$$

where S_i is the initial specific activity, S_f is the final specific activity, and B is the initial amount of ^{31}P in the solution added to the soil (Olsen and Sommers 1982).

Anion Exchange Resin P

The extraction of P from soils using an anion exchange resin was performed in the laboratory of J. W. B. Stewart at the Saskatchewan Institute of Pedology. The procedure followed was that described by Sibbesen (1977).

Intercept Labile P and the Equilibrium Phosphorus Concentration

The equilibrium phosphorus concentration (EPC) and intercept labile P were determined from adsorption/desorption isotherms using the method described by Kunishi and Taylor (1977). The development of an adsorption/desorption curve involves equilibrating a soil with solutions having a range of P concentrations and plotting the change in soil P (P adsorbed or desorbed) as a function of the final equilibrium solution P level. In this experiment, the adsorption/desorption measurements were made simultaneously with the isotopically exchangeable labile P determinations. The four levels of carrier P (0, 1.24, 6.20, and 3.10 ug P/g in solution) used in the labile P method described above were the initial solution P concentrations. After the 24-hour equilibration period, the final solution P concentrations were measured as described previously and the calculated change in soil P was plotted as a function of the final solution P level to obtain an adsorption/desorption curve. The EPC, corresponding to the concentration of P in solution at which there is no net gain or loss of P from the solution, was determined from the intercept of the adsorption/desorption curve with the abscissa. An estimate of labile P was obtained by extrapolating the tangent of the curve at the EPC to the ordinate.

Olsen, Bray I, and Mehlich I Soil Tests for P

Soil samples were sent to several State university soil testing laboratories, where the Olsen (NaHCO$_3$ extraction), Bray I, and Mehlich I soil tests were performed on all soils in duplicate using standard soil test procedures. The Olsen soil test (Olsen et al. 1954) was performed at the University of Nebraska, North Dakota State University, and Kansas State University; the Bray I test (Bray and Kurtz 1945) was performed at the Universities of Minnesota and Nebraska and at Kansas State University; and the Mehlich I soil test (Sabbe and Breland 1974) was performed at Auburn University and at the Virginia Polytechnic Institute and State University.

LABILE P MEASUREMENTS AND THE RELATIONSHIP BETWEEN LABILE P AND EPC

Effects of Different Levels of Carrier P on Isotopically Determined Labile P

Introduction

The most traditional method of measuring labile P in soils is by isotopic exchange. However, there are several experimental problems involved with this method which could lead to inaccurate measurements of the labile P pool. One of the problems involves the effect of the level of carrier P used on the labile P determination. The objective of this part of the study was to evaluate this effect. A brief discussion of the theory behind the measurement of labile P by isotopic exchange and some of the difficulties involved with this technique are as follows.

The general relationships involving P in the soil and soil solution are described by the equation

$$\text{soil solution P} \rightleftharpoons \text{labile P} \rightleftharpoons \text{nonlabile P} \tag{3}$$

where labile P refers to the quantity of the soil P which equilibrates rapidly with the soil solution, and nonlabile P refers to the portion of soil P which reaches equilibrium slowly with the labile fraction (Larsen 1967). In most soils, the labile fraction is only a small portion of the total P present.

Because of the complexity of the reactions occurring in the soil system, a clear distinction between the labile and nonlabile P components of the soil does not exist and the equilibrium relationship described in Equation 3, particularly between labile and non-labile P, is probably never achieved (Olsen and Khasawneh 1980). However, the labile P pool may be defined as that which involves reactions occurring within a specified short period of time, while the reactions between the labile and nonlabile pools are those which occur more slowly (Olsen and Khasawneh 1980).

The determination of labile P in soils by equilibration with ^{32}P is based on the exchange reaction

$$^{31}P_{surface} + {}^{32}P_{solution} \rightleftharpoons {}^{32}P_{surface} + {}^{31}P_{solution} \tag{4}$$
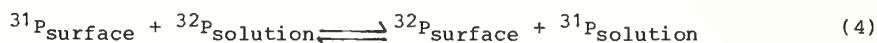
which occurs when the radioactive isotope, ^{32}P, is added to a soil-solution system (Russell et al. 1954). The $^{31}P_{(surface)}$ represents that portion of the soil P which is readily exchangeable with ^{32}P. At equilibrium,

$$\frac{(^{31}P_{surface})\ (^{32}P_{solution})}{(^{32}P_{surface})\ (^{31}P_{solution})} = 1 \tag{5}$$

and $^{31}P_{surface}$ may be determined from the equation,

$$^{31}P_{surface} = \frac{(^{32}P_{surface})(^{31}P_{solution})}{(^{32}P_{solution})} \tag{6}$$

By definition, labile P is equal to the isotopically exchangeable soil P plus the P in solution (Russell et al. 1957), and the working formula for determining labile P becomes

$$\text{labile P} = \frac{^{31}P_{solution}}{f} \tag{7}$$

where f is the fraction of ^{32}P remaining in solution after equilibrium has been achieved (Olsen and Sommers 1982).

While the concept of labile P described here is relatively straightforward and theoretically sound, experimentally there are several difficulties involved. One difficulty involves the assumption that equilibrium between ^{32}P and soil P has been reached. Phosphorus may be held in the soil in many different forms, and the exchange reaction between ^{32}P in solution and soil ^{32}P will occur at different rates making the point at which equilibrium is reached difficult to establish (Russell et al. 1954). Many researchers have demonstrated that the fast reactions between $^{32}P_{solution}$ and $^{31}P_{surface}$ are complete within 24 hours and are followed by a slow reaction which continues for days (McAuliffe et al. 1947, Russell et al. 1954, Seatz 1954, 1958). As a consequence, a 24-hour equilibration period has been recommended for the determination of labile P by ^{32}P (Olsen and Sommers 1982).

Another difficulty with the procedure involves the determination of labile P on soils which have either a high capacity to adsorb P or those which have low solution levels of P. In soils which have a high adsorption capacity for P, the ^{32}P added to the solution may react irreversibly with some of the soil components (Amer 1962, Amer et al. 1969). As a result, the equilibrium specified by Equation (5) is not achieved. Consequently, the calculated labile P value will be an overestimate of the actual exchangeable P. In soils where the solution P concentration is low, the difficulty in making labile P

measurements lies in the decreased accuracy for solution P measurements (Russell et al. 1954, Olsen and Sommers 1982).

To overcome these difficulties, the addition of ^{31}P carrier with ^{32}P has been recommended (Amer 1982, Russell et al. 1954, Sommers and Olsen 1982). The addition of the carrier allows the solution P concentration to be measured with greater accuracy and decreases the effect that the irreversible adsorption of ^{32}P by the soil has on the determination of labile P. However, the addition of carrier P to the soil, while alleviating some experimental problems involved with the determination of labile P, may create others. Several researchers have demonstrated that the kinetics of exchange of P in soils may be modified by the solution level of P with which a soil is equilibrating (Amer 1962, Talibudeen 1957). As the solution level of P is increased, the time required to reach equilibrium increases (Talibudeen 1957). In some instances, it has been shown that this affects the calculation of the labile P values (Amer 1962), while in other instances no effect has been noted (Amer 1962, Russell et al. 1954). The results of these studies are difficult to interpret, however, because of the wide range of carrier concentrations used, the differences in equilibration time, and the differences among the soils studied.

In this study, to investigate the effect of carrier P on labile P determinations, labile P was measured on all soils using four levels of carrier P ranging from 0 to 3100 ug P/L solution, giving 0 to 77.5 ug P/g soil. The highest level chosen is that recommended by Olsen and Sommers (1982) as the carrier level to be used for soils with very low solution P levels.

Results and Discussion

The labile P measurements made at different levels of carrier P are shown in Table 2. In many instances, the increase in level of carrier P resulted in decreased labile P, while in others no effect of the carrier was noted. The carrier P effect was most notable on the low P calibration plots of each soil. Table 3 shows the means of the labile P values determined at different P carrier levels over all soils and on soils separated on the basis of the low, medium or high P calibration plots. As may be seen, the labile P values determined at the four different rates of carrier are significantly different when an analysis of variance is performed over all soils as well as when performed on soils from the low P calibration plots. However, the differences among labile P values decrease on soils from the higher P calibration plots. On soils from the plots containing the highest P level, only the labile P values determined with the largest amount of carrier (77.5 ug P/g soil) are significantly different from the others. The general indication from these results is that the addition of carrier P may have a significant effect on the labile P determination on soils where P is low, while the effect decreases in significance on soils to which medium or high rates of P have been applied. Despite these differences, the labile P measurements made at the 0, 3.1 and 15.5 ug P/g soil level of carrier were highly correlated with one another (r values of 0.95 or higher) while the correlations of these determinations with labile P measurements at the highest carrier rate were slightly lower (r values of 0.91 or higher).

The decrease in the measured labile pool with the addition of carrier P noted on some of the soils may be due to a decrease in the relative amount of ^{32}P irreversibly adsorbed by the soil; to the greater accuracy in the measurement of solution P as carrier P is increased; or to the effect that the carrier P has on the rate at which the isotopic exchange reaction reaches equilibrium. It is likely that all of these effects are operative to some degree, although the relative importance of each will vary with the particular soil as well as with the specific level of carrier P used.

One group of researchers (Amer 1962, Amer et al. 1969) has demonstrated that the irreversible adsorption of ^{32}P by soils low in P, and particularly on those soils with a large capacity to "fix" P, will lead to an overestimate of the labile P pool. It is probable that this effect is occurring in at least some of the soils used in this study as well. For example, the data indicate that labile P in the Davidson soil decreases with the increased levels of P in the calibration plots (Table 1). This trend was observed when labile P was determined at all but the highest rate of carrier P. In addition to this effect, the calculated labile P values are extremely high. The indication is that P is irreversibly adsorbed by the soil, to the greatest extent on the low P

Table 2
Labile P determinations (ug P/g soil) at different levels of carrier P

Soil series	Level of fertilizer P	Carrier level of P ug P/g soil			
		0	3.1	15.5	77.5
Benndale	1	6.7	5.3	2.5	-4.5
	2	6.2	4.1	4.1	-7.4
	3	12.0	11.2	9.0	-1.1
	4	12.0	11.6	7.6	5.2
	5	34.3	26.8	29.5	25.9
Cecil	1	28.6	14.6	5.6	-12.2
	2	13.6	10.2	4.8	-12.6
	3	16.3	13.0	8.9	-11.2
	4	15.6	13.4	10.7	-8.7
	5	21.1	201.6	19.2	-0.3
Cisne	1	16.4	9.4	4.0	-13.6
	2	18.8	17.6	14.3	0.1
	3	22.6	22.4	19.4	4.7
	4	27.7	25.4	22.5	13.8
	5	57.5	56.9	57.4	47.2
Creldon	1	25.9	17.7	20.4	11.9
	2	24.4	28.0	26.6	23.8
	3	45.4	44.2	39.4	37.1
Davidson	1	667.8	446.4	276.2	73.3
	2	324.1	304.3	218.0	76.1
	3	215.1	160.8	149.0	66.0
	4	142.2	118.0	130.8	95.0
Dickson	1	51.5	30.8	18.6	7.0
	2	38.3	35.0	46.0	20.9
	3	54.7	56.4	53.3	52.6
	4	80.6	85.0	83.5	74.9
Flanagan (corn)	1	21.7	16.4	12.3	-2.1
	2	26.7	24.5	19.2	5.4
	3	40.0	40.7	36.5	24.8
Flanagan (soybean)	1	16.7	14.1	9.6	-0.6
	2	30.0	26.6	22.6	16.6
	3	48.8	52.6	41.8	33.6
Freehold	1	19.7	15.5	15.9	5.4
	2	68.5	77.9	73.5	54.4
Hagerstown (no-till)	1	28.4	28.3	25.7	12.5
	2	30.9	32.5	27.6	15.4
	3	35.5	37.1	32.3	21.7
Hagerstown (conv. till)	1	28.8	24.8	22.2	6.6
	2	27.7	26.3	24.2	12.5
	3	35.2	35.0	30.5	20.7
Hartsells	1	15.4	11.6	5.8	1.4
	2	9.3	9.5	5.8	1.6
	3	14.6	13.6	9.4	6.2
	4	20.4	14.5	12.0	4.9
	5	33.8	31.7	29.3	27.7
Hastings	1	37.6	38.6	40.4	37.3
	2	71.0	75.1	70.8	68.4
	3	62.0	63.4	62.6	63.0

Table 2--Continued
Labile P determinations (ug P/g soil) at different levels of carrier P

Soil series	Level of fertilizer P	Carrier level of P ---------- ug P/g soil ------------			
		0	3.1	15.5	77.5
Mattapex	1	48.3	32.5	38.2	37.2
	2	51.9	48.6	30.2	52.8
	3	88.5	89.9	81.8	71.4
Pacolet	1	6.84	6.39	2.34	-11.32
	2	5.33	5.14	2.35	-15.23
Plano	1	28.0	26.0	21.1	16.0
	2	280.3	26.5	21.4	17.2
	3	30.7	30.0	26.9	21.9
Portsmouth	1	5.5	5.0	3.0	-2.2
	2	11.3	11.3	10.0	23.8
	3	64.8	42.9	65.0	72.2
Raub	1	11.0	11.3	8.5	6.3
	2	24.3	16.5	18.5	17.5
	3	83.0	83.7	78.1	69.0
Red Bay	1	13.7	13.6	9.5	6.8
	2	13.5	15.0	13.1	9.6
	3	23.1	26.9	23.2	11.3
Sharpsburg	1	26.0	24.3	22.3	22.6
	2	27.5	28.4	25.9	26.7
	3	35.4	37.6	34.2	33.9
Tatum	1	35.5	37.0	2.7	0.7
	2	29.2	23.6	6.2	6.8
	3	30.7	30.4	26.6	19.6
	4	42.1	38.3	32.4	32.1
	5	100.2	100.7	103.5	101.8
Webster (IA)	1	16.9	17.2	15.2	19.0
	2	25.3	21.5	31.9	33.8
	3	64.9	65.0	60.3	63.3
Webster (MN)	1	17.1	16.7	15.1	11.5
	2	28.4	30.5	31.1	22.7
	3	40.1	43.3	42.1	39.2
Winfield	1	12.7	11.9	10.8	7.5
	2	19.7	19.6	18.5	16.8
	3	33.3	34.3	31.3	26.7
Woodson	1	15.6	15.0	10.8	6.9
	2	25.5	19.8	19.1	13.1
	3	30.3	30.0	31.4	22.0
Wooster (corn)	1	15.1	9.6	6.5	2.0
	2	21.8	17.0	23.2	5.3
	3	24.8	23.5	22.2	16.6
Wooster (soybean)	1	24.0	20.1	11.1	4.9
	2	25.3	22.0	20.1	12.2
	3	28.4	240.8	22.2	20.5

Table 3
Means of labile P values (ug P/g soil) determined at different levels of carrier P over all soils and on soils from low, medium and high P fertility[1]

Level of carrier P (ug P/g soil)	All plots[2]	P fertility level		
		Low P plots	Medium P plots	High P plots
0	32.10 A	22.80 A	27.00 A	46.49 A
3.1	29.78 B	18.79 B	25.63 AB	44.93 A
15.5	27.40 C	14.24 C	23.90 B	44.06 A
77.5	21.39 D	7.63 D	18.04 C	38.51 B

[1] Means followed by the same letter are not significantly different at the 5% level of probability by the Duncan's multiple range test.

[2] Cv's for labile P values over all soils were 15.1, 8.8, 19.0 and 20.5%, respectively, for the low to high levels of carrier P.

plot, leading to an overestimate of labile P. In addition, the difficulty in measuring the low levels of solution P may have contributed to the observed effect.

On soils where the capacity to irreversibly adsorb P is extremely high, the determination of labile P using isotopic dilution techniques may be inappropriate. Even the addition of large amounts of carrier is insufficient to offset the fixation of significant quantities of ^{32}P and, as a result, labile P will be over-estimated. Similar to the Davidson soil, the labile P values for the low calibration plots of the Pacolet, Tatum and Dickson soils were also larger than the high P plots of these same soils when the determinations were made at the zero level of carrier P (Table 2). However, this effect was reversed when carrier P was used in the measurement of labile P.

Another effect observed on some of the soils in this study was the occurrence of negative labile P values at the high level of carrier P (Table 2). This effect has been noted by others (Thompson et al. 1960, White and Taylor 1977) and several explanations have been offered. White and Taylor (1977) suggested that in acid soils, aluminophosphate complexes may be present in the soil solution. The labelled complexes would be measured by scintillation counting, but the P present in the complexes would not be measured colorimetrically. As a result, the final specific activity (S_f) would be overstimated and could, in fact, be larger than the initial specific activity (S_f). If this were the case, the labile P as calculated using Equation 2 would be negative. A similar situation would result if labeled organic compounds were present in the soil solution (Olsen et al. 1961). Alternatively, Amer (1962) suggested that the decreased sensitivity of the method when large amounts of carrier are used could account for the negative values reported in the literature. He suggested that minimum amounts of carrier be used when determining labile P in soils.

Summary and Conclusions

From the above discussion and from the results in Tables 2 and 3, it is apparent that the selection of a carrier level at which the "true" labile P values were determined for all of the soils used in this study is difficult. When no carrier has been added, the irreversible adsorption of P by some soils along with the difficulty of measuring low P levels in solution may lead to an overestimate of labile P. The addition of carrier would decrease, although not eliminate, the effect of the irreversible adsorption of ^{32}P and allow solution P levels to be measured with greater accuracy. On the other hand, the effect of large amounts of carrier P added to the soil may be to change the rate at which equilibrium is obtained and, as a result, underestimate labile P.

The most logical solution is to select a low level of carrier P which allows for a more accurate determination of labile P in low P soils without leading to an underestimate of this quantity which may occur when the carrier is applied at high rates. For these reasons, the labile P values determined at the low level of carrier P (3.1 ug P/g soil) were selected as the ones to be used in this study for comparison with the other soil test P and EPC values. Because of the obviously extreme labile P values determined for the Davidson soil, the values from these samples were not included in the comparative analyses.

Comparison of Labile P Measurements

Introduction

While the labile pool for P has traditionally been determined using isotopic exchange techniques, it can be determined by any method which measures the amount of soil P in rapid equilibrium with solution P. One alternative to isotopic exchange is the estimation of labile P from adsorption/desorption isotherms (Kunishi and Taylor 1977). In this approach, the curve defining the relationship between P adsorbed by or desorbed from the soil and the solution P concentration is extrapolated to the ordinate. The point of interception represents the amount of P that must be desorbed from the soil to give zero levels of P in solution and is taken as a measure of labile P. Another approach is to use an anion exchange resin to extract P from the soil. The resin acts as a continuous sink for P and is considered by some to behave in a manner similar to the way in which a plant root obtains P from the soil (Amer et al. 1955).

The objective of this part of the study was to evaluate the relationships among measurements of labile P determined 1) by isotopic exchange, 2) from adsorption/desorption isotherms (intercept P) and 3) by resin extraction (resin P).

Results and Discussion

The equations describing the relationships among the three measurements of labile P are shown in Table 4. While all relationships were good ($r^2 > .80$), the highest correlation was found between labile ^{32}P and resin P ($r^2 = .89$). It is interesting to note that the slope of the equation describing the relationship between these two variables approaches 1.00, suggesting that the same labile P pool is being measured. In contrast, the quantity of labile P determined from the adsorption/desorption isotherm procedure was approximately one-half of that removed by the labile ^{32}P and resin P techniques.

As seen in Table 4, the intercepts of the equations describing the relationships of both intercept P and resin P with labile ^{32}P were significantly different than zero. The experimental difficulties involved in the determination of isotopically exchangeable labile P on low P soils, as discussed previously, may account for this observation. If this is true, it may be that the measurement of P in soils by the resin exchange procedure will give a more accurate

Table 4
Equations describing the relationships among labile P measurements

	Equation[1]	r^2
Labile ^{32}P	$= 5.75_* + 1.08$ Resin P	0.88
Labile ^{32}P	$= 6.50_* + 2.35$ Intercept P	0.84
Resin P	$= 2.31_{ns} + 1.99$ Intercept P	0.80

[1]ns and * indicate, respectively, that the intercept is not significantly different and is significantly different from zero at the 5% level of probability.

assessment of labile P than will the more traditionally used isotopically exchangeable P technique.

Summary and Conclusions

It is evident from these results that while all three methods of measuring labile P in soils are highly correlated, the isotopic exchange and resin extraction procedures measure approximately the same labile P pool while the P estimated from adsorption/desorption isotherms measure on the order of one-half of this quantity.

Until experiments are performed on these soils evaluating the relationships between the three measures of labile P and the biological availability of P, it is impossible to select the "best" measurement of labile P. Currently, all three methods are being used by researchers to evaluate the P status of soils. For this reason, the relationships developed involving labile P in the remainder of this paper will include all three measurements discussed here.

Relationships Between Labile P Measurements and EPC

Introduction

For a soil at a specified labile P or solution P value, the relationship between labile P and EPC is described by the equation

$$Labile\ P = M(EPC) \tag{8}$$

where M is the soil's phosphate buffer capacity. For most soils, the phosphate buffer capacity decreases as the quantity of P in the soil increases (Amer et al. 1955). Consequently, the relationship between labile P and soil solution P is curvilinear over a wide range of solution P concentrations.

The primary soil properties affecting the phosphate buffer capacity are 1) the clay content and mineralogy, 2) the presence of Fe and Al oxides, 3) the amount of exchangeable aluminum, and 4) the organic matter content (Baldovinos and Thomas 1967, Olsen and Watanabe 1963, Sanchez and Uehara 1980). While the presence of each of these components may be determined by direct measurement, an estimate of the relative amounts present in soils may be made on the basis of other information that is more readily available. For example, soil grouped according to their 1) textural class, 2) taxonomic classification, and/or 3) geographic location might be expected to have similar properts and P buffering capacities.

While soil texture, soil order and geographic location are not entirely independent of one another, when the soils used in this study were separated into the above three groups, the most successful relationships between labile P measurements and EPC were found on soils grouped according to geographic location. For the purposes of this study, separation of soils into regional groups also provides the most readily usable information since the soil test for P used by soil testing laboratories will be dependent upon geographic location.

In this section, the relationships between each measurement of labile P and EPC on soils from different geographic regions will be discussed. When appropriate, the effect of soil texture and/or soil order on these relationships will be included in the discussion.

Separation of Soils into Geographic Regions

The soils used in this study were separated into three geographic regions--North Central, Southeastern and Northeastern--on the basis of the climatic and geolcgic factors which have influenced their development. The distributions of the soil orders and texture groups within these geographic regions are shown in Table 5.

States from which soils were collected in the North Central region were Iowa, Illinois, Indiana, Missouri, Nebraska, and the southern parts of Minnesota and Wisconsin. Most of the soils from this region developed under grassland vegetation in an area characteristically having a seasonal moisture deficit. The predominant parent material of the soils from this region is lcess. As a consequence of these factors, soils have developed which have a relatively high

Table 5
Distribution of orders and textures of soils collected from the North Central, Southeast and Northeast regions of the United States[1]

Geographic region	Soil texture[2]	Ultisols[3]	Alfisols	Mollisols
North Central	Fine	--	--	4 (12)
	Medium	--	3 (11)	5 (15)
	Coarse	--	--	--
Southeast	Fine	2 (7)	--	--
	Medium	3 (12)	--	--
	Coarse	5 (18)	--	--
Northeast (PA and OH)	Fine	--	--	--
	Medium	--	2 (12)	--
	Coarse	--	--	--

[1]First number refers to total number of soil series and number in parentheses refers to total number of soil samples.

[2]Fine, medium, and coarse textured soils refer to moderately fine, medium and moderately coarse plus coarse textured soils respectively.

[3]Davidson soil not included.

base status and organic matter content and have clay mineralogy dominated by 2:1 layer silicates. Eight of the soils collected for this study from this region were Mollisols, with half of these classified as medium and the other half as moderately fine textured (Table 5). The other three soils from this region were medium textured Alfisols (Table 5) with two of these classified in the Mollic subgroup.

Agricultural soils from the Southeastern United States developed primarily under forest vegetation in one of two regions--the Coastal Plain or the Piedmont Plateau. The Coastal Plain extends from Texas to New England. As a result, New Jersey and Maryland, generally considered Northeastern States, have for the purpose of this study been included in the Southeastern region. Other states in this region from which soils were collected were Virginia, North Carolina, South Carolina, Georgia, Alabama, and Florida.

In general, soils from these states have undergone extensive weathering. As a consequence, they are characteristically low in exchangeable bases and organic matter and are relatively high in exchangeable Al and in Fe and aluminum oxides. All of the soils collected from this region were Ultisols, with all but one of these being medium or moderately coarse textured (Table 5).

The last group of soils were Alfisols from Pennsylvania and Ohio. While Ohio is commonly grouped with the North Central States, many of the soils in this region developed from glaciated parent material and under forest vegetation. As a result, Alfisols from this region are similar to Pennsylvania Alfisols which developed under the same climatic and vegetative conditions and are distinctly different from the Mollisols and associated Alfisols of the North Central United States which developed from loess deposits and under prairie vegetation.

Results and Discussion

The relationships between all labile P measurements and EPC on soils from the North Central U.S. were curvilinear and not significantly affected by either the soil order or texture. The relationships were most successfully described by performing log transformations on both the X (EPC) and Y (labile ^{32}P, resin P and intercept P) variables. The equations describing the relationships between the logs of labile ^{32}P, intercept P and resin P and the log of EPC are given in the top part of Table 6. As seen in the Table, there are strong relationships

Table 6
Relationships between measurements of labile P (y, ug/g) and EPC (x, ug/L) on
North Central United States soils

Labile measurement	Range EPA (ug/L)	Range Labile P (ug/g)	N_{To}[1]	N_{Se}[2]	Equation[3]	r^2
Full Range						
Labile [32]P	5-3250	9-85	38	12	$\log y = .688_* + .343 \log x$	0.86
Resin P	5-3250	6-75	38	12	$\log y = .450_* + .401 \log x$	0.89
Intercept P	5-3250	1-40	38	12	$\log y = -.02_{ns} + .488 \log x$	0.85
Low Range						
Labile [32]P	5-400	9-45	30	11	$y = 14.17_* + .085 x$	0.58
Resin P	5-400	6-37	30	11	$y = 9.26_* + .079 x$	0.67
Intercept P	5-400	1-19	30	11	$y = 3.44_* + .043 x$	0.73
High Range						
Labile [32]P	>499-3250	>45-85	8	6	$y = 35.75_* + .015 x$	0.89
Resin P	>400-3250	>37-75	8	6	$y = 31.17_* + .013 x$	0.87
Intercept P	>400-3250	>19-400	8	6	$y = 10.28_* + .007 x$	0.65

[1]Total number of samples included in the analyses.

[2]Number of soil series represented in the analyses.

[3]ns and * indicate, respectively, that intercept is not significantly different
and is significantly different than zero at the 5% level of probability.

($r^2 \geq 0.85$) between the logs of all measures of labile P and the log of EPC.
It should be noted that the intercepts of the equations describing the
relationships between the logs of labile ^{32}P and resin P and the log of EPC are
significantly different than zero, although theoretically both variables should
go to zero together. The non-zero intercept may be explained at least in part
by the experimental difficulties involved in measuring labile P in soils low in
P. This is most particularly true for isotopically exchangeable labile P.
Another difficulty is the lack of data points in the extremely low P range.
When the slope of the curve is constantly changing, as in the labile P/EPC
relationship, it is critical that data points approaching zero be present in
order to accurately describe the relationship in this region.

While the log-log transformations shown in Table 6 provide good relationships
between labile P measurements and the EPC values over the entire range of data,
for many purposes it is more convenient to have the data described directly by
linear equations. One way to do this is to divide the curve into parts which
approximate linearity.

The relationships between labile ^{32}P and EPC are approximately linear in the
ranges above and below the 400 ug/L EPC level. This level also represents a
convenient point of separation from an agronomic standpoint. In general,
solution P concentrations less than or equal to 400 ug/L are the maximum
required to produce optimum yields of crops on soils having the same textures as
these (Kamprath and Watson 1980, Sanchez and Uehara 1980).

The equations describing the relationships between the measurements of labile P
and EPC on the low (less than 400 ug/L EPC) and high (greater than 400 ug/L EPC)
ranges of the curve are shown in Table 6. On soils in the low EPC range, the
resin P and intercept P relationships with EPC were the strongest (r^2 values of

0.67 and 0.73, respectively) while on soils in the high EPC range, the strongest relationships with EPC were found with the labile ^{32}P and resin P measurements. Again, the intercepts of the low range soils were significantly different than zero. In addition to the reasons cited above, the use of linear equations to describe data which may be slightly curvilinear will contribute to this effect.

On the Southeastern soils good relationships were found between all labile P measurements and EPC with the exception of two outlier soils. One of the outliers was a Benndale fine sandy loam to which high rates of fertilizer P had been applied. The other was a Dickson silt loam which had received large quantities of manure. It is likely that the increased organic matter content of this soil effectively altered the phosphate buffer capacity allowing the soil to maintain a higher solution P level for a given quantity of labile P. Neither of these soils was included in the regression analyses performed between the labile P measurements and EPC on this group of soils.

Unlike the North Central soils where differences in texture were unimportant in influencing the labile P/EPC relationships, texture had a significant effect on the relationship between labile ^{32}P and EPC on the Southeastern soils. A similar textural effect was observed on the relationship between resin P and EPC on this group of soils but was less apparent on the relationship between intercept P and EPC. The equations describing the relationships between all measurements of labile P and EPC on the Southeastern soils are shown in Table 7. Results of a general linear F test performed on the data showed that both the slopes and intercepts of the equations describing the labile P^{32} and resin P relationships with EPC were significantly affected by texture. In contrast, only the intercepts of the equations describing the relationships between intercept P and EPC on the two textural groups were found to be significantly different.

The slopes (or buffer capacities) of the equations describing the labile P/EPC relationships on the medium textured Southeastern soils were greater than those describing these relationship on both the Southeastern coarse textured soils and on the low P range of soils from the North Central states (see Tables 6 and 7). These results are as would be expected based on an understanding of the factors

Table 7
Relationships between labile P measurements (y, ug/g) and EPC (x, ug/l) on Southeastern United States soils[1]

Labile P Measurement	Texture[2]	Range EPC (ug/L)	Range Labile P (ug/g)	N_{To}[3]	N_{Se}[4]	Equation[5]	r^2
Labile ^{32}P	Medium	3–460	5–100	18	5	y = 18.21* + 0.182 x	0.74
	Coarse	4–560	4–80	17	5	y = 8.44* + 0.125 x	0.88
Resin P	Medium	3–460	3–90	18	5	y = 5.64* + 0.175 x	0.92
	Coarse	4–560	3–70	17	5	y = 4.8* + 0.117 x	0.95
Intercept P	Medium	3–460	1–30	18	5	y = 5.67* + 0.053 x	0.52
	Coarse	4–560	1–35	17	5	y = 1.42$_{ns}$ + 0.059 x	0.91

[1]Benndale soil receiving high rate of fertilizer P, Dickson soil receiving manure treatment and Davidson soil not included in the analyses.

[2]Medium refers to medium and moderately-fine textured soils. Coarse refers to coarse and moderately-coarse textured soils.

[3]Total number of soil samples included in the analysis.

[4]Total number of soil series represented in the analyses.

[5]* and ns indicate, respectively, that intercepts are and are not significantly different than zero at the 5% level of probability.

responsible for influencing the phosphate buffer capacity of soils having these textures and which have developed in different regions of the United States.

The last group of soils examined in this study was from the Northeast (Pennsylvania and Ohio). Only two soil series were represented in this group and both were classified as medium textured Alfisols (see Table 5). The linear relationships between EPC and each of the labile P measurements on these soils are described in Table 8. In general, the relationships were good ($r^2 > 0.77$). The slightly steeper slopes (or buffer capacities) observed on these soils in comparison to the medium textured Ultisols of the Southeast is likely due to the differences in the labile P and EPC ranges covered by the two groups of soils. While the range of labile P and EPC values represented by the Pennsylvania and Ohio soils used in this study were low (Table 8), data from studies performed by others on soils similar to these may be used to extend these ranges and develop equations which describe the labile P/EPC relationship. Table 8a shows the resin P, EPC and intercept P values determined on a Hagerstown soil from Maryland which had been collected from conventional tillage and no-till plots. When these data points were included with those from this study, the relationships between the labile P measurements and EPC were distinctly curvilinear and most successfully described by the log-log equations shown in Table 8b. As seen in the table, there were strong relationships ($r^2 > 0.92$) between the logs of both measurements of labile P and the log of EPC.

Because of the curvilinear nature of the data, the equations given in Table 8b are more appropriate than those in Table 8 for describing the intercept P or resin P relationship with EPC when the data extend beyond the ranges of labile P and EPC values given in Table 8.

Summary and Conclusions

The results from this part of the study indicate that good to excellent relationships can be developed between all labile P measurements examined (labile ^{32}P, resin P and intercept P) and EPC when soils are separated into groups on the basis of geographic location and further by texture for soils of the Southeast.

For the Southeastern and North Central soils, the relationships are adequately described over the labile P and EPC ranges considered to be of greatest agricultural importance. Only a small group of soils from Pennsylvania and Ohio was represented and data from a limited range of labile P and EPC values was available. However, the inclusion of data collected by others was used to develop the relationships of resin P and intercept P with EPC over a wider range of values.

Table 8
Relationships between measurements of labile P (y, ug/g) and EPC (x, ug/L) on soils from Pennsylvania and Ohio

| Labile P measurement | Range | | N_{To}[1] | N_{Se}[2] | Equation[3] | r^2 |
	EPC (ug/L)	Labile P (ug/g)				
Labile [32]P	1–100	10–40	12	2	y = 6.47* + .202 x	0.81
Resin P	1–100	6–30	12	2	y = 9.65* + .163 x	0.77
Intercept P	1–100	1–15	12	2	y = 3.04* + .092 x	0.79

[1]Total number of samples included in the analysis.

[2]Number of soil series represented in the analysis.

[3]* indicates that intercept is significantly different than zero at the 5% level of probability.

65

Table 8a
Resin P, Intercept P, and EPC values for Hagerstown soils collected from
conventional till and no-till plots in Maryland[1]

Tillage treatment	Resin P (ug/g)	Intercept P (ug/g)	EPC (ug/L)
Conventional	11.3	13.0	50.0
	39.3	20.6	287.
No-till	62.3	42.4	1330.
	67.7	50.6	1520.

[1]Data provided by H. M. Kunishi, Agricultural Research Service, United States
Department of Agriculture, Beltsville, Maryland.

Table 8b
Equations describing the relationships of Resin P and Intercept P (y, ug/g) to
EPC (x, ug/L) on soils from Pennsylvania, Ohio and Maryland[1]

| Labile P measurement | Range | | N_{To}[2] | N_{Se}[3] | Equation[4] | r^2 |
	EPC (ug/L)	Labile P (ug/g)				
Resin P	1-1520	6-67	16	2	$\log y = 0.687_* + .348 \log x$	0.92
Intercept P	1-1520	1-50	16	2	$\log y = 0.032_{ns} + .526 \log x$	0.91

[1]The soils from Pennsylvania and Ohio are those collected as part of this study.
The soils from Maryland are those described in Table 8a.

[2]Total number of soil samples included in the analysis.

[3]Number of soil series represented in the analysis.

[4]* and ns indicate, respectively, that intercepts are and are not significantly
different than zero at the 5% level of probability.

SOIL TEST P RELATIONSHIPS WITH LABILE P AND EPC

Comparison of Olsen, Bray and Mehlich Soil Tests
Performed in Different States

Introduction

While standard procedures exist for measuring P by the Olsen, Bray I and Mehlich
I soil tests (Bray and Kurtz 1945, Olsen et al. 1954, Sabbe and Breland 1974),
the use of slightly different techniques by different laboratories may result in
variable measures of P even when the same procedure is performed. The objective
of this part of the study was to evaluate the agreement among different
laboratories performing the Olsen, Bray I and Mehlich I soil tests for P on
soils having a wide range of properties.

Results and Discussion

The results of the regression analysis describing the relationships among the Olsen, Bray I and Mehlich I soil test values as determined by different state laboratories are shown in Table 9. The differences in P values among states performing the Bray I or Mehlich I soil tests were, for the most part, small and the coefficients of determination (r^2 values) describing the relationships among these values were high. In general, the regression equations had intercepts close to zero and slopes approaching one.

Larger differences existed among the Olsen P values determined by the various states although all were highly correlated, having r^2 values greater than or equal to 0.90. The slopes from the equations relating the Olsen values from Kansas to those from Nebraska and North Dakota are much smaller than one indicating that on the whole the Olsen soil test procedure in Kansas yields a proportionately greater amount of P from the soil than the same soil test performed in the other two states. On the other hand, the equation describing the relationship between Olsen soil test values from Nebraska and those from North Dakota had a slope close to one indicating that the tests performed in these two states extract a similar amount of P from the soil.

Summary and Conclusions

In general, the agreement among laboratories performing the Olsen, Bray I and Mehlich I soil tests was very good. Differences among the laboratories were small and, when present, involved differences in calibration rather than correlation. For the ease of discussion, only one set of values for each of the soil tests will be included in the remaining discussion concerning the relationships between the Olsen, Bray I and Mehlich I soil tests and other measures of soil P. The soil test values from Nebraska, Kansas and Virginia for the Olsen, Bray I and Mehlich I soil tests, respectively, will be used to describe these relationship in the sections that follow.

Relationships Between Labile P Measurements and Soil Tests for P

Introduction

As discussed in the introduction to this paper, one of the primary objectives of this study was to evaluate the relationships between labile P and several routine soil tests for P. The most commonly performed soil tests in the North Central, Northeast, and Southeast regions of the United States are Olsen's $NaHCO_3$, Bray I, and Mehlich I. A discussion of the relationships between each of the soil tests and each measurement of labile P will be presented here.

Table 9
Relationships between P soil test values (lb/acre) determined by different states[1]

Soil test	Equation	r^2
Olsen	Olsen (NE) = 5.25 + 1.09 Olsen (ND)	0.94
	Olsen (NE) = 5.94 + 0.71 Olsen (KN)	0.90
	Olsen (ND) = 1.00 + 0.65 Olsen (KN)	0.92
Bray	Bray (MN) = -2.11 + 0.97 Bray (KN)	0.95
	Bray (MN) = 2.28 + 0.89 Bray (NE)	0.97
	Bray (KN) = 7.44 + 0.88 Bray (NE)	0.94
Mehlich	Mehlich (AL) = 1.65 + 1.05 Mehlich (VA)	0.97

[1]State from which the determination was made is in parentheses following the name of the soil test in the equation.

Results and Discussion

The equations describing the relationships between each measurement of labile P and soil test P for all soils are shown in Table 10. The Olsen and Mehlich I soil tests for P were highly correlated with all labile P measurements (r^2 values $\geq$ 0.73) while the correlations between measurements of labile P and Bray I P were much lower ($r^2 \leq$ 0.62). When soils were separated into groups on the basis of geographic location, most of the soil test P/labile P relationships improved substantially. Tables 11, 12 and 13 show the relationships between soil test P and labile P on soils from the North Central and Southeastern regions of the United States and on soils from Ohio and Pennsylvania.

Bray I is the most commonly used soil test for P in the North Central region. As shown in Table 11, this test was also the best predictor of all labile P measurements made on soils from these states. The other soil tests, however, were highly correlated with the labile P measurements as well.

The equations describing the relationships between each labile P measurement and soil test P on the Southeastern soils are shown on Table 12. Soil texture had a significant effect on all of the relationships with the exception of the relationship between resin P and Bray P. In all instances but two, the intercepts were significantly affected by texture; in only a few instances the textural effect on the slopes of the equations was significant. In general, a smaller fraction of the labile P pool was extracted from soils of medium texture in comparison to the coarse-textured soils. While all soil tests for P were highly correlated with each labile P measurement on the moderately coarse textured soils, the Mehlich I and Olsen soil tests were the best predictors of the labile P measurements on the medium textured soils.

Table 13 shows the equations describing the relationships between measurements of labile P and soil test P on the soils from Ohio and Pennsylvania. Again, Bray I is the test most commonly used in these states and, in general, was the one most highly correlated with the three measurements of labile P.

Summary and Conclusions

The results from this study demonstrate that labile P measurements may be successfully predicted by the commonly used soil tests for P. In general, when soils were separated into groups on the basis of geographic location and, for

Table 10
Equations describing the relationships between measurements of labile P (y, ug/g) and soil test P (x, ug/g) on all soils[1]

Labile P measurement (ug/g)	Soil test P (ug/g)	Equation[2]	r^2
Labile ^{32}P	Olsen	$y = 5.91_* + 1.61\ x$	0.77
	Bray I	$y = 14.35_* + 0.39\ x$	0.57
	Mehlich I	$y = 5.77_* + 1.02\ x$	0.81
Resin P	Olsen	$y = 0.069_{ns} + 1.49\ x$	0.88
	Bray I	$y = 8.34_* + 0.349\ x$	0.60
	Mehlich I	$y = -0.048_{ns} + 0.937$	0.91
Intercept P	Olsen	$y = 0.80_{ns} + 0.615\ x$	0.73
	Bray I	$y = 3.59_* + 0.160\ x$	0.62
	Mehlich I	$y = 0.677_{ns} + 0.389\ x$	0.77

[1]Davidson soil not included in the analyses.

[2]* and ns indicate, respectively, that intercepts are and are not significantly different from zero at the 5% level of probability.

Table 11
Equations describing the relationships between measurements of labile P (y, ug/g) and soil test P (x, ug/g) on North Central soils.

Labile P measurement (ug/g)	Soil test P (ug/g)	Equation[1]	r^2
Labile ^{32}P	Olsen	$y = 5.14_* + 1.81 \, x$	0.88
	Bray I	$y = 7.89_* + 0.80 \, x$	0.93
	Mehlich I	$y = 6.69_* + 0.98 \, x$	0.82
Resin P	Olsen	$y = 0.635_{ns} + 1.70 \, x$	0.94
	Bray I	$y = 3.64_* + 0.744 \, x$	0.96
	Mehlich I	$y = 1.48_{ns} + 0.953 \, x$	0.92
Intercept P	Olsen	$y = 0.741_{ns} + 0.715 \, x$	0.81
	Bray I	$y = 1.87_* + 0.317 \, x$	0.85
	Mehlich I	$y = 1.62_{ns} + 0.378 \, x$	0.71

[1]* and ns indicate, respectively, that intercepts are and are not significantly different than zero at the 5% level of probability.

Table 12
Equations describing the relationships between measurements of labile P (y, ug/g) and soil test P (x, ug/g) on Southeastern soils[1]

Labile P measurement (y, ug/g)	Soil test P (x, ug/g)	Texture[2]	Equation[3]	r^2
Labile ^{32}P	Olsen	Medium	$y = 8.18_* + 1.85 \, x$	0.89
		Coarse	$y = 0.8_{ns} + 1.18 \, x$	0.82
	Bray I	Medium	$y = 15.15_* + 0.43 \, x$	0.68
		Coarse	$y = 1.94_{ns} + 0.33 \, x$	0.91
	Mehlich I	Medium	$y = 8.29_* + 1.14 \, x$	0.88
		Coarse	$y = 1.17_{ns} + 0.86 \, x$	0.92
Resin P	Olsen	Medium	$y = -1.76_{ns} + 1.59 \, x$	0.94
		Coarse	$y = -3.16_* + 1.22 \, x$	0.97
	Bray I	Medium	$y = 4.05_{ns} + 0.37 \, x$	0.72
		Coarse	$y = -0.49_{ns} + 0.31 \, x$	0.90
	Mehlich I	Medium	$y = -1.88_{ns} + 0.99 \, x$	0.94
		Coarse	$y = -1.20_{ns} + 0.80 \, x$	0.90
Intercept P	Olsen	Medium	$y = 2.52_{ns} + 0.57 \, x$	0.70
		Coarse	$y = -2.27_* + 0.59 \, x$	0.88
	Bray I	Medium	$y = 3.45_* + 0.15 \, x$	0.74
		Coarse	$y = -1.78_* + 0.16 \, x$	0.98
	Mehlich I	Medium	$y = 2.23_{ns} + 0.36 \, x$	0.75
		Coarse	$y = -2.12_* + 0.42 \, x$	0.98

[1]Davidson soil not included in the analyses.

[2]Medium refers to medium and moderately-fine textured soils. Coarse refers to coarse and moderately coarse textured soils.

[3]* and ns indicate, respectively, that intercepts are and are not significantly different than zero at the 5% level of probability.

Table 13

Equations describing the relationships between measurements of labile P (y, ug/g) and soil test P (x, ug/g) on soils from Ohio and Pennsylvania.

Labile P measurement (ug/g)	Soil test P (ug/g)	Equation[1]	r^2
Labile ^{32}P	Olsen	$y = 6.17_{ns} + 1.75 x$	0.78
	Bray I	$y = 11.86_* + 0.61 x$	0.82
	Mehlich I	$y = 1.05_{ns} + 1.43 x$	0.78
Resin P	Olsen	$y = 1.14_{ns} + 1.43 x$	0.76
	Bray I	$y = 5.83_* + 0.500 x$	0.80
	Mehlich I	$y = -4.34_{ns} + 1.24 x$	0.86
Intercept P	Olsen	$y = -0.824_{ns} + 0.722 x$	0.62
	Bray I	$y = 1.36_{ns} + 0.259 x$	0.70
	Mehlich I	$y = -2.40_{ns} + 0.555 x$	0.56

[1]* and ns indicate, respectively, that intercepts are and are not significantly different than zero at the 5% level of probability.

the Southeastern soils, texture, the most successful relationship developed were between the labile P measurements and the soil test for P most commonly used in the given region. Bray I was the best predictor of labile P on the North Central soils and on soils from Pennsylvania and Ohio. On the Southeastern soils, both the Mehlich I and Olsen soil tests for P were good predictors of labile P when soils from this region were separated into textural groups.

Relationships Between EPC and Soil Test P

Introduction

Commonly the relationships between measurements of labile P and the equilibrium phosphorus concentration are expressed in the form of Equation 9:

$$\text{Labile P} = a + m(\text{EPC}) \tag{9}$$

where a is the intercept and m represents the soil's phosphate buffer capacity. The equation in this form is useful in that it allows comparisons of the buffer capacities among many different soils or groups of soils to be made. The objective of this part of the study, however, was to develop relationships whereby estimates of the equilibrium solution P concentration could be made using readily obtainable soil test data. Consequently, the relationships developed here are presented in the form:

$$\text{EPC} = a + b(\text{soil test P}) \tag{10}$$

where a and b represent the intercept and slope of the equation, respectively, and soil test P refers to the P extracted by the Olsen, Bray I or Mehlich I soil tests. For comparative purposes, the relationships between EPC and the three measurements of labile P are also presented here in this form.

Results and Discussion

The equations describing the relationships between EPC and the labile P and soil test P measurements on all soils collected from the North Central regions are shown in Table 14. The relationships between these variables were curvilinear and, as discussed in a previous section are most successfully described by log transformations of both the x and y variables. As shown in Table 14, the correlations between the log of EPC and the logs of P extracted by the three soil tests were good ($r^2 \geq 0.81$), although slightly lower than those between the log EPC and the logs of the labile P measurements ($r^2 \geq 0.86$).

Table 14

Equations describing the relationships of EPC (y, ug/L) to measurements of labile P (x, ug/g) and soil test P (x, ug/g) over full range of North Central soils.

Labile P or soil test P measurement	Range EPC (ug/L)	Labile P or Soil Test P (ug/g)	N_{To}[1]	N_{Se}[2]	Equation[3]	r^2
Labile P Measurement						
Labile ^{32}P	5-3250	9-85	38	12	Log y = -1.41* + 2.50 log x	0.86
Resin P	5-3250	6-75	38	12	Log y = -0.75* + 2.21 log x	0.89
Intercept P	5-3250	1-40	38	12	Log y = 0.36* + 1.90 log x	0.86
Soil Test P						
Olsen	5-3250	4-40	38	12	Log y = -0.148ns + 2.15 log x	0.82
Bray I	5-3250	7-90	38	12	Log y = -0.46* + 1.94 log x	0.85
Mehlich I	5-3250	7-70	38	12	Log y = -0.550* + 2.07 log x	0.81

[1] Total number of soil samples included in the analyses.

[2] Total number of soil series represented in the analyses.

[3] * and ns indicate, respectively, that intercepts are and are not significantly different than zero at the 5% level of probability.

As discussed previously, linear and perhaps more useful relationships between these variables may be obtained when the soils are separated into groups representative of the high and low ranges of P. The equations describing these relationships are shown in Table 15. Of all soil tests, the Bray I extractant was the most successful predictor of EPC on soils from both the low and high P ranges (r^2 values of 0.72 and 0.81, respectively), although the Olsen and Mehlich I soil tests were good predictors on the low and high P soils, respectively. While the Olsen soil test is occasionally performed in this region, Bray I is the soil test most commonly used.

The equations describing the relationships of EPC with labile P and soil test P on the Southeastern soils are given in Table 16. Texture was found to have a significant effect on the relationships between labile P measurements and EPC but not on the relationships between soil test P and EPC. This difference may be explained by the influence that soil texture has on the amount of the labile P pool extracted by the soil tests as discussed in the previous section. Of the three soil tests, the highest correlations were found between EPC and the P removed by the Olsen and Mehlich I extracts (r^2 values of 0.92 and 0.85, respectively). Mehlich I is the soil test most commonly used within this region.

The relationships of EPC with labile P and soil test P on the Ohio and Pennsylvania soils are shown in Table 17. While all relationships were good ($r^2 \geq 0.68$), the best predictor of EPC on these soils was the P extracted by the Bray I soil test. This test is also the one used by the State universities in Pennsylvania and Ohio to test soils for P.

Summary and Conclusions

The results from this study indicate that EPC can be successfully predicted from readily obtainable soil test P measurements when soils are separated into groups according to geographic location. On soils from the North Central region and from Pennsylvania and Ohio, Bray soil test P was the best predictor of EPC; but, for soils from the Southeast region, EPC was most successfully predicted by the Olsen and Mehlich I soil tests.

Table 15

Equations describing the relationships of EPC (y, ug/L) to measurements of labile P (x, ug/g) and soil test P (x, ug/g) on low and high P ranges of North Central soils

Labile P or soil test P measurement	EPC (ug/L)	Labile P or Soil Test P (ug/g)	N_{To}[1]	N_{Se}[2]	Equation[3]	r^2
Labile P Measurement						
Labile ^{32}P	5–400	9–45	30	11	$y = -51.33_@ + 6.86\ x$	0.58
Resin P	5–400	6–37	30	11	$y = -42.63_@ + 8.47\ x$	0.67
Intercept P	5–400	1–19	30	11	$y = -29.8_@ + 16.93\ x$	0.73
Labile ^{32}P	>400–3250	>45–85	8	6	$y = -19.43_* + 59.03\ x$	0.89
Resin P	>400–3250	>37–75	8	6	$y = -1900_* + 67.42\ x$	0.87
Intercept P	>400–3250	>19–40	8	6	$y = -382.0_{ns} + 91.69\ x$	0.65
Soil Test P						
Olsen	5–400	4–23	30	11	$y = -38.40_* + 14.30\ x$	0.72
Bray I	5–400	7–42	30	11	$y = -30.41_@ + 7.16\ x$	0.72
Mehlich I	5–400	7–34	30	11	$y = -9.18_{ns} + 6.70\ x$	0.49
Olsen	>400–3250	>23–40	8	6	$y = -1187_{ns} + 94.27\ x$	0.49
Bray I	>400–3250	>42–90	8	6	$y = -1197_@ + 43.79\ x$	0.81
Mehlich I	>400–3250	>34–70	8	6	$y = -1478_{ns} + 49.85\ x$	0.70

[1]Total number of soil samples included in the analysis.

[2]Total number of soil series represented in the analysis.

[3]* and @ indicate, respectively, that intercepts are significantly different at the 5 and 10% levels of probability. ns indicates intercepts are not significantly different at the 1% level of probability.

Table 16

Equations describing the relationships of EPC (y, ug/L) to measurements of labile P (X, ug/g) and soil test P (x, ug/g) on Southeastern soils[1]

Labile P or soil test P measurement	Texture	Range EPC (ug/L)	Range Soil P (ug/g)	N_{To}[3]	N_{Se}[4]	Equation[5]	r^2
Labile P							
Labile ^{32}P	Medium	3-460	5-100	18	5	$y = -51.04_{@} + 4.04\ x$	0.74
	Coarse	4-560	4-80	17	5	$y = -49.97_{*} + 7.07\ x$	0.88
Resin P	Medium	3-460	3-90	18	5	$y = -22.42_{@} + 5.23\ x$	0.92
	Coarse	4-560	3-70	17	5	$y = -34.79_{*} + 8.08\ x$	0.95
Intercept P	Medium	3-460	1-30	18	5	$y = -14.60_{ns} + 9.77\ x$	0.52
	Coarse	4-560	1-35	17	5	$y = -14.45_{ns} + 15.44\ x$	0.91
Soil Test P							
Olsen	--	3-560	3-60	35	10	$y = -51.79_{*} + 9.81\ x$	0.92
Bray I	--	3-560	4-205	35	10	$y = -15.45_{ns} + 2.07\ x$	0.70
Mehlich I	--	3-560	5-80	35	10	$y = -39.77_{*} + 5.64\ x$	0.85

[1]Benndale soil receiving high rate of fertilizer P, Dickson soil receiving manure treatment and Davidson soil not included in the analyses.

[2]Medium refers to medium and moderately-fine textured soils. Coarse refers to coarse and moderately-coarse textured soils.

[3]Total number of samples included in the analysis.

[4]Total number of soil series represented in the analysis.

[5]* and @ indicate that intercepts are significantly different than zero at the 5 and 10% levels of probability, respectively. ns indicates that intercept is not significantly different than zero at the 1% level of probability.

73

Table 17

Relationships betwen EPC (y, ug/L) and measurements of labile P (x, ug/g) and soil test P (x, ug/g) on soils from Pennsylvania and Ohio.

	Range					
	EPC (ug/L)	Labile P (ug/g)	N_{To}[1]	N_{Se}[2]	Equation[3]	r^2
Labile P Measurement						
Labile ^{32}P	1-100	10-40	12	2	$y = -58.42_* + 4.03\ x$	0.81
Resin P	1-100	6-30	12	2	$y = -36.01_* + 4.75\ x$	0.77
Intercept P	1-100	1-15	12	2	$y = -17.23_{ns} + 8.63\ x$	0.79
Soil Test P						
Olsen	1-100	3-17	12	2	$y = -36.71_{ns} + 7.37\ x$	0.68
Bray I	1-100	6-40	12	2	$y = -20.48_* + 2.93\ x$	0.94
Mehlich I	1-100	10-25	12	2	$y = -63.39_* + 6.30\ x$	0.76

[1]Total number of soil samples included in the analysis.

[2]Total number of soil series represented in the analysis.

[3]* and ns indicate, respectively, that intercepts are and are not significantly different than zero at the 5% level of probability.

SUMMARY AND CONCLUSIONS

The most biologically available forms of P in soils are the labile P fraction and the P in the soil solution. While laboratory measurements of both labile P and solution P are time consuming and expensive, State and commercial soil testing laboratories routinely perform low-cost soil tests for P for making fertilizer recommendations. The relationships developed in this study allow the labile P and solution P estimates to be made from readily available soil test data.

The relationships among three soil tests for P (Olsen's $NaHCO_3$, Bray I, and Mehlich I), three measurements of labile P (labile ^{32}P, resin P and intercept P) and EPC were examined for a diverse group of noncalcareous agricultural soils. All measurements of labile P were highly correlated with one another ($r^2 \geq$ 0.83). When soils were grouped according to geographic location, good relationships were found betwen each labile P measurement and each soil test for P and between EPC and both labile P and soil test P measurements. Bray I was the best predictor of labile P on the North Central and Northeastern soils ($r^2 \geq 0.82$) while the Olsen and Mehlich I soil tests most successfully predicted labile P on soils from the Southeast ($r^2 \geq 0.85$).

From both a soil fertility and environmental perspective there is a growing concern over the loss of P from agricultural land. In conjunction with agriculture management models, the relationships developed in this study provide a tool for evaluating the effects of different soil and water management systems on the loss of the most biologically available P fractions from land.

ACKNOWLEDGMENTS

in South Carolina, Larry Parks in Tennessee, George Jones in Virginia, and Emmett Schulte in Wisconsin.

The soil tests were performed under the supervision of John Grava at the University of Minnesota, Dave Whitney at Kansas State University, William Dahnke at North Dakota State University, Delno Knudsen at the University of Nebraska, C. E. Evans at Auburn University, and Steve Donohue at Virginia Polytechnic Institute and State University.

REFERENCES

Amer, F. 1962. Determination of phosphorus-32 exchangeable phosphorus in soils (pp. 43-58). In Radioisotopes in soil-plant nutrition studies. International Atomic Energy Agency, Vienna.

Amer, F., D. R. Bouldin, C. A. Black, and F. R. Duke. 1955. Characterization of soil phosphorus by anion exchange resin adsorption and P^{32} equilibration. Plant and Soil (VI)4:391-408.

Amer, F., S. Mahdi, and A. Alradi. 1969. Limitations in isotopic measurements of labile phosphate in soils. J. Soil Sci. 20:91-100.

Baldovinos, F., and G. W. Thomas. 1967. The effect of clay content on phosphorus uptake. Soil Sci. Soc. Am. Proc. 31:680-682.

Brady, N. C. 1974. The Nature and Properties of Soils. 8th edition. MacMillan Publishing Co., Inc., New York.

Buol, S. W. (ed.). 1973. Soils of the Southern States and Puerto Rico. Southern Cooperative Series Bulletin No. 174. A joint regional publication by the agricultural experiment stations of the southern states and Puerto Rico land-grant universities with cooperative assistance by the Soil Conservation Service of the U.S.D.A.

Bray, R. H., and L. T. Kurtz. 1945. Determination of total, organic and available forms of phosphorus in soils. Soil Sci. 59:39-45.

Kamprath, E. J., and M. E. Watson. 1980. Conventional soil and tissue tests for assessing the phosphorus status of soils. pp. 433-470. In F. E. Khasawneh, E. C. Sample, and E. J. Kamprath (eds.), The Role of Phosphorus in Agriculture. Am. Soc. of Agron., Madison, Wis.

Krusekopf, H. H. 1960. Major soil groups of the North Central Region. In Soils of the North Central Region of the United States. North Central Regional Publication No. 76. Agric. Exp. Sta., Univ. of Wisconsin, Madison, Wis. Bul. No. 544. June, 1960.

Kunishi, H. M., and A. W. Taylor. 1977. Predicting pollution potential of phosphorus at heavy application rates. Proc. of the international seminar on soil environment and fertility management in intensive agriculture. Tokyo, Japan.

Larsen, S. 1967. Soil phosphorus. Adv. Agron. 19:191-210.

McAuliffe, C. D., N. S. Hall, L. A. Dean, and S. B. Hendricks. 1947. Exchange reactions between phosphates and soils: hydroxylic surfaces of soil minerals. Soil Sci. Soc. Proc. 12:119-122.

Miller, F. T., and L. A. Quandt. 1984. Soil Classification System. p. 15-22. In R. L. Cunningham and E. J. Ciolkosz (eds.). Soils of the Northeastern United States. Northeastern Regional Res. Pub. Bull. 848. The Pennsylvania Agri. Exp. Stn., University Park, Pa.

Olsen, S. R., and F. E. Khasawneh. 1980. Use and limitations of physical-chemical criteria for assessing the status of phosphorus in soils. In F. E. Khasawneh, E. C. Sample, E. J. Kamprath (eds.), The Role of Phosphorus in Agriculture. Am. Soc. of Agron. pp. 361-410.

Olsen, S. R., and L. E. Sommers. 1982. Phosphorus. In A. L. Page, R. H. Miller, D. R. Keeney (eds.), Methods of Soil Analysis. Part 2. Chemical and Microbiological Properties. Second ed. Agronomy 9:403-430. Am. Soc. of Agron., Madison, Wis.

Olsen, S. R., and F. S. Watanabe. 1963. Diffusion of phosphorus as related to soil texture and plant uptake. Soil Sci. Soc. Am. Proc. 27:648-653.

Olsen, S. R., C. V. Cole, F. S. Watanabe, and L. A. Dean. 1954. Estimation of available phosphorus in soils by extraction with sodium bicarbonate. U.S.D.A. Circ. 939.

Olsen, S. R., F. S. Watanabe, and R. E. Danielsen. 1961. P adsorption by corn roots as affected by moisture and P concentration. Proc. Soil Sci. Soc. Am. 25:289-294.

Russell, R. S., J. B. Rickson, and S. N. Adams. 1954. Isotopic equilibria between phosphates in soil and their significance in the assessment of fertility by tracer methods. J. Soil Sci. 5:85-105.

Russell, R. S., E. W. Russell, and P. G. Marais. 1957. Factors affecting the ability of plants to absorb phosphate from soils. I. The relationships between labile phosphate and absorption. J. Soil Sci. 5:85-105.

Sabbe, W. E., and H. L. Breland. 1974. Procedures used by state soil testing laboratories in the southeastern region of the United States. South. Coop. Ser. Bull. 190.

Sanchez, P. A., and G. Uehara. 1980. Management considerations for acid soils with high phosphorus fixation capacity. pp. 471-514. In F. E. Khasawneh, E. C. Sample, and E. J. Kamprath (eds.), The Role of Phosphorus in Agriculture. Am. Soc. of Agron.

Seatz, L. F. 1954. Phosphate activity measurements in soils. Soil Sci. 77:43-51.

Sibbesen, E. 1977. A simple ion-exchange resin procedure for extracting plant-available elements from soil. Plant and Soil 46:665-669.

Talibudeen, O. 1957. Isotopically exchangeable phosphorus in soils. II. Factors influencing the estimation of 'labile' phosphorus. Soil Sci. 8:86-96.

Talibudeen, O. 1958. Isotopically exchangeable phosphorus in soils. III. The fractionation of soil phorphorus. J. Soil Sci. 9:120-129.

Thompson, E. J., A. L. F. Oliveira, U. S. Moser, and C. A. Black. 1960. Evaluation of laboratory indexes of absorbtion of soil phosphorus by plants. III. Plant and Soil XIII(1):28-38.

White, R. E., and A. W. Taylor. 1977. Effect of pH on phosphate adsorption and isotopic exchange in acid soils at low and high additions of soluble phosphate. J. of Soil Sci. 28:48-61.

ESTIMATING SOLUBLE PHOSPHORUS FROM GREEN CROPS

AND THEIR RESIDUES IN AGRICULTURAL RUNOFF

J. D. Schreiber[1]

ABSTRACT

The leaching of crop residues and green crops contributes significant quantities of soluble plant nutrients to agricultural runoff and, thus, must be considered an essential component of a small watershed chemical transport model. Past research on nutrient release from crop residues has largely focused on the chemical and physical changes of the residue itself. Few studies are concerned with the release of plant nutrients from crop residues as an influence on water chemistry. Crop residue decomposition is discussed in light of the factors which influence the nutrient content of crop residues and microbial activity, i.e., moisture, temperature, soil fertility, residue management, and nutrient ratios. Various models are presented for the decomposition of crop residues and nutrient release. Also the leaching and washoff of green plants by rainfall may add significant amounts of nutrients to agricultural runoff during the growing season. A model to describe the leaching of nutrients from growing plants is more complex than models describing the release of nutrients from crop residues, as the physiological aspects of plant growth must be considered. The model must include components for plant growth and nutrient uptake, leachability of living tissue as a function of plant age, rainfall dynamics which include rainfall distribution (plant recovery time), intensity and amount, and the dynamics of leaching chemistry as a function of time.

INTRODUCTION

The Water Quality and Management Program under Section 208 of P. L. 92-500 requires that each State plan and implement programs to achieve water quality goals by decreasing both point and nonpoint pollution. In some cases, mathematical models are being used to predict the movement of water, sediment, and agricultural chemicals from farmlands. One of the primary needs for 208 planning is models for assessing the effectiveness of land management practices on sediment and agricultural chemical transport from croplands. As the leaching of green crops and residues contributes significant and variable quantities of soluble plant nutrients, this process must be an essential component of a small watershed chemical transport model.

For the United States, crop residues result in the incorporation of approximately 8 - 10 t dry matter/ha/yr (Reddy, 1980). Residue from dryland wheat amounts to 2 - 8 t/ha/yr (Black and Reitz, 1972) compared with 2 - 16 t/ha/yr for corn stalks (Larson et al., 1972). On an annual basis, crop residues release significant quantities of phosphorus (P) to soil systems. For example, residues of corn, soybean, small grain, and cotton in the United States account for 225,700, 81,200, 107,700, and 14,300 metric tons P per year, respectively (Power and Legg, 1978).

Past research on nutrient release from crop residues has largely focused on the chemical and physical changes of the residue itself. Few studies were concerned with nutrient release from crop residues as an influence on water chemistry. The release or mineralization of nutrients during residue decomposition is principally a microbial process and is thus influenced by factors that affect microbial activity, i.e., temperature, moisture, pH, and energy supply.

---

[1]Soil Scientist, USDA-ARS, USDA Sedimentation Laboratory, Airport Road, P. O. Box 1157, Oxford, MS 38655.

Moisture

In general, adequate soil mositure and high relative humidity increased the degradation rate of surface applied straw residues (Sain and Broadbent, 1975; Shields and Paul, 1973). Soil respiration rates usually achieve a maximum between 0.05 and 0.33 bar soil moisture tension, with decreasing rates of residue decomposition at either high or low soil moisture tension values (Reddy et al., 1980). Compared to continuously moist conditions, alternate periods of residue drying and wetting may also increase the release of inorganic P leached from plant tissue (Cowen and Lee, 1973; Jones and Bromfield, 1969). However, under laboratory conditions, neither the amounts of CO_2 released nor P mineralized differed significantly over a 4-fold range in residue moisture content (Floate, 1970c). Soil moisture may also influence the uptake of P through root systems. For example, at 3 soil P fertility levels, soil mositure influenced the total quantity and percent P in soybean tops (Marais and Wiersma, 1975). Many plant residue degradation models contain a component to describe the effects of soil moisture on decomposition rates (Gilmour et al., 1977; Hunt, 1977; Reddy et al., 1980). While both live and dead plant tissues release plant nutrients upon soaking or when subjected to fine mists, little research has focused on the leaching of nutrients from plant residues under controlled conditions of rainfall intensity, duration, and distribution.

Temperature

The optimim temperatures for the biological decomposition of plant residues range from 30–40 C (Alexander, 1977). If temperatures are below this optimum range, a temperature increase will usually increase the rate of decomposition. At low temperatures reaction rates may increase 2 – 4 times for each 10 C rise in temperature, compared to 1.5 times for increases at higher temperatures (Reddy et al., 1980). At 30, 10, and 5 C the amount of CO_2 released after a twelve week period was 48, 31, and 17%, respectively, of the carbon originally present in the plant material. Similarly, the net amounts of P mineralized were also reduced (Floate, 1970b). While temperature may influence rates of decomposition, rapid or slow heating or bare or mulched soil had little effect on the P content of wheat tissue (Smika and Ellis, 1971). Other temperature effects, such as freezing and thawing cycles, may also increase the release of P from plant residues (Timmons et al., 1970). Many plant-residue-degradation models contain a component to correct for temperature effects on the decomposition rate (Gilmour et al., 1977; Hunt, 1977; Reddy et al., 1980).

Biological Factors

The presence of growing plants may affect the release of P from residue added to soil systems. The presence of growing oat plants led to a significant increase in the net release of ^{32}P added as labeled plant material to a high and low P soil (Blair and Boland, 1978). Similarly, the presence of growing plants was thought to act as a driving force to shift less labile P forms to solution P forms which were more readily available for plant uptake (Dalal, 1979).

Soil Fertility

Soil fertility can directly, and indirectly, affect the release of plant nutrients. Optimum soil fertility will increase not only crop yield, and hence, residue amounts, but also the nutrient content of the plant tissue. In addition, optimum soil fertility and soil reaction asure an adequate microbial population, essential to residue decomposition. Under cropping conditions of low P fertility (no P applications for 24 years) corn residues contained 0.28% P compared with 0.43% P when corn was fertilized with 49 kg/ha P (Nielsen and Barber, 1978). Similarly, established clover grown for 19 days on a low P soil contained 0.16% P compared with 0.33% for clover grown on a high P soil (Blair and Boland, 1978). However, at 3 levels of soil-applied P on 2 different soils, there was no difference in the tissue P content of corn or small grain (Murdock and Wells, 1978).

Residue Management

Residues incorporated into the soil are placed in intimate contact with microorganisms and, hence, undergo faster rates of decomposition (k). For example, k values for wheat straw decomposition increased in the order buried > on surface > above surface (Brown and Dickey, 1970; Douglas et al., 1980). However, a bare or mulched soil had little influence on the P content of wheat grown to heading stage (Smika and Ellis, 1971). Additional studies also indicate that incorporation of residues into the soil increases k values and the total quantity of residue decomposed (Parker, 1962; Sain and Broadbent, 1977). The chopping of straw residues had no influence on rates of decomposition.

In addition to the direct release and leaching of P from residues undergoing decomposition, residues would also be expected to increase the equilibrium phosphorus concentration (EPC) of surface soils. For example, in laboratory studies, several PO_4-P sources, including chemical, chemical plus straw, straw, manure, and other organic residues, markedly increased the EPC values of several soils (Dalal, 1979; Moser, 1942; Reddy et al., 1978; Singh and Jones, 1976). In part, decomposition of crop residues may have produced organic acids which can form stable complexes with Fe and Al thereby blocking P sorption sites (Dalton, et al., 1952; Gaur, 1969; Vyas, 1964).

Crop Factors and Nutrient Ratios

Quantities of residue appear not to influence the kinetics of decomposition; that is, loss rates (% C day^{-1}) are independent of loading rate (Jenkinson, 1965; Pal and Broadbent, 1975b). However, the percentage of decomposition of wheat straw was inversely related to the loading rate, and the absolute values of k (first order rate constant) decreased as the loading rate increased (Brown and Dickey, 1970). Total CO_2 losses can be a linear function of loading rates (Pal and Broadbent, 1975b).

Net P mineralization from plant residues depends upon the C concentration or energy supply and P concentration, i.e., a given C/P ratio. As with N, there is a critical level of P in carbonaceous material which serves as a balance point between immobilization and mineralization (Reddy, 1980). For natural carbonaceous products, this balance point is about 0.2% P (Alexander, 1977; Black and Reitz, 1972). Thus, P mineralization should follow C mineralization provided the C/P ratio of the carbonaceous material is below a critical level, about 200:1 or less (Blair and Boland, 1978; Dalal, 1979; Koelling and Kucera, 1965). In laboratory studies, the net P mineralization correlated with the orginal P content of plant tissue. The critical P value decreased as the incubation period increased form 2 - 12 weeks (Floate, 1970a). The critical value of P in residues during soil P sorption – desorption studies was 0.3%. Residues with < 0.3% P decreased labile soil P and increased sorption by soil after 75 - 150 days' incubation (Singh and Jones, 1976).

Ratios of C/N are also important in the decomposition of plant residues. Critical N contents are 1.5 - 2%, and C/N ratios of 20-25 are needed for decomposition of proceed (Smith and Douglas, 1968). In soil column studies, the leachate C/N ratios for wheat straw alone exceeded 20:1 on several occasions, with a maximum of 56. Leachate C/N ratios from 1-, 2-, and 4-cm-deep soil columns with surface applied wheat straw ranged up to 55:1, 30:1, and 22:1, respectively (Cochran et al., 1980). Many plant residue decomposition models estimate the initial portion of residue susceptible to degradation from the C/N ratio (Hunt, 1977; Reddy et al., 1980). Recent crop residue decomposition investigations indicate that the difference between actual and potential rates of residue decomposition reflects a reduction in the rate of decomposition when not enough N is available, i.e., (dc/dt) actual = µN (dc/dt) potential. The term µN is a reduction factor which is a function of the ratio of the potential rate of C residue decomposition to the total amount of N available (N potentially released from the residues during decomposition plus inorganic N available) (Molina et al., 1983).

While C:N:P ratios are important in determining the amount of net P mineralized, knowledge is also required of the total amount and forms of P

present in residue tissue when estimating the quantities of P released during decomposition. In general, agricultural crops contain 0.05 to 0.5% P in their tissues (Alexander, 1977). Of the total P present in frozen or non-green vegetation, 60 to 80%, may be leached with water compared with 69 to 78% of the total P in hayed-off pasture plants, of which 90% was inorganic P (Jones and Bromfield, 1969). Inorganic P was 59 and 63% of the total P present in Nordus and Agrostus grass, respectively, the remainder organic P (Floate, 1970a). Wheat seedlings contained mostly inorganic P, about 80% as PO_4-P (Bhatti and Loneragan, 1970). The P content in plant tissue of several major agronomic crops is presented in Table 1. These data represent a wide range of geographic areas, agricultural practices, plant growth stage, and fertility practices. Based on these data, the average P content of corn, soybeans, small grains, grasses, legumes and cotton is 0.25, 0.26, 0.19, 0.29, and 0.34%, respectively.

Crop Residue Decomposition Model

Models which describe the decomposition of crop residues must take into account the major processes shown in the following:

(AFTER REDDY ET AL., 1980)
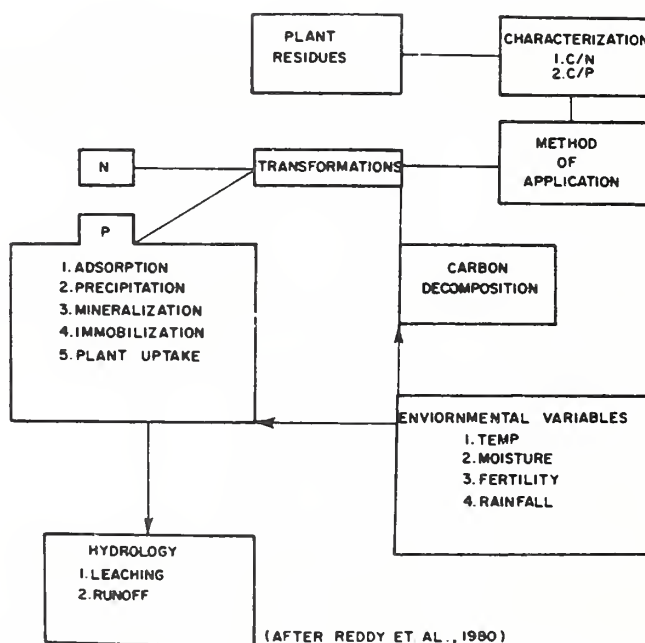
Experimental evidence indicates that decomposition of crop residues best follows the rate equation for a first-order reaction; thus,

$$- \frac{d(A)}{dt} = k(A)$$

where k = first order rate constant and has the dimensions of reciprocal time. If the concentration of A is $(A)_1$ at t_1 and $(A)_2$ at t_2 then,

$$- \int_{(A)_1}^{(A)_2} \frac{d(A)}{(A)} = k \int_{t_1}^{t_2} dt$$

or

$$\ln \frac{(A)_1}{(A)_2} = k(t_2 - t_1)$$

If $t_1 = 0$, then

$$\ln \frac{(A)_o}{(A)} = kt$$

or

$$(A) = (A)_o e^{-kt}$$

Another important equation describes the time period ($t_{1/2}$) when one-half of Ao has disappeared from the reaction, then:

$$k = \frac{0.693}{t_{1/2}}$$

Decomposition of ^{14}C labeled wheat straw followed the expression $C_t = C_o e^{-rt}$, where C_o = % residue at t = 0, t = time in years, C_t = % residue remaining at time t, and r = $\ln 2/t_{1/2}$ (Douglas et al., 1980; Sauerbeck and Gonzales, 1977). After an initial rapid loss of C, the mineralization of P from ^{14}C and ^{32}P labeled white clover buried in soil closely followed C mineralization according to first order kinetics (Dalal, 1979). Simple power functions also describe cumulative carbon losses as a function of time (Pal and Broadbent, 1975b; Sain and Broadbent, 1975). However, simple power or first order kinetic equations do not take into account variables such as temperature, soil moisture, and immobilization. A recent model designed to describe the degradation of plant residues and other organic wastes takes into account some of these variables (Gilmour et al., 1977):

where
$$k = 2.303/(t_2 - t_1) \log C_1/C_2$$
k = reaction velocity constant
t_1 = initial time
t_2 = final time
C_1 = input carbon at t_1
C_2 = residual carbon at t_2

Corrections are made for temperature:

$$t_{1/2} = \frac{0.693}{k \times 0.933^{-(\text{Annual Heat Units}/365-(T_2 - T_1))}}$$

Annual Heat Units = (MAT - 5) x 365

$$\text{MAT} = \sum_{\text{Day 1}}^{\text{Day 365}} \left(\frac{\text{Max. Day Temp. } ^\circ C + \text{Min. Day Temp. } ^\circ C}{2} \right) \times \frac{1}{365}$$

$$t_{1/2} = \frac{0.693}{k \frac{M_2}{M_1}}$$

M_1 = soil moisture for optimum mineralization (% of water holding capacity)

M_2 = actual soil moisture (% of water holding capacity)

Plant residue decomposition may involve both slow and fast reactions, reflecting the relative ease of degradation for different organic constituents. Thus, often a double exponential equation gives the best fit to residue decomposition data, i.e., $Y = Ae^{-k_1 t} + (100 + A) e^{-k_2 t}$, where Y is the % C remaining in the soil at time t (Cheshire et al., 1979). Rye grass decomposition followed a double exponential equation of the form $Y = 70.9e^{-2.83t} + 29.1e^{-0.087t}$, where Y = % retention of the organic matter added in the soil, and t = time in years. Seventy percent of the plant material decomposed with $t_{1/2} = 0.25$ years; and for the remaining material $t_{1/2} = 0.8$ years. This same equation also described the degradation of plant residues in the tropics, but reaction rates were four times as fast (Jenkinson and Ayanoba, 1977).

For grassland ecosystems it was recognized that decomposition for a pure substance at a constant temperature and water tension could be represented by simple first order reaction kinetics, i.e., $x_t = x_o e^{-kt}$. However, it was also acknowledged that decomposition of grasses involved two different fractions, each with a different rate constant. One fraction (labile), consisting of sugars, starches, and proteins, underwent decomposition relatively rapidly compared to a second more resistant fraction, consisting of cellulose, lignins, fats, tannins, and waxes. Thus, the final form of the equation is similar to that presented earlier (Hunt, 1977).

$$At = Se^{-kt} + (1-S) e^{-ht}$$

where S = the initial portion of labile material, 1-S = the proportion of resistant material, k and h = reaction rate constants for labile and resistance components, respectively. Values of S can be estimated by the C:N ratio of the carbonaceous material; that is, $S = 0.70 + 1.11 (N/C)^{1/3}$, $r^2 = 0.98$. The complete model also corrects for soil moisture, added nitrogen, and temperature, which is given by $E = e^{(-5.66 + 0.240T - 0.00239T^2)}$, where T is temperature in °C ($0 < T < 38$) (Hunt, 1977).

A model, very similar to that presented above, has been developed to describe the decomposition of crop residues and other wastes. As before, decomposition is assumed to follow first order kinetics for different phases of decomposition.

$$-\frac{dC_i}{dt} = k_i C_i$$

$$C_{t_i} = C_i e^{-k_i t}$$

where i = decomposition phase I, II, or III

C_i = organic C at beginning of phase I

C_{t_i} = organic C remaining

k_i = first order rate constant

t = time in days

The residue amount available for decomposition in phase I is represented as D_1 (labile fraction, easily decomposable) and phase III and D_3 (residual fraction). No phase II decomposition was observed for plant residues. The quantity D_1 was related to, and could be estimated from, the C/N ratio, where

$$D_1 = 86.64 - 13.95 \ln (C/N)$$

This model also provides corrections for temperature, soil moisture, and method of application:

Temperature

$$k_{i2} = k_{i1}\theta^{(T_2-T_1)}$$, where θ ranges from 1.04 to 1.12, with an average of $1.07 \pm .03$

Soil Moisture

$$Fm = 1.223 + 0.201 \ln \psi \text{ for } (0.02 \leq \psi \leq 0.33)$$

$$Fm = 0.874 - 0.115 \ln \psi \text{ for } (0.33 \leq \psi \leq 10.0)$$, where ψ is soil

moisture tension in bars

Method of Residue Application (F_{ma})

Residue	Incorporated	Surface Applied
Corn stalks	1.0	0.51
Wheat straw	1.0	0.37
Rice straw	1.0	0.63

Thus, when all corrections are taken into consideration, the final equation for the reaciton rate constant becomes

$$\overline{k}_{i2} = k_{i1}\theta^{(T_2-T_1)} F_m \cdot F_{ma} \qquad \text{(Reddy et al., 1980)}$$

Values of k and h (a second rate constant) can be assumed to be fairly constant for different organic residues with their values depending more on temperature, soil water, soil aeration, soil fertility and pH (Hunt, 1977). For the decomposition model developed by Reddy, k_1 values were related to D_1, the percent of added C decomposed in phase I (Reddy et al., 1980).

LEACHING OF GREEN CROPS

The leaching and washoff of green plants by rainfall may also add nutrients, including PO_4-P, to runoff during the growing season (Dalbro, 1957; Mann and Wallace, 1924; Morgan and Tukey, 1964; Tukey et al., 1958). Leaching of PO_4-P from green plants may contribute to the storm to storm variability of PO_4-P concentrations in runoff from agricultural areas. For example, significant quantities of PO_4-P leached from prairie vegetation during the month of April were attributed to water soluble PO_4-P extracted from growing plants by precipitation (White, 1973a). Similarly, moisture retained on leaves after a rainstorm contained significant quantities of soluble PO_4-P (Cowen and Lee, 1973). While nutrients are leached from young leaves with difficulty, up to 80% of the nutrient content of old leaves can be leached with ease. Major pathways of nutrient losses include the cuticle, plasmodesmata, and ectodesmata (Tukey, Jr., and Tukey, 1962).

When the physiological aspects of plant growth are considered, a model to describe the leaching of nutrients from growing plants is more complex than one describing the release of nutrients from crop residues. A model to describe the leaching of plant nutrients such as P from growing plants must include components of (1) plant growth and nutrient uptake, (2) leachability of living tissue by rainfall as a function of plant age (P extraction coefficient), (3) rainfall dynamics which include rainfall distribution (plant recovery time), intensity, amount, and (4) dynamics of leaching chemistry as a function of time. While a complete model which describes these processes is not presented, these topics will be discussed briefly in the remainder of this section.

Plant growth models may be relatively general, such as

$$\text{Yield} = \frac{10\text{Eta}}{Kt} \cdot Qs \cdot Qv$$

where   Yield = t/ha/yr

    Eta = actual evaportranspiration, mm/yr
    Kt = water transpired by plant per ton of dry matter produced
    Q_s = soil quality index
    Q_v = shoot index (Husz, 1978)

Other plant growth models such as GOSSYM (Gossypium, cotton simulator) are more complex and require inputs of air temperature, total solar energy, evaporation, infiltration water, plant population and spacing, soils data, and fertilizer applications. However, evidence indicates the theory of growth and morphogenesis described in GOSSYM can be generalized and applied to other crops. This model can provide for a daily output of plant height, weight, fruit load, and nutritional status (Baker et al., 1976).

Dry matter accumulation in corn plants tends to follow a characteristic sigmoid shaped growth curve (Nelson, 1956). For specific time periods, dry matter and P accumulation may be expressed as linear functions of time. In addition, P accumulation usually parallels dry matter accumulation (Hanway, 1962; Nelson, 1956). Values of I max (maximal P influx to root) were measured for five single crosses of corn and ranged from 0.13 to 0.34 pmoles P/cm/sec. These data were used to predict the P content (mmoles/plant) of similar corn plants grown under field conditions. For the 22 to 38 day interval, observed P = 0.27 + 1.38 predicted P, r^2 = 0.90; and for the 22 to 51 day interval, observed P = 0.45 + 0.64 predicted P, r^2 = 0.98 (Nielson and Barber, 1978).

Except during very early and late (senescence) stages of soybean growth, accumulation of P in vegetative parts (stems, petioles, leaves) was essentially linear over time during the growing season (Henderson and Kamprath, 1970; Scott and Brewer, 1980). For 1966, 1967, and 1968 these relationships were Y = 0.12X - 3.83, r^2 = 0.99; Y = 0.21X - 7.53, r^2 = 0.99; and Y = 0.20X - 7.34, r^2 = 0.99, where Y = P uptake, kg/ha, and X = time, days (Scott and Brewer, 1980). Using the mechanistic Cushman model (Cushman, 1979), which contains three soil and eight plant parameters, predicted P uptake by the three soybean cultivars agreed closely with observed P uptake over a time period of 0-28 days (Silberbush and Barber, 1983). As with many other crops, translocation of P and other nutrients within the plant can be expected during periods of reproductive growth (Henderson and Kamprath, 1970).

For winter wheat, daily growth equations (mg/cm^2) estimating photosynthesis and respiration were developed based on net CO_2 exchange measurements. The photosynthesis and respiration equations were developed from meteorological data. The only crop parameter required was leaf area index. The resulting growth equations predicted dry matter production that agreed favorably with observed dry matter accumulation (Hodges and Kanemasu, 1977). Maximum P content (16±2 mg/plant) occurred at the soft dough growth stage, and then decreased rapidly as the plant matured. In general, P accumulation paralleled that at dry matter. Grain contained 75% of the total plant P at maturity (Waldren and Flowerday, 1979). Other equations have also related dry matter accumulation to time. For example, from spring to harvest time for winter wheat Y = 15.6 + 11.4X^5 - 2.26X + 0.0285X^2 - 0.000148X^3, r^2 = 0.97, where Y = dry matter, t/ha, and X = time, days since dormancy. Phosphorus concentrations in both living and senescing leaves decreased as a function of time for the same period. For living leaves Y_2 = 0.433 - 0.0023X, r^2 = 0.59; and for senescing leaves Y = 0.243 - 0.015X^5, r^2 - 0.38, where Y = %P, and X = time, days since dormancy. Once P uptake into a plant is expressed as a function of time and/or dry matter accumulation, a rainfall P extraction coefficient must be determined. A P extraction coefficient defines how much of the plant total P is susceptible to leaching by rainfall.

The loss of nutrients from squash and bean leaves was a linear function of time, and indicated a significant replacement of nutrients into the leaf by translocation during leaching. For squash leaves, < 1% of the P applied as P was leached (Tukey, Jr., et al., 1958). Other studies indicate that nutrients are lost from plant foliage throughout the growing season, with

quantities lost increasing just before maturity and death of the foliage (Long et al., 1956; Sharpley, 1981). Throughout the active growing season for corn, the total P in separate plant parts was signficantly correlated with water soluble P. For corn leaves, Y = 0.67X - 0.02, r = 0.97; leaf sheaths, Y = 0.77X - 0.01, r = 0.96; and for stalks, Y = 0.87X, r = 0.98, were Y = % water soluble P, and X = % total P. Thus, about 67, 75, and 87% of the total P in leaves, leaf sheaths, and stalks, respectively, were water soluble. Water soluble P was determined by shaking 0.50 g samples of oven dry (65°C) plant material for 30 min in 100 ml H_2O (Hanway, 1962). In other plant materials, water soluble P can account for 69 to 78% of the total P (Jones and Bromfield, 1969).

In a most comprehensive study, simulated rainfall was applied at 6 cm/hr to growing cotton, sorghum, and soybean plants as a function of soil type and time interval between rainfall events. The amounts of soluble P in the plant leachate was found to increase with plant age and soil - water stress. A period of 24 hours between rainfall events was needed for P to reaccumulate on the leaf surface. With an increase in plant age from 42 to 82 days, the contribution of plant leachate P to soil surface runoff P increased from 20 to 60% (Sharpley, 1981).

Data in Fig. 1 are from a preliminary study on the leaching of soluble nutrients from green cotton plants by artifical rainfall. Rain was applied at (a) 2.5 cm/hr for 1 hr, (b) same plant after a 4 hr wait, 2.5 cm/hr for 1 hr, (c) same plant after a 24 hr wait, 2.5 cm/hr for 2 hr, and (d) on a second new plant, 2.5 cm/hr for 3 hr. This experiment was conducted late in the growing season; plant senescence and defoliation were rapidly approaching. No organophosphate insecticides were applied to the cotton during the growing season. As cotton plant leaves are probably the major source of P during rainfall leaching, a P extraction coefficient was calculated based on the assumption that mature cotton plant leaves weigh 26.28 ± 13.14 g (G. W. Willis, personal communication) and have a P content of 0.34% (Table 1). All data were corrected for background nutrient values throughout the event. Assuming no P replacement, during the first, second, and third rainfall applications, about 4.50, 2.21, and 2.91%, respectively, of the plant total P were leached by rainfall. While a knowledge of P extraction coefficients is essential, information is also required on plant-runoff-P concentration relationships. For example, the first hour of rainfall, the plant-runoff-weighted PO_4-P concentration was about 0.15 mg/l, a relatively high value, and decreased to 0.05 mg/l during the last two hours (Fig. 1). Concentrations of PO_4-P in the plant runoff show relatively good agreement between the two different cotton plants (Fig. 1).

Concentrations of PO_4-P in plant runoff are related to time (Fig. 1) and cumulative plant runoff volumes as logarithmic functions. Accumulative quantities of PO_4-P in plant runoff were related to accumulative runoff volumes as linear functions.

For quantities of PO_4-P leached from the plant at equal volumes of cumulative runoff, the plant showed a 49 and 34% recovery at the end of 4 and 24 hours, respectively. At this one intensity (2.5 cm/hr) the results indicate that cumulative quantities of PO_4-P leached are the linear function of time; similar results were observed for the loss of Ca from squash leaves by leaching with distilled water (Tukey, et al., 1958). Data (not presented) are similar for ammonium (NH_4-N) and total organic carbon (TOC).

Research is needed to further evaluate the leaching of nutrients from green crops as functions of the probability of rainfall and runoff, crop growth stage (leaf area) and plant recovery time. Under natural rainfall, nutrients like PO_4-P leached from the growing plant become part of the soil-water P matrix and are sorbed by the soil, leached from the runoff extraction zones, and/or transported in runoff.

REFERENCES

Agarwal, A. S., B. R. Singh, and Y. Kanchiro. 1971. Soil nitrogen and carbon mineralization as affected by drying-rewetting cycles. Soil Sci. Soc. Am. Proc. 35:96-100.

Alexander, M. 1977. Introduction to soil microbiology. John Wiley and Sons, New York. 467 p.

Allison, F. E. and R. M. Murphy. 1963. Comparative rates of decomposition in soil of wood and bark particles of several species of pine. Soil Sci. Soc. Am. Proc. 27:309-312.

Anderson, O. E., R. L. Carter, H. F. Perkins, and J. B. Jones. 1971. Plant nutrient survey of selected plants and soils of Georgia. Georgia Agric. Exp. Stat. Res. Rep. 102. 29 p.

Baker, D. N., J. R. Lambert, C. J. Phene and J. M. McKinion. 1976. GOSSYN: A simulator of cotton crop dynamics. Computers applied to the management of large scale agricultural enterprises: Papers and proceedings of a US-USSR seminar. Moscow, Riga, Kishinev.

Bartholomew, W. V. 1954. Availability of organic nitrogen and phosphorus from plant residues, manures and soil organic matter. Soil Microbiology Conference, Purdue University.

Bartholomew, W. V. 1965. Mineralization and immobilization of nitrogen in the decomposition of plant and animal residues. Agronomy 10:285-306. Am. Soc. Agron., Madison, Wisconsin.

Bartlett, J. B. and A. G. Norman. 1938. Changes in the lignin of some plant materials as a result of decomposition. Soil Sci. Soc. Am. Proc. 3:210-216.

Beeson, K. C. 1941. The mineral composition of crops with particular reference to the soils in which they were grown: A review and compilation. USDA Miscellaneous Pub. No. 369. 117 p.

Bhatti, A. S. and J. F. Loneragan. 1970. Phosphorus concentrations in wheat leaves in relation to phosphorus toxicity. Agron. J. 62:288-290.

Black, A. L. and L. L. Reitz. 1972. Phosphorus and nitrate-nitrogen immobilization by wheat straw. Agron. J. 64:782-785.

Black, A. L. 1973. Soil property changes associated with crop residue management in a wheat-fallow rotation. Soil Sci. Soc. Am. Proc. 37(6):943-946.

Black, A. L. and F. H. Siddoway. 1979. Influence of tillage and wheat straw residue management on soil properties in the Great Plains. J. Soil and Water Cons. 34:220-223.

Blair, G. J. and O. W. Boland. 1978. The release of phosphorus from plant material added to soil. Aust. J. Soil Res. 16:101-111.

Broadbent, F. E. and W. V. Bartholomew. 1948. The effect of quantity of plant material added to a soil on its rate of decomposition. Soil Sci. Soc. Am. Proc. 13:271-274.

Broadbent, F. E. and T. Nakashima. 1974. Mineralization of carbon and nitrogen in soil amended with carbon-13 and nitrogen-15 labeled plant material. Soil Sci. Soc. Am. Proc. 38:313-315.

Brown, P. L. and D. D. Dickey. 1970. Losses of wheat straw residue under simulated field conditions. Soil Sci. Soc. Am. Proc. 34:118-121.

Burwell, R. E., D. R. Timmons, and R. F. Holt. 1975. Nutrient transport in surface runoff as influenced by soil cover and seasonal periods. Soil Sci. Soc. Am. Proc. 39:523-528.

Cochran, V. L., L. F. Elliott, and R. I. Papendick. 1980. Carbon and nitrogen movement from surface-applied wheat (Triticum aestivum) straw. Soil Sci. Soc. Am. J. 44:978-982.

Cowen, W. F. and G. Fred Lee. 1973. Leaves as source of phosphorus. Environ. Sci. and Technol. 7:853-854.

Chase, F. E. and P. H. H. Gray. 1957. Applications of the Warburg respirometer in studying activity in soil. Can. J. Microbiol. 3:335-349.

Cheshire, M. W., G. P. Sparling and R. H. E. Inkson. 1979. The decomposition of straw in soil. p. 65-71. In E. Grosebard (ed.), Straw decay and its effect on disposal and utilization. John Wiley and Sons, Chichester.

Cushman, J. H. 1979. An analytical solution to solute transport near root surfaces for low initial concentrations. I. Equations development. Soil Sci Soc. Am. J. 43:1087-1090.

Dalal, R. C. 1979. Mineralization of carbon and phosphorus from carbon-14 and phosphorus-32 labeled plant material added to soil. Soil Sci. Soc. Am. J. 43:913-916.

Dalbro, S. 1957. Leaching of nutrients from apple foliage. Rept. 14th International Hort. Cong. (1955):770-778.

Dalton, J. D., G. C. Russell, and D. H. Shelling. 1952. Effect of organic matter on phosphate availability. Soil Sci. 73:173-181.

Douglas, C. L., R. R. Allmaras, P. E. Rasmussen, R. E. Ramig and N. C. Roager, Jr. 1980. Wheat straw composition and placement effects on decomposition in dryland agriculture of the Pacific Northwest. Soil Sci. Soc. Am. J. 44:833-837.

Epstein, E. 1956. The effect of organic matter on soil aeration with particular reference to nutrient uptake by plants. Ph.D. Thesis. Purdue University, West Lafayette, IN. Diss. Abstr. 16:841.

Floate, M. J. S. 1970a. Decomposition of organic materials from hill soils and pastures. II. Comparative studies on the mineralization of carbon, nitrogen, and phosphorus from plant materials and sheep faeces. Soil Biol. Biochem. 2:173-185.

Floate, M. J. S. 1970b. Decomposition of organic materials from hill soils and pastures. III. The effect of temperature on the mineralization of carbon, nitrogen, and phosphorus from plant materials and sheep faeces. Soil Biol. Biochem. 2:187-196.

Floate, M. J. S. 1970c. Decomposition of organic materials from hill soils and pastures. IV. The effects of moisture content on the mineralization of carbon, nitrogen, and phosphorus from plant materials and sheep faeces. Soil Biol. Biochem. 2:275-283.

Fribourg, E. A., and W. V. Bartholomew. 1956. Availability of nitrogen from crop residues during the first and second years after application. Soil Sci. Soc. Am. Proc. 20:505-508.

Führ, R. and D. Sauerbeck. 1968. Decomposition of wheat straw in the field as influenced by cropping and rotation. p. 241-250. In Isotopes and radiation in soil organic matter studies. Proc. IAEA/FAO Symp. Vienna, Austria.

Gaur, A. C. 1969. Studies on the availability of phosphate in soil as influenced by humic acid. Agronchimica. 14:62-65.

Gaur, A. C., K. V. Sadasivam, O. P. Vimal, and R. S. Mathur. 1971. The study on the decomposition of organic matter in an alluvial soil: CO_2

evolution, microbiological and chemical transformations. Plant and Soil 34:17-28.

Gilmour, C. M., F. E. Broadbent, and S. M. Beck. 1977. Recycling of carbon and nitrogen through land disposal of various wastes. In Soils for Management of Organic Wastes and Waste Waters. Am. Soc. Agro., Madison, WI, pp. 173-194.

Gooding, T. H. and T. M. McCalla. 1945. Loss of carbon dioxide and ammonia from crop residue during decomposition. Soil Sci. Soc. Am. Proc. 10:185-190.

Grimes, D. W. and J. J. Hanway. 1967. An evaluation of the availability of K in crop residue. Soil Sci. Soc. Am. Proc. 31:705-706.

Haas, H. J. and C. E. Evans. 1957. Nitrogen and carbon changes in Great Plains soils as influenced by cropping and soil treatments. Tech. Bull. 1164. U. S. Dept. Agr., Washington, D. C. 58 p.

Halm, B. J., J. W. B. Stewart, and R. H. Halstead. 1972. The phosphorus cycle in a native grassland ecosystem. p. 571-589. In Isotopes and radiation in soil-plant relationships including forestry. Proc. IAEA/FAO Symp. Vienna, Austria.

Hanway, J. J. 1962. Corn growth and composition in relation to soil fertility. II. Uptake of N, P, and K and their distribution in different plant parts during the growing season. Agron. J. 54:217-222.

Harley, C. P., H. H. Moon, and L. O. Regeimbal. 1951. The release of certain nutrient elements from simulated orchard grass mulch. Am. Soc. of Hort. Sci. 57:17-23.

Heber, V. 1967. Freezing injury and uncoupling of phophorylation from electron transport in chloroplasts. Plant Physiol. 42:1343-1350.

Henderson, J. B. and F. J. Kamprath. 1970. Nutrient and dry matter accumulation by soybeans. North Carolina Agric. Exp. Sta. Tech. Bull. 197. 27 p.

Hodges, T. and E. T. Kanemasu. 1977. Modeling daily dry matter production of winter wheat. Agron. J. 69:974-978.

Hunt, H. W. 1977. A simulation model for decomposition in grasslands. Ecology 58:469-484.

Husz, G. S. 1978. Agro-ecosystems in South America. p. 244-276. In M. J. Fressel (ed.), Cycling of mineral nutrients in agricultural ecosystems. Elsevier Scientific Publishing Co., Amsterdam.

Jackman, R. H. 1955. Organic phosphorus in New Zealand soils under pasture. II. Relation between organic phosphorus content and some soil characteristics. Soil Sci. 79:293-299.

Jenkinson, D. S. 1960. The production of ryegrass labeled with carbon-14. Plant Soil 13:279-290.

Jenkinson, D. S. 1965. Studies on the decomposition of plant material in soil. I. Losses of carbon from ^{14}C-labeled ryegrass incubated with soil in the field. J. Soil Sci. 16:104-115.

Jenkinson, D. S. 1977. Studies on the decomposition of plant material in soil. V. The effects of plant cover and soil type on the loss of carbon from ^{14}C-labeled ryegrass decomposing under field conditions. J. Soil Sci. 28:424-434.

Jenkinson, D. S. and A. Ayanoba. 1977. Decomposition of Carbon-14 labeled plant material under tropical conditions. Soil Sci. Soc. Am. J. 41:912-915.

Jones, O. L. and S. M. Bromfield. 1969. Phosphorus change during the leaching and decomposition of hayed-off pasture plants. Aust. J. Agric. Res. 20:653-663.

Jung, G. A. and D. Smith. 1961. Trends of cold resistance and chemical changes over winter in the roots and crowns of alfalfa and medium red clover. I. Changes in certain nitrogen and carbonhydrate fractions. Agron. J. 53:359-363.

Karlen, D. L. and D. A. Whitney. 1980. Dry matter accumulation, mineral concentrations, and nutrient distribution in winter wheat. Agron. J. 72:281-288.

Kaushik, N. K. and H. B. N. Hynes. 1971. The fate of the dead leaves that fall into streams. Arch. Hydrobiol. 68:465-515.

Koelling, M. R. and C. L. Kucera. 1965. Dry matter losses and mineral leaching in bluestem standing crop and litter. Ecology 46:529-532.

Larson, W. E., C. E. Clapp, W. H. Pierre, and Y. B. Morachan. 1972. Effects of increasing amounts of organic residues on continuous corn: II. Organic carbon, nitrogen, phosphorus, and sulfur. Agron. J. 64:204-208.

LeClerc, J. A. and J. F. Breazeale. 1908. Plant food removed from growing plants by rain or dew. U. S. Dept. Agr. Ybk. Agr. 389-402.

Long, W. G., D. V. Sweet and H. B. Tukey. 1956. The loss of nutrients from plant foliage by leaching as indicated by radioisotopes. Science: 1039-1040.

Lyda, S. D. and G. D. Robinson. 1969. Soil respiratory activity and organic matter depletion in an arid Nevada soil. Soil Sci. Am. Proc. 33:92-94.

Maas, F. E. and R. M. Adamson. 1972. Resistance of sawdusts, peats, and bark to decomposition in the presence of soil and nutrient solution. Soil Sci. Soc. Am. Proc. 36: 769-772.

Mann, C. E. T. and T. Wallace. 1924. The effects of leaching with cold water on the foliage of the apple. Jour. Pomol. Hort. Sci. 4:146-161.

Marais, J. N. and D. Wiersma. 1975. Phosphorus uptake by soybeans as influenced by moisture stress in the fertilized zone. Agron. J. 67:777-781.

McCalla, T. M. and F. L. Duley. 1943. Disintegration of crop residue as influenced by sub-tillage and plowing. J. Am. Soc. Agron. 35:306-315.

McCalla, T. M. 1948. The decomposition of _Carex filifolia_. Soil Sci. Soc. Am. Proc. 13:284-286.

Mes, M. G. 1951. Excretion (recretion) of phosphorus and other mineral elements under the influence of rain. S. African Jour. Sci. 50:167-172.

Millar, H. C., F. B. Smith, and P. E. Brown. 1936. The rate of decomposition of various plant residues in soils. J. Am. Soc. Agron. 28:914-923.

Molina, J. A. E., C. E. Clapp, M. J. Shaffer, F. W. Chichester, and W. E. Larson, 1983. NCSOIL, a model of nitrogen and carbon transformation in soil: description, calibration, and behavior. Soil Sci. Soc. Am. J. 47:85-91.

Morgan, J. V. and J. B. Tukey, Jr. 1964. Characterization of leachate from plant foliage. Plant Physiol. 39:590-593.

Moser, F. 1942. Influence of leguminous plant additions to the organic matter content and available nutrient supply of southern soils. J. Am. Soc. Agron. 34:711-719.

Murdock, L. W. and K. L. Wells. 1978. Yields, nutrient removal, and nutrient concentrations of double-cropped corn and small grain silage. Agron. J. 70:573-576.

Nelson, L. B. 1956. The mineral nutrition of corn as related to its growth and culture. In Advances in Agronomy. VIII:321-375. Academic Press Inc.

Nielsen, N. E. and S. A. Barber. 1978. Differences among genotypes of corn in the kinetics of P uptake. Agron. J. 70:695-698.

Norman, A. G. 1929. The biological decomposition of plant materials. Biochem. J. 23:1367-1384.

Nyhan, J. W. 1975. Decomposition of carbon-14 labeled plant materials in a grassland soil under field conditions. Soil Sci. Soc. Am. Proc. 39:643-648.

Nyhan, J. W. 1976. Influence of soil temperature and water tension on the decomposition rate of carbon-14 labeled herbage. Soil Sci. 121:288-293.

Pal, D. and F. E. Broadbent. 1975a. Influence of moisture on rice straw decomposition in soils. Soil Sci. Soc. Am. Proc. 39:59-63.

Pal, D. and F. E. Broadbent. 1975b. Kinetics of rice straw decomposition in soils. J. Environ. Qual. 4:256-260.

Parker, D. T. 1962. Decomposition in the field of buried and surface-applied cornstalk residue. Soil Sci. Soc. Am. Proc. 26:559-562.

Parnas, H. 1975. Model for decomposition of organic material by microorganisms. Soil Biol. Biochem. 7:161-169.

Pinck, L. A., F. E. Allison, and M. W. Sherman. 1950. Maintenance of soil organic matter. II. Losses of carbon and nitrogen from young and mature plant materials during decomposition in soil. Soil Sci. 69:391-401.

Power, J. F. and J. O. Legg. 1978. Effect of crop residues on soil chemical environment and nutrient availability. In Crop Residue Management Systems. Am. Soc. Agro., Madison, WI. pp. 85-100.

Reddy, K. R. and W. H. Patrick, Jr. 1975. Effect of alternate aerobic and anaerobic conditions on redox potential, organic matter decomposition, and nitrogen loss in a flooded soil. Soil Biol. Biochem. 7:87-94.

Reddy, G. Y., E. O. McLean, G. D. Hoyt and T. J. Logan. 1978. Effects of soil, cover crop, and nutrient source on amounts and forms of phosphorus movement under simulated rainfall conditions. J. Environ. Qual. 7:50-54.

Reddy, K. R. 1980. Land areas receiving organic wastes: transformations and transport in relation to nonpoint source pollution. p. 243-274. In M. R. Overcash and J. M. Davidson (ed.), Environmental impact of nonpoint source pollution. Ann Arbor Science, Ann Arbor, MI.

Reddy, K. R., R. Khaleel, and M. R. Overcash. 1980. Carbon transformations in the land areas receiving organic wastes in relation to nonpoint source pollution: a conceptual model. J. Environ. Qual. 9:434-442.

Richards, E. H. and A. G. Norman. 1931. The biological decomposition of plant materials. V. Some factors determining the quality of nitrogen immobilized during decomposition. Biochem. J. 25:1769-1778.

Rovira, A. D. 1953. The use of the Warburg apparatus in soil metabolism studies. Nature 172:29.

Sain, P., and F. E. Broadbent. 1975. Moisture absorption, mold growth, and decomposition of rice straw at different relative humidities. Agron. J. 67:759-762.

Sain, P. and F. E. Broadbent. 1977. Decomposition of rice straw as affected by some management factors. J. Environ. Qual. 6:96-100.

Sauerbeck, D. R. and M. A. Gonzales. 1977. Field decomposition of ^{14}C-labeled plant residues in different soils of Germany and Costa Rica. In International Symposium on Soil Organic Matter Studies, sponsored by FAO/IAEA/Agrochimica. (Braunschweig, 1976).

Scott, H. D. and D. W. Brewer. 1980. Translocation of nutrients in soybeans. Soil Sci. Soc. Am. J. 44: 566-569.

Sharpley, A. N. 1981. The contribution of phosphorus leached from crop canopy to losses in surface runoff. J. Environ. Qual. 10:160-165.

Shields, J. A. and E. A. Paul. 1973. Decomposition of ^{14}C-labeled plant material under field conditions. Can. J. Soil Sci. 53:297-306.

Silberbush, M., and S. A. Barber. 1983. Prediction of phosphorus and potassium uptake by soybeans with a mechanistic mathematical model. Soil Sci. Soc. Am. J. 47:262-265.

Singh, B. B. and J. P. Jones. 1976. Phosphorus sorption and desorption characteristics of soil as affected by organic residues. Soil Sci. Soc. Am. J. 40:389-394.

Smika, D. E. and R. Ellis, Jr. 1971. Soil temperature and wheat straw mulch effects on wheat plant development and nutrient concentration. Agron. J. 65:388-391.

Smith, J. H. and C. L. Douglas. 1968. The influence of residual nitrogen on wheat straw decomposition in the field. Soil Sci. 106:456-459.

Smith, J. H. and C. L. Douglas. 1971. Wheat straw decomposition in the field. Soil Sci. Soc. Am. Proc. 35:269-272.

Tam. R. H. and O. C. Magistad. 1936. Chemical changes during decomposition of pineapple trash under field conditions. Soil Sci. 41:315-327.

Terman, G. L., P. M. Giordano and S. E. Allen. 1972. Relationships between dry matter yields and concentrations of Zn and P in young corn plants. Agron. J. 64:684-687.

Terman, G. L. and J. C. Noggle. 1973. Nutrient concentration changes in corn as affected by dry matter accumulation with age and response to applied nutrients. Agron. J. 65:941-945.

Terman, G. L. 1977. Yields and nutrient accumulation by determinate soybeans as affected by applied nutrients. Agron. J. 69:234-238.

Terry, R. E., D. W. Nelson, and L. E. Sommers. 1979. Carbon cycling during sewage sludge decomposition in soils. Soil Sci. Soc. Am. J. 43:494-499.

Tester, C. F., L. J. Sikora, J. M. Taylor and J. F. Parr. 1979. Decomposition of sewage sludge compost in soil: III. Carbon, nitrogen, and phosphorus transformations in different sized fractions. J. Environ. Qual. 8:79-82.

Thomas, B., W. B. Holmes, and J. L. Clapperton. 1955. A study of meadow hays from the Cockle Park plots. Part II. Ash constituents. Emp. J. Exp. Agric. 23:101-108.

Timmons, D. R., R. F. Holt, and J. J. Latterell. 1970. Leaching of crop residues as a source of nutrients in surface runoff water. Water Resour. Res. 6:1367-1375.

Timmons, D. R., R. E. Burwell, and R. F. Holt. 1973. Nitrogen and phosphorus losses in surface runoff from agricultural land as influenced by placement of broadcast fertilizer. Water Resour. Res. 9:658-667.

Timmons, D. R. and R. F. Holt. 1977. Nutrient losses in surface runoff from a native prairie. J. Environ. Qual. 6:369-373.

Tukey, H. B., S. H. Wittwer, and H. B. Tukey, Jr. 1957. Leaching of nutrients from plant foliage as determined by radio-isotopes. Proc. International Conf. Radio-isotopes in Scientific Research, UNESCO, Paris.

Tukey, H. B., Jr., H. B. Tukey, and S. H. Wittwer. 1958. Loss of nutrients by foliar leaching as determined by radioisotopes. Proc. Am. Soc. Hort. Sci. 71:496-506.

Tukey, H. B., Jr. and J. A. Romberger. 1959. The nature of substances leached form foliage. Plant Physiol. 34:vi.

Tukey, H. B., Jr. and H. b. Tukey. 1962. The loss of organic and inorganic materials by leaching from leaves and other above-ground plant parts. In: Radioisotopes in Soil-Plant Nutrition Studies. Intern. Atomic Energy Agency. Vienna. p. 289-302.

Unger, P. W. 1976. Surface residue, water application, and soil texture effects on water acumulation. Soil Sci. Soc. Am. J. 40:298-300.

Van Diest, A. and C. A. Black. 1959. Soil organic phosphorus and plant growth. II. Organic phosphorus mineralized during incubation. Soil Sci. 87:145-154.

Vyas, K. K. 1964. Availability and uptake of phosphorus by wheat under different moisture and organic matter levels. Current Sci. 33:756-757.

Waksman, S. A. and F. C. Gerretson. 1931. Influence of temperature and moisture upon the nature and extent of decomposition of plant residues by micro-organisms. Ecol. 12:33-60.

Waldren, R. P. and A. D. Flowerday. 1979. Growth stages and distribution of dry matter, N, P, and K. Agron. J. 71:391-397.

White, E. M. 1973a. Overwinter changes in the percent Ca, Mg, K, P, and N in vegetation and mulch in an eastern South Dakota Prairie. Agron. J. 65:680-691.

White, E. M. 1973b. Water-leachable nutrients from frozen or dried prairie vegetation. J. Environ. Qual. 2:104-107.

Whitfield, C. J. 1962. (A Committee Report). A standardized procedure for residue sampling. USDA, ARS. 41-68.

Wild, A. and O. L. Oke. 1966. Organic phosphate compounds in calcium chloride extracts of soils: Identification and availability to plants. J. Soil Sci. 17:356-371.

Zayed, M. N., S. M. Taha, and M. A. Azazy. 1971. Bacteriological and chemical studies in rice straw compost. V. Effect of phosphorus. Zentralbl. Bakteriol. Parastenkd. Abt. 2. 126:678-686.
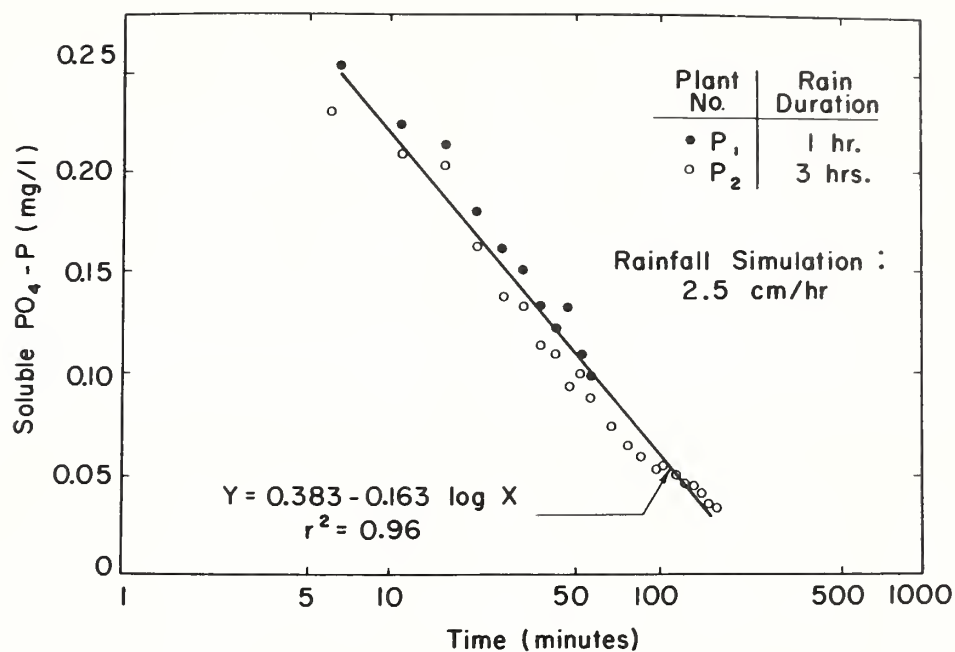
Figure 1
Soluble PO_4-P concentrations in cotton canopy runoff as a function of time
for two different cotton plants.

Table 1
Nutrient contents of selected crops

Crop	P	C	N	C/N	C/P	Age	Plant Part	Ag Practice	Reference
Corn	–	–	–	102	–	–	stover	–	Reddy et al., 1980
	0.30	40	–	57	–	–	–	–	Parker, 1962
	0.28	–	1.15	–	–	–	–	–	Reddy, 1980
	0.43	–	3.69	–	–	x̄ of 22–51 days	aerial	low P fert	Nielsen and Barber, 1978
	0.22	–	3.85	–	–	x̄ of 22–51 days	aerial	high P fert	Nielsen and Barber, 1978
	0.27	–	–	–	–	–	stalks	–	Singh and Jones, 1976
	0.27	–	1.29	–	–	mature	whole plant	high P fert & N	Murdock and Wells, 1978
	0.30	–	1.15	–	–	mature	whole plant	med. P fert & N	Murdock and Wells, 1978
	0.11	–	0.99	–	–	8 weeks	whole plant	low P fert & N	Murdock and Wells, 1978
	0.14	–	–	–	–	–	leaves & stalks	–	Terman et al., 1972
	0.35	–	–	–	–	–	stalks	–	Larson et al., 1972
	–	–	0.40	102	–	–	top leaves	–	Terman and Noggle, 1973
	–	44	–	–	–	–	stover	–	Pinck et al., 1950
	0.15	–	–	–	–	–	stover	–	Beeson, 1941
	0.12	–	–	–	–	–	stover	–	Beeson, 1941
Soybeans	0.37	–	5.05	–	–	3 months	top leaves	–	Terman, 1977
	0.30	–	2.30	–	–	3 months	bottom leaves	–	Terman, 1977
	0.23	–	–	–	–	6 weeks	——	low P fert	Marais and Wiersma, 1975
	0.17	–	–	–	–	6 weeks	——	med. P fert	Marais and Wiersma, 1975
	0.24	–	–	–	–	6 weeks	——	high P fert	Marais and Wiersma, 1975
Small grain									
rice	0.25	40	0.43	93	160	–	whole plant	–	Reddy, 1980
winter wheat	0.10	–	–	–	–	95 days after dormancy	whole plant	–	Karlen and Whitney, 1975
wheat	0.21	–	2.33	–	–	–	straw	–	Singh and Jones, 1976
wheat	0.17	–	–	–	–	heading stage	whole plant	–	Smika and Ellis, 1971
barley-wheat-oat	0.30	–	1.97	–	–	–	whole plant	high P fert & N	Murdock and Wells, 1978
barley-wheat-oat	0.27	–	1.60	–	–	–	whole plant	med. P fert & N	Murdock and Wells, 1978
barley-wheat-oat	0.26	–	1.16	–	–	–	whole plant	low P fert & N	Murdock and Wells, 1978
wheat	–	43.1	0.6	73	–	–	straw	–	Pinck et al., 1950
wheat	0.08	–	–	–	–	–	straw	–	Beeson, 1941
oat	0.11	–	–	–	–	–	straw	–	Beeson, 1941
rye	0.10	–	–	–	–	–	straw	–	Beeson, 1941
Grasses & Legumes									
alfalfa	0.50	40	4.0	10	80	–	–	–	Reddy, 1980
alfalfa	0.38	–	–	–	–	–	–	–	Singh and Jones, 1976
alfalfa	0.25	–	2.6	–	–	–	–	–	Larson et al., 1972
alfalfa	0.30	–	–	–	–	–	–	–	Beeson, 1941
blue grass	0.22	–	–	–	–	–	–	–	Beeson, 1941
orchard grass	0.50	39	2.9	13	78	–	–	–	Reddy, 1980
nordus grass	0.11	40	1.9	45	365	1 year	cuttings	–	Floate, 1970
agrostis grass	0.13	41	1.4	30	315	1 year	cuttings	–	Floate, 1970
clover	0.16	–	–	–	–	–	–	low P fert	Blair and Boland, 1978
clover	0.33	–	–	–	–	–	–	high P fert	Blair and Boland, 1978
grasses	0.27	–	–	–	–	mature	–	–	Thomas et al., 1985
Cotton	0.34	–	–	–	–	mature	leaves	–	Anderson et al., 1971

Table 2
Selected constants for crop residue decomposition models

Crop	Percent of added C decomposed in phase I	K_1	K_3	Other Variables	References
Corn					
stover	27	0.0449 day-1	0.0011 day-1	-	Hunt, 1977
stover	27	0.0082 day-1	0.0015 day-1	Temp @ 30°C	Reddy et al., 1980
stalks	-	0.0119 day-1	0.0018 day-1	Temp @ 35°C	Bartlett and Norman, 1938
stalks	-	0.0085 day-1	0.0013 day-1	Temp @ 30°C	Bartlett and Norman, 1938
stalks	22	0.0088 day-1	0.0014 day-1	-	Reddy, 1980
Oats					
straw	60	0.0437 day-1	0.00052 day-1	-	Hunt, 1977
straw	-	0.0192 day-1	0.0096 day-1	Temp @ 35°C	Richards and Norman, 1931
straw	28	0.0137 day-1	0.0068 day-1	Temp @ 30°C	Richards and Norman, 1931
Wheat					
straw	-	0.0058 day-1	0.0012 day-1	Temp @ 28°C	Reddy et al., 1980
straw	23	0.0068 day-1	0.0014 day-1	Temp @ 30°C	Reddy et al., 1980
straw	-	0.026 month-1	-	N=0.78%, residue on surface	Douglas et al., 1980
straw	-	0.015 month-1	-	N=0.49%, residue on surface	Douglas et al., 1980
straw	-	0.009 month-1	-	N=0.19%, residue on surface	Douglas et al., 1980
straw	-	0.084 month-1	-	N=0.78%, residue buried	Douglas et al., 1980
straw	-	0.061 month-1	-	N=0.49%, residue buried	Douglas et al., 1980
straw	-	0.070 month-1	-	N=0.19%, residue buried	Douglas et al., 1980
straw	32	0.0236 day-1	0.00074 day-1	-	Hunt, 1977
Rye					
straw	41	0.090 day-1	0.00028 day-1	> two different soils	Cheshire et al., 1979
straw	35	0.053 day-1	0.00066 day-1	> two different soils	Cheshire et al., 1979
straw	-	0.0199 day-1	0.0039 day-1	Temp @ 35°C	Norman, 1929
straw	29	0.0142 day-1	0.0028 day-1	Temp @ 30°C	Norman, 1929
Rice					
straw	28	0.0054 day-1	0.0013 day-1	Temp @ 30°C aerobic	Reddy and Patrick, 1975
Soybeans					
residue	-	0.0168 day-1	0.0007 day-1	Temp @ 28°C	Reddy et al., 1980
residue	53	0.0196 day-1	0.0008 day-1	Temp @ 30°C	Reddy et al., 1980
residue	60	0.0482 day-1	.00019 day-1	-	Hunt, 1977
Grasses					
bluegrass	58	0.0463 day-1	0.00057 day-1	-	Hunt, 1977
bluegrass	-	0.0163 day-1	0.0011 day-1	Temp @ 28°C	Reddy et al., 1980
bluegrass	52	0.0190 day-1	0.0013 day-1	Temp @ 30°C	Reddy et al.1980
rye grass	62	0.0053 day-1	0.00050 day-1	-	Jenkinson, 1965

ESTIMATING TRANSFER OF AMMONIUM BETWEEN SOLUTION AND SEDIMENT IN
STREAM CHANNELS AND THE ORGANIC-N/ORGANIC-C RATIO USED IN SWAM

R. R. Schnabel

ABSTRACT

A materials balance approach is used to predict equilibrium ammonium concentra-
tion and ammonium adsorption isotherms for composite suspensions of sediment
slurries. Such mixed suspensions occur at stream confluences and when surface
runoff flows into a stream. Adsorption isotherms are determined for three soil
mixtures, and these are compared with the predicted isotherms. A procedure,
based on the Gapon cation exchange equation, is presented for estimating
isotherm parameters from readily obtained soil properties.

INTRODUCTION

As streams converge or runoff enters a stream, sediment-associated chemicals in
each flow component are exchanged with the mixed solution and indirectly with
each other. Estimates of the postmixing solution concentration and mass of
chemical retained by the suspended solids must be obtained to predict the mass
of a chemical transported downstream, from the point of mixing, as transforma-
tions occur in solution and as sediment settles.

Three of the most widely used equations to describe the partitioning of chemicals
between fluid and solid phases are the linear, Freundlich, and Langmuir
isotherms. The linear isotherm is appealing due to its computational simplicity.
However, at higher solution concentrations the exchange data is expected to be
curvilinear, making the Freundlich or Langmuir isotherms the more appropriate
forms.

The purpose of this paper is to demonstrate a tool to predict the partitioning of
ammonium between soluble and adsorbed phases of mixed suspensions as occur at
stream confluences, and to describe a method for estimating the slope of linear
isotherms prior to mixing.

PROGRAM DEVELOPMENT

Complete mixing without transformations at the confluence is assumed to determine
the equilibrium solution concentration and an adsorption isotherm for the mixed
suspension. It is further assumed that adsorption-desorption kinetics are
nonlimiting.

The total mass of a chemical at a confluence is the sum of the masses in the
solution and solid phases. If no transformations occur and adsorbed chemical
is the only solid phase, the change of mass in solution is equal and opposite
to the change in the mass of chemical adsorbed. This expression is given in
Eq. [1] for a two component confluence with zero-intercept linear adsorption
isotherms,

$$-TV*(X_{eq}-X_m) = S_a*M_a*(X_{eq}-X_{oa}) + S_b*M_b*(X_{eq}-X_{ob}),$$ [1]

where TV = total water volume $(V_a + V_b)$; L^3

   V = volume

   X_{eq} = equilibrium solution concentration ; M/L^3

   X_m = weighted average solution concentration ; M/L^3
   $= (V_a*X_{oa} + V_b*X_{ob})/(V_a + V_b)$

Soil Scientist, USDA-ARS, Northeast Watershed Research Center, University Park,
PA 16802.

X_o = solution concentration prior to mixing ; M/L^3

S = isotherm slope ; L^3/M
M = mass of suspended solids ; M
a and b refer to components at the confluence.

The equilibrium solution concentration of the combined flows, from Eq. [1], is

$$X_{eq} = (X_m+(S_a*M_a*X_{oa} + S_b*M_b*X_{ob})/TV)/(1+(S_a*M_a + S_b*M_b)/TV).$$ [2]

When mixing the suspensions causes no change in the adsorption characteristics of the components, the total mass of chemical adsorbed at equilibrium is

$$\text{Adsorbed chemical} = S_a*M_a*X_{eq} + S_b*M_b*X_{eq}$$ [3]

and the slope of the isotherm for the mixed suspension reduces to

$$S = (S_a*M_a + S_b*M_b)/(M_a+M_b).$$ [4]

The equilibrium solution concentration and mixed-suspension isotherm slope for a multicomponent confluence are given by Eqs. [5] and [6]:

$$X_{eq} = (X_m+(\Sigma S_i*M_i*X_{oi})/TV)/(1+(\Sigma S_i*M_i)/TV),$$ [5]

$$S = \Sigma S_i*M_i/\Sigma M_i.$$ [6]

When the exchange process is better described by Langmuir adsorption isotherms, the linear adsorption terms in Eq. [1] are replaced with Langmuir terms, yielding Eq. [7]. The equilibrium concentration is then determined using the bisection method (Hornbeck, 1975) to find the root of Eq. [7]:

$$-TV*(X_{eq}-X_m) = X_{eq}*Q_{ma}/(X_{eq}+K_a)-X_{oa}*Q_{ma}/(X_{oa}+K_a)$$

$$+ X_{eq}*Q_{mb}/(X_{eq}+K_b)-X_{ob}*Q_{mb}/(X_{ob}+K_b)$$ [7]

where Q_m = adsorption maximum ; M/M
K = the half-saturation concentration ; M/L^3

The adsorption maximum of the mixed suspensions is taken to be a weighted average of the components, and the half-saturation constant is calculated by rearranging the Langmuir equation:

$$Q_m = \Sigma Q_{mi}*M_i/\Sigma M_i$$

$$K = X_{eq}*(Q_m/Q - 1)$$ [8]

where Q = mass chemical adsorbed at equilibrium/mass sediment ; M/M

The above analysis was not performed using Freundlich adsorption isotherms, since there are two unknowns, only a single equation, and no simple means of eliminating either of the unknowns.

Calculation of Isotherm Parameters

When assigning values to the isotherm parameters the best possible situation is for the user to have measured values for the soil of interest. When measured values are not available an alternate means of determining values for the adsorption isotherm parameters is required which uses more readily available data. A method of calculating the slope of the linear adsorption isotherm is presented based on the Gapon cation exchange equation.

The Gapon cation exchange equation for the exchange of ammonium and calcium may be written as Eq. [9],

$$\frac{[NH_4X]}{[Ca_{1/2}X]} = \frac{K_g \ (NH_4)}{(Ca)^{1/2}} \ , \tag{9}$$

where $[NH_4X]$ = ammonium associated with the exchanger (meq/g)

   $[Ca_{1/2}X]$ = calcium associated with the exchanger (meq/g)

   (NH_4) = soluble ammonium   (mmole/L)

   (Ca) = soluble calcium   (mmole/L)

   K_g = Gapon exchange constant $(mmole/L)^{-1/2}$.

Rearranging equation [9] gives a linear expression for ammonium exchange similar to one given by Jackson et al. (1980) for the exchange of trace quantities of radionuclides,

$$[NH_4X] = \frac{K_g \ [Ca_{1/2}X] \ (NH_4)}{(Ca)^{1/2}} \ . \tag{10}$$

Let

$$S = \frac{K_g \ [Ca_{1/2}X]}{(Ca)^{1/2}} \ , \tag{11}$$

then

$$[NH_4X] = S * [NH_4] \ . \tag{12}$$

To calculate the slope, Eq. [11], of the linear exchange equation, Eq. [12], assume that all counterions behave as calcium, then

$$CEC = [NH_4X] + [Ca_{1/2}X] \ . \tag{13}$$

If $Ca >> NH_4$; $CEC = [Ca_{1/2}X]$ $\tag{14}$

   and (Ca) = solution concentration. $\tag{15}$

The solution concentration may be estimated (United States Salinity Laboratory Staff, 1954) from the electrical conductivity as

   solution concentration = 10 * EC. $\tag{16}$

Units on solution concentration and EC are meq/L and mmhos/cm, respectively. Since the solution is assumed to be predominantly calcium, a divalent cation, the solution concentration is estimated as five times the EC. Convenient units for (NH_4) and $[NH_4X]$ are mg/L and mg/kg, respectively. Substituting Eqs. [14], [15], and [16] into Eq. [11] and converting units, the final form of the expression for the slope of the isotherm, S, is

$$S = (K_g *CEC*1000)/(5*EC)^{1/2} \ ; \ \text{units L/kg.} \tag{17}$$

The slope of the isotherm is now expressed as a function of more common soil chemistry parameters. Possible sources for the values of CEC, EC, and K_g are the national and State soil characterization laboratories and the USDA Salinity Laboratory. A list of suggested default values for CEC, EC, and K_g is given in Table 1.

When a Langmuir or Freundlich isotherm describes the adsorption process better than a linear equation, it is assumed that the user had the isotherm parameters available in order to make that judgment.

Table 1
Default values for K_g, CEC, and EC for estimating the slope of a
linear adsorption isotherm

Gapon Exchange Constant:
  Default value = 0.01   assume ammonium : calcium exchange
  Source: Bohn et al. (1979)

Cation Exchange Capacity:
  Default value: CEC = -0.92 + 2.24*(% OC) + 0.56*(% clay)

                 CEC - cation exchange capacity ; meq/g
                 OC - organic carbon   ; %

  Source: Helling et al. (1964)

  Relationship at pH 6

Electrical Conductivity:
  Default value = 0.1 to 1.0 mmhos/cm east to west across
                 country

Ratio - Organic Nitrogen to Organic Carbon Ratio:
  Default value = 0.06 to 0.09
                west to east
                south to north
  Source: Brady, N. C. (1974)

Estimation of Organic Nitrogen

Nitrogen transformations enroute from field edge to stream bank are not simulated
in this model, and travel times in these small watershed streams are thought to
be sufficiently short to allow nitrate and organic nitrogen to be treated as
conservative substances. Therefore, the outflow nitrate nitrogen concentration
is simply the volume weighted average of the inflow concentrations. In this
version of the program the inflow organic nitrogen concentrations are taken to
be a fraction of the organic carbon concentration and are calculated by multi-
plying organic carbon content by the ratio of organic nitrogen to organic carbon
in each soil.

This approach is taken for the reason that organic carbon is a variable common
to a number of other submodels, including the pesticide and impoundment models,
and a small range of values for the ratio of nitrogen to carbon applies to a
great many soils. Much research regarding the carbon to nitrogen ratio has been
performed over the years, and the Soil Conservation Service, the Soil Character-
ization Laboratory, and State soil laboratories should be valuable sources of
data for many soils. In addition, data sets organized for other national or
regional modeling efforts such as EPIC (Williams et al., 1982) may provide input
data about soils of interest. Suggestions for default values for the ratio of
organic nitrogen to organic carbon are presented in Table 1.

METHODS AND MATERIALS

Adsorption isotherms of ammonium for six soils were determined at 23 C by batch
equilibrium techniques. Triplicate 1:5 mixtures of 5 grams of soil to 25 ml of
solution containing 1, 2, 5, 10, 20, or 50 ppm ammonium in 0.001, 0.003, 0.005,
or 0.01 M $CaCl_2$ were used in the adsorption studies. The soil and solution
were placed in 50-ml polyethylene centrifuge tubes sealed with screw caps. Each
tube was shaken for one hour, and a 10-ml aliquot removed for analysis by steam
distillation (Bremner and Keeney, 1965). The adsorption data were fit to
equations for linear, Freundlich, and Langmuir isotherms. The data were fit to
Freundlich and Langmuir isotherms by linearizing the equation prior to linear
least squares analysis and by nonlinear least squares analysis (SAS, 1982).
The linear form of the Langmuir equation is Eq. [10] of Veith and Sposito
(1977). Adsorption isotherms were also determined for mixtures of the original
soils, and these were compared with predicted isotherms for the mixed
suspensions.

RESULTS AND DISCUSSION

The soil materials used for this experiment were collected in a small watershed in central Pennsylvania and from a strip mine spoil pile. A shaking time study indicated that a one hour shaking period was sufficient to bring the samples to "equilibrium."

The isotherms determined with the raw data all had negative intercepts as a result of originally adsorbed ammonium. Therefore, the adsorption data for three of the soils, and 1:1 mixtures for each pair of the soil materials, Figure 1(a-c), were made to pass through the origin by adding the intercept of a straight line fit to the first three points of each plot. The goodness of fit as defined by the standard deviation about the nontransformed line (Syx), Table 2, shows that over the range of concentrations used, the adsorption data for the WG and Berks soil materials are best fit by the Langmuir adsorption equation, while a straight line equation gives a somewhat better fit for the mine spoil material. The mixtures with WG also show the best fit by the Langmuir equation, while the Berks:spoil pair, like the spoil alone, is fit somewhat better by a straight line.

All components at a confluence must have isotherms of the same form to use this technique. Based on the standard deviation of the points from the best fit lines for all the soil materials, the Langmuir isotherm appeared to be the most appropriate form to use. Therefore, following the procedure described in the development section, Langmuir equations were calculated for each of the mixed soil suspensions. The best fit Langmuir iostherms for the data from each member of a pair, the mixture, and the predicted lines are also plotted in Figure 1(a-c). Root mean square deviations of the measured from predicted lines (Table 3) show that over a range of ammonium concentrations up to 40 ppm, the error made using the predicted line to describe ammonium partitioning is similar to that using the measured line. The predicted and measured lines are more similar for mixtures where both members of the pair conformed more closely to the Langmuir isotherm. When little information is available to calculate adsorption isotherms, the linear isotherm seems a logical choice. However, greater differences were calculated between estimates of adsorbed ammonium made using measured and estimated isotherms when adsorption was assumed to be linear (Table 3).
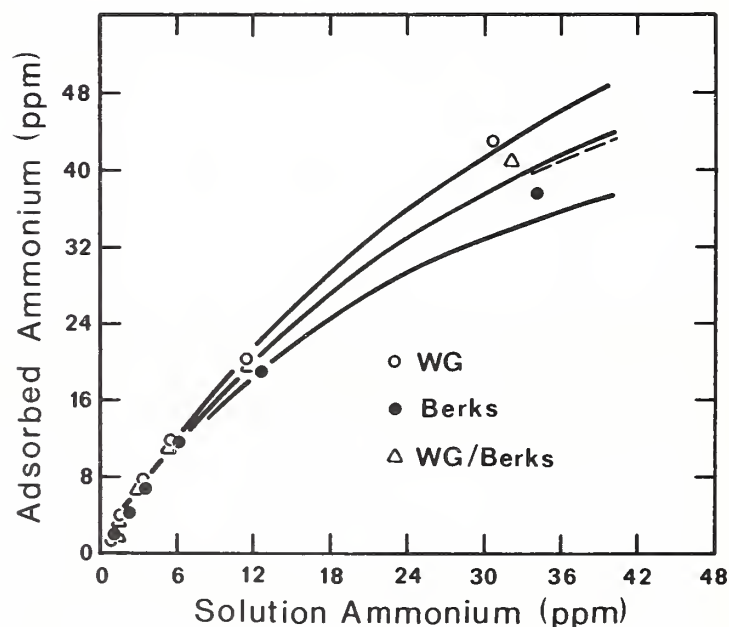
Figure 1a
Ammonium adsorption data and best fit Langmuir isotherms for the mixed suspensions, WG/Berks; each component of the mixture, and the isotherm predicted for the mixture with Eq. [8] (dashed line).
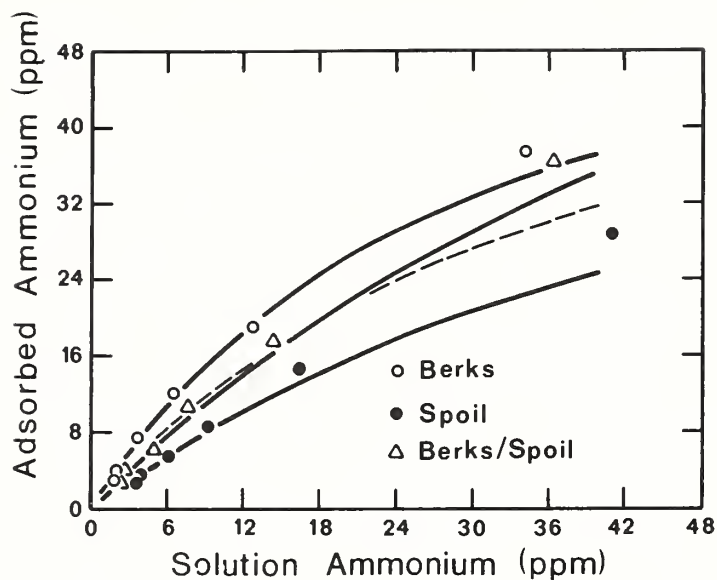
Figure 1b
Ammonium adsorption data and best fit Langmuir isotherms
for the mixed suspensions, Berks/Spoil; each component
of the mixure, and the isotherm predicted for the mixture
with Eq. [8] (dashed line).
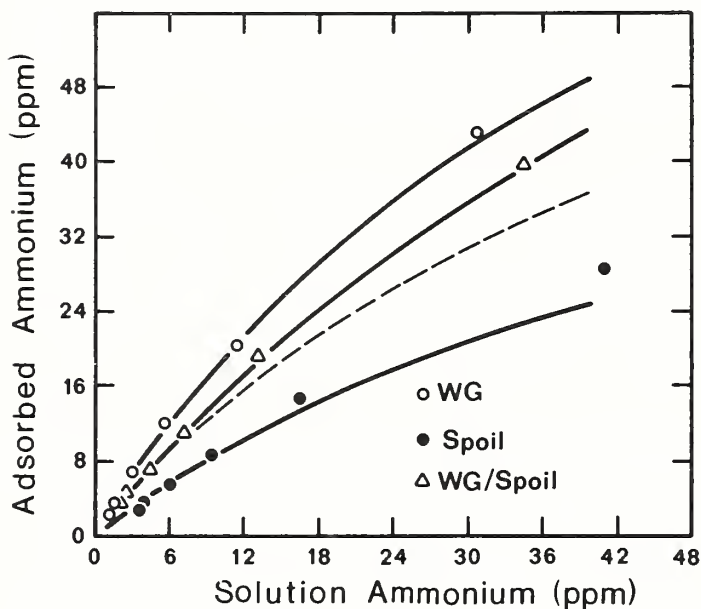
Figure 1c
Ammonium adsorption data and best fit Langmuir isotherms
for the mixed suspensions, WG/Spoil; each component of
the mixture, and the isotherm predicted for the mixture
with Eq. [8] (dashed line).

Table 2
Fitting parameters of adsorption isotherms for soil materials

Isotherm Form	Soil Material					
	WG	Berks	Spoil	WG:Berks	WG:Spoil	Berks:Spoil
-------------------- Adsorption data --------------------						
Linear						
Slope	1.34	1.02	0.67	1.21	1.10	0.97
Syx	1.79	2.20	1.30	1.70	1.37	1.27
Freundlich						
K	2.23	2.22	0.99	2.18	1.82	1.31
n	0.89	0.83	0.93	0.86	0.88	0.94
Syx	2.22	2.52	1.61	1.75	1.24	1.65
Langmuir						
Qmax	110.56	66.27	63.34	93.83	125.61	103.30
K	50.72	31.16	62.00	45.11	76.32	76.94
Syx	0.67	1.44	1.67	0.84	0.22	1.65

Table 3
Root mean square deviations of measured and predicted Langmuir and linear equations for mixed suspensions

Mixture	RMS Deviation				
	measured line from data		predicted from measured line		measured from predicted conc
	Langmuir	linear	Langmuir	linear	Langmuir
------------------------- ppm -------------------------					
WG:Berks	0.84	1.74	0.20	0.71	0.12
WG:Spoil	0.22	1.37	2.54	2.12	0.36
Berks:Spoil	1.65	1.27	0.80	2.82	0.63

Note: These RMS deviations are for solution concentrations of 1 to 40 ppm.

Equilibrium concentrations for the mixtures and solutions used during the experimental determination of the adsorption isotherms were calculated with Eq. [7]. Good agreement was obtained between the measured and predicted concentrations (Figure 2), as indicated by the root mean square deviation (Table 3) of the data. The good agreement is an indication that the Langmuir equation adequately describes the exchange of ammonium and that the exchange exhibits little hysteresis. Because the isotherms for each component of a mixture and not the isotherm predicted for the mixture are used to estimate equilibrium solution concentration, the agreement between measured and predicted concentrations is better than that between fit and predicted adsorption isotherms.

When the adsorption data were fit to either the Freundlich or Langmuir isotherms, the equations were linearized and the data appropriately transformed prior to linear least squares analysis. Linear regression of transformed data to linearized equations introduces bias into the analysis by weighting some of the data more heavily than others. As an example, linear regression of the log of the data, as was done for the Freundlich isotherm, results in larger values of adsorbed ammonium being weighted more heavily than the rest (i.e., 0.1 is no nearer to 1 than 1 is to 10 in the least squares sense). Bias in such analyses can be avoided by performing nonlinear least squares regression. A comparison
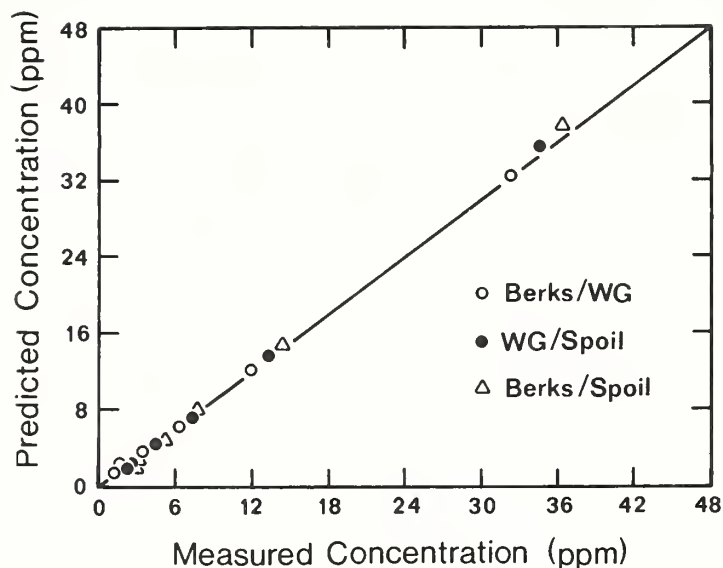
Figure 2
Measured equilibrium ammonium concentrations for mixed
suspensions of the soil materials and concentrations
predicted with Eq. [7]. There is a 1:1 correspondence
between measured and predicted values for points
falling on the line.

of the standard deviations about the nontransformed lines (Figure 3, a-b)
reveals that in addition to the elimination of bias, nonlinear regression
resulted in a better fit to the data than did linear regression of the
transformed data. This was true for every case, whether the data were fit
to Freundlich or Langmuir isotherms. Given the availability of nonlinear
regression packages and the improved fit which may be obtained through their
use, nonlinear regression should be used to determine best fit adsorption
isotherms.

Isotherms were fit to data measured in solutions with background $CaCl_2$ concen-
trations of 0.001, 0.003, 0.005, and 0.01 M. The slopes of the linear
isotherms fit to these data were used to evaluate estimates of isotherm
slopes made using Eq. [17]. The fit and estimated slopes for one of the
soils are shown in Figure 4. When all of the ammonium data for each $CaCl_2$
solution were used to fit the isotherm, the estimated slopes matched the fit
slopes well at high $CaCl_2$ concentrations, EC in the range 0.3 to 1.0 mmhos/cm,
but matched quite poorly at lower $CaCl_2$ concentrations. Since the only
variable considered to be independent in Eq. [17] is the electrical conduc-
tivity of the $CaCl_2$, a possible reason for the poor fit at the lower $CaCl_2$
concentrations is that the ammonium in solution made a significant, unaccount-
ed for contribution to solution electrical conductivity. When the data
measured in the three lower ammonium concentration solutions only were used
to fit the isotherms, the agreement between fit and estimated slopes was
somewhat better; however, it was still poor at low $CaCl_2$ concentrations. The
poor agreement at the lower $CaCl_2$ concentrations likely indicates that the
Gapon exchange coefficient is not a constant value over this range of solution
concentrations. This is also demonstrated by the curvilinear nature of all
the adsorption isotherms. A value of 0.01 is suggested for the Gapon exchange
coefficient in Table 1. The data collected indicate that a value of 0.03 is
more suitable for these soils.

Linear–Nonlinear Comparison
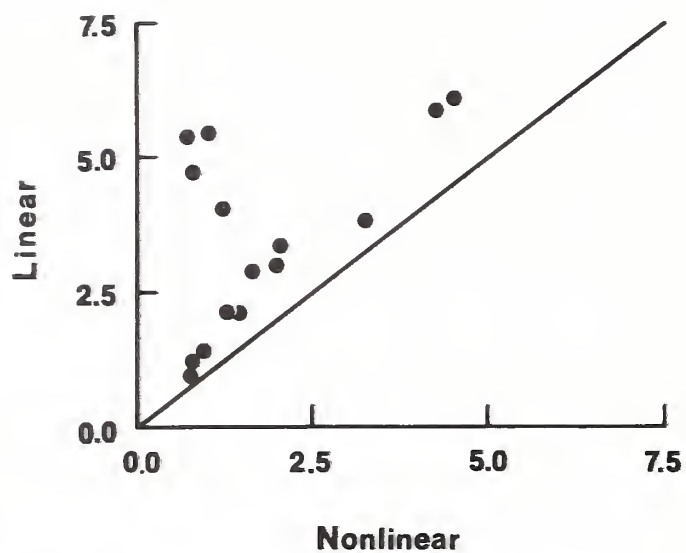
Figure 3a
Comparison of root mean square deviations when data were
fit with linear and nonlinear regression analysis;
Langmuir isotherms.

Linear–Nonlinear Comparsion
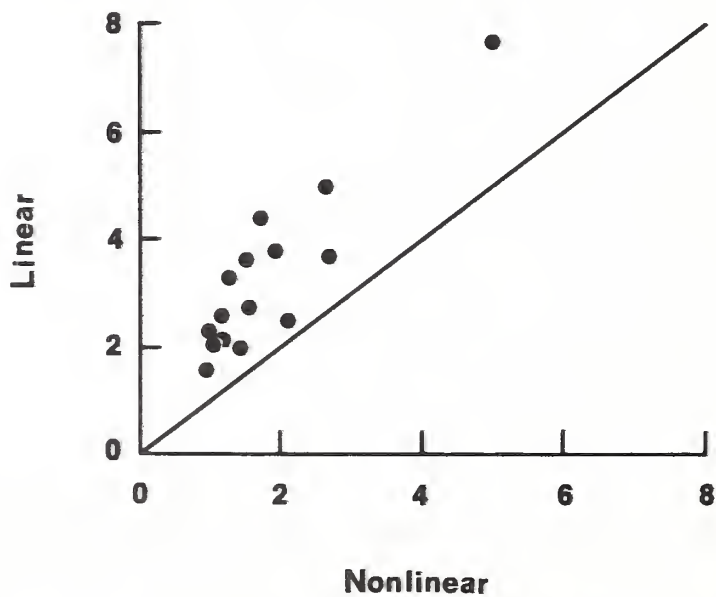
Figure 3b
Comparison of root mean square deviations when data were
fit with linear and nonlinear regression analysis;
Freundlich isotherms.
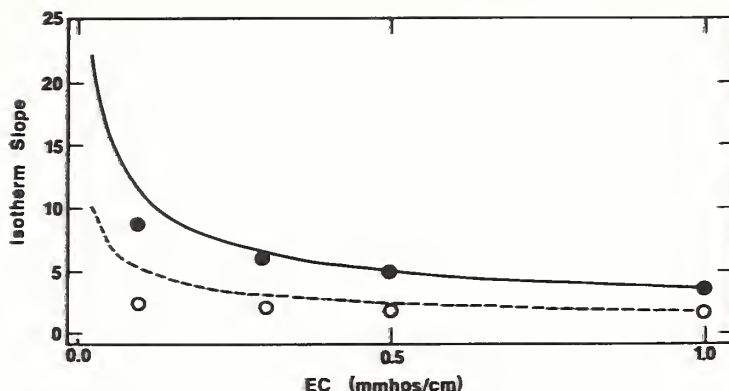
Figure 4
Best fit and estimated slopes to ammonium adsorption
isotherms in solutions of varying CaCl$_2$ concentration.
EC equals molarity of CaCl$_2$/5. The upper set of
points results when the three most dilute ammonium
solutions only are used. The lower set of points
results when all six ammonium solutions are used.

SUMMARY

A simple procedure is presented which can be used to accurately describe the
partitioning of a chemical between solution and adsorbed phases at stream
confluences. The partitioning is an obligatory step in the estimation of
downstream transport. Langmuir isotherms were found to fit the adsorption
data better than either Freundlich or linear isotherms, and nonlinear regres-
sion improved the fit to the data as compared with linear regression of
transformed data. In the absence of adsorption data, an assumption is made
that a linear isotherm adequately describes the adsorption-desorption
phenomenon of ammonium. A method is presented for estimating the slope of
linear adsorption isotherms for the case where no data exist. For the soils
used in this study, estimating ammonium adsorption with linear isotherms
resulted in an overall loss of accuracy. Although ammonium is used in this
example, the approach could be applied to any chemical exhibiting a well
defined "adsorption" isotherm.

REFERENCES

Bohn, H., B. McNeal, and G. O'Connor. 1979. Soil Chemistry. Wiley
Interscience, NY.

Brady, N. C. 1974. The Nature and Properties of Soils. 8th Edition.
MacMillin, NY.

Bremner, J. M., and D. R. Keeney. 1965. Steam distillation methods for the
determination of ammonium, nitrate and nitrite. Anal. Chim. Acta. 32:485-495.

Helling, G., G. Chesters, and R. Corey. 1964. Contributions of organic
matter and clay to soil cation exchange capacity as affected by the pH
of the saturating solution. Soil Sci. Soc. Am. J. 28:517-520.

Hornbeck, R. W. 1975. Numerical Methods. Quantum Publishers, Inc., NY.

Jackson, R. E., K. J. Inch, R. J. Patterson, and others. 1980. Adsorption of
radionuclides in a fluvial-sand aquifer: measurements of the distribution
coefficients K_c^{Sr} and K_d^{Cs} and identification of mineral adsorbents. In R. A.
Baker, ed., Contaminants and Sediments, Volume 1. Ann Arbor Science, Ann
Arbor, MI.

SAS Institute. 1982. SAS users guide: statistics. SAS Institute, Inc., Cary, NC.

United States Salinity Laboratory Staff. 1954. Diagnosis and improvement of saline and alkali soils. Agriculture Handbook No. 60, USDA. U. S. Government Printing Office, Washington, DC.

Veith, J. A., and G. Sposito. 1977. On the use of the Langmuir equation in the interpretation of "adsorption" phenomena. Soil Sci. Soc. Am. J. 41:697-702.

Williams, J. R., P. T. Dyke, and C. A. Jones. 1982. EPIC -- A model for assessing the effects of erosion on soil productivity. Paper presented at the Third International Conference on State-of-the-Art in Ecological Modelling, Colorado State University, May 24-28, 1982.

MODEL FOR THE REDISTRIBUTION AND STREAM TRANSPORT OF
LABILE SEDIMENT-ADSORBED AND SOLUTION PHOSPHORUS

H. M Kunishi, H. B. Pionke, and R. J. DeAngelis

ABSTRACT

A model was developed to describe the transport of labile sorbed P and
solution P in small watersheds. The core of the model, an algorithm for
calculating the amounts of P redistributed, gained, and lost during transport,
is presented and the underlying logic detailed.

INTRODUCTION

In seeking to develop productive and efficient farm management practices, the
U. S. Department of Agriculture (USDA) seeks also to make certain that these
practices are environmentally safe. Thus, through its Soil Conservation
Service, USDA has established a program to evaluate the effects of different
management practices on the potential for fertilizers and pesticides to leak
from farm fields into our water supplies. To help make this evaluation, USDA
researchers in the Agricultural Research Service have developed process-
oriented models for simulating the transport/loss of water, soil, and
chemicals, as induced by individual rainfall events. One such model, CREAMS2
(Smith and Knisel, 1985), estimates the amounts of these materials transported
from agricultural fields; another, SWAM (Alonso and De Coursey, 1985; Pionke
et al., 1985) to their further transport from fields through streams,
impoundments, and groundwater to the watershed outlet. SWAM is designed for
use on small watersheds--ideally less than 10 km^2.

P, present naturally in soil minerals and plant materials and added as
fertilizer to improve crop yields, is one of the nutrients transported with
runoff and its suspended load (sediment). In lakes, ponds, and estuaries,
high concentrations of P are often associated with dense microplankton
growth. Through death, submergence, and decay, such growth can adversely
affect water use and fish populations, cause premature aging of these bodies
of water, and lead to the decline of desirable submerged aquatic vegetation.
Good management of P is therefore necessary, and this involves supplying
enough P for efficient crop production while controlling P loss to drainage
waters. To help managers assess this type of P loss, we developed a labile-P
algorithm for use as a submodel within SWAM. The algorithm was developed from
data obtained previously (Kunishi et al., 1972) for the Mahantango watershed,
a 26-km^2 watershed in central Pennsylvania. We focused on labile P because
it comprises those forms of P--solution P and available sorbed P--that are
readily available to plants and microplankton and are essential to their
productivity. When used with the appropriate hydrologic and
sediment-transport models of SWAM (Alonso and De Coursey, 1985) or available
data from other sources, the algorithm has the capability to compute
redistributions, gains, and losses of solution and sorbed P caused by (1)
sediment deposition, resuspension, or admixture with sediments from different
sources (e.g., fields) or (2) groundwater discharge, streamflow recharge of
groundwater, or the mixing of outflows from different sources (e.g., fields,
streams). Computations are made for individual rainfall events on designated
stream segments, which separate distinct source areas. Although the algorithm
is a component model of SWAM, it can be used separately, provided it is
supplied with the following data: the volumes of runoff, with water loss and
gain enroute; mass of sediment derived from erosion, with sediment loss and
gain enroute; and particle-size distribution of eroding soil and sediment.

Kunishi is a soil scientist, USDA-ARS, Environmental Chemistry
Laboratory, Beltsville, MD 20705; Pionke is a soil science
research leader, USDA-ARS, Northwest Watershed Research Laboratory,
The Pennsylvania State University, University Park, PA 16802; and
DeAngelis is a mathematician, USDA-ARS, also at the Northwest
Watershed Research Laboratory.

The objectives of this paper are to present (1) the P algorithm and underlying logic in detail and (2) the stand-alone version of the model for possible use by others.

FOUNDATIONS OF THE ALGORITM

The algorithm has been described by Kunishi and Pionke (1985) and has four main features: P sorption isotherms, a governing equation, a fixation coefficient, and the use of specific surface to quantify transported sediment. These features are examined in detail below.

P Sorption Isotherm

The P sorption isotherm of a soil or sediment sample is a plot of the amounts of P the sample adsorbs from or releases into solutions of different P concentrations under near equilibrium conditions (Taylor and Kunishi, 1971). Specific analytic procedures for constructing a P isotherm have been given by Kunishi and Pionke (1985), and its pertinent features are explained in Figure 1. The isotherm relates the equilibrium P concentration (EPC) and the intercept (I), which is equal to the labile P concentration of the sample (available sorbed P). In Figure 1, the equation of the isotherm for soil DE-6 is

$$Y = 80 * EPC - 24, \tag{1}$$

where Y is available sorbed P.

Wolf et al. (1985, this vol.) examined the relationship between EPC and soil test P values (Bray P, Olsen P, and Mehlich No. 1 P) and between I and soil test values. The correlations for both comparisons were high when these tests were made on groups of soils from a limited geographic region. These high correlations suggest that the soil test values can be used to estimate P sorption isotherms, but that these values be verified for the particular area.
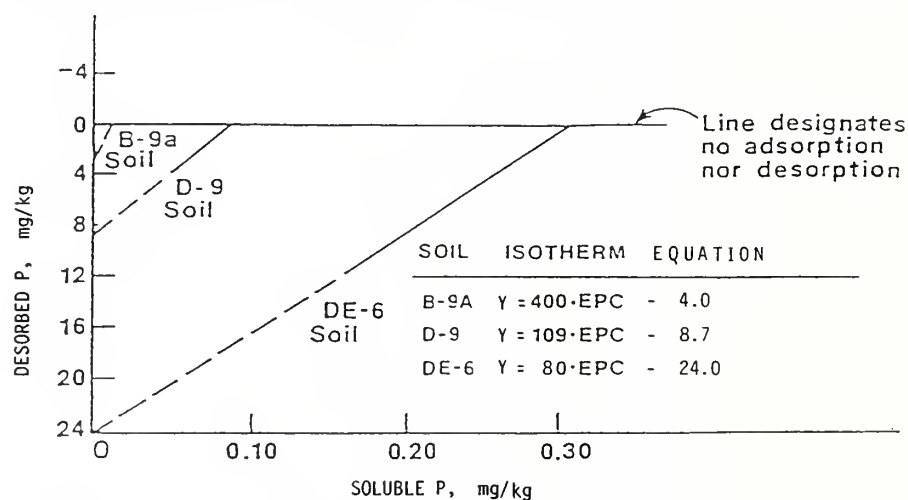
Figure 1
Phosphorus sorption isotherms and their pertinent features, as determined for three Schuylkill soils from the Mahantango watershed, PA.

Governing Equation

Examination of the P sorption isotherms previously determined for soils of the Mahantango watershed and covering a range of P enrichment levels showed that a single equation could be derived to relate all of the isotherms (Kunishi and Pionke, 1985). The equation was thus called the controlling, or governing, equation. Derivation of this equation may be illustrated with data presented in Figure 1. The EPC and I values for the three soils are plotted as shown in Figure 2, and the equation for the line is then derived. For the family of isotherms to which the three soils belong, the governing equation is

$$Y_{ge} = 69.3 * EPC + 3.2 \qquad (2)$$

where Y_{ge} is in milligrams P per kilogram sediment and EPC is in milligrams P per kilogram solution. By using this equation, the sorption isotherm of any soil or sediment mixture within the Mahantango watershed can be predicted so long as either its I or EPC value is known. As will be shown later, this condition is met in the P algorithm, so use of the governing equation greatly reduces the number of computations that would otherwise be required. The coefficient and constant of the governing equation can vary from one watershed to another if the watersheds differ substantially in soil mineralogy or particle-size distribution of the materials they erode. In fact, we observed that governing equations, while mostly linear, were different for each of several watersheds studied (Kunishi and Pionke, 1985); therefore a governing equation must be determined for each watershed being modeled.
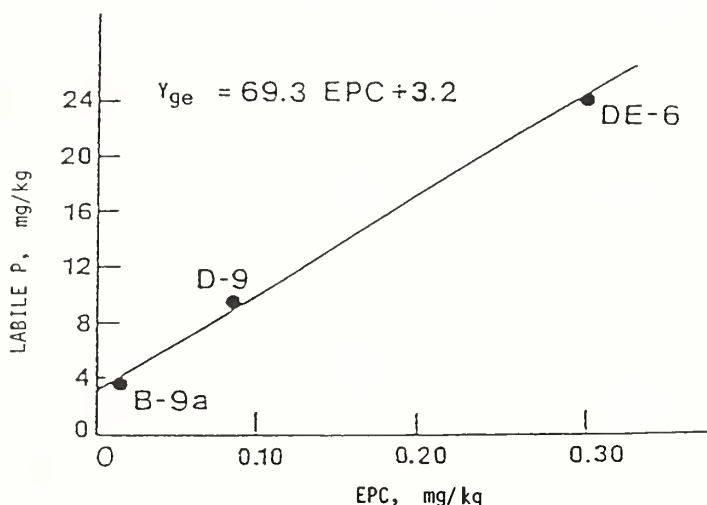
Figure 2
Governing equation for the Mahantango watershed soils as determined from the isotherms shown in Figure 1.

P Fixation Coefficient

Griffin and Hanna (1967) and Peck et al. (1971) reported that for New Jersey and Illinois soils, respectively, between 2 and 10 units of fertilizer P had to be added to raise the value of soil extractable P by one unit. Kunishi et al. (1972) reported that in the Mahantango watershed, significant amounts of solution P were sorbed by sediment and made nonlabile. These reports show that P fixation can be sizable and must be accounted for. In the P algorithm, P fixation is defined specifically as the loss of labile P in a channel segment. Thus, P fixation can occur when a P-poor sediment mixes either with a sediment rich in labile P or with an inflow containing a high concentration of P. As will be shown later, the P algorithm computes the amount of P fixation that occurs under these conditions through the use of a P fixation coefficient (FRACFX). This coefficient can be estimated experimentally for a watershed by mixing a high-P soil with a low-P soil according to Taylor and Kunishi (1971). The calculated amount of P fixed is proportional to the product of the difference in I values for the sediments and the fixation coefficient.

The reverse of P fixation--P release from fixed sites--can occur also. P release is expected to be considerably smaller in magnitude than P fixation, but it too is accounted for in the P algorithm. This is done through use of the governing equation.

Soil Specific Surface

Erosion and sediment deposition are processes that are influenced by particle size. That is, it is usually the finest soil particles that are the most likely to escape redeposition in stream beds. Also, concerning particle size,

the labile P concentration of a given soil or sediment sample increases with decreasing particle size when expressed, as conventionally done, in milligrams P per kilogram of sample. Evidence for these effects of sediment transport processes on particle size and P concentration has been provided by Menzel (1980) and Sharpley (1980), who reported that labile P content was higher for transported sediments than for the soils they derived from.

The governing equation relationship discussed earlier (equation 2) was based on labile P expressed in units of milligram P per kilogram sediment and relates EPC to I values of sediments with the same particle size distribution. When the particle size distribution changes, as noted above, the EPC and I (labile P) relationship in the governing equation is affected. If the governing equation is to be unaffected by changes in particle size distribution of the sediment particles, the labile P concentration of the sediment must be expressed in terms of surface area of the sediment. When this concentration is expressed in milligrams P per square meter of sediment, the sorption isotherm changes only with changes in the P enrichment level of the sediment, and the governing equation for the Mahantango watershed becomes

$$Y_{ge} = 0.191 * EPC + 0.009 \tag{3}$$

Because data on sediment loads are obtained in mass units (kg) of sand, silt, and clay, they are first converted to specific surface units, (SS, m^2/kg), by the following equation (Young and Onstad, 1976)

$$SS = 1000 \ (2.0 * \% \ clay + 0.4 * \% \ silt + 0.005 * \% \ sand) \tag{4}$$

where SS units (m^2/kg) multiplied by total mass of sediment yield surface area units (m^2). The relationship shown in equation 4 was developed specifically for kaolinite clay mineral which has no internal surface. This is consistent with P adsorption on edge surfaces and not at interlayer locations.

OPERATION OF THE ALGORITHM

The algorithm operates on a segmented stream, with each segment bounded by nodes. A node is defined as the site of a hydrologic event that may result in a net P addition to or deletion from the stream. With only a few exceptions, only one such event is allowed for each segment. Moreover, the chemical reactions and mixing at the node are assumed to be complete before the reactions and mixing at the next node downstream take place.

The program for the algorithm is written in BASIC for a Wang computer and has five options for entering data on the type of hydrologic event occurring at a given node (see appendix for definition of terms used in the program). Each option is used for a specific type of event, as shown in the following tabulation:

Option No.   Event

   1. Mixing of sediment plus water from each of two sources.
   2. Resuspension of sediment (gain of sediment) without loss or gain of water.
   3. Loss of water, as groundwater, without loss or gain of sediment.
   4. Gain of water, from groundwater, without loss or gain of sediment.
   5. Deposition of sediment (loss of sediment) without loss or gain of water.

For option 1 the sources of the sediment and water may be two fields, two channels, or a field and a channel. Regardless, they are designated as fields A and B. After data entry, the computer automatically designates the source with the higher EPC as field B. For options 2-5, the convention is to designate the stream segment entering the node as field A and the hydrologic or sediment change occurring at the node field B. If sediments are involved, however, the computer is programmed to automatically designate the source with the higher EPC as field B.

As applicable to the hydrologic or sediment change, the computer calculates total P entering the node (PIN) from the sum of sediment P (PSED) and solution P (PSOL); within-node P redistribution, gain, or loss due to the amounts of P fixed (PFIXED), deposited (PDEP), resuspended (PRESUS), or lost or gained via groundwater (PGW); and total P leaving the stream node (POUT) from the sum of sediment P (PSED) and solution P (PSOL). PFIXED is calculated by difference

$$PFIXED = PIN + PDEP + PGW + PRESUS - POUT \qquad (5)$$

Although the P algorithm operates as a complete subroutine, input and output data can be transferred as needed to other SWAM subroutines. These subroutines are (1) input of hydrologic and erosion files to the P algorithm at each node from the hydrologic and erosion submodels (Alonso, 1985); (2) input of field or source-area chemical information from CREAMS2 (Smith and Knisel, 1985) at each node; (3) transfer of the P data files used to compute P transport, gain, and losses from node to node; and (4) output of computed P data compiled at each node to the model user.

In the discussion that follows, a specific example is presented to show the operation of the P algorithm. In the example, the hydrologic event is the mixing of sediment and water from two source areas. This type of event was chosen because it is computationally the most involved. The computations are made sequentially according to three mixing steps:

1. Mixing of the two sediments only, the computations accounting for the redistribution of sorbed P between the sediments after correcting for any P fixation. Since the liquid phase is not considered in this step, the P concentration obtained for the mixture of sediments is still tentative and is so indicated by the prefix "UA."
2. Mixing of the two solutions only, the computations accounting for the P concentrations of the combined solutions.
3. Mixing of the combined sediments and combined solutions, the computations accounting for the final (equilibrium) distribution of P between the two phases.

The computations for the three mixing steps are presented below, and a typical printout for an option-1 type hydrologic event is presented in the appendix.

Step 1. In step 1, the computer calculates a tentative value for the labile P concentration of the end sediment mixture (UACSED, or the I value of the sorption isotherm, expressed in mg P/m^2) from the labile P concentrations (CSEDA and CSEDB) of the component sediments, A and B. To make this calculation the computer simulates the mixing of the sediments according to one of two schedules that make up the sediment mixing scheme. Schedule A/B is used when the surface area of sediment A (MA) is larger than the surface area of sediment B (MB), and schedule B/A when MB is larger than MA. In either schedule, the sediment with the higher labile P concentration is called sediment B. Also in either schedule, a sediment mixture containing equal parts of A and B is first made; then, as necesseary through successive "backcrossing" operations, the mixture is enriched in one component (i.e., A in schedule A/B and B in schedule B/A) until the composition of the end mixture is obtained. For example, if the end mixture consists of 7 parts B and 1 part A (expresed as product 7B-A), schedule B/A is used, and the following series of operations are carried out:

1. 1 unit B + 1 unit A ----> 2 units B-A
   (where ratio of MB/MA in product = N = 1)
2. 2 units B + 2 units B-A - -> 4 units 3B-A
   (where N = 3)
3. 4 units B + 4 units 3B-A ---> 8 units 7B-A
   (where N = 7)

At the same time that the mixing operation is being simulated, the computer also accounts for any appreciable P fixation taking place by including the FRACFX term in the equations shown in Table 1. The number of equations used in a mixing schedule depends on the value of N or N', a maximum of four equations being used in schedule B/A (N > 7) and of two equations in schedule A/B (N' > 1).

After calculating UACSED, the computer uses it in the governing equation to calculate a corresponding tentative EPC value, which is called UAEPCX (mg/kg):

$$UACSED = 0.191 * UAEPCX + 0.009 \qquad (6)$$

Together, UACSED and UAEPCX define the parameters of the sorption isotherm of the end mixture when it is in equilibrium with the solution phase (step 3):

$$CSEDX = (UACSED/UAEPCX) * EPCX - UACSED \qquad (7)$$

where CSEDX is the labile sediment P concentration of the end mixture (mg P/kg solution). This equation is one of two simultaneous equations to be solved in step 3.

Table 1
Equations used to calculate the labile P concentrations (I values of sorption isotherms) for sediment mixtures prepared according to mixing schedules B/A and A/B from sediments A and B[1] [2].

Value of N or N[3]	Equation(s) used	Equation number
Schedule B/A		
N = 1	I1 = (IA + (IB - (IB - IA) (FRACFX)))/2	1
3 > N > 1	I1 = (IA + (IB - (IB - IA) (FRACFX)))/2	1
	IN = (2I1 + (N - 1) (IB - I1)(FRACFX)))/(N + 1)	2
7 > N > 3	I1 = (IA + (IB - IA)(FRACFX)))/2	1
	I3 = (2I1 + (3 - 1)(IB - (IB - I1)(FRACFX)))/(3 + 1)	2
	IN = (4I3 + (N - 3)(IB - (IB - I3)(FRACFX)))/(N + 1)	3
N > 7	I1 = (IA + (IB - (IB - IA)(FRACFX)))/2	1
	I3 = (2I1 + (3 - 1) (IB - (IB - I1)(FRACFX)))/(3 + 1)	2
	I7 = (4I3 + (7 - 3) (IB - (IB - I3)(FRACFX)))/(7 + 1)	3
	IN = (8I7 + (N - 7)(IB))/(N + 1)	4
Schedule A/B		
N' = 1	I1 = (IA + (IB - (IB - IA)FRACFX))/2	1
N' > 1	I1 = (IA + (IB - (IB - (IA)(FRACFX)))/2	1
	IN' = (2I1 + (N' -1)(IA))/(N' + 1)	1'

[1] Equations contain the term "FRACFX," which accounts for any significant P fixation. FRACFX for the Mahantango watershed, Pennsylvania, is 0.55 (Kunishi and Pionke, 1985).

[2] Labile P concentrations expressed in milligrams P per square meter of sediment B.

[3] N = ratio of MB/MA in sediment mixture, and N' = ratio of MA/MB in mixture.

Step 2. In step 2 the computer combines the P inputs of the waters (solutions) associated with sediments A and B and derives a solution P concentration for the combined solutions:

$$CSOLAB = (CSOLA * VA + CSOLB * VB/VA + VB) \qquad (8)$$

where CSOLAB = volume-weighted solution P concentration
VA = volume of solution from source A
VB = volume of solution from source B
CSOLA = solution P concentration of source A
CSOLB = solution P concentration of source B.

The P concentration of the combined solutions (CSOLAB) can be less than, equal to, or greater than the EPCX of the sorption isotherm obtained in step 1. When CSOLAB is less than EPCX, the sediment mixture releases some P to the combined solutions. When CSOLAB is greater than EPCX, the sediment mixture sorbs additional amounts of P from solution. To determine the direction of labile P movement, if any, between the sediment mixture and solution when these two phases mix and to also calculate the amount of labile P involved in such a movement (step 3), a second relationship must be defined in terms of CSOLAB and the relative quantities of solution and sediment (solution:sediment ratio, SSR). This ratio is the slope of a line that intersects the sorption isotherm obtained in step 1-- CSEDX = (UACSED/UAEPCX) * EPCX - UACSED--at a common EPCX point. Sharing the same X and Y axes as this isotherm, the line intersects the X axis at CSOLAB (i.e., CSEDX = 0) and the Y axis at SSR * CSOLAB (i.e., CSOLAB = 0). Thus, the second simultaneous equation to be used in step 3 is

$$CSEDX = SSR * CSOLAB - SSR * EPCX \qquad (9)$$

Step 3. In this step, the two equations CSEDX = (UACSED/UAEPCX) * EPCX - UACSED and CSEDX = SSR * CSOLAB - SSR * EPCX are solved simultaneously for EPCX, where EPCX is the solution P value at the intersection of these two equations. This EPCX value is then used in the governing equation to calculate CSEDX. The process of combining sediments and solutions from sources A and B is now complete.

Once both EPCX and CSEDX are obtained, PSOLX AND PSEDX can be calculated. EPCX is the same as CSOLX, and CSOLX multiplied by (VA + VB) yields PSOLX; CSEDX multiplied by MAB yields PSEDX, where MAB is the surface area equivalent of the combined sediments A and B. The sum of PSOLX and PSEDX represents the total labile P, POUT, that exits this channel segment.

REFERENCES

Alonso, C. V. 1985. Chemical flow routing in the SWAM model p. 353-357. In D. G. De Coursey (ed). Proc. Natural Resources Modeling Symposium, Pingree Park, CO, 16-21 Oct. 1983. USDA, Agric. Res. Service, ARS-30.

Alonso, C. V., and D. G. De Coursey. 1985. Small watershed model. p. 40-46. In D. G. De Coursey (ed), Proc. Natural Resources Modeling Symposium, Pingree Park, CO, 16-21 Oct. 1983. USDA, Agric. Res. Service, ARS-30.

Griffin, G. F. and W. H. Hanna. 1967. Phosphorus fixation and profitable fertilization: lime fixation in New Jersey soil. Soil Sci. 103:202-208.

Kunishi, H. M., A. W. Taylor, W. R. Heald, and others. 1972. Phosphorus movement from an agricultural watershed during two rainfall periods. J. Agric. Food Chem. 20:900-905.

Kunishi, H. M. and H. B. Pionke. 1985. The use of sorption isotherms to characterize stream transport of phosphorus in watersheds. p. 146-150. In D. G. De Coursey (ed.), Proc. Natural Resources Modeling Symposium, Pingree Park, CO, 16-21 Oct. 1983. USDA, Agric. Res. Service, ARS-30.

Menzel, R. G. 1980. Enrichment ratios for water quality modeling. Chapt. 12. In CREAMS, a field scale model for chemicals, runoff, and erosion from agricultural management systems. Vol. 3, USDA-SEA-Conserv. Res. Report.

Peck, T. R., L. T. Kurtz, and H. L. Tandon. 1971. Changes in Bray P-1 soil phosphorus test values resulting from applications of phosphorus fertilizer. Soil Sci. Am. Proc. 35:595-598.

Pionke, H. B., H. M. Kunishi, R. R. Schnabel, and others. 1985. SWAM--the chemical models used in the channel system. p. 220-226. In D. G. De Coursey (ed.) Proc. Natural Resources Modeling Symposium, Pingree Park, CO, 16-21 Oct. 1983. USDA, Agric. Res. Service, ARS-30.

Sharpley, A. N. 1980. The enrichment of soil phosphorus in runoff sediments. J. Environ. Qual. 9:521-526.

Smith, R. E. and W. G. Knisel. 1985. Summary of methodology in CREAMS2 model. p. 33-36. In D. G. De Coursey (ed.), Proc. Natural Resources Modeling Symposium, Pingree Park, CO, 16-21 Oct. 1983. USDA, Agric. Res. Service, ARS-30.

Taylor, A. W. and H. M. Kunishi. 1971. Phosphate equilibria on stream sediment and soil in a watershed draining an agricultural region. J. Agric. Food Chem. 19:827-831.

Wolf, A. M., D. E. Baker, H. B. Pionke, and H. M. Kunishi. 1985. Soil tests for estimating labile soluble, and algae-available phosphorus in agricultural soils. J. Environ. Qual. 14:341-348.

Young, R. A. and C. A. Onstad. 1976. Predicting particle-size composition of eroded soil. Transactions of the ASAE 19:1071-1075.

APPENDIX

Glossary of Terms

Terms for Data Entered Into Program

Line No.	Term	Definition	Units	Origin[1]
2	CMAH	Intercept, governing equation	mg/kg	User
3	SLMAH	Slope, governing equation	none	User
4	EPCA	Equilibrium phosphorus concentration, field A	mg/kg	File or user
5	CSEDA	Equilibrium labile P concentration, field A	mg/kg	File or user
6	CLA	Clay mass, field A	kg	CREAMS2 ES (S and K)
7	SNDA	Sand mass, field A	kg	CREAMS2 ES (S and K)
8	SLTA	Silt mass, field A	kg	CREAMS2 ES (S and K)
9	VA	Runoff water volume, field A	kg	CREAMS2 H (S and K)
10	CSOLA	Solution P concentration of VA (at equilibrium = EPCA)	mg/kg	File or user
11	FRACFX	Factor (0-1.0) for computing labile P conversion to nonlabile forms	dimensionless	User
12	FIELDS	No. of input/output units	dimensionless	User
13	EPCB	Same as EPCA except pertains to field B	mg/kg	File or user
14	CSEDB	Same as CSEDA except pertains to field B	mg/kg	File or user
15	CLB	Same as CLA except pertains to field B[2]	kg	CREAMS2 ES (S and K)
16	SNDB	Same as SNDA except pertains to field B[2]	kg	CREAMS2 ES (S and K)
17	SLTB	Same as SLTA except pertains to field B[2]	kg	CREAMS2 ES (S and K)
18	VB	Same as VA except pertains to field B	mg/kg	File or user
19	CSOLB	Same as CSOLA except pertains to field B	mg/kg	File or user

[1] CREAMS2 ES = CREAMS2 erosion-sediment submodel; CREAMS2 H = CREAMS2 hydrology submodel; S and K = Smith and Knisel, (1985).

[2] May be negative if water withdrawal, recharge to groundwater, or sediment deposition.

Other Terms Used in Program

Line No.	Term	Definition	Units
35	MA, MB, MAB	Surface areas of sediment A, sediment B, and sediment A plus sediment B	m^2
37	PSOLA	Amount of solution P entering the node from field A	mg
38	PSOLB	Amount of solution P entering the node from field B	mg
39	PSEDA	Amount of sediment P entering node from field A	mg
40	PSEDB	Amount of sediment P entering the node from field B	mg
41	PIN	Amount of total P entering the node via sediment and solution	mg
47	I1	Sediment P concentration when exactly one part of sediment from field A and one part of sediment from field B, are mixed.	mg/m^2
49	I3	Sediment P concentration when exactly one part of sediment from field A and three parts of sediment from field B are mixed	mg/m^2
54	UACSED	A tentative P concentration calculated for the combined "dry" mixture of sediments from fields A and B; it yields CSEDX when corrected for any P redistribution resulting from mixing of the combined solutions	mg/m^2
55	UAEPCX	A tentative equilibrium P concentration calculated for the combined solutions from fields A and B; it yields EPCX when corrected for any P redistribution resulting from mixing of the combined sediment with the combined solutions	mg/kg
56	CSOLAB	Solution P concentration of mixture of water from source A and source B	mg/kg
57	SSR	Solution to sediment ratio	kg/m^2
59	EPCX	Calculated value of P in solution after solution has equilibrated with sediment; to be reinitialized as EPCA and used in the iteration at the next node	mg/kg
63	CSEDX	Calculated value of the P concentration on sediment after sediment has equilibrated with solution phase; it is to be reinitialized as CSEDA and used in the iteration at the next node	mg/m^2
63	PSEDX	Amount of sediment leaving the node	mg
65	PFIXED	AMOUNT OF P fixed	mg
65	POUT	Amount of total P leaving the node, via sediment and solution	mg
66	PGW	Amount of solution P in groundwater	mg
66	PRESUS	Amount of P resuspended from channel segment	mg
72	VAB	The combined runoff water mass from field A and field B	

Annotations to Program

Lines

Lines	
2-19	Data entered, with source of data as user, file, or CREAMS 2
20-24	Option selected based on hydrologic event
26-33	Sediment units converted from mass (kg) to specific surface (m^2/kg)
34-41	Total P input computed from P input concentrations
42-52	Sediments from fields A and B combined according to schedule B/A
53-55	Sorption isotherm calculated for "dry" sediment mixture
56-57	Solution:sediment ratio derived
58-60	Equations from lines 55 and 57 solved simultaneously for EPCX; CSEDX then calculated from EPCX
61-67	P output calculated
68-73	Resultant P values for sediment and water mixtures assigned to field A
44-47	Sediments from fields A and B combined according to schedule A/B

MODELING THE TRANSPORT OF PHOSPHORUS AND RELATED ADSORBED CHEMICALS:
A KINETIC APPROACH

A. N. Sharpley, L. R. Ahuja and H. B. Pionke

ABSTRACT

A lack of accuracy in predicting nutrient and pesticide transport in runoff
using equilibrium relationships has led to an evaluation of the use of
non-equilibrium functions. Equations describing the kinetics of soil P
desorption were evaluated for a wide range of soils and used to predict
soluble P loss in runoff from several cropped and grassed Southern Plains
watersheds. The constants of a logarithmic equation were related to the ratio
of Fe: or clay:organic C content of acidic soils and $CaCO_3$: or clay:organic C
content of basic calcareous soils. Using these relationships, depth of
surface soil-runoff interaction, runoff volume, and Bray-I available P, the
kinetic equation gave accurate predictions of the soluble P concentrations of
runoff for a range of watershed management practices, soil types, and
vegetative covers. The use of similar kinetic equations to describe the loss
of pesticides and herbicides dissolved in runoff is discussed, along with
future developments of the kinetic approach, which may improve predictions of
the transport of adsorbed chemicals in runoff.

INTRODUCTION

Due to the high cost and long time needed to obtain reliable data on nutrient
and pesticide losses in runoff, increasing efforts are being made to model the
processes associated with their transport in runoff, in conjunction with
existing models for hydrologic and sediment loss (Donigian et al., 1977;
Williams and Hann, 1978; Frere et al., 1980; Leonard and Wauchope, 1980). Two
recently developed models which include phosphorus (P), pesticides, and
herbicides, are the ARM (Agricultural Runoff Management) model (Donigian et
al., 1977) and the CREAMS (Chemicals, Runoff, and Erosion from Agricultural
Management Systems) model (Knisel, 1980). Both these models are physically
based descriptions of the processes involved in chemical transport. Limited
field testing of the ARM and CREAMS models, however, has shown that the
prediction of both adsorbed and solution phase chemicals is not satisfactory
(Donigian et al., 1977; Davis and Donigian, 1979; Frere et al., 1980; Leonard
and Wauchope, 1980).

The importance of partitioning between soluble and particulate (sediment
bound) forms of adsorbed chemicals transported in runoff to the modeling of
these losses is well recognized (Wauchope, 1978; Davis and Donigian, 1979;
Sharpley et al., 1981a; Ahuja et al., 1982b). In the ARM model, first-order
kinetics is assumed to operate between the adsorbed reactions and solution P
forms in soil. Computation of the forward and backward reactions is done
numerically for small time steps (Donigian and Crawford, 1976). The reaction
constants are considered independent of the water to soil ratio. In the
CREAMS model, the kinetics of P release is not invoked, per se. It is assumed
that the soil contains a certain amount of readily soluble P and that the P
buffering capacity of the soil maintains a certain concentration in runoff,
percolating water and the soil water. Ahuja et al. (1982b) tested the above
concepts of the ARM and CREAMS on runoff data for several soils under
simulated rainfall of 30-min duration and 6 cm/hr intensity and found them to
be inadequate. A quasi-empirical higher order kinetic model (Sharpley et al.,
1981b; Sharpley and Ahuja, 1983) was found to be more appropriate.
In the CREAMS model, the release of pesticides from soil is modeled by
assuming a constant partition coefficient between the adsorbed and solution
concentrations at any given time (Leonard and Wauchope, 1980; Steenhuis and
Walter, 1980). In the ARM model, a nonlinear isotherm is taken as the basis
for partitioning (Donigian et al., 1977). In both cases, an instantaneous

Sharpley and Ahuja are soil scientists, Oklahoma State Agricultural Experiment
Station and USDA-ARS, Water Quality and Watershed Research Laboratory, Durant,
OK 74702-1430; respectively; Pionke is research leader, USDA-ARS, Northeast
Watershed Research Laboratory, The Pennsylvania State University, University
Park, PA 16802.

equilibrium between the adsorbed and solution phases is assumed to exist. The field tests of both these models have indicated problems with the partitioning mechanisms employed. Leonard and Wauchope (1980) found that the partition coefficient increased with time. Studies on the movement of pesticides through soil columns have shown that instantaneous equilibrium may be assumed at low water flow velocities but not at high velocities (Van Genuchten et al., 1974; James and Rubin, 1979). The velocities of overland flow are much larger than those of flow through soils. A diffusion controlled kinetic release is more likely to operate. A few laboratory studies on the kinetics of pesticide adsorption and desorption reported in the literature, which were reviewed earlier (Ahuja et al., 1982b), support the above statement. Some detailed experimental studies relating the kinetics of desorption in the laboratory with the release of several pesticides to runoff are needed to verify this.

In the present paper, the application of desorption kinetics in predicting the transport of adsorbed chemicals (P and pesticides) in runoff water is examined. The current state of the art regarding desorption kinetics, the new information available on these processes, and their practical application to field situations will be reviewed and analyzed.

REVIEW OF THE KINETIC MODEL

Simplified kinetic models describing the desorption of soil P have been recently developed. One such model is the modified Elovich equation (Chien and Clayton, 1980):

$$P_d = (1/a) \ln(ba) + (1/a) \ln t \qquad\qquad [1]$$

where P_d is the amount of soil P desorbed (μg P/g soil) in time t (min), and a and b are constants. According to Eq. [1], a plot of P_d versus natural logarithm of time should yield a straight line. More recently, Sharpley et al. (1981b) suggested the following equation to describe the desorption of soil P to water:

$$P_d = KP_o t^\alpha W^\beta \qquad\qquad [2]$$

where W is the water:soil ratio (cm^3/g soil) of the system in which P_d is desorbed, P_o is the initial amount (μg P/g soil) of desorbable or available P present in the soil, and K, α, and β are constants for a given soil. The term P_o does not represent an absolute measure of the desorbable P, since there is a continuous range of energies with which P is held on the soil (Posner and Bowden, 1980). For practical purposes P_o can be represented by an estimate of available P (e.g., Olsen, Bray I, or water extractions) (Sharpley et al., 1981b). Although the value of constant K (Eq. [2]) will vary with the method of estimating P_o, this will not be important as long as one consistent method is used. The important features of Eq. [2], in contrast with Eq. [1], are that factors known to influence the rate of P desorption (P_o, t and W) are included. According to Eq. [2], log P_d is linearly related to log t (slope = α) at any given W and P amendment, and to log, W (slope = β) at any given t and P amendment. In addition, P_d is directly proportional to P_o (slope = $K t^\alpha W^\beta$). Equation [2] gave a reasonably good description of P desorption from several soils and provided similar values of the constants K, α, and β for each soil over a range of t (5 to 180 min), W (10:1 to 1000:1) and P_o (2 to 140 μg P/g soil) (Sharpley et al., 1981b).

The simplified power-form Eq. [2] may be theoretically derived, assuming that P desorption is diffusion controlled and is a case of nonlinear diffusion (Sharpley and Ahuja, 1983). The basic desorption rate equation is formulated as a diffusion equation, with the diffusion coefficient taken as a power function of the fraction of P_o yet to be desorbed. The development utilized some empirical deductions from the literature.

The model (Eq. [2]) was subsequently developed to describe the transport of soluble P in runoff from soil boxes under simulated rainfall of constant rate (Sharpley et al., 1981b), where steady runoff began very shortly after the start of rainfall:

$$\bar{P}_r = \frac{K \, P_o \, S \, t^\alpha \, W^\beta}{V} \qquad [3]$$

where $\bar{P}_R$ is the storm-average soluble P concentration of runoff (μg P/1), t is the storm duration, S is the mass of soil in the interacting zone (g), and V is the total rainfall during the event (cm). For practical field applications, the model would be more useful if rewritten in terms of mean soluble P concentration in runoff per unit area for a certain rainstorm as a function of storm size, average rainfall intensity, slope length, and relevant soil parameters. Equation [3] was, thus, modified by Ahuja et al. (1982a) to:

$$\bar{P}_r = KP_o(EDI \cdot BD) \, (\frac{I + 0.5LQ}{EDI \cdot BD})^\beta \, \frac{V^\alpha - V_i^\alpha}{I^\alpha(V-V_i)} \qquad [4]$$

where EDI is the effective depth of interaction between surface soil and runoff in soluble P transport (cm), BD is the bulk density of soil (g/cm^3), I is the average rainfall intensity during the storm (cm/min), L is the slope length (cm), Q is the average rainfall excess rate available for runoff (cm/min), and V_i is the volume of rainfall that infiltrates into the soil before runoff begins (cm). In Eq. [4], W has been set equal to the term [(I + 0.5LQ)/(EDI · BD)], where 0.5LQ is the average depth of overland flow along the slope length L (cm), and (I + 0.5LQ) represents the total average volume of water per unit area, due to both rainfall and accumulated water, that interacts with soil mass (S = EDI . BD) at any instant of time under steady continuous flow conditions. Details are explained by Ahuja et al. (1982a). Equation [4] is very useful in that it can account for the effects of rainfall intensity, volume, and amount which infiltrates prior to runoff initiation.

The effective depth of interaction (EDI) has been shown to depend upon kinetic energy of the raindrop impact on soil surface, soil slope, slope length, soil surface shaping, and presence of clods at the soil surface (Sharpley et al., 1981a; Ahuja et al., 1982a; Ahuja et al., 1983). Vegetative cover and tillage methods will, thus, change the EDI. At the present stage of modeling, a constant value of EDI may be used for a watershed, but a calibration for the prevailing management system may be necessary to obtain this value.

The kinetic models Eq's. [2] and [4] may also be useful for describing desorption of other adsorbed chemicals, such as pesticides and herbicides, to runoff. The net adsorption of 2,4-D on several different soil minerals (Hague and Sexton, 1968) under conditions of simultaneous opposing reactions of adsorption and desorption was found to be described by the following equation of Faya and Eyring (1956):

$$d\phi / dt = 2A(1 - \phi) \, Sin \, h \, C \, (1 - \phi) \qquad [5]$$

where ϕ is the fraction of the total adsorbable amount that has been adsorbed at any time, and A and C are constants. This equation is similar to Eq. [2] in that the rate of desorption depends upon the distance from equilibrium or the final state and the hyperbolic sine function is similar in shape to a power function. We found that our Eq. [2] was consistent with the experimental data on net cumulative adsorption with time for 2,4-D, isocil or bromocil on different surfaces (Hague and Sexton, 1968; Lindstrom et al., 1970), and for carbaryl and parathion on organic matter (Leenheer and Ahlrichs, 1971).

At the moment, however, application of the equation is restrictive, due to the fact that the constants have to be determined for a given soil prior to their use. It may be possible to estimate values of the model constants from soil physical and chemical properties. Although Chien et al. (1980) observed that

the constants of Eq. [1] (a and b) were related to the reactive Al content of several acid Columbian soils, no information is available for neutral or alkaline soils or for the constants of Eq. [2] (K, α, and β). The following experimental analysis investigates the dependence of the equation constants on soil properties for a wide range of soils and demonstrates their practical application to modeling soluble P losses in runoff from agricultural watersheds.

MATERIALS AND METHODS

Surface samples (0-10 cm) of 60 soils were collected from throughout the United States, encompassing all the soil groups except Histosols. Volcanic ash from from the May 19, 1980, eruption of Mount St. Helens was collected from a 1.5 cm thick deposit. The soils were air dried, sieved (2 mm) and stored until analysis. The location, soil family, and subgroup of the selected soils have been presented by Sharpley et al. (1982a).

The particle size distribution of the soils was determined by pipet analysis (Day, 1965), following dispersion of the samples with sodium hexametaphosphate. Soil pH was measured with a glass electrode using a 5:1 water:soil ratio (weight:weight). Organic carbon was determined by the dichromate wet-combustion method (Raveh and Avnimelech, 1972) and $CaCO_3$ equivalent by the acid-neutralization method of Allison and Moodie (1965). Exchangeable Ca and Al contents were measured by atomic absorption of filtered extracts following end-over-end shaking of 1 g of soil for 2 hours with 1 $\underline{N}$ KCl (Heald, 1965; McLean, 1965). Extractable Fe and Al contents were similarly determined after 10 g of soil was allowed to stand in 100 ml of 1 $\underline{N}$ NH_4OAc (adjusted to pH 4.8) for 2 hours (Olsen, 1965; McLean, 1965).

Bray-1 available P was determined by extracting 2 g of soil with 20 ml of 0.02 $\underline{N}$ NH_4 F and 0.025 $\underline{N}$ HCl for 5 min (Bray and Kurtz, 1945). The extracts were centrifuged (266 $\overline{km}$/s for 5 min) and filtered (0.45 μm). The total P content of the selected soils was determined by extraction of ignited samples with 0.5 $\underline{N}$ H_2SO_4 (Walker and Adams, 1958). Desorption of P from the selected soils was investigated by incubating 25 g of soil with various amounts of P(0-200 μgP/g of soil), added as a solution of K_2HPO_4 at 25 $^{\circ}$C for 4 weeks. The soils were wetted to field capacity and allowed to dry slowly. The soils were rewetted with deionized water when dry. At the end of the incubation period the dry soils were sieved (2 mm). The amounts of P desorbed by distilled water at water:soil ratios of 10:1, 40:1, 100:1, 200:1, 400:1, and 1000:1, on an end-over-end shaker at 25 $^{\circ}$C for 5 min to 180 min, were determined. The constants of the semilogarithmic Eq. [1] (a and b) were determined from the slope (1/a) with intercept [(1/a) ln (b a)] of the linear relationship between P desorbed and logarithm of time (Chien and Clayton, 1980). The constants of the logarithmic Eq. [2] (K, α, and β) were determined from the slope of the linear relationships between log P_d and log t (for α) and log W (for β). Constant K was calculated from the slope of a linear relationship between P_d and initial soil P (P_o) represented by Bray-I available P (Sharpley et al., 1981b).

For all samples, the concentration of P was determined colorimetrically on filtered samples by the molybdenum-blue method (Murphy and Riley, 1962). Acidic or alkaline filtrates were neutralized prior to P determination.

RESULTS AND DISCUSSION

Model Constants

The range, mean, and standard deviation of several physical and chemical properties of the 60 soils and ash are given in Table 1. A wide range of properties is evident. Values of these properties for each soil have been presented by Sharpley et al. (1982a). The range, mean, and standard deviation of the constants of Eqs. [1] and [2], describing the kinetics of P desorption for the soils, are given in Table 2. The constants were not correlated to any single soil property associated with P adsorption or desorption, such as Al, Fe, Ca, clay or organic C content (Table 3). The highest correlation

Table 1
Mean and range of several physical and chemical properties of the
60 soils and ash.

Soil property	Mean	Range
$CaCO_3$, %	1.14	0-3.96
Clay, %	23	6-53
Exchangeable Al, mg/g	0.9	0.2-2.4
Exchangeable Ca, mg/g	1.72	0.09-9.43
Extractable Al, mg/g	5.5	0.9-14.8
Extractable Fe, mg/g	10.3	3.7-38.0
Organic C, %	1.16	0.07-4.93
pH	6.8	5.1-9.1
Bray-I P, μg/g	26.5	2.7-92.6
Total P, μg/g	465	63-1062

Table 2
Mean and range of the constants of the kinetic models (Eq. [1]
and [2]) for the 60 soils and ash.

Constant	Mean	Range
Equation [1]		
a (hr^{-1})	1.03	0.02-5.73
b [g P/(g/hr)]	196.9	10.8-552.0
Equation [2]		
K	0.085	0.016-0.262
α	0.167	0.045-0.319
β	0.551	0.204-0.850

coefficients were between K, α, and β (Eq. [2]) and organic C content although
it explained only 37, 33, and 29%, respectively, of the variation in the
constants. Little improvement on the correlation was obtained when all the
soil properties were used in a multiple regression with the constants (data
not presented).

Table 3
Correlation coefficients of several soil properties and constants of
the kinetic equations [1] (a and b) and [2] (K, α, and β) for the 60
soils and ash.

Soil property	P desorption contants				
	a	b	K	α	β
Exchangeable Al	N.S.	N.S.	N.S.	N.S.	N.S.
Extractable Al	N.S.	N.S.	N.S.	N.S.	N.S.
Extractable Fe	N.S.	N.S.	N.S.	N.S.	N.S.
Exchangeable Ca	N.S.	N.S.	N.S.	N.S.	N.S.
Percent clay	N.S.	N.S.	0.312**	0.308**	0.356**
Organic carbon	N.S.	N.S.	0.606***	0.571***	0.543***

, *   Designate significance (n=61) at the 99.0 and 99.9% levels,
respectively.

N.S.   Not significant

When the soils were grouped into acidic and basic calcareous soils,
significant (at the 99.9% level) relationships were obtained between constants
a and b (Eq. [1]) and extractable Al and $CaCO_3$ equivalent, respectively (Table
4).   Similarly, Chien et al. (1980) observed that the constants a and b were
significantly related (at the 99.9% level) to the reactive Al content of
several acid Columbian soils.

Table 4
Relationship between constants a and b (Eq. [1]) and extractable Al
and $CaCO_3$ equivalent of acidic and basic calcareous soils, respectively.

Regression equation	r^+
Acidic soils - pH < 7.0 (n=43)	
$\quad a = 21.317 \text{ Ext Al}^{-2.235}$	0.74
$\quad b = 31.301 \text{ Ext Fe} - 49.917$	0.76
Basic calcareous soils - pH > 7.0, $CaCO_3$ > 0.0 (n=18)	
$\quad a = 1.501 \text{ CaCO}_3^{-1.168}$	0.68
$\quad b = 118.362 \text{ CaCO}_3^{-0.950}$	0.70

[+]   All relationships were significant at the 99.9% level.

The values of constants a and b given in Table 2 were calculated from P
desorbed at a water:soil ratio of 40:1 and P addition of 100 μ g P/g soil. A
decrease in the value of a and increase in b was calculated from the amounts
of P desorbed with an increase in water:soil ratio and soil P addition (Fig.
1).   Bernow fine sandy loam is given as an example, with the other soils
behaving similarly.

Because the solution:soil ratio can change rapidly during interaction between the surface soil and runoff and fertilizer P applications will change soil P status, the effect of water:soil ratio and P addition on P desorption must be accounted for in water quality models. Consequently, use of the modified Elovich equation (Eq. [1]) is impractical for describing soil P desorption to runoff, as the constants change with water:soil ratio and P addition unless these two parameters are included. The use of the log-log model (Eq. [2]) is preferred, as the effect of water:soil ratio and P addition on P desorption is accounted for, and the parameters K, α, and β are constant for a given soil.
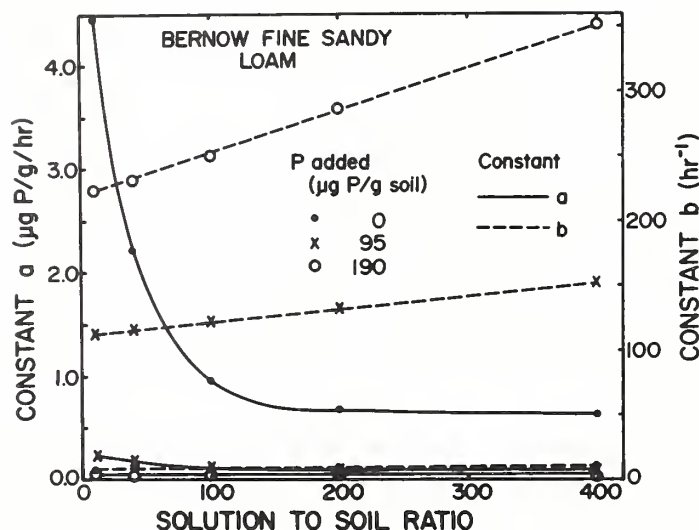
Figure 1
Constants a and b of Eq. [1] as a function
of solution:soil ratio and soil P addition
for Bernow fine sandy loam.

The constants of Eq. [2] were highly correlated with the extractable Fe:organic C content ratio of the acidic soils (Fig. 2) and CaCO₃ equivalent:organic C content ratio of the basic calcareous soils[3] (Fig. 3). Similar relationships were obtained between the ratio of clay:organic C content and equation constants for both acidic and basic soils (data not presented). The ratio of extractable Fe:, CaCO₃:, or clay:organic C content is used in this case to represent the interactive surface area of a soil, involved in P adsorption and desorption. In this respect, the most interactive soil surfaces are those of sesquioxide or mineral nature (Larsen and Widdowson, 1970; Sharpley et al., 1982a) and the least interactive are those of organic matter (Dalton et al., 1952; Moshi et al., 1974; Singh and Jones, 1976). Consequently, the effective surface area, which is interactive, may be correlated with the ratio of percent clay, extractable Fe, or CaCO₃ and organic C content. Since extractable Fe content is not usually available from soil survey analyses, percent clay was used so that Eq. [2] may have wider application.

Constant K (Eq. [2]) represents a P desorbability (or capacity) term expressing the proportion of available P (P_o) that can be desorbed from a soil under given t and W conditions. An increase in the value of K indicates that the proportion of P_o desorbed from a soil will increase. This may be attributed to a decrease in the P adsorption capacity of a soil, which is consistent with the data of Fig. 4, where a decrease in clay:organic C represents a decrease in interactive surface area. Constant α (Eq. [2]) represents a P desorption rate term, such that with an increase in α the rate of P desorption will increase. With a decrease in the clay: organic C ratio, representing a decrease in interactive surface area and thus P adsorption, desorption of added P will increase. Constant β (Eq. [2] represents a P buffering (or intensity) term, in that as β increases, dilution of the interacting soil and water has a greater effect on P release. This is consistent with the data in Fig. 4, where a decrease in clay:organic C represents a decrease in the sorption of added P, and thus dilution will less affect P desorption.
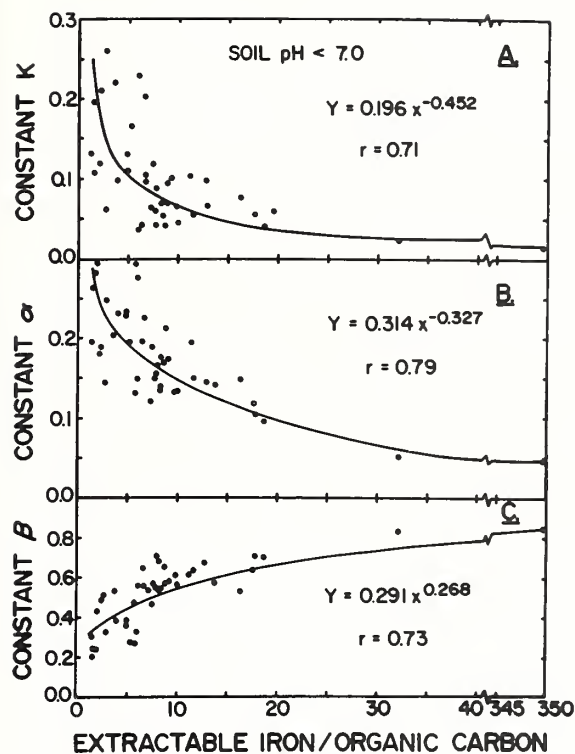
Figure 2
Relationship between the constants
of Eq. [2] and the ratio of
extractable iron:organic carbon
content of the acidic soils.
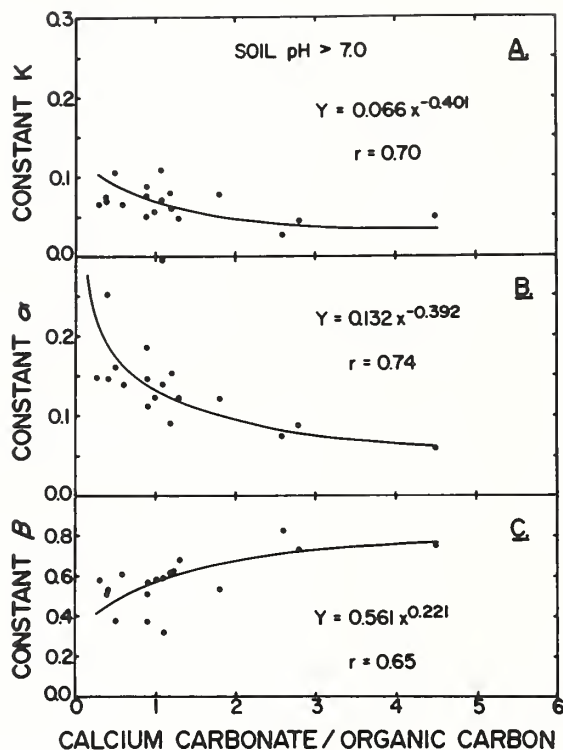
Figure 3
Relationship between the constants
of Eq. [2] and the ratio of calcium
carbonate:organic carbon content of
the basic calcareous soils.
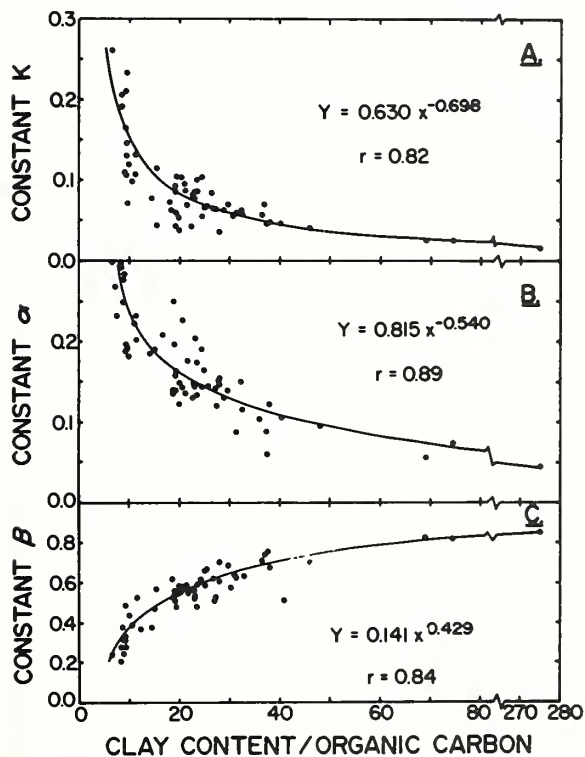
Figure 4
Relationship between the constants
of Eq. [2] and the ratio of clay:
organic carbon content of the 60
soils and ash.

A similar relationship between interactive surface area of a soil, represented by the calculated specific surface of a soil and a measure of pesticide adsorption, and the partition coefficients (K_d) of several pesticides between soil and water phases was found for a range of soils (Harris and Sheets, 1965; Upchurch et al., 1966; Mustafa and Gamar, 1972; Pionke and DeAngelis, 1980). For general field application of Eq. [2], therefore, the constants K, α, and β for a given soil can be calculated from percent clay:organic C content using the following relationships:

$$K = 0.630 \text{ (percent clay:organic C)}^{-0.698} \qquad [6]$$

$$\alpha = 0.815 \text{ (percent clay:organic C)}^{-0.540} \qquad [7]$$

$$\beta = 0.141 \text{ (percent clay:organic C)}^{0.429} \qquad [8]$$

Field Application of the Kinetic Model

Phosphorus

The soluble P concentration of runoff from several Southern Plains watersheds was predicted using Eq. [3]. Equation [4] was not used due to a lack of soil and rainfall data. Detailed descriptions of the watersheds discussed are given by Sharpley et al. (1982) and the parameters of Eq. [3] for each major soil type at each watershed location are presented in Table 5. Values of the constants K, α, and β were calculated from the percent clay:organic carbon content using Eqs. [6], [7], and [8], respectively. Storm duration, t, was set at 30 min, an approximate value for an average storm size. Actual storm duration data were not available. The effective depths of interactions used in the present testing were measured with simulated rainfall (6 cm/hr) and a fine screen covering the soil to simulate vegetative cover (Sharpley et al., 1981a). Bulk densities were obtained from field measurements. Annual runoff volume and available P (Bray-1) content of surface soil (0-1 cm depth) from the watersheds used in Eq. [3] are given in Table 6. Available P content was measured in March each year. Runoff volume was used in Eq. [3] and not rainfall volume, since the amount of rainfall infiltrating the soil before runoff begins is not known.

Soluble P prediction was good over a wide range of concentrations (30-500 μg/l), fertilizer and management practices, soil types, and vegetative covers (Table 7). Predicted concentrations at the El Reno, Bushland, and Woodward watersheds, however, were slightly higher than measured values (Fig. 5). In contrast, predicted concentrations for the Riesel watersheds were generally lower than the measured values (Fig. 5). In the present testing, only one estimate of available P was used each year, due to a lack of field data. The available P content of the surface soil will change during a growing season with fertilizer P addition, plant wash-off and decay, organic P mineralization and formation, plant uptake, and conversion to unavailable forms. It is expected, therefore, that more frequent measurement of available P or interfacing SWAM with models simulating soil P cycling, such as EPIC (Williams et al., 1983), will improve the prediction of soluble P concentration in runoff.

Observed discrepancies between measured and predicted values may also result from the fact that contributions from plant and residue wash-off to soluble P transport in runoff (McDowell et al., 1980; Sharpley, 1981) are not included in the present testing. As only a portion of the incident rainfall leaves a watershed as runoff, predicted soluble P concentrations will have been smaller than those shown in Table 7 if rainfall volume rather than runoff volume had been used in Eq. [3]. In addition, effective depth of interaction between surface soil and runoff was constant for each watershed location in the present analysis. As model application becomes more refined, changes in effective depth of interaction with rainfall and management characteristics may improve the predictions.

Close predictions were also obtained using the P extraction coefficient of the CREAMS model (Sharpley et al., 1982b). The present results indicate, however, that if sufficient soil and rainfall data were available to allow use of Eq. [4], more reliable estimates may be obtained with a wide range in climatic and soil conditions.

Table 5
Parameters used in the kinetic equation (Eq. [3]) to predict soluble P
concentration of runoff from the watersheds.

Location	Major soil type	Kinetic constants			Effective depth of interaction	Bulk density
		K	α	β		
					cm	g/cm^3
Bushland, TX	Pullman cl.	0.113	0.118	0.657	0.030	1.30
El Reno, OK	Kirkland sil.	0.378	0.299	0.313	0.030	1.40
Riesel, TX	Houston Black cl.	0.155	0.150	0.541	0.030	1.35
Woodward, OK	Woodward l.	0.125	0.127	0.619	0.030	1.40

Table 6
Annual runoff and available P content of surface soil from the watersheds.

Watershed location		Runoff[+]				Available P			
		1977	1978	1979	1980	1977	1978	1979	1980
		---------------------- cm ----------------------				------- mg P/g -------			
FR-1	El Reno,	5.10 (2)[¶]	3.98 (2)	6.62 (4)	5.10 (3)	3.5	2.2	2.8	3.2
FR-2	OK	3.02 (2)	2.99 (2)	4.42 (4)	8.35 (6)	1.3	1.8	2.3	10.0
FR-3		4.50 (2)	3.50 (2)	6.40 (4)	6.77 (5)	1.2	1.6	2.7	2.7
FR-4		5.26 (2)	2.56 (2)	4.08 (4)	6.82 (4)	2.4	1.6	5.4	8.3
FR-5		2.48 (2)	1.34 (1)	8.06 (6)	1.90 (6)	1.6	1.3	10.4	2.5
FR-6		--	2.10 (1)	5.46 (6)	0.23 (3)	---	2.2	6.5	2.0
FR-7		1.15 (2)	1.68 (2)	6.75 (9)	1.89 (5)	1.4	2.6	11.5	1.8
FR-8		1.44 (2)	2.67 (2)	3.57 (7)	2.69 (7)	1.5	2.6	4.2	1.7
G-11	Bushland,	---	38.11 (8)	1.60 (1)	2.50 (3)	---	4.4	4.0	2.3
G-10	TX	---	29.15 (8)	3.67 (5)	1.61 (3)	---	6.6	4.1	6.2
G-12		---	33.30 (8)	-- (5)	1.06 (1)	---	6.9	5.0	2.4
W-1	Woodward,	1.58 (3)	5.47 (12)	3.31 (5)	3.41 (1)	2.4	3.1	2.8	2.8
W-2	OK	8.01 (5)	21.06 (15)	20.10 (12)	7.73 (4)	2.6	3.5	3.7	3.5
W-3		2.40 (4)	5.81 (10)	9.45 (6)	2.27 (3)	2.0	2.7	3.1	3.8
W-4		3.77 (3)	11.80 (10)	13.80 (9)	2.73 (6)	2.7	2.9	3.1	3.7
Y	Riesel,	1486 (8)	901.25 (3)	2816 (18)	1140 (8)	6.2	3.8	6.0	7.1
Y-2	TX	493 (4)	469 (2)	1359 (12)	409 (5)	7.0	4.3	5.5	5.9
Y-6		40.57 (3)	31.29 (1)	94.79 (8)	---	2.2	3.2	2.7	4.3
Y-8		40.40 (1)	62.09 (3)	137 (6)	46.47 (4)	2.4	2.7	2.0	5.1
Y-10		---	115.22 (4)	147.6 (9)	15.26 (1)	---	2.6	2.8	2.5
Y-14		18.33 (5)	25.43 (2)	76.08 (14)	30.40 (8)	2.0	3.2	5.8	3.0
W-10		36.30 (1)	62.22 (2)	257.21 (9)	46.50 (2)	3.3	4.8	6.4	2.2
SW-11		11.12 (4)	9.92 (1)	30.27 (11)	11.65 (4)	3.7	4.4	3.3	5.2

+ Number of runoff events each year is given in parenthesis.
¶ Available P content of surface soil (0-1 cm) measured as Bray-I extractable P.

Table 7
Measured and predicted mean annual flow-weighted soluble P concentration of runoff from the watersheds using the kinetic equation (Eq. [3]).

Watershed location		1977 Meas.	Pred.[+]	1978 Meas.	Pred.	1979 Meas.	Pred.	1980 Meas.	Pred.
		------------------------------- µg/l -------------------------------							
FR-1	El Reno,	170	187	145	139	100	125	129	171
FR-2	OK	68	99	104	145	80	135	348	311
FR-3		70	70	80	111	100	123	84	119
FR-4		117	125	104	137	320	336	472	501
FR-5		147	140	104	174	410	405	72	263
FR-6		---	---	203	216	290	331	163	188
FR-7		179	208	211	297	490	506	137	190
FR-8		168	191	181	217	280	286	83	114
G-10	Bushland,	---	---	93	104	171	210	115	138
G-11	TX	---	---	152	171	207	216	420	433
G-12		---	---	148	171	---	---	72	195
W-1	Woodward,	163	212	173	170	170	186	179	184
W-2	OK	95	130	116	121	120	130	140	177
W-3		100	122	100	117	100	97	197	217
W-4		109	138	92	96	90	96	194	213
Y	Riesel,	120	118	90	91	100	85	132	117
Y-2	TX	150	148	90	93	80	73	137	136
Y-6		50	54	70	90	50	45	61	68
Y-8		60	67	50	62	30	32	99	122
Y-10		---	---	30	42	50	41	86	104
Y-14		60	45	60	62	110	68	42	54
W-10		112	102	130	115	80	80	62	60
SW-11		70	80	70	77	30	45	112	108

+ Values predicted using the kinetic equation.
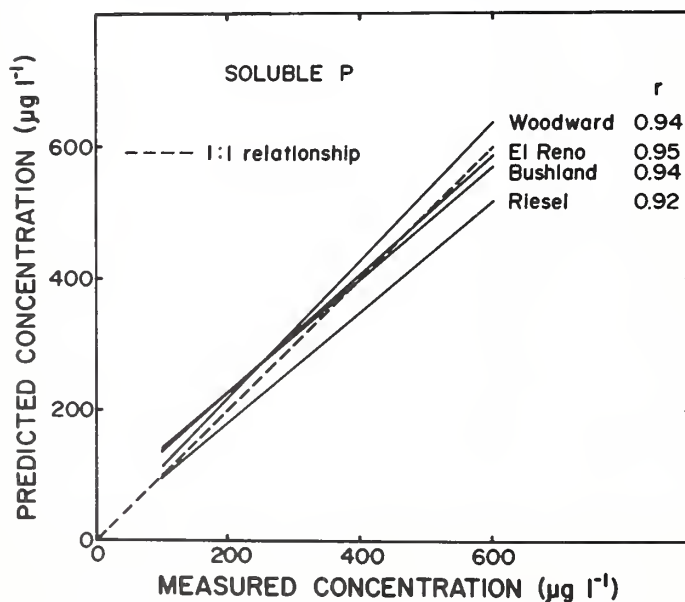
Figure 5
Relationship between measured and predicted (using Eq. [3]) mean annual soluble P concentration of runoff for four watersheds. All relationships are significant at the 95% level.

Pesticide

Unlike the case for P, a lack of experimental studies relating the kinetics of desorption in the laboratory with the release of several pesticides to runoff, precludes model testing. The applicability of the kinetic equation to modeling pesticide release to runoff has been recently discussed by Ahuja et al. (1982b). Using data of Baker et al. (1979) on the movement of propachlor, atrazine, and alachlor in runoff from field plots under simulated rainfall, Ahuja et al. (1982b) observed that a log-log plot of pesticide concentration and time was linear. These data, along with similarly treated data on 2, 4-D losses in runoff (White et al., 1976), are presented in Fig. 6. The linear form of the log-log plot is the same as that observed for P (Sharpley et al., 1981a) and is in agreement with the kinetic model. This is in contrast to a semilog plot of pesticide concentration in runoff as a function of time, which showed a definite curvature (White et al., 1976; Ahuja et al., 1982b). The data suggest, therefore, that kinetic Eq. [2] and its modifications (Eqs. [3] and [4]) may be applicable to pesticide transport in runoff.
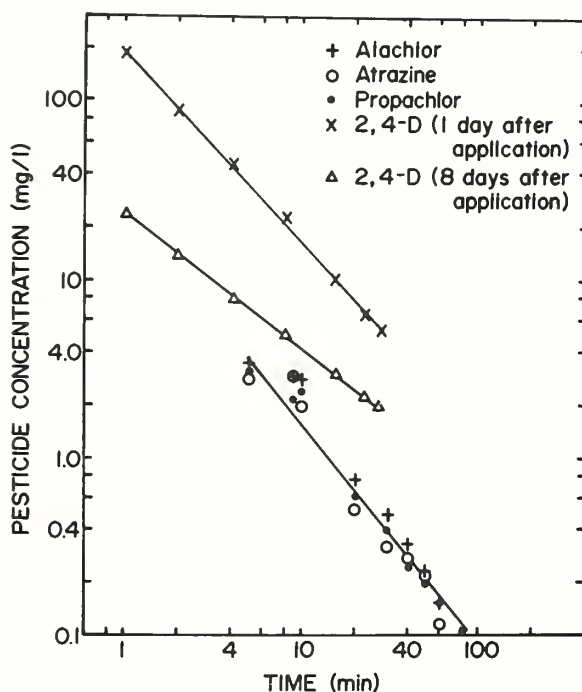
Figure 6
Log-log plot of pesticide concentration in runoff as a function of time during a rainfall event, as a test of the kinetic model. Alachlor, atrazine, and propachlor are from Baker et al. (1979) and 2,4-D) from White et al. (1976).

CONCLUSIONS

A lack of accuracy in predicting nutrient and pesticide transport in runoff using equilibrium relationships has led to an evaluation of the use of nonequilibrium functions. Recently developed equations describing the desorption of soil P as a function of available soil P, water:soil ratio, and reaction time, may, thus, be important to water quality modeling. Research was, therefore, initiated to evaluate the application of desorption kinetics. The findings of this research were:

1. The constants of the modified Elovich equation (a and b, Eq. [1]) were significantly related to the extractable Al and $CaCO_3$ contents of acidic and basic soils, respectively. The constants varied, however, with soil and P status and water:soil ratio of the extracting medium in which they were determined. Consequently, the use of Eq. [1] in modeling adsorbed chemical

transport is limited unless these two parameters are included. As the effect of water:soil ratio and soil P status on P release is accounted for in Eq. [2], its use in water quality models is recommended.

2. The constants of Eq. [2] (K, α, and β) for a given soil may be estimated from the ratio of percent clay and organic C content of the soil using the following relationships:

K = 0.630 percent clay/organic $C^{-0.698}$
α = 0.815 percent clay/organic $C^{-0.540}$
β = 0.141 percent clay/organic $C^{0.429}$

3. The kinetic model of Eq. [3] was used to predict the soluble P concentration of runoff from several cropped and grassed Southern Plains watersheds. Model parameters were determined from laboratory (effective depth of interaction) and field studies (bulk density, runoff volume, and available P) and constants K, α and β calculated with the above relationships. Even though available P (Bray-I) content was measured once a year (March), prediction of mean annual soluble P concentrations of runoff was a good over a wide range of concentrations (30-500 μg/l), fertilizer and watershed management practices, soil types, and vegetative covers.

4. With more frequent estimates of the available P content of surface soil from a watershed, an improved prediction of soluble P concentration is expected.

5. Linear logarithmic relationships between the concentration of pesticide dissolved in runoff and time during a runoff event were obtained for several pesticides. This indicates that the kinetic model describing soil P desorption may also be applicable to pesticide desorption.

6. As the kinetic model incorporates parameters describing the depth of surface soil-runoff interaction, storm size, and runoff water:soil (or suspended sediment) ratio, it is expected to be more versatile in describing adsorbed chemical transport than partition coefficients or equilibrium relationships.

Further research is needed in the following areas to improve model application and prediction:

1. The application of the kinetic model to pesticide desorption should be evaluated with laboratory batch experiments, as used for P. It is hoped that the parameters K, α, and β will be constant for a given soil and pesticide. Several pesticides must be evaluated due to the great variation in pesticide chemistry.

2. The kinetic approach may also be applicable to describing processes occurring after the adsorbed chemical leaves the edge of the field. As reaction time between river or lake sediment and overlying water will be longer than that for surface soil and runoff, equilibrium relationships may be more appropriate. Comparative research is needed, however, to establish which procedure should be used.

3. For application of the kinetic model to a field situation, input data (runoff volume) and parameters (K, α, and β) may be predicted from hydrologic models and soil properties, respectively. Since frequent estimates of available P are needed, models simulating the soil P cycle should be developed and interfaced with SWAM.

4. As plant and residue wash-off can contribute soluble P to runoff, the kinetic equation must be interfaced with relationships estimating these contributions.

5. Sufficient field data must be obtained from watersheds so that the kinetic model may be used on a storm to storm basis and the predicted values compared with measured values. These data must be obtained from a wide area of the country, covering different soil types and land management practices.

REFERENCES

Ahuja, L. R., O. R. Lehman, and A. N. Sharpley. 1983. Bromide and phosphate in runoff water from shaped and cloddy soil surfaces. Soil Sci. Soc. Am. J. 47:746-748.

Ahuja, L. R., A. N. Sharpley, and O. R. Lehman. 1982a. Effect of slope and rainfall characteristics on P released to runoff. J. Environ. Qual. 11:9-13.

Ahuja. L. R., A. N. Sharpley, R. G. Menzel, and S. J. Smith, 1982b. Modeling the release of phosphorus and related adsorbed chemicals from soil to overland flow. In Proc. of Int. Symp. on Rainfall-Runoff Modeling, May 1981, Mississippi State Univ., MS. pp. 463-484.

Ahuja, L. R., A. N. Sharpley, M. Yamamoto, and R. G. Menzel. 1981. The depth of rainfall-runoff-soil interaction as determined by ^{32}P. Water Resour. Res. 17:969-974.

Allison. L. E., and C. D. Moodie. 1965. Carbonate. In C. A. Black (ed.), Methods of soil analysis. Part 2. Agronomy 9:1379-1394. Am. Soc. of Agron., Madison, WI.

Baker, J. L., J. M. Laflen, and R. O. Hartwig. 1979. Effects of corn residue and herbicide placement on herbicide runoff losses. Paper No. 79-2050a, 22 pp., Am. Soc. of Agric. Engr. St. Joseph, MO.

Black, C. A. (ed.). 1965. Methods of soil analysis. Part 2. Agronomy 9:1379-1394. Am. Soc. of Agron., Madison, WI.

Bray, R. H., and L. T. Kurtz. 1945. Determination of total, organic and available forms of phosphorus in soils. Soil Sci. 59:39-45.

Bruce, R. R., L. A. Harper, R. A. Leonard, W. W. Snyder, and A. W. Thomas. 1975. A model for runoff of pesticides from small upland watersheds. J. Environ. Qual. 4:541-548.

Chien, S. H., and W. R. Clayton. 1980. Application of Elovich equation to the kinetics of phosphate release and sorption in soils. Soil Sci. Soc. Am. J. 44:265-268.

Dalton, D., G. Russell, and D. Sieling. 1986. Effect of organic matter on phosphate availability. Soil Sci. 73:173-181.

Davis, H. H., Jr., and A. S. Donigian, Jr. 1979. Simulating nutrient movement and transformations with the ARM model. Trans, of the Am. Soc. of Agric. Engr. 22:1081-1087.

Day, P. R. 1965. Particle fractionation and particle size analysis. In C. A. Black (ed.), Methods of soil analysis. Part 1. Agronomy 9:545-567. Am. Soc. of Agron., Madison, WI.

Donigian, A. S., Jr., and N. H. Crawford. 1976. Modeling pesticides and nutrients on agricultural lands. Report No. EPA 600/2-76-043, 317 pp. Environ. Res. Lab., U.S. EPA, Athens, GA.

Donigian, A. S., Jr. D. C. Beyerlein, H. H. Davis, and N. H. Crawford. 1977. Agricultural runoff management (ARM) model version II: Refinement and testing. Report No. EPA 600/3-77-098, 293 pp. Environ. Res. Lab., U.S. EPA, Athens, GA.

Fava, A., and H. Fyring. 1956. Equilibrium kinetics of detergent adsorption--a generalized equilibration theory. J. Phys. Chem. 60:890-898.

Frere, M. H., J. D. Ross, and L. J. Lane. 1980. The nutrient submodel. Chapt. 4 In Knisel, W. G. (ed.), CREAMS: A Field Scale Model for Chemicals, Runoff, and Erosion from Agricultural Management Systems. Cons. Res. Rep. No. 26, pp. 65-87, U.S. Dept. of Agric., Washington, DC.

Hague, R., and R. Sexton. 1968. Kinetic and equilibrium study of adsorption of 2, 4-dichlorophenoxyacetic acid on some surfaces. J. Colloid and Interface Sci. 27:818-827.

Harris, C. I., and T. J. Sheets. 1965. Influence of soil properties on adsorption and phytotoxicity of CIPC, diuron, and simazine. Weeds 13:215-219.

Heald, W. R. 1965. Calcium and magnesium. In C. A. Black (ed.), Methods of soil analysis. Part 2. Agronomy 9:999-1010. Am. Soc. of Agron., Madison, WI.

James, R. V., and J. Rubin. 1979. Applicability of the local equilibrium assumption to transport through soils of solute affect by ion exchange. Am. Chem. Soc. Symp. Series, N. ASCV061, pp. 225-235.

Knisel, W. G. (ed.). 1980. CREAMS: A Field Scale Model for Chemicals, Runoff, and Erosion from Agricultural Management Systems. Cons. Res. Rep. No. 26, 643 pp., U.S. Dept. of Agric., Washington, DC.

Larsen, S., and A. E. Widdowson. 1970. Evidence of dicalcium phosphate precipitation in calcareous soil. J. Soil Sci. 21:365-367.

Leenheer, J. A., and J. L. Ahlrichs. 1971. A kinetic and equilibrium study of the adsorption of carbaryl and parathion upon soil organic matter. Soil Sci. Soc. Am. Proc. 35:700-705.

Leonard, R. A., and R. D. Wauchope. 1980. The pesticide submodel. Chapt. 5 In Knisel, W. G. (ed.), CREAMS: A Field Scale Model for Chemicals, Runoff, and Erosion from Agricultural Management Systems. Cons. Res. Rep. No. 26, pp. 88-112, U.S. Dept. of Agric., Washington, DC.

Lindstrom, F. T., R. Hague, and W. R. Coshow. 1970. Adsorption from solution. III. A new model for the kinetics of adsorption-desorption processes. J. Phy. Chem. 74:495-502.

McDowell, L. L., Schreiber, J. D., and Pionke, H. B. 1980. Estimating soluble (PO_4-P) and labile phosphorus in runoff from croplands. Chapt. 14. In Knisel, W. G. (ed.) CREAMS: A Field Scale Model for Chemicals, Runoff, and Erosion from Agricultural Management Systems. Vol. III. Supporting Documentation. Cons. Res. Rep. No. 26, pp. 509-533. U.S. Dept. of Agric., Washington, DC.

McLean, E. D. 1965. Aluminum. In C. A. Black (ed.), Methods of soil analysis. Part 2. Agronomy 9:978-998. Am. Soc. of Agron., Madison, WI.

Moshi, A. O., A. Wild, and D. S. Greeland. 1974. Effect of organic matter on the charge and phosphate adsorption characteristics of Kikuyu red clay from Kenya. Geoderma 11:275-285.

Murphy, J., and J. P. Riley. 1962. A modified single solution method for the determination of phosphate in natural waters. Anal. Chim. Acta. 27:31-36.

Mustafa, M. A., and Y. Gamar. 1972. Adsorption and desorption of diuron as a function of soil properties. Soil Sci. Soc. Am. Proc. 36:561-565.

Olsen, R. V. 1965. Iron. In C. A. Black (ed.), Methods of soil analysis. Part 2. Agronomy 9:963-973. Am. Soc. of Agron., Madison, WI.

Pionke, H. B., and R. J. DeAngelis. 1980. Method for distributing pesticide loss in field runoff between the solution and the adsorbed phase. Chapt. 19. In Knisel, W. G. (ed.), CREAMS: A Field Scale Model for Chemicals, Runoff, and Erosion from Agricultural Management Systems. Cons. Res. Rep. No. 26, pp. 607-643, U.S. Dept. of Agric., Washington, DC.

Posner, A. M., and J. W. Bowden. 1980. Adsorption isotherms: Should they be split? J. Soil Sci. 31:1-10.

Raveh, A., and Y. Avnimelech. 1972. Potentiometric determination of soil organic matter. Soil Sci. Soc. Am. Proc. 36:967.

Sharpley, A. N. 1981. The contribution of phosphorus leached from crop canopy to losses in surface runoff. J. Environ. Qual. 10:160-165.

Sharpley, A. N., and L. R. Ahuja. 1983. A diffusion interpretation of soil phosphorus desorption. Soil Sci. 135:322-326.

Sharpley, A. N., L. R. Ahuja, and R. G. Menzel. 1981a. The release of soil phosphorus to runoff in relation to the kinetics of desorption. J. Environ. Qual. 10:386-391.

Sharpley, A. N., L. W. Reed, and D. Simmons. 1982a. Relationships between available soil P forms and their role in water quality modeling. Okla. State Univ. Bull. T157.

Sharpley, A. N., S. J. Smith, and R. G. Menzel. 1982b. Prediction of phosphorus losses in runoff from Southern Plains watershed. J. Environ. Qual. 11:247-251.

Sharpley, A. N., L. R. Ahuja, M. Yamamoto, and R. G. Menzel. 1981b. The kinetics of phosphorus desorption from soil. Soil Sci. Soc. Am. J. 45:493-496.

Singh, B. B., and J. P. Jones. 1976. Phosphorus sorption and desorption characteristics of soil as affected by organic residues. Soil Sci. Soc. Am. J. 40:389-394.

Steenhuis, T. S., and M. F. Walter. 1980. Closed form solution for pesticide loss in runoff water. Trans. of Am. Soc. of Agric. Engr. 23:615.
Upchurch, R. P., Selman, F. L., Manson, D. D., and Kamprath, E. J. 1966. The correlation of herbicidal activity with soil and climatic factors. Weeds 14:42-49.

Van Genuchten, M. T., J. M. Davidson, and P. J. Wierenga. 1974. An evaluation of kinetic and equilibrium equations for the prediction of pesticide movement through porous media. Soil Sci. Soc. Am. Proc. 38:29-35.

Walker, T. W., and A. F. R. Adams. 1958. Studies on soil organic matter. I. Influence of phosphorus content of parent material on accumulation of carbon, nitrogen, sulfur, and organic phosphorus in grassland soils. Soil Sci. 85:307-318.

Wauchope, R. D. 1978. The pesticide content of surface water draining from agricultural fields - A Review. J. Environ. Qual. 7:459-472.

White, A. W., Jr., L. E. Asmussen, E. W. Hauser, and J. W. Turnbull. 1976. Loss of 2,4-D in runoff from plots receiving simulated rainfall and from a small agricultural watershed. J. Environ. Qual. 5:487-490.

Williams, J. R., and R. W. Hann, Jr. 1978. Optimal operation of large agricultural wateshed with water quality constraints. Tech. Rep. No. 96, 152 pp. Water Resour. Res. Inst., Texas A & M Univ., College Station, TX.

Williams, J. R., P. T. Dyke, and C. A. Jones. 1983. EPIC - A model for assessing the effects of erosion on soil productivity. Proc. Third Int. Conf. on State-of-the-Art in Ecology Modeling. May 24-28, 1982. Ft. Collins, CO.

FACTORS AFFECTING EPC MEASUREMENTS AND THEIR RELATIONSHIPS TO P IN RUNOFF

R. C. Wendt

ABSTRACT

The EPC and the slope of the P adsorption isotherm used in determining EPC are useful for assessing relative differences in pollution potential among soils and sediments. Results of EPC determinations for soil are also potentially useful as input parameters for water quality models. However, several factors, including the period and temperature of equilibration, amount of P adsorbed, solution-to-soil ratio, vigor of mixing, microbial activity, type and amount of electrolyte in the equilibrating solution and the extent of particle aggregation will influence the results obtained and, thus, their relationships to P in runoff. If results of EPC determinations are to be used to describe P reactions in runoff, conditions used in determining EPC should approximate those in runoff as closely as possible. Although many of these conditions may be roughly approximated, unaccounted for variations in each are likely to contribute to prediction errors.

INTRODUCTION

The equilibrium phosphate concentration (EPC) is defined for soils and sediments as the dissolved orthophosphate (P) concentration at which no net adsorption or desorption of P occurs (Taylor and Kunishi 1971). It is estimated by extrapolating an experimentally derived segment of P adsorption-desorption isotherm to the dissolved P concentration corresponding to zero change in adsorbed P (Figure 1). Equilibrium phosphate concentrations and slopes of isotherm segments used in EPC determinations have been used extensively as a means of assessing relative differences in pollution potential among soils and sediments (Green et al. 1978, Kunishi et al. 1972, McCallister and Logan 1978, McDowell and McGregor 1980, Reddy et al. 1978, Taylor and Kunishi 1971). The EPC of surface soil has also been shown to be related to the dissolved P concentrations in surface runoff (McDowell et al. 1980). Similar approaches have shown P in runoff to be related to amounts of soil P equilibrating with
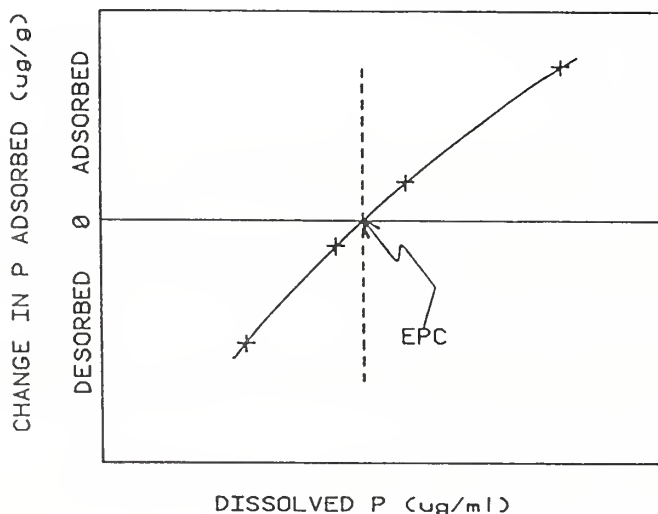
Figure 1.
Typical segment of P adsorption-desorption isotherm from which the EPC is estimated by extrapolation.

Soil scientist, USDA-ARS, Watershed Research Unit, 269 Agricultural Engineering, Columbia, MO 65211. Currently Environmental Scientist, Warzyn Engineering Inc., Madison, WI 53705.

water or dilute electrolyte solutions (McDowell et al. 1980, Sharpley et al. 1982, Sharpley et al. 1978). These results suggest that relatively simple soil analyses, such as the EPC, in combination with the appropriate empirical factor or factors, may be useful for predicting runoff concentrations of dissolved P.

It has been suggested that sediment labile P in runoff is the primary solid-phase P form influencing dissolved P levels and that, except at low sediment concentrations where reaction rates may be limiting, dissolved P concentrations in runoff approach a steady state with sediment labile P (Logan 1980). Under these conditions, slopes of adsorption isotherms used in EPC determinations may be useful for predicting the distribution of total labile P between dissolved and adsorbed forms. Potentially useful approaches have been described by Mulkey and Falco (1977), Steenhuis and Walter (1980), and Haith (1980).

The rate and extent of P adsorption-desorption reactions on soil and sediment depend on several factors, including the period and temperature of equilibration, amount of P adsorbed, solution-to-soil ratio, vigor of mixing, microbial activity, type and amount of electrolyte in the equilibrating solution and extent of particle aggregation. Variations in these factors may influence the values of EPC and isotherm slope obtained and, as a result, their relationships to P in runoff. This paper will briefly discuss several of these factors.

PERIOD OF EQUILIBRATION

The EPC has been shown to be relatively insensitive to the period of equilibration (Taylor and Kunishi 1971, White and Taylor 1977). However, slopes of isotherm segments, such as that illustrated in Figure 1, tend to increase with equilibration time, pivoting approximately on the EPC as adsorption and desorption reactions continue. Hence, slope values, often termed "P buffering capacities", will depend on the equilibration time used.

Rates of P adsorption and desorption on soils and soil constituents are initially rapid, followed by a period of slower reaction rates. The more rapid reactions are usually considered to approach completeness within a few minutes or hours of equilibration (Barrow and Shaw 1975a, Evans and Jurinak 1976, Kuo and Lotse 1972, Muljudi et al. 1966, Ryden et al. 1977), but slower reactions may continue for days or months (Enfield and Bledsoe 1975, Munns and Fox 1976). For many purposes it is useful to place reaction rates into either the fast or slow category. However, this distinction is somewhat arbitrary as there is no apparent boundary between fast and slow reaction rates (Enfield and Bledsoe 1975).

Most runoff events occur over a period of a few hours or less, and, thus, the fast reactions will dominate P adsorption and desorption on soil particles in runoff in most cases. Therefore, for application to runoff systems, EPC measurements should be directed at characterizing the fast reactions. Equilibration times of sufficient length to encompass the majority of fast reactions should provide isotherm slopes useful for estimating a maximum expected buffering capacity. Although the selection of an appropriate equilibration time may be somewhat arbitrary, buffering capacity estimates consistent with observed amounts of P desorbed have been obtained using a 6-hour time period (Taylor and Kunishi 1971).

The fast reactions will not occur instantaneously. Thus, buffering capacities estimated in the above manner will only be useful for predicting the distribution of labile P between dissolved and adsorbed forms in runoff as a steady state between these forms is approached. However, this limitation may not greatly diminish the usefulness of the buffering capacity estimate. It has been suggested that knowledge of P distributions between dissolved and adsorbed forms is of little value prior to the time runoff enters receiving streams (Ryden et al. 1973). Streams (defined as water flowing in a natural channel) represent greatly diluted, different and probably more homogeneous systems in which dissolved and adsorbed P forms are expected to rapidly readjust. In streams, silt- and clay-sized particles, which contain the majority of P adsorbing surface in soils, are considered to travel in the wash load at the velocity of the flowing water (Johnson and Moldenhauer 1970). Under these conditions, a steady state between dissolved and adsorbed P forms should be approached for which the EPC buffering capacity estimates may be applicable.

Appropriate adjustments for any particle sorting which has occurred would be needed.

TEMPERATURE

In describing effects of temperature on P reactions in soils, it is convenient to divide P into three forms (Barrow 1979, Barrow and Shaw 1975a):

dissolved P $\leftrightarrow$ adsorbed P $\leftrightarrow$ firmly held P

Phosphate dissolved in solution is assumed to equilibrate with adsorbed P. Firmly held or nonlabile P is assumed to equilibrate with adsorbed P, but not directly with P in solution. The division of solid phase P between adsorbed and firmly held forms is based primarily on kinetic considerations. Thus, quantities of P in the adsorbed and firmly held categories are somewhat analogous to quantities associated with the fast and slow adsorption-desorption reactions, respectively.

In reviewing the literature describing effects of temperature on P adsorption-desorption reactions, Barrow (1979) has identified three effects: 1) an effect on the equilibration between dissolved and adsorbed P, 2) an effect on the rate of transfer from adsorbed to firmly held forms and 3) an effect on the rate of transfer from firmly held to adsorbed forms. Although increasing temperature increases rates of conversion between adsorbed and firmly held P forms, the effects on forward and reverse rates are approximately equal (Barrow 1979). Hence, the distribution between these forms at equilibrium is relatively insensitive to temperature. However, increasing temperature results in a shift in the distribution between dissolved and adsorbed forms toward the former. An approximately twofold increase in the EPC determined at 25°C compared with that determined at 10°C has been observed for an Australian soil (Barrow and Shaw 1975a).

EPC determinations are usually made using short equilibration times so that dissolved and adsorbed P are the primary forms involved. The above observations indicate that an increase in the temperature of measurement will increase the value of the EPC attained and probably reduce the slope of the isotherm segment used for estimating buffering capacity. Similar effects would be expected with temperature variations in runoff. However, sufficient data are not available to estimate the magnitude of these effects over a variety of soil types.

AMOUNT OF P ADSORBED

Adsorption isotherms relating the change in P adsorbed per unit mass of soil or sediment to dissolved P levels in solution may be approximately linear over short segments such as those used for determining EPC (Taylor and Kunishi 1971, White and Taylor 1977). Over wide ranges of dissolved and adsorbed P, however, adsorption isotherms are typically curved, having positive slopes that decrease with increasing amounts of P adsorbed. Hence, slopes of isotherm segments are expected to decrease with increasing EPC for a given soil (Figure 2). As a result, the usefulness of buffering capacity estimates for predicting the distribution of P between dissolved and adsorbed forms may diminish as dissolved P concentrations out of the range used for EPC measurement are approached. This could occur in runoff with P desorption as sediments are greatly diluted, with P adsorption as P leached from growing or decomposing plants is adsorbed by sediments, or by both mechanisms at stream confluences, where sediments of widely different P saturations and buffering capacities may mix.

Error resulting from extrapolation outside the range of measurement may be partially overcome by using nonlinear adsorption models to describe the relationship between dissolved and adsorbed P forms. However, simple adsorption models, such as the commonly used Langmuir (Equation 1) and Freundlich (Equation 2) equations, may not fully describe P adsorption over wide concentration ranges (Barrow 1978). The reason is that assumptions inherent in their development are oversimplifications of the adsorption process. Thus, some extrapolation error would still be expected. However, these errors, even though substantial, may be small relative to those introduced in the hydrologic or sediment transport models or by the assumptions on spatial variability.
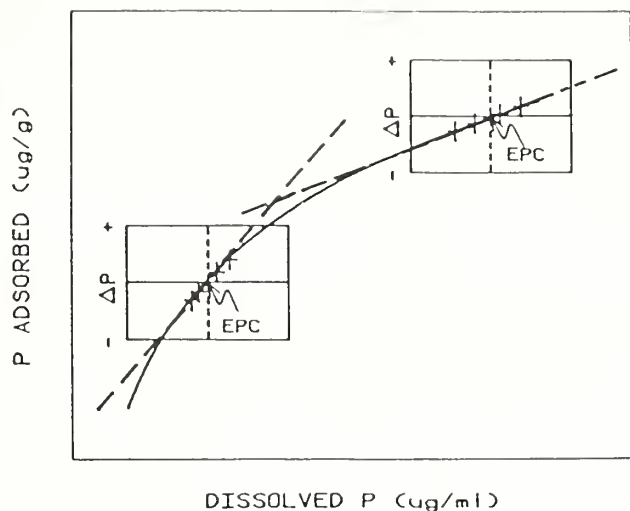
Figure 2.
P adsorption isotherm illustrating changes in P
buffering capacity with EPC.

$$x = a\ x_m\ c/(1 + a\ c) \tag{1}$$

    x = amount of P adsorbed by soil ($\mu g/g$)

    c = P concentration in solution ($\mu g/ml$)

    x_m = P adsorption maximum ($\mu g/g$)

    a = coefficient

$$x = kc^b \tag{2}$$

    x, c = as for equation 1

    k, b = coefficients

Several improvements of the simple models have been proposed. For example,
multisurface Langmuir models (Equation 3) have been developed that better
describe data than the simple Langmuir model (Holford et al. 1974, Syers et al.
1973). Similarly, an improved fit of data to the Freundlich equation has been
obtained by adding a term to account for native labile P (Equation 4) (Fitter
and Sutton 1975, White and Taylor 1977). The improvements, however, usually
have the disadvantage of increasing the number of equation parameters, some of
which are not easily obtained.

$$x = \sum_{i=1}^{n} a_i x_{mi}\ c/(1 + a_i c) \tag{3}$$

    x, c = as for equation 1

    x_{mi} = P adsorption maximum for ith
         adsorption surface

    a_i = coefficient for the ith adsorption
        surface

137

$$x = kc^b - d \qquad\qquad (4)$$

x, k, b, c = as for equation 2

d = native labile P

In comparing adsorption models using 31 Australian soils, Barrow (1978) found the simple Freundlich to be superior to both the simple and two-surface Langmuir models. On two Danish soils, Sibbesen (1981) found the Freundlich equation as modified by Fitter and Sutton (1975) to be superior to the simple Freundlich and the simple and two-surface Langmuir models.

HYSTERESIS

Several researchers have observed P adsorption isotherms to exhibit hysteresis in which less P is desorbed for equivalent changes in P concentration than is adsorbed (Figure 3) (Barrow and Shaw 1975b, Fox and Kamprath 1970, Hingston et al. 1974, Kafkafi et al. 1967, Ryden and Syers 1977). Because the majority of points on the P adsorption isotherm used for determining EPC are derived by making P additions, the implication is that isotherm slopes so determined overestimate the buffering capacity for P desorption. The cause of the hysteresis is thought to be the continued, slow conversion of added P to more firmly held forms that are less readily desorbed (Barrow and Shaw 1975b, Madrid and Posner 1979, Munns and Fox 1976, White and Taylor 1977). When sufficient time for desorption reactions is allowed (Madrid and Posner 1979), or when equilibration times are sufficiently short for slow reactions to be negligible (White and Taylor 1977), adsorption and desorption reactions appear to be essentially reversible. An exception to the latter may be when disequilibrium conditions (within-sample heterogeneity with respect to P) exist in soil due to recent fertilizer P additions or severe depletion of P from localized areas by plant roots. EPC measurements primarily involve the fast reactions, and, in the case of runoff, results are applied to a system in which slow reactions are expected to have a minor effect. Hence, for this application, the assumption of isotherm reversibility should not result in major errors.
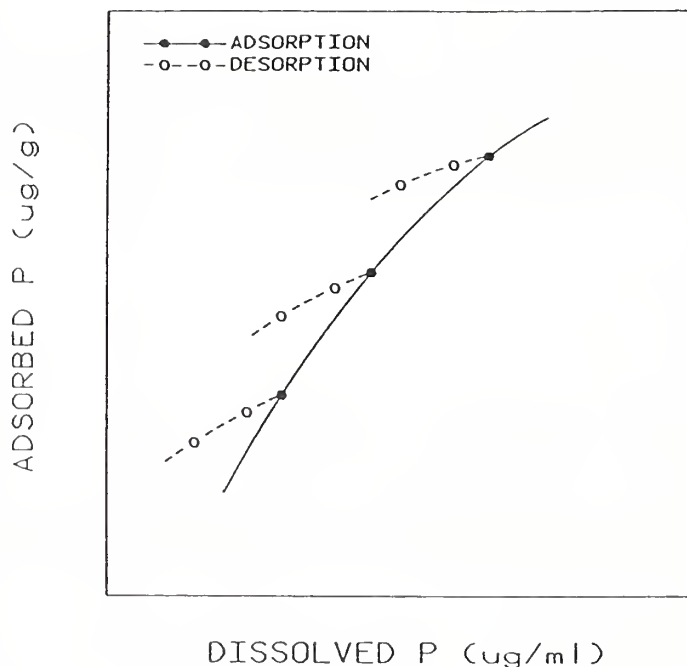
Figure 3.
P adsorption isotherm showing hysteresis frequently observed with subsequent P desorption.

SOLUTION-TO-SOIL RATIO

Phosphate adsorption isotherms have been shown to vary with the ratio of water to soil or sediment, often termed the "solution-to-soil ratio", used in their determination. Hence, relationships between concentrations of dissolved and adsorbed P determined at standard solution-to-soil ratios may often be in error when applied to sediments in runoff over a range of sediment concentrations. The reported effects of solution-to-soil ratio on P adsorption isotherms are, however, inconsistent. In comparing adsorption isotherms at solution-to-soil ratios of 50 to 1 or lower, White (1966) observed greater amounts of P adsorbed per gram of soil at equivalent dissolved P concentrations at higher ratios. This was attributed to the disequilibrium condition of the soil. When soils were allowed to equilibrate in a moist state at constant temperature for extended time periods (>105 days), there was no apparent effect of solution-to-soil ratio on P adsorption isotherms. Neither was there an effect for disequilibrium soils among solution-to-soil ratios of 50 to 1 or greater. Hope and Syers (1976) observed less P adsorbed per gram of soil at equivalent dissolved P concentrations at higher solution-to soil ratios. They attributed this to slower rates of P adsorption at the higher solution-to-soil ratios and indicated that little effect of solution-to-soil ratio on P adsorption isotherms would be expected as equilibrium was approached. More recently, Barrow and Shaw (1979b) concluded that the influence of solution-to-soil ratio on P adsorption was due to the breakup of aggregated soil particles during shaking. At lower solution-to-soil ratios, greater breakup was postulated to occur, which exposed additional sites for P adsorption and increased amounts of P adsorbed. This mechanism is consistent with the observation that dispersion of aggregated soil particles with shaking is more rapid at lower solution-to-soil ratios (Edwards and Bremner 1967). The effect of solution-to-soil ratio on P adsorption isotherms was found by Barrow and Shaw (1979b) to vary with vigor of shaking and soil type, the latter presumably due to differences in aggregate stability between soils.

For application of results of adsorption studies to field soils, Barrow and Shaw (1979b) have recommended that equilibration procedures that minimize particle breakdown be used for soils with aggregates of low stability. Soil particles in runoff, however, have experienced some dispersive forces during detachment and entrainment. Thus, special precautions to minimize breakdown during equilibration may not be appropriate. But because the magnitude of dispersive forces is expected to vary with event, it is not possible to recommend a single solution-to-soil ratio or method of agitation that would be directly applicable in all cases.

MICROBIAL ACTIVITY

The two main ways that microbial activity can affect dissolved P levels and, thus, the determination of EPC, are by 1) biological immobilization of P and 2) the production of acid compounds which solubilize P (Larsen 1967). For short equilibration times, effects of microorganisms are likely to be small. White (1964), however, has suggested that P immobilization may be significant for equilibration times greater than 1 or 2 hours, particularly for soils which have been air-dried. In contrast, Larsen (1967) has suggested that any changes in dissolved P levels due to biological immobilization are likely to be small and well buffered by solid phase P forms. Although organic acids produced by microorganisms have been suggested to have little effect on soil P (Larsen 1967), carbon dioxide produced by microorganisms has been observed to accumulate during 16-hour equilibrations in closed containers, resulting in lowered pH and increased dissolved P levels (Larsen and Widdowson 1964). Carbon dioxide buildup could be prevented by aerating samples with moist air.

In many studies of P reactions in soils, microbial inhibitors such as chloroform or toluene have been included in equilibrating solutions in order to reduce microbial activity. Barrow et al. (1965) compared the effectiveness of the above mentioned plus mecuric chloride and observed that each reduced the amounts of P retained by the solid phase relative to samples receiving no inhibitor, presumably by reducing biological immobilization. However, use of chloroform (Birch 1961, Hedley and Stewart 1982) or toluene (Thompson and Black 1947) may result in the solubilization of P from organic or microbial sources. Thus, there is uncertainty regarding the cause of differences observed with some microbial inhibitors.

Short equilibration times without the use of microbial inhibitors appear to be the most logical way of avoiding effects of microbial activity and any secondary effects of the inhibitors. Potential effects of enhanced microbial activity during equilibration of air-dried soils can be reduced by preequilibrating soils in a moist state. However, the long time periods used by White (1964) will be impractical in most cases. Recently, Barrow and Shaw (1980) observed effects of air drying on P adsorption to be almost eliminated when soils were preequilibrated at 12.5% moisture for 24 hours. This method may be a more practical alternative.

TYPE AND AMOUNT OF ELECTROLYTE

Increasing the concentration of neutral salt in aqueous, supporting solutions increases amounts of P adsorbed by soil and soil constituents (Barrow 1972, Clark and Peach 1960, Rajan and Fox 1972, Ryden and Syers 1975, Wild 1950). Several mechanisms have been proposed to account for this phenomenon, including a constant product of the ion activities of P and the neutral salt cation (Clark and Peach 1960), a kinetic effect which diminishes as equilibrium is approached (Ryden and Syers 1975), a surface complex of Ca with P reducing mutual repulsion of adjacent, adsorbed P ions (Helyar et al. 1976), and reduced electrostatic potentials near the surface of negatively charged adsorbent particles due to increased ionic strength (Barrow et al. 1980). Increasing the concentration of neutral salt can also reduce the solution pH (Rajan and Fox 1972, Ryden and Syers 1975, Ryden et al. 1977), which can influence amounts of P adsorbed. However, Ryden and Syers (1975) suggest that this effect is small relative to changes in P adsorption associated with different concentrations of supporting electrolyte. Differences in P adsorbed among electrolyte solutions of the same ionic strength have been associated with decreased distances between cations and negatively charged surfaces, with those closest resulting in greater P adsorption (Barrow and Shaw 1979a). Specific adsorption of Ca has also been suggested as a factor responsible for increasing P adsorption when Ca salts are employed (Ryden and Syers 1975).

It is clear from these results that the choice of the amount and type of electrolyte in equilibrating solutions will influence the results of EPC determinations. Numerous studies of P adsorption on soils and soil constituents have been performed using an equilibrating solution of 0.01 $\underline{M}$ $CaCl_2$. Calcium is the predominant exchangeable cation in many agricultural soils and, for many soils, this solution is a reasonable approximation of the Ca concentration in soil solution (Olsen and Khasawney 1980). Thus, it may be useful when P concentrations in equilibrating solutions are to be used for estimating dissolved P levels in soil solution. However, lower Ca concentrations are expected in runoff water due to dilution. Moss (1963) has observed Ca concentrations in soil water to decrease rapidly with dilution up to solution-to-soil ratios of approximately 1 to 1 and to decline less rapidly with further dilution. At a solution-to-soil ratio of 100 to 1, Ca concentrations for two acid soils and the Ca plus Mg concentration for a calcareous soil were approximately 1/20 that at a solution-to-soil ratio of 0.4 to 1. Calcium concentrations less than 3×10^{-4} $\underline{M}$ have been reported in runoff (Schreiber et al. 1976, Timmons et al. 1977), but substantially higher concentrations may result if a portion of the runoff water is derived from subsurface flow through calcareous material (Jones et al. 1977).

If results of EPC determinations are to be used for comparing intrinsic differences among soil and sediment samples, a salt concentration, such as 0.01 $\underline{M}$ $CaCl_2$, which is sufficient to damp out effects of naturally occurring salts in nonbrackish or nonsaline systems, is a logical choice. But, for the direct application of results to runoff, this salt concentration will probably be excessive in most instances. Equilibrations in water at sufficiently wide solution-to-soil ratios to avoid the region where Ca concentrations change rapidly with dilution may be more appropriate.

DISCRETE PARTICLE SIZE AND AGGREGATION

Because of greater surface area per unit mass, smaller-sized, discrete soil particles should contain greater quantities of labile P and sites for P adsorption. Hence, they should contribute disproportionately more to the ability of the soil to buffer changes in solution P concentrations than should the larger particles. However, aggregation of the smaller discrete particles

may influence amounts of labile P and P buffering capacity by reducing reaction rates with internal particles. Phosphate adsorption on 0.5-μm aggregates has been shown to be limited to aggregate surfaces during at least the first hour of equilibration (Evans and Syers 1971). Factors limiting rates of P desorption from soil after initial fast reactions, although complex and poorly understood, have been suggested to involve P diffusion within aggregates (Bache and Ireland 1980). Several other studies have implied an effect of aggregation by suggesting that aggregate disruption exposes sites for P adsorption that would not otherwise be accessible (Barrow and Shaw 1975a, Barrow and Shaw 1979b, Beckett and White 1964).

The effect of aggregation on P adsorption has been observed to vary with size of the aggregate. After of 2-hour equilibration period, Alberts et al. (1983) found P buffering capacities for aggregates of similar discrete particle composition to decrease with increasing aggregate size. When compared to buffering capacities for dispersed aggregates, results suggested little effect of aggregation for aggregates less than 50 μm in diameter for the soil studied.

Because smaller-sized particles tend to be eroded preferentially (Neal 1944, Stoltenberg and White 1953), differences in amounts of labile P among sizes of aggregated or dispersed soil particles are important considerations for predicting labile P movement in runoff. Preferential removal of small particles results in sediments having both greater labile P concentrations at equivalent dissolved P levels and greater P buffering capacities than those indicated from EPC determinations on the source soil. It may be possible to obtain appropriate correction factors, termed "enrichment ratios", from relatively simple functions of sediment concentration as is done for total P (Menzel 1980). However, because much of the sediment in runoff may be in the form of water stable aggregates (Alberts and Moldenhauer 1981, Young 1980), predicted enrichment based on changes in the proportion of discrete particles may result in overestimation where aggregation significantly restricts reaction rates on some particles.

OVERVIEW

If EPC determinations are used for making comparisons of P status among samples or as input to empirical predictive models, effects of the above factors on results should not be critical. For the former application, standardized procedures for all samples will eliminate most effects from the comparisons made. For the latter, differences in the EPC associated with methodology will be compensated for in the calibration constants. If results are to be used to describe P reactions in runoff, the conditions of measurement affecting P reactions should approximate those expected in runoff as closely as possible. Although many of these conditions may be roughly approximated, unaccounted for variations in each in runoff are likely to contribute to prediction errors.

REFERENCES

Alberts, E. E., and Moldenhauer, W. C. 1981. Nitrogen and phosphorus transported by eroded soil aggregates. Soil Sci. Soc. Am. J. 45:391-396.

Alberts, E. E.; Wendt, R. C.; and Piest, R. F. 1983. Physical and chemical properties of eroded soil aggregates. Transactions of the ASAE 26:465-471.

Bache, B. W., and Ireland, C. 1980. Desorption of phosphate form soils using anion exchange resins. J. Soil Sci. 31:297-306.

Barrow, N. J. 1972. Influence of solution concentration of calcium on the adsorption of phosphate, sulfate, and molybdate by soils. Soil Sci. 113:175-180.

Barrow, N. J. 1978. The description of phosphate adsorption curves. J. Soil Sci. 29:447:462.

Barrow, N. J. 1979. Three effects of temperature on the reactions between inorganic phosphate and soil. J. Soil Sci. 30:271-279.

Barrow, N. J.; Bowden, J. W.; Posner, A. M.; and Quirk, J. P. 1980. Describing the effects of electrolyte on adsorption of phosphate by a variable charge surface. Aust. J. of Soil Res. 18:395-404.

Barrow, N. J.; Ozanne, P. G.; and Shaw, T. C. 1965. Nutrient potential and capacity I. the concepts of nutrient potential and capacity and their application to soil potassium and phosphorus. Aust. J. Agric. Res. 16:61-76.

Barrow, N. J., and Shaw, T. C. 1975a. The slow reactions between soil and anions: 2. effect of time and temperature on the decrease in phosphate concentrations in soil solution. Soil Sci. 119:167-177.

Barrow, N. J., and Shaw, T. C. 1975b. The slow reactions between soil and anions: 5. effects of period of prior contact on the desorption of phosphate from soils. Soil Sci. 119:311-320.

Barrow, N. J., and Shaw, T. C. 1979a. Effects of ionic strength and nature of the cation on desorption of phosphate from soil. J. Soil Sci. 30:53-65.

Barrow, N. J., and Shaw, T. C. 1979b. Effects of solution: soil ratio and vigour of shaking on the rate of phosphate adsorption by soil. J. Soil Sci. 30:67-76.

Barrow, N. J., and Shaw, T. C. 1980. Effect of drying soil on the measurement of phosphate adsorption. Comm. in Soil Sci. and Plant Anal. 11:347-353.

Beckett, P.H.T., and White, R. E. 1964. Studies on the phosphate potentials of soils III. the pool of labile inorganic phosphate. Plant and Soil 21:253-282.

Birch, H. F. 1961. Phosphorus transformations during plant decomposition. Plant and Soil 15:347-366.

Clark, J. S., and Peach, M. 1960. Influence of neutral salts on the phosphate ion concentration in soil solution. Soil Sci. Soc. Am. J. 24:346-348.

Edwards, A. P., and Bremner, J. M. 1967. Microaggregates in soils. J. Soil Sci. 18:65-73.

Enfield, C. G., and Bledsoe, B. E. 1975. Kinetic model for orthophosphate reactions in mineral soils. USEPA Report (EPA-660/2-75-022).

Evans, R. L., and Jurinak, J. J. 1976. Kinetics of phosphate release from a desert soil. Soil Sci. 121:205-211.

Evans, T. D., and Syers, J. K. 1971. The application of autoradiography to study the spacial distribution of ^{33}P-labelled orthophosphate added to soil crumbs. Soil Sci. Soc. Am. J. 35:906-909.

Fitter, A. H., and Sutton, C. D. 1975. The use of the Freundlich isotherm for soil phosphate sorption data. J. Soil Sci. 26:241-246.

Fox, R. L., and Kamprath, E. J. 1970. Phosphate sorption isotherms for evaluating the phosphate requirements of soils. Soil Sci. Soc. Am. J. 34:902-907.

Green, D. B.; Logan, T. J.; and Smeck, N. E. 1978. Phosphate adsorption-desorption characteristics of suspended sediments in the Maumee river basin of Ohio. J. Environ. Qual. 7:208-212.

Haith, D. A. 1980. A mathematical model for estimating pesticide losses in runoff. J. Environ. Qual. 9:428-433.

Hedley, M. J., and J. W. B. Stewart. 1982. Method to measure microbial phosphate in soils. Soil Biol. and Biochem. 14:377-385.

Helyar, K. R.; Munns, D. N.; and Buran, R. G. 1976. Adsorption of phosphate by gibbsite I. effects of neutral chloride salts of calcium, magnesium, sodium, and potassium. J. Soil Sci. 27:307-314.

Hingston, F. J.; Posner, A. M.; and Quirk, J. P. 1974. Anion adsorption by goethite and gibbsite II. desorption of anions from hydrous oxide surfaces. J. Soil Sci. 25:16-26.

Holford, J. C. R.; Wedderburn, R. W. M.; and Mattingly, G. E. G. 1974. A Langmuir two-surface equation as a model for phosphate adsorption by soils. J. Soil Sci. 25:242-255.

Hope, G. D., and Syers, J. K. 1976. Effects of solution:soil ratio on phosphate sorption by soils. J. Soil Sci. 27:301-306.

Johnson, H. P., and Moldenhauer, W. C. 1970. Pollution by sediment: sources and the detachment and transport processes. In T. L. Willrich and G. E. Smith (eds.), Agricultural Practices and Water Quality pp. 3-20. The Iowa State Univ. Press. Ames, Ia.

Jones, L. A.; Smeck, N. E.; and Wildung, L. P. 1977. Quality of water discharged from three small agronomic watersheds in the Maumee river basin. J. Environ. Qual. 6:296-302.

Kafkafi, U.; Posner, A. M.; and Quirk, J. P. 1967. Desorption of phosphate from kaolinite. Soil Sci. Soc. Am. J. 31:348-353.

Kunishi, H. M.; Taylor, A. W.; Heald, W. R.; Gburek, W. J.; and Weaver, R. N. 1972. Phosphate movement from an agricultural watershed during two rainfall periods. J. Agr. Food Chem. 20:900-905.

Kuo, S., and Lotse, E. G. 1972. Kinetics of phosphate adsorption by calcium carbonate and Ca-kaolinite. Soil Sci. Soc. Am. J. 36:725-729.

Larsen, S. 1967. Soil phosphorus. Adv. Agron. 19:151-210.

Larsen, S., and Widdowson, A. E. 1964. Effect of soil/solution ratio on determining the chemical potentials of phosphate ions in soil solutions. Nature 203:942.

Logan, T. J. 1980. The role of soil and sediment chemistry in modeling nonpoint sources of phosphorus. In M. R. Overcash and J. M. Davidson (eds.), Environmental Impact of Nonpoint Source Pollution, pp. 189-208. Ann Arbor Science, Ann Arbor, Mich.

Madrid, L., and Posner, A. M. 1979. Desorption of phosphate from goethite. J. Soil Sci. 30:697-707.

McCallister, D. L., and Logan, T. J. 1978. Phosphate adsorption-desorption characteristics of soils and bottom sediments in the Maumee River basin of Ohio. J. Environ. Qual. 7:87-92.

McDowell, L. L., and McGregor, K. C. 1980. Nitrogen and phosphorus losses in runoff from no-till soybeans. Transactions of the ASAE 23:643-648.

McDowell, L. L.; Schreiber, J. D.; and Pionke, H. B. 1980. Chapter 14. Estimating soluble (PO_4-P) and labile phosphorus in runoff from croplands. In Vol. III, Supporting Documentation CREAMS-A Field Scale Model for Chemicals Runoff and Erosion from Agricultural Management Systems, pp. 509-533. USDA Conservation Research Report No. 26.

Menzel, R. G. 1980. Enrichment ratios for water quality modeling. In Vol. III. Supporting Documentation CREAMS-A Field Scale Model for Chemicals Runoff and Erosion from Agricultural Management Systems, pp. 486-492. USDA Conservation Research Report No. 26.

Moss, P. 1963. Some aspects of the cation studies of soil moisture I. the ratio law and soil moisture content. Plant and Soil 18:99-113.

Muljudi, D.; Posner, A. M.; and Quirk, J. P. 1966. The mechanism of phosphate adsorption by kaolinite, gibbsite and pseudoboehmite I. the isotherms and the effect of pH on adsorption. J. Soil Sci. 17:212-228.

Mulkey, L. A., and Falco, J. W. 1977. Sedimentation and erosion control implications for water quality management. In Proceedings National Symposium on Soil Erosion and Sedimentation by Water, pp 69-90. Am. Soc. Ag. Eng., St. Joseph, Mich.

Munns, D. N., and Fox, R. L. 1976. The slow reactions which continue after phosphate adsorption: kinetics and equilibrium in some tropical soils. Soil Sci. Soc. Am. J. 40:46-57.

Neal, O. R. 1944. Removal of nutrients from the soil by crops and erosion. J. Am. Soc. Agron. 36:601-607.

Olsen, S. R., and Khasawneh, F. E. 1980. Use and limitations of physical-chemical criteria for assessing the status of phosphorus in soils. In F. E. Khesawneh, E. C. Sample, E. J. Kamprath (eds.), The Role of Phosphorus in Agriculture, pp. 361-410. American Society of Agronomy, Madison, Wisc.

Rajan, S. S. S., and Fox, R. L. 1972. Phosphate adsorption by soils I. influence of time and ionic environment on phosphate adsorption. Comm. in Soil Sci. and Plant Anal. 3:493-504.

Reddy, G. Y.; McLean, E. O.; Hoyt, G. D.; and Logan, T. J. 1978. Effects of soil, crop cover, and nutrient source on amounts and forms of phosphorus movement under simulated rainfall conditions. J. Environ. Qual. 7:50-54.

Ryden, J. C., and Syers, J. K. 1975. Rationalization of ionic strength effects on phosphate sorption by soils. J. Soil Sci. 26:395-406.

Ryden, J. C., and Syers, J. K. 1977. Desorption and isotopic exchange relationships of phosphate sorbed by soils and hydrous ferric oxide gel. J. Soil Sci. 28:596-609.

Ryden, J. C.; McLaughlin, J. R.; and Syers, J. K. 1977. Time-dependent sorption of phosphate by soils and hydrous ferric oxides. J. Soil Sci. 28:585-595.

Ryden, J. C.; Syers, J. K.; and Harris, R. F. 1973. Phosphorus in runoff and streams. Adv. Agron. 25:1-45.

Ryden, J. C.; Syers, J. K.; and McLaughlin, J. R. 1977. Effects of ionic strength on chemisorption and potential-determining sorption of phosphate by soils. J. Soil Sci. 28:62-71.

Schreiber, J. D.; Duffy, P. D.; and McClurkin, D. C. 1976. Dissolved nutrient losses in storm runoff from five southern pine watersheds. J. Environ. Qual. 5:201-205.

Sharpley, A. N.; Smith, S. J.; and Menzel, R. G. 1982. Prediction of phosphorus losses in runoff from Southern Plains watersheds. J. Environ. Qual. 11:247-251.

Sharpley, A. N.; Syers, J. K.; and Tillman, R. W. 1978. An improved soil-sampling procedure for the prediction of dissolved inorganic phosphate concentrations in surface runoff from pasture. J. Environ. Qual. 7:455-456.

Sibbesen, E. 1981. Some new equations to describe phosphate sorption by soils. J. Soil Sci. 32:67-74.

Steenhuis, T. S., and Walter, M. F. 1980. Closed form solution for pesticide loss in runoff water. Transactions of the ASAE 23:615-620.

Stoltenberg, N. L., and White, J. L. 1953. Selective loss of plant nutrients by erosion. Soil Sci. Soc. Amer. J. 16:353-356.

Syers, J. K.; Browman, M. G.; Smillie, G. W.; and Corey, R. B. 1973. Phosphate sorption by soils evaluated by the Langmuir adsorption equation. Soil Sci. Soc. Am. J. 37:358-363.

Taylor, A. W., and Kunishi, H. M. 1971. Phosphate equilibria on stream sediment and soil in a watershed draining an agricultural region. J. Agr. Food Chem. 19:827-831.

Thompson, L. M., and Black, C. A. 1947. The effect of temperature on the mineralization of soil organic phosphorus. Soil Sci. Soc. Am. J. 11:323-326.

Timmons, D. R.; Verry, E. S.; Burwell, R. E.; and Holt, R. F. 1977. Nutrient transport in surface runoff and interflow from an Aspen-Birch forest. J. Environ. Qual. 6:188-192.

White, R. E. 1964. Studies on the phosphate potentials of soil II. microbial effects. Plant and Soil 20:184-193.

White, R. E. 1966. Studies on the phosphate potential of soils IV. the mechanism of the "soil/solution ratio effect". Aust J. Soil Res. 4:77-85.

White, R. E., and Taylor, A. W. 1977. Reactions of soluble phosphate with acid soils: the interpretation of adsorption-desorption isotherms. J. Soil Sci. 28:314-328.

Wild, A. 1950. The effect of exchangeable cations on the retention of phosphate by clay. J. Soil Sci. 4:72-85.

Young, R. A. 1980. Characteristics of eroded sediment. Transactions of the ASAE 23:1139-1146.

INSTREAM WATER TEMPERATURE: PHYSICAL PROCESSES
AND MATH MODELS

Fred T. Theurer

ABSTRACT

The temperatures of water in a stream system are very important in determining
its quality from an environmental perspective. This paper presents analytical
descriptions of the physical processes that affect stream water temperature.
The model that simulates these processes uses solar energy, meteorological data,
and site specific stream characteristics to estimate the flux and movement of
heat through the stream system.

INTRODUCTION

This paper discusses each of the physical processes that affect instream water
temperatures and their mathematical descriptions so that engineers and
scientists can understand the behavior of the model and determine the
applicability of the model, the utility of linking the model with other models,
and the validity of results.

The instream water temperature model incorporates (1) a complete solar model
that includes both topographic and riparian vegetation shade; (2) an adiabatic
meteorological correction model to account for the change in air temperature,
relative humidity, and atmospheric pressure as a function of elevation; (3) a
complete set of heat flux components to account for all significant heat
sources; (4) a heat transport model to determine longitudinal water temperature
changes; (5) regression models to smooth or complete known water temperature
data sets at measured points for starting or interior validation/calibration
temperatures; (6) a flow mixing model at tributary junctions; and (7)
calibration equations and tips to help eliminate bias and/or reduce the probable
errors at interior calibration nodes.

Further information concerning the various model components can be found in the
following sources (see references at end of report):

Tennessee Valley Authority 1972 - Solar radiation and subsequent alternatives

Tennessee Valley Authority 1972 - Heat flux components

Grenney and Kraszewski 1981 - Heat transport

Quigley 1981 - Shade

Information concerning a fully dynamic flow and water temperature model may be
found in Johnson and Keifer (1979). However, the fully dynamic model is not a
network model and has all the execution difficulties associated with dynamic
flow models.

SOLAR RADIATION

The solar radiation model has four parts: (1) extraterrestrial radiation; (2)
correction for atmospheric conditions; (3) correction for cloud cover; and (4)
correction for reflection from the water surface. The extraterrestrial
radiation, when corrected for both the atmosphere and cloud cover, predicts the
average daily solar radiation received at the ground on a horizontal surface of
unit area. Therefore, it is the total amount of solar energy per unit area that
projects onto a level surface in a 24-hour period. It is expressed as a
constant rate of heat energy flux over a 24-hour period even though there is no
sunshine at night and the actual solar radiation varies from zero at sunrise and
sunset to maximum intensity at solar noon.

Soil Conservationist, USDA-SCS-Engineering Division, Cotton Annex, P.O. Box
2890, Washington, D.C. 20013.

Extraterrestrial Radiation

The extraterrestrial radiation at a site is a function of the latitude, general topographic features, and time of year. The general topographic features affect the actual time of sunrise and sunset at a site. Therefore, the effect of solar shading due to hills and canyon walls can be quantified. The time of year directly predicts the angle of the sun above or below the equator (declination) and the distance between the earth and the sun (orbital position). The latitude is a measure of the angle between horizontal surfaces along the same longitude at the equator and the site.

The extraterrestrial solar radiation equation is

$$H_{sx,i} = (q_s/\pi) \ \{[(1 + e \cos\Theta_i)^2/(1-e^2)]\} \tag{1}$$

$$\{[h_{s,i}(\sin\phi \ \sin\delta_i)] + [\sinh_{s,i}(\cos\phi \ \cos\delta_i)]\}$$

where
q_s = solar constant = 1377 $(J/m^2/sec)$

e = orbital eccentricity = 0.0167238 (dimensionless)

Θ_i = earth orbit position about the sun (radians)

ϕ = site latitude for day i (radians)

δ_i = sun declination for day i (radians)

$h_{s,i}$ = sunrise/sunset hour angle for day i (radians)

$H_{sx,i}$ = average daily extraterrestrial solar radiation for day i $(J/m^2/sec)$

The extraterrestrial solar radiation can be averaged over any time period:

$$\overline{H}_{sx} = [\sum_{i=n}^{N} H_{sx,i}]/[N-n + 1] \tag{2}$$

where
$H_{sx,i}$ = extraterrestrial solar radiation for day i $(J/m^2/sec)$

N = last day in time period (Julian days)

n = first day in time period (Julian days)

i = day counter (Julian day)

$\overline{H}_{sx}$ = extraterrestrial solar radiation averaged over time period n to N $(J/m^2/sec)$

The earth orbit position and sun declination as a function of the day of year are

$$\Theta_i = [(2\pi/365) \ (D_i-2)] \tag{3}$$

$$\delta_i = 0.40928 \cos [(2\pi/365) \ (172-D_i)] \tag{4}$$

where
D_i = day of year (Julian days) D_i=1 for January 1 and D_i=365 for December 31

Θ_i = earth orbit position for day i (radians)

δ_i = sun declination for day i (radians)

The sunrise/sunset hour angle is a measure of time, expressed as an angle, between solar noon and sunrise/sunset. Solar noon is when the sun is at its zenith. The time from sunrise to noon is equal to the time from noon to sunset only for symmetrical topographic situations. However, for simplicity, the average of the solar positions at sunrise/sunset is used. Therefore, the sunrise/sunset hour angle (see Figure 1) is

$$h_{s,i} = \arccos \{[\sin\alpha_s - (\sin\phi \sin\delta_i)]/[\cos\phi \cos\delta_i]\} \tag{5}$$

$$\bar{h}_s = [\sum_{i=n}^{N} h_{s,i}]/[N-n+1] \tag{6}$$

where

ϕ ≡ site latitude (radians)

δ_i ≡ sun declination for day i (radians)

α_s ≡ average solar altitude at sunrise/sunset (radians)
α_s = 0 for flat terrain, α_s > 0 for hilly or canyon terrain

$h_{s,i}$ ≡ sunrise/sunset hour angle for day i (radians)

$\bar{h}_s$ ≡ average sunrise/sunset hour angle over the time period n to N (radians)

n ≡ first day of time period (Julian days)

N ≡ last day of time period (Julian days)

i ≡ day counter (Julian day)

It is possible for some sites to be completely shaded from the sun during winter months. This is why snow often lasts on the north slopes of hillsides. Therefore, certain restrictions are imposed on α_s; i.e., $\alpha_s \leq (\pi/2) - \phi + \delta_i$.

The average solar position at sunrise/sunset is a measure of the obstruction of topographic features. It is determined by measuring the average angle from the horizon to the point where the sun rises and sets. The shade model accounts for local sunrise and sunset independently.
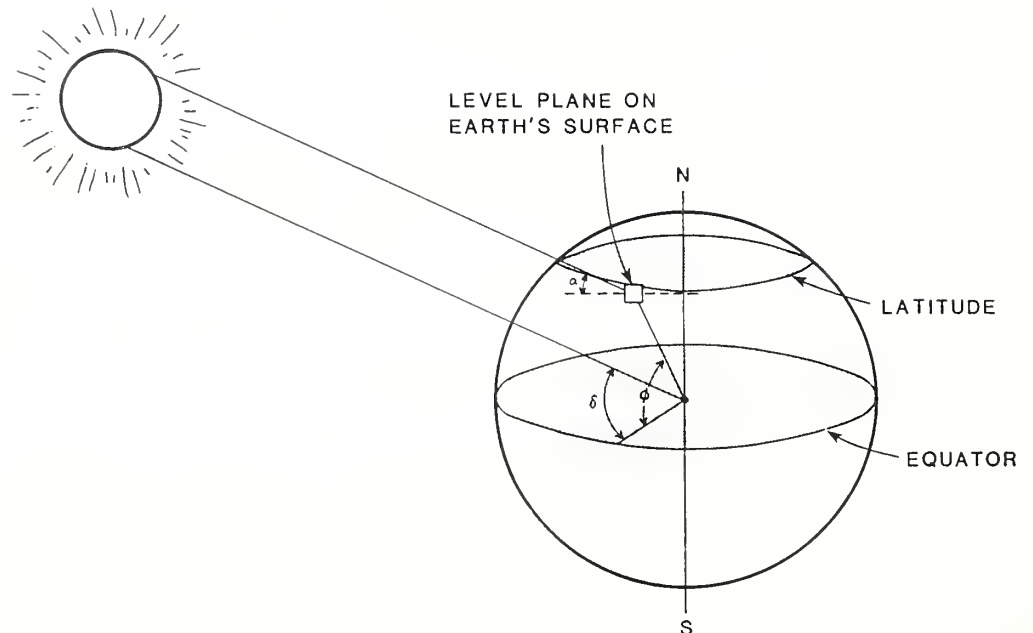
Figure 1. Solar angle measurements.

Sunrise to Sunset Duration

The sunrise to sunset duration at a specific site is a function of latitude, time of year, and topographic features. It can be computed directly from the sunrise/sunset hour angle $h_{s,i}$. The average sunrise to sunset duration over the time period n to N is

$$S_o = (12/\pi) \, \bar{h}_s \tag{7}$$

where

$S_o \equiv$ average sunrise to sunset duration at the specific site over the time period n to N (hours)

$\bar{h}_s \equiv$ average sunrise to sunset hour angle over the time period n to N (radians)

Atmospheric Correction

The extraterrestrial solar radiation is attenuated on its path through the atmosphere by scattering and absorption when encountering gas molecules, water vapor, and dust particles. Furthermore, radiation is reflected from the ground back into the sky, where it is again scattered and reflected back to the ground.

The attenuation of solar radiation due to the atmosphere can be approximated by Beer's law

$$H_{sa} = (e^{-\eta z}) \, H_{sx} \tag{8}$$

where

$H_{sx} \equiv$ average daily extraterrestrial solar radiation ($J/m^2/sec$)

$H_{sa} \equiv$ average daily solar radiation corrected for atmosphere only ($J/m^2/sec$)

$\eta \equiv$ absorption coefficient (1/m)

$z \equiv$ path length (m)

While Beer's law is valid only for monochromatic radiation, it is useful to predict the form of, and significant variables for, the atmospheric correction equation. Repeated use of Beer's law and recognition of the importance of the optical air mass (path length), atmospheric moisture content (water vapor), dust particles, and ground reflectivity result in a useful empirical atmospheric correction approximation:

$$e^{-\eta z} = [a'' + (1-a'-d)/2]/[1-R_g(1-a'+d)/2] \tag{9}$$

where

$a' \equiv$ mean atmospheric transmission coefficient for dust-free moist air after scattering only (dimensionless)

$a'' \equiv$ mean distance transmission coefficient for dust-free moist air after scattering and absorption (dimensionless)

$d \equiv$ total depletion coefficient of the direct solar radiation by scattering and absorption due to dust (dimensionless)

$R_g \equiv$ total reflectivity of the ground in the vicinity of the site (dimensionless)

The two transmission coefficients can be calculated by

$$a' = \exp \{-[0.465 + 0.134 \, w] \, [0.129 + 0.171 \exp (-0.880 \, m_p)] \, m_p\} \tag{10}$$

$$a'' = \exp \{-[0.465 + 0.134 \, w] \, [0.179 + 0.421 \exp (-0.721 \, m_p)] \, m_p\} \tag{11}$$

where

$w \equiv$ precipitable water content (cm)

$m_p \equiv$ optical air mass (dimensionless)

The precipitable water content, w, of the atmosphere can be obtained using the following pair of formulas:

$$(1.0640^{T_d})/(T_d+273.16) = (R_h 1.0640^{T_a})/(T_a+273.16) \qquad (12)$$

$$w = 0.85 \exp(0.110 + 0.0614\ T_d) \qquad (13)$$

where
$T_a \equiv$ average daily air temperature (C)

$R_h \equiv$ relative humidity (dimensionless)

$T_d \equiv$ mean dew point (C)

$w \equiv$ precipitable water content (cm)

The optical air mass is the measure of both the path length and absorption coefficient of a dust-free dry atmosphere. It is a function of the site elevation and instantaneous solar altitude. The solar altitude varies according to the latitude of the site, time of year, and time of day. For practical application, the optical air mass can be time averaged over the same time period as the extraterrestrial solar radiation. The solar altitude function is

$$\alpha_i = \arcsin\{[\sin\phi\ \sin\delta_i] + [\cosh(\cos\phi\ \cos\delta_i)]\} \qquad (14)$$

$$\bar{\alpha} = \{\sum_{i=n}^{N} [(\int_o^{h_{s,i}} \alpha_i\ dh)/h_{s,i}]\}/[N-n+1] \qquad (15)$$

where
$\phi \equiv$ site latitude (radians)

$\delta_i \equiv$ sun declination on day i (radians)

$h \equiv$ instantaneous hour angle (radians)

$h_{s,i} \equiv$ sunrise/sunset hour angle for day i (radians)

$n \equiv$ first day in time period (Julian day)

$N \equiv$ last day in time period (Julian day)

$i \equiv$ day counter (Julian day)

$\alpha_i \equiv$ instantaneous solar altitude during day i (radians)

$\bar{\alpha} \equiv$ average solar altitude over time period n to N (radians)

Equations (14) and (15) can be solved by numerical integration to obtain a precise solution. However, if the time periods do not exceed a month, a reasonable approximation to the solution is

$$\tilde{\alpha}_i = \arcsin\{[\sin\phi\ \sin\delta_i] + [\cos\phi\ \cos\delta_i\ \cos(h_{s,i}/2)]\} \qquad (16)$$

$$\bar{\alpha} \approx [\sum_{i=n}^{N} \tilde{\alpha}_i]/[N-n+1] \qquad (17)$$

where
$\tilde{\alpha}_i \equiv$ average solar altitude during day i (radians)

The corresponding optical air mass is

$$m_p = \{[(288-0.0065Z)/288]^{5.256}\}/$$
$$\{\sin\bar{\alpha} + 0.15[(180/\pi)\ \bar{\alpha} + 3.885]^{-1.253}\} \qquad (18)$$

where
$Z \equiv$ site elevation above mean level (m)

$\bar{\alpha} \equiv$ average solar altitude for time period n to N (radians)

$m_p \equiv$ average optical air mass (dimensionless)

The dust coefficient d and ground reflectivity R_g can be estimated from Tables 1 and 2, respectively, or they can be calibrated to published solar radiation data (Cinquemani et al. 1978) after cloud cover corrections have been made.

Seasonal variations appear to occur in both d and R_g. These seasonal variations can be expressed analytically, resulting in reasonable estimates of ground solar radiation.

The dust coefficients d of the atmosphere can be seasonally distributed by the following empirical relationship:

$$d = d_1 + \{[d_2 - d_1] \sin [(2\pi/365) (D_i - 213)]\} \qquad (19)$$

where
$d_1 \equiv$ minimum dust coefficient occurring in late July - early August (dimensionless)

$d_2 \equiv$ maximum dust coefficient occurring in late January - early February (dimensionless)

$D_i \equiv$ day of year (Julian day); $D_i=1$ for January 1 and $D_i=365$ for December 31

Table 1
Dust coefficient d (Tennessee Valley Authority 1972:2.15)

Season	Washington, DC		Madison, Wisconsin		Lincoln, Nebraska	
--------	$m_p=1$	$m_p=2$	$m_p=1$	$m_p=2$	$m_p=1$	$m_p=2$
Winter	-	0.13	-	0.08	-	0.06
Spring	0.09	0.13	0.06	0.10	0.05	0.08
Summer	0.08	0.10	0.05	0.07	0.03	0.04
Fall	0.06	0.11	0.07	0.08	0.04	0.06

Table 2
Ground reflectivity R_g (Tennessee Valley Authority 1972:2.15).

Ground Condition	R_g
Meadows and fields	0.14
Leaf and needle forest	0.07 - 0.09
Dark, extended mixed forest	0.045
Heath	0.10
Flat ground, grass-covered	0.25 - 0.33
Flat ground, rock	0.12 - 0.15
Sand	0.18
Vegetation, early summer, leaves with high water content	0.19
Vegetation, late summer, leaves with low water content	0.29
Fresh Snow	0.83
Old Snow	0.42 - 0.70

The ground reflectivity R_g can be seasonally distributed by the following empirical relationship:

$$R_g = R_{g1} + \{[R_{g2} - R_{g1}] \sin [(2\pi/365) (D_i - 244)]\} \qquad (20)$$

where $\quad R_{g1} \equiv$ minimum ground reflectivity occurring in mid-September (dimensionless)

$\quad R_{g2} \equiv$ maximum ground reflectivity occurring in mid-March (dimensionless)

$\quad D_i \quad =$ day of year (Julian day); $D_i=1$ for January 1 and $D_i=365$ for December 31

The average minimum-maximum values for both the dust coefficient and ground reflectivities can be calibrated to actual recorded solar radiation data. Summaries of recorded solar radiation data are available in Cinquemani et al. (1978).

Cloud Cover Correction

Cloud cover significantly reduces direct solar radiation and somewhat reduces diffused solar radiation. The preferred measure of the effect of cloud cover is the "percent possible sunshine" recorded value (S/S_o) as published by the National Oceanic and Atmospheric Administration in their local climatological data (LCD's). It is a direct measurement of solar radiation duration:

$$H_{sg} = [0.22 + 0.78 (S/S_o)^{2/3}] H_{sa} \qquad (21)$$

where $\quad H_{sg} \equiv$ daily solar radiation at ground level

$\quad H_{sa} \equiv$ solar radiation corrected for atmospheric only

$\quad S \quad \equiv$ actual sunshine duration on a cloudy day

$\quad S_o \quad \equiv$ sunrise to sunset duration at the specific site

If direct S/S_o values are not available, then S/S_o can be obtained from estimates of cloud cover C_1:

$$S/S_o = 1 - C_1^{5/3} \qquad (22)$$

where $\quad C_1 \equiv$ cloud cover (dimensionless)

Diurnal Solar Radiation

Obviously, the solar radiation intensity varies throughout the 24-hour daily period. It is zero at night, increases from zero at sunrise to a maximum at noon, and decreases to zero at sunset. This diurnal variation can be approximated by

$$H_{night} = 0 \qquad (23)$$

$$H_{day} = (\pi/\overline{h}_s) H_{sg} \qquad (24)$$

where $\quad H_{night} \equiv$ average nighttime solar radiation ($J/m^2/sec$)

$\quad H_{day} \quad \equiv$ average daytime solar radiation ($J/m^2/sec$)

$\quad H_{sq} \quad \equiv$ average daily solar radiation at ground level ($J/m^2/sec$)

$\quad \overline{h}_s \quad \equiv$ average sunrise/sunset hour angle over the time period n to N (radians)

Solar Radiation That Penetrates the Water

Solar or shortwave radiation can be reflected from a water surface. The relative amount of solar radiation reflected (R_t) is a function of the solar angle and the proportion of direct to diffused shortwave radiation. The average solar angle α is a measure of the angle, and the percent possible sunshine S/S_o reflects the direct-diffused proportions:

$$R_t = A(S/S_o) \ [\bar{\alpha}(180/\pi)]^{B(S/S_o)}; \ 0 \leq R_t \leq 0.99 \qquad (25)$$

where

R_t $\equiv$ solar-water reflectivity coefficient (dimensionless)

$\bar{\alpha}$ $\equiv$ average solar altitude (radians)

$A(S/S_o)$ $\equiv$ coefficient as a function of S/S_o

$B(S/S_o)$ $\equiv$ coefficient as a function of S/S_o

S/S_o $\equiv$ percent possible sunshine (dimensionless)

Both $A(S/S_o)$ and $B(S/S_o)$ are based on values given in Tennessee Valley Authority (1972:Table 2.4). The following average high and low cloud values were selected from this table to fit the curves:

C_1	S/S_o	A	A'	B	B'
0	1	1.18	-	-0.77	-
0.2	0.932		2.20	-0.97	0
1	0	0.33	-	-0.45	-

where $A' = dA/dC_1$ and $B' = dB/dC_1$

The resulting curves are

$$A(S/S_o) = [a_0 + a_1 \ (S/S_o) + a_2 \ (S/S_o)^2]/[1 + a_3 \ (S/S_o)] \qquad (26)$$

$$B(S/S_o) = [b_0 + b_1 \ (S/S_o) + b_2 \ (S/S_o)^2]/[1 + b_3 \ (S/S_o)] \qquad (27)$$

where

$a_0 = 0.3300$ $b_0 = -0.4500$

$a_1 = 1.8343$ $b_1 = -0.1593$

$a_2 = -2.1528$ $b_2 = 0.5986$

$a_3 = -0.9902$ $b_3 = -0.9862$

The amount of solar radiation actually penetrating an unshaded water surface is

$$H_{sw} = (1-R_t) \ H_{sg} \qquad (28)$$

where

H_{sw} $\equiv$ daily solar radiation entering water ($J/m^2/sec$)

R_t $\equiv$ solar-water reflectivity (dimensionless)

H_{sg} $\equiv$ daily solar radiation at ground level ($J/m^2/sec$)

SOLAR SHADE

The solar shade factor is a combination of topographic and riparian vegetation shading. The model is a major modification and extension of Quigley's (1981) work. It distinguishes between topographic and riparian vegetation shading and does so for each side of the stream. Quigley's work was also modified to include the intensity of the solar radiation throughout the entire day and is completely consistent with the heat flux components used with the water temperature model.

Topographic shade dominates the shading effects because it determines the local time of sunrise and sunset. Riparian vegetation is important for shading between local sunrise and sunset only if it casts a shadow on the water surface.

Topographic shade (see Figure 2) is a function of the (1) time of year; (2) stream reach latitude; (3) general stream reach azimuth; and (4) topographic altitude angle. The riparian vegetation parameters of (1) height of vegetation; (2) crown measurement; (3) vegetation offset; and (4) vegetation density. The model allows for different conditions on opposite sides of the stream.

The time of the year (D_i) and stream reach latitude (ϕ) parameters were explained as part of the solar radiation section. The remaining shade parameters are necessary only to determine the shading effects.

The general stream reach azimuth (A_r) is a measure of the average departure angle of the stream reach from a north-south (N-S) reference line when looking south. For streams oriented N-S, the azimuth is 0°; for streams oriented NW-SE, the azimuth is less than 0°; and, for stream oriented NE-SW, the azimuth is greater than 0°. Therefore, all stream reach azimuth angles are bounded between -90° and $+90^\circ$. The direction of flow has no effect on determining the azimuth; i.e., two streams with a 180° flow direction difference can have exactly the same azimuth.

The east side of the stream is always on the left-hand side because the azimuth is always measured looking south for streams located in northern latitudes. Note that an E-W oriented stream dictates the east or left-hand side by whether the azimuth is a -90° (left-hand is the north side) or $+90^\circ$ (left-hand is the south side).
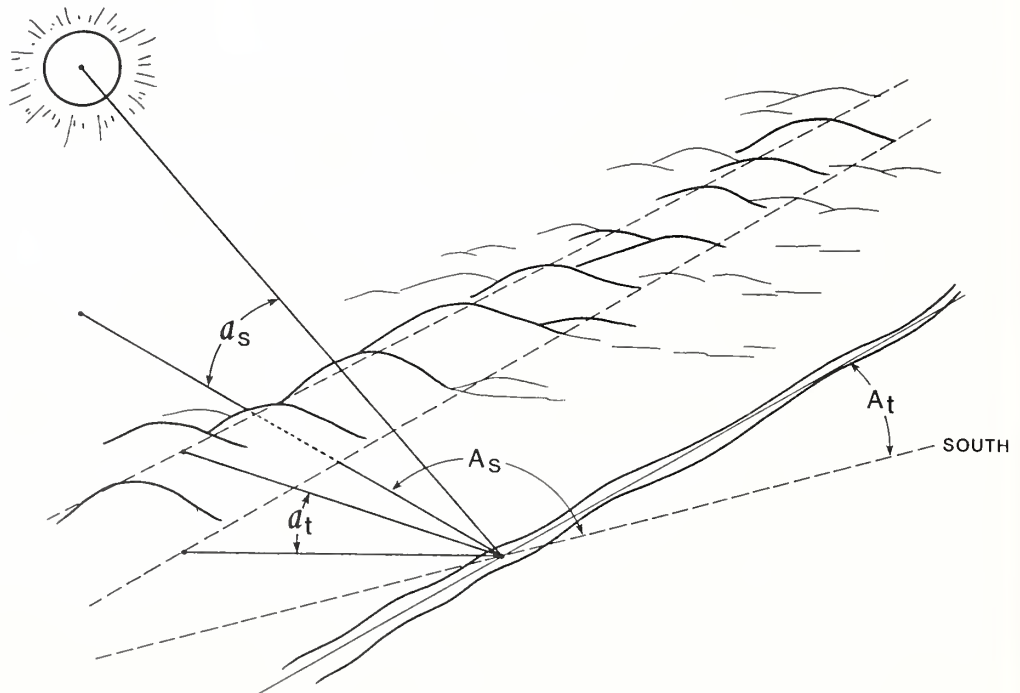
Figure 2. Local solar and stream orientation angle measurements.

The topographic altitude angle (α_t) is the vertical angle from a level line at the streambank to the general top of the local terrain when looking at a $90°$ angle from the general stream reach azimuth. There are two altitude angles, one for the left-hand side and one for the right-hand side. The altitude is 0 for level plain topography; $\alpha_t > 0$ for hilly or canyon terrain. The altitudes for opposite sides of the stream are not necessarily identical; sometimes streams tend to one side of a valley or they may flow past a bluff line.

The height of vegetation (V_h) is the average maximum existing or proposed height of the overstory riparian vegetation above the water surface. If the height of vegetation changes dramatically (e.g., due to a change in type of vegetation), then subdividing the reach into smaller subreaches may be warranted.

Crown measurement (V_c) is a function of the crown diameter of the vegetation and accounts for overhang. Crown measurement is the average of the maximum diameter of the riparian vegetation immediately adjacent to the stream (Figure 3).

Vegetation offset (V_o) is the average distance of the tree trunks from the water's edge. The net overhang is determined by vegetation offset, together with crown measurement. This net overhang, $(V_c/2)-V_o$, must always be equal to or greater than zero.

Vegetation density (V_d) is a measure of the screening of sunlight that would otherwise pass through the shaded area determined by the riparian vegetation. It accounts for both the continuity of riparian vegetation along the stream bank and the filtering effect of leaves and stands of trees along the stream. For example, if only 50% of the left side of the stream has riparian vegetation (trees) and if those trees actually screen only 50% of the sunlight, then the vegetation density for the left-hand (east) side is 0.25. V_d must always be between 0 and 1.

The solar shade model allows for separate topographic altitudes and riparian vegetation parameters for both the east (left-hand) and west (right-hand) sides of the stream.

The solar shade model is calculated in two steps. First, the topographic shade is determined according to the local sunrise and sunset times for the specified time of the year. Then, the riparian shade is calculated between the local sunrise and sunset times.

Vc ≡ average maximum diameter

Vd ≡ ratio of shortwave radiation eliminated to incoming over entire reach shaded area
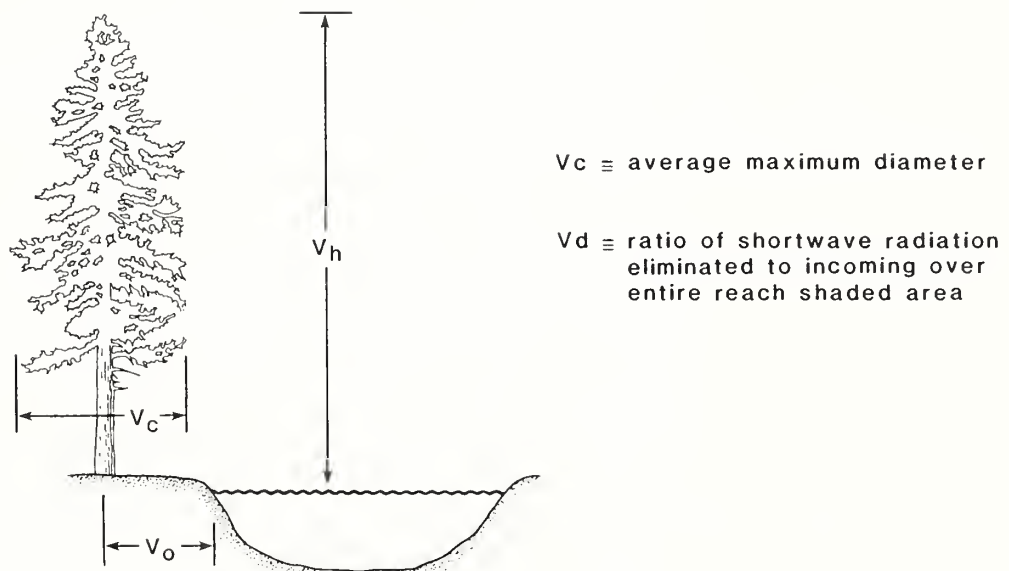
Figure 3. Riparian vegetation shade parameters.

Topographic shade is defined as the ratio of that portion of solar radiation excluded between level-plain and local sunrise/sunset to the total solar radiation between level-plain sunrise and sunset.

Riparian vegetation shade is defined as the ratio of that portion of the solar radiation over the water surface that is intercepted by the vegetation between local sunrise and sunset to the total solar radiation between level-plain sunrise and sunset.

The following math models are based on the previous rationales. There are five groupings of these models: (1) level-plain sunrise/sunset hour angle and azimuth (h_s and A_{so}); (2) local sunrise/sunset altitude (α_{sr} and α_{ss}); (3) topographic shade (S_t); (4) riparian vegetation shade (S_v); and (5) total solar shade (S_h).

Indicator function notation, $I[\bullet]$, is used. If the relationship shown within the brackets is true, the value of the indicator function is 1; if false, the value is 0. Definitions for each variable are given after the last grouping of math models.

The global conditions of latitude and time of year determine the relative movements of the sun, which affects all subsequent calculations. These conditions were explained in the solar radiation section. The time of year directly determines the solar declination, which is the starting point for the following math models.

Level-Plain Sunrise/Sunset Hour Angle and Azimuth

The level-plain sunrise/sunset group of math models are used to determine the hour angle and corresponding solar azimuth at sunrise and sunset. The solar movements are symmetrical about solar noon; i.e., the absolute values of the sunrise and sunset parameters are identical; they differ only in sign. The math model is

$$\delta = 0.40928 \cos[(2\pi/365)\ (172 - D_i)] \tag{29}$$

$$h_s = \arccos\ [-(\sin\phi\ \sin\delta)/(\cos\phi\ \cos\delta)] \tag{30}$$

$$A_{so} = \arcsin\ (\cos\delta\ \sin h_s) \tag{31}$$

The level-plain sunrise hour angle is equal to $-h_s$; the sunset hour angle is h_s. The hour angles are referenced to solar noon ($h = 0$). Therefore, the duration from sunrise to solar noon is the same as from solar noon to sunset. One hour of time is equal to 15° of hour angle.

The solar azimuth at sunrise is $-A_{so}$; the sunset azimuth is A_{so}. Azimuths are referenced from the north-south line looking south for streams located in northern latitudes. The absolute values of A_{so} are between 0° and 90° from autumn until spring ($S \leq 0$) and between 90° and 180° from spring until autumn ($S \geq 0$).

Local Sunrise/Sunset Altitudes

Local sunrise and sunset are functions of the local topography, as well as the global conditions. Furthermore, the local terrain may not be identical on both sides of the stream. Also, some streams are oriented such that the sun may rise and set on the same side of the stream during part or even all of the year. The following local sunrise/sunset models properly account for the relative location of the sun with respect to each side of the stream.

The model for the local sunrise is

$$\alpha_{tr} = \alpha_{te}\ I[-A_{so} \leq A_r] + \alpha_{tw}\ I[A_{so} > A_r] \tag{32}$$

$$h_{sr} = -\arccos\ \{[\sin\alpha_{sr} - (\sin\phi\ \sin\delta)]/\cos\phi\ \cos\delta]\} \tag{33}$$

$$A_{sr} = -\arcsin\ [(\cos\delta\ \sin h_{sr})/(\cos\alpha_{sr})] \tag{34}$$

$$\alpha_{sr} = \arctan\ \{(\tan\alpha_{tr})\ [\sin(A_{sr} - A_r)]\} \tag{35}$$

but, $\sin \alpha_{sr} \leq (\sin \phi \sin \delta) + (\cos \phi \cos \delta)$.

The model for the local sunset is

$$\alpha_{ts} = \alpha_{te} \ I[A_{so} \leq A_r] + \alpha_{tw} \ I[A_{so} > A_r] \tag{36}$$

$$h_{ss} = \arccos \ \{[\sin \alpha_{ss} - (\sin \phi \sin \delta)]/[\cos \phi \cos \delta]\} \tag{37}$$

$$A_{ss} = \arcsin \ [(\cos \delta \sin h_{ss})/(\cos \alpha_{ss})] \tag{38}$$

$$\alpha_{ss} = \arctan \ \{(\tan \alpha_{ss}) \sin(A_{ss} - A_r)]\} \tag{39}$$

but, $\sin \alpha_{ss} \leq (\sin \phi \sin \delta) + (\cos \phi \cos \delta)$.

The reason for the restriction on the $\sin \alpha_{sr}$ and $\sin \alpha_{ss}$ is that the sun never rises higher in the sky than indicated for that latitude and time of year, regardless of the actual topographic altitude. For example, an E-W oriented stream in the middle latitudes could be flowing through a deep canyon that casts continuous shade for a portion of the winter months.

Topographic Shade

Once the level-plain and local sunrise and sunset times are known, the topographic shade can be computed directly in closed form. The definition for topographic shade leads to the following:

$$S_t = \left\{ \left[\int_{-h_s}^{h_s} \sin \alpha \ dh \right] - \left[\int_{h_{sr}}^{h_{ss}} \sin \alpha \ dh \right] \right\} \Big/ \left\{ \int_{-h_s}^{h_s} \sin \alpha \ dh \right\} \tag{40}$$

which also can be expressed as

$$S_t = 1 - \left\{ \left[\int_{h_{sr}}^{h_{ss}} \sin \alpha \ dh \right] \Big/ \left[\int_{-h_s}^{h_s} \sin \alpha \ dh \right] \right\} \tag{41}$$

and which can be integrated directly to

$$S_t = 1 - \left\{ \left[(h_{ss}-h_{sr})(\sin \phi \sin \delta) \right] + \left[(\sin h_{ss} - \sin h_{sr})(\cos \phi \cos \delta) \right] \right\} \Big/ \\ \left\{ 2 \left[(h_s \sin \phi \sin \delta) + (\sin h_s \cos \phi \cos \delta) \right] \right\} \tag{42}$$

Riparian Vegetation Shade

The determination of riparian vegetation shade requires keeping track of the shadows cast throughout the sunlight time because only that portion of sunlight over the water surface is of interest. The model must account for side of the stream where the sun is located and the length of the shadow cast over the water. The model is

$$V_c = V_{ce} \ I[A_s \leq A_r] + V_{cw} \ I[A_s > A_r] \tag{43}$$

$$V_d = V_{de} \ I[A_s \leq A_r] + V_{dw} \ I[A_s > A_r] \tag{44}$$

$$V_h = V_{he} \ I[A_s \leq A_r] + V_{hw} \ I[A_s > A_r] \tag{45}$$

$$V_o = V_{oe} \ I[A_s \leq A_r] + V_{ow} \ I[A_s > A_r] \tag{46}$$

$$\alpha = \arcsin \ [(\sin \phi \sin \delta) + (\cos \phi \cos \delta \cos h)] \tag{47}$$

$$A_s = \arcsin \ [(\cos \delta \sin h) / (\cos \alpha)] \tag{48}$$

$$B_s = \{(V_h \cot \alpha) \ [\sin(A_s \cdot A_r)]\} + [(V_c/2) - V_o)] \tag{49}$$

but,
$$(V_c/2) - V_o \geq 0$$

$$0 \leq B_s \leq \bar{B}$$

$$S_v = \left\{ \int_{h_{sr}}^{h_{ss}} (V_d \, B_s \, \sin \alpha) dh \right\} \Big/ \left\{ \int_{-h_s}^{h_s} (\bar{B} \, \sin \alpha) dh \right\} \tag{50}$$

It is not possible to integrate equation (50) completely, so a numerical integration method is required. The suggested numerical approximation is

$$S_v = \left\{ \left[\sum_{h_{sr}}^{h_{ss}} (V_d \, B_s \, \sin \alpha) \right] \Delta h \right\} \Big/$$

$$\left\{ 2\bar{B} \, [(h_s \, \sin \phi \, \sin \delta) + (\sin h_s \, \cos \phi \, \cos \delta)] \right\} \tag{51}$$

Equations (43) through (49) are used to determine the jth value of V_d, B_s, and α for $h_j = h_{sr} + j\Delta h$. Sixteen intervals, or $\Delta h = (h_{ss} - h_{sr})/16$, result in better than 1% precision when using the trapezoidal rule and better than 0.01% precision when using Simpson's rule for functions without discontinuities. However, the function will have a discontinuity if the stream becomes fully shaded due to riparian vegetation between sunrise and sunset. Even so, the numerical error will generally have a negligible effect on water temperatures.

Solar Shade Factor

The solar shade factor is simply the sum of the topographic and riparian vegetation shading:

$$S_h = S_t + S_v \tag{52}$$

Because the solar declination and subsequent solar-related parameters depend on the time of year, it is necessary to calculate the various shade factors for each day of the time period to obtain the average factor for the time periods. This results in shade factors that are completely compatible with the heat flux components. This is done by

$$S_h = \left[\sum_{i=n}^{N} (S_{t,i} + S_{v,i}) \right] \Big/ \left[N - n + 1 \right] \tag{53}$$

Definitions

The following definitions pertain to all the variables used in this solar shade section:

α $\equiv$ solar altitude (radians)

α_{sr} $\equiv$ local sunrise solar altitude (radians)

α_{ss} $\equiv$ local sunset solar altitude (radians)

α_{te} $\equiv$ east side topographic altitude (radians)

α_{tr} $\equiv$ sunrise side topographic altitude (radians)

α_{ts} $\equiv$ sunset side topographic altitude (radians)

α_{tw} $\equiv$ west side topographic altitude (radians)

A_r $\equiv$ stream reach azimuth (radians)

A_s $\equiv$ local azimuth at time h (radians)

A_{so} $\equiv$ level-plain sunset azimuth (radians)

A_{sr} ≡ local sunrise solar azimuth (radians)

A_{ss} ≡ local sunset solar azimuth (radians)

$\bar{B}$ ≡ average stream width (m)

B_s ≡ stream solar shade width (m)

D_i ≡ time of year (Julian day)

S_i ≡ solar declination (radians)

h ≡ solar hour angle (radians)

h_s ≡ level-plain sunset hour angle (radians)

h_{sr} ≡ local sunrise hour angle (radians)

h_{ss} ≡ local sunset hour angle (radians)

i ≡ day counter (Julian day)

n ≡ first day in time period (Julian days)

N ≡ last day in time period (Julian days)

ϕ ≡ stream reach latitude (radians)

S_h ≡ total solar shade (decimal)

S_t ≡ topographic shade (decimal)

S_v ≡ riparian vegetation shade (decimal)

V_c ≡ riparian vegetation crown measurement (m)

V_{ce} ≡ east side crown measurement (m)

V_{cw} ≡ west side crown measurement (m)

V_d ≡ riparian vegetation density factor (decimal)

V_{de} ≡ east side density (decimal)

V_{dw} ≡ west side density (decimal)

V_h ≡ riparian vegetation height above water surface (m)

V_{he} ≡ east side height (m)

V_{hw} ≡ west side height (m)

V_o ≡ riparian vegetation waterline offset distance (m)

V_{oc} ≡ east side offset (m)

V_{ow} ≡ west side offset (m)

METEOROLOGY

There are five meteorological parameters used in the instream water temperature model: (1) air temperature; (2) humidity; (3) sunshine ratio or cloud cover; (4) wind speed; and (5) atmospheric pressure. The first four parameters are input data for a specific elevation in the basin. The meteorology model assumes adiabatic conditions to transpose the air temperature and humidity vertically throughout the basin. Atmospheric pressure is calculated directly from reach elevations. Sunshine ratio or cloud cover and wind speed are assumed constant throughout the basin.

Adiabatic Correction Model

The atmospheric pressure for each reach can be computed with sufficient accuracy directly from the respective reach elevations. The formula is

$$P = 1013[(288-0.0065Z)/288]^{5.256} \qquad (54)$$

where

$P \equiv$ atmospheric pressure at elevation Z (mb)

$Z \equiv$ average reach elevation (m)

Air temperatures generally decrease $2^{\circ}F$ for every 1,000 ft. increase in elevation. Therefore, correcting for the metric system, the following formula is used:

$$T_a = T_o + C_T (Z-Z_o) \qquad (55)$$

where

$T_a \equiv$ air temperature at elevation E (C)

$T_o \equiv$ air temperature at elevation E_o (C)

$Z \equiv$ average elevation of reach (m)

$Z_o \equiv$ elevation of station (m)

$C_T \equiv$ adiabatic temperature correction coefficient = -0.00656 C/m

Both the mean annual air temperature and the actual air temperature for the desired time period must be corrected for elevation.

The relative humidity can also be corrected for elevation, assuming that the total moisture content is the same over the basin and the station. Therefore, the formula is a function of the original relative humidity and the two different air temperatures. It is based on the ideal gas law:

$$R_h = R_o \{[1.0640^{(T_o-T_a)}] [(T_a+273.16)/(T_o+273.16)]\} \qquad (56)$$

where

$R_h \equiv$ relative humidity for temperature T_a (dimensionless)

$R_o \equiv$ relative humidity at station (dimensionless)

$T_a \equiv$ air temperature of reach (C)

$T_o \equiv$ air temperature at station (C)

$0 \leq R_h \leq 1.0$

The sunshine factor is assumed to be the same over the entire basin as over the station. There is no known way to correct the windspeed for transfer to the basin. Certainly local topographic features will influence the windspeed over the water. However, the station windspeed is, at least, an indicator of the basin windspeed. Because the windspeed affects only the convection and evaporation heat flux components and these components have the least reliable coefficients in these models, the windspeed can be used as an important calibration parameter when actual water temperature data are available.

Average Afternoon Meteorological Conditions

The average afternoon air temperature is greater than the daily air temperature because the maximum air temperature usually occurs during the middle of the afternoon. This model assumes that

$$\overline{T}_{ax} = [(5T_{ax}) + (11\overline{T}_a)]/16 \qquad (57)$$

where $\overline{T}_{ax}$ ≡ average daytime air temperature between noon/sunset (C)

T_{ax} ≡ maximum air temperature during the 24-hour period (C)

$\overline{T}_a$ ≡ average daily air temperature during the 24-hour period (C)

A regression model was selected to incorporate the significant daily meteorological parameters to estimate the incremental increase of the average daytime air temperature above the average daily air temperature. The resulting average daytime air temperature model is

$$T_{ax} = \overline{T}_a + [a_0 + a_1 H_{sx} + a_2 R_h + a_3 (S/S_0)] \tag{58}$$

where T_{ax} ≡ maximum air temperature (C)

$\overline{T}_a$ ≡ daily air temperature (C)

H_{sx} ≡ extraterrestrial solar radiation ($J/m^2/sec$)

R_h ≡ relative humidity (decimal)

S/S_0 ≡ percent possible sunshine (decimal)

a_0 through a_3 ≡ regression coefficients

Some regression coefficients were determined for the "normal" meteorological conditions at 16 selected weather stations. These coefficients and their respective coefficient of multiple correlations R, standard deviation of maximum air temperature $S.T_{ax}$, and probable differences δ are given in Table 3.

The corresponding afternoon average relative humidity is

$$R_{hx} = R_h [1.0640^{(\overline{T}_a - \overline{T}_{ax})}] [(\overline{T}_{ax} + 273.16)/(\overline{T}_a + 273.16)] \tag{59}$$

where R_{hx} ≡ average afternoon relative humidity (dimensionless)

R_h ≡ average daily relative humidity (dimensionless)

$\overline{T}_a$ ≡ daily air temperature (C)

$\overline{T}_{ax}$ ≡ average afternoon air temperature (C)

Table 3. Regression coefficients for maximum daily air temperatures.

Station name	$\overline{R}$	(C) $S.T_{ax}$	(C) δ	Regression coefficients			
				a_0	a_1	a_2	a_3
Phoenix, AZ	.936	0.737	0.194	11.21	-.00581	- 9.55	3.72
Santa Maria, CA	.916	0.813	0.243	18.90	-.00334	-18.85	3.18
Grand Junction, CO	.987	0.965	0.170	3.82	-.00147	- 2.70	5.57
Washington, DC	.763	0.455	0.219	6.64	-.00109	- 7.72	4.85
Miami, FL	.934	0.526	0.140	29.13	-.00626	-24.23	-7.45
Dodge City, KA	.888	0.313	0.107	7.25	-.00115	- 5.24	4.40
Caribou, ME	.903	0.708	0.226	0.87	.00313	0.09	7.86
Columbia, MO	.616	0.486	0.286	4.95	-.00163	- 2.49	4.54
Great Falls, MT	.963	1.220	0.244	9.89	.00274	- 9.56	1.71
Omaha (North), NE	.857	0.487	0.187	9.62	-.00279	- 9.49	6.32
Bismarck, ND	.918	1.120	0.332	11.39	-.00052	-13.03	5.97
Charleston, SC	.934	0.637	0.170	9.06	-.00325	- 8.79	7.42
Nashville, TN	.963	0.581	0.117	5.12	-.00418	- 4.55	9.47
Brownsville, TX	.968	0.263	0.049	9.34	-.00443	- 4.28	0.72
Seattle, WA	.985	1.180	0.153	-9.16	.00824	12.79	3.86
Madison, WI	.954	0.650	0.145	1.11	.00219	1.80	3.96
ALL	.867	1.276	0.431	6.64	-.00088	- 5.27	4.86

HEAT FLUX

There are five basic thermal processes recognized by the heat flux relationships: (1) radiation; (2) evaporation; (3) convection; (4) conduction; and (5) the conversion of energy from other forms to heat (see Figure 4).

Thermal Sources

Heat flux sources are considered mutually exclusive; and when they are added together, each accounts for the heat budget of a single column of water. A heat budget analysis would be applicable for a stationary tank of continuously mixed water. However, the transport model is necessary to account for the spatial location of the column of water at any point in time.

Radiation

Radiation is an electromagnetic mechanism, which allows energy to be transported at the speed of light through regions of space that are devoid of matter. The physical phenomena causing radiation are sufficiently well understood to provide very dependable source-component models. Radiation models have been theoretically derived from both thermodynamics and quantum physics and have been experimentally verified with a high degree of precision and reliability. Radiation is the most dependable component of the heat flux submodel and, fortunately, is also the most important source of heat exchange. Solar, back radiation from the water, atmosphere, riparian vegetation, and topographic features are the major sources of radiation heat flux. There is interaction between these various sources; e.g., riparian vegetation screens both solar and atmospheric radiation while replacing it with its own radiation.

ATMOSPHERIC RADIATION

SOLAR RADIATION

TOPOGRAPHIC RADIATION

WATER BACKRADIATION

RIPARIAN VEGETATION RADIATION

REFLECTION

SHADE

ALSO: (1) HEAT LOSS DUE TO EVAPORATION

(2) HEAT GAIN DUE TO FLUID FRICTION

(3) HEAT EXCHANGE DUE TO AIR CIRCULATION (CONVECTION)

STREAMBED CONDUCTION
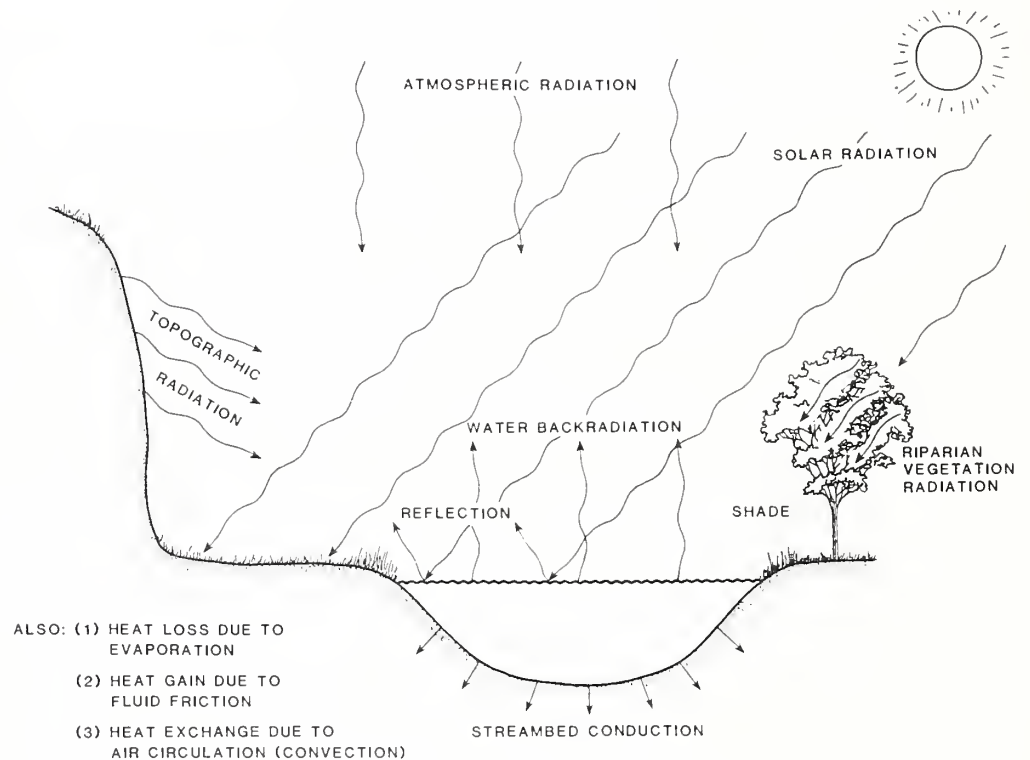
Figure 4. Heat flux sources.

Solar Radiation Corrected for Shading

The solar radiation penetrating the water must be further modified by local shading due to riparian vegetation and other sources. The resulting model is

$$H_s = (1-S_h) \ H_{sw} \tag{60}$$

where
$S_h \equiv$ solar shade factor (decimal)

$H_{sw} \equiv$ average daily solar radiation entering unshaded water ($J/m^2/sec$)

$H_s \equiv$ average daily solar radiation entering shaded water ($J/m^2/sec$)

Atmospheric Radiation

The atmosphere emits longwave radiation (heat). There are five factors affecting the amount of longwave radiation entering the water: (1) the air temperature is the primary factor; (2) the atmospheric vapor pressure affects the emissivity; (3) the cloud cover converts the shortwave solar radiation into additional longwave radiation, which are "hot spots" in the atmosphere; (4) the reflection of longwave radiation at the water-air interface; and (5) the interception of longwave radiation by vegetative canopy cover or shading. An equation that approximates longwave atmospheric radiation entering the water is

$$H_a = (1-r_1)(1-S_a)(1+kC_1^2) \ [\epsilon_a \ \sigma(T_a+273.16)^4] \tag{61}$$

where
$C_1 = [1-(S/S_0)]^{3/5} \equiv$ cloud cover (decimal)

$S/S_0 \equiv$ sunshine ratio (decimal)

$k \equiv$ type of cloud cover factor ($0.04 \le k \le 0.24$)

$\epsilon_a \equiv$ atmospheric emissivity (decimal)

$S_a \equiv$ atmospheric shade factor (decimal)

$r_1 \equiv$ longwave radiation reflection (decimal)

$T_a \equiv$ air temperature (C)

$\sigma = 5.672 \times 10^{-8} \ (J/m^2/sec/K^4) \equiv$ Stefen-Boltzman constant

The preferred estimate of ϵ_a is

$$\epsilon_a = a+b \ \sqrt{e_a} \quad \text{(decimal)} \tag{62}$$

$$a = 0.61$$

$$b = 0.05$$

$$e_a \equiv \text{vapor pressure} = R_h \ [6.60(1.0640)^{T_a}] \ \text{(mb)} \tag{63}$$

An alternate estimate of ϵ_a is

$$\epsilon_a = 9.062 \times 10^{-6} \ (T_a + 273.16)^2 \ \text{(decimal)} \tag{64}$$

The preferred estimate accounts for water vapor, which also absorbs solar radiation (shortwave) which, in turn, is converted into longwave radiation. If the absorption of solar radiation is overpredicted, then some of the overprediction is returned as longwave and vice versa. Therefore, errors in shortwave radiation tend to be compensated for by errors in longwave radiation. The alternate form for ϵ_a is mentioned in the literature as a simpler model and

possibly a better predictor of longwave radiation alone. However, for the purpose of predicting water temperatures, the form of radiation (shortwave or longwave) ultimately makes little difference, as long as the total heat exchange is accurately predicted. The alternate form is only used when a desired solution technique requires simple steps.

Assuming $k = 0.17$, $r_1 = 0.03$, and using the preferred estimate of ϵ_a, this equation reduces to

$$H_a = (1-S_a)(1+0.17C_1^2)[3.36+0.706(R_h \times 1.0640^{T}a)^{1/2}][10^{-8}(T_a+273.16)^4] \qquad (65)$$

The atmospheric shade factor (S_a) is assumed to be identical to the solar shade factor (S_h).

Topographic Features Radiation

Currently, the radiation from topographic features is assumed to be included as a part of the riparian vegetation radiation. Therefore, no separate component model is used.

Riparian Vegetation Radiation

The riparian vegetation intercepts all other forms of radiation and radiates its own form. Essentially, it totally eliminates the estimated shade amount of solar radiation, but replaces the other longwave sources with its own longwave source. The difference is mostly in the emissivity between the different longwave sources. The model is

$$H_v = (\epsilon_v \sigma) S_v (T_a+273.16)^4 \qquad (66)$$

where
$\epsilon_v \equiv$ vegetation emissivity = 0.9526 (decimal)

$\sigma \equiv$ Stefen-Boltzman constant = $5.672 \ 10^{-8} \cdot J/m^2/sec/K^4$

$H_v \equiv$ riparian vegetation radiation $(J/m^2/sec)$

$S_v \equiv$ riparian vegetation shade factor (decimal)

$T_a \equiv$ riparian vegetation temperature, assumed to be the ambient air temperature (C)

The riparian vegetation shade factor (S_v) is assumed to be identical to the solar shade factor (S_h).

Water Radiation

The water emits radiation, and this is the major balancing heat flux that prevents the water temperature from increasing without bonds. The model is

$$\hat{H}_w = \epsilon_w \sigma (T_w+273.16)^4 \qquad (67)$$

where
$\hat{H}_w$ = water radiation $(J/m^2/sec)$

T_w = water temperature (C)

ϵ_w = water emissivity = 0.9526 (decimal)

σ = Stefan-Boltzman constant = $5.672 \times 10^{8} \ J/m^2/sec/K^4$

A first-order approximation to equation (67) with less than $\pm 1.8\%$ error of predicted radiation for $0 \ C \leq T_w \leq 40 \ C$ is

$$\hat{H}_w = 300 + 5.500 \ T_w \qquad (68)$$

where
$\hat{H}_w$ = approximate water radiation $(J/m^2/sec)$

T_w = water temperature (C)

Evaporation and its counterpart, condensation, require an exchange of heat. The isothermal (same temperature) conversion of liquid water to vapor requires a known fixed amount of heat energy called the heat of vaporization. Conversely, condensation releases the same amount of heat. The rate of evaporation (the amount of liquid water converted to vapor) is a function of both the circulation and vapor pressure (relative humidity) of the surrounding air. If the surrounding air is at 100% relative humidity, no net evaporation occurs. If there is no circulation of air, then the air immediately above the water surface quickly becomes saturated and no further net evaporation occurs.

Evaporation, while second in importance to radiation, is a significant form of heat exchange. Most available models are derived from lake environments and are probably the least reliable of the thermal processes modeled. However, one model was derived from a single set of open channel flow data. Both model types are included below. They differ only in the wind function used. The wind function for the flow-type model was adjusted by approximately 75% to better match recorded field data.

The first model was obtained largely from lake data and is used only for small, hand-held calculator solution techniques. The second model is the preferred one. It was obtained from open channel flow data and is used for all but the simplest solution technique.

The lake-type model is

$$H_e = (26.0W_a)[R_h(1.0640)^{T_a} - (1.0640)^{T_w}] \tag{69}$$

The flow-type model is

$$H_e = (40.0 + 15.0W_a)[R_h(1.0640)^{T_a} - (1.0640)^{T_w}] \tag{70}$$

where

$H_e \equiv$ evaporation heat flux ($J/m^2/sec$)

$W_a \equiv$ wind speed (m/sec)

$R_h \equiv$ relative humidity (decimal)

$T_a \equiv$ air temperature (C)

$T_w \equiv$ water temperature (C)

Convection

Convection can be an important source of heat exchange at the air-water interface. Air is a poor conductor, but the ability of the surrounding air to circulate, either under forced conditions from winds or freely due to temperature differences, results in constant exchanges of the air at the air-water interface. Convection affects the rate of evaporation and, therefore, the two models are related. But the actual heat exchanges due to the two different sources are mutually exclusive. Convection is not quite as important as evaporation as a source of heat flux but is still significant. The available convection models suffer from the same defects because they both used the same circulation model.

The current convection models are largely based on lake data but are used here. The convection model is based on the evaporation model, using the Bowen ratio:

$$\text{Bowen ratio} = B_f \, P(T_w - T_a)/(e_s - e_a) \tag{71}$$

where

$P \equiv$ atmospheric pressure (mb)

$T_w \equiv$ water temperature (C)

$T_a \equiv$ air temperature (C)

$e_s \equiv$ saturation vapor pressure (mb)

$e_a \equiv$ air vapor pressure (mb)

$B_f \equiv$ Bowen ratio factor

Air convection heat exchange is approximated by the product of the Bowen ratio and the evaporation heat exchange:

$$H_c = RH_e \qquad (72)$$

where
$H_c \equiv$ air convection heat flux ($J/m^2/sec$)

$R \equiv$ Bowen ratio (decimal)

$H_e \equiv$ evaporated heat flux ($J/m^2/sec$)

Because the air convection heat flux is a function of the evaporation heat flux, two models are offered. The first, the simplest, is a lake-type model. The second, the preferred, is a flow-type model.

The lake-type model is

$$H_c = (2.55 \times 10^{-3} W_a) \; P(T_w - T_a) \qquad (73)$$

The flow-type model is

$$H_c = (3.75 \times 10^{-3} + 1.40 \times 10^{-3} W_a) \; P(T_w - T_a) \qquad (74)$$

where
$H_c \equiv$ air convection heat flux ($J/m^2/sec$)

$W_a \equiv$ wind speed (m/sec)

$P \equiv$ atmospheric pressure (mb)

$T_w \equiv$ water temperature (C)

$T_a \equiv$ air temperature (C)

Streambed Conduction

Conduction occurs when a temperature gradient (temperature difference between two points) exists in a material medium in which there is molecular contact. The only important conduction heat flux component is through the streambed. The thermal processes are reasonably well understood, although some of the necessary data may not be easily obtained without certain assumptions. However, the importance of this component, while not negligible, is that it does allow for some liberties, and suitable predictions can be made for most applications.

Streambed conduction is a function of (1) the difference in temperature between the streambed at the water-streambed interface and the streambed at an equilibrium ground temperature at some depth below the streambed elevation, (2) the equilibrium depth, (3) and the thermal conductivity of the streambed material. The equation is

$$H_d = K_g [(T_g - T_w)/\Delta Z_g] \qquad (75)$$

where
$H_d \equiv$ conduction heat flux ($J/m^2/sec$)

$K_g \equiv$ thermal conductivity of the streambed material ($J/m^2/sec$)

$T_g \equiv$ streambed equilibrium temperature (C)

$T_w \equiv$ streambed temperature at the water-streambed interface, assumed to be the water temperature (C)

$\Delta Z_g \equiv$ equilibrium depth from the water-streambed interface (m)

$K_g \equiv$ 1.65 J/m/sec/C for water-saturated sands and gravel mixtures (Pluhowski 1970)

The two terms $K_g/\Delta Z_g$, when combined, are called the streambed thermal gradient.

Heat is generated by fluid friction as the water flows downstream, either as work done on the boundaries or as internal fluid shear. That portion of the potential energy (elevation) of the flowing water that is not converted to other uses (e.g., hydroelectric generation) is converted to heat. When ambient conditions are below freezing, the fact that water in a stream is still flowing may be due partly to this generation of heat due to friction. The available model is straightforward, simple to use, and solidly justified by basic physics. Fluid friction is the least significant source of heat flux, but it can be noticeable for steep mountain streams during cooler conditions.

The stream friction model is

$$H_f = 9805 \ (Q/\bar{B}) S_f \tag{76}$$

where

$H_f \equiv$ fluid friction heat flux $(J/m^2/sec)$

$S_f \equiv$ rate of heat energy conversion, generally the stream gradient (m/m)

$Q \equiv$ discharge (cms)

$\bar{B} \equiv$ average top width (m)

Net Heat Flux

The various heat flux components, when added together, form the net heat flux equation:

$$H_n = H_a + H_c + H_d + H_e + H_s + H_v - H_w \tag{77}$$

where

$H_n \equiv$ net heat flux

When the equations for the separate components are substituted into equation (77), it can be reduced to

$$H_n = A(T_w + 273.16)^4 = BT_w + C \ (1.0640)^{T_w} - D \tag{78}$$

where

$A = 5.40 \times 10^{-8}$

$B = (C_r \times C_e \ P) + (K_g / \Delta Z_g)$

$C = (40.0 + 15.0 W_a)$

$D = H_a + H_f + H_s + H_v + (Cr \times C_e \ PT_a) +$

$\qquad [T_g (K_g / \Delta Z_g)] + [C_e \ R_h \ (1.0640^{T_a})]$

$C_e = a + bW_a + c \ \sqrt{W_a}$

$C_r = B_f / 6.60$

The equilibrium water temperature T_e is defined as the water temperature when the net heat flux is zero for a constant set of input parameters:

$$A(T_e + 273.16)^4 + BT_e + C \ (1.0640)^{T_e} - D = 0 \tag{79}$$

The solution of equation (79) for T_e, given A, B, C, and D, is the equilibrium water temperature of the stream for a fixed set of meteorologic, hydrologic, and stream geometry conditions. A physical analogy is that, as a constant discharge of water flows downstream in a prismatic stream reach under a constant set of

meteorologic conditions, the water temperature will asymptotically approach the equilibrium water temperature regardless of the initial water temperature.

The first-order thermal exchange coefficient K_1 is the first derivative of equation (78) (dH/dT_w) taken at T_e:

$$K_1 = 4A(T_e+273.16)^3 + B + [Cln\ (1.0640)]\ (1.0640)^{T_e} \qquad (80)$$

The second-order thermal exchange coefficient is the coefficient for a second-order term that collocates the actual heat flux at the initial water temperature (T_o) with a first-order Taylor series expansion about T_e:

$$K_2 = \{[A(T_o+273.16)^4 + BT_o + C(1.0640)^{T_o} - D] - [K_1(T_o-T_e)]\}/[(T_o-T_e)^2] \qquad (81)$$

Therefore, a first-order approximation of equation (78), with respect to the equilibrium temperature, is

$$H_n = K_1\ (T_e - T_w) \qquad (82)$$

A second order approximation of equation (78), with respect to the equilibrium temperature is

$$H_n = K_1\ (T_e - T_w) + K_2\ (T_e - T_w)^2 \qquad (83)$$

Heat Transport

The heat transport model is based on the dynamic temperature - steady flow equation. This equation, when expressed as an ordinary differential equation, is identical in form to the less general steady-state equation. However, it requires different input data and requires tracking the mass movement of water downstream. The simultaneous use of the two identical equations with different sets of input data is acceptable because the actual water temperature equals the average daily water temperature twice each day, once at night and once during the day.

The steady-state equation assumes that the input parameters are constant for each 24-hour period. Therefore, the solar radiation, meteorological, and hydrology parameters are 24-hour averages. It follows, then, that the predicted water temperatures are also 24-hour averages. Hence, the term "average daily" means 24-hour averages, from midnight to midnight for each parameter.

The dynamic model allows the 24-hour period to be divided into night and day times. Although the solar radiation and meteorological parameters for nighttime and daytime are different, they are considered constant. Because the dynamic model is a steady flow model, the discharges are constant over the 24-hour period.

The water temperature is at a minimum at sunrise and continually rises during the day, with the average daily water temperature occurring near noon. At sunset, the water temperature is at its maximum; then it begins to cool, with the average daily temperature again occurring near midnight. Just before sunrise, the temperature returns to the minimum.

The steady-state equation, with input based on 24-hour averages, can be used to predict the average daily water temperatures throughout the entire stream network. Because these average daily values actually occur near midnight and midday, the dynamic model can be used to track the column of water between midnight and sunrise and between midday and sunset to determine the minimum nighttime and maximum daytime water temperatures, respectively. Of course, the proper solar radiation and meteorological parameters reflecting night and daytime conditions must be used for the dynamic model.

A minimum/maximum simulation model requires that the upstream average daily water temperature stations at midnight/midday for the respective sunrise/sunset stations be simulated. This step is a simple hydraulic procedure, requiring only a means to estimate the average flow depth.

Dynamic Temperature - Steady Flow

A control volume for the dynamic temperature - steady flow equation is shown in Figure 5. It allows for lateral flow. To satisfy the fundamental laws of physics regarding conservation of mass and energy, the heat energy in the incoming waters less the heat energy in the outgoing water plus the net heat flux across the control volume boundaries must equal the change in heat energy of the water within the control volume. The mathematical expression is

$$\{[pc_p(QT)_i - pc_p(QT)_o] + [pc_p q_1 T_1 \Delta x] + [(B\Sigma H) \Delta x]\}\Delta t$$

$$= \{pc_p(\partial(AT)/\partial t)]\Delta t\}\Delta x \qquad (84)$$

where

$p \equiv$ water density (M/L^3)

$c_p \equiv$ specific heat of water $(E/M/T)$

$Q \equiv$ discharge (L^3/t)

$T \equiv$ water temperature (T)

$q_1 \equiv$ lateral flow (L^2/t)

$T_1 \equiv$ lateral flow temperature (T)

$x \equiv$ distance (L)

$t \equiv$ time (t)

$A \equiv$ flow area (L^2)

$i \equiv$ inflow index

$o \equiv$ outflow index

$B \equiv$ stream top width (L)

$\Sigma H \equiv$ net heat flux across control volume $(E/L^2/t)$

note: units are

M - mass
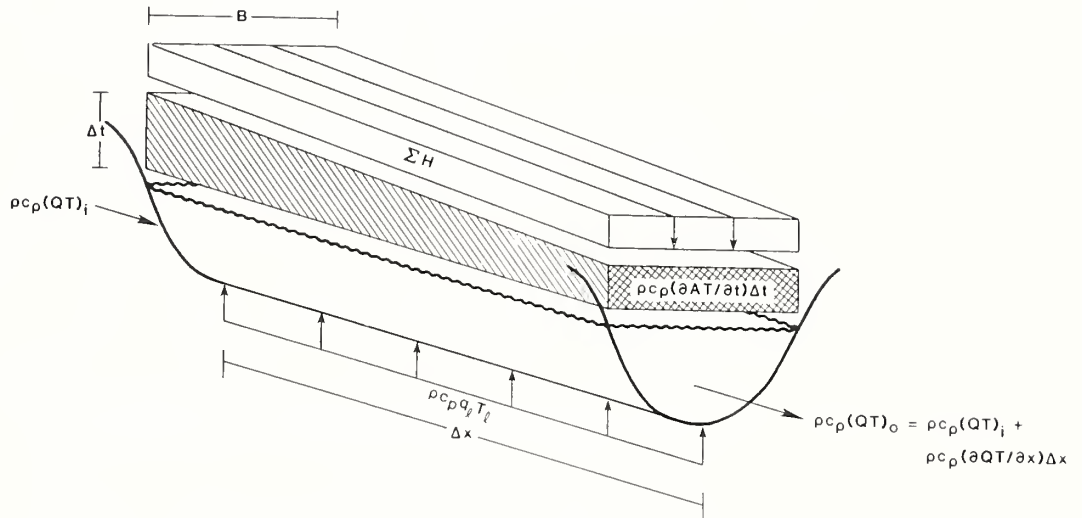
Figure 5. Dynamic energy control volume.

T - temperature

L - length

t - time

E - heat energy

Equation (84) reduces to

$$\partial(AT)/\partial t + \partial(QT)/\partial x = q_1 T_1 + (\bar{B}\Sigma H)/(pc_p) \qquad (85)$$

Assuming steady flow ($\partial A/\partial t = 0$), letting $H_n = \Sigma H$, recognizing $q_1 \equiv \partial Q/\partial x$, and dividing through by Q, leads to

$$(A/Q)\ (\partial T/\partial t) + \partial T/\partial x = [(q_1/Q)\ (T_1 - T)] + [(\bar{B}H_n)/(Qpc_p)] \qquad (86)$$

<———————>|<———————————————————————>
dynamic   steady-state equation
  term

<———————————————————————————————>
dynamic temperature - steady flow equation

If the dynamic temperature term is neglected ($\partial T/\partial t = 0$), then the steady-state equation is left. Because the steady-state equation contains only a single independent variable x, it converts directly into an ordinary differential equation with no mathematical restrictions:

$$dT/dx = [(q_1/Q)\ (T_1 - T)] + [(\bar{B}H_m)/(Qpc_p)] \qquad (87)$$

If the dynamic temperature term is not neglected ($\partial T/\partial t = 0$), then equation (86) can still be solved using the classical mathematical technique known as the Method of Characteristics. If for notational purposes only, we substitute

$$\Phi = [(q_1/Q)\ (T - T)] + [(\bar{B}H_m)/(Qpc_p)] \qquad (88)$$

into equation (86) and use the definition of the total derivative for the dependent variable T, a resulting pair of dependent simultaneous first-order partial differential equations emerge:

$$(A/Q)\ (\partial T/\partial t) + (1)\ (\partial T/\partial x) = \Phi \qquad (89)$$

$$(dt)\ (\partial T/\partial t) + (dx)\ (\partial T/\partial x) = dT \qquad (90)$$

Because the equations are dependent, the solution of the coefficients matrix is zero:

$$\begin{bmatrix} (A/Q) & 1 \\ dt & dx \end{bmatrix} = 0$$

which leads to the characteristic line equation

$$dx = (Q/A)dt \qquad (91)$$

For the same reason, the solution matrix is also zero:

$$\begin{bmatrix} \Phi & 1 \\ dt & dx \end{bmatrix} = 0$$

which leads to the characteristic integral equation

$$dT/dx = [(q_1/Q)(T_1-T)] + [(\bar{B}H_m)/(Qpc_p)] \tag{92}$$

when Φ is replaced by its original terms of equation (88).

Equation (92) is identical in form to equation (87) and is valid for dynamic temperature conditions when solved along the characteristic line equation [equation (91)]. This presents no special problem because equation (91) simply tracks a column of water downstream, an easily simulated task.

Closed-form solutions for the ordinary differential equation forms [equations (91) and (92)] of the dynamic temperature-steady flow equations are possible with two important assumptions: (1) uniform flow exists; and (2) first and/or second-order approximations of the heat flux versus water temperature relationships are valid.

First-Order Solutions

First-order solutions are possible for all three cases of q_1: Case 1, $q_1 > 0$; Case 2, $q_1 < 0$; and Case 3, $q_1 = 0$. The ordinary differential equation with the first-order substitution is

$$dT/dx = [(q_1/Q)(T_1-T)] + [K_1(T_e - T)\bar{B}/(pc_pQ)] \tag{93}$$

Case 1, $q_1 > 0$

Because $Q = Q_o + q_1 x$, equation (93) becomes

$$[Q_o + q_1 x] \, dT/dx = \{[q_1 T_1] + [(\bar{K}_1 B)/(pc_p)]T_e\} - \{q_1 + [(K_1 W)/pc_p)]\}T \tag{94}$$

If we let $\quad a = [q_1 T_1] + [(K_1 \bar{B})/(pc_p)]T_e$

$$b = q_1 + [(K_1 \bar{B})/(pc_p)]$$

Then equation (94) becomes

$$(Q_o + q_1 x) \, dT/dx = a - bT \tag{95}$$

Using separation of variables,

$$\int_{T_o}^{T_w} \frac{dT}{a-bT} = \int_0^{x_o} \frac{dx}{Q_o + q_1 x} \tag{96}$$

The solution is

$$T_w = (a/b) - [(a/b) - T_o][1 + (q_1 x_o/Q_o)]^{(-b/q_1)} \tag{97}$$

Case 2, $q_1 < 0$

If $q_1 < 0$, then $T_1 = T$, and equation (93) becomes

$$[Q_o + q_1 x_o] \, dT/dx = [(K_1 \bar{B})/(pc_p)][T_e - T] \tag{98}$$

The solution is

$$T_w = T_e - [T_e - T_o][1 + (q_1 x_o/Q_o)]^{[(q_1-b)/q_1]} \tag{99}$$

171

Case 3, $q_1 = 0$

If $q_1 = 0$, then $Q \neq Q(x)$, and equation (93) becomes

$$dT/dx = [(K_1B)/(pc_pQ)] [T_e - T] \tag{100}$$

The solution is

$$T_w = T_e - [T_e - T_o] \exp [-(K_1\bar{B}x_o)/(pc_pQ)] \tag{101}$$

Second-Order Solutions

A second-order solution for case 3 is as follows:

Letting $q_1 = 0$ and using equation (83) results in

$$dT/dx = [K_1(T_e - T) + K_2 (T_e - T)^2]\bar{B}/(pc_pQ_o) \tag{102}$$

The solution is

$$T_w = T_e - \frac{(T_e - T_o) \exp [-(K_1\bar{B}x_o)/(pc_pQ_o)}{1 + (K_2/K_1) (T_e - T_o) \{1 - \exp [-(K_1Bx_o)/(pc_pQ_o)]\}} \tag{103}$$

Using the first-order solution and making second-order corrections according to the form suggested by equation (103) results in

$$T_w = T_e' - [(T_e' - T_o) R]/[1 + (K_2/K_1) (T_e' - T_o) (1-R)] \tag{104}$$

where

$$a = [q_1T_1] + [(K_1\bar{B})/(pc_p)]T_e \tag{105}$$

$$b = q_1 + (K_1\bar{B})/(pc_p) \tag{106}$$

Case 1, $q_1 > 0$

$$T_e' = a/b \tag{107}$$

$$R = [1 + (q_1x_o/Q_o)]^{(-b/q_1)} \tag{108}$$

Case 2, $q_1 < 0$

$$T_e' = T_e \tag{109}$$

$$R = [1 + (q x_o/Q_o)]^{[(q_1-b)/q_1]} \tag{110}$$

Case 3, $q_1 = 0$

$$T_e' = T_e \tag{111}$$

$$R = \exp [-(bx_o)/Q_o] \tag{112}$$

172

Figure 6 shows a typical longitudinal water temperature profile.

Time Periods

The basic math model for the overall basin network is a steady-state model
because it assumes that the input is a constant over an indefinite period of
time. Conceptually, it assumes that the input conditions exist sufficiently
long for the steady-state results to reach the lowest point in the network. If
the travel time from the uppermost point upstream to the downstream end of the
network becomes significant compared to the time period, the results become less
reliable.

If the travel time to the lowest point is 30 days, it should be recognized that
the water passing this point on the first day of the 30-day period originated
upstream 30 days earlier. Therefore, the meteorological conditions that
determine downstream daily water temperatures on the first day are not included
in the time period averages. In fact, only the last day's water column was
influenced entirely by the meteorologic data used as input for the time period.

One way to overcome this problem is to redefine the time periods as smaller
increments (as small as a day, if necessary) and track each day's water column
movement, using the previous day's results as the initial conditions for the
current day.

Diurnal Fluctuations

The following relationships can be solved explicitly at any study site or point
of interest to determine the maximum temperature rise of the water above the
average. They are based on the fact that the water temperature equals the
average temperature twice each day, that the average water temperature occurs
approximately half way through the day, and that the remainder of the day the
water temperature increases steadily to a maximum close to sunset. The same
logic is used to determine the minimum water temperature by substituting
nighttime conditions in lieu of daytime conditions:

$$d = \{[(Q/\bar{B})n]/[\sqrt{S}_e]\}^{3/5} \tag{113}$$

$$t_x = (S_o/2)\ 3600 \tag{114}$$

$$T_{ox} = T_{ed} - \{(T_{ed} - T_{wd})\ \exp\ [(K_d t_x)/(pc_p d)]\} \tag{115}$$

$$T_{wx} = T_{ex} - \{(T_{ex} - T_{ox})\ \exp\ [-(K_x t_x)/(pc_p d)]\} \tag{116}$$
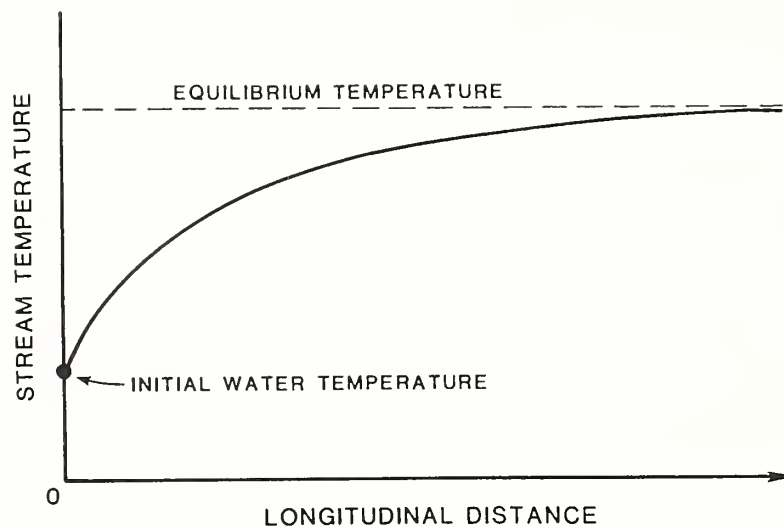
Figure 6.—Typical longitudinal water temperature profile
predicted by the heat transport equation.

where
        d ≡ average flow depth (m)

        n ≡ Manning's n value

        Q ≡ discharge (cm)

        $\bar{B}$ ≡ average top width (m)

        S_e ≡ energy gradient (m/m)

        t_x ≡ travel time from noon at sunset (sec)

        S_o ≡ duration of possible sunshine from sunrise to sunset (hours)

        T_{ed} ≡ equilibrium temperature for average daily conditions (C)

        T_{ex} ≡ equilibrium temperature for average daytime conditions (C)

        T_{wd} ≡ average daily water temperature (at solar noon) at point of interest (C)

        T_{ox} ≡ average daily water temperature at travel time distance upstream from point of interest (C)

        T_{wx} ≡ average maximum daytime water temperature (at sunset) at point of interest (C)

        K_d ≡ first-order thermal exchange coefficient for daily conditions ($J/m^2/sec/C$)

        K_x ≡ first-order thermal exchange coefficients for daytime conditions, $J/m^2/sec/C$

        p ≡ density of water = 1000 kg/m^3

        c_p ≡ specific heat of water = 4182 J/kg/C

Because of the symmetry assumed for the daytime conditions, it is only necessary to calculate the difference between the maximum daytime and average daily water temperatures to obtain the minimum water temperature:

$$T_{wn} = T_{wd} - (T_{wx} - T_{wd}) \tag{117}$$

where
        T_{wn} ≡ average minimum nighttime water temperature (at sunrise) at point of interest (C)

        T_{wx} ≡ average maximum daytime water temperature (at sunset) at point of interest (C)

        T_{wd} ≡ average daily water temperature (at solar noon) at point of interest (C)

Flow Mixing

The equation for determining the final downstream water temperature when flows of different temperatures and discharges met is:

$$T_J = (T_B Q_B + T_T Q_T)/(Q_B + Q_T) \tag{118}$$

where
        T_J ≡ water temperature below junction

        T_B ≡ water temperature above junction on the mainstream (branch node)

        T_T ≡ water temperature above junction on the tributary (terminal node of the tributary)

        Q_B ≡ discharge above junction on the mainstream (branch node)

        Q_T ≡ discharge above junction on the tributary (terminal node on the tributary)

174

REGRESSION MODELS

Regression models are commonly used to smooth data and/or fill in missing data. They are used as a part of the instream water temperature model to provide initial water temperatures at headwaters or point sources to start the transport mode and as an independent prediction of water temperatures at interior network points for purposes of validation and calibration. Obviously, regression models are only useful at the points of analysis and cannot be used in lieu of the longitudinal heat transport model. Two regression models are included in the instream water temperature model package: (1) a standard regression model; and (2) a transformed regression model. Each model requires measured or known water temperatures as the dependent variable, along with associated meteorological, hydrological, and stream geometry independent parameters. However, the standard regression model requires less detail than the transformed model. The standard model is satisfactory for most applications, but the transformed version has a better physical basis. The choice becomes a matter of judgement.

Standard Regression Model

Instream Flow Group (IFG) studies during model development showed that the following simple linear multiple regression model provides a high degree of correlation for natural conditions:

$$\hat{T}_w = a_0 + a_1 T_a + a_2 W_a + a_3 R_h + a_4 (S/S_o) + a_5 H_{sx} + A_6 Q$$
$$+ b_1 T_a^2 + b_2 W_a^2 + b_3 R_h^2 + b_4 (S/S_o)^2 + b_5 H_{sx}^2 + b_6 Q^2 \quad (119)$$

where

$\hat{T}_w$ ≡ estimate of water temperature (C)

a_0-a_6 ≡ regression coefficients for linear independent variables

b_1-b_6 ≡ regression coefficients for second-order independent variables

T_a ≡ air temperature (C)

W_a ≡ wind speed (mps)

R_h ≡ relative humidity (decimal)

S/S_o ≡ sunshine ratio (decimal)

H_{sx} ≡ extraterrestrial solar radiation (J/m^2/sec)

Q ≡ discharge (cm)

It is recommended that the meteorological parameters and the solar radiation at the meteorological station be used for each regression analysis. Obviously, the discharge, Q, and the dependent water temperature variables must be obtained at the point of analysis.

These six independent variables are readily obtainable and are also necessary for the transport model. A minimum of seven data sets are necessary to obtain a solution, if the second-order terms are neglected. However, a greater number is desirable for statistical validity. Also, it needs to be emphasized that the resulting regression model is only valid at the point of analysis and only if upstream hydrologic conditions do not change. For example, if a reservoir has been constructed upstream subsequent to the data set, the model is not likely to be valid because the release temperatures have been affected.

Transformed Regression Model

The best regression model is one that not only uses the same parameters as the best physical-process models but has the same, or nearly the same, mathematical form. That is, the regression model equation uses physical-process transformed parameters as the independent variables. This transformed regression model uses all of the input parameters used in the transport model except for stream distance and initial water temperature.

The first-order approximation of the constant-discharge heat transport model was chosen as the basis for the physical-process regression model. Water temperature and discharge data at the specified location, together with the corresponding time period meteorologic data from a nearby station, are needed. The meteorologic data are used to determine the equilibrium temperature (T_e) and first-order thermal exchange coefficient (K_1). The T_e and K_1 are combined with the corresponding time period discharges as independent variables to determine the regression coefficients for estimating the corresponding time period water temperature dependent variable. An estimate of the average stream width W above the site location is necessary as an arbitrary constant in the regression. The resulting regression coefficients are tantamount to synthetically determining an upstream source water temperature as a function of time and the distance to the source.

The constant discharge heat transport model is

$$T_w = T_0 + (T_e - T_0) \{1 - \exp[-(K_1 \bar{B} x_0)/(pc_p Q)]\}$$
(120)

where

$T_e \equiv$ equilibrium water temperature (C)

$T_0 \equiv$ initial water temperature (C)

$T_w \equiv$ water temperature at x_o (C)

$K_1 \equiv$ first-order thermal exchange coefficient ($J/m^2/sec/C$)

$\bar{B} \equiv$ average stream width (m)

$x_0 \equiv$ distance from T_0 (m)

$p \equiv$ water density = 1000 kg/m^3

$c_p \equiv$ specific heat of water = 4182 J/kg

$Q \equiv$ discharge (cm)

The definition of exp $(x) = e^x$ is

$$e^x = 1 + x + x^2/2! + x^3/3! + \ldots$$
(121)

If T_0 is a function of the time period only, then it can be approximated as

$$T_0 = \bar{T}_0 + \Delta T_0 \cos[(2\pi/365)(D_i - 213)]$$
(122)

where

$\bar{T}_0 \equiv$ average initial water temperature over all time periods (C)

$\Delta T_0 \equiv$ half initial temperature range over all time periods (C)

$D_i \equiv$ average Julian day for i^{th} time period; January 1 = 1 and December 31 = 365

Let

$$Z_1 = -(K_1 \bar{B})/(pc_p Q)$$
(123)

$$Z_2 = -T_e$$
(124)

$$Z_3 = \cos[(2\pi/365)(D_i - 213)]$$
(125)

If equations (122) through (125) are substituted into equation (120), using (121), and the terms rearranged, then T_w can be expressed as

$$
\begin{aligned}
T_w = T_0 &+ (\Delta T_0)Z_3 + (T_0 x_0)Z_1 + (\Delta T_0 x_0)Z_1 Z_3 \\
&+ (x_0)Z_1 Z_2 + (\bar{T}_0^2 x_0^2/2)Z_1^2 + (\Delta T_0 x^2/2)Z_1^2 Z_3 \\
&+ (x_0^2/2)Z_1^2 Z_2 + (\bar{T}_0 x_0^3/6)Z_1^3 + (\Delta T_0 x_0^3/6)Z_1^3 Z_3 \\
&+ (x_0^3/6)Z_1^3 Z_2 + (\bar{T}_0 x_0^4/24)Z_1^4 + (\Delta T_0 x_0^4/24)Z_1^4 Z_3 \\
&+ (x_0^4/24)Z_1^4 Z_2 + \ldots
\end{aligned}
\tag{126}
$$

If the converging power series is truncated after the final fourth-order term and the following substitutions are made, a possible multiple linear regression model results.

Let

$$a_0 = \bar{T}_0$$

$$a_1 = \Delta T_0 \qquad\qquad X_1 = Z_3$$

$$a_2 = \bar{T}_0 x_0 \qquad\qquad X_2 = Z_1$$

$$a_3 = \Delta T_0 x_0 \qquad\qquad X_3 = Z_1 Z_3$$

$$a_4 = x_0 \qquad\qquad X_4 = Z_1 Z_2$$

$$a_5 = \bar{T}_0 x_0^2/2 \qquad\qquad X_5 = Z_1^2$$

$$a_6 = \Delta T_0 x_0^2/2 \qquad\qquad X_6 = Z_1^2 Z_3$$

$$a_7 = x_0^2/2 \qquad\qquad X_7 = Z_1^2 Z_2$$

$$a_8 = \bar{T}_0 x_0^3/2 \qquad\qquad X_8 = Z_1^3$$

$$a_9 = \Delta T_0 x_0^3/6 \qquad\qquad X_9 = Z_1^3 Z_3$$

$$a_{10} = x_0^3/6 \qquad\qquad X_{10} = Z_1^3 Z_2$$

$$a_{11} = \bar{T}_0 x_0^4/2 \qquad\qquad X_{11} = Z_1^4$$

$$a_{12} = \Delta T_0 x_0^4/24 \qquad\qquad X_{12} = Z_1^4 Z_3$$

$$a_{13} = x_0^4/24 \qquad\qquad X_{13} = Z_1^4 Z_2$$

If the resulting independent transformed variables X_1 through X_{13} are regressed on the dependent variable T_w, the following regression equation results:

$$
\hat{T}_w = a_0 + a_1 X_1 + \ldots + a_{13} X_{13}
\tag{127}
$$

The best estimates of the synthetic physical-process parameters are

$$
\bar{T}_0 = a_0
\tag{128}
$$

$$
\Delta T_0 = a_1
\tag{129}
$$

$$
x_0 = a/a_0
\tag{130}
$$

VALIDATION

Regression Model Validation

There were 15 U.S. Geological Survey (USGS) gauges within the Upper Colorado
River Basin (UCRB) study area that had some useful instream water temperature
data. However, none of the gauge data were developed from accurate 24-hour
averages. The USGS published temperatures can be assumed only to represent
water temperatures somewhere between the minimum and maximum on the day
recorded. Frequently, published temperature data were missing for several days
a month at each gauge. Therefore, accurate monthly means of the average daily
water temperatures for a specific year at any given gauge were not obtainable.

The transformed regression model was used at each gauge to smooth the data. The
published water temperature data were treated as the dependent variable. The
corresponding discharge and prevailing meteorological parameters obtained from
published data at the Grand Junction weather station were transformed into the
independent variables. Data from 1964 through 1979 were used for the
regression.

Table 4 identifies the respective gauges and their associated adjusted
correlation coefficients (R) and probable difference (δ). The correlation
coefficient is the ratio of explained variation of the predicted temperature to
the total variation of the published temperature. The probable difference is
the expected difference range of the published temperature with respect to the
predicted temperatures; i.e., 50% of the published temperatures fall within the
probable difference limits of the predicted temperature.

The regression models for the headwater gauges were used to determine the
initial water temperatures necessary for the instream water temperature
transport model. The regression models for the validation/calibration gauges
were used to calibrate and measure the performance of the transport model.

Heat Transport Model Validation

The regression models for the validation gauges were compared to the net
transport model (Theurer and Voos 1982). Table 5 gives the mean difference (Δ)
and probable difference range (δ), before calibration, by months for the years
1964 to 1979. Table 6 gives the same statistics for "normal" discharges and
meteorological conditions. The probable difference range is the 50% confidence
limits about the mean difference; i.e., 50% of the data from the validation
gauge regression model will fall within $\Delta \pm \delta$ of the transport model.

Care must be taken not to assume that the differences represent errors. Where
there is a difference, it can only be said that both temperatures cannot be
correct. Errors do exist in both the regression and transport models. It has
been pointed out that the published water temperature data do not necessarily
represent the average daily water temperatures (Theurer and Voos 1982).
Therefore, it can only be expected that the regression model predictions
generally fall within the minimum/maximum daily water temperatures. See Theurer
et al. (1982) for a discussion of application of the model.

CALIBRATION

Calibration is defined as adjusting one or more input parameters or internally
defined model coefficients to meet certain specified objective functions.
Desirable objective functions include eliminating the mean errors, minimizing
the square of the errors, or both. A well defined objective function is subject
to the number of independent data sets available, the number of input parameters
or internal coefficients considered as candidates, and, of course, the
tractability of solution. The instream water temperature model includes two
calibration models: (1) ground level solar radiation and (2) transport model
water temperature predictions. Of course, regression models automatically
include calibration concepts as their mathematical basis; i.e., least squares or
minimizing the square of the errors, as well as no net mean error.

Table 4
Transformed regression model statistics.

USGS gauge name and number	Location	R	δ (C)
Headwater gauges			
Flaming Corge 09234500	Green River near Creendale, UT	.7304	1.17
Maybell 09251000	Yampa River near Maybell, CO	.9483	1.78
Lily 09260000	Little Snake River near Lily, CO	.9505	1.74
Duschesne 09302000	Duschesne River near Randett, UT	.9682	1.32
Watson 09302000	White River near Watson, UT	.9764	1.13
Price 09314500	Price River at Woodside, UT	.8950	2.82
San Rafael 09328500	San Rafael River near Creen River, UT	.9791	1.21
Cameo 09095500	Colorado River near Cameo, CO	.9567	1.90
Dolores 09180000	Dolores River near Cisco, UT	.9818	1.07
Crand Junction 09152500	Gunnison River near Crand Junction, CO	.9864	0.74
Validation/calibration gauges			
Jensen 09261000	Creen River near Jensen, UT	.9799	0.91
Creen River 09315000	Creen River near Green River, UT	.9838	1.07
State line 09163530	Colorado River near CO-UT State line	.9808	0.99
Cisco 09180500	Colorado River near Cisco, UT	.9876	0.84
UT163 09182880	Colorado River at UT163 near Maob, UT	.9802	1.20

Table 5
Heat transport model statistics for 1964-1979 before calibration (after Theurer
and Voos 1982).

		Jensen	Green River	State line	Cisco	UT163
January	Δ	0.78	0.21	- 0.04	0.05	- 0.60
	δ	± 0.57	± 0.41	± 0.29	± 0.11	± 0.51
February	Δ	0.44	0.27	- 0.16	- 0.04	- 0.31
	δ	± 0.59	± 0.51	± 0.57	± 0.54	± 0.92
March	Δ	0.70	0.46	0.21	- 0.08	0.30
	δ	± 0.59	0.37	± 0.51	± 0.35	± 0.53
April	Δ	0.10	0.19	- 0.13	- 0.10	0.82
	δ	± 0.74	± 0.37	± 0.90	± 0.68	± 0.54
May	Δ	- 1.96	- 1.01	0.00	0.39	- 0.73
	δ	± 0.91	± 0.57	± 0.49	± 0.48	± 0.78
June	Δ	- 1.46	- 1.48	- 0.55	- 0.11	- 1.77
	δ	± 0.80	± 0.57	± 0.43	± 0.41	± 0.94
July	Δ	0.12	- 1.78	- 0.74	- 0.35	- 1.23
	δ	± 1.03	± 0.52	± 0.53	± 0.55	± 0.66
August	Δ	- 0.26	- 1.67	- 0.66	- 0.56	- 0.75
	δ	± 0.94	± 0.32	± 0.41	± 0.52	± 0.63
September	Δ	- 0.01	- 0.97	- 0.58	- 0.70	- 1.03
	δ	± 0.80	± 0.38	± 0.68	± 0.63	± 0.62
October	Δ	- 0.13	- 0.91	- 0.28	- 0.72	- 0.79
	δ	± 0.47	± 0.45	± 0.38	± 0.51	± 1.03
November	Δ	0.06	- 0.90	- 0.86	- 1.17	- 1.84
	δ	± 0.53	± 0.34	± 0.37	± 0.44	± 0.78
December	Δ	0.76	- 0.21	- 1.03	- 0.97	- 2.64
	δ	± 0.71	± 0.36	± 0.35	± 0.35	± 0.86
Annual	Δ	- 0.08	- 0.65	- 0.40	- 0.35	- 0.84
	δ	± 0.91	± 0.67	± 0.56	± 0.55	± 0.92

Table 6
Heat transport model statistics, normals before calibration (after Theurer and Voos 1982).

		Jensen	Green River	State line	Cisco	UT163
January	Δ	1.11	0.00	0.27	0.25	- 0.88
February	Δ	0.76	0.52	0.02	- 0.14	- 1.01
March	Δ	0.92	0.65	0.25	- 0.10	- 0.03
April	Δ	0.61	0.39	0.18	0.11	0.45
May	Δ	- 1.19	- 0.49	0.15	0.63	- 0.46
June	Δ	- 1.36	- 1.24	- 0.13	0.55	- 1.63
July	Δ	0.52	- 1.48	- 0.18	0.19	- 1.05
August	Δ	0.52	- 1.49	- 0.26	- 0.70	- 0.49
September	Δ	0.36	- 1.13	- 0.64	- 1.03	- 1.50
October	Δ	0.17	- 0.71	- 0.32	- 0.99	- 1.85
November	Δ	- 0.10	- 1.07	- 0.96	- 1.46	- 2.64
December	Δ	0.54	- 0.65	- 1.11	- 1.26	- 3.38
Annual	Δ	0.24	- 0.56	- 0.23	- 0.33	- 1.21
	δ	± 0.53	± 0.53	± 0.31	± 0.49	± 0.73

Solar Calibration

Solar radiation can be calibrated at ground level by using SOLMET data. The U.S. Department of Energy has compiled and summarized (Cinquemani et al., 1978) several years of solar radiation data at many weather stations throughout the United States. Normal solar radiation at ground level by months is available. These data can be used to calibrate the dust and/or ground reflectivity coefficients. Table 7 shows the monthly normal meteorology at the Grand Junction weather station, together with a summary of the measured solar radiation. Initial estimates of the dust and ground reflectivity coefficients were made from Tables 1 and 2 and adjusted by trial and error until satisfactory agreement with the published solar data was reached. The resulting final values of dust and ground reflectivity are assumed to be valid over the UCRB without change from year to year. However, the changes between time periods are maintained.

The meteorologic station at Grand Junction is located at longitude 39° 07' and elevation 1476 m. The dust coefficients were determined from the annual cycle formula [equation (19)] assuming $d_1 = 0.10$ and $d_2 = 0.20$. The monthly normal meteorological values in columns 2, 3, and 4 of Table 7 were obtained from the 1977 Grand Junction, Colorado LCD's. The solar radiation data at ground level value in column 5 were obtained from measured data (Cinquemani et al. 1978).

The solar radiation parameters in columns 6, 8, 9, and 10 were calculated using the HP-41C solar radiation model. The atmospheric attenuation coefficient in column 7 was calculated according to equation (131). And finally, the ground reflectivity was calibrated to reproduce the solar radiation at ground level according to equation (132). Therefore, the final dust and ground reflectivity coefficients reproduce the normal solar radiation at ground level for normal meteorologic conditions and are assumed to be valid for the entire UCRB, regardless of the year simulated.

Table 7
Solar calibration using normal meteorology.

| | Monthly normals at Grand Junction | | | | | | $d_1 = 0.10$ | | | |
| | Lat: 39° 01' | | | Elev: 1476 m | | | $d_2 = 0.20$ | | | |

1	2	3	4	5	6	7	8	9	10	11
	C	dec.	dec.	$J/m^2/sec$	$J/m^2/sec$	dec.	dec.	dec.	dec.	dec.
Time period	T_a	R_h	S/S_o	H_{sg}	H_{sx}	$e^{-\eta z}$	$1-a'$	a''	d	R_g
Jan	- 3.0	0.718	0.58	103.9	184.8	.7374	.1711	.7254	.1989	.1899
Feb	0.9	0.590	0.64	147.0	243.4	.7556	.1530	.7448	.1989	.2539
Mar	5.1	0.475	0.64	204.1	325.7	.7840	.1368	.7640	.1925	.3707
Apr	10.9	0.400	0.67	260.9	407.7	.7830	.1295	.7725	.1797	.2941
May	16.8	0.363	0.71	312.6	464.7	.8009	.1306	.7692	.1613	.4025
June	21.8	0.295	0.79	342.4	486.6	.7937	.1317	.7671	.1389	.2812
July	25.9	0.328	0.78	324.5	473.5	.7779	.1443	.7464	.1137	.1614
Aug	24.1	0.345	0.76	286.6	425.7	.7742	.1458	.7450	.1128	.1269
Sep	19.6	0.363	0.79	241.0	350.7	.7751	.1473	.7454	.1381	.2269
Oct	12.7	0.430	0.74	176.7	265.3	.7761	.1562	.7372	.1607	.3346
Nov	4.3	0.570	0.63	120.6	196.4	.7741	.1709	.7234	.1791	.4045
Dec	- 1.4	0.680	0.60	96.1	166.6	.7444	.1797	.7160	.1922	.2503
annual	11.5	0.465	0.70	217.9	333.0	.7837	.1381	.7596	.1500	.2662

The following equations were used to supplement the HP-41C solar radiation model:

$$e^{-\eta z} = H_{sg}/\{[0.22 + 0.78(S/S_o)^{2/3}]H_{sx}\} \qquad (131)$$

$$R_g = \{2-[(1-a'-d + 2a'')/e^{-\eta z}]\}/\{1-a' + d\} \qquad (132)$$

Single-Parameter Heat Transport Calibration

It is possible to calibrate the heat transport model to closely match the mean water temperature data at any of the validation gauges by adjusting a single, but significant, parameter. There are several candidate parameters within the meteorological (e.g., solar), hydrology (e.g., source temperature), and stream geometry variables (e.g., stream width). If the assumption is made that the validation gauge regression models are accurate, one calibration technique would involve adjusting the wind speed to account for both the transposition of the wind speed from the weather station to each reach in the basin and to possibly better determine the evaporation coefficient used in the heat flux components.

Tables 8 and 9 show how a wind speed factor can be used to reduce or entirely eliminate the monthly mean differences, Δ, at validation gauges. No attempt was made to calibrate UT163 because the data are considered unreliable. Obviously, if the mean differences for all months are reduced or eliminated at a specific gauge, the annual mean differences are also reduced or eliminated. However, a probable difference range for each month will generally remain. In other words, calibration can only reduce the bias, not necessarily remove all differences.

Table 10 shows the monthly mean differences at each validation gauge for the normal (mean monthly average) calibrated conditions. They could have just as easily been calibrated on the normals and the results compared to the historical temperatures.

Table 8
Wind calibration factors

	Jensen	Green River	State line	Cisco
January	1.85	1.6	1	1
February	1.22	1.05	0.94	1.05
March	1.3	1.08	1.06	0.8
April	1.06	1.07	0.95	1
May	0	0.83	1	1.7
June	0	0.75	0.7	1.5
July	1.08	0.505	0.79	1.05
August	0.76	0.65	0.85	0.9
September	1	0.715	0.85	0.78
October	0.9	0.62	0.9	0.4
November	1.02	0.34	0.6	0
December	1.3	0.48	0.4	0.6

Note: The input wind speed at each node was set equal to the associated wind calibration factor times the wind speed at the meteorological station for the proper year and time period. Nodes were associated with the first radiation/calibration node encountered downstream.

Table 9
Heat transport model after single-parameter (wind) calibration statistics:
1964-1979.

		Jensen	Green River	State line	Cisco	UT163
January	Δ	0.01	0.09	- 0.04	0.05	- 0.60
	δ	± 0.31	± 0.22	± 0.29	± 0.11	± 0.51
February	Δ	0.00	0.01	- 0.01	- 0.04	- 0.30
	δ	± 0.59	± 0.47	± 0.57	± 0.54	± 0.92
March	Δ	0.00	0.01	0.02	- 0.01	0.62
	δ	± 0.55	± 0.38	± 0.51	± 0.34	± 0.57
April	Δ	0.01	- 0.04	0.03	- 0.01	0.88
	δ	± 0.73	± 0.37	± 0.90	± 0.67	± 0.54
May	Δ	- 1.37	- 0.01	0.00	0.05	- 1.43
	δ	± 1.19	± 0.82	± 0.49	± 0.65	± 0.61
June	Δ	- 0.46	- 0.02	0.00	- 0.00	- 2.04
	δ	± 1.46	± 0.67	± 0.53	± 0.44	± 0.80
July	Δ	0.01	0.06	- 0.01	0.04	- 1.10
	δ	± 0.99	± 0.48	± 0.55	± 0.51	± 0.65
August	Δ	0.00	- 0.04	- 0.02	0.01	- 0.21
	δ	± 1.12	± 0.30	± 0.44	± 0.52	± 0.65
September	Δ	- 0.01	0.00	- 0.03	- 0.02	- 0.17
	δ	± 0.80	± 0.38	± 0.70	± 0.64	± 0.66
October	Δ	0.06	- 0.00	- 0.02	- 0.04	0.42
	δ	± 0.47	± 0.35	± 0.36	± 0.46	± 0.92
November	Δ	0.02	0.00	- 0.02	0.02	- 0.16
	δ	± 0.54	± 0.29	± 0.34	± 0.38	± 0.69
December	Δ	0.00	- 0.04	0.00	- 0.05	- 1.52
	δ	± 0.76	± 0.36	± 0.28	± 0.27	± 0.69
Annual	Δ	- 0.15	0.00	- 0.01	0.01	- 0.47
	δ	± 0.87	± 0.44	± 0.51	± 0.47	± 0.89

Table 10
Heat transport model after single-parameter (wind) calibration statistics: normals.

		Jensen	Green River	State line	Cisco	UT163
January	Δ	- 0.28	0.00	0.27	0.25	- 0.88
February	Δ	0.27	0.21	0.15	- 0.06	- 0.99
March	Δ	0.20	0.18	0.08	- 0.06	0.23
April	Δ	0.50	0.17	0.33	0.20	0.53
May	Δ	- 0.56	0.65	0.15	0.37	- 1.04
June	Δ	- 0.55	0.26	0.35	0.75	- 1.72
July	Δ	0.40	- 0.07	0.35	0.57	- 0.79
August	Δ	0.95	0.17	0.35	- 0.15	0.10
September	Δ	0.36	- 0.09	- 0.07	- 0.53	- 1.02
October	Δ	0.38	0.30	0.01	- 0.23	- 0.55
November	Δ	- 0.15	- 0.06	- 0.08	- 0.21	- 0.88
December	Δ	- 0.22	- 0.41	0.02	- 0.13	- 2.25
Annual	Δ	0.11	0.11	0.16	0.06	- 0.77
	δ	$\pm$ 0.31	$\pm$ 0.18	$\pm$ 0.11	$\pm$ 0.25	$\pm$ 0.53

Multiple-Parameter Heat Transport Calibration

The single-parameter calibration scheme can only eliminate bias (mean error) or only minimize the standard deviation of the errors, for example. The multiple-parameter scheme can not only eliminate bias but also minimize the probable differences. By spreading the amount of calibration over multiple parameters, no single variable requires as much change as it does in the single-parameter scheme. This latter feature reduces the tendency of the final calibrated values to exceed reasonable, or even physical, limits.

If known water temperature data are available, together with matching time period meteorological data for several time periods, then multiple-parameter calibration of either or both the regression and heat transport models is possible. The objective of calibration of the regression model is to minimize the probable differences because the mean difference is automatically zero. However, the objective of calibration of the heat transport model is twofold: first, to eliminate bias (set the mean difference to zero) and, second, to minimize the probable differences.

The multiple-parameter heat transport calibration scheme is based on the first-order solution of the constant discharge heat transport model, the same as the transformed regression model.

Element Correction

A first-order correction formula for a single element from a paired data set is

$$T_{wi} - \hat{T}_{wi} = (\partial T_w/\partial z_1)\Delta z_1 + (\partial T_w/\partial z_2)\Delta z_2 + \ldots + (\partial T_w/\partial z_n)\Delta z_n \tag{133}$$

where $T_{wi} \equiv$ ith known water temperature

$\hat{T}_{wi} \equiv$ ith predicted water temperature

z_i thru $z_n \equiv$ ith dummy variables to represent an n-dimensional multiple-parameter data set

In order to linearize equation (133) and to more easily apply constraints, the individual dummy corrections (Δz_i) are noted as

$$\Delta z_i = b_{o,i} + b_{1,i} z_i \tag{134}$$

where $\Delta z_i \equiv$ ith dummy correction term

$z_i \equiv$ ith actual value dummy term

$b_{o,i} \equiv$ ith calibration constant

$b_{1,i} \equiv$ ith calibration factor

Partial Derivatives

In order to solve the correction formula, it is necessary to determine the partial derivatives for each of the calibration parameters. These derivatives are based on the heat transport equation:

$$T_w = T_o + (T_e - T_o) [1-\exp(\bullet)] \tag{135}$$

where $\exp(\bullet) = \exp[-(K_1 x_o B)/p\bar{c}_p Q)]$

T_o is determined by

$$T_o = T_e - [(T_e - T_w)/\exp(\bullet)] \tag{136}$$

where $T_w \equiv$ known water temperature

T_e and $\exp(\bullet)$ are calculated using current input data

The parameter x_o can be obtained from the original transformed regression model analysis and is treated as a given constant during calibrations; p and c_p are physical constants. Q is treated as an independent given variable not subject to calibration. This leaves T_e, K_1, and B subject to calibration. The average stream width is a function of, at most, discharge. However, T_e and K_1 are functions of many physical constants and parameters. Only seven parameters are considered significant for calibration. They are

$$T_e = f_1 (H_{sw}, T_a, W_a, R_h, \bar{B}, S_h, K_g/\Delta Z_g)$$

$$K_1 = f_2 (W_a, K_g/\Delta Z_g)$$

Because of the mathematical relationship between some of the physical constants and parameters, one parameter may serve as a surrogate for others. For example, wind speed (W_a) and the evaporation coefficient (C_b) are not separable. Also, ground temperature (T_g) and the streambed thermal gradient ($K_d/\Delta Z_g$) are surrogates for each other.

The change in water temperature with respect to any dummy variable is

$$\partial T_e / \partial z = \{[(T_e + 273.16)^4 (\partial A / \partial z)] + [T_e (\partial B / \partial z)]$$

$$+ [(1.0640^{T}e)(\partial C / \partial z)] - [\partial D / \partial z]\} / -K_1 \qquad (137)$$

$$\partial \exp(\ )/ \partial z = [-x_o / (pc_p Q)][\exp(\bullet)]\{[\bar{B}(\partial K_1 / \partial z)] + [K_1 (\partial \bar{B} / \partial z)]\} \qquad (138)$$

$$\partial K_1 / \partial z = \{[12A(T_e + 273.16)^2 + C(1.0640^{T}e)\ln^2(1.0640)][\partial T_e / \partial z]\}$$

$$+ \{\partial B / \partial z\} + \{[(1.0640^{T}e)\ln(1.0640)][\partial C / \partial z]\}$$

$$+ \{[4(T_e + 273.16)^3 (\partial A / \partial z)]\} \qquad (139)$$

$$\partial T_w / \partial z = \{[1 - \exp(\bullet)][\partial T_e / \partial z]\} - \{[T_e - T_o][\partial \exp(\bullet) / \partial z]\} \qquad (140)$$

$$\partial \bar{B} / \partial z = I[z = \bar{B}] \qquad (141)$$

where

$$A = 5.40 \times 10^{-8} \qquad (142)$$

$$B = [C_c\, C_e\, P] + [K_g / \Delta Z_g] \qquad (143)$$

$$C = C_e \qquad (144)$$

$$D = H_a + H_f + H_s + H_v$$

$$+ [C_c\, C_e\, PT_a]$$

$$+ [T_g (K_g / \Delta Z_g)]$$

$$+ [C_e\, R_h\, (1.0640^{T}a)] \qquad (145)$$

$$C_e = a + bW_a + cW_a^2 \qquad (146)$$

$$C_c = B_f / 6.60 \qquad (147)$$

$$H_a = (1 - S_h)(1 + 0.17C_1^2)[3.36 + 0.706\,(R_h\,1.0640^{T}a)^{1/2}]$$

$$[10^{-8}(T_a + 273.16)^4] \qquad (148)$$

$$H_f = [9805\,(Q/\bar{B})\,S_f] \qquad (149)$$

$$H_s = [(1 - S_h)\,H_{sw}] \qquad (150)$$

$$H_v = [(5.24 \times 10^{-8})\,S_h\,(T_a + 273.16)^4 \qquad (151)$$

Let

$$H_a' = [(1 - S_h)\,(1 + 0.17C_1^2)\,(3.36 \times 10^{-8})\,(T_a + 273.16)^4] \qquad (152)$$

When

$$z_1 = H_{sw},$$

$$\partial \bar{B} / \partial H_{sw} = 0 \qquad (153)$$

$$\partial A / \partial H_{sw} = 0 \qquad (154)$$

$$\partial B / \partial H_{sw} = 0 \qquad (155)$$

$$\partial C / \partial H_{sw} = 0 \qquad (156)$$

$$\partial D / \partial H_{sw} = (1 - S_h) \qquad (157)$$

When $z_2 = T_a$,

$$\partial \bar{B}/\partial T_a = 0 \tag{158}$$

$$\partial A/\partial T_a = 0 \tag{159}$$

$$\partial B/\partial T_a = 0 \tag{160}$$

$$\partial C/\partial T_a = 0 \tag{161}$$

$$\partial D/\partial T_a = [4(H_a + H_v)/(T_a + 273.16)]$$
$$+ \{[(H_a - H_a')/2]\ [\ln(1.0640)]\}$$
$$+ [C_c\ C_e\ P]$$
$$+ [C_e\ \ln(1.0640)(1.0640^{T}a)] \tag{162}$$

When $z_3 = W_a$,

$$\partial \bar{B}/\partial W_a = 0 \tag{163}$$

$$\partial A/\partial W_a = 0 \tag{164}$$

$$\partial B/\partial W_a = C_c\ [b + 2\ cW_a]\ P \tag{165}$$

$$\partial C/\partial W_a = b + 2\ cW_a \tag{166}$$

$$\partial D/\partial W_a = [C_c\ (b + 2\ cW_a)\ P] + [b + 2\ cW_a\ R_h\ (1.0640^{T}a)] \tag{167}$$

When $z_4 = R_h$,

$$\partial \bar{B}/\partial R_h = 0 \tag{168}$$

$$\partial A/\partial R_h = 0 \tag{169}$$

$$\partial B/\partial R_h = 0 \tag{170}$$

$$\partial C/\partial R_h = 0 \tag{171}$$

$$\partial D/\partial R_h = [(H_a - H_a')/(2\ R_h)] + [C_e\ (1.0640^{T}a)] \tag{172}$$

When $z_5 = K_g/\Delta Z_g$,

$$\partial \bar{B}/\partial (K_g/\Delta Z_g) = 0 \tag{173}$$

$$\partial A/\partial (K_g/\Delta Z_g) = 0 \tag{174}$$

$$\partial B/\partial (K_g/\Delta Z_g) = 1 \tag{175}$$

$$\partial C/\partial (K_g/\Delta Z_g) = 0 \tag{176}$$

$$\partial D/\partial (K_g/\Delta Z_g) = T_g \tag{177}$$

When $z_6 = \bar{B}$,

$$\partial\bar{B}/\partial\bar{B} = 1 \qquad (178)$$

$$\partial A/\partial\bar{B} = 0 \qquad (179)$$

$$\partial B/\partial\bar{B} = 0 \qquad (180)$$

$$\partial C/\partial\bar{B} = 0 \qquad (181)$$

$$\partial D/\partial\bar{B} = -H_f/\bar{B} \qquad (182)$$

When $z_7 = S_h$,

$$\partial\bar{B}/\partial S_h = 0 \qquad (183)$$

$$\partial A/\partial S_h = 0 \qquad (184)$$

$$\partial B/\partial S_h = 0 \qquad (185)$$

$$\partial C/\partial S_h = 0 \qquad (186)$$

$$\partial D/\partial S_h = (H_v/S_h) - [(H_a + H_s)/(1-S_h)] \qquad (187)$$

The objective function is as follows:

Let

$$\Delta_j = \hat{T}_{w,j} - T_{w,j}$$

$$x_i = (\partial T_w/\partial z_i) \, [I(k_i=1) + z_i I(1_i=1)]$$

Then

$$\Delta_j = c_1 x_{1,j} + c_2 x_{2,j} + \cdots + c_n x_{n,j}$$

where

$$c_i = b_{o,i} I(k_i=1) + b_{1,i} I(1_i=1)$$

$$k_i = 0 \text{ if ith constant is zero, 1 otherwise}$$

$$1_i = 0 \text{ if ith factor is zero, 1 otherwise}$$

To eliminate bias

$$\sum_{j=1}^{J} \, [\Delta_j - (c_1 x_{1,j} + c_2 x_{2,j} + \cdots + c_n x_{n,j})] = 0 \qquad (189)$$

To minimize the probable differences,

$$\text{Min.} : S = \sum_{j=1}^{J} \, [\Delta_j - (c_1 x_{1,j} + c_2 x_{2,j} + \cdots + c_n x_{n,j})]^2 \qquad (190)$$

requires

$$\partial S/\partial c_i = 0$$

Therefore

$$S = [\Delta - (c_1 x_1 + c_2 x_2 + \cdots c_n x_n)]^2$$

$$= [\Delta_1 - (c_1 x_1 + c_2 x_{2,1} + \cdots c_n x_{n,1})]^2$$

$$+ [\Delta_2 - (c_1 x_{1,2} + c_2 x_{2,2} + \cdots c_n x_{n,2})]^2 + \cdots$$

$$+ [\Delta_j - (c_1 x_{1,j} + c_2 x_{2,j} + \cdots + c_n x_{n,j})]^2$$

$$\partial S / \partial c_i = \sum_{j=1}^{J} \{2\, x_{i,j} [\Delta_j - (c_1 x_{1,j} + c_2 x_{2,j} + \cdots$$

$$+ c_1 x_{1,j} + c_n x_{n,j})]\} = 0 \qquad (191)$$

And

$$\sum [\Delta_j - (c_1 x_1 + c_2 x_2 + \cdots + c_n x_n)] = 0$$

becomes

$$\Sigma\Delta = c_1 \Sigma x_1 + c_2 \Sigma x_2 + \cdots + c_n \Sigma x_n \qquad (192)$$

and

$$\Sigma\Delta\, x_i = c_1 \Sigma(x_1 x_i) + c_2 \Sigma(x_2 x_i) + \cdots + c_i \Sigma x_i^2 + \cdots c_n \Sigma[x_i x_n)]$$

The above probable difference equations can be expressed in matrix for as

$$\begin{bmatrix} \Sigma(x_1^2) & \Sigma(x_1 x_2) & \cdots & \Sigma(x_1 x_n) \\ \Sigma(x_2 x_1) & \Sigma(x_2^2) & \cdots & \Sigma(x_2 x_n) \\ \cdot & \cdot & & \cdot \\ \cdot & \cdot & & \cdot \\ \cdot & \cdot & & \cdot \\ \Sigma(x_n x_1) & \Sigma(x_n x_2) & \cdots & \Sigma(x_n^2) \end{bmatrix} \begin{bmatrix} c_1 \\ c_2 \\ \cdot \\ \cdot \\ \cdot \\ c_n \end{bmatrix} \begin{matrix} = \\ = \\ \cdot \\ \cdot \\ \cdot \\ = \end{matrix} \begin{bmatrix} \Sigma(x_1\Delta) \\ \Sigma(x_2\Delta) \\ \cdot \\ \cdot \\ \cdot \\ \Sigma(x_n\Delta) \end{bmatrix} \qquad (193)$$

and the bias equation is

$$c_1 \Sigma x_1 + c_2 \Sigma x_2 + \cdots + c_n \Sigma x_n = \Sigma\Delta \qquad (194)$$

the solution of which eliminates bias and minimizes the probable differences. If all seven parameters are chosen for calibration, a minimum of seven data sets are required; more are required if both the constant and factor calibration terms for any parameter are nonzero.

The solution of the above multiple-parameter calibration scheme is dependent on which equation is eliminated from the set of equations. If the first equation (bias equation) is eliminated, a residual bias will remain, but the probable differences will be at the absolute minimum. The elimination of one of the probable differences equations locates the bias equation in the matrix. This will eliminate bias but will result in a different probable difference for each choice for the eliminated equation. The best choice will depend on both the magnitude of the errors and the range of the regression coefficients. For example, the wind coefficient should not be less than 0 because negative winds have no physical meaning.

STATISTICAL DEFINITIONS

A small set of statistical parameters are used to measure the performance of various portions of the instream water temperature model. The coefficient of multiple correlation (R) and the probable difference (δ) are used as the measures of performance of the regression model. The mean difference (Δ) and probable difference (δ) are used as the measures of performance of the physical-process model at validation and calibration points within the network. The standard deviation (S_T) and modified standard difference of estimate ($S_{T.X}$) are intermediate statistical parameters used to calculate the probable difference. All measurements are for temperature; therefore, the units are Celsius except for R, which is dimensionless.

Standard Deviation

The standard deviation is a measure of the dispersion or variation of published water temperature data about their mean. All standard deviations calculated by this model are modified to give the best estimate of the population standard deviation from the set of published temperature (sample) data. Consequently, this parameter is, by convention, the sample standard deviation. The formula is

$$S_T = \sqrt{[\Sigma(T_i - \overline{T})^2]/[N-1]} \tag{195}$$

where

$S_T \equiv$ standard deviation of sample set (C)

$T_i \equiv$ ith published temperature from sample set (C)

$\overline{T} \equiv$ mean temperature of sample set $= \Sigma T_i/N$ (C)

$N \equiv$ number of temperatures in sample set

Modified Standard Difference of Estimate

The modified standard difference of estimate is analogous to the standard deviation. It is a measure of the dispersion of the differences between the published temperatures and the predicted regression model values and between the predicted regression and heat transport models. The standard differences calculated by this model are modified by the number of degrees of freedom. The number of degrees of freedom, when comparing the regression model to the physical-process model, is one before calibration and two after. The number of degrees of freedom, when comparing published temperatures to predicted regression model values, is the number of terms used in the regression model; e.g., a single-independent-variable regression model has two terms, and a two-independent-variable multiple regression model has three terms.

Convention usually calls this parameter the standard error of estimate. However, there are errors in using the published recorded water temperatures (even when "smoothed") as accurate estimates of the average daily water temperature, as well as inherent errors in any prediction model. The typical published water temperatures are assumed to be taken at some variable unknown time of day and represent, at best, a water temperature somewhere between the minimum and the maximum of the diurnal cycle. If the published temperatures were really taken at random times, then use of the regression model would smooth or approach the 24-hour average. However, the most that reasonably can be assumed is that the heat transport model will generally predict temperatures that fall within the diurnal temperature cycle, about the predicted value from the regression model, and, maybe, the mean differences between the two will be minimized (calibration).

Heat Transport Model

The formula for the best estimate of the standard difference of estimate for the heat transport model is

$$S_{T.X} = \sqrt{[\Sigma(T_j - T_i)^2]/[N-1]} \tag{196}$$

where $S_{T.X}$ ≡ modified standard difference of estimate (C)

               T_j ≡ jth predicted temperature from regression model (C)

               T_i ≡ ith predicted temperature from heat transport model (C)

               N ≡ number of temperatures in sample set

               i = j

Regression Model

The formula used for the best estimate of the standard difference of estimate for the regression model is an alternate form of equation F:

$$S_{T.X} = S_T \sqrt{[(1-R^2)\ (N-1)]/[N-n]} \tag{197}$$

where $S_{T.X}$ ≡ modified standard difference of estimate (C)

               S_T ≡ standard deviation of sample set (C)

               R ≡ coefficient of multiple correlation

               N ≡ number of temperatures in sample set

               n ≡ number of terms in regression model

Coefficient of Multiple Correlation

The coefficient of multiple correlation is a measure of the explained variation to the total variation. This definition is only valid when the variations are about the same mean. Therefore, the coefficient of multiple correlation is only applicable to the regression model because the mean of the predicted heat transport temperatures is generally different from the mean of the published water temperatures. The formula is

$$R = \sqrt{[\Sigma(T_i - \overline{T})^2]/[\Sigma(T_j - \overline{T})^2]} \tag{198}$$

where   R ≡ coefficient of multiple correlation

               T_j ≡ jth published temperature from sample set (C)

               T_i ≡ ith predicted temperature from regression model (C)

               $\overline{T}$ ≡ mean temperature of sample set (C)

               i = j

Mean Difference

The mean difference is the average of the differences between the predicted regression and heat transport models. The mean difference of the regression model, with respect to the published temperatures, is automatically zero because of the mathematical restrictions imposed by the regression conditions. However, the heat transport model, when compared to predicted regression model temperatures, generally has a bias because of independent errors inherent in both. One purpose of calibration is to eliminate these mean differences. The formula is

$$\Delta = [\Sigma(T_i - T_j)]/N \tag{199}$$

where Δ = mean difference (C)

T_j = jth predicted temperature from regression model (C)

T_i = ith predicted temperature from heat transport model (C)

N $\equiv$ number of predicted temperatures in sample set

i $\equiv$ j

Probable Difference

The probable difference is used to determine how well the various models are performing. It sets the 50% confidence limits; i.e., 50% of the actual water temperatures fall within $\Delta \pm \delta$ of the model predictions. Again, for the regression model Δ always equals zero; but generally Δ does not equal zero for the heat transport model without calibration. The formula is

$$\delta = 0.6745 \ S_{T.X} \qquad (200)$$

where δ $\equiv$ probable difference (C)

$S_{T.X}$ $\equiv$ modified standard difference of estimate (C)

CONVERSIONS AND PHYSICAL CONSTANTS

The standard units used for the water temperature model are metric units. In addition, all physical constants and internal processing algorithms are computed using metric units. However, for user convenience, the input/output model portions of the computer model have a user-specified option that allows the user to request English units. This option requires that all standard input/output displays be in English units. Internal processing, which is transparent to the user, remains in metric units. If the English units option is specified, then (1) the computer input model converts all English units to metric units; (2) the computer processing model performs the necessary calculations in metric units; and (3) the computer output model converts the metric units to English units for output display. Note that only the computer model has an English units option. The other solution techniques (HP-34C and HP-41C), because of their limited processing capabilities, operate entirely in metric units. Table 11 can be used to convert commonly used English units to standard metric units.

The physical constants in the instream water temperature model range from well established constants used in physics (e.g., the solar constant) to empirically derived coefficients (e.g., the evaporation coefficient). The physics constants have a single value for any situation. However, the empirically derived coefficients frequently are expressed as a range of possible values. Table 12 gives the single-valued constants and the chosen constant value for empirically derived coefficients.

Table 11
Conversions from English to metric units.

Parameter		English units	Metric units	
H_{sr}	1	$BTU/ft^2/day$	0000.1313	$J/m^2/sec$
	1	langley/day	0000.4842	$J/m^2/sec$
	1	$kcal/m^2/day$	0000.04842	$J/m^2/sec$
	1	$KJ/m^2/day$	0000.01157	$J/m^2/sec$
W	1	ft/sec	0000.3048	m/sec
	1	mile/hr	0000.4470	m/sec
P	1	in H_g	0033.86	mb
	1	mm H_g	0001.333	mb
	1	psi	0068.95	mb
	1	atm	1013.00	mb
v	1	ft/sec	0000.3048	m/sec
d	1	ft	0000.3048	m
q	1	ft^2/sec	0000.09290	m^2/sec
Q	1	ft^3/sec	0000.02832	m^3/sec
A	1	ft^2	0000.09290	m^2
T	1	T_f	$32 + [(915)T_C]$	

Table 12
Physical constants.

Parameter	Physical constants

C_b evaporation coefficient, $1 \leq C_b \leq 5$; use $C_b = 1.681$

C_T adiabatic temperature correction coefficient; use $C_T = -0.00656$ C/m

c_p specific heat of water = 4182 J/kg/C

e orbital eccentricity = 0.0167238

K_g thermal conductivity coefficient; use $K_g = 1.65$ J/m/sec/C for water-saturated sands and gravel mixtures

k type of cloud cover factor, $0.04 \leq k \leq 0.24$; use $k = 0.17$

q_s solar constant = 1377 $J/m^2/sec$

r_1 longwave radiation reflection; use $r = 0.03$

T_{ab} absolute zero correction = 273.16 (C)

p density of water = 1000 kg/m^3

σ Stefan-Boltzman constant = 5.672 10^{-8} $J/m^2/sec/K^4$

ϵ_w water emissivity; use $\epsilon_w = 0.9526$

ϵ_v vegetation emissivity; use $\epsilon_v = 0.9526$

REFERENCES

Cinquemani, V., J. R., Owenby, and R. G. Baldwin. 1978. Input data for solar systems. U.S. Dept. of Energy. Environ. Resour. and Assessments Branch. 192 pp.

Grenney, W. J., and A. K. Kraszewski. 1981. Description and application of the stream simulation and assessment model. Version IV (SSAM IV). Instream Flow Inf. Pap. 17, U.S. Fish and Wildl. Serv. FWS/OBS-82/46. 199 pp.

Johnson, H. E., and T. N. Keefer. 1979. Modeling highly transient flow, mass, and heat transport in the Chattahoochee River near Atlanta, Georgia. U.S. Geol. Surv. Prof. Pap. 1136. 41 pp.

Pluhowski, E. J. 1970. Urbanization and its effect on the temperature of the streams on Long Island, New York. U.S. Geol. Surv. Prof. Pap. 627-D. 110 pp.

Quigley, T. M. 1981. Estimating contributions of overstory vegetation to stream surface shade. Wildl. Soc. Bull. 9(1):22-27.

Spiegel, M. R. 1961. Schaum's outline series - theory and problems of statistics. McGraw-Hill Book Co., New York. 360 pp.

Tennessee Valley Authority. 1972. Heat and mass transfer between a water surface and the atmosphere. Water Resour. Res. Lab. Rep. 14. Norris, TN. 166 pp.

Theurer, F. D. and K. A. Voos. 1982. IFG's instream water temperature model validation. Pages 513-518 in F. Kilpatrick and D. Matchett (eds.). Proceedings of the Conference on water and energy technical and policy issues. Am. Soc. of Civil Engineers.

Theurer, F. D., K. A. Voos, and C. G. Prewitt. 1982. Application of IFG's instream water temperature model in the Upper Colorado River. International Symposium on Hydrometeorology, Denver, CO, June 13-17, 1982. Am. Wat. Resour. Assoc. Pages 287-292.

CONCEPTUAL PROCESS FOR DISSIPATION OF PESTICIDES IN PONDS

Ralph G. Nash and Allan R. Isensee

ABSTRACT

This paper describes the processes that regulate the inputs and outputs of pesticides to a pond. It describes the important partitioning and dissipation processes, their mathematical form (i.e., partition coefficients and rate values, respectively), how to obtain or estimate these processes, and how to develop a mathematical model of the pond pesticide process.

THE POND PROCESS FOR PESTICIDES

Pesticides may reach ponds through runoff from adjacent pesticide-treated fields, pesticide-contaminated streams, pesticide accidents, and possibly through contaminated rain or aerial condensation of pesticides. Regardless of the contamination pathway, a method is required to assess the pesticide contamination in a pond at any given time. This paper addresses pesticide concentration in a pond at any given time.

The concept of a pond as visualized here is a small body of water (usually on a farm) which receives runoff waters but usually has little water outflow. The SWAM pesticide model is predicated on the premise that an estimate of the pesticide concentration in pond water can be calculated for any given time. Simplified, this means that the amount of pesticide entering and leaving a pond and the pond processes that alter the amount of pesticide in the water are known or can be estimated. Two approaches can be taken: (1) determine the pesticide in pond water with time (monitoring) and (2) estimate the pesticide in pond water by mathematical expressions after identifying as many individual processes and parameters as possible that affect the pesticide concentration, determining or measuring the effect each process or parameter has, and summing
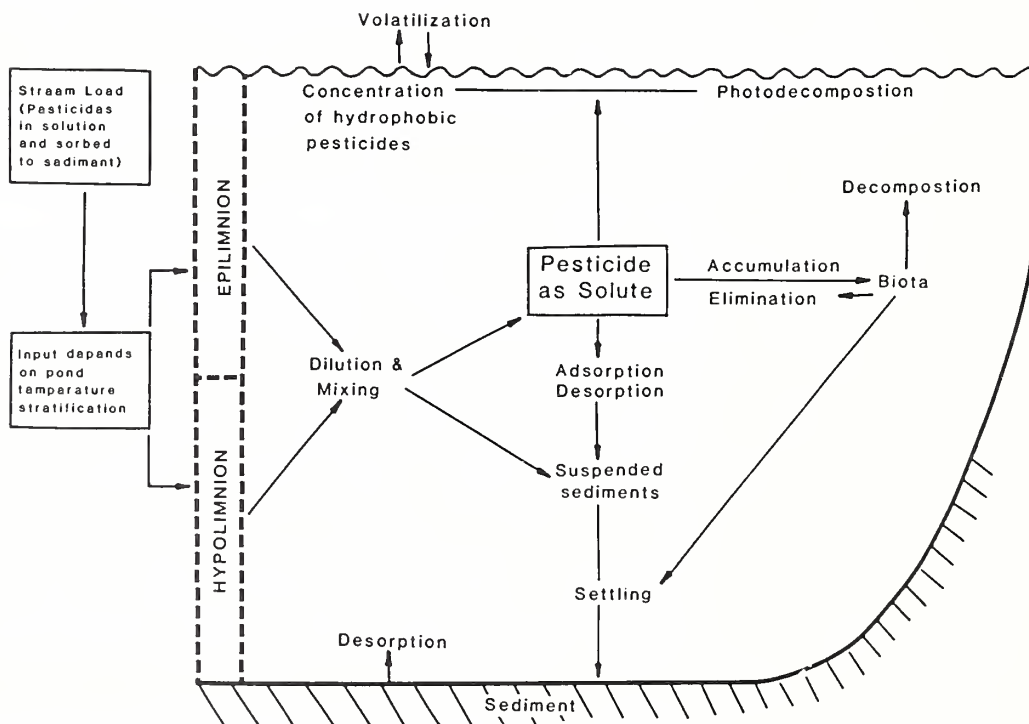
Figure 1.--Schematic representation of the conceptualized pond process for pesticides.

Soil scientist and plant physiologist, USDA-ARS, Pesticide Degradation Laboratory, Beltsville, MD 20705.

the results (mechanistic). Mathematical expressions generally are of two types: (1) theoretical, based on thermodynamics or kinetics and (2) empirical, based on regression or pseudo kinetics. Monitoring the pesticide is probably the superior method, but obviously the time and expense of monitoring tens of thousands of ponds would overwhelm our resources. Further, it is important to predict what will happen under an array of land management practices, and to do this an estimate must be calculated. This section will deal primarily with the mathematical methods used to estimate pesticide concentration in ponds.

Schematic of Pond Pesticide Model

A schematic of the conceptualized pond processes for pesticides is given in figure 1 and represents a column of pond water with 1 m^2 surface area. Briefly, a given load of pesticide will enter the pond either in the epilimnion (upper surface water) or hypolimnion (subsurface water), depending upon entering water temperatures and whether the pond is temperature stratified. The likelihood of a pond or impoundment being stratified is dependent on depth, amount of water flowing out of the pond, and whether surface or deep-water discharge occurs (deep-water discharge may alter normal stratification).

The pesticide load upon entering the pond will mix and affect dilution either of the incoming pesticide load or the pesticide in the pond. A portion of the pesticide will be adsorbed to sediment particles, which will begin to settle. Some portion of adsorbed pesticide will desorb, even after settling to the bottom. A portion of the pesticide will enter into solution (plus that desorbed from contaminated sediment), which will be considered the center for all pond pesticide processes. The processes that affect pesticide concentration in the pond water are discussed in greater detail elsewhere.

Nearly all pond processes tend to act to reduce pesticide concentration in the water. For organic pesticides the single most important process is sorption or partitioning between the water and biotic or abiotic solids suspended in the pond water or the pond walls (Baughman and Lassiter, 1978). Plankton both adsorb and absorb pesticides, eventually die, and settle. Likewise, macrophytes, vertebrates, and invertebrates accumulate (absorb and adsorb) pesticides to some equilibrium concentration (which ranges widely, depending on the compound) with water. Release back to water depends on changes in the water concentration (reequilibration), properties of the chemical, and metabolism rates in the organisms. Regardless of the process, release is usually slow and rarely total, and ultimately "binding" or degradation may take place in the sorbed state.

In addition to the pond sorptive processes, the physical and chemical properties of the pesticide play an important role in reducing its concentration. Many chemical processes, such as oxidation, reduction, hydrolysis, and photolysis, may occur to alter the structure of the pesticide, often forming a transformation product or degradation products of simpler structure. The transformation or degradation products frequently undergo more rapid alterations which ultimately result in nonidentifiable pesticide-related compounds.

Some pesticides may have the potential to combine chemically by polymerizing (joining of molecules to make larger molecules) or complexing with other substances. Polymerization is pesticide-specific and usually is considered of little or no importance in pond water chemistry because of the extreme dilution of the pesticide. Complexation, which usually is an irreversible process, can be very important in pond water chemistry and may lead to "bound residues" (Kaufman et al., 1976).

Chemical oxidation and reduction reactions are usually pesticide-specific, but often are enhanced by biological processes. Oxidation or reduction may or may not be important in pond water chemistry. Usually oxidation occurs in the pond water while reduction is more important in pond sediment, because of the corresponding oxidized or reduced environments. Hydrolysis is an important chemical process for many pesticides in pond water.

Many pesticides tend to concentrate near the pond water surface either because they partition into nonpolar organic surface films or because they are hydrophobic (such as DDT) and concentrate at the water/surface interface. When the pesticide concentrates on the pond surface, volatilization is greatly

enhanced over that predicted from Henry's law constant in a uniformly mixed system (Bowman et al., 1964). Photodecomposition is important for many pesticides in the surface pond water and depends on turbidity, latitude, and season.

A simplified pond pesticide model is shown in figure 2. There are four major components that influence the pesticide concentration in pond water: (1) the pesticide's physical, chemical, and biological properties, (2) the pond parameters and behavior (physical, chemical, and biological), (3) the climatic parameters, and (4) the pesticide load in stream inflow and in pond outflow water. All act and interact upon the others. Two of these components, stream pesticide load and climatic parameters, can be considered exogenous to the pond and hence are provided by other submodels of SWAM. Pesticide properties and pond parameters and behavior can be considered endogenous to the pond. The pond parameters and portions of pond behavior are provided by other submodels of SWAM.

A more detailed description of the four components that influence pesticide concentration in pond water is given in table 1. The stream pesticide load is all of the pesticide in solution and that adsorbed to inorganic sediment and that sorbed (primarily adsorbed) to organic material expressed as amount per volume. Among the climatic parameters listed, relative humidity probably is of little direct importance, because it does not affect pesticide volatilization from water (Chiou, 1980); however, it is important in computing volume of stored water and outflow from the pond.

Several approaches can be taken to describe the fate of a chemical in an environmental component. Usually, the approach is as follows: Estimate the initial pesticide in each compartment (for a pond: water, sediment, biota, abiota, and air above); estimate the rate of pesticide loss from each compartment; estimate pesticide advection [pesticide flow rate out (and in) divided by pond volume]; and, finally, combine these estimates in a manageable mathematical expression to estimate pesticide concentration and amount in outflow and all pond compartments at any time.

Pond Pesticide Approach

In an ideal situation, pesticide concentration in pond water could be estimated thermodynamically—or, better, kinetically because time is involved. By knowing the pesticide's physical and chemical properties and the environmental properties of the pond, classical kinetic equations could be used to estimate pesticide concentrations in pond water at any given time. Unfortunately, the pond parameters are so complex that it is unlikely that all parameters can be determined exactly. For example, can ponds with a heavy load of biota or abiota ever be exactly defined? At best, certain upper and lower limits can be
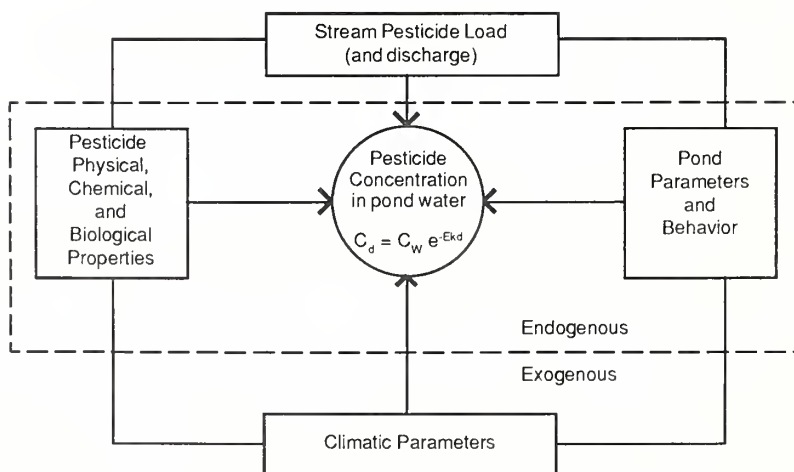
Figure 2.--Simplified schematic representation of the pond pesticide model.

198

Table 1.—Outline of the four components that influence pesticide concentration in pond water.

A. Stream Pesticide Load (amount per given item)
   1. Pesticide in solution
   2. Pesticide adsorbed to sediment
   3. Water
   4. Sediment
   5. Organic carbon

B. Climatic parameters
   1. Average daily temperature
   2. Average daily wind velocity
   3. Average daily relative humidity
   4. Average daily solar radiation

C. Pond parameters and behavior
   1. Volume
   2. Surface area
   3. Water pH
   4. Stratification
      a. Epilimnion depth and temperature
      b. Hypolimnion depth and temperature
   5. Turbulence
   6. Turbidity in epilimnion
   7. Biomass
      a. Microphytes
      b. Macrophytes
      c. Invertebrates
      d. Vertebrates
      e. Ratio of biomass surface area

D. Pesticide's physical, chemical, and biological properties
   1. Molecular weight (MW)
   2. Transition temperatures (T)
      a. Melting point
      b. Boiling point
      c. Decomposition
   3. Vapor pressure (VP)
   4. Water solubility (WS)
   5. Partition coefficients
      a. Octanol/water (K_{ow})
      b. Adsorption
         (1) Soil/sediment (K_d)
         (2) Organic carbon (K_{oc})
      c. Henry's law (K_h)
      d. Bioconcentration factor (K_{bcf})
   6. Disassociation
      a. Acid (pK_a)
      b. Base (pK_b)
   7. Rate reactions
      a. Volatilization
         (1) water/air (k_v)
         (2) soil/air (k_a)
      b. Photolysis (k_p)
      c. Hydrolysis (k_w)
      d. Reduction (k_r)
      e. Oxidation (k_o)
      f. Complexation (k_e)
      g. Polymerization (k_m)
      h. Biodegradation (k_i)
      i. Diffusion (k_f)
      j. Bioelimination (k_l)
      k. Desorption (k_d)
      l. Biosorption (k_b)

set for these parameters. Further, at the present time there are few pesticides in which all the needed physical and chemical properties are known. Because of this deficiency, a whole book has been devoted to estimating such properties (Lyman et al., 1982).

Nevertheless, most mathematical modelers use the kinetic approach to estimate pesticide concentration in pond water. Several models have been developed and tested:

Acronym: EXAMS
Name: Exposure Analysis Modeling System
Type: Hydrologic model to predict "steady-state" or "pulse-load" behavior of organic toxicants in aquatic ecosystems
Developer: U.S. EPA Environmental Research Laboratory, Athens, Georgia

Acronym: TOXI-WASP
Name: Toxics Water Analysis Simulation Package
Type: Dynamic compartment model to predict the fate of pesticides which enter the aquatic environment in pulses
Developer: U.S. EPA Environmental Research Laboratory, Athens, Georgia

Acronym: WASTOX
Name: Real Time WASP: Toxics Model
Type: Hydrologic, time variable model which analyzes the physical-chemical behavior of toxic chemicals in aquatic systems
Developer: John P. Connolly, Manhattan College, Bronx, New York, for the U.S. EPA Environmental Research Laboratory, Gulf Breeze, Florida and Duluth, Minnesota

Acronym: FUGACITY
Name: Fugacity
Type: Based on fugacity (pesticide partial pressure) and used to estimate pond compartment partitioning
Developer: Donald Mackay and Sally Paterson, Dept. of Chemical Engineering and Applied Chemistry, University of Toronto, Toronto, Ontario

Acronym: MASS-BALANCE
Name: Mass-balance
Type: Particle transport, as well as kinetic transfer and transport process
Developer: Dominic DiToro et al. (1982). HydroQual, Inc., Mahwah, New Jersey and Manhattan College, Bronx, New York

Acronym: HSPF
Name: Hydrological Simulation Program - Fortran
Type: Simulates water flow over and under land and through streams, rivers, and shallow lakes
Developer: Robert C. Johanson et al. (1980), School of Engineering, University of the Pacific, Stockton, California 95211, for U.S. EPA, Athens, Georgia

The EXAMS model (Burns et al., 1979) probably has received the most attention and testing, even though its design was broader in scope than just for a pond. All models have been programmed for computers and have been discussed elsewhere.

The primary purpose of this paper is to identify the inputs required for most of the models. All the models generally take the form of pesticide input and output (as well as water and sediment), partitioning or equilibrium balance between pond compartments, and transfer or transport (dissipation or loss from a compartment whether by degradation or transfer out of the compartment) rate out of each compartment. Input, output, advection processes, sediment settling, biota bloom, turbidity, as well as weather conditions are components of other papers and models and hence will not be considered here. This paper will be confined to pesticide partitioning within the pond as it influences pesticide concentration in the water compartment and those dissipation processes that reduce pesticide concentration in a compartment, primarily the water. In certain situations desorption, diffusion, or elimination of pesticide into water from abiota, sediment, or biota may be important, but for a first approach these usually can be ignored. Most models make provisions for these processes if they are known.

Because partitioning (K = partitioning coefficient) is such an important process (especially for nonpolar, high molecular weight, hydrophobic pesticides) in controlling the aqueous pesticide concentration, this will be discussed more fully than the various dissipation (k = loss rate) processes. The user is directed to where some of the K and k values may be found. When literature values are not available, an estimate may be calculated from equations found in the literature. Again the user is directed to these sources. As a general rule, calculating the model parameter values (K and k) is a more formidable task than using the pesticide submodel.

Pesticide Partitioning Between the Pond Water and Sediment, Biota, and Atmosphere

Partitioning of a pesticide in a pond is the separating of the pesticide into the pond components: water, sediment (includes abiota and pond walls), biota, and atmosphere. The water is the central component and interfaces with the sediment, biota, and atmosphere. Therefore, the partitioning of the pesticide will be between the water and the sediment, biota, and atmosphere as described by their partition coefficients, respectively,

$$K_d = \frac{P_S}{P_W} \; ; \qquad K_{bcf} = \frac{P_B}{P_W} \; ; \qquad \text{and } K_h = \frac{P_A}{P_W}$$

where P = pesticide, W = water, S = sediment, B = biota, and A = air. P_W is defined as the concentration of pesticide in solution in pond water on some given day; for example, the day the pesticide enters the pond, assuming little or no pesticide is already in the pond. Upon entering the pond the pesticide will be mixed and diluted; and a K_d, K_{bcf}, and K_h will be established. If the pesticide is ionic, or an acid or base, an ionization equilibration will become established, depending upon the pesticide and pond temperature and pH. Upon equilibration, a concentration P_W will be established and remain constant until some other process becomes active. For most (especially hydrophobic) pesticides, the equilibration process is rapid relative to losses. We can let P_i = inflow pesticide load, P_p = pesticide load in pond water prior to inflow, V_i = pond volume. Therefore,

$$P_W = P_{i+p} \, (V_{i+p} + K_d S_{i+p} + K_{bcf} B_{i+p})^{-1} \qquad\qquad [1]$$

where P_{i+p}, V_{i+p}, S_{i+p}, and B_{i+p} = total (from inflow and already present in pond) pesticide, water, sediment, and biota. Under pond conditions, the atmosphere becomes a sink (Glotfelty, 1978). Therefore, K_h becomes a dynamic rather than a partitioning process.

Partitioning Coefficients (K)

Partitioning coefficients (K_d, K_{bcf}, and K_h) for several pesticides can be found in the literature. The senior author has compiled a list of pesticide partition coefficients, which has been placed into a computerized database at Beltsville, Maryland. Further listing of K_d's can be found in Green and Karickhoff (this volume). Unfortunately, because many pesticide partition coefficients have not been measured, an estimate must be calculated.

Estimating Partitioning Coefficients (K)

Water/sediment (sorption-K_d and desorption-k_d). Sorption (or desorption) of pesticides and related chemicals to biotic and abiotic surfaces in the aquatic environment is a pivotal process that directly or indirectly controls distribution, fate, and behavior of these compounds. The magnitude of the sorption controls the degree to which other processes will be affected. For example, once in the aquatic environment, a chemical will rapidly equilibrate between water and available surfaces (abiotic and biotic), thus affecting the water concentration. Some ionic and highly hydrophobic compounds are irreversibly bound and unavailable for degradation or loss (Steen et al., 1980). Most, however, will be less tenaciously held and may (1) desorb (k_d) kinetically, (2) be transported to other locations or settle to the bottom in the adsorbed state, (3) partition into living aquatic organisms, and (4) enter one of several degradation or dissipation pathways.

Sorption itself is dependent on the chemical properties of the pesticide, water, and the absorbing surface. Of these, the properties of the adsorbing

surface are the most complex and least understood. For example, Hamaker and Thompson (1972) describe eight intermolecular interactions that influence the bonding of organic and inorganic molecules to different types of surfaces. Fortunately, adsorption isotherms empirically incorporate into one or several parameters many of the different bonding types for most compounds of interest. The most frequently used isotherm is the one described by the Freundlich equation:

$$pa^{-1} = KC^{1n^{-1}} \qquad [2]$$

where pa^{-1} = amount of pesticide (p) adsorbed per unit amount of adsorbent (a), K = equilibrium constant, C = equilibrium concentration, and n = the degree of nonlinearity. However, when $n \simeq 1$;

$$K_d = \frac{\mu g \text{ pesticide (g adsorbent}^{-1})}{\mu g \text{ pesticide (g water}^{-1})} \qquad [3]$$

where K = sorption coefficient, μg pesticide (g adsorbent^{-1}) = concentration of adsorbed pesticide, and μg pesticide (g water^{-1}) = equilibrium concentration of pesticide in solution.

These equations have been used extensively to describe adsorption of pesticides to soils (Hamaker and Thompson, 1972; Pionke and De Angelis, 1980) and increasingly for adsorption to sediments. Since soil adsorption data are extensive (compared to sediments), utilization of this existing information for the pond model would be most useful. Several approaches appear to be available and it is suggested the approach of Green and Karickhoff (this volume) would be the most appropriate.

The first is to convert the sorption coefficient (K_d) to K_{oc}:

$$K_{oc} = \frac{\mu g \text{ chemical (g organic carbon}^{-1})}{\mu g \text{ chemical (g water}^{-1})} \qquad [4]$$

$$K_{oc} = \frac{K_d}{\% \text{ organic carbon}} \times 100\% \qquad [5]$$

Many researchers have reported a correlation between adsorption and various soil properties, such as clay (quantity and type), pH, cation exchange capacity, hydrated metal oxides, and organic carbon content. However, of these factors, organic carbon content has been shown to be the single most important property affecting the sorption of neutral organic compounds to both soil and sediments (Hamaker and Thompson, 1972; Karickhoff et al., 1979; McCall et al., 1981). Another important merit of the K_{oc} is that it is roughly independent of soil or sediment type. For example, McCall et al. (1979) reported that the coefficient of variation (CV) for the sorption of nine pesticides by three soils (0.7 to 2.0% O.C. content) was only 17% CV for K_{oc} compared to 44% CV for K_d. In general, the percent CV for K_{oc} may be expected to vary by 20 to 50% over a range in K_{oc} of 1 to 1×10^6 between different compounds.

Another advantage of the K_{oc} value is that it can be estimated from other physical properties. The K_{oc} value is a measure of the degree to which a hydrophobic molecule partitions between water and the organic carbon in soil or sediment. Other laboratory measurements that also express this partitioning include (1) octanol/water partitioning coefficient (K_{ow}), (2) water solubility (K_w) and (3) the retention time on a reverse phase high-pressure liquid chromatographic column (R_t). The authors have examined several of the published correlations between K_{oc}, K_{ow}, and K_w. Correlations between K_{oc} and K_{ow} have been developed by Karickhoff et al. (1979) (based on 10 aromatic and chlorinated hydrocarbon chemicals):

$$\log K_{oc} = \log K_{ow} - 0.21 \text{ or } K_{oc} = 0.63 K_{ow} \qquad [6]$$

and by Hassett et al. (1980) (based on 14 energy-related organic chemicals):

$$\log K_{oc} = \log K_{ow} - 0.317 \text{ or } K_{oc} = 0.48 K_{ow}. \qquad [7]$$

Both of these correlations gave good fits with measured K_{oc} values. The relationship reported by Hassett et al. (1980) for K_w ($\mu g \text{ ml}^{-1}$):

$$\log K_{oc} = -0.686 \log K_w + 4.273 \text{ or } K_{oc} = 18,750 \, K_w^{-0.686} \tag{8}$$

fit the measured K_{oc} values almost as well as the K_{ow} correlation.

The correlation developed by Kenaga and Goring (1980) for K_w was based on 170 chemicals:

$$\log k_{oc} = 3.64 - 0.55 \log K_w \text{ or } K_{oc} = 4,365 \, K_w^{-0.55} \tag{9}$$
$$[\pm 1.23 \text{ orders of magnitude (OM)}].$$

Equation 9, later tested on 100 compounds (mostly pesticides) with known K_{oc} values, was found to fit well (i.e., standard deviations for 87% of the pesticides fell within one OM and 96% fell within two OM). However, equation 8, generally overestimated measured K_{oc} values when applied to Kenaga's (1980) compounds, while equation 9 generally underestimated measured K_{oc} values when applied to Hassett et al. (1980) compounds. K_{oc} values do not adequately describe adsorption for some ionic pesticides and for sediments or soils that have low organic carbon contents in combination with medium to high swelling clay contents (Hassett et al., 1980).

Sorption phenomenon is dependent on both the sorbate and sorbant properties, sorbant surface area, and sorbant flocculates (in which diffusion may be more limiting to the transport process between compartments than absorption or desorption). Therefore, another approach for the utilization of soil data is to use the calculated specific surface correlation as described by Pionke and De Angelis (1980):

$$K_d = m \, SS \tag{10}$$

where K_d = pesticide distribution between soil and water, m = slope, and SS = specific surface = 100 X % organic carbon (oc) + 2.0 X % clay (c) + 0.4 X % silt (si) + 0.005 X % sand (s). This correlation, which was designed to estimate pesticide distribution between soil and runoff waters, is theoretically more useful than the K_{oc} value since it combines both the organic and inorganic fractions. Its usefulness is potentially best under conditions of low % oc – high clay contents or the predominance of high specific surface clays. The SS method does not appear to have the flexibility of the K_{oc} method for estimating pesticide partitioning in the aquatic environment, primarily because particle size data are often not as readily available as oc data.

For details on the methodology of laboratory K_{oc} determination, the reader is referred to McCall et al. (1981). Further discussion on K_d may be found in Burns et al. (1979), Lyman (1982), Pionke and De Angelis (1980), and Green and Karickhoff (this volume). K_d values and methods for estimating K_d values (or K_{oc} or K_{ss}) may be found in Lyman (1982), Pionke and De Angelis (1980), and Green and Karickhoff (this volume).

At the present time, it appears that K_{oc} values estimated by correlation with K_{ow} are superior to those estimated by correlations with K_w.

Partitioning (K) as treated here assumes that the rate (k) of the sorption process is fast relative to the time interval under consideration. If so, sorption would be mostly complete and the equilibrium approach is appropriate. However, sorption is not an instantaneous process, but usually takes place over a period of hours, sometimes days or weeks (Karickhoff, 1983). Therefore, a sorption rate may need to be considered. If so, the overall sorption process should be second-order like, i.e., K_d for sorption and k_d for desorption rate. K_d would be proportional to the organic carbon or specific surface as discussed above, and k_d would be dependent upon time.

Water/Biota (Bioconcentration factor—K_{bcf} and bioelimination—k_e). The bioconcentration factor (K_{bcf}) is defined as the concentration of a chemical in aquatic organisms (wet weight) divided by the mean concentration of the chemical in water when the system is at equilibrium:

$$K_{bcf} = \frac{\mu g \ g^{-1} \text{ chemical in organisms}}{\mu g \ g^{-1} \text{ chemical in water}} \tag{11}$$

This factor expresses the potential for a chemical to accumulate in aquatic organisms when exposed to a known concentration of the chemical in water. The extent of the partitioning into the biota depends on the hydrophilic, lipophilic, and organophilic characteristics of the chemical under consideration. It is this direct response of an organism to a chemical that makes the K_{bcf} useful. Other measures of the partitioning potential of a chemical, such as water solubility or octanol-water partition coefficient, are often good indicators of accumulation but would not predict, for example, that two or more species of aquatic organisms might accumulate or metabolize a chemical at different rates. Unfortunately, laboratory determinations of K_{bcf} are often time consuming and therefore expensive. As a result, K_{bcf} values often have to be estimated from the very measures of partitioning potential that sometimes fail to give accurate results. A much more thorough discussion of K_{bcf} may be found in Bysshe (1982) and Burns et al. (1979).

For the purpose of this model, we will very briefly describe three of the estimation methods.

(1) If the octanol-water partition coefficient (K_{ow}) for an organic chemical is known, then the following equation, derived by Veith et al. (1979), is recommended:

$$\text{Log } K_{bcf} = 0.85 \log K_{ow} - 0.70 \quad \text{or} \quad K_{bcf} = 0.2 \, K_{ow}^{0.85} \qquad [12]$$

This regression equation was derived from the results of laboratory experiments using several species of fish and 84 different organic chemicals. Mackay (1982) presents an equation giving similar results.

(2) If water solubility (WS) of an organic chemical is known, then the following equation derived by Kenaga and Goring (1980) can be used:

$$\text{Log } K_{bcf} = 2.791 - 0.564 \log WS \quad \text{or} \quad K_{bcf} = 618 \, WS^{-0.564} \qquad [13]$$

This regression equation was derived from laboratory experiments using several species of fish and 36 organic chemicals. An additional equation has been provided by Mackay (1982), which corrects for insoluble compounds.

(3) Another regression equation has been derived using soil adsorption coefficients (K_{oc}):

$$\text{Log } K_{bcf} = 1.12 \log K_{oc} - 1.58 \quad \text{or} \quad K_{bcf} = 0.026 \, K_{oc}^{1.12} \qquad [14]$$

This equation developed by Kenaga (1980) was based on 26 organic chemicals.

It should be understood that all of these methods only estimate K_{bcf} to within one order of magnitude under the best of conditions, with higher levels of uncertainty likely. Verschueren (1983) is an important source for K_{bcf} values.

Like sorption (K_d), bioconcentration is not an instantaneous process, and therefore kinetics are involved. Presumably this could be considered second-order like because K_{bcf} is proportional to the biota amount.

Water/atmosphere (Henry's Law-K_h)

Although water/air is a partitioning process expressed by Henry's Law (K_h), it is not a true partitioning because the atmosphere is more of a sink where the pesticide decreases with time rather than a compartment (Glotfelty, 1978). K_h expresses a potential for partitioning and is useful for estimating pesticide volatilization as will be discussed in a later Section.

Very few K_h values can be found for pesticides in the literature and therefore must be estimated. One of the more simple estimate methods is given by Thomas (1982) in equation 15-8:

$$K_h = (VP)(WS)^{-1} \qquad [15]$$

where VP = vapor pressure in Pa and WS = water solubility in mol^{-3}. Unfortunately, the vapor pressures of many pesticides have either not been

determined or are estimates themselves. Grain (1982) has provided methods (see methods 1 and 2, pages 14-7 to 14-8) for estimating the vapor pressure. The answer from methods 1 and 2 above must be multiplied by mm Hg x 133.32 = Pa to change pressure to pascals.

Pesticide Dissociation in Water (pK_a)

Several pesticides are ionizable in aqueous solutions. Ionization affects the degree of sorption. The degree of ionization is usually dependent upon the pond pH value, and hence the degree of pesticide ionization will affect its partitioning into the pond compartments and the rate of exchange between the pond components.

Pesticide ionization is described by the dissociation constant K_a or K_b: $HA = H^+ + A^-$, where HA is the nonionized pesticide, H^+ the hydrogen ion and, A^- the pesticidal anion:

$$K_a = \frac{[H^+][A^-]}{[HA]} \qquad [16]$$

and when expressed logarithmically,

$$pK_a = pH - \log \frac{[A^-]}{[HA]} \qquad [17]$$

Conversely,

$$pK_b = pH - \log \frac{[H+][B]}{[HB^+]} \qquad [18]$$

Pionke and De Angelis (1980) provide pK values for several acid and base herbicides. 2,4-D acid, for example, has a pK_a of 2.8. However, in non-stagnant pond water, the pH would not be expected to fall much below pH 5 in the Eastern United States or above pH 8 in the Western States (Harris, 1982a); hence, 2,4-D acid would be >99.4% ionized in pond water. pH values for stagnant pond water, hypolimnion, sediment, and particulate surfaces may be much different and change with the seasons.

If pesticide ionization is suspected and a pK_a is not provided, then follow the steps in Harris and Hayes (1982), pages 6-10, 6-16, and 6-21.

The percent dissociation (D) for anionic (acidic) pesticides is found from the following by substituting D in equation 17 for $[A^-]/[HA]$:

$$\log D = pH - pK_a \qquad [19]$$

and

$$\% D = \frac{D \times 100}{D + 1} \qquad [20]$$

For protonated (basic) pesticides $[H^+][B]/[HB^+]$ pK_a is found from pK_b by

$$pK_a = 14 - pK_b \qquad [21]$$

and % D found as above. For a more thorough discussion on dissociation, refer to Harris and Hayes (1982).

Pesticide Dissipation From the Pond: (Rate Constants-k)

Ponds are not static, especially during the summer. Pesticides volatilize, with little of the vaporous pesticide returning to the pond. Pesticides hydrolyze irreversibly. Various other transformations and degradation processes occur, which all reduce P_W. These processes usually go in one direction and usually are relatively slow compared to equilibration, i.e., the partitioning and dissociation. Therefore,

$$\frac{dP_W}{dt} = -(k_v+k_p+k_w+k_e+k_r+k_o+k_m+k_b)P_W + (K_1-k_i)P_B + (k_f+k_d)P_S + (P_iQ_i/V) \qquad [22]$$

where P = pesticide concentration in a medium; W = water, B = biota, and S = sediment and suspended sediment (SS) masses, both biotic and abiotic; P_i and Q_i = pesticide inflow and water inflow rate, respectively; V = pond volume; and k_v = volatilization, k_p = photolysis, k_w = hydrolysis, k_e = complexation, k_r = reduction, k_o = oxidation, k_m = polymerization, k_b = biosorption, k_l = bioelimination, k_i = biodegradation, and k_f = diffusion. Bioelimination (k_l), desorption (k_d), and diffusion (k_f) (from water in sediment and desorption from sediment) are the only processes identified here whereby a pesticide enters back into the pond water from another compartment. All (k_l, k_d, and k_f) are not only time-dependent, but may be mass- (biota, suspended sediment, and sediment) dependent also, which would result in positive pseudo second-order kinetics with respect to pesticide concentration in the pond and need be considered only under long-term situations. Over the short-term fast equilibration period, both k_e and k_d cannot be separated from sorption or bioconcentration and therefore are measured as a partial component of K_d and K_{bcf}, respectively (Kahn, 1977; Matsumura, 1977; Metcalf, 1977).

Several of the rate constants (k_v, k_o, k_r, k_w, k_p, k_e, k_m) may be reversible, given the proper conditions and energy; but under practical pond conditions, the reversibility is so small that it can be ignored. Some rate values represent opposite transitions (k_r vs. k_o), and some are of little or no importance or can be combined, which greatly simplifies the required input values for the pesticide submodel. For example, k_r is usually not important in pond water but can be important in microbiologically active pond sediments, and hence would be a dissipation process in the sediment compartment. Both k_r and k_o are usually associated with other rate processes, i.e., biological reduction or oxidation and photooxidation. Therefore k_r and k_o probably can be ignored in the water compartment. The general pathway in reduction/oxidation transformations is often initial reduction of highly halogenated pesticides followed by oxidation.

Polymerization (k_m) rarely, if ever, occurs in pond water because pesticide concentration is normally low and therefore can be ignored. Complexation (k_e) may be extremely important when pesticides chemically bind to clay minerals and biotic materials or when conjugated biologically. Complexation is a special case for the pyridinium herbicides diquat and paraquat and clay minerals. Complexation or "bound residues" have received attention only within the past 15 years (Kaufman et al., 1976). Although k_e values have not received a great deal of attention in measuring P_w values, it is likely k_e values should be given more emphasis in future considerations for several pesticides. Biosorption (k_b) or bioaccumulation is often measured in model aquatic systems. More often than not, bioaccumulation has been measured as an equilibrium constant called bioaccumulation ratio or bioconcentration factor (K_{bcf}). When measured as a ratio it then becomes a partial component of K_{oc}.

By combining and omitting some of the pond pesticide processes, equation 22 can be simplified. In its most complex form,

$$\frac{dp_W}{dt} = -(k_v+k_p+k_w)P_W + k_fP_S - k_iP_B + k_dP_{SS} + (P_iQ_i/V) \qquad [23]$$

In most cases, though, one or more of these rate constants can be omitted as not contributing significantly to the overall process for the particular pesticide under consideration.

To simplify equation 23, the pesticide inflow and water inflow components (P_i and Q_i) are controlled by hydrology flow rates and not chemical kinetics. Therefore, advection is treated on a per-instance basis with information provided by the hydrologics portion of SWAM. Hence equation 23 becomes

$$\frac{dP_W}{dt} = -(k_v+k_p+k_w)P_W + k_fP_S - k_iP_B + k_dP_{SS} \qquad [24]$$

It is generally assumed that k_v, k_p, and k_w can be expressed as pseudo first-order kinetics (Burns et al., 1979; Harris, 1982a, 1982b; Mackay and Leinonen, 1975; Mackay and Paterson, 1981; Neely, 1980; Smith et al., 1980;

Thomas, 1982; Szeto and Sundaram, 1982; Zepp and Cline, 1977; and Zepp et al., 1975). The biodegradation rate (k_i) is generally assumed monod kinetics (Baughman and Lassiter, 1978; Paris et al., 1981) (probably where the substrate is the primary source of carbon and at high concentrations), but more recently it has been shown to follow pseudo second-order kinetics in natural waters; in some cases it is reported as pseudo first-order kinetics (Scow, 1982).

Therefore, equation 24 when considered as pseudo first-order kinetics becomes

$$C_d = P_W e^{(-k_v-k_p-k_w)d} + P_S e^{k_f d} + P_B e^{-k_i d} + P_{SS} e^{k_d d} \qquad [25]$$

when d = time and C_d = concentration of pesticide in water on day d between flow events. P_S and P_{SS} would be correspondingly depleted of pesticide.

Determining or Estimating Rate Constants (k)

Rate constants (k) must be determined experimentally under controlled conditions. Whether the dissipation rate is true kinetics or kinetics-like depends upon what causes the pesticide per se to be lost from the compartment. True kinetics is random dissipation and proportional to the concentration left with time as defined by

$$\frac{dC}{dt} = -k \, C_o^{\, n} \qquad [26]$$

where C and C_o = concentrations at time (t) and time zero (t_o), respectively, and n = nth order of dissipation. Many environmental pesticide dissipations are not true kinetics, because of the complexity of the conditions in the environment. However, regression analysis of dissipation data more often than not indicates that a simple exponential equation will describe the data satisfactorily with a high degree of statistical confidence (Nash, 1980). The simple exponential equation is the same equation as for first-order kinetics; therefore, pseudo first-order or first-order-like kinetics can be used for dissipation rates in those situations where true first-order kinetics cannot be accurately described.

Measuring pesticide amount with time then determining an equation (from regression analysis) that fits the data is probably the best method for describing pesticide dissipation from an environmental compartment, provided the researcher has good control of all the experimental parameters. In many cases measuring is the only adequate way to obtain a rate constant in complex interacting systems where many processes are going on simultaneously. Unfortunately, the time and expense are so great that it has been feasible to measure rate processes for only a few pesticides. Consequently, estimating a rate constant from theoretical and empirical considerations of the several compartments of a system is often performed. A discussion of rate constants is beyond the scope of this section and has been thoroughly reviewed by Lyman et al. (1982) and others. All rate constants (k) here are on a per day basis.

The senior author has compiled a list of k values for pesticides, which has been placed into a computerized database. It is suggested that various individual computer programs for determining a k value be incorporated as a subroutine or data bank for obtaining k values.

Rate of volatilization (k_v). Pesticide volatilization from a pond is not a simple process and depends upon water and air temperatures, wind velocity, and pesticide diffusion through both the water and air [usually referred to as the two-boundary-layer (Liss and Slater, 1974)]. However, as indicated by Thomas (1982) and reviewed by Burns et al. (1979), volatilization can often be reduced to pseudo first-order kinetics, presumably because some other process, such as desorption or diffusion, may be the rate-limiting process for volatilization in slowly mixed water bodies.

Thomas (1982) lists the volatilization rate for a few pesticides in table 15-4. To change the values in table 15-4 to day^{-1}, use the following conversion factor:

$$k_v = \frac{0.693 \times 24}{t_{1/2}{}^h} \qquad [27]$$

If a volatilization (k_v) from water is not given, follow the procedure of Thomas (1982) pages 15-27 to 15-31. An alternative to the Thomas (1982) methods is provided by Wolff and Van der Heijde (1982). The model has been computer programmed.

Another procedure is that of Smith et al. (1980), which is based upon oxygen aeration of a water body. "The measured parameter is the ratio of the evaporation rate constant of the chemical to the oxygen reaeration rate constant, $k_v/k_v°$, which has been shown to be constant for volatile substances over a wide range of conditions. If the oxygen reaeration rate constant, $k_v°$, can be estimated or measured in a natural water body ..., then the volatilization rate constant of the chemical under the same conditions can be estimated by multiplying the value of the ratio by the environmental value of $k_v°$." The following is suggested for lakes and ponds (Smith et al., 1980):

$$k_v = (k_v/k_v°)_{lab}^{1.6} \ (k_v°)_{env}$$ [28]

It is suggested that the Smith et al. (1980) procedure be adopted as a first alternative, followed by the Wolff and Van der Heijde (1982) procedure for pesticide volatilization from a pond.

Rate of photolysis (k_p). Photolysis is dependent upon the light energy available and the ability of the pesticide to absorb the energy. Many factors affect the energy available for photolysis in ponds.

Pesticide photolysis rate in water has been reviewed by Harris (1982b) and Burns et al. (1979). Harris (1982b) lists the photolysis rate for several pesticides in table 8-12. To change the values in table 8-12 to day^{-1} use the following conversion factors:

for hours $$k_p = \frac{0.693 \times 24}{t_{1/2}h}$$ [29]

for years $$k_p = \frac{0.693}{t_{1/2}y \times 365}$$ [30]

where h and y are hours and years, respectively.

For pesticides not given in table 8-12, a laboratory determination has to be conducted under controlled conditions before an estimate of a pond environment can be obtained. Harris (1982b) explains this, beginning on page 8-22.

When using k_p (or $t_{1/2}$) values, the user should be aware of whether the k_p was determined under laboratory or field conditions. Pesticide photolysis is determined under near ideal laboratory conditions, which usually differ greatly from natural conditions. Light attenuation (from pond depth), turbidity, season and latitude, and cloud cover all reduce the energy available for photolysis. Zepp and Cline (1977) have an equation, which has been computer programmed, that is suggested for use where pesticide photolysis has been demonstrated or suspected.

Wolfe et al. (1982) provide equations for light attenuation and cloud cover, which can be used in the EXAMS model. Light attenuation resulting from pond depth is given by

$$k_p(PD) = k_p \frac{1-e^{-KPD}}{KPD}$$ [31]

where $k_p(PD)$ is the average photolysis rate constant in a water column of depth PD, k_p is the near surface photolysis rate constant (laboratory rate), and K is the mean diffuse attenuation coefficient of the water body (Smith and Tyler, 1976). Wolfe et al. (1982) suggest a value of 2 m^{-1} for a pond. Cloud cover is described by Mo and Green (1974) as,

$$F = 1 - 0.056C$$ [32]

where F = ratio of the light intensity in the presence and absence of clouds and C = cloud cover in tenths. Further discussion on photolysis can be found in Lemaire et al. (1982).

Conversely, Zepp and Schlotzhauer (1983) have shown that certain algae enhance photodegradation through photoinduction upon pesticide adsorption to the algae. They showed that total photolysis in the presence of algae-induced photolysis (k_{ap}) was described by a hyperbolic relationship:

$$k_{ap} = \frac{A}{1 + B[P]^{-1}} \qquad [33]$$

where A and B are constants and [P] the pesticide concentration. However, total photolysis (k_{ap}) at low pesticide concentrations was a function of direct photolysis (k_p and normally first-order) and algae-induced photolysis (k_{ap} and proportional to the algae concentration), also. Therefore, second-order kinetics applied:

$$k_{ap} = k_p + k_a C_a \qquad [34]$$

where C_a = algae concentration (mg of chlorophyll algae per L). They point out that algae concentrations in most natural fresh waters are several orders of magnitude less than used in their study; hence direct photolysis (k_p) was more dominant than algae-induced photolysis (k_a). However, the data suggested that algae-induced photolysis may be important for hydrophobic compounds that adsorb onto algae to a greater extent.

More recently, West et al. (1983) have determined dissipation half-lives of fluridone, an aquatic herbicide, in 40 ponds from Canada to Panama. They found that latitude has little effect on fluridone photodegradation and that pond depth explained only 63% of the variation. By incorporating only dissolved oxygen and turbidity into the regression equation, they found an average error of only 3 days for 10 ponds in the United States. They reasoned that turbidity would have the same effect as pond depth on sunlight penetration; and the amount of dissolved oxygen affected photolysis.

Rate of hydrolysis (k_w). Pesticide hydrolysis rate in water has been reviewed by Harris (1982a) and Burns et al. (1979). The following is the suggested approach for SWAM:

1. Ascertain whether a hydrolysis rate for the pesticide under question has been determined from table 7-11 (Harris, 1982a). If so, correct for pond temperature (°C) by interpolation from the following factors:

    a. 1° change use factor 0.1
    b. 10° change use factor 2.5
    c. 25° change use factor 10

    Use the following equation for temperatures greater than those given in table 7-11:

    $$\text{k value} + (\text{k} \times \text{factor}) = \qquad [35]$$

    and for temperatures less than those given in table 7-11:

    $$\text{k value} - \frac{\text{k} \times \text{factor}}{1 + \text{factor}} = \qquad [36]$$

2. Convert $M^{-1} s^{-1}$ (seconds) or s^{-1} to d^{-1} (day) by

    multiplying by 8.64×10^4 $\qquad [37]$

3. Examples:

    - for malathion in a neutral ($k_o = 7.7 \times 10^{-9}$ at 27° C) pond at 30° C:

    $$[7.7 + (7.7 \times 0.7)] \times 10^{-9} \simeq 13 \times 10^{-9} \text{ s}^{-1} \qquad [34]$$

    $$13 \times 10^{-9} \times 8.64 \times 10^4 \simeq 1.13 \times 10^{-3} \text{ d}^{-1} \qquad [36]$$

- for malathion in a neutral pond at 17° C:

$$[7.7 - \frac{7.7 \times 2.5}{1 + 2.5}] \times 10^{-9} \simeq 2.2 \times 10^{-9} \text{ s}^{-1} \qquad [35]$$

$$2.2 \times 10^{-9} \times 8.64 \times 10^4 \simeq 1.94 \times 10^{-4} \text{ d}^{-1} \qquad [36]$$

4. If the pesticide is not listed in table 7-11 and hydrolysis is suspected to contribute significantly to pesticide dissipation or a more accurate k_w value than that provided above is required, then the procedure of Harris (1982a) beginning on page 7-21 should be followed.

Rate of biodegradation (k_b). Biodegradation (as defined here) goes beyond simple transformations. It is one of the more complicated rate processes to describe because in natural waters several biological species are usually present and, depending upon all of the pond parameters as well as the pesticide, there is a fluctuating population density. Biodegradation (limited to microbial here) is not only time-dependent but is proportional to the microbial population. Therefore, biodegradation rate is usually found by monod kinetics (Baughman and Lassiter, 1978; Paris et al., 1981; Scow, 1982). However, in ponds where pesticide concentration is low, monod kinetics reduces to pseudo second-order kinetics. And when second-order microbial degradation is involved, the rate of pseudo first-order microbial degradation (k_b) can be found, providing the microbial concentration is given:

$$k_i = k_{ii} (MC) \qquad [38]$$

where k_{ii} = second-order kinetics in mL (cell)$^{-1}$ day^{-1} and MC = microbial concentration. (Microbial concentration may be in other suitable units as well if the units are the reciprocal of the k_{ii} units.) For example, from Paris et al. (1981) a mean second-order value for 2,4-D butoxyethyl ester (2,4-DBE) degradation in lake water was $k_{ii} = (3.6 \pm 0.7) \times 10^{-6}$ over a 2,4-DBE concentration range of 0.01 to 1 µg mL^{-1} and a bacterial concentration range of 2.1×10^6 to 2×10^8 organisms mL^{-1}. For 2,4-DBE degradation in the presence of 10^6 to 10^8 bacterial cells mL^{-1}, $k_i = 3.6 \pm 0.3$ and 360 ± 30, respectively. Hence, a $C_{1/2}$ value (time for 2,4-DBE to degrade to one-half its concentration) would vary from 2.1×10^{-1} to 1.8×10^{-3} days, respectively.
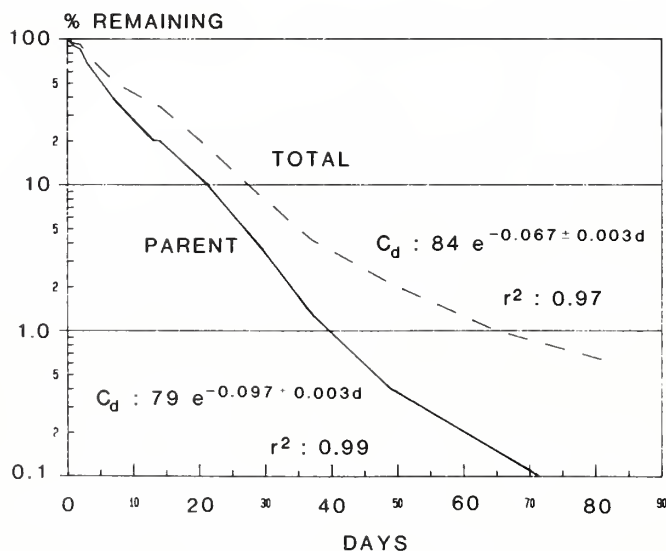
Figure 3.--Dissipation of chlorpyrifos-methyl
(parent) and chlorpyrifos-methyl
plus 3,5,6-trichloro-2-pyridinal
(total) in lake water and clean soil
at 15°C (Szeto and Sundaram, 1982).

Scow (1982) (table 9-16) lists first-order (exponential) or day^{-1} k_i's for several pesticides. When $t_{1/2}$ is given, convert to k_i by:

$$k_i = \frac{0.693}{t_{1/2}} \qquad [39]$$

However, microorganisms in ponds probably do not depend upon the pesticide as a primary source of carbon in most cases. More likely, the pesticide is a tertiary or quartic source of carbon for most pond microbial populations. If so, microbial pesticide degradation is only incidental, which results in degradation being proportional to the pesticide remaining and not necessarily to the biomass; hence pseudo first-order kinetics prevail (figure 3).

Rate of diffusion from sediment (k_f). Diffusion of pesticides from sediments into water probably cannot be separated from sorption partitioning for most pesticides. Diffusion may become important in those situations where a large quantity of a long-lived pesticide is washed into a pond along with a heavy silt load. In such a situation where most of the pesticide is partitioned into the sediment, the diffusion of the pesticide back into the water could be very slow over a long period of time.

Presumably, the equations given by Jury et al. (1980) for liquid diffusion could be used for sediment to water transport.

Rate of complexation (k_c). Complexation as defined here is all those processes which essentially bind a pesticide to abiota or biota such that it will not desorb from, diffuse out of, or be excreted from solid material into the pond water. Complexation can be considered an encompassing of "bound residues" as given in Kaufman et al. (1976) and pesticide losses that cannot be explained or accounted for, i.e., a catchall or undefined pesticide loss with time. The complexation rate (k_c) will be assumed pseudo first-order.

Estimating Pesticide Dissipation, From Pond Sediment, Biota, and Suspended Sediment

To have mass balance, the pesticide concentration (C_x) (on any day) in each pond compartment (sediment, biota, and suspended sediment) must be determined in addition to the water compartment. These (sediment, biota, and suspended sediment) comprise the last three elements of equation 25 presented again below. Their initial concentrations (P_S, P_B, and P_{SS}) would be those obtained at equilibrium, as described in previous sections on water/sediment and water/biota partitioning systems. However, it should be recognized that "inplace" biodegradation (k_i) and complexation (k_e) may be even more dominant dissipation pathways from these compartments than transport to the water compartment, especially over long time intervals. When biodegradation and complexation are known, $-k_i$ and/or $-k_e$ can be entered into each element of equation 25 and the concentration (C_x) estimated, which in turn provides a new estimated value for P_S, P_B, and P_{SS} for use in equation 25 (see table 2).

Estimating Pesticide Dissipation From Pond Water

Equation 25 is the basic dissipation pesticide submodel:

$$C_d = P_w e^{(-k_v-k_p-k_w)d} + P_S e^{k_f d} + P_B e^{-k_i d} + P_{SS} e^{k_d d} \qquad [25]$$

where C_d = pesticide concentration in water on day d and P_w, P_S, P_B, and P_{SS} = pesticide concentrations in water, sediment, biota, and suspended sediments, respectively, at their maximum on some day following d = 0.

Pesticide concentration (C_d) in pond water can now be estimated for any day, d, when inflow and outflow are known (see table 3).

Table 2.--Pesticide submodel physical, chemical, and biological input requirements

Item	Symbol	Value	Units	Reference or calculated from abbreviation, Vol: pages (year)		
Chemical		////////	////////////	///////////////////////		
Molecular Weight	MW		$g\ mol^{-1}$	///////////////////////		
Water Solubility	WS		$g\ m^{-3} = \mu g\ g^{-1}$ $mol\ m^{-3}$	,	:	( )
Vapor Pressure	VP		Pa (133.32 X mm Hg)	,	:	( )
Temperature	T		$^{\circ}K\ (^{\circ}C + 273)$	,	:	( )
Sorption Coefficient	K_d (K_{oc} or K_{ss})		$\frac{\mu g\ P\ (g\ adsorbent^{-1})}{\mu g\ P\ (g\ water^{-1})}$		:	( )
Suspended Solids Concentration	SS_C		$\mu g\ cm^{-3} = g\ m^{-3}$	,	:	( )
SS & Sediment Density	SS_D		$g\ cm^{-3}$ (1.5 suggested)	,	:	( )
Bioconcentration Factor	K_{bcf}		$\frac{\mu g\ P\ (g\ biota^{-1})}{\mu g\ P\ (g\ water^{-1})}$	,	:	( )
Biota Concentration	B_C		$\mu g\ cm^{-3} = g\ m^{-3}$	,	:	( )
Biota Density	B_D		$g\ cm^{-3}$ (1 suggested)	,	:	( )
Air Density	A_D		$g\ cm^{-3}$ (1.2×10^{-3} suggested)	,	:	( )
Henry's Law Constant	K_h		$Pa\ m^3\ mol^{-1}$	,	:	( )
Pond Surface Area	PSA		m^2	,	:	( )
Pond Depth (mean)	PD		m	,	:	( )
Pond pH	pH		10^{-pH}	,	:	( )
Pesticide dissociation	pK_a		10^{-pK_a}	,	:	( )
Pond Pesticide Input	P_i		mol	,	:	( )
Pond Pesticide Output	P_o		mol	,	:	( )

Classifying Dominant Mechanisms Governing Pesticide Fate

Usually one fate mechanism predominates over all other possible mechanisms for pesticide fate in or loss from a pond. An identification of the dominant mechanism(s) should be possible from the physicochemical properties of the pesticide. One scheme is to classify the pesticide into three general tendency categories:

I. Those that adsorb onto particulate or organic matter (i.e., bipyridilium quaternary salts, chlorinated hydrocarbons) and usually bioaccumulate (i.e., chlorinated hydrocarbons)

II. Those that are soluble in water (i.e., acids, including their esters; phenols; organophosphates; s-triazines; phenylcarbanilates; phenylureas; substituted anilides)

III. Those that volatilize (i.e., dinitroanilines, thiocarbamates, chlorinated hydrocarbons)

Category I pesticides are those pesticides which have a tendency to adsorb onto particulate and organic matters (K_d) and bioaccumulate (K_{bcf}). Partitioning is generally a fast process; hence pesticide rate of loss from the pond system may be minimal over a short time period (<1 week). However, over a longer time period (>1 week), pesticide loss rate may predominate, hence one or more of the following may be the more important considerations for the submodel: Volatilization (k_v), photolysis (k_p), hydrolysis (k_h), or biodegradation (k_b). Furthermore, over even longer time periods (>1 month), the loss rate may be governed by one or more of the following: Desorption (k_d), possibly bioelimination (k_l), or diffusion from sediment (k_f). When k_d, k_e, or k_f actually governs admittance of the pesticide into the water compartment from the suspended particulates, biota, and sediment compartments, the actual loss mechanism (volatilization, photolysis, hydrolysis, or biodegradation) need not be considered.

Category II pesticides are those that tend to solubilize in water. Therefore, Category II pesticide loss from a pond would be governed primarily by photolysis (k_p), hydrolysis (k_w), or biodegradation (k_i).

Category III pesticides are those that tend to volatilize. Category III would include not only the high-vapor-pressure pesticides (i.e., dinitroanilines, thiocarbamates), but also some low-vapor-pressure pesticides, such as the chlorinated hydrocarbons, which also tend to fit Category I but not Category II or the dissipation pathways associated with Category II pesticides.

This classification system does not suggest that less dominant mechanisms should be ignored, but rather serves as an aid to identify the one or two mechanisms that one should focus on. Table 4 presents a scheme to aid in categorizing a pesticide as to the dominant fate mechanism.

Table 3.--Pesticide submodel rate constants input requirements

Rate Constant	Symbol (d^{-1})	Value	Reference abbreviation, or calculated from Vol:pages (year)
Volatilization	$-k_v$		, : ( )
Photolysis	$-k_p$		, : ( )
Hydrolysis	$-k_w$		, : ( )
Biodegradation	$-k_i$		, : ( )
	$-k_{ii}$[1]		, : ( )
Complexation	$-k_e$		, : ( )
(Other)	$-k$		, : ( )

[1]k_{ii} can be converted to k_i: $k_i = k_{ii}$ (MC), when the microbial concentration is known.

Summary and Conclusions

A pesticide entering a pond will partition rapidly between the water, sediment, and biota primarily, with some partitioning into air. Subsequently, dissipation from each pond compartment (water, sediment, suspended particulates, and biota) will occur but usually at a slower rate.

Pesticide partitioning depends upon the organic content of the sediment amount (and in some cases the surface area of the clay), the concentration of the biota, and the pesticide hydrophobicity; it usually increases with increased organic content and pesticide hydrophobicity. Several empirically derived estimation methods exist (based on pesticide water solubility and sediment or biota sorption relationships) to describe pond pesticide partitioning. From this partitioning, a pesticide concentration in pond water can be estimated.

Several pesticide dissipation processes in ponds are first-order kinetic like (hydrolysis, photolysis), and others (biodegradation, volatilization) often can be reduced to pseudo first-order kinetics. Therefore, by estimating pond pesticide concentration as a result of partitioning processes, pesticide concentration in pond water can be estimated for any given time.

For purposes of the SWAM model, pesticide concentration in the pond water will initially be calculated by the pesticide partitioning algorithm [number (1)] and then by the pesticide dissipation algorithm [number (25)] to determine pesticide concentration on any given day. Values for the algorithms will come from databases, the literature, and from computed estimates.

Several mathematical models exist for estimating pond pesticide concentration. The EXAMS model has received the most testing. Presumably several should be investigated, tried, selected, and modified to meet the user's needs.

Table 4.--Scheme for classifying a pesticide as to the probable dominant process that will govern its fate in a pond[1]

Item	Symbol	Units	Classification[2] I Value	I (x)[3]	II Value	II (x)[3]	III Value	III (x)[3]
Water Solubility	WS	μg g^{-1}	<1	( )	>50	( )	<50	( )
Vapor Pressure	VP	Pa	<0.01	( )	>0.01	( )	>0.05	( )
Octanol-water	K_{ow}	$\frac{\mu g\ P\ (octanol^{-1})}{\mu g\ P\ (water^{-1})}$	>1000	( )	<100	( )	<200	( )
Sorption Coefficient	K_d	$\frac{\mu g\ P\ (g\ adsorbent^{-1})}{\mu g\ P\ (g\ water^{-1})}$	>10	( )	<5	( )	<10	( )
	K_{oc}	$\frac{\mu g\ P\ (g\ adsorbent^{-1})}{\mu g\ P\ (g\ water^{-1})}$	>100	( )	<50	( )	<100	( )
Bioconcentration Factor	K_{bcf}	$\frac{\mu g\ P\ (g\ biota^{-1})}{\mu g\ P\ (g\ water^{-1})}$	>1000	( )	<100	( )	<500	( )
Sum of (x's)				( )		( )		( )

[1]Values arbitrarily selected from Garten and Trabalka (1983), Kenaga and Goring (1980). Pionke and De Angelis (1980), and Weed and Weber (1974).

[2]See Classifying Dominant Mechanisms Governing Pesticides Fate Section.

[3]Place an "x" for each classification a pesticide falls into.

The fugacity model is the simplest model and can readily be operated with a desk calculator or personal computer. The fugacity model can be used to indicate gross pesticide partitioning into the various pond compartments. Subsequently, dissipation from pond water can be estimated from the several individual pseudo first-order rates of dissipation. For this gross approach, rates of partitioning and desorption or bioelimination are ignored, and, once accomplished, no further transport of pesticide back into water from any compartment (air, biota, abiota, sediment) is considered. At best, this is only a gross indication of pesticide disposition in pond water.

Regardless of which model is selected, certain information on the pesticide is required. One way to organize the collection and recordkeeping of this information is to use tables 2 and 3.

Probably more critical than the models per se is the lack of various model input values (sorption, bioconcentration, volatilization, biodegradation, and so forth etc.) required to operate all the models. As a result, many estimation procedures for determining these values have been proposed and have been brought together in one volume.

Recommendations

1. Initially the model should be kept as simple as possible while taking advantage of the few good physical, chemical, and biological properties available.

2. Algorithms describing processes which are temperature-dependent should be modified to account for temperature.

3. The model should be computerized and the computerization should first check a database and second allow estimate input values to be selected from subroutines.

4. There is a critical need for testing a few pesticides in a pond situation to determine pesticide disposition, and this should be done in conjunction with a modeler and potential user.

5. Adequate physical, chemical, and biological properties are not available for most pesticides (especially for those processes that are temperature-dependent) and should be determined in conjunction with a modeler who can help identify the most important processes and the needed sensitivities.

REFERENCES

Baughman, G. L., and Lassiter, R. R. 1978. Prediction of environmental pollutant concentration. In J. Cairns, K. L. Dickson, A. W. Maki (eds.), Estimating the Hazard of Chemical Substances to Aquatic Life, pp. 35-54. ASTM, 1916 Race St., Philadelphia, Pennsylvania 19103.

Bowman, M. C.; Acree, F., Jr.; Lofgren, C. S.; and Beroza, M. 1964. Chlorinated insecticides: Fate in aqueous suspensions containing mosquito larvae. Science 46:1480-1481.

Burns, L. A.; Cline, D. M.; and Lassiter, R. R. 1979. Exposure Analysis Modeling System (EXAMS): User Manual and System Documentation. Environmental Research Laboratory, U.S. Environmental Protection Agency, Athens, Georgia 30613.

Bysshe, S. E. 1982. Bioconcentration factor in aquatic organisms. In W. J. Lyman, W. F. Reehl, and D. H., Rosenblatt (eds.), Handbook of Chemical Property Estimation Methods. McGraw-Hill Book Co., New York.

Chiou, C. T. 1980. On the validity of the codistillation model for the evaporation of pesticides and other solutes from water solution. Environ. Sci. Technol. 14:1253-1254.

DiToro, D. M.; and O'Connor, D. J.; Thomann, R. V.; and St. John, J. P. 1982. Simplified model of the fate of partitioning chemicals in lakes and streams. In K. L. Dickson, A. W. Maki, and J. Cairns, Jr. (eds.), Modeling the Fate of Chemicals in the Aquatic Environment. Ann Arbor Science, Michigan.

Garten, C. T., and Trabalka, J. R. 1983. Evaluation of models for predicting terrestrial food chain behavior of xenobiotics. Environ. Sci. Technol. 17:590-595.

Glotfelty, D. E. 1978. The atmosphere as a sink for applied pesticides. J. Air Pollut. Control Assoc. 28:917-921.

Grain, C. F. 1982. Vapor pressure. In W. J. Lyman, W. F. Reehl, and D. H. Rosenblatt (eds.), Handbook of Chemical Property Estimation Methods, Ch. 14. McGraw-Hill Book Co., New York.

Hamaker, J. W., and Thompson, J. M. 1972. Adsorption. pp. 49-143. In C. A. I. Goring, and J. W. Hamaker (eds.), Organic Chemicals in the Soil Environment, Ch. 2, Vol. 1, Marcel Dekker, Inc., New York.

Harris, J. C. 1982a. Rate of hydrolysis. In W. J. Lyman, W. F. Reehl, and D. H. Rosenblatt (eds.), Handbook of Chemical Property Estimation Methods, Ch. 7. McGraw-Hill Book Co., New York.

Harris, J. C. 1982b. Rate of photolysis. In W. J. Lyman, W. F. Reehl, and D. H. Rosenblatt (eds.), Handbook of Chemical Property Estimation Methods, Ch. 8. McGraw-Hill Book Co., New York.

Harris, J. C., and Hayes, M. J. 1982. Acid dissociation constant. In W. J. Lyman, W. F. Reehl, and D. H. Rosenblatt (eds.), Handbook of Chemical Property Estimation Methods, Ch. 6. McGraw-Hill Book Co., New York.

Hassett, J. J.; Means, J. C.; Banwart, W. L.; and Wood, S. G. 1980. Sorption properties of sediments and energy-related pollutants, EPA-600/3-80-041, 132 pp.

Johanson, R. C.; Imhoff, J. C., and Davis, H. H., Jr. 1980. User's Manual for Hydrological Simulation Program – FORTRAN (HSPF). Environmental Research Laboratory, Athens, Georgia, EPA 600/9-80-015, 678 pages.

Jury, W. A.; Glover, R.; Spencer, W. F.; and Farmer, W. J. 1980. Modeling vapor losses of soil-incorporated triallate. Soil Sci. Soc. Am. J. 44:445-450.

Kahn, M. A. Q. 1977. Elimination of pesticides by aquatic animals. In M. A. O. Kahn (ed.), Pesticides in Aquatic Environments, pp. 107-125. Plenum Press, New York.

Karickhoff, S. W. 1983. Sorption kinetics of hydrophobic pollutants in natural sediments. 186th ACS Nat'l. Meet. Washington, D.C. Pestic. Div. Abstr. No. 65.

Karickhoff, S. W.; Brown, D. S.; and Scott, T. A. 1979. Sorption of hydrophobic pollutants on natural sediments. Water Res. 13:241-248.

Kaufman, D. D.; Still, G. G.; Paulson, G. D.; and Bandal, S. K. 1976. Bound and Conjugated Pesticide Residues. ACS Symp. Ser. 29, Washington, D.C.

Kenaga, E. E. 1980. Predicted bioconcentration factors and soil sorption coefficients of pesticides and other chemicals. Ecotoxicol. Environ. Safety 4:26-38.

Kenaga, E. E., and Goring, C. A. I. 1980. Relationship between water solubility, soil sorption, octanol-water partitioning, and concentration of chemicals in biota. In J. C. Eaton, P. R. Parrish, and A. C. Hendricks (eds.), Aquatic Toxicology ASTM STP 707. American Society for Testing and Materials, Philadelphia, PA.

Lemaire, J.; Campbell, I.; Hulpke, H.; Guth, J. A.; Merz, W.; Philip, J.; and von Waldow, C. 1982. An assessment of test methods for photodegradation of chemicals in the environment. Chemosphere 11:119-164.

Liss, P. S., and Slater, P. G. 1974. Flux of gasses across the air-sea interface. Nature 247:181-184.

Lyman, W. J. 1982. Adsorption coefficient for soils and sediments. In W. J. Lyman, W. F. Reehl, and D. H. Rosenblatt (eds.), Handbook of Chemical Property Estimation Methods, Ch. 4. McGraw-Hill Book Co., New York

Lyman, W. J.; Reehl, W. F.; and Rosenblatt, D. H. 1982. Handbook of Chemical Property Estimation Methods. McGraw-Hill Book Co., New York.

Mackay, D. 1982. Correlation of bioconcentration factors. Environ. Sci. Technol. 16:274-278.

Mackay, D., and Leinonen, P. J. 1975. Rate of evaporation of low-solubility contaminants from water bodies to atmosphere. Environ. Sci. Technol. 9:1178-1180.

Mackay, D., and Paterson, S. 1981. Calculating fugacity. Environ. Sci. Technol. 15:1006-1014.

Matsumura, F. 1977. Absorption, accumulation, and elimination of pesticides by aquatic organisms. In M. A. 1. Khan (ed.), Pesticides in Aquatic Environments, pp. 77-105. Plenum Press, New York.

McCall, P. J.; Laskowski, D. A.; Swann, R. W.; and Dishburger, H. J. 1981. Measurement of sorption coefficients of organic chemicals and their use in environmental fate analysis. In Test Protocols for Environmental Fate and Movement of Toxicants, AOAC, ISBN 0-935584-20-X, pp. 89-109.

McCall, P. J.; Swann, R. L.; Laskowski, D. A.; Vrona, S. A.; Unger, S. M.; and Dishburger, H. J. 1979. Prediction of chemical mobility in soil from sorption coefficients. In Aquatic Toxicology and Hazard Assessment, Proceedings of the fourth annual symposium on aquatic toxicology. ASTM Chicago, Illinois.

Metcalf, R. L. 1977. Biological fate and transformation of pollutants in water, pp. 195-221. In I. H. Suffet (ed.), Fate of Pollutants in the Air and Water Environments. Part 2. John Wiley and Sons, New York.

Mo, T., and Green, A. E. S. 1974. A climatology of solar erythema dose. Photochem. Photobiol. 20:483-496.

Nash, R. G. 1980. Dissipation rate of pesticides from soils. In W. G. Knisel (ed.), CREAMS: A Field Scale Model for Chemicals, Runoff, and Erosion from Agricultural Management Systems. U.S. Gov't. Printing Office: 0-310-945/SEA-15. Vol. 3: 560-594 (Technical Research Report).

Neely, W. B. 1980. Chemicals in the Environment, Distribution, Transport, Fate, Analysis. Marcel Dekker, Inc., New York.

Paris, D. F.; Steen, W. C.; Baughman, G. L.; and Barnett, J. T., Jr. 1981. Second-order model to predict microbial degradation of organic compounds in natural waters. Appl. Environ. Microbiol. 41:603-609.

Pionke, H. B., and De Angelis, R. J. 1980. Method for distributing pesticide loss in field runoff between the solution and adsorbed phase. In W. G. Knisel (ed.), CREAMS: A Field Scale Model for Chemicals, Runoff, and Erosion from Agricultural Management Systems, pp. 607-643. U.S. Gov't. Printing Office: 0-310-945/SEA-15.

Scow, K. M. 1982. Rate of biodegradation. In W. J. Lyman, W. F. Reehl, and D. H. Rosenblatt (eds.), Handbook of Chemical Property Estimated Methods, Ch. 9. McGraw-Hill Book Co., New York.

Smith, J. H.; Bomberger, D. C.; and Hayes, D. L. 1980. Prediction of the volatilization rates of high-volatility chemicals from natural water bodies. Environ. Sci. Technol. 14:1332-1337.

Smith, R. C., and Tyler, J. E. 1976. Transmission of solar radiation into natural waters. Photochem. Photobiol. Rev. 1:117-155.

Steen, W. C.; Paris, D. F.; and Baughman, G. L. 1980. Effects of sediment sorption on microbial degradation of toxic substances. In R. A. Baker (ed.), Contaminants and Sediments. Vol. 1. Ann Arbor Sci. Publ.

Szeto, S. Y., and Sundaram, K. M. S. 1982. Behavior and degradation of chlorpyrifos-methyl in two aquatic models. J. Agric. Food Chem. 30:1032-1035.

Thomas, R. G. 1982. Volatilization from water. In W. J. Lyman, W. F. Reehl, and D. H. Rosenblatt (eds.), Handbook of Chemical Property Estimated Methods, Ch. 15. McGraw-Hill Book Co., New York.

Veith, G. D.; DeFoe, D. L.; and Bergstedt, B. V. 1979. Measuring and estimating the bioconcentration factor of chemicals in fish. J. Fish. Res. Board Can. 36:1040-1048.

Verschueren, K. 1983. Handbook of Environmental Data on Organic Chemicals, 2nd ed. Van Nostrand Reinhold Co., New York.

Weed, S. B., and Weber, J. B. 1974. Pesticide-organic matter interactions. In W. D. Guenzi (ed.), Pesticides in Soil and Water, Ch. 3. Soil Sci. Soc. Am., Inc., Madison, Wisconsin.

West, S. D.; Burger, R. O.; Poole, G. M.; and Mowrey, D. H. 1983. Bioconcentration and field dissipation of the aquatic herbicide fluridone and its degradation products in aquatic environments. J. Agric. Food Chem. 31:579-585.

Wolfe, N. L.; Zepp, R. G.; Schlotzhauer, P.; and Sink, M. 1982. Transformation pathways of hexachlorocyclopentadiene in the aquatic environment. Chemosphere 11:91-101.

Wolff, C. J. M., and Van der Heijde, H. B. 1982. A model to assess the rate of evaporation of chemical compounds from surface waters. Chemosphere 11:103-117.

Zepp, R. G., and Cline, C. M. 1977. Rates of direct photolysis in aquatic environment. Environ. Sci. Technol. 11:359-366.

Zepp, R. G.; Wolfe, N. L.; Gordon, J. A.; and Baughman, G. L. 1975. Dynamics of 2,4-D esters in surface waters, hydrolysis, photolysis, and vaporization. Environ. Sci. Technol. 9:1144-1150.

Zepp, R. G., and Schlotzhauer, P. F. 1983. Influence of algae on photolysis rates of chemicals in water. Environ. Sci. Technol. 17:462-468.

A GROUNDWATER SUBSYSTEM FOR SWAM

Donn G. DeCoursey and William L. Gburek

ABSTRACT

Water that percolates into groundwater aquifers carries with it soluble materials. Diffusion, convection, and the rising and falling of the water table mix and transport the water and chemicals in a down gradient direction. Eventually the water and chemicals exit the aquifer into a receiving stream or reservoir. Discharge rates of typical flow paths can be simulated by accounting for recharge from specific fields and determining the amount and quality of outflow as a function of the elevation of the water table and average concentrations of solutes in the aquifer at its junction with its outlet. Seepage rates from the bottom of the root zone provide estimates of recharge. The recession rate of the aquifer (as a function of the saturated hydraulic conductivity, aquifer thickness, porosity, length of the flow path and elevation of water table at the divide relative to the elevation in the channel) was obtained by simulating the response of a two dimensional model under a wide range of conditions and relating the response to aquifer characteristics.

INTRODUCTION

This paper describes the groundwater flow and quality subsystem developed for SWAM. It accepts the water and associated solutes that percolate below the root zone as recharge, and routes them through a saturated groundwater zone to a receiving stream channel. Only conservative chemicals are considered. Numerous models have been developed to solve the Laplace equation for saturated groundwater flow. Finite-difference or finite-element models are the most widely employed methods of solving the equation (Amerman and Naney, 1982; Freeze, 1971). However, their computational time is prohibitive for systems with the large number of elements needed to describe the groundwater response from a mixed-land-use watershed. This paper describes an operational system requiring minimal computation time yet simulating the water and soluble chemicals concentrations of groundwater contributions to the channel from a small ($\sim 10 km^2$)mixed-land-use catchment. It is derived from concepts presented by Liong and DeCoursey, (1982), and Liong et al.,(1982).

The subsurface saturated flow region of a catchment is visualized areally as consisting of numerous non-interacting flow paths, both parallel and convergent, that carry water to the channel (see Figure 1 parts a, b, and c). Total daily flow, distributed along the channel, is determined by simulating the response of each path. Concentrations of soluble materials within the groundwater below identifiable land use zones (all three zones in Fig. 1c) are also simulated. Since the purpose of the model is to simulate response from ungauged catchments, it must require a minimum of input information yet be reasonably accurate.

GENERAL EXPRESSION OF GROUNDWATER FLOW

Smith and Hebbert (1983) developed a general expression for groundwater flow from a hillslope segment (Figure 2) with saturated flow, $h(x,t)$, forming above the surface of a confining (crosshatched) soil layer. Thickness of soil above the confining layer is $y(x)$. The extent of saturation is a function of the unsaturated vertical inflow rate, $q(x,t)$, vertical seepage rate through the confining layer, $q_1(x,t)$, slope of the confining layer, s_i, the length of the hillslope segment, L, saturated conductivity, in the direction of the confining layer K_h, and effective porosity ϕ_e. The degree of convergence (or divergence) is indicated by the angle ω, and flow is assumed to be sufficiently parallel to the lower boundary that Dupuit theory may be applied. The distance, x, is measured along the slope, positive in the downslope direction. The width and depth of saturated flow at the outlet into the channel are w_z and h_{out}, respectively. At $x=0$ (the watershed divide) the slope of the water surface with respect to that of the confining layer is γ. Water in the capillary fringe is assumed to move downslope; its thickness, z_b, is an "effective"

$$(a) \qquad\qquad (b)$$

$$(c)$$
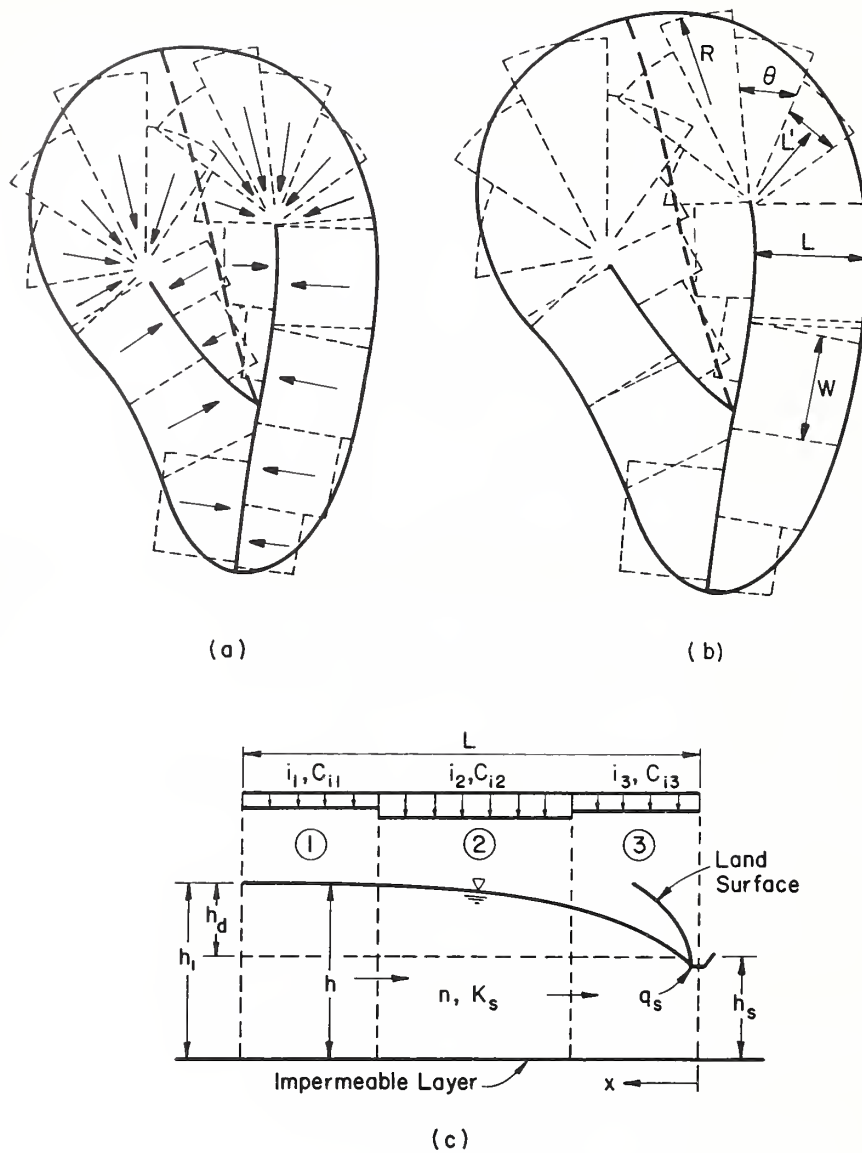
Figure 1
Groundwater flow as visualized in a) the real watershed; b) the model;
and c) a vertical cross section of a typical segment.

saturated thickness which, for small flow rates, is approximately equal to the
bubbling pressure. Thus, the total head of water is $H = h + z_b$. The basic
dynamic equation of Dupuit flow from this hillslope segment is defined by Smith
and Hebbert as:

$$q_n(x,t) = - K_h \left[H \cos \gamma \frac{\partial^2 h}{\partial x^2} + \cos \gamma \left(\frac{\partial h}{\partial x}\right)^2 - \frac{\partial h}{\partial x}\left(s_i - \frac{H}{w}\cos\gamma\frac{\partial w}{\partial x}\right) - \frac{s_i H}{w}\left(\frac{\partial w}{\partial x}\right)\right] + \phi_e \frac{\partial H}{\partial t} \tag{1}$$

in which $q_n(x,t)$ is the flow rate at any point along the flow path. The
steady-state profile of the water surface for any given inflow rate and
thickness of the saturated layer at $x = L$ is obtained by solving equation (1)
with $\partial h/\partial t = 0$. An analytical expression is possible for nonconvergent flow,

Figure 2
Definition sketch of Smith-Hebbert hillslope model.

Figure 3
Water surface profile for steady state and long term drainage
conditions.

($\omega=0$), but not for convergent or divergent cases (Smith and Hebbert, 1983). It
is also not possible to obtain an analytical solution to the general
differential equation, (1). Smith and Hebbert solved the expression using a
finite difference scheme.

A spatially homogeneous aquifer, similar to the one described in Figure 2, that
receives periodic uniform recharge displays a water surface profile that falls
between two extremes. The extremes are the steady-state profile and the water
table surface after long periods of continuous drainage with no recharge. An
example of these extreme profiles with the same boundary conditions at the ends
of the flow section is shown in Figure 3. The profiles are for nonconverging
sections 420 meters in length with a horizontal impervious surface. Flow rates

for the steady-state and draining conditions are 0.088 and 0.078 m^3/day-m, respectively. The profiles were obtained using the finite-difference solution of Smith and Hebbert. Since the profile of the steady-state solution can be obtained analytically, a comparison was made between the finite-difference and the analytical solutions. Maximum error was 0.09 m at the upslope end of the profile; this represents the cumulative error of the finite-difference solution. Errors between the end points appear to be linearly distributed with distance from the downstream starting point.

A comparison was also made between the Smith and Hebbert model and the three-dimensional finite-difference model of Freeze (1971). Model responses were nearly identical if the effective thickness of the capillary fringe was appropriately selected. The best estimate of this value is obtained by calculating "effective" saturation of the capillary fringe and converting this to a head using the moisture tension/saturation curve of the soil material. The "effective" saturation is the first moment of the entire saturation conductivity curve, of the given soil, about the saturated hydraulic conductivity axis.

The Smith-Hebbert model is computationally much faster than the Freeze model, but is still not very efficient when a large number of flow paths are needed to describe watershed-scale groundwater response. The balance of this paper describes a simple model that can be used for areas larger than a single hillslope. The Smith-Hebbert model was used to obtain parameters of the model apropos to a wide range of field conditions.

SIMPLE EXPRESSION OF GROUNDWATER FLOW

Liong and DeCoursey (1982) analyzed the response of a phreatic aquifer in dimensionless terms. In their analysis, the discharge of a representative flow path (Figure 1c) into a stream channel is the dependent variable; independent variables consist of twenty descriptors of (1) the geometry of the system, (2) infiltration or recharge, (3) soil properties, (4) fluid properties, (5) the driving force, and (6) time. After a dimensional analysis and elimination of the least significant variables, flow rate into the channel was described as (see Figure 1c)

$$\frac{q_s}{K_s L} = f \left(\frac{t K_s}{L} , \frac{h_u}{L} , \frac{h_s}{L} , \frac{h_d}{L} , \frac{i_e}{K_s} , \frac{t_i K_s}{L} , n_s \right) \tag{2}$$

in which q_s is the flow rate into the stream channel

K_s is the saturated hydraulic conductivity

L is the length of the flow path

t is the time elapsed between observations (generally 24 hours)

h_u is the depth of the unsaturated zone

h_s is the saturated flow depth at the channel

h_d is the elevation of the water above the channel evaluated at the divide and considered a constant for any one period

i_e is the effective recharge rate

t_i is the duration of infiltration

n_s is the effective porosity or specific yield

Saturated hydraulic conductivity, K_s, and length of the flow path, L, were selected as repeating variables.

In a later paper, Liong et al. (1982) presented an analysis of expression (2) for two different situations: one in which the system response was observed with no infiltration starting at a steady-state condition and the second being the same as the first but adding infiltration. The Freeze (1971) model was used to represent aquifer response. Six groups of numerical experiments were evaluated, each consisted of several runs in which only one dimensionless parameter at a time was varied. Model output in dimensionless units, $q^* = q_s/K_s L$, was plotted against dimensionless time, $t^* = t K_s/L$, for each of the

experiments. The results were exponential as expected.

$$q^* = A \exp(-Bt^*) \qquad (3)$$

in which A and B are functions of the flow field descriptors.

A similar expression was obtained for the difference between flow with and without infiltration. They further showed that continuous simulation can be obtained by using the two equations, which collectively require three parameters: A, B, and C. Values of each of the parameters were obtained by nonlinear regressions on the dimensionless variables.

Model structure and its attempted use showed several weaknesses. The first is discussed by Liong et al. (1982). Assuming Darcian conditions, the rate of change in head at the divide, h_d, should be the same as the rate of change in q_s. However, the parameter B, which is the proportionality constant between values at two different times, is not a function of the head at the divide as it should be to conform with Darcy's law.

Another weakness in the structure of the model is that simulation of daily flows is similar to the unit hydrograph method with a very long tail, thus requiring incremental values of change in flow, due to infiltration, to be carried for very long periods before they become insignificant. If inflow were to last for extended periods, computation would become very unwieldy.

A third point, flow in the unsaturated zone above the capillary fringe was considered a part of the Liong model. Current thinking is that flow in the unsaturated zone of SWAM should be a part of the recharge system rather than part of the groundwater model.

THE OPERATIONAL MODEL

The operational model, developed herein, is based on the following assumptions and results of previous work.

Assumptions

(i)   Each of the flow paths is independent and its response is calculated individually.

(ii)   Flow is Darcian.

(iii)   Flow paths are relatively long such that the Dupuit assumption of horizontal flow is valid.

(iv)   The flow profile is assumed to be more representative of steady-state than of a draining state.

(v)   Even though the water table is allowed to rise and fall, the shape of the surface profile can be described at all times by the steady-state expression.

(vi)   The aquifer is homogeneous, isotropic and unconfined.

(vii)   There is no flow across the left and lower boundaries of the profile shown in Figure 1c. Flow simulated at the right boundary is assumed stream discharge.

(viii)   The impervious lower boundary is horizontal (this requirement may be relaxed in future versions of the model).

(ix)   Depth of saturated zone at the channel does not change.

(x)   Recharge from the unsaturated zone does not have to be spatially uniform, but for flow simulation the total from all recharge segments is assumed to be distributed uniformly over the surface.

(xi)   Concentrations of dissolved materials within identifiable groundwater regions are assumed to be mixed instantaneously with concentrations coming from upslope and from recharge at the surface.

(xii)   Both the initial volume of water in the aquifer and the effective hydraulic conductivity are based on streamflow records from the site in question or adjacent streams.

Model Development

The operational model described herein is simple in concept and similar to that described by Liong and DeCoursey (1982) except that outflow is determined directly from a change in storage within the aquifer by rearranging continuity

$$Q_j = Q_{j-1} + i_j - q_j \tag{4}$$

$$q_j = Q_{j-1} + i_j - Q_j \tag{5}$$

in which Q_j and Q_{j-1} are the volumes in storage at times j and j-1, i_j is the recharge for the jth day and q_j is the outflow volume for the jth day. Volumes in storage Q_j and Q_{j-1} are functions of the water surface profile and depth defined by h in Figure 1c. The water surface profile, assumed to be described by steady-state expressions, is evaluated by integration over the length of the stream tube. Recharge volume, i_j, is added to Q_{j-1}. A procedure similar to that of Liong et al. (1982) is then used to show the effect of drainage on change in volume from one day to the next. Change is based on water table elevation at the divide, $h_d = h_1 - h_s$ (see figure 1c). Thus, before outflow for day j, q_j, can be determined, the water table profile must be determined for the volume $Q_{j-1} + i_j$. An expression is presented to show the drop in h_d that would be expected from one day's drainage. It is a function of K_s, n_s, L, h_d, h_s, and other physical conditions. Based on the drop in h_d the volume in storage after drainage, Q_j, is then evaluated, and q_j is calculated using expression (5). Since all values are expressed in terms of aquifer volume, flow in the channel is calculated as $q_{e_j} = n_s q_j$. With this brief description of the model's operation, we will now describe model development in more detail.

Water Surface Profile in Parallel and Convergent Conditions

Referring to Figure 1c and using the assumptions listed above, flow at any point, x, is

$$q_x = K_s h \frac{dh}{dx} \tag{6}$$

Since flow is assumed to be at steady-state, it must equal the recharge rate upslope of x

$$q_x = i (L-x) \tag{7}$$

in which i is the average effective steady-state recharge rate over the entire flow path.

Combining the expressions

$$K_s h \frac{dh}{dx} = i (L-x) \tag{8}$$

separating variables, and integrating yields

$$\frac{K_s h^2}{2} = i Lx - \frac{i x^2}{2} + C \tag{9}$$

When x = 0, and h = h_s, C = $\frac{K_s h_s^2}{2}$; thus

$$h^2 = \frac{2i Lx}{K_s} - \frac{i x^2}{K_s} + h_s^2 \tag{10}$$

If $h = h_1$ when $x = L$ (x measured positively from the channel), then

$$h_1^2 = \frac{i\,L^2}{K_s} + h_s^2 \qquad \text{or} \qquad h_1^2 - h_s^2 = \frac{i\,L^2}{K_s} \tag{11}$$

Substituting in equation (10) yields

$$h^2 = h_s^2 + \frac{2x}{L}(h_1^2 - h_s^2) - \frac{x^2}{L^2}(h_1^2 - h_s^2) \tag{12}$$

which is a general expression for the profile given elevations at the end points. Equation (11) relates the elevation at the end points to the saturated hydraulic conductivity, the steady-state recharge rate and the specific yield n_s. Specific yield enters into the relationship because $i = i_e/n_s$. Equation (11) also shows that for any given flow path of given length, L, and aquifer thickness at the channel, h_s, there is a definite relation between steady-state recharge, i; specific yield, n_s; the saturated hydraulic conductivity, K_s; and the elevation of the water table at the upstream boundary, h_1. Any three of the four can be defined, and the fourth will be dependent on these three.

Water surface profiles for convergent flow can be obtained in a way similar to those for parallel flow. Referring to Figure 4, lateral steady-state flow, q_r, at any point, r, is defined as

$$q_r = i\,\frac{\theta}{2}(R^2 - r^2) \tag{13}$$

in which i is the recharge rate, i_e/n_s; θ is the angle of convergence in radians; and R is the radial length to the upstream end of the flow section. The cross-sectional area of flow at a radial distance r is $\theta r h$; thus the Darcian flow at that point is

$$q_r = K_s\,\theta r h\,\frac{dh}{dr} \tag{14}$$
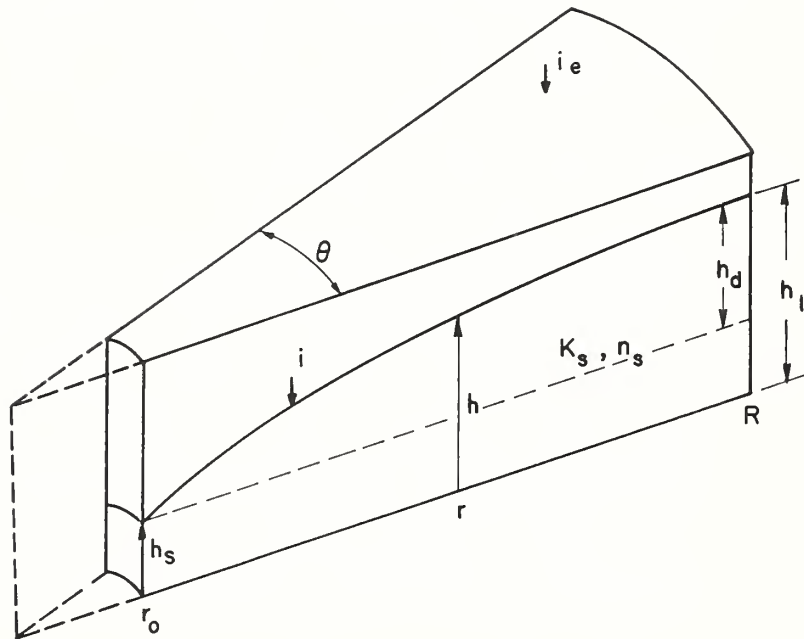
Figure 4
Schematic of converging flow showing nomenclature used in model.

Since the system is steady-state, recharge and flow must be equal thus

$$K_s \theta r h \frac{dh}{dr} = \frac{i \theta}{2} (R^2 - r^2) \tag{15}$$

Separation of variables and integration yields

$$h^2 = \frac{i R^2}{K_s} \ln r - \frac{i r^2}{2K_s} + C \tag{16}$$

When $r = r_o$, $h = h_s$ and

$$C = h_s^2 - \frac{i R^2}{K_s} \ln r_o + \frac{i r_o^2}{2K_s} \tag{17}$$

Thus

$$h^2 = \frac{i}{K_s} R^2 (\ln r - \ln r_o) - \frac{i}{2K_s} (r^2 - r_o^2) + h_s^2 \tag{18}$$

when $r = R$, $h = h_1$ and

$$h_1^2 = h_s^2 + \frac{i R^2}{K_s} \ln \left(\frac{R}{r_o}\right) - \frac{i}{2K_s} (R^2 - r_o^2) \tag{19}$$

Rearranging equation (18)

$$h^2 = \frac{i R^2}{K_s} \ln r - \frac{i r^2}{2K_s} + h_s^2 - \frac{i R^2}{K_s} \ln r_o + \frac{i r_o^2}{2K_s} \tag{20}$$

and letting

$$A = \frac{i R^2}{K_s}$$

$$B = \frac{-i}{2K_s}$$

and $C = h_s^2 - \frac{i R^2}{K_s} \ln r_o + \frac{i r_o^2}{2K_s}$

$$h = (A \ln r + Br^2 + C)^{1/2} \tag{21}$$

Equation (19) is similar to equation (11) in that it relates the elevation of the groundwater table at the end points to length of the flow path, $R-r_o$; saturated hydraulic conductivity, K_s; steady-state recharge rate i; and since $i-i_e/n_s$, porosity, n_s. Thus, given aquifer thickness at the channel, h_s, and flow length defined by R and r_o, equation (19) can be used to calculate either K_s, h_1, i, or n_s, given the other three parameters. In the model, i will be based on channel flow records, n_s will be based on pump tests or records of well testing, and h_1 will be calculated from the aquifer volume which is based on streamflow records and estimates of h_s, thus K_s will be calculated using equation (19). A methodology for accomplishing all this is described later in this paper.

Solving equation (19) for K_s

$$K_s = \frac{i \, R^2 \ln\left(\frac{R}{r_o}\right) - \frac{i}{2} (R^2 - r_o^2)}{h_1^2 - h_s^2} \tag{22}$$

and substituting this expression for K_s in the expressions for A, B, and C in equation (21) provides an expression for calculating the steady-state water surface profile in terms of h_1, h_s, R, and r_o. In this development, i falls out because it is not possible to specify both K_s and i given h_1 as mentioned above. Expressions for A, B, and C obtained with this substitution are

$$A = \frac{(h_1^2 - h_s^2)}{\ln(\frac{R}{r_o}) + \frac{r_o^2}{2 \, R^2} - \frac{1}{2}}$$

$$B = \frac{(h_1^2 - h_s^2)}{2 \, R^2 \ln(\frac{R}{r_o}) - (R^2 - r_o^2)}$$

$$C = h_s^2 - A \ln r_o - B \, r_o^2$$

And the expression for the water table elevation at any point r is

$$h = (A \ln r + Br^2 + C)^{1/2} \tag{23}$$

Aquifer Storage Volume

Equations (12) and (23) can be used to define the surface configuration of all flow paths in any given catchment. Thus the volume of water stored within each flowpath is obtained by integration as shown in the following paragraphs.

For parallel flow the width of flow is assumed to be unity, thus the volume becomes the area under the surface profile

$$Q_{j-1} = \int_{x = 0}^{x = L} h \, dx \tag{24}$$

where h is defined by equation (12). The resulting expression is

$$Q_{j-1} = \frac{(2cx + b)\sqrt{X}}{4c} - \frac{4ac - b^2}{8 \, c\sqrt{-c}} \sin^{-1} \frac{2cx + b}{\sqrt{b^2 - 4ac}} \Bigg|_{x = 0}^{x = L} \tag{25}$$

in which

$$a = h_s^2$$

$$b = \frac{2 \, (h_1^2 - h_s^2)}{L}$$

$$c = - \frac{(h_1^2 - h_s^2)}{L^2}$$

and $X = a + bx + cx^2$

227

For converging flow, the total volume stored under a wedge-shaped surface such as shown in Figure 4 is

$$Q_{j-1} = \int_{r=r_o}^{r=R} \theta r \, h \, dr \qquad (26)$$

in which $\theta r h$ is the cross-sectional area of flow at any point, r, and h is defined by equation (23).

$$Q_{j-1} = \int_{r=r_o}^{r=R} \theta r \, (A \ln r + B \, r^2 + C)^{1/2} \, dr \qquad (27)$$

This expression cannot be solved explicitly; thus a numerical integration method such as Gausian Quadrature (Carnahan et al., 1969) must be used.

Equations (25) and (27), for parallel and convergent conditions respectively, define the total volume in the aquifer above the impervious layer. Thus these volumes must be adjusted to account for the undrainable volume that lies between the impervious layer and the level of water in the stream channel, before being reconciled with aquifer volumes based on streamflow records.

Recharge and Elevation of the Water Table at the Divide After Recharge

At this point the water table configuration and storage volume, Q_{j-1}, have been determined, and a recharge rate, i_e, is assumed known. The recharge rate is converted to an aquifer volume over the surface of the flow domain, i.e., using equations (7) and (13) with $i = i_e \, n_s$, and added to the volume in storage to determine storage, Q_j, at time j. The method used to estimate outflow, as described previously, depends upon the elevation of the water table at the divide, h_1. Thus, h_1, must be determined as a function of Q_j. For parallel or convergent flow this means solving equations (25) and (27), respectively, for h_1 given Q_j. There is no direct solution; thus h_1 is obtained by iteration.

Drainage and Decline in the Water Table

As discussed previously, Liong et al. (1982) used a simple regression model calibrated by output from the Freeze model to study time-varying drainage as an aquifer responds to recharge and natural drainage. The study showed that flow recession and decline in water table height at the divide could be predicted quite accurately. Therefore we decided to use this concept for the parallel flow case.

Recession in the Water Surface Profile for Parallel Sections Flow

Liong et al. (1982) found that daily decline in water table elevation could be expressed in terms of dimensionless time and space by the expression

$$\Delta h_d^* = \exp(-B_p t^*) \qquad (28)$$

in which Δh_d^* is the proportional drop in elevation expressed in dimensionless terms, i.e., $\Delta h_d^* = h_{d_j}^* / h_{d_{j-1}}^*$ where j and $j-1$ represent values of h_d^* on adjacent days and $h_d^* = h_d / L$ where h_d is the elevation of the water table at the divide above the level of the stream, i.e., $h_d = h_1 - h_s$; and t^* is one day expressed in dimensionless time, i.e., $t^* = t \, K_s / L = K_s$. B_p is a recession parameter that is a function of h_s, n_s, h_d, and L. Numerical experiments used to obtain the functional relationship are described in the appendix of this paper. Equation (28) is similar to one frequently used to describe base flow recession, thus one should expect it to hold for recession of water table rates if Darcian conditions are assumed realistic.

Equation (28) defines the day to day change of the water table for draining parallel or nonconverging flow conditions. The change in storage, from which we determine outflow, is directly proportional to change in h_1, and is obtained by differencing solutions of equation (25) using values of h_1 before and after daily recession. During times of no recharge, the value of h_1, before recession, is the value of h_1 at the end of the previous day. During times of recharge, the value of h_1, before recession, is the value of h_1 after adding recharge (see previous section of this report).

Recession in the Water Surface Profile for Converging Flow Sections

In the case of a converging flow section, outflow rate, and thus change in storage, i.e., change in volume of water stored above the elevation of the water in the channel, h_s, is proportional to a change in the integral product of surface area and $(h-h_s)$. To define an expression for converging flow paths, it was assumed that the rate of decline, B_c, for converging conditions could be related to that for nonconverging cases by

$$B_c = R_B B_p \qquad\qquad\qquad (29)$$

in which R_B is a multiplying factor. A series of numerical experiments using the Smith-Hebbert model confirmed the theory and were used to develop a functional relationship in which R_B was found to be a function of r_o/R. The derivations are presented in appendix B.

B_c from equation (29) is substituted for B_p in equation (28) to obtain the daily decline in the water table for converging flow paths. Change in storage, from which we get converging section outflow, is obtained by differencing the solutions of equation (27) using values of h_1 before and after daily recession.

A comparison of values obtained using Equation (B-4) (see appendix B) and values obtained from use of the Smith-Hebbert model is presented in Table B-4. The average error of prediction is about 2.5 percent. Having calculated R_B using equation (B-4), B_c for converging flow is calculated from equation (B-1) or equation (29).

As in the case of non-converging flow, during times of no recharge, the value of h_1, before recession, is the value of h_1 at the end of the previous day. During times of recharge, the value of h_1, before recession, is the value of h_1 after adding recharge (see previous section of this report).

Flow Rate into the Channel

Using equation (28); and equation (29) for converging flow cases; it is possible to calculate the rate of decline in the water table from one day to the next for any parallel or convergent flow conditions given h_s, h_d, n_s, r_o, θ, R, L, and K_s. Having made these calculations to get h_1, the new water table elevation at the divide after one day's drainage; equation (25) or (27) is used with this value of h_1 to determine Q_j. The volume discharged to the channel for day j, q_j, is then determined from equation (5), and the relationship q_{e_j} = $n_s q_j$ to convert from aquifer volume to flow volume.

The procedures described in the previous five sections of this report are used repeatedly from day to day to calculate volume of water discharged to the channel from representative flow paths. Values obtained for parallel flow are per unit width and must be scaled to the effective width of the flow path. Values for convergent flow are for the whole area and are not scaled.

MAINTENANCE OF CONTINUITY AND PARAMETER IDENTIFICATION

In the previous discussion of surface profiles, equations (11) and (19) express a relation between the steady-state water surface profile and recharge rate, i, specific yield, n_s, and saturated hydraulic conductivity K_s. Aquifer thickness

at the channel, h_s, is assumed known or estimated. Since the objective of the groundwater component of SWAM is to provide estimates of continuing groundwater flow to the channel, it is necessary to have the component response coupled to its parameters in such a way that it accurately simulates both streamflow levels and streamflow recession rates. Therefore the model relies on flow records from the watershed of concern, or other hydrologically similar watersheds, and equations (11) and (19) to estimate its parameter values.

In the following paragraphs we show how flow records, estimates of water table elevation, and specific yield are used to identify aquifer storage volumes and parameter values. The parameters we want to identify are i, n_s, h_1, and K_s however we also need representative streamflow recession rates and aquifer storage volumes. First we show how to estimate i from streamflow records, then how h_1 and n_s are obtained from static well elevations and volumes of storage in the aquifer. Finally K_s is obtained from equations (11) and (19) using the values of h_1, h_s, and an initial recharge rate, i, estimated from streamflow records.

It is not possible to independently assign all parameter values and meet the constraints of equations (11) and (19). However, it is possible to fix those parameters that are best known, and use the equations to provide estimates of the others. In most cases, the parameter least known is the effective saturated hydraulic conductivity of the flow section, so the model is formulated to calculate K_s using equations (11) and (19) after obtaining estimates of h_s, h_1 and i. At present, observed streamflow data probably provide more information about the volume of water in the aquifer than does anything else. Therefore data from nearby gauging stations are used to estimate aquifer storage volumes, initial recharge rates and parameter values.

First we'll convert the initial streamflow rate into an equivalent steady-state recharge and then show how to calculate the initial aquifer volume using flow rates equal to initial boundary conditions, i.e., flow rates assumed in the channel at the beginning of the simulation period. Since the model assumes a steady-state condition, the base flow rate selected to be representative of stream conditions at the starting date, q_o, can be converted to a recharge rate, i_e in meters or feet per day, this rate is converted to an effective recharge depth, i, in the soil by $i = i_e / n_s$. Values of n_s are obtained from old pump tests or similar documents.

Periods of groundwater recession are frequently expressed as

$$q_i = q_{i-ti}e^{-Dt_i} \tag{30}$$

in which q_i and q_{i-t_i} are flow rates t_i days apart and D is a recession parameter. The advantage of using this expression is that the drainable volume of water in the aquifer, Q_o, at time zero when the flow rate is q_o can be obtained by integrating equation (30):

$$Q_o = q_o / D \tag{31}$$

Thus, by choosing a representative base flow recession period from the streamflow record, it is possible to use equation (30) to calculate the recession parameter, D, from consecutive observations of flow t_i days apart. Equation (31) is then used to calculate the drainable volume of the aquifer, Q_o at the time of the recession from the flow rate q_o. Note that the flow rate at the start of simulated q_o does not have to correspond to the period used to calculate the recession parameter.

Our previous discussion has shown that base flow rate and aquifer volume are not as simple as expression 30 would indicate, however for establishing initial conditions the simple expression is satisfactory. If recession rates for the representative stream appear to vary somewhat, as they frequently do, it may be advisable to select several recession periods with flow rate approximately

equal to the conditions at the start of simulation. Late fall, winter or early spring conditions would probably be the best times to use because riparian vegetation would not be removing water giving a false measure of the groundwater flow rates. An average or representative value of D should then be selected from those evaluated and used in equation (31) along with, q_o, to calculate the volume of water stored in the aquifer at the time when the flow rate is q_o.

The drainable volume is assumed to be distributed over the drainage area in such a way that the volume in a unit width segment or a converging flow segment can be obtained by a ratio of the segment's area to that of the watershed.

Lastly we'll calculate the value of h_1 using the information just obtained on aquifer storage. Equations (25) and (27) express the volume in storage as functions of the elevation of the water table at both ends of the segment and the flow path length; for converging flow, the angle of convergence is also needed. Given the segment volume, determined by apportioning Q_o, the saturated flow depth at the channel, h_s, the length of the flow path and angle of convergence; equations (25) and (27) may be used to calculate the starting elevation of the water Table, h_1, at the upstream end of the flow path. One must remember to add the undrainable volume (the volume in storage above the impermeable layer and below the stream elevation represented as thickness h_s) to the drainable volume obtained from stream-flow records before using the two equations. Before adding Q_o to the undrainable volume both must be expressed in terms of aquifer storage volume, thus it is necessary to adjust Q_o for the effective porosity, storativity, or specific yield, n_s, in order to obtain the volume in the aquifer Q_o^*, i.e., $Q_o^* = Q_o / n_s$. Solution of equations (25) and (27) for h_1 is not direct, but h_1 and the volume in storage are nearly linearly related over narrow ranges, thus iterative solutions used in the model provided are very rapid.

Values of h_1 obtained from solution of equations (25) and (27) are functions of the assumed value of storativity n_s; thus if storativity is not well known, one should attempt to obtain records of h_1 from groundwater observation wells, and the value of n_s chosen such that the values obtained from equations (25) and (27) are as close as possible to those observed in the well records.

The above procedure provides a means of maintaining continuity between the water surface profile, the internal physical characteristics of the flow domain, and streamflow observations. It is also important to maintain continuity between recharge, i, and outflow, q_i, when establishing parameter values under steady-state conditions at the start of simulation. In the model's present configuration outflow is obtained by change in the volume of storage, but there is no guarantee that this will equal recharge if K_s is chosen independently. However, it is possible to force steady-state outflow to be equal to recharge by the proper selection of K_s. This is done through the use of equations (28) and (29), and the values of B_p or B_c.

For parallel flow conditions, change in elevation of the water table at the divide as a result of drainage was shown to be

$$\Delta h_d^* = \exp(-B_p t^*) \tag{32}$$

We know that

$$t^* = \frac{t K_s}{L} \tag{33}$$

Thus,

$$\Delta h_d^* = \exp\left(\frac{-B_p t K_s}{L}\right) \tag{34}$$

or

$$\ln (\Delta h_d^*) = \frac{-B_p \, t \, K_s}{L} \tag{35}$$

and

$$K_s = - \frac{L \ln (\Delta h_d^*)}{B_p \, t} \tag{36}$$

Since we are forcing a continuity of recharge and outflow, i.e., $i_e = q_j$, all of the parameters needed to solve equation (36) are known. The value of h_d is taken as the level of the water table at the divide, $h_1 - h_s$, at the simulation starting time. Assuming steady-state conditions, we want the calculated proportional decline in the water table, Δh_d^*, to produce a volume equal to the average observed base flow rate at the start of simulation. Therefore, we calculate the volume in storage at h_d, $h_{d_{j-1}}$, using equation (25), reduce this volume by the observed daily equivalent of base flow, q_j, and use the iterative scheme, described in the section of this report on recharge, to calculate the new value of h_d, h_{d_j}.

The ratio, $h_{d_j}/h_{d_{j-1}}$ of these two values, or their dimensionless form h_d^* / h_d; is Δh_d^*. The parameter B_p is calculated as described in appendix A, and all other inputs, h_d^*, h_s^*, and n_s are known. The time interval t is 1.0 day, so equation (36) gives the required K_s directly. This procedure for calculating K_s forces the model to maintain continuity between recharge and outflow, while at the same time maintaining continuity between the water surface profile and internal physical features.

The procedure outlined above is for the parallel flow case. An identical procedure is used for converging flow except that B_p in equations (32), (34), (35), and (36) is replaced by B_c; equation (25) is replaced by equation (27); B_c is calculated as described in appendix B; and equation (11) is replaced by equation (19).

CONCENTRATION OF SOLUTES

The model simulates concentration of dissolved, conservative chemicals in the groundwater discharged to the stream, as well as within the groundwater body itself. Whereas flow simulation lumps recharge, effectively neglecting the partitions (i.e., compartments) within flow segments resulting from variable recharge rates or different concentrations (see Figure 5), the quality routine utilizes individual partition characteristics.

Water Mass Balance

A day-by-day mass balance of water is calculated for each partition including exchanges between partitions and the actual amount of upslope recharge. Water balance operates between beginning and ending water surface profiles of a time step; the intermediate water table position of the flow model, from which drainage is calculated, is neglected. The difference between beginning and ending volumes of water within a partition for a given day, $Q_{i,t-1} - Q_{i,t}$, is calculated by applying equations (25) or (27) with limits of integration corresponding to partition boundaries. Change of storage, which can be either positive or negative, must equal the sum of the inflows and outflows during the same day, i.e., recharge added directly to the partition, plus inflow to the partition from the next partition upslope, minus partition outflow to the next partition downslope.
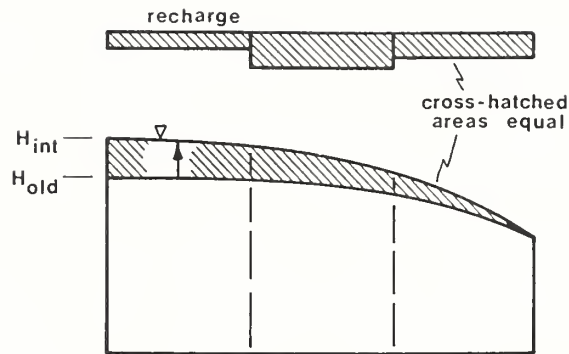
1) Recharge volume added to previous groundwater volume
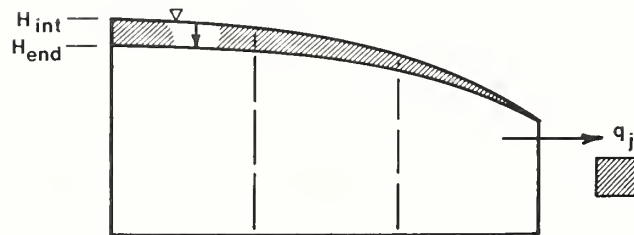
2) Drained volume is section outflow

Figure 5
Schematic of water balance in the ground water model.
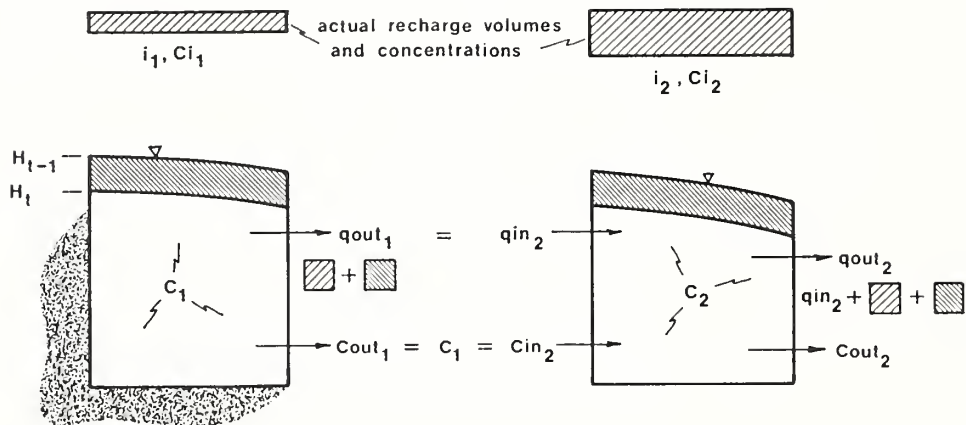
Figure 6
Schematic of solute mixing in the groundwater model.

Considering the most upslope partition first (see Figure 6), the only input is recharge, so change in saturated volume within the partition during a time step must equal recharge minus partition outflow. Recharge volume is calculated using the actual recharge rate, i_1, applied to the partition length. Since change in storage is known from beginning and ending water surface profiles, transfer of water to the next partition downslope, $qout_1$, may be calculated directly. A similar water balance is carried out for the next partition, except its inflow from upslope is equal to outflow from the next upslope

partition. Exchange of water between partitions calculated this way considers a combination of real water volumes (spatially varied recharge) and mathematical water volumes (resulting from the flow-model water surface profile assumptions), and thus reflects to some extent, variable recharge over the watershed.

These partition-oriented water balances use a form of equation (5) including partition-to-partition exchange terms

$$\text{qout}_{i,t} = Q_{i,t-1} + i_{i,t} + \text{qout}_{i-1,t} - Q_{i,t} \tag{37}$$

where subscript i indicates partition and quot is partition volume output. The qout of the partition adjacent to the channel is identical to q_j of equation (5).

The outcome of such routing is that groundwater within the section will move slower through zones which have little or no recharge upslope, and faster through zones having the bulk of the recharge upslope. As an example, if a relatively high chemical concentration is input to the most upslope partition by an extremely small amount of recharge, while greater recharge is being applied to partitions downslope, the higher concentration input will be modeled as moving relatively slowly toward the zone of higher recharge. Once in this zone however, its rate of transport to the stream would increase. At the extreme, if a watershed was at steady-state with all recharge occurring near the stream, a high-concentration groundwater zone at the watershed divide would never affect the stream since there is no recharge above it causing partition-to-partition exchange of water. However in a drainage condition, i.e., a period of no recharge, a water volume equal to $Q_{i,t-1} - Q_{i,t}$ and associated solute would move downslope.

Chemical Mass Balance

The partition-based water balance is the basis for chemical routing. Chemicals are balanced by multiplying each flow component in equation (37) by its respective solute concentration, partition concentration at the end of the time step being the unknown. Recharge concentration and partition concentration at the start of the time step are known. To begin simulation, all partition concentrations are initialized to user-specified values and each partition's outflow concentration is set equal to the partition concentration itself. Solution for the partition's concentration at the end of the time step is

$$C_{i,t} = (Q_{i,t-1} * C_{i,t-1} + i_{i,t} * C_{i,t} + \text{qout}_{i-1,t} * C_{i-1,t-1} +$$
$$\text{qout}_{i-1,t} * C_{i-1,t-1} - \text{qout}_{i,t} * C_{i,t-1}) / Q_{i,t} \tag{38}$$

where C is concentration and i designates the partition number.

Equation (37) is used to compute a partition-to-partition water balance over the entire flow section during each time interval. In a like manner, equation (38) is used to compute the partition-to-partition chemical balance.

The concentration of solute entering the stream is the concentration of the adjacent partition during each time step. Within-partition concentrations reflect the distribution of recharge inputs to the section in both time and space, and could be used, to a limited extent, to assess impact of watershed land use on groundwater quality.

No watershed data have been used to test the model; however, it can be tested for mass balance and its output compared to travel times calculated for given section configurations. In Figure 7, a constant flux of 0.2 ft/day is applied to the lower 800 ft of a 1,000-ft section with water surface elevations as shown. Initial groundwater concentrations are assumed to be 0.0 ppm. Beginning on day 2 and continuing for 10 days thereafter, recharge over partition 3 (200 ft to 300 ft from the stream) is given a concentration of 100 ppm; total chemical load input is 20,000 ft^3-ppm. When integrated over a 60-day period, the water entering the channel had a chemical load of 19,840 ft^3-ppm, showing that continuity of chemical mass is well-maintained.

Figure 8 shows outflow concentration at the stream for the four flux-concentration configurations shown. Solute concentrations in the groundwater zones beneath the recharge areas were initialized at 100 ppm.
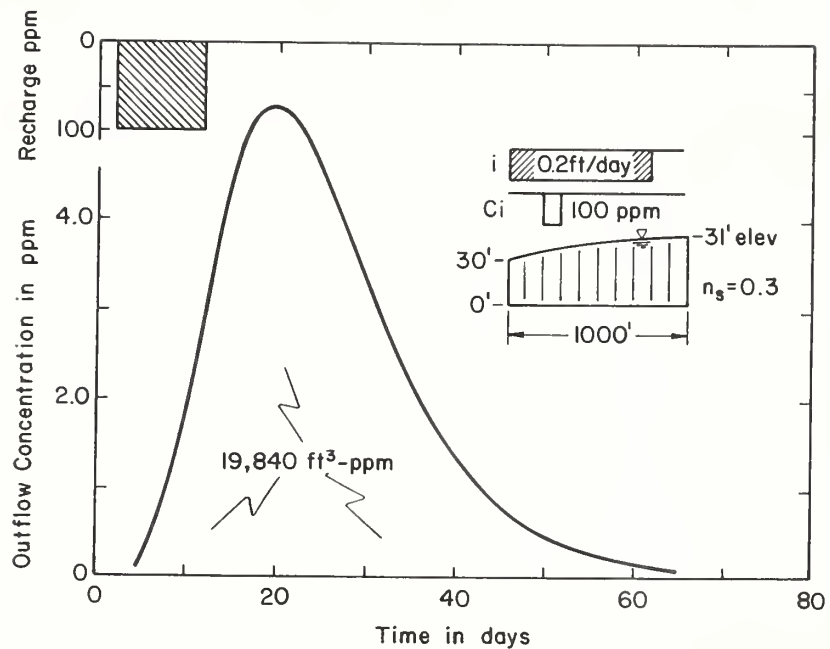
Figure 7
Concentration in outflow as a function of time - used to test for continuity.
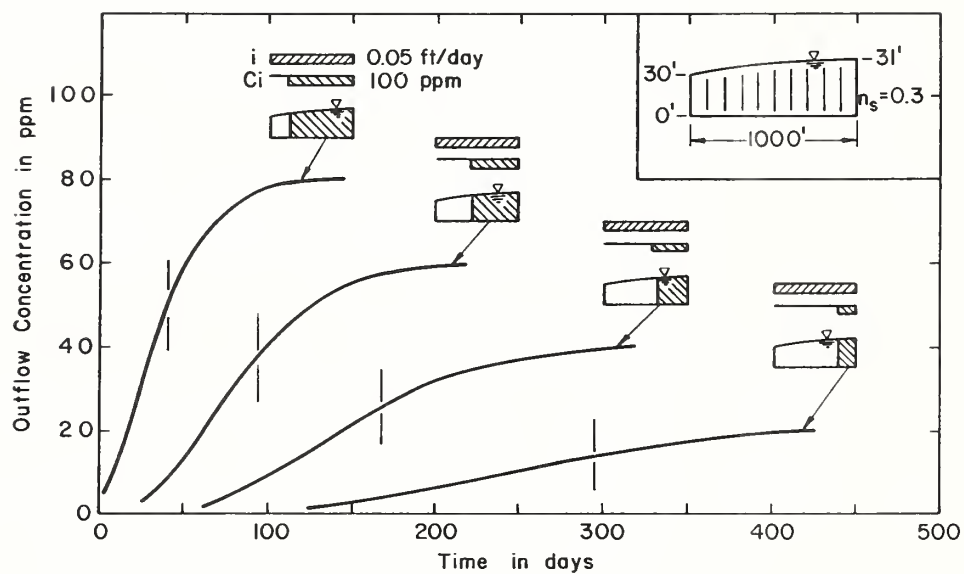
Figure 8
Concentration of outflow response as a function of location of recharge area. Timelines indicate analytically derived travel time.

Equilibrium concentrations at the outlet are as expected, and the lag in response is dependent on distance from the stream to the area receiving the high solute concentration recharge. Also shown on the figure are analytically derived travel times from location of the initial chemical front to the stream. Travel times were determined by numerical integration of the velocity distribution under the Forchheimer ellipse describing the flow model's water table equation (12). It can be seen that the travel times intersect the model responses consistently at about 60% of equilibrium concentration.

Figure 9 shows the results of runs designed to give approximately uniform velocities between the initial chemical front and the stream. Flux and initial groundwater concentration of 100 ppm are applied only to an area above 200, 400, 600, or 800 ft from the stream, but the flux rate applied is such that an outlet flow of 50 ft^3/day/ft is maintained for all runs. Since the flow section is almost uniform in depth, varying from 30 ft at the stream to 31 ft at the watershed divide 1,000 ft away, velocity of flow through the media is approximately 5.4 ft/day (50 ft^2/day / 30.5 ft/n_s). Travel times given on Figure 9 are distance from the stream to the chemical front divided by this velocity. It can be seen that model output gives an almost uniformly increasing delay in response from the 200-ft no-flux zone to the 800-ft no-flux zone. Response-travel time intersections are similar to those previously described.

Recognizing that the breakthrough type curve response pattern produced by the model is primarily due to numerical dispersion resulting from partitioning the section and assuming fully mixed partitions, the effect of number of partitions was examined. Figure 10 shows the results of runs using the section geometry of Figure 8 and three different partitioning groupings: 2 partitions of 500 ft each, 4 partitions of 250 ft each, and 10 partitions of 100 ft. each. Water flux was applied over the entire section; initial groundwater concentration and recharge concentrations of 100 ppm were applied only above the 500-ft mark. Response of the configuration using two 500-ft partitions shows an extremely rapid initial response, followed by a rather gradual rise to equilibrium. Conversely, the configuration of 10 100-ft partitions gives a greater initial delay, a steeper rise following the delay, and a quicker approach to equilibrium.

Based on this limited testing, the groundwater quality routine appears to behave reasonably well. Chemical mass input in recharge is fully conserved, equilibrium output concentrations are as expected, and responses with time correspond to calculated travel times. Further testing and application to field situations are needed, but data appropriate for verification will be hard to find.

OPERATIONAL IMPROVEMENTS

The previous material describes the structure of a model that can be used to simulate the subsurface contribution of a catchment to its stream system. However, refinements are needed to make it easy to use. The first is to appropriately select the flow paths to minimize the number of different elements in each and make all of the rectangular and convergent flow paths equal in surface area to the real catchment to which it is being fitted. In rectangular sections this is done by fixing either the length or the width of the path and determining the other dimension by dividing the surface area measured on the watershed map by the fixed dimension.

In a converging flow situation, it can be shown algebraically that the parameters θ, r_o, and R can be obtained from two dimensionless terms, w_s' and w_1', and the measured surface area. The dimensionless terms are

$$w_s' = \frac{w_s}{w_1 - w_s} \tag{39}$$
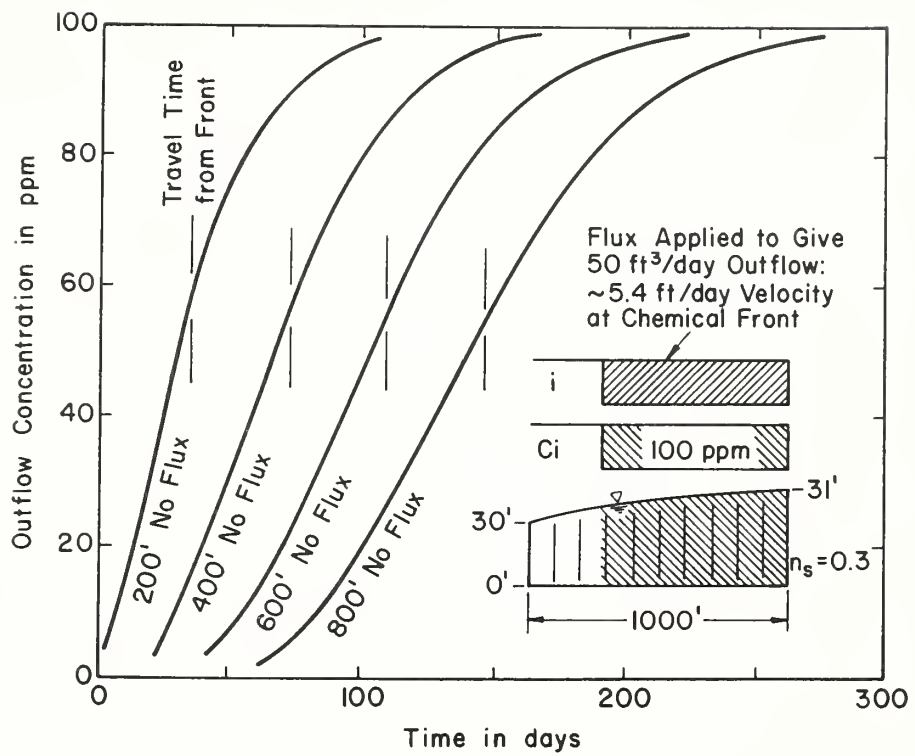
Figure 9
Arrival times for chemical fronts that originate at different
distances from the channel.
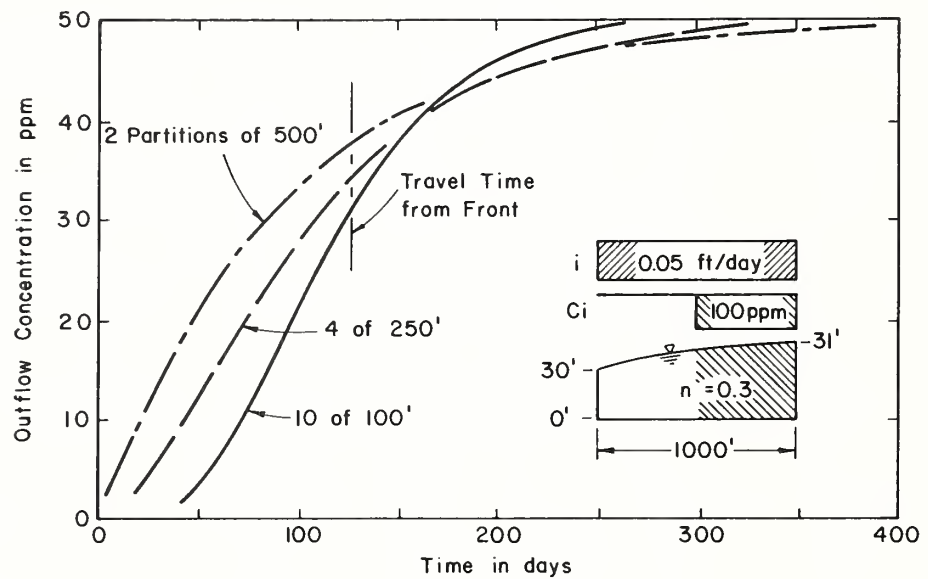
Figure 10
Concentration of outflow response as a function of the number of
partitions.

237

$$\text{and } w_1' = \frac{w_1}{w_1 - w_s} \tag{40}$$

in which w_1 and w_s are two parallel lines measuring the width of the converging section; w_s is width at the channel and w_1 is width at a distance L' upslope. These measures of w_s, w_1, and L' are illustrated in Figure 1b. It may be shown that the angle θ, in radians, is

$$\theta = 2 \tan^{-1} \left(\frac{w_1}{2 w_1' L'}\right) \tag{41}$$

the radial distance from the focal point to the channel, r_o, is

$$r_o = \frac{w_s' L'}{\cos (\theta/2)} \tag{42}$$

and radial distance to the end of a flow path equal in area to that of a segment of the catchment is given by

$$R = \left(\frac{2 A_c}{\theta} + r_o^2\right)^{1/2} \tag{43}$$

in which A_c is the area of the catchment to be included.

The terms w_s, w_1, and L' make it easy to obtain all of the parameters needed to use the model in a converging flow situation. It is also possible to use expressions (41), (42), and (43) to find the radial distance to intermediate points that correspond to the breaks between different fields. All one has to do is start with the channel and define the areas of consecutive fields and use equation (43) to find the distance.

ILLUSTRATED EXAMPLES

The water flow component of the model was tested by comparing it with response from two watersheds, one in Oklahoma and the other in Pennsylvania.

Watershed 5142 Near Chickasha, Oklahoma

Watershed, Number 5142, is a small grassland watershed near Chickasha, Oklahoma. The watershed and 29 flow paths selected to represent the groundwater flow are shown in Figure 11. The length of channel receiving groundwater contribution was determined by field observation. Above the point of converging flow, the water table lies below the bed of the channel and no base flow was observed. Naney et al., (1978), used this same watershed in illustrating a similar type model. In their paper they describe the 1.45 Km^2 (0.57 mi^2) watershed as having little alluvium and deeply incised channels. Water levels in drill holes and observation wells indicated that the groundwater levels at the divide were 3-4.5 m (10-15 ft) above the water surface in the channel. Depth of the saturated zone contributing water to the channel, h_s, was estimated to be about 5.2 m (17 ft). Porosity or specific yield is very low and was estimated at 0.002. An initial flow rate at the outlet of the watershed of 2.8 x 10^{-4} m^3/sec (0.01 ft^3/sec) was converted to a steady-state recharge of 1.7 x 10^{-5} m/day (5.5 X10^{-5}/ft/day) to establish the depth at the divide, h_d, saturated conductivity, K_s, and initial flow rate in the system. An analysis of streamflow recession patterns showed that an average recession constant, D, of 0.009 sec^{-1} could be used to determine the aquifer storage volume/outflow rate. Table 1 shows physical characteristics of each of the 29 flow paths. Since the objective of the test was simply to
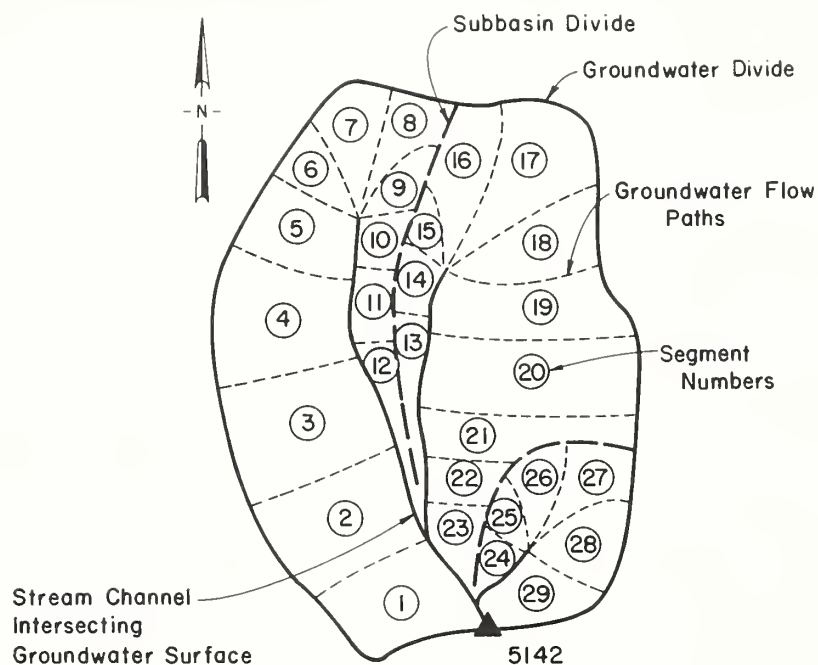
Figure 11
Groundwater basin of ARS Watershed 5142 near Chickasha, Ok.

Table 1
Physical characteristics of flow paths for watershed 5142
near Chickasha, Oklahoma

Element No.	Length L meters	Width w meters	Angle θ degrees	Calculated h_d meters	K_s m/day
1	360	280	0	1.3	.003
2	440	300	0	1.3	.005
3	460	300	0	1.3	.005
4	400	300	0	1.3	.004
5	320	200	0	1.3	.003
6	280	10	30	1.0	.006
7	400	10	45	1.0	.014
8	360	10	35	1.0	.010
9	240	10	30	1.1	.004
10	120	140	0	1.0	.0004
11	100	200	0	1.3	.0003
12	60	400	0	1.4	.0001
13	60	500	0	1.4	.0001
14	120	180	0	1.3	.0004
15	160	10	40	1.0	.002
16	300	10	30	1.0	.007
17	500	10	40	1.0	.023
18	440	10	30	1.0	.016
19	540	160	0	1.3	.008
20	600	220	0	1.3	.009
21	600	120	0	1.3	.009
22	200	120	0	1.4	.001
23	180	200	0	1.3	.0009
24	80	140	0	1.3	.0002
25	160	10	45	1.1	.002
26	260	10	35	1.0	.005
27	340	10	45	1.0	.010
28	260	10	55	1.1	.005
29	180	200	0	1.3	.0009

demonstrate the performance of the groundwater model, and not the ability to generate dates and rates of recharge, the recharge rate, date, and duration of recharge were estimated from flow records on the watershed (see Figure 12). Also note that the calculated values of h_d are in the range of 1.3 meters, whereas observations would have placed h_d at 3-4.5 meters. Thus the estimate of n_s is likely low and should have been about 0.006. Values of K_s obtained from the simulation are reasonable. Recharge values used in the simulation are shown in Table 2. Results of the simulation using these estimated recharge rates are shown in Figure 12.
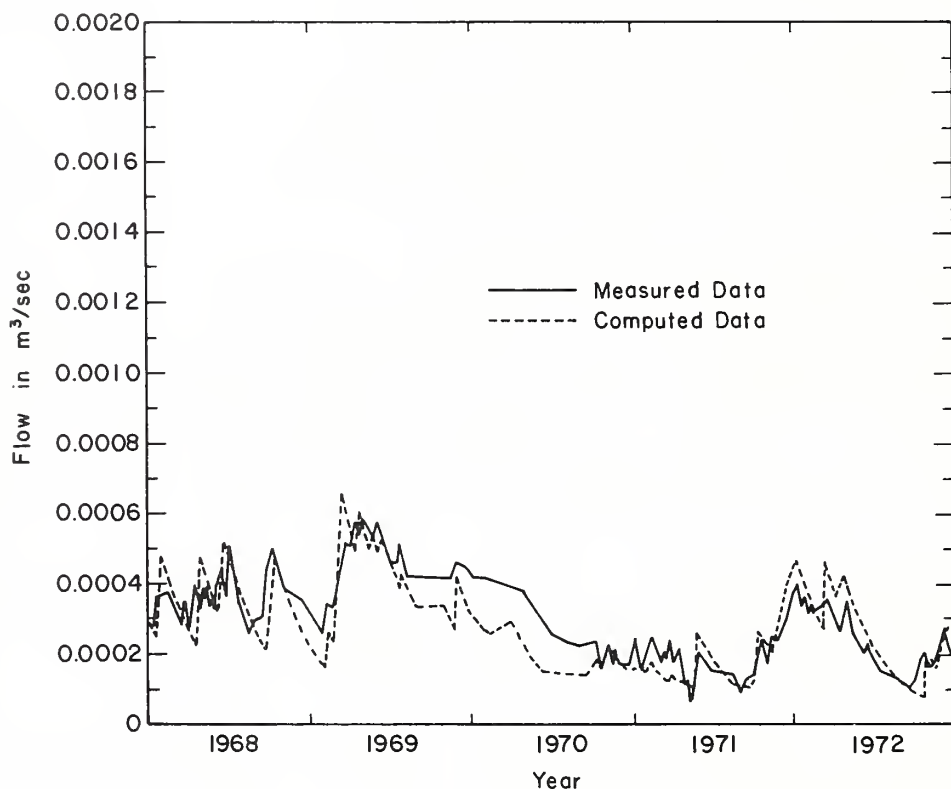
Figure 12
Base flow of watershed 5142 in Oklahoma (measured and computed).

Table 2
Recharge rates by date and length of period (m/day)

1968		1969		1970		1971		1972	
20/10	2.0×10^{-4}	40/10	7.0×10^{-5}	50/50	5.0×10^{-6}	1/10	1.5×10^{-5}	1/20	7.0×10^{-5}
110/10	2.0×10^{-4}	60/20	2.0×10^{-4}	270/30	1.0×10^{-5}	40/10	3.0×10^{-5}	80/5	3.0×10^{-4}
160/20	1.0×10^{-4}	110/10	1.5×10^{-4}	310/10	2.4×10^{-5}	90/10	1.8×10^{-5}	110/20	5.0×10^{-5}
270/20	2.0×10^{-4}	140/10	7.0×10^{-5}			120/5	3.0×10^{-5}	310/5	1.0×10^{-4}
		160/10	7.0×10^{-5}			155/5	2.0×10^{-4}	335/30	3.0×10^{-5}
		210/5	1.0×10^{-4}			260/30	1.0×10^{-5}		
		250/60	1.2×10^{-5}			290/10	1.0×10^{-4}		
		335/5	2.0×10^{-4}			330/35	5.0×10^{-5}		

Starting flow rate = 2.83×10^{-4} m^3/sec = 1.66×10^{-5} m/day recharge.

The first column of each year lists the beginning day and duration in days of the recharge rate listed in the second column.

Mahantango Creek Watershed, Pennsylvania

A second test of the model was carried out using data from a Mahantango Creek subwatershed in Pennsylvania. The research watershed is mixed land use: 8 percent pasture, 57 percent crop land and 35 percent forest. The drainage area is 7.4 Km^2 (2.85 mi^2 sq.) The watershed showing the subdivisions used in simulation is shown in Figure 13.

Testing a subsurface model such as the one described in this report is not as easy as testing a surface runoff model, because we do not know recharge amounts or rates on an event or daily basis. In the case of this study, streamflow and well records were used to estimate the recharge, values were then adjusted to get recharge and outflow volumes compatible.

The data set was constructed using streamflow records from the watershed for calendar years 1983 and 1984. Total streamflow was separated into base flow and direct runoff components for the entire period of record by extending all hydrograph recessions back in time to under the peak, and then connecting this point to the initial hydrograph rise. The resulting data set consists of daily "base flow" for the entire two-year period.
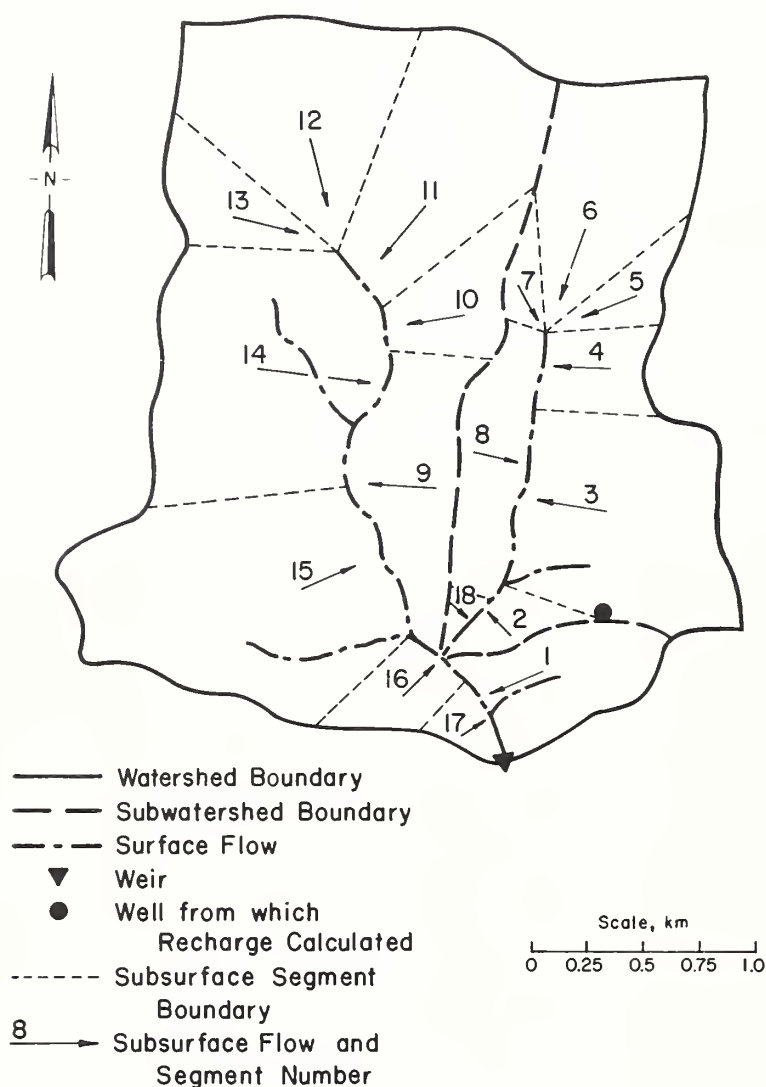
Figure 13
Mahantango Creek watershed in Pennsylvania.

241

Initial estimates of recharge to the model were developed using these base flow data and records from an observation well which is typical of overall watershed response to precipitation. Total base flow for the two-year period was assumed to equal total recharge, because beginning and ending groundwater levels were approximately equal. The assumption was then made that the well indicates active recharge whenever it is rising. Daily readings were abstracted from the total well record, and all daily rises (day-end level>day-beginning level) were accumulated for the two years of record, a total of 8.1m (24.8 ft). Total base flow for the two-year period is equivalent to 0.74m (2.3 ft) of recharge over the watershed, so a ratio of 0.09 meters recharge / meter groundwater rise was used to develop the recharge data set. That is, every day there was an observed rise in groundwater level in the indicator well, recharge was assumed to occur at 0.09 m / m of rise. Preliminary analyses of results using these estimates of recharge showed that even though total volumes of a recharge matched outflow, there were large discrepancies in individual values, thus recharge rates were adjusted to give better event and sustained base flow balance.

The period selected to start simulation was a prolonged recession in July 1983. There was 46mm (1.8 in) of rain on June 28 and none again until July 16. We chose to begin simulation on July 13, when base flow was at 0.026 m^3/sec (0.91 cfs). A plot of the daily streamflow records for this recession period showed that the exponential recession rate was 0.051 day^{-1}, indicating that the volume in aquifer storage at the start of simulation (0.91 cfs x 86400 sec/day)/ 0.051 is 1.54 x 10^6 ft^3 distributed over the watershed. This translates to 0.019 ft, and assuming a storage constant of 0.01, a saturated depth of water available for drainage averaging 1.9 ft in thickness. The 0.01 value for the storage coefficient was used based on results of pumping tests and other studies on the watershed. Results of the simulation showed that this volume was equivalent to elevations at the divide of about 0.6 meters (2.0 ft). Observed values of h_d are about 6 meters (20 ft). The discrepancy comes from the fact that the impervious layer on the watershed is sloping and the model is not able to simulate that feature.

Results of the simulation (Figure 14) show an overall satisfactory simulation with excellent simulation of sustained base flows, which the model is primarily designed to simulate. The plot also shows that the watershed has sizable
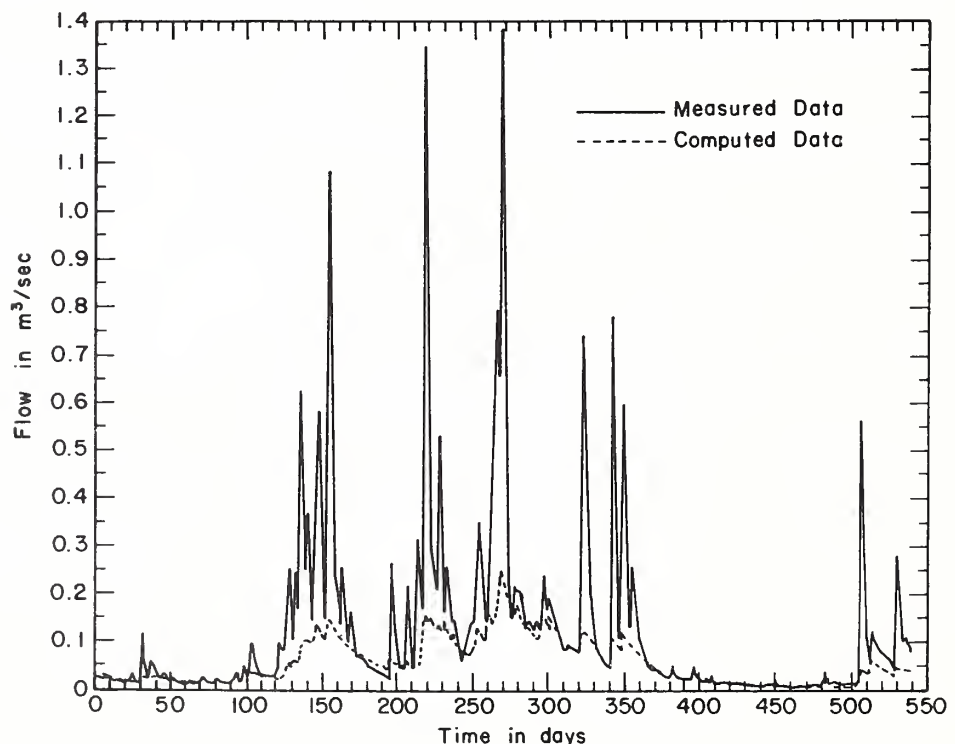
Figure 14
Base flow of Mahantango Creek Watershed (measured and computed).

volumes of rapid subsurface return flow which are not simulated by the present model. The model was modified for application to another site in which rapid return subsurface flow was evident. In this case, the deep aquifer of the watershed was assumed to be overlain with a much more responsive leaky aquifer. The two combined worked very well, but the current model does not include a leaky aquifer because at present, calibration of the two models to determine the leak rate, (recharge to the deep aquifer), is a trial and error process.

SUMMARY

This paper presents a simple model of the subsurface flow and quality contribution of a catchment to its stream system for use in SWAM. The model parameters have been determined such that its response is representative of that of a complete finite-difference model of the same processes. The flow system is visualized as consisting of parallel and converging paths that contribute directly to the stream. Subsurface flow to the channel from any segment is a function of the length of the flow path, thickness of the aquifer at the channel, elevation of the water table at the divide, saturated hydraulic conductivity, effective porosity or specific yield, width of the flow path, and angle of convergence. Simulation is based on recharge, the volume of water in aquifer storage, and the elevation of the water table at the upstream divide. Recharge to the groundwater table adds directly to the volume in storage, thereby raising the water table level. The outflow rate from day to day is a function of the rate of decline in the water table at the divide. Provision has been made to partition the flow paths into sections, each representative of the aquifer below different land uses. This enables the model to be used to simulate the concentrations of dissolved materials and their movement through the aquifer to the channel. Plug flow and instantaneous mixing are assumed. Methods of obtaining the input parameters are described, and a simple scheme is presented for getting the shape of the schematic flow paths. The method is illustrated by comparing it to periods of record from watersheds in Oklahoma and Pennsylvania.

The actual model is summarized as follows: Flow rate from day to day is calculated using equation (5). Water surface profiles used to determine volumes in storage are calculated using equation (12) or (23); and volumes in storage are determined using equation (25) or (27), depending upon whether the flow sections are parallel or converging, respectively. Change in storage, and thus the outflow rate, is determined by using equation (28). The rate of decline for parallel or converging flow is calculated with equations (A-1) or (B-1), respectively. Parameters to calculate the recession constant for parallel flow in equation (A-1) are evaluated using equations (A-2) through (A-14), and for convergent flow in equation (B-1) using equation (B-4). Equation (36) is used to calculate the saturated hydraulic conductivity.

REFERENCES

Amerman, C.R., and J.W. Naney. 1982. Subsurface flow and groundwater systems. In Hydrologic Modeling of Small Watersheds, Ch. 7, pp. 277-293. American Soc. Agric. Eng. St. Joseph, MI.

Carnahan, B., H. A. Luther, and J. O. Wilkes. 1969. Applied numerical methods. John Wiley and Sons, New York, NY. pp. 101-105.

Freeze, R. A. 1971. Three-dimensional, transient, saturated-unsaturated flow in a groundwater basin. Water Resources Res. 7:347-366.

Liong, S.Y., and D.G. DeCoursey. 1982. Development of prediction equations for a phreatic aquifer in response to infiltration: Dimensional Analysis. Water Resources Bull. 18(2):307-310.

Liong, S.Y., D.G. DeCoursey, E.H. Seely, 1982. Response function for subsurface flow, rainfall-runoff relationships. In Proceedings of the International Symposium on Rainfall-Runoff Modeling, Mississippi State University, MS. May 1981. pp. 285-300.

Muskat, M., and R.D. Wyckoff. 1937. The flow of homogenous fluids through porous media. McGraw-Hill, New York, NY, pp. 630-642.

Naney, James W., Donn G. DeCoursey, Bill B. Barnes, and others. 1978. Predicting base blow using hydrogeologic parameters. Water Resources Bulletin 14(3):640-650.

Smith, R. E., and R. H. B. Hebbert. 1983. Mathematical simulation of interdependent surface and subsurface hydrologic processes. Water Resources Research. 19(4):987-1001.

It is possible that an analytical solution to relate the groundwater table recession rate B_p to watershed and aquifer features exists. However since no readily obvious solutions could be found, we ran a series of experiments with the Smith-Hebbert (1982) model to evaluate B_p as a function of h_s^*, h_d^*, and n_s. For converging flow situations, B_c, as a function of B_p, is described in appendix B. A range in values of the parameters h_s^*, h_d^*, and n_s was selected for the experiments to encompass most real situations. Table A-1 shows the values selected. Six dimensionless values of the depth of the aquifer at the channel, h_s^*, ranging from 0.005 to 0.16 were used. For each of these values, nine different effective porosities, n_s, ranging from 0.001 to 0.60 were considered. Collectively, these represent 54 combinations. Values of K_s were adjusted to be representative of materials with porosities similar to the values selected for n_s (values of K_s ranged from 0.02 to 5.0 cm / hr). Lengths of flow paths, L, varied from 50 to 1,000 meters. Since the Smith-Hebbert model fixes the steady-state profile as a function of the flow rate, q_s, three and in some cases four different flow rates, each an order of magnitude apart, were selected to provide a range in h_d^* values. Values of h_d^* obtained did not cover as broad a range as q_s, but were several orders of magnitude apart for any combination of n_s and h_s^*. The total range in h_d^* was 0.000002 to about 0.8. The parameter, B_p, in expression (28) was evaluated from the output of the Smith-Hebbert model. It was obtained by starting from a steady-state condition and noting the change in h_d after one day of drainage with no recharge. It was our opinion that the normal groundwater surface profile was more nearly like a steady-state profile than a drainage profile. Therefore values of B_p selected were average values taken within a few days of the start of simulation, rather than letting the simulation run for many days before selecting a value. Values taken from the simulations were very stable, changing very gradually with time and drop in the water table elevation. Table A-1 shows values of the parameter B_p obtained from the experiment. The values were plotted against h_d^*, and it was found that for any given h_s and n_s value, the relationship with h_d^* was linear as one would expect if Darcy's Law is valid (see Figure A-1). Figure A-1 shows values of B_p vs. h_d^* for experimental runs with $h_s^* = 0.01$ and $n_s = 0.001$ to 0.60. Plots from the other five sets of runs are similar, showing a linear relation between B_p and h_d^*. An analytical solution for B_p as a function of h_s^*, n_s and h_d^* was obtained by calculating the slope and intercept of the relation between B_p and h_d^* as functions of n_s and h_s^*, i.e.,

$$B_p = a + b\, h_d^* \tag{A-1}$$

Values of a and b taken from the plots are shown in Table A-2. A plot of the intercept, a, vs. h_s^* for a given value of n_s, showed a family of lines with similar features, but decreasing slope with decreasing n_s. In an attempt to collapse the family of lines, the intercept values were divided by the intercept at $h_s^* = 0.16$. Figure A-2 is a plot of the "dimensionless" intercept as a function of h_s^*. In this figure there appears to be two distinct groups of lines that diverge at an h_s^* of 0.04. The right hand group of lines encompass most of the more common values of n_s; therefore the line chosen to represent the family of lines was selected to go through the mean of the right

hand group at $h_s^* = 0.04$. It is shown as the heavy dashed line in Figure A-2. Breaks in the line were defined at $h_s^* = 0.003$, 0.04, 0.08, and 0.16. Expressions for the various segments are

$$a/a_{.16} = 0.0 \qquad\qquad\qquad\qquad h_s^* \leq 0.003 \qquad (A-2)$$

$$a/a_{.16} = 10.8 \, (h_s^* - 0.003) \qquad 0.003 \leq h_s^* \leq 0.04 \qquad (A-3)$$

$$a/a_{.16} = 0.4 + 2.68 \, (h_s^* - 0.04) \qquad 0.04 \leq h_s^* \leq 0.08 \qquad (A-4)$$

$$a/a_{.16} = 0.507 + 6.16 \, (h_s^* - 0.08) \quad 0.08 \leq h_s^* \qquad (A-5)$$

The fact that nearly all of the lines go through the same point at $h_s^* = 0.08$ means that equation (A-5) can probably be extrapolated beyond $h_s^* = 0.16$ without serious error.

Since we used $a_{0.16}$ as the means of collapsing the family of lines, we must find an expression to estimate its value for all n_s values. The intercepts at $h_s^* = 0.16$, $a_{0.16}$, for all n_s are plotted on Figure A-3.

The intercepts for values of n_s less than 0.05 increase rapidly as n_s gets smaller. It does not appear that they depart much from a straight line, therefore straight line segments were used to fit the data in this range of n_s values. An exponential equation was used to fit the data for n_s greater than 0.05. The resulting expressions are:

$$a_{.16} = (n_s - 0.0108) \, / -0.0000148 \qquad\qquad n_s \leq 0.01 \qquad (A-6)$$

$$a_{.16} = (n_s - 0.0632) \, / -0.00104 \qquad\quad 0.01 \leq n_s \leq 0.05 \qquad (A-7)$$

$$a_{.16} = -0.272 + 982 \exp\,(-8.21 \, n_s^{.213}) \qquad 0.05 \leq n_s \qquad (A-8)$$

These equations are shown on Figure A-3.

The slope, b, of the relation between B_p and h_d^* in equation (A-1) was plotted against h_s^* for each value of n_s. The resulting family of curves were similar. One interesting feature of the lines was the fact that all of the curves showed very little change in the value of b for h_s^* values greater than 0.04. Thus for all practical purposes, the response for dimensionless depth to the impermeable layer greater than 0.04 approaches that of an infinite aquifer. In an attempt to collapse the curves onto one line, the values of slope were divided by the average of the values of the slope at $h_s^* = 0.04$, 0.08, and 0.16. These values are shown on Table A-2 as the reference values. Figure A-4 is a plot of the "dimensionless" slope as a function of h_s^*. Below a value of $h_s^* = 0.005$, the relation was assumed to be linear and approach a value of zero as h_s^* approached zero. In the range between h_s^* values of 0.005 and 0.04, an exponential expression was used. Following are the equations used to express the dimensionless slope b/b_{ave} of the line as a function of h_s^*:

$$b \, / \, b_{ave} = 132.\,h_s^* \qquad\qquad\qquad\qquad 0.0 \leq h_s^* \leq 0.005 \qquad (A-9)$$

$$b \, / \, b_{ave} = 685. - 684. \exp[112.(0.04 - h_s^*)^{3.68}] \; 0.005 \leq h_s^* \leq 0.04 \qquad (A-10)$$

$$b \, / \, b_{ave} = 1.0 \qquad\qquad\qquad\qquad\qquad 0.04 \leq h_s^* \qquad (A-11)$$

Since b_{ave} was used to collapse all of the lines onto one, we must find a way of calculating its value for all n_s. All the average values of the slope, b, at $h_s^* = 0.04$, 0.08, and 0.16, b_{ave}, are plotted on Figure A-5; they increase rapidly as values of n_s decrease below 0.05. There is no indication that they depart from a straight line; therefore straight line segments were used to fit the data in this range of n_s values. An exponential equation was used to fit the data for n_s greater than 0.05. The resulting expressions are

$$b_{ave} = (n_s - 0.0107) / -0.0000058 \qquad\qquad n_s \leq 0.01 \qquad\qquad (A-12)$$

$$b_{ave} = (n_s - 0.0702) / -0.000478 \qquad 0.01 \leq n_s \leq 0.05 \qquad (A-13)$$

$$b_{ave} = 0.874 + 1278.\exp(-8.19\, n_s^{0.291}) \qquad 0.05 \leq n_s \qquad (A-14)$$

These equations are shown on Figure A-5.

Given the above expressions for $a_{.16}$ and b_{ave}, it is possible to calculate the slope and intercepts of equation (A-1) using equations (A-2) through (A-5) and (A-9) through (A-11), respectively. The recession parameter B_p can then be calculated using equation (A-1). The expressions for a and b were tested by picking values from the lines in Figure A-1 and those of the other runs and comparing them to values calculated using expressions (A-1) through (A-14). The values obtained in testing are presented in Table A-3. The average absolute error is 8.5 percent.

Table A-1

B_p values obtained in experiments with the Smith and Hebbert model for parallel flow

Run No	L (m)	K_s (cm/hr)	n_s	h_s^* (cm)	low q_s (m³/sec)	low h_d^*	low B_p	med q_s (m³/sec)	med h_d^*	med B_p	high q_s (m³/sec)	high h_d^*	high B_p	xhigh q_s (m³/sec)	xhigh h_d^*	xhigh B_p
C-1	1000	0.02	0.15	0.005	0.000002	.00072	0.10	0.00002	.0054	0.13	0.0002	0.026	0.27			
-2		0.10	0.30		0.000001	.00077	0.04	0.0001	.0057	0.05	0.001	0.027	0.11			
-3		5.0	0.40		0.0004	.00075	0.02	0.004	.0053	0.03	0.04	0.024	0.08			
-4		0.20	0.50		0.00005	.0019	0.02	0.0005	.011	0.29	0.005	0.046	0.08			
-5		1.4	0.60		0.0005	.0027	0.02	0.005	.014	0.03	0.05	0.056	0.10			
-6		0.2	0.001		0.0000005	0.0000204	19.0	0.000005	0.000201	19.3	0.00005	0.00179	21.9	0.005	0.0453	90.2
-7		2.0	0.01		0.00001	0.0000455	1.29	0.0001	0.000440	1.34	0.001	0.00351	1.73	0.10	0.0650	9.25
-8		0.05	0.10		0.00005	0.00565	0.21	0.0005	0.0267	0.480	0.005	0.0645	1.01			
-9		0.05	0.05		0.0001	0.0095	0.54	0.001	0.0400	1.42	0.01	0.0645	2.19			
D-1	200	0.02	0.15	0.010	0.000002	.0013	0.29	0.00002	.010	0.36	0.0002	0.055	0.75			
-2		0.10	0.30		0.00001	.0015	0.11	0.0001	.011	0.15	0.001	0.057	0.33			
-3		5.00	0.40		0.0004	.0017	0.06	0.004	.012	0.09	0.04	0.055	0.21			
-4		0.05	0.50		0.00005	.0040	0.05	0.0005	.025	0.08	0.005	0.102	0.23			
-5		1.40	0.60		0.0005	.0056	0.10	0.005	.032	0.10	0.05	0.124	0.29			
-6		0.2	0.001		0.0000005	0.0000376	56.2	0.000005	0.000372	56.8	0.00005	0.00342	61.8	0.005	0.0959	216.
-7		2.0	0.01		0.00001	0.0000939	3.46	0.0001	0.000912	3.57	0.001	0.00743	7.87	0.10	0.145	22.2
-8		0.05	0.10		0.00005	0.0114	0.66	0.0005	0.0574	1.49	0.005	0.207	4.39			
-9		0.05	0.05		0.0001	0.0195	1.75	0.001	0.0869	4.40	0.01	0.207	9.28			
E-1	100	0.02	0.15	0.02	0.000001	.00066	0.64	0.00001	.0062	0.69	0.0001	0.043	1.07			
-2		0.10	0.30		0.000005	.00075	0.25	0.00005	.0069	0.28	0.0005	0.046	0.46			
-3		5.0	0.40		0.0002	.00090	0.12	0.002	.0079	0.15	0.02	0.046	0.27			
-4		0.20	0.50		0.00002	.0018	0.09	0.0002	.015	0.12	0.002	0.078	0.25			
-5		1.4	0.60		0.0002	.0026	0.10	0.002	.020	0.14	0.02	0.098	0.30			
-6		0.2	0.001		0.0000002	0.0000147	120.	0.000002	0.000146	121.	0.00002	.00144	123.	0.002	0.0689	236.
-7		2.0	0.01		0.000005	0.0000464	7.23	0.00005	0.000406	7.48	0.0005	0.00430	7.87	0.05	0.128	24.1
-8		0.05	0.10		0.00002	0.00561	1.23	0.0002	0.0389	1.90	0.002	0.174	4.66			
-9		0.05	0.05		0.0005	0.0738	5.51	0.005	0.297	14.7	0.05	0.413	19.9			
F-1	50	0.02	0.15	0.04	0.000002	.0013	1.53	0.00002	.013	1.67	0.0002	0.086	2.54			
-2		0.10	0.30		0.00001	.0015	0.60	0.0001	.015	0.66	0.001	0.092	1.06			
-3		5.0	0.40		0.0004	.0018	0.27	0.004	.016	0.31	0.04	0.091	0.54			
-4		0.20	0.50		0.00002	.0044	0.23	0.0002	.035	0.30	0.002	0.179	0.64			
-5		1.4	0.60		0.0002	.0064	0.23	0.002	.047	0.32	0.02	0.224	0.70			
-6		0.2	0.001		0.0000002	0.0000133	272.	0.000002	0.000133	273.	0.00002	0.00131	274.	0.002	0.740	376.
-7		2.0	0.01		0.000005	0.0000436	16.3	0.00005	0.000434	16.5	0.0005	0.00418	16.9	0.05	0.147	34.1
-8		0.05	0.10		0.00005	0.00581	2.72	0.0005	0.0456	3.57	0.004	0.2294	7.48			
-9		0.05	0.05		0.0005	0.0915	9.42	0.005	0.395	22.6	0.05	0.822	41.3			
H-1	100	0.02	0.15	0.08	0.00001	.0026	1.81	0.0001	.023	2.05	0.001	0.151	3.52			
-2		0.10	0.30		0.0001	.0054	0.79	0.001	.45	0.99	0.01	0.244	1.99			
-3		5.0	0.40		0.001	.0013	0.47	0.01	.012	0.51	0.1	0.084	0.72			
-4		0.20	0.50		0.001	.0138	0.36	0.01	.097	0.55	0.1	0.433	1.33			
-5		1.4	0.60		0.001	.0042	0.35	0.02	.036	0.42	0.1	0.201	0.77			
-6		0.2	0.001		0.0000002	0.00000051	369.	0.000002	0.0000051	370.	0.00002	0.000509	370.	0.002	0.0404	411
-7		2.0	0.01		0.000005	0.00000141	25.0	0.00005	0.0000141	25.0	0.0005	0.00140	25.1	0.05	0.0878	35.8
-8		0.05	0.10		0.00002	0.0029	3.45	0.0002	0.0202	3.83	0.04	0.132	6.18			
-9		0.05	0.05		0.0005	0.0451	9.16	0.005	0.244	17.7	0.05	0.802	41.8			
I-1	100	0.02	0.15	0.16	0.00002	.0029	3.50	0.0002	.027	3.80	0.002	0.192	5.77			
-2		0.10	0.30		0.0001	.0060	1.54	0.001	.053	1.78	0.01	0.318	3.14			
-3		5.0	0.40		0.001	.0013	0.95	0.01	.012	0.99	0.1	0.099	1.25			
-4		0.20	0.50		0.002	.015	0.70	0.02	.117	0.94	0.2	0.578	2.03			
-5		1.4	0.60		0.002	.0044	0.68	0.02	.040	0.76	0.2	0.255	1.23			
-6		0.2	0.001		0.0000002	0.00000257	659	0.000002	0.0000257	660.	0.00002	0.000257	660.	0.002	0.0235	694.
-7		2.0	0.01		0.000005	0.00000697	510	0.00005	0.0000697	51.1	0.0005	0.000695	51.1	0.05	0.0569	55.5
-8		0.05	0.10		0.00002	0.00121	6.63	0.0002	0.0117	6.86	0.002	0.0952	8.66			
-9		0.05	0.05		0.0005	0.0280	15.1	0.005	0.194	22.3	0.05	0.866	51.5			

Table A-2
Intercepts and slopes in the functional relation between B_p and h_d^* as functions of h_s^*, h_1^*, and n_s

Intercept

$n_s \backslash h_s^*$	.005	.01	.02	.04	.08	.16
.001	18.7	56.0	119.6	272.1	368.5	659.0
.01	1.28	3.45	7.2	16.2	24.8	51.0
.05	.24	.96	2.31	5.55	7.4	14.1
.1	.13	.46	1.13	2.57	3.39	6.65
.15	.094	.273	.63	1.51	1.78	3.47
.3	.036	.103	.248	.591	.766	1.505
.4	.018	.055	.123	.263	.471	.950
.5	.015	.036	.091	.219	.326	.665
.6	.012	.041	.098	.218	.338	.675

Slope

$n_s \backslash h_s^*$	.005	.01	.02	.04	.08	.16	Ref.Values [1]
.001	1640	1670	1690	1410	1030	1490	1670
.01	123	130	130	123	100	78.1	126
.05	30.3	40	42.7	40	43.5	44.1	42.1
.1	13.7	18.9	20.8	20.8	20.8	20.8	20.8
.15	6.64	8.54	10.2	11.8	11.5	12.16	11.82
.3	2.85	3.93	4.57	5.09	5.01	5.14	5.08
.4	2.40	2.86	2.92	3.02	3.01	3.02	3.02
.5	1.32	1.87	2.11	2.34	2.28	2.35	2.32
.6	1.51	1.99	2.09	2.21	2.22	2.18	2.20

[1] Except for n_s = 0.001 and 0.01 the reference value is the average of values for h_s^* = 0.04, 0.08, and 0.16. It is used to reduce all values to a dimensionless term in the range zero to one.

Table A-3
Values of recession parameter, B_p, obtained using the Smith-Hebbert model and using equation (A-1)

Porosity n_s	Depth h_s^*	Head h_d^*	B_p (eq.A-1)	B_p S/H 1/	% error
			Recession Parameter		
0.001	0.005	0.010	25.3	35.0	-27.6
0.010	0.005	0.010	1.93	2.52	-23.2
0.050	0.005	0.010	0.552	0.540	2.24
0.100	0.005	0.010	0.267	0.267	-0.051
0.150	0.005	0.010	0.164	0.160	2.47
0.300	0.005	0.010	0.063	0.065	-2.72
0.400	0.005	0.010	0.041	0.043	-5.64
0.500	0.005	0.010	0.028	0.029	-2.88
0.001	0.010	0.010	63.5	73.0	-13.1
0.010	0.010	0.010	4.88	4.75	2.72
0.050	0.010	0.010	1.29	1.35	-4.12
0.100	0.010	0.010	0.630	0.650	-3.04
0.150	0.010	0.010	0.389	0.360	7.97
0.300	0.010	0.010	0.148	0.142	4.38
0.400	0.010	0.010	0.093	0.082	12.98
0.500	0.010	0.010	0.062	0.055	12.11
0.001	0.020	0.010	137	137	0.500
0.010	0.020	0.010	10.6	8.60	23.0
0.050	0.020	0.010	2.72	2.70	0.548
0.100	0.020	0.010	1.33	1.29	2.82
0.150	0.020	0.010	0.820	0.735	11.5
0.300	0.020	0.010	0.311	0.295	5.37
0.400	0.020	0.010	0.192	0.152	26.2
0.500	0.020	0.010	0.125	0.112	11.6
0.001	0.040	0.010	280	286	-1.95
0.010	0.040	0.010	21.7	17.6	23.1
0.050	0.040	0.010	5.45	6.10	-10.7
0.100	0.040	0.010	2.67	2.78	-4.04
0.300	0.040	0.010	0.624	0.645	-3.29
0.400	0.040	0.010	0.382	0.295	29.4
0.500	0.040	0.010	0.245	0.243	0.943
0.001	0.080	0.010	351	376	-6.64
0.010	0.080	0.010	27.1	26.2	3.50
0.050	0.080	0.010	6.79	7.50	-9.44
0.100	0.080	0.010	3.33	3.62	-8.09
0.300	0.080	0.010	0.778	0.815	-4.59
0.400	0.080	0.010	0.475	0.502	-5.34
0.500	0.080	0.010	0.304	0.350	-13.1
0.001	0.160	0.010	676	674	0.250
0.010	0.160	0.010	52.3	51.8	0.948
0.050	0.160	0.010	12.98	8.60	50.97
0.100	0.160	0.010	6.37	6.86	-7.21
0.150	0.160	0.010	3.94	3.60	9.46
0.300	0.160	0.010	1.49	1.57	-5.32
0.400	0.160	0.010	0.905	0.980	-7.63
0.500	0.160	0.010	0.576	0.690	-16.5
0.001	0.005	0.030	47.5	67.6	-29.8
0.010	0.005	0.030	3.6	4.95	-27.3
0.050	0.005	0.030	1.11	1.14	-2.35
0.100	0.005	0.030	0.534	0.540	-1.09
0.150	0.005	0.030	0.327	0.292	11.9
0.300	0.005	0.030	0.128	0.122	4.54
0.400	0.005	0.030	0.084	0.092	-8.7
0.500	0.005	0.030	0.061	0.055	10.3
0.001	0.010	0.030	90.6	106	-14.6
0.010	0.010	0.030	6.92	7.35	-5.86
0.050	0.010	0.030	1.98	2.16	-8.22
0.100	0.010	0.030	0.958	1.12	-14.5
0.150	0.010	0.030	0.588	0.550	6.98
0.300	0.010	0.030	0.227	0.220	3.22
0.400	0.010	0.030	0.146	0.140	4.21
0.500	0.010	0.030	0.101	0.092	10.3

Table A-3--Continued
Values of recession parameter, B_p, obtained using the Smith-Hebbert model and using equation (A-1)

			Recession Parameter		
Porosity	Depth	Head	B_p	B_p	% error
n_s	h_s^*	h_d^*	(eq.A-1)	S/H [1]	
0.001	0.020	0.030	169	171	-0.763
0.010	0.020	0.030	13.0	11.2	16.2
0.050	0.020	0.030	3.53	3.54	-0.323
0.100	0.020	0.030	1.71	1.75	-2.06
0.150	0.020	0.030	1.06	0.940	12.3
0.300	0.020	0.030	0.404	0.385	4.96
0.400	0.020	0.030	0.255	0.210	21.3
0.500	0.020	0.030	0.172	0.155	11.0
0.001	0.040	0.030	314	315	-0.199
0.010	0.040	0.030	24.2	20.1	20.3
0.050	0.040	0.030	6.3	6.80	-7.37
0.100	0.040	0.030	3.07	3.23	-4.87
0.300	0.040	0.030	0.721	0.745	-3.19
0.400	0.040	0.030	0.448	0.355	26.1
0.500	0.040	0.030	0.294	0.290	1.55
0.001	0.080	0.030	385	400	-3.92
0.010	0.080	0.030	29.6	28.7	3.27
0.050	0.080	0.030	7.64	8.20	-6.8
0.100	0.080	0.030	3.73	4.05	-7.85
0.300	0.080	0.030	0.875	0.915	-4.37
0.400	0.080	0.030	0.541	0.561	-3.57
0.500	0.080	0.030	0.354	0.395	-10.5
0.001	0.160	0.030	709.4	704.4	0.715
0.010	0.160	0.030	54.8	53.3	2.74
0.050	0.160	0.030	13.8	15.4	-10.2
0.100	0.160	0.030	6.77	7.25	-6.61
0.150	0.160	0.030	4.19	3.81	9.9
0.300	0.160	0.030	1.58	1.67	-5.16
0.400	0.160	0.030	0.971	1.02	-4.8
0.500	0.160	0.030	0.626	0.735	-14.9
0.001	0.005	0.050	69.6	101	-30.8
0.010	0.005	0.050	5.26	7.43	-29.2
0.050	0.005	0.050	1.67	1.74	-3.77
0.100	0.005	0.050	0.801	0.816	-1.8
0.500	0.005	0.050	0.093	0.080	16.4
0.001	0.010	0.050	118	139	-15.4
0.010	0.010	0.050	8.96	10.0	-10.4
0.050	0.010	0.050	2.67	2.97	-10.1
0.100	0.010	0.050	1.29	1.41	-8.82
0.150	0.010	0.050	0.788	0.700	12.6
0.300	0.010	0.050	0.306	0.300	1.98
0.400	0.010	0.050	0.199	0.198	0.583
0.500	0.010	0.050	0.141	0.130	8.70
0.001	0.020	0.050	201	204	-1.46
0.010	0.020	0.050	15.4	13.8	11.6
0.050	0.020	0.050	4.34	4.47	-2.86
0.100	0.020	0.050	2.10	2.12	-0.875
0.300	0.020	0.050	0.497	0.477	4.26
0.400	0.020	0.050	0.318	0.270	17.7
0.500	0.020	0.050	0.219	0.195	12.4
0.001	0.040	0.050	348	343	1.47
0.010	0.040	0.050	26.7	22.5	18.7
0.050	0.040	0.050	7.15	7.60	-5.94
0.100	0.040	0.050	3.48	3.62	-3.94
0.300	0.040	0.050	0.819	0.845	-3.12
0.400	0.040	0.050	0.513	0.415	23.7
0.500	0.040	0.050	0.344	0.338	1.69
0.001	0.080	0.050	418	420	-0.368
0.010	0.080	0.050	32.2	31.2	3.07
0.050	0.080	0.050	8.49	9.40	-9.65
0.100	0.080	0.050	4.14	4.42	-6.40
0.300	0.080	0.050	0.972	1.02	-4.19

Table A-3--Continued
Values of recession parameter, B_p, obtained using the Smith-Hebbert model and using equation (A-1)

		Recession Parameter			
Porosity	Depth	Head	B_p	B_p	% error
n_s	h_s^*	h_d^*	(eq.A-1)	S/H 1/	
0.400	0.080	0.050	0.607	0.598	1.47
0.500	0.080	0.050	0.403	0.440	-8.47
0.001	0.160	0.050	743	733	1.39
0.010	0.160	0.050	57.3	54.9	4.37
0.050	0.160	0.050	14.7	16.3	-9.91
0.100	0.160	0.050	7.18	7.67	-6.45
0.150	0.160	0.050	4.43	4.10	8.14
0.300	0.160	0.050	1.68	1.76	-4.47
0.400	0.160	0.050	1.04	1.10	-5.74
0.500	0.160	0.050	0.675	0.785	-14.0
0.001	0.005	0.070	91.8	133	-31.2
0.010	0.005	0.070	6.93	9.70	-28.61
0.050	0.005	0.070	2.24	2.33	-4.06
0.100	0.005	0.070	1.07	1.08	-1.06
0.001	0.010	0.070	145	167	-13.4
0.010	0.010	0.070	11	12.6	-13
0.050	0.010	0.070	3.36	3.76	-10.7
0.100	0.010	0.070	1.61	1.69	-4.53
0.300	0.010	0.070	0.385	0.380	1.26
0.500	0.010	0.070	0.181	0.165	9.78
0.001	0.020	0.070	234	238	-1.75
0.010	0.020	0.070	17.8	16.5	7.98
0.050	0.020	0.070	5.16	5.30	-2.72
0.100	0.020	0.070	2.49	2.54	-2.01
0.500	0.020	0.070	0.266	0.240	10.9
0.001	0.040	0.070	381	371	2.86
0.010	0.040	0.070	29.2	25.0	16.9
0.050	0.040	0.070	8	8.60	-6.99
0.100	0.040	0.070	3.88	4.06	-4.37
0.300	0.040	0.070	0.916	0.949	-3.47
0.400	0.040	0.070	0.579	0.475	21.9
0.500	0.040	0.070	0.393	0.385	2.05
0.001	0.080	0.070	452	440	2.59
0.010	0.080	0.070	34.7	36.0	-3.67
0.050	0.080	0.070	9.34	10.1	-7.5
0.100	0.080	0.070	4.54	4.88	-6.93
0.300	0.080	0.070	1.07	1.12	-4.04
0.400	0.080	0.070	0.673	0.680	-1.09
0.500	0.080	0.070	0.452	0.485	-6.82
0.001	0.160	0.070	777	763	1.82
0.010	0.160	0.070	59.8	56.5	5.88
0.050	0.160	0.070	15.5	16.7	-6.98
0.100	0.160	0.070	7.58	8.10	-6.42
0.150	0.160	0.070	4.68	4.30	8.85
0.300	0.160	0.070	1.78	1.86	-4.37
0.400	0.160	0.070	1.10	1.17	-5.76
0.500	0.160	0.070	0.724	0.815	-11.2

Average Error is 8.5%

1/ S.H. stands for values obtained using plots obtained from use of the Smith-Hebbert model.
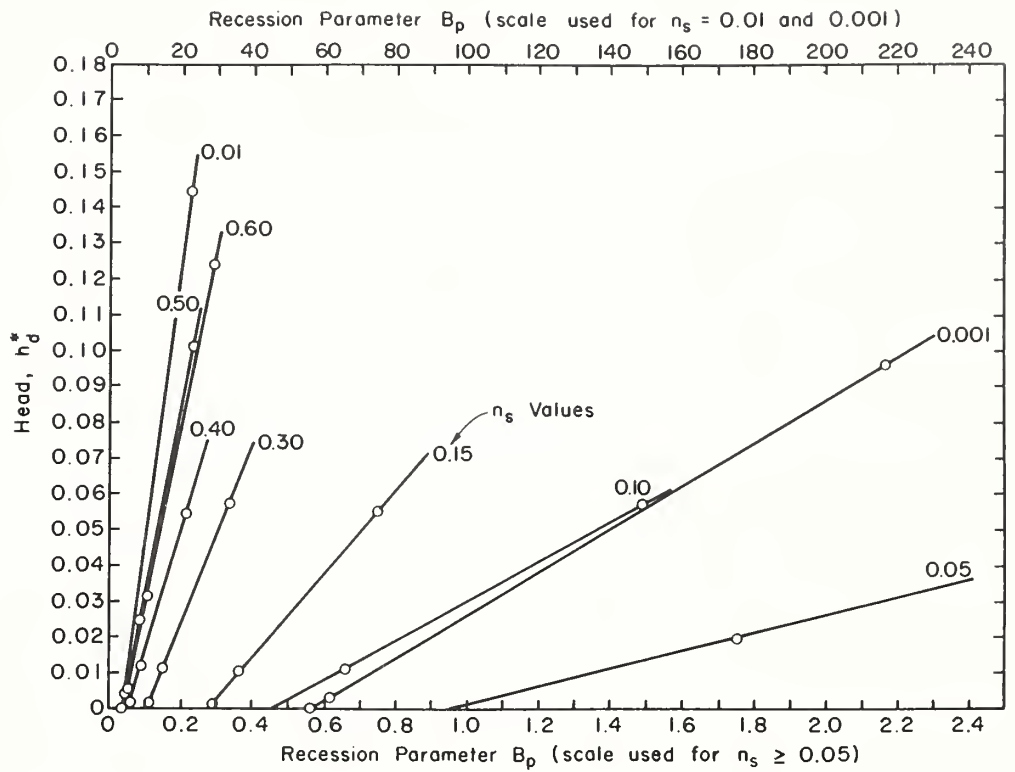
Figure A-1
Values of B_p as a function of dimensionless head h_d*; $h_s* = 0.01$; n_s values are as noted.
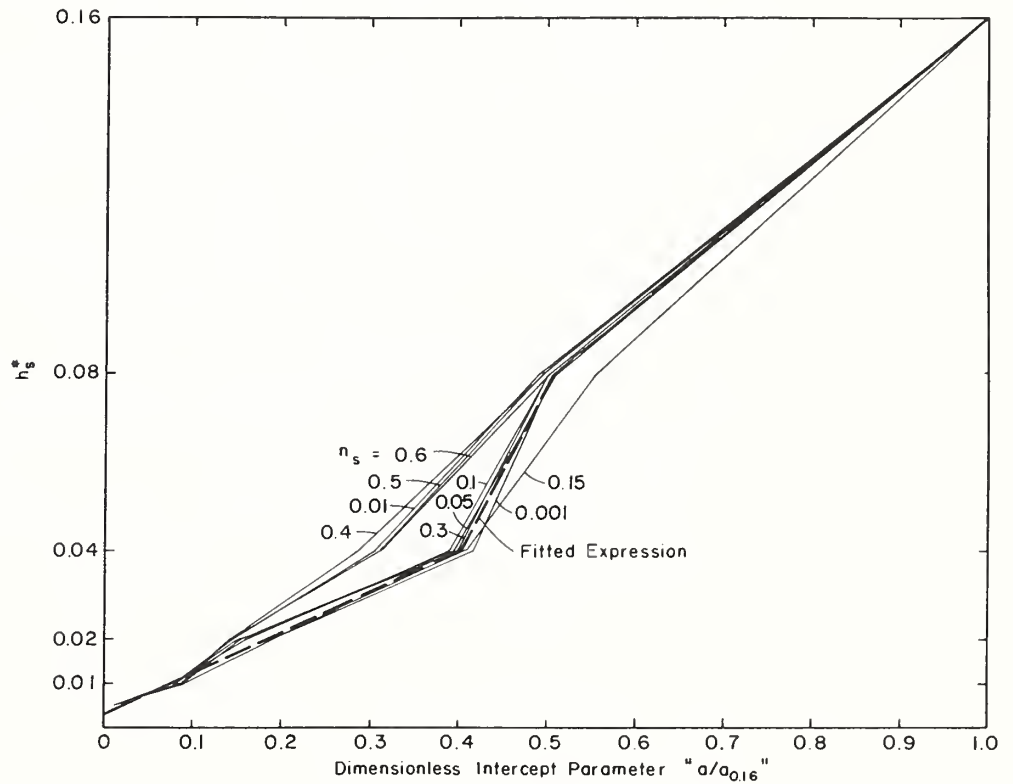
Figure A-2
Plot of dimensionless intercept parameter $a/a_{0.16}$ vs. h_s*.
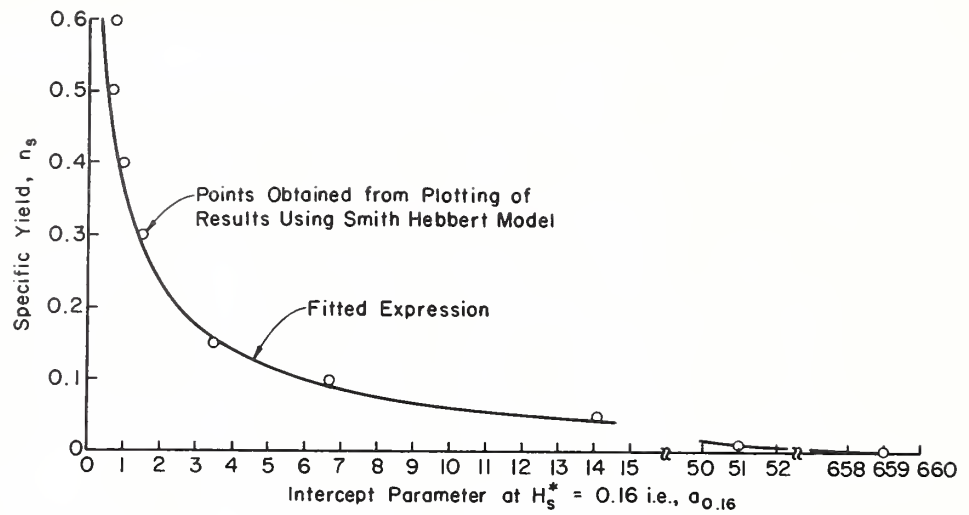
Figure A-3
Plot of the intercept parameter, $a_{0.16}$, at $h_s{}^* = 0.16$ vs. specific yield, n_s.
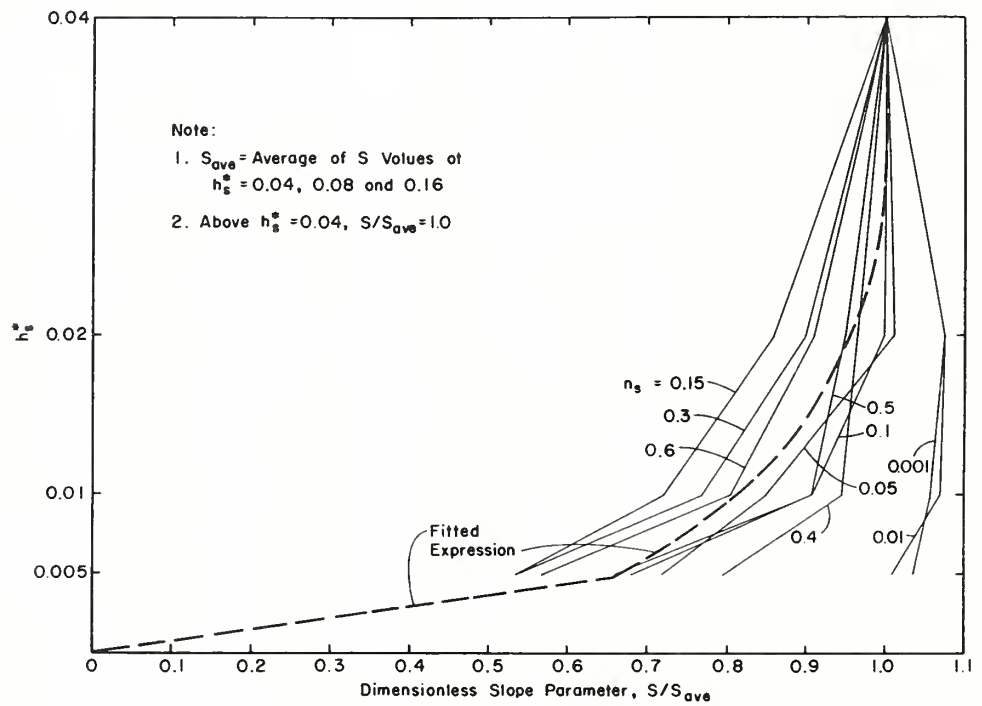
Figure A-4
Plot of dimensionless slope parameter S/S_{ave} vs. $h_s{}^*$ for a range of effective porosity or specific yield.
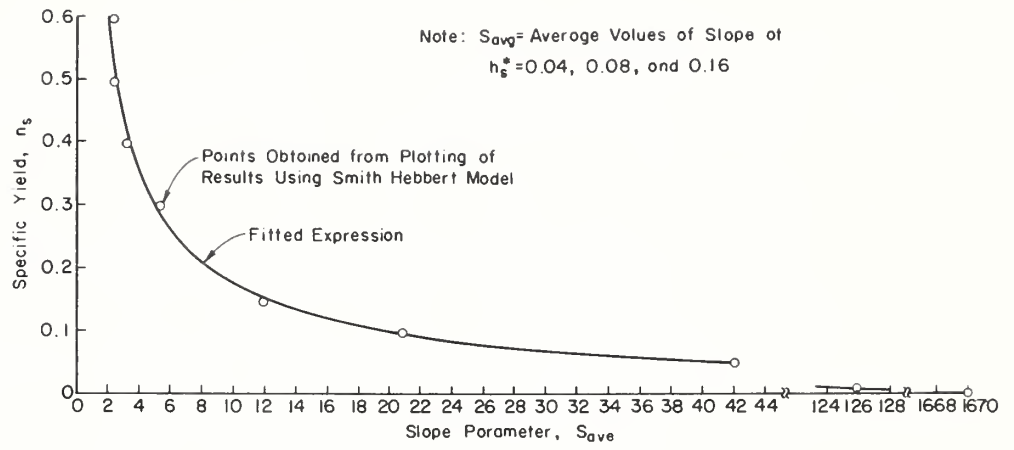
Figure A-5
Plot of slope parameter, S_{ave}, vs. specific yield, n_s.

APPENDIX B -- RELATION BETWEEN RECESSION RATES FOR PARALLEL AND CONVERGING FLOW

The rate of decline in the water table at the watershed divide, B_c, in regions of converging flow is different from that of parallel flow, B_p. However it was assumed that it could be related to that of parallel flow, i.e.:

$$B_c = R_B B_p \qquad\qquad\qquad (B-1)$$

in which R_B is a multiplying factor. A series of experiments with the Smith-Hebbert model were used to develop the functional value of R_B.

The flow domain used to describe the system included the circular width of the converging section at the outlet, $w = \theta r_o$; the length of the flow path, $L = R - r_o$; the angle of convergence, θ; the depth of flow at the channel, h_s^*; and the head on the aquifer at the divide, h_d^*. The range of parameter values used in the analysis was selected to encompass most real situations. Four values of length to width ratio, L/w, were selected; they were 5, 10, 25 and 100. For each value of L/w values of 0°, 2°, 4°, 6°, 10°, 20°, 30°, 45°, 60°, 90°, 135°, and 180° were selected for the angle of convergence, θ. For each of these 48 combinations of L/w and θ, 12 different values of h_d^* between 0.003 and 0.02 were selected to determine if the thickness of the aquifer would be significant in the ratio, R_B. Four different values of h_s^* were used.

The Smith-Hebbert model was run using these combinations, and the parameter B_c was evaluated from rate of change in flow rate. The ratio, R_B, of B_c vs. the B_p value for any given combination of L/w, θ, and h_d was calculated. The values of B_c, B_p and their ratio, R_B, are shown in Table B-1. Plots of B_c vs. B_p for any combination of L/w and θ for all h_d show a straight line with 0, 0 intercepts. This is verified by the ratio, R_B, which does not appear to be a function of h_d, but fluctuates randomly about the mean value for a given combination of L/w and θ by less than about 0.5 percent.

Muskat and Wyckoff (1937) in their analyses of radial flow toward a sink used the ratio of the radii to compare responses of different wells. This same concept was used in an attempt to reduce the families of curves represented by the data in Table B-1 to a common base. We have already shown that it is possible to use the value of R_B averaged over all h_d to reduce the amount of data presented in Table B-1. The angle, θ; width, w; and length L from Table B-1 were used to calculate values of r_o/R where r_o is the radial distance to the groundwater entry point into the channel and R is the radial distance to the watershed divide (see Figure 4). Values of r_o and R are calculated as

$$r_o = w/[2.0 \sin (\theta/2)] \quad \theta \text{ in degrees} \qquad\qquad (B-2)$$

$$R = r_o + L \qquad\qquad\qquad (B-3)$$

Values from Table B-1 of r_o/R were plotted against R_B. This plot is shown as Figure B-1. An expression of the form

$$R_B = a + (1-a)(r_o/R)^b \qquad\qquad\qquad (B-3)$$

was fitted to the data in Figure B-1. Optimal values of the parameters yield the expression

$$R_B = 0.108 - 0.892 (r_o/R)^{0.477} \qquad\qquad\qquad (B-4)$$

The expression is shown in figure B-1. In Table B-2 Values of R_B calculated using equation (B-4) are shown along with values taken from the experimental data in Table B-1 for the 48 combinations of L/w and θ. The percent error ranges from 0.1 to 14.2 percent, with an average absolute error of 2.5 percent.

Table B-1
Values of B_p and B_c the ratio, R_B, of B_c/B_p obtained with the Smith-Hebbert model

$d(\ln Q^*)/dt^* \times 10^3$

Length L (meters)	Width w (meters)	L/w	Head (hd) meters	B_p 0°	B_c 2°	R_B 2°/0°	B_c 4°	R_B 4°/0°	B_c 6°	R_B 6°/0°	B_c 10°	R_B 10°/0°	B_c 20°	R_B 20°/0°	B_c 30°	R_B 30°/0°	B_c 45°	R_B 45°/0°	B_c 60°	R_B 60°/0°	B_c 90°	R_B 90°/0°	B_c 135°	R_B 135°/0°	B_c 180°	R_B 180°/0°
304.8	3.05	100	1.52	-.1000	-.0530	.530	-.0440	.440	-.0390	.390	-.0326	.326	-.0269	.269	-.0242	.242	-.0223	.223	-.0215	.215	-.0197	.197	-.0189	.189	-.0183	.183
			1.78	-.1040	-.0570	.548	-.0460	.442	-.0400	.385	-.0343	.330	-.0284	.273	-.0255	.245	-.0237	.228	-.0223	.214	-.0208	.200	-.0200	.192	-.0194	.187
			2.03	-.1100	-.0600	.545	-.0490	.445	-.0410	.373	-.0361	.328	-.0300	.273	-.0269	.245	-.0250	.227	-.0236	.215	-.0221	.201	-.0210	.191	-.0205	.186
			2.29	-.1150	-.0630	.548	-.0510	.443	-.0440	.383	-.0379	.330	-.0315	.274	-.0283	.246	-.0261	.227	-.0248	.216	-.0232	.202	-.0221	.192	-.0214	.186
			2.54	-.1200	-.0660	.550	-.0525	.438	-.0470	.392	-.0390	.325	-.0330	.275	-.0299	.249	-.0274	.228	-.0260	.217	-.0243	.206	-.0231	.193	-.0223	.186
			2.79	-.1230	-.0700	.569	-.0550	.447	-.0490	.398	-.0411	.334	-.0343	.279	-.0310	.252	-.0287	.233	-.0272	.221	-.0253	.206	-.0240	.195	-.0232	.189
			3.05	-.1300	-.0730	.562	-.0580	.446	-.0510	.392	-.0433	.333	-.0360	.277	-.0326	.251	-.0300	.231	-.0284	.218	-.0266	.205	-.0252	.194	-.0243	.187
			3.30	-.1370	-.0770	.563	-.0605	.442	-.0530	.387	-.0452	.330	-.0374	.273	-.0341	.249	-.0313	.228	-.0297	.217	-.0276	.205	-.0263	.192	-.0254	.185
			3.56	-.1410	-.0790	.560	-.0630	.447	-.0550	.390	-.0472	.335	-.0392	.278	-.0355	.252	-.0327	.232	-.0307	.218	-.0287	.204	-.0272	.193	-.0263	.187
			3.81	-.1460	-.0805	.551	-.0660	.452	-.0570	.390	-.0489	.335	-.0405	.277	-.0368	.252	-.0340	.233	-.0320	.219	-.0299	.205	-.0283	.194	-.0273	.187
			4.06	-.1500	-.0820	.547	-.0680	.453	-.0590	.393	-.0507	.338	-.0420	.280	-.0382	.255	-.0352	.235	-.0330	.220	-.0311	.207	-.0294	.196	-.0283	.189
			4.32	-.1600	-.0870	.544	-.0710	.444	-.0610	.381	-.0531	.332	-.0439	.274	-.0399	.249	-.0364	.228	-.0342	.214	-.0323	.202	-.0304	.190	-.0293	.185
			4.57	-.1640	-.0900	.549	-.0730	.445	-.0630	.384	-.0545	.332	-.0453	.276	-.0411	.251	-.0379	.228	-.0355	.216	-.0333	.203	-.0314	.196	-.0303	.186
			Ave			.551		.445		.388		.331		.275		.249		.230		.217		.203		.193		.186
152.4	6.09	25	0.51	-.2200	-.1720	.782	-.1490	.677	-.1370	.623	-.1120	.509	-.0900	.409	-.0800	.364	-.0720	.327	-.0650	.295	-.0600	.273	-.0540	.245	-.0520	.236
			0.64	-.2310	-.1800	.779	-.1560	.675	-.1420	.615	-.1160	.502	-.0960	.416	-.0850	.368	-.0750	.325	-.0680	.294	-.0630	.273	-.0570	.247	-.0540	.234
			0.76	-.2450	-.1910	.780	-.1650	.673	-.1500	.612	-.1220	.498	-.1000	.408	-.0880	.358	-.0790	.322	-.0720	.294	-.0660	.269	-.0610	.249	-.0570	.233
			0.89	-.2550	-.2010	.788	-.1720	.675	-.1540	.604	-.1290	.506	-.1050	.412	-.0920	.361	-.0830	.325	-.0750	.298	-.0690	.271	-.0630	.247	-.0600	.235
			1.02	-.2650	-.2050	.774	-.1800	.679	-.1620	.611	-.1350	.509	-.1090	.411	-.0970	.366	-.0860	.325	-.0790	.302	-.0720	.272	-.0660	.249	-.0630	.238
			1.14	-.2750	-.2160	.785	-.1860	.676	-.1680	.611	-.1400	.509	-.1140	.415	-.1000	.364	-.0890	.328	-.0830	.300	-.0750	.273	-.0690	.251	-.0650	.236
			1.27	-.2870	-.2240	.780	-.1920	.669	-.1730	.603	-.1460	.510	-.1180	.411	-.1050	.366	-.0940	.323	-.0860	.300	-.0780	.272	-.0720	.251	-.0680	.237
			1.52	-.3100	-.2420	.781	-.2070	.668	-.1830	.590	-.1580	.510	-.1270	.410	-.1140	.368	-.1000	.323	-.0930	.296	-.0840	.269	-.0770	.248	-.0730	.235
			1.78	-.3380	-.2600	.769	-.2240	.663	-.2000	.592	-.1700	.503	-.1360	.402	-.1220	.361	-.1090	.323	-.1000	.300	-.0910	.269	-.0840	.249	-.0780	.231
			2.03	-.3530	-.2750	.779	-.2390	.677	-.2140	.606	-.1800	.510	-.1450	.411	-.1290	.365	-.1160	.329	-.1070	.303	-.0970	.275	-.0890	.252	-.0840	.238
			2.29	-.3800	-.2950	.776	-.2550	.671	-.2250	.592	-.1930	.508	-.1550	.408	-.1380	.363	-.1230	.324	-.1140	.300	-.1030	.271	-.0950	.250	-.0890	.234
			2.59	-.4220	-.3250	.770	-.2770	.657	-.2480	.588	-.2060	.488	-.1660	.395	-.1470	.348	-.1300	.308	-.1230	.291	-.1110	.261	-.1020	.242	-.0960	.227
			Ave			.779		.672		.604		.505		.409		.363		.324		.297		.271		.248		.235
609.5	60.9	10	3.05	-.4400	-.3900	.875	-.3600	.818	-.3350	.761	-.2900	.659	-.2400	.545	-.2100	.477	-.1800	.409	-.1700	.386	-.1470	.334	-.1310	.298	-.1200	.273
			3.56	-.4700	-.4100	.872	-.3800	.809	-.3600	.766	-.3050	.649	-.2550	.543	-.2200	.468	-.1950	.414	-.1800	.383	-.1580	.336	-.1390	.296	-.1290	.274
			4.06	-.4950	-.4400	.889	-.3990	.806	-.3700	.747	-.3250	.657	-.2700	.545	-.2300	.465	-.2050	.414	-.1900	.384	-.1660	.335	-.1470	.297	-.1360	.275
			4.57	-.5200	-.4600	.885	-.4250	.817	-.3900	.750	-.3400	.654	-.2800	.538	-.2500	.481	-.2200	.423	-.1990	.383	-.1750	.337	-.1550	.298	-.1440	.277
			5.08	-.5500	-.4830	.878	-.4500	.818	-.4100	.745	-.3520	.640	-.2980	.542	-.2600	.473	-.2300	.418	-.2100	.382	-.1840	.335	-.1630	.296	-.1500	.273
			5.59	-.5700	-.5000	.877	-.4620	.811	-.4300	.754	-.3700	.649	-.3120	.547	-.2750	.482	-.2400	.421	-.2200	.386	-.1940	.340	-.1720	.302	-.1580	.277
			6.10	-.5900	-.5200	.881	-.4820	.817	-.4510	.764	-.3850	.653	-.3200	.542	-.2800	.475	-.2500	.423	-.2280	.386	-.2000	.339	-.1780	.302	-.1670	.283
			6.60	-.6200	-.5500	.887	-.5000	.806	-.4700	.758	-.4000	.645	-.3400	.548	-.3000	.484	-.2600	.419	-.2390	.385	-.2110	.340	-.1860	.300	-.1750	.282
			7.11	-.6500	-.5800	.892	-.5240	.809	-.4950	.762	-.4200	.646	-.3500	.538	-.3100	.477	-.2750	.423	-.2480	.382	-.2210	.340	-.1960	.302	-.1800	.277
			7.62	-.6800	-.6000	.882	-.5500	.816	-.5120	.753	-.4400	.647	-.3650	.537	-.3250	.478	-.2900	.426	-.2590	.381	-.2300	.339	-.2050	.301	-.1890	.278
			8.64	-.7350	-.6500	.884	-.6000	.813	-.5600	.762	-.4800	.653	-.4000	.544	-.3450	.469	-.3100	.421	-.2820	.384	-.2500	.340	-.2210	.301	-.2050	.279
			9.65	-.8000	-.7100	.888	-.6500	.812	-.6000	.756	-.5250	.656	-.4300	.538	-.3750	.469	-.3400	.425	-.3100	.388	-.2690	.336	-.2370	.296	-.2220	.278
			Ave			.883		.812		.756		.651		.542		.475		.420		.384		.337		.299		.277
76.2	15.2	5	0.25	-.6400	-.6000	.938	-.5700	.891	-.5400	.844	-.5000	.781	-.4300	.672	-.3800	.594	-.3400	.531	-.3130	.489	-.2750	.430	-.2450	.383	-.2250	.352
			0.36	-.6700	-.6300	.940	-.6000	.896	-.5700	.851	-.5200	.776	-.4500	.672	-.4000	.597	-.3600	.537	-.3300	.493	-.2900	.439	-.2600	.388	-.2400	.358
			0.46	-.7000	-.6600	.943	-.6300	.900	-.6000	.857	-.5500	.786	-.4800	.686	-.4200	.600	-.3800	.543	-.3470	.496	-.3070	.445	-.2740	.391	-.2520	.360
			0.56	-.7300	-.6900	.945	-.6600	.904	-.6300	.863	-.5700	.781	-.5000	.685	-.4400	.603	-.4000	.548	-.3650	.500	-.3250	.436	-.2880	.395	-.2660	.364
			0.66	-.7800	-.7300	.936	-.7000	.897	-.6600	.846	-.6100	.782	-.5200	.667	-.4700	.603	-.4200	.543	-.3830	.491	-.3400	.441	-.3020	.387	-.2800	.364
			0.76	-.8400	-.7900	.940	-.7600	.905	-.7200	.857	-.6600	.786	-.5700	.679	-.4900	.607	-.4400	.548	-.4020	.501	-.3570	.446	-.3180	.393	-.2940	.359
			0.86	-.8800	-.8300	.943	-.7900	.898	-.7500	.852	-.6900	.784	-.6000	.682	-.5100	.602	-.4600	.545	-.4210	.499	-.3750	.443	-.3320	.395	-.3070	.363
			0.97	-.9300	-.8700	.935	-.8300	.892	-.7900	.849	-.7300	.785	-.6300	.677	-.5300	.592	-.4800	.538	-.4390	.492	-.3900	.435	-.3450	.392	-.3200	.365
			1.07	-.9800	-.9300	.949	-.8800	.898	-.8300	.847	-.7700	.786	-.6600	.673	-.5600	.585	-.5000	.531	-.4580	.487	-.4050	.431	-.3580	.385	-.3340	.364
			1.17	-1.060	-1.000	.943	-.9500	.896	-.9000	.849	-.8200	.774	-.7100	.670	-.5800	.568	-.5200	.528	-.4770	.472	-.4220	.415	-.3730	.381	-.3440	.359
			1.27	-1.180	-1.012	.949	-1.05	.890	-1.000	.851	-.9100	.781	-.7800	.661	-.6200	.597	-.5600	.500	-.5000		-.4400		-.3860	.364	-.3600	.351
			1.37																							-.340
			Ave			.942		.897		.851		.781		.675		.597		.536		.492		.436		.387		.358

257

Table B-2
Values of R_B for different values of r_o/R

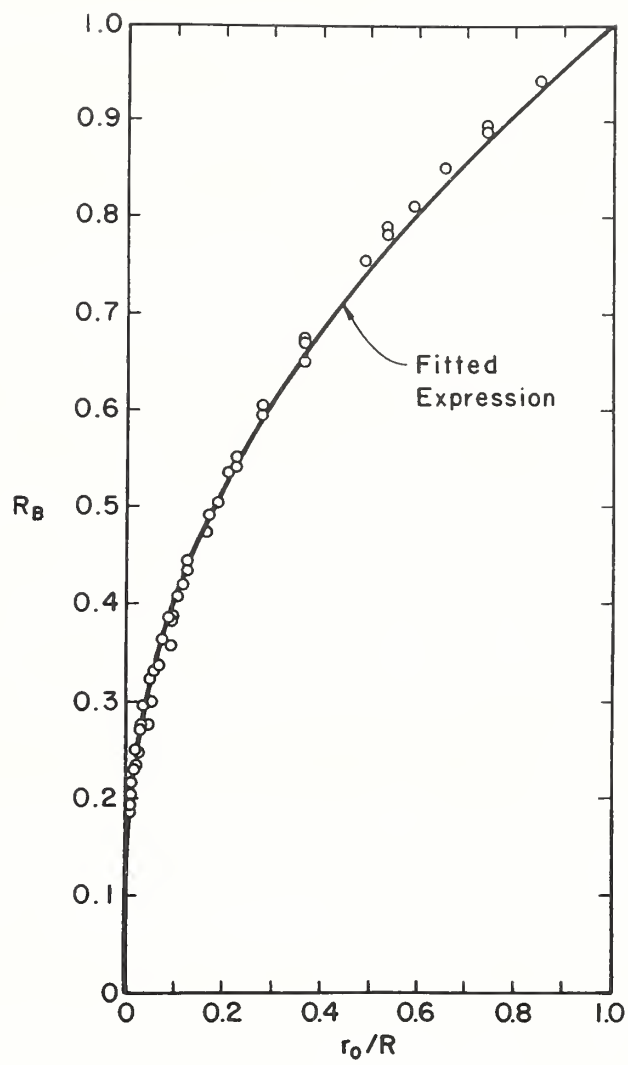| Length L (meters)	Width W (meters)	Convergence Angle (degrees)	r_o/R	R_B Ratio from Experimental Data	R_B Ratio from Regression Equation	R_B Percent Error
		0	- -	1.000	1.000	0.00
		2	0.2220	0.551	0.543	1.50
		4	0.1250	0.445	0.438	1.48
		6	0.0870	0.388	0.386	0.55
		10	0.0541	0.331	0.329	0.48
304.8	3.04	20	0.0279	0.275	0.269	2.07
		30	0.0189	0.249	0.242	2.86
		45	0.0129	0.230	0.219	4.57
		60	0.0099	0.217	0.207	4.76
		90	0.0070	0.203	0.191	5.83
		135	0.0054	0.193	0.179	7.38
		180	0.0050	0.186	0.179	3.90
		0	- -	1.000	1.000	0.00
		2	0.5338	0.779	0.769	1.28
		4	0.3640	0.672	0.659	2.00
		6	0.2762	0.604	0.591	2.22
		10	0.1865	0.505	0.508	-0.60
152.4	6.09	20	0.1032	0.409	0.410	-0.13
		30	0.0717	0.363	0.361	0.46
		45	0.0496	0.324	0.320	1.10
		60	0.0384	0.297	0.296	0.35
		90	0.0275	0.271	0.268	1.03
		135	0.0212	0.248	0.249	-0.58
		180	0.0196	0.235	0.244	-3.93
		0	- -	1.000	1.000	0.00
		2	0.7411	0.883	0.881	0.21
		4	0.5887	0.812	0.801	1.40
		6	0.4883	0.756	0.741	1.92
		10	0.3643	0.651	0.659	-1.20
609.6	60.9	20	0.2234	0.542	0.544	-0.38
		30	0.1618	0.475	0.482	-1.43
		45	0.1155	0.420	0.426	-1.47
		60	0.0908	0.384	0.392	-1.98
		90	0.0660	0.337	0.352	-4.31
		135	0.0513	0.299	0.324	-8.32
		180	0.0476	0.277	0.316	-14.18
		0	- -	1.000	1.000	0.00
		2	0.8514	0.942	0.934	0.84
		4	0.7414	0.897	0.881	1.75
		6	0.6563	0.851	0.838	1.58
		10	0.5345	0.781	0.769	1.48
		20	0.3654	0.675	0.660	2.28
76.2	15.24	30	0.2788	0.597	0.593	0.71
		45	0.2072	0.536	0.529	1.37
		60	0.1667	0.492	0.487	0.99
		90	0.1239	0.436	0.437	-0.24
		135	0.0976	0.387	0.402	-3.77
		180	0.0909	0.358	0.392	-9.43
				average absolute error		2.50

Figure B-1
R_B as a function of r_o/R.

MODELING TECHNIQUES FOR ASSESSING THE IMPACTS OF SEEPAGE ON GROUND WATER FLOW
NEAR EARTHEN-FILLED DAMS

J. W. Naney and C. R. Amerman

ABSTRACT

Some effects of seepage from earthen-filled dams are presented, qualitatively.
Theoretical development of subsurface flow models are discussed, as well as
some of the hydraulic constraints encountered in modeling subsurface flow in
the presence of seepage. Modeling techniques are identified which may be used
to quantify the impact of seepage on the flow of a watershed containing an
earthen-filled dam.

INTRODUCTION

Seepage, as implied herein, means water temporarily stored as suface water in
a reservoir environment and introduced to the ground water flow system by
means of flow through a porous medium, at some later time. Damaging effects
of such seepage may result from, or be worsened by, the construction of an
earthen-filled dam across a stream. Therefore, an estimate of seepage effects
should be made in any hydrologic model which predicts flows where such
structures either exist or may be built during the predictive period of the
model. The purpose of this paper is to identify the impacts of seepage on the
hydrologic system being modeled and document some modeling approaches
available for quantifying both the on-site and downstream effects of seepage.

BACKGROUND

The number of earthen-filled dams built under the Soil Conservation Service,
USDA assistance programs as of June 30, 1969, includes 5,282 multipurpose
structures, 9,751 flood water retarding structures, 23,400 diversions, 45,211
irrigation storage structures, and 1,700,353 farm ponds, including "dugouts"
(SCS 1970). The type and magnitude of problems associated with seepage are
varied and depend on local environmental factors such as geology, soil,
hydrology, geochemistry, meteorology, and biology.

The types of problems associated with seepage are shown qualitatively in
figure 1, and interrelations of land and water use problems associated with
seepage are shown in figure 2 (Yost and Naney 1975; Naney 1983). Studies of
water quality at six earthen-filled dam sites on Sugar Creek watershed in
southwestern Oklahoma showed mineralization of seepage waters to be nearly 5
times that of water above the dams (Yost and Naney, 1974).

Such increases in total dissolved solids (TDS), as well as increases in most
of the chemical constituents in seepage, indicate that salinity buildup
downstream from earthen dams may deteriorate both soil and water quality to a
degree that such resources become unusable, particularly in areas of semiarid
or arid climate.

THEORY OF MODEL DEVELOPMENT AND AVAILABLE MODELS

Bachmat et al. (1980) presented an inventory of 193 numerical models used to
solve ground water management problems. The models reported are categorized
as follows: flow (138), mass transport (39), heat transport (9), deformation
(8), and other (6). Nineteen are identified as stream-aquifer relation
models, and 9 are flow pattern models.

Geologist, USDA-ARS, Water Quality and Watershed Research Laboratory, Durant,
OK 74702, and Research Hydraulic Engineer, USDA-ARS, Peoria, IL 61604
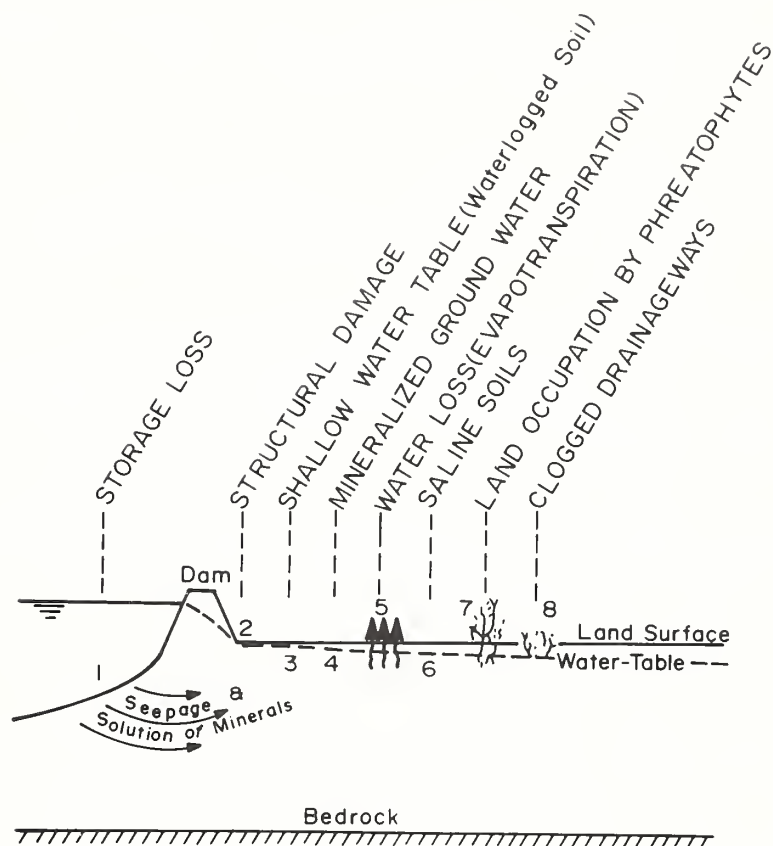
Figure 1
Some seepage problems associated with earthern-filled
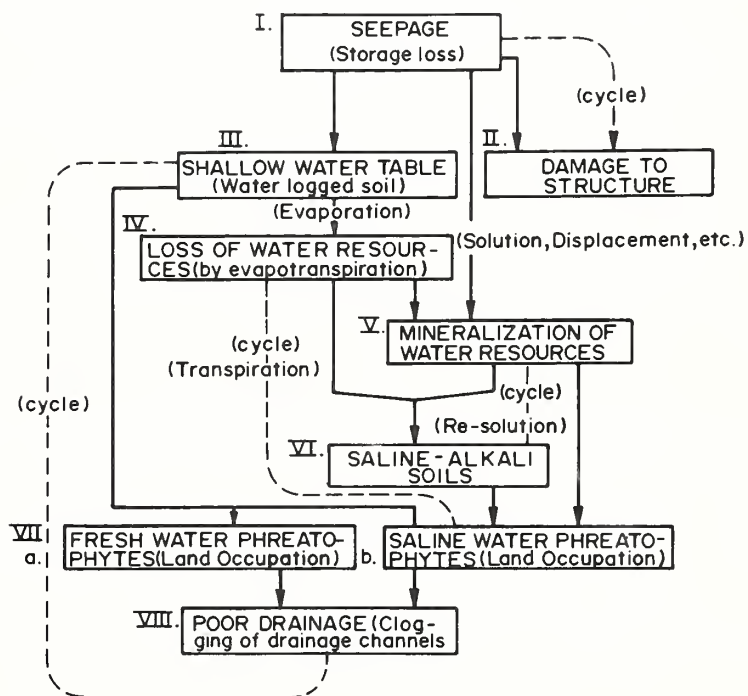dams. (From Yost and Naney 1975.)

Figure 2
Interrelated land and water conditions associated
with seepage. (From Yost and Naney 1975.)

261

Amerman and Naney (1982) traced the development of subsurface water flow theory from the discovery of Darcy's law (Taylor 1948), through the subsequent linking of Darcy's law with the continuity equation (Childs 1969). The Laplace equation for saturated flow which resulted:

$$\frac{\partial^2 H}{\partial x^2} + \frac{\partial^2 H}{\partial y^2} + \frac{\partial^2 H}{\partial z^2} = 0$$

where x, y, z = distances parallel to the major axes of the Cartesian

coordinate system;

and   H = hydraulic head;

is the foundation of much of the analyses of ground water flow. Numerical techniques, i.e., finite difference and finite elements, as well as analog methods are available for obtaining an approximate solution to the Laplace equation.

Equation (1) can be used to solve problems associated with unconfined aquifers, but several features of confined aquifers necessitated a different form of equation. Jacob (1950) derived the needed equation:

$$\frac{\partial^2 H}{\partial x^2} + \frac{\partial^2 H}{\partial y^2} + \frac{\partial^2 H}{\partial z^2} = \frac{\theta \gamma_o}{K} (\beta + \frac{\alpha}{\theta}) \frac{\partial H}{\partial t} \qquad (2)$$

where θ = porosity;

γ_o = speficic weight of water;

β = compressibility of water;

α = vertical compressibility of the media;

K = hydraulic conductivity;

and t = time.

The Dupuit-Forchheimer (1863) assumption of horizontal flow in which dH/dz is insignificant allows equation (2) to take on this form. Van Schilfgaarde (1974) presented the D-F assumptions and the restrictions of their applicability in the presence of a falling water table.

Amerman and Naney (1982) followed the development of equation (2) by Jacob (1950) through the form in which S/T appears; shown here as

$$\frac{\partial^2 H}{\partial x^2} + \frac{\partial^2 H}{\partial y^2} = \frac{S}{T} \frac{\partial H}{\partial t} \qquad (3)$$

where S = $\theta \gamma_o b (\beta + \alpha/\theta)$;

T = Kb;

and b = aquifer thickness.

The term S is called the coefficient of storage and is the volume of water released from storage by a unit decrease in head in a vertical column of unit cross-sectional area. The term T is called transmissivity or transmissibility.

Prickett and Lonnquist (1971), Trescott et al. (1976), and others added a volumetric flux term to equation (3), removed the assumption of isotropy, and oriented the coordinate axes parallel to the principal components of the transmissivity tensor, giving

$$\frac{\partial}{\partial x}(T_x \frac{\partial H}{\partial x}) + \frac{\partial}{\partial y}(T_y \frac{\partial H}{\partial y}) = S \frac{\partial H}{\partial t} + W \qquad (4)$$

where T_x and T_y = x and y components of transmissivity;

and $\qquad$ W = volumetric flux of recharge or withdrawal per unit

$\qquad$ surface area

At steady state flow, $\partial H/\partial t = 0$; and if $W = 0$ then equation (4) becomes a Laplace equation provided the coordinates are distorted to account for anisotropy (Childs 1969) and the solution methods previously discussed can be applied.

Prickett and Lonnquist (1971) and Trescott et al. (1976) developed two-dimensional finite difference models for equation (4); while Gupta et al (1975) presented a three-dimensional finite element model based on it. Numerous other models have been developed as well, as indicated earlier. The U. S. Geological Survey is active in the development of ground water models and recently summarized the status of several of these models, both operational and developmental (Appel and Bredehoeft 1976).

Four types of numerical solutions, each employing finite-difference techniques for solving the ground water flow equations listed above were described by Trescott et al. (1976). These are line successive over-relaxation, line successive over-relaxation plus two-dimensional correction, alternating direction implicit procedure, and strongly implicit procedure. The authors also compared numerical results of the four finite difference techniques.

Another solution to the ground water flow equation (4) is found in the finite difference technique used by Nelson (1962). Nelson used both over-relaxation and under-relaxation techniques, employing the Gauss-Seidel predictor-corrector method for a node-by-node solution of the difference equation beginning with an initial head estimate. The predictor-corrector technique is detailed by Remson et al. (1977) in which the authors made a comparison between exact analytical and finite difference solutions to the equation for ground water flow to a tile drain, assuming the D-F assumption to hold and the diameter of the drains to be negligibile. This procedure is also useful for the study of unconfined ground water flow between trenches (Hornberger et al. 1969) and for the study of the interaction of water between a stream and an unconfined aquifer (Hornberger et al. 1970).

Winter (1976) modeled two-dimensional porous media flow systems for which one or more lakes were included on the upper boundary. Later, he expanded the study to include three dimensions and solved a variation of the steady state form of equation (4) by finite differences (Winter 1978).

Hall (1976) defined three general methods for determining ground water inflow into large lakes, which when modified are also applicable to small bodies of water. They are 1) base-flow analysis of stream networks tributary to lakes, 2) use of analytical techniques for application of Darcy's law, derivation of flow nets, and the solution of appropriate differential equations, and 3) the average long-term water-balance method. Method 3), when expanded to include net inflow (Zektzer 1973), is applicable to small water bodies (Manson et al. 1968: Allred et al. 1971).

MODEL APPLICATION

Winter (1976) applied modeling techniques to lakes in a glacially deposited environment and used vertical strips to generate piezometric heads upgradient from, beneath, and downgradient from such lakes. He found the existence and position of the stagnation point -- i.e., the point of minimum head on the divide separating a zone of local flow from larger magnitude flows -- to be a major factor controlling both the occurrence and rate of seepage from these lakes. A barrier to water seeping from the lake into the ground water system is established when a stagnation point is present with head greater than the lake. An example of how the presence of a stagnation point beneath one lake in a two lake system affects lake seepage is shown in figure 3.

Winter (1976) also found the parameter K_h/K_v, ratio of horizontal to vertical hydraulic conductivity, often determines whether a lake loses water to the

ground water system or not. He found lakes on strata with ratio < 100 rarely lose water, whereas those with K_h/K_v >1000 often lose water. The presence or absence of seepage from lakes with intermediate ratios of 100 to 1000 usually was influenced by other factors.

Additionally, he investigated the effects of such factors as the height of water table in relation to the lake surface, ratio of the hydraulic conductivity of aquifers to that of surrounding till, position and size of aquifers, and lake depth, on the position and head of the stagnation point relative to lake level. Flow simulations for a variety of glacial deposit settings where a series of lakes were modeled along sloping terrain were also presented.

Naney (1974) adapted a model developed by Nelson (1962) to predict seepage flow and direction of flow from a Soil Conservation Service floodwater retarding structure on a sandy alluvium in the southern plains of the United States. He found an important feature of seepage to be its impact on the direction of flow near the lake, and downstream from the dam for several hundred feet (Naney et al. 1976). The changes in flow direction which may result in longer flow paths in many geologic environments may increase both residence time in the subsurface and the opportunity for an increase in either chemical or nutrient content. In some instances both chemical and nutrient contents of the subsurface waters returning to an open channel downstream from a dam are increased.

The method used to study ground-water travel time requires a flow net of hydraulic potential contour lines and stream lines, shown conceptually for a small watershed without and with a lake in figure 4.
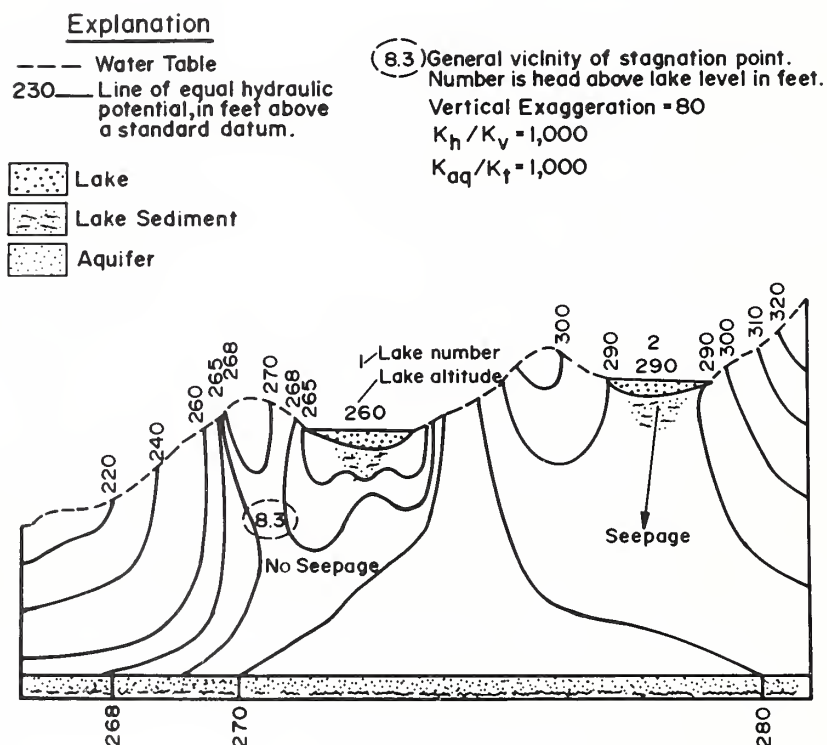

Figure 3
Diagram showing the effect of a stagnation point on lake seepage in the presence of a highly permeable aquifer at depth. (Modified from Winter 1976).
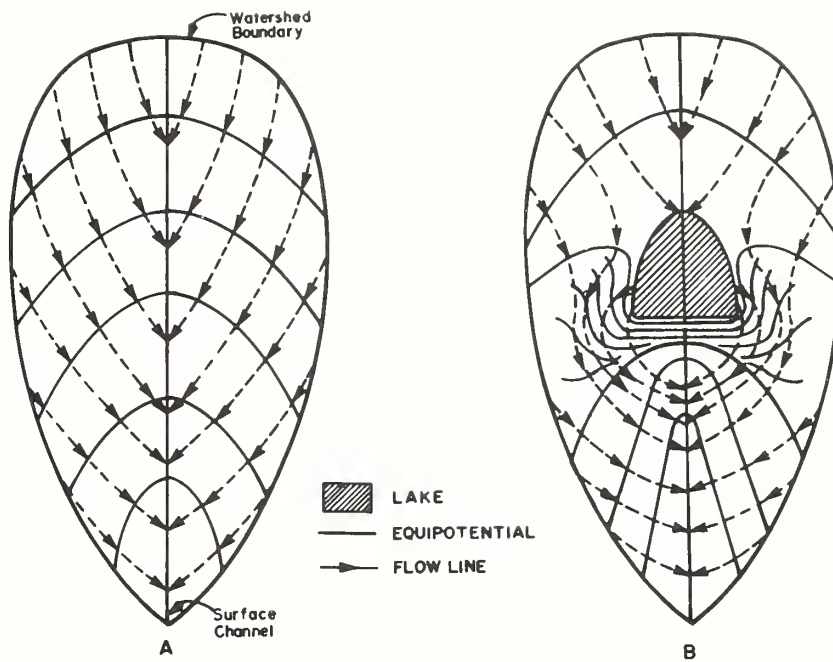
264

Figure 4
Ground water flow network without (A) and with (B) dam.

Seepage velocities can then be computed directly from the flow net. Darcy's equation used to describe the seepage velocity within an element of the flow net is

$$v_i = \frac{L_i}{\Delta t_i} = \frac{-K_i \; \Delta \phi_i}{P_i \; L_i} \qquad (5)$$

where v_i = seepage velocity of flow in an element of the flow tube, ft/day;

K_i = saturated permeability for the element, ft/day;

$\Delta \phi_i$ = potential drop across the element, ft;

P_i = porosity, dimensionless;

L_i = length across the element, ft;

Δt_i = time of travel across the element, days.

Thus:

$$T = \sum_{i=1}^{n} \frac{L_i}{v_i} \qquad (6)$$

where T = total time of travel along the flow tube, days;

and n = number of flow tube elements.

The travel time along any flow tube, between the reservoir and the intersection of the tube with the surface channel is developed from equation 6. The flow nets of the measured water surface elevations and of the predicted water surface elevations were used for the computation of travel times. Reservoir seepage determined by the analyses of the flow nets for modeled and measured conditions at the floodwater retarding structure was 13.0

and 11.5 acre-ft/yr, respectively, compared to a water budget analysis estimate of seepage for the same reservoir conditions of 21.9 acre-ft/yr (Naney and Thompson 1979).

Based on his analysis of the variables controlling flow from the subsurface to an open channel, Hall (1981) found that residence time is not a constant and that, therefore, the system is nonlinear for most small watersheds. Liong and DeCoursey (1982) investigated the subsurface contribution to streamflow by applying dimensional analysis to determine the functional relationship between the dependent and independent variables involved. Their study showed the dependence of subsurface contributions to streamflow on the dimensions of such factors as flow domain, soil properties, infiltration rate and duration, and the initial water table gradient. Gburek and Liong (personal communication) are investigating the use of both a water balance technique and a prediction equation developed by Liong and DeCoursey (1982) to estimate the contribution of subsurface flow to the open channel. Their approach uses the Dupuit-Forhheimer approximation for ground water storage changes within the watershed. Their method defines sections of the subsurface flow regime and applies subsurface flow characteristics by section in a manner similar to earlier applications of the theory for predicting base flow in a stream by Aron and Borrelli (1973) and Naney et al. (1978).

SUMMARY

The effects of seepage from an earthen-filled dam vary with geologic, climatologic, and hydrologic conditions of the dam site. In the case of small agricultural watersheds these effects may significantly alter the quality and quantity of downstream waterflow. For this reason, a mathematical model developed for predicting water, sediment, or chemical-nutrient discharge from such watersheds should also be capable of predicting the impacts of seepage within the modeled system.

The changes in ground water flow which occur as a result of seepage may influence both the residence time and the horizontal and vertical movement of water in the subsurface. Therefore, to the extent possible, data for any watershed to be studied should include the hydraulic characteristics of the subsurface flow regime and a definition of boundary conditions near any earthen-filled dam site.

The model should serve to enhance understanding of the hydrologic response of a small watershed to precipitation events. To do so, it should describe the processes involved and adequately predict changes in the amount or character of subsurface flow to the open channel from small watersheds whenever earthen-filled dams are present or may be constructed.

The authors have presented theoretical and physical factors to be considered when modeling seepage flow. Additionally, some examples are presented of efforts to improve the understanding of such flows, through the use of modeling techniques.

REFERENCES

Allred, E. R.; Manson, P. W.; Schwratz, G. M.; Golany, Pinhas; and Rienke, J. W. 1971. Continuation of studies on the hydrology of ponds and small lakes. Univ. Minnesota Agric. Experi. Station Tech. Bull. 274.

Amerman, C. R., and Naney, J. W. 1982. Subsurface flow and ground water systems. Chapt. 7 In Hydrologic Modeling of Small Watersheds, pp. 277-293. American Soc. of Agric. Engr., St. Joseph, Michigan.

Appel, C. A., and Bredehoeft, J. D. 1976. Status of ground-water modeling in the U. S. Geological Survey. USGS Circular 737.

Aron, G, and Borrelli, J. 1973. Stream baseflow prediction by convolution of antecedent rainfall effects. Water Resour. Bull. 9(2):360-365.

Bachmat, Yehuda; Bredehoeft, J. D.; Andrews, Barbara; Holtz, David; and Sebastian, Scott. 1980. Groundwater management: the use of numerical models. Water Resour. Monograph 5, p. 127. Amer. Geophysical Union, Washington, D. C.

Childs, E. C. 1969. An introduction to the physical basis of soil water phenomena. John Wiley and Sons, Ltd., London.

Dupuit, J. 1863. Etude theoriques et pratiquies sur le mouvement des eaux. Second ed., Dunod, Paris.

Gupta, S. K.; Tanji, K. K.; and Luthin, J. N. 1975. A three-dimensional finite element ground water model. Univ. of California-Davis, Calfornia Water Resources Center Contribution 152.

Hall, F. R. 1976. Relationships between small water bodies and groundwater. In Advances in Groundwater Hydrology, pp. 248-261. American Water Resour. Assoc., Minneapolis, Minnesota.

Hall, F. R. 1981. Subsurface water contributions to streamflow. In Rainfall-Runoff Relationship, pp. 237-244. Water Resour. Pub., Littleton, Colorado.

Hornberger, G. M.; Remson, I.; and Fungaroli, A. A. 1969. Numeric studies of a composite soil moisture ground-water system. Water Resour. Res. 5(4):797-802.

Hornberger, G. M.; Ebert, J.; and Remson, I. 1970. Numerical solution of the Boussinesq equation for aquiferstream interaction. Water Resour. Res. 6(2):601-608.

Jacob, C. E. 1950. Chapter V. Flow of ground water. In Rouse, Hunter (ed.)., Engineering Hydraulics, pp. 321-386. John Wiley and Sons, New York.

Liong, S. Y. and DeCoursey, D. G. 1982. Development of prediction equations for a phreatic aquifer in response to infiltration. Dimensional Analysis. Water Resour. Bull. 18(2):307-310.

Manson, P. W.; Schwartz, G. M.; and Allred, E. R. 1968. Some aspects of hydrology of ponds and small lakes. Univ. Minnesota Agric. Experi. Stat. Tech. Bull. 257.

Naney, J. W. 1974. The determination of the impact of an earthen-fill dam on the ground-water flow using a mathematical model. 119. pp. Masters thesis, Oklahoma State University, Stillwater.

Naney, J. W. 1983. Groundwater movement and quality, Section 12. In Hydrology, Erosion and Water Quality Studies of the Southern Great Plains Research Watershed, Washita River, Caddo and Grady Counties, Oklahoma, 1961-1979, pp. 134-141. USDA Science and Education Administration, Agric. Res. Results, Southern Region Series, New Orleans, LA.

Naney, J. W.; Kent, D. C.; and Seely, E. H. 1976. Evaluating ground-water paths using hydraulic conductivities. Ground Water 14(4):205-213. Nat'l Water Well Ass'n. Tech. Div., Worthington, Ohio.

Naney, J. W.; DeCoursey, D. G.; Barnes, B. B.; and Gander, G. A. 1978. Predicting baseflow using hydrogeologic parameters. Water Resour. Bull. 14(3):640-650. Am. Water Resour. Assn., Litho Crafters, Inc., Chelsea, MI.

Naney, J. W., and Thompson, T. B. 1979. Estimating seepage from a reservoir from change in hydraulic head. J. Hydr. 40:201-213. North-Holland Publishing Co., Amsterdam, The Netherlands.

Nelson, R. W. 1962. Steady darcian transport of fluids in heterogenous partially saturated porous media, Part I, Mathematical and numerical formulation. AEC Research and Development Report HW-72335 TT.I.

Prickett, T. A., and Lonnquist, C. G. 1971. Selected digital computer techniques for groundwater resource evaluation. Ilinois State Water Survey Bull. 55.

Remson, I.; Hornberger, G. M.; and Molz, F. J. 1971. Numerical methods in subsurface hydrology. Wiley-Inter-science, New York.

Soil Conservation Service, U. S. Department of Agriculture. 1970. Title. Soil Conservation 35(6):139.

Taylor, D. W. 1948. Fundamentals of soil mechanics. John Wiley and Sons, New York.

Trescott, P. C.,; Pinder, G. F.; and Larson, S. P. 1976. Chapter C1. Finite difference model for aquifer simulation in two dimensions with results of numerical experiments. In Techniques of Water Resources Investigations of the U. S. Geological Survey, pp. 2-33. Automated Data Processing and Computations, Box 7, USGS.

Van Schilfgaarde, J. 1974. Nonsteady flow to drains. In Agronomy No. 17 Drainage for Agriculture, pp. 245-307. American Society of Agronomy, Madison, WI.

Winter, T. C. 1976. Numerical simulation analysis of the interaction of lakes and ground water. USGS Prof. Paper 1001.

Winter, T. C. 1978. Numerical simulation of steady state three-dimensional groundwater flow near lakes. Water Resour. Res. 14(2):245-254.

Yost, Coyd, Jr., and Naney, J. W. 1974. Water Quality effects of seepage from earthen dams. Jour. of Hydrology 21:15-26. North-Holland Publishing Co., Amsterdam, The Netherlands.

Yost, Coyd, Jr., and Naney, J. W. 1975. Earth-dam seepage and related land and water problems. Jour. of Soil and Water Conservation 30(2):87-91. Soil Conser. Soc. Am., Ankeny, Iowa.

Zektzer, I. S. 1973. Studying the role of groundwater flow in water and salt balances of lakes. Internatl. Assoc. Hydrol. Sci. Pub. No. 109. pp. 197-201.

GENERATION OF DAILY WEATHER DATA

C. W. Richardson

ABSTRACT

A computer simulation model is described that can be used to generate daily values of precipitation, maximum temperature, minimum temperature, solar radiation, and wind speed. The weather data that are generated are representative of the weather at a specific site and may be used as input to hydrologic models. An example application of the model is given, and data generated with the model are compared with actual weather data.

INTRODUCTION

The general climate of an area and the day-to-day variations in weather have a major influence on hydrologic processes. Climate and weather strongly influence the surface and subsurface movement of water, the movement of sediment, the transportation and disposition of chemicals, and other related processes. Many hydrologic models require the input of weather data to calculate the output of the various processes that are simulated. For many sites, actual weather data are not available in sufficient detail or in sufficient length to permit the desired simulation. When such is the case, the capability to generate weather data that have the same statistical properties as the actual weather at the site offers an attractive alternative. This paper describes a procedure that may be used to generate daily weather data at an arbitrary site.

The procedure is called WGEN (Weather Generator) and is capable of generating daily values of precipitation, maximum temperature, minimum temperature, solar radiation, and wind speed. The procedure is a modification of the weather generation model described by Richardson (1981) with a wind speed component added. Two options are provided for the user. With option 1, daily values of all five weather variables are generated. With option 2, actual rainfall data are used and daily values of the other variables are generated. Option 2 is provided because long records of rainfall data are available at many locations without corresponding data for the other variables.

WEATHER GENERATION PROCEDURE

Daily values of precipitation (p), maximum temperature (t_{max}), minimum temperature (t_{min}), solar radiation (r), and wind speed (v) are generated with WGEN. Precipitation and wind speed are generated independent of the other variables. Maximum temperature, minimum temperature, and solar radiation are generated conditioned on the wet or dry status of the day.

Precipitation

A first-order Markov chain is used to generate the occurrence of wet or dry days. The probability of rain on a given day is conditioned on the wet or dry status of the previous day. A wet day is defined as a day with 0.2 mm of rain or more. Let $P_i(W/W)$ be the probability of a wet day on day i, given a wet day on day i-1; and let $P_i(W/D)$ be the probability of a wet day on day i, given a dry day on day i-1. Then

$$P_i(D/W) = 1 - P_i(W/W) \tag{1}$$

$$P_i(D/D) = 1 - P_i(W/D)$$

where $P_i(D/W)$ and $P_i(D/D)$ are the probabilities of a dry day, given a wet day on day i-1, and the probability of a dry day, given a dry day on day i-1, respectively. Therefore, the transition probabilities are fully defined, given $P_i(W/W)$ and $P_i(W/D)$.

Agricultural Engineer and Laboratory Director, USDA-ARS, Grassland, Soil and Water Research Laboratory, Temple, TX 76502.

A two-parameter gamma distribution is used to describe the distribution of precipitation amounts on wet days. The density function of the two-parameter gamma distribution is given by

$$f(p) = \frac{\beta^{\alpha} p^{\alpha-1} e^{-\beta p}}{\Gamma(\alpha)} \quad , \qquad p > 0 \tag{2}$$

where α and β are distribution parameters and $\Gamma(\alpha)$ is the gamma function of α. The α and β are shape and scale parameters, respectively.

The values of $P(W/W)$, $P(W/D)$, α, and β vary seasonally for most locations. In WGEN each of the four precipitation parameters is held constant for a given month but is varied from month to month. Let $P_j(W/W)$, $P_j(W/D)$, α_j, and β_j be defined as the values of the parameters for month j. The values of each of the four parameters have been determined by month for numerous locations in the United States and are given in Richardson and Wright (1984). The parameters are used with a Markov chain generation procedure and the gamma generation procedure described by Haan (1977) to generate daily precipitation values.

Temperature and Solar Radiation

The procedure that is used in WGEN for generating daily values of t_{max}, t_{min}, and r is described by Richardson (1981). The procedure is based on the weakly stationary generating process given by Matalas (1967). The equation is

$$\chi_i(k) = A\chi_{i-1}(k) + B\varepsilon_i(k) \tag{3}$$

where $\chi_i(k)$ is a 3 X 1 matrix for day i whose elements are values of t_{max} (k = 1), t_{min} (k = 2), and r (k = 3) with the seasonal means and standard deviations removed (residuals), ε_i is a 3 X 1 matrix of independent random components, and A and B are 3 X 3 matrices whose elements are defined such that the new sequences have the desired serial correlation and cross correlation coefficients. The A and B matrices are given by

$$A = M_1 M_0^{-1} \tag{4}$$

$$BB^T = M_0 - M_1 M_0^{-1} M_1^{\ T} \tag{5}$$

where the superscripts -1 and T denote the inverse and transpose of the matrix. M_0 and M_1 are matrices containing the lag-zero cross correlation coefficients and the lag-one serial correlation coefficients, respectively.

The seasonal and spatial variations in the correlation coefficients were found by Richardson (1982) to be relatively small. If the small variations are neglected and the average values of the correlation coefficients given by Richardson (1982) are used, the A and B matrices become

$$A = \begin{bmatrix} 0.567 & 0.086 & -0.002 \\ 0.253 & 0.504 & -0.050 \\ -0.006 & -0.039 & 0.244 \end{bmatrix} \tag{6}$$

$$B = \begin{bmatrix} 0.781 & 0 & 0 \\ 0.328 & 0.637 & 0 \\ 0.238 & -0.341 & 0.873 \end{bmatrix} \tag{7}$$

The A and B matrices given in equations (6) and (7) are used with equation (3) in WGEN to generate new sequences of t_{max}, t_{min}, and r that are serially correlated and cross correlated.

The final daily generated values of t_{max}, t_{min}, and r are determined by adding a seasonal mean and standard deviation to the residual elements generated with equation (3) using the equation

$$t_i(k) = \chi_i(k) \cdot s_i(k) + m_i(k) \tag{8}$$

where $t_i(k)$ is the daily value of t_{max} ($k = 1$), t_{min} ($k = 2$), and
r ($k = 3$); $s_i(k)$ is the standard deviation; and $m_i(k)$ is the mean for day
i. The values of $m_i(k)$ and $s_i(k)$ are conditioned on the wet or dry status,
as determined from the precipitation component of the model. By expressing
equation (8) in terms of the coefficient of variation ($c = s/m$) rather than the
standard deviation, the equation becomes

$$t_i(k) = m_i(k) [\chi_i(k) \cdot c_i(k) + 1] \tag{9}$$

The seasonal change in the means and coefficients of variation may be described
by

$$u_i = \bar{u} + C \cos(0.0172 (i - T)) , i = 1, ..., 365 \tag{10}$$

where u_i is the value of the $m_i(k)$ or $c_i(k)$ on day i, $\bar{u}$ is the mean of
u_i, C is the amplitude of the harmonic, and T is the position of the harmonic
in days (Figure 1). Values of $\bar{u}$, C, and T have been determined for the mean
and coefficient of variation of each weather variable (t_{max}, t_{min}, r) and
for the wet or dry condition. These values were determined from the daily
weather data for many locations. There were no detectable differences in the
means and coefficients of variation to t_{min} on wet or dry days.

Some of the parameters were strongly location dependent while other parameters
did not change significantly with location. The values of T for all of the
descriptors of temperature (means and coefficients of variation of t_{max} and
t_{min}) were near 200 days for all locations. Similarly, the T values for r
were about 172 days (summer solstice) for all locations. Therefore, in WGEN
all of the T values for temperature are assumed to be 200 days, and all the T
values for solar radiation are assumed to be 172 days.

The $\bar{u}$ and C values vary with location. The values for each parameter have been
mapped and are given in Richardson and Wright (1984). An example is given in
Figure 2.

Wind

The wind component of WGEN provides for the generation of daily values of mean
wind speed. Daily wind speed may be related to the daily temperature, solar
radiation, or precipitation values. However, in WGEN the correlation between
daily wind speed and the other variables is assumed negligible, and wind speed
is generated independent of the other variables. Wind speed is generated using
a two-parameter gamma distribution expressed as

$$f(v) = \frac{\gamma_j^{\lambda_j} v^{\lambda_j - 1} e^{-\gamma_j v}}{\Gamma(\lambda_j)} \tag{11}$$

where λ_j and γ_j are distribution parameters for month j, and v is daily
wind speed. The values of λ_j and γ_j are estimated, using the method of
moments, by

$$\lambda_j = \bar{v}_j^2 / s_j^2 \tag{12}$$

and

$$\gamma_j = \bar{v}_j / s_j^2 \tag{13}$$

where $\bar{v}_j$ is the mean daily wind speed and s_j is the standard deviation of
daily wind speed. "The Climatic Atlas of the United States" (U.S. Department
of Commerce, 1968) contains values of $\bar{v}_j$ for many locations. The mean annual
wind speed ($\bar{v}_y$) and the standard deviation of hourly wind speed on an annual
basis (s_h) are also available in the climatic atlas. By experimenting with
the standard deviation of hourly and daily wind speeds for several locations, a
correction factor of 0.7 was found to be appropriate for converting the
standard deviation of hourly wind speed to the standard deviation of daily wind
speed.

If the coefficient of variation of daily wind speed (c_v) for a location is assumed to be constant over the year, c_v may be estimated by

$$c_v = 0.7 \, s_h \, / \, \bar{v}_y \, .\hspace{4cm}(14)$$

The s_j values may be calculated by

$$s_j = c_v \cdot \bar{v}_j \, .\hspace{4cm}(15)$$

The $\bar{v}_j$ and s_j values are used with the gamma generation procedure (Haan, 1977) to generate daily wind speeds.

EXAMPLE

The procedure for generating the daily weather variables will be illustrated by generating a 30-year sample of weather data for Columbia, MO. The parameters used to generate the data are given in Tables 1a, 1b, and 1c. The precipitation parameters were obtained from a 20-year (1951-70) sample of rainfall data for Columbia. The temperature and solar radiation parameters were obtained from maps, developed by the author, that give the spatial patterns of the parameters. The wind parameters were obtained from the climatic atlas.

The generated data and the actual data are compared in Tables 2-5. The mean monthly precipitation amounts and the mean number of wet days for each month are shown in Table 2 for the generated and observed data. The mean precipitation amount for each month and that for the year from the generated data are very similar to those obtained from the observed data. The mean monthly precipitation amounts from the generated data were not significantly different from the observed means for any of the months. Similarly, the mean number of wet days per month from the generated data did not differ significantly from the observed mean for any month.

Many applications of hydrologic models are related to processes, such as surface runoff, sediment movement, and chemical transport, that are strongly influenced by excessive rainfall amounts. The mean number of days per month with excessive rainfall amounts (> 50 mm) from the generated data are compared to the number of observed excessive rainfall days in Table 2. The number of excessive rainfall days from the generated data is very close to that from the observed data. Both the generated and observed data show a strong tendency for the excessive rainfall amounts to occur during the summer months at Columbia.

Maximum and minimum temperatures and solar radiation data generated with WGEN are compared with the observed data in Table 3. The mean daily maximum temperature from the generated data was about the same as that from the observed data for all months. The largest difference was 1.9°C for October. The mean daily maximum temperature on an annual basis was only 0.3°C less than that from the observed data. The mean daily minimum temperatures and mean daily solar radiation from the generated data also compared favorably with the observed means. None of the differences in the means of the observed and generated data for maximum temperature, minimum temperature, or solar radiation were significant (5% level).

The average annual extreme temperatures and the number of days with extreme temperatures are compared in Table 4. The average annual maximum temperature from the generated data was only 1.0°C greater than that from the observed data. The average annual minimum temperature from the generated data was 0.9°C less than the observed. The average number of days per year with freezing temperatures and that with temperatures above 35°C from the generated data also compared closely with those from the observed data.

The mean monthly wind speeds from the generated data are shown in Table 5 and compared favorably with those from the observed data.

SUMMARY

WGEN can be used to generate daily weather variables that are required for various hydrologic models. The generation procedure produces daily values of precipitation, maximum temperature, minimum temperature, solar radiation, and wind speed that approximate the actual weather for a site.

Application of WGEN to a particular site requires that the generation parameters be determined. The precipitation parameters have been defined for many locations, and the temperature and radiation parameters have been mapped for the United States. The wind speed parameters may be obtained from the "Climatic Atlas of the United States" (U.S. Department of Commerce, 1968).

The climatic atlas and the maps and tables that have been developed describe the large scale variation in parameters. Careful judgment should be used in applying WGEN in areas where small scale changes may occur due to physiographic features such as high elevations or orientation of mountain ranges. If weather data of relatively short length are available for the site, the parameters can be defined from the data and the parameter values used to generate weather sequences of greater length.

REFERENCES

Haan, C. T. 1977. Statistical Methods in Hydrology. The Iowa State University Press, Ames, Iowa, 378 pp.

Matalas, N. C. 1967. Mathematical assessment of synthetic hydrology. Water Resources Res. 3(4):937-945.

Richardson, C. W. 1981. Stochastic simulation of daily precipitation, temperature, and solar radiation. Water Resources Res. 17(1):182-190.

Richardson, C. W. 1982. Dependence structure of daily temperature and solar radiation. Trans. ASAE 25(3):735-739.

Richardson, C. W. and D. A. Wright. 1984. WGEN: A model for generating daily weather variables. USDA-ARS, ARS-8, 80 pp.

U.S. Department of Commerce. 1968. Climatic atlas of the United States. Environmental Science Services Administration, Environmental Data Service, 80 pp.

Table 1a
Parameters for generating daily precipitation
(mm) for Columbia, MO.

Month	Parameter			
	P(W/W)	P(W/D)	α	β
Jan.	0.412	0.181	0.643	8.0
Feb.	.405	.224	.712	8.1
Mar.	.456	.274	.695	9.1
Apr.	.477	.309	.816	9.5
May	.445	.279	.803	12.8
June	.473	.279	.677	15.1
July	.454	.243	.706	15.4
Aug.	.340	.205	.662	14.4
Sept.	.415	.199	.612	20.4
Oct.	.403	.182	.585	18.9
Nov.	.353	.163	.735	9.4
Dec.	.424	.208	.750	7.0

Table 1b
Parameters for generating daily maximum and minimum temperatures
(°C) and solar radiation (ly) for Columbia, MO.

Statistic	Wet/Dry	$\bar{u}$	C	T
	Maximum Temperature			
Mean	Dry	18.6	14.2	200
Mean	Wet	17.2	14.2	200
Coefficient of variation	Dry/wet	0.18	−0.13	200
	Minimum Temperature			
Mean	Dry/wet	6.7	13.1	200
Coefficient of variation	Dry/wet	.27	−.30	200
	Solar Radiation			
Mean	Dry	430	225	172
Mean	Wet	259	225	172
Coefficient of variation	Dry	0.24	−0.08	172
Coefficient of variation	Wet	0.48	−0.13	172

Table 1c
Parameters for generating daily wind speed for Columbia, MO.

Parameter	Month	Speed, m/sec
Mean annual speed, $\bar{v}_y$	--	4.2
Std. dev. of hourly speed, s_h	--	2.3
Mean monthly speed, $\bar{v}_j$	Jan.	4.5
	Feb.	4.9
	Mar.	5.4
	Apr.	5.4
	May	4.0
	June	4.0
	July	3.6
	Aug.	3.6
	Sept.	3.6
	Oct.	3.6
	Nov.	4.5
	Dec.	4.9

Table 2
Average precipitation amount, average number of wet days, and average number
of excessive rainfall days (>50 mm) by month from actual data (1951-70) and
generated data (30 years), Columbia, MO.

Month	Precipitation amount, mm		Number of wet days		Number of days with precipitation >50 mm	
	Observed	Generated	Observed	Generated	Observed	Generated
Jan.	35.8	32.2	7.1	6.1	0	0
Feb.	42.7	42.7	7.6	7.3	0	0
Mar.	63.7	75.4	10.4	10.8	.05	0
Apr.	92.2	86.4	11.4	11.0	.10	0
May	113.0	104.6	10.5	10.6	.10	.17
June	105.4	121.7	10.4	10.9	.25	.27
July	100.3	112.5	9.3	9.4	.15	.27
Aug.	72.1	79.7	7.5	7.0	.20	.23
Sept.	101.6	100.1	7.9	7.3	.40	.30
Oct.	79.2	85.3	7.6	7.1	.20	.17
Nov.	40.1	43.9	6.2	6.1	0	0
Dec.	42.2	47.2	8.3	8.6	0	0
Annual	888.5	931.9	104.2	102.2	1.45	1.41

Table 3
Mean daily maximum temperature, minimum temperature, and solar radiation by month and for the year from data generated with WGEN (30 years) and from observed data (1951-70), Columbia, MO.

Month	Max. temp., °C Observed	Max. temp., °C Generated	Min. temp., °C Observed	Min. temp., °C Generated	Solar rad., ly Observed	Solar rad., ly Generated
Jan.	3.4	4.2	-6.8	-6.2	186	193
Feb.	6.2	5.5	-4.3	-5.3	261	258
Mar.	10.9	9.9	-0.3	-0.9	348	343
Apr.	19.0	17.7	7.0	6.5	440	452
May	24.3	24.0	12.4	12.4	531	541
June	28.9	30.4	17.4	17.7	571	581
July	31.5	32.1	19.7	19.6	584	578
Aug.	30.8	30.6	18.7	18.1	523	516
Sept.	26.9	25.6	14.2	13.4	427	403
Oct.	20.7	18.8	8.2	7.0	322	287
Nov.	12.3	11.6	1.2	0.5	212	207
Dec.	5.6	6.7	-3.9	-4.0	161	153
Year	18.4	18.1	7.0	6.5	381	377

Table 4
Average annual maximum temperature, minimum temperature, number of days per year with temperature greater than 35°C, and number of days per year with temperature less than 0°C from data generated with WGEN (30 years) and from observed data (1951-70), Columbia, MO.

Variable	Observed	Generated
Average annual max. temp., °C	37.8	38.8
Average annual min. temp., °C	-20.6	-21.5
Average no. days per year $\geq$ 35°C	13.5	14.4
Average no. days per year $\leq$ 0°C	108.1	113.1*

* The generated mean is significantly different from the observed mean at the 5% level.

Table 5
Mean daily wind speed by month and for the year from observed data (1971-75) and generated data (30 years), Columbia, MO.

Month	Wind speed, m/sec. Observed	Wind speed, m/sec. Generated
Jan.	4.7	4.7
Feb.	5.3	4.7*
Mar.	5.5	5.4
Apr.	5.1	5.3
May	3.8	4.1
June	4.0	4.2
July	3.7	3.6
Aug.	3.3	3.6*
Sept.	3.6	3.7
Oct.	3.8	3.4*
Nov.	4.4	4.4
Dec.	4.6	5.1*
Year	4.3	4.3

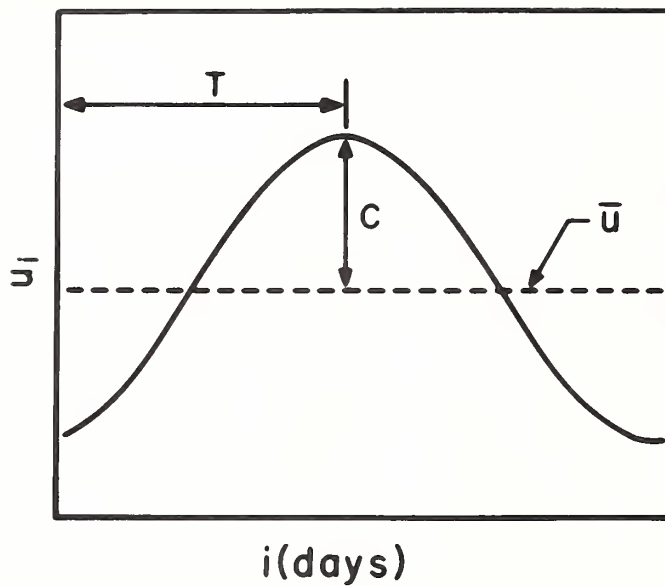* The generated mean is significantly different from the observed mean at the 5% level.

Figure 1
Definition of variables in seasonal description
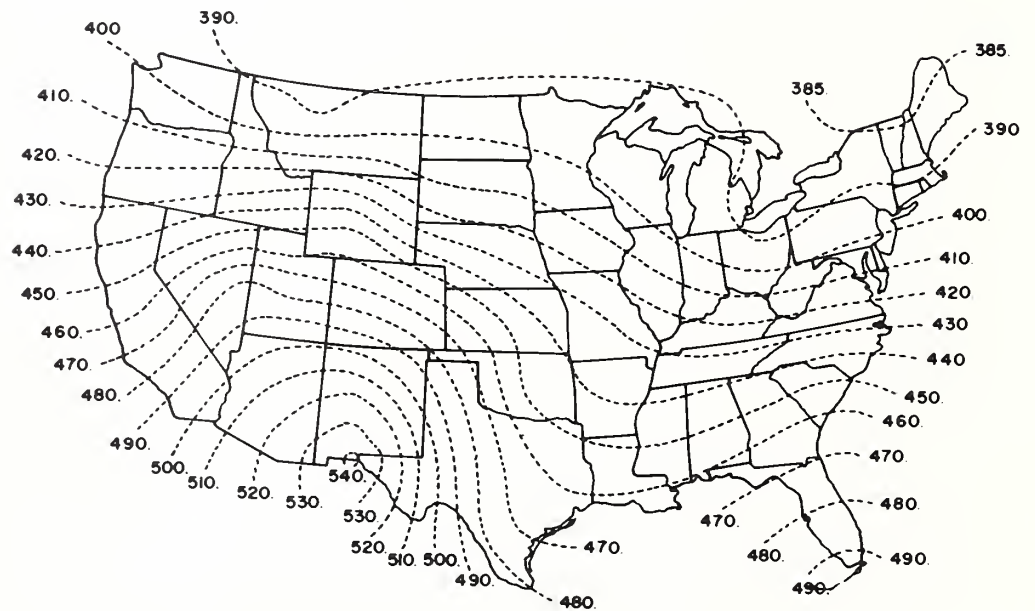of temperature and solar radiation.

Figure 2
Example map of weather generation parameters. (Mean daily solar
radiation on dry days, 1y.)